TECHNICAL REPORT

# Hydrologic and Carbon Services in the Western Ghats: Response of Forest and Agro-ecosystems to Extreme Rainfall Events

Submitted to:

**Ministry of Earth Sciences**,
Government of India


# Hydrologic and Carbon Services in the Western Ghats: Response of Forest and Agro-ecosystems to Extreme Rainfall Events

TECHNICAL REPORT

June 2017

Submitted to:

Ministry of Earth Sciences,

Government of India

Edited by

Jagdish Krishnaswamy, Nick Chappel, Ravinder Singh Bhalla, Mahesh Sankaran, Srinivas Vaidyanathan, Shrinivas Badiger, and Susan Varghese

**Implementing Institute:** Ashoka Trust for Research in Ecology and the Environment (ATREE)

**Collaborating Institutes:** Foundation for Ecological Research, Advocacy and Learning (FERAL) and National Centre for Biological Sciences (NCBS)

**The Changing Water Cycle programme was set up in 2010 and was the first UK Natural Environment Research Council (NERC) and Ministry of Earth Sciences (MoES) India's joint collaborative research programme that ran from 2010 – 2016. The Changing Water Cycle in South Asia programme aimed to develop a UK-India integrated, quantitative understanding of the changes taking place in the global water cycle, involving all components of the earth system, improving predictions for the next few decades of regional precipitation, evapotranspiration, soil moisture, hydrological storage and fluxes.**

**The programme worked to understand how local to regional scale hydrological and biogeochemical processes respond to changing climate and land use, together with their consequent impacts on the sustainable use of soil and water. It also investigated the consequences of the changing water cycle for water-related natural hazards, including floods and droughts, improving prediction and mitigation of these hazards.**

**Five UK-India projects were funded under the programme and one of those funded was the current project titled "Hydrologic and carbon services in the Western Ghats: Response of forests and agro-ecosystems to extreme rainfall events"**

**(UK Principal Investigator: Professor Michael Bonell (deceased), Dundee and replaced by Dr Nick Chappell, University of Lancaster; Indian Principal Investigator: Dr Jagdish Krishnaswamy, ATREE, Bangalore)**


**Contributors**

**Project scientists**: Jagdish Krishnaswamy, Nick Chappell, Mike Bonell (late), Ravi S Bhalla, Mahesh Sankaran, Shrinivas Badiger, John Rowan, Wlodek Tych, Srinivas Vaidyanathan, Susan Varghese, Naresh Vissa, Trevor Page, Tim Jones, and Ciaran Broderick.

**Project researchers**: Saravanan S, Kumaran K, Vivek Ramachandran, Siva Kumar, Shivona Bhojwani, Manish Kumar, Vidyadhar Atkore, Tarun Nair.

**Field staff**: Kamalraj S, Senthil Kumar, Yogisha Bhat, Manohar Kalal, Vinayaka, Mahesha.

**Lab staff**: Vindhya NG

**Interns**: Vaijayanti Vijayaraghavan and Prachi Ghatwai.



Suggested citation:

Krishnaswamy J, Chappel N, Bhalla RS, Sankaran M, Vaidyanathan S, Badiger S & Varghese S.(2017). Hydrologic and Carbon Services in the Western Ghats: Response of Forest and Agro-ecosystems to Extreme Rainfall Events. Technical Report submitted to Ministry of Earth Sciences, Government of India. 67pp.

Dedicated to Professor Michael (Mike) Bonell 1943-2014

# ACKNOWLEDGEMENTS

We thank Dr. Vijay Kumar of the Ministry of Earth Sciences for his excellent administrative support throughout the project. Professor Vinod Gaur who served as an advisor to the Ministry of Earth Sciences was a pillar of support and encouragement to the India and UK Principal Investigators and for ensuring an intellectually stimulating environment for the research teams. We are grateful to the Forest Departments of Karnataka and Tamil Nadu for giving us research permits and for installation of instrumentation in the forest areas. The distinguished panel of our international advisory group consisting of Prof. Dr. L.A. (Sampurno) Bruijnzeel, Dr. Wouter Buytaert (Imperial College) and Prof. David Schultz (University of Manchester) gave us critical and insightful suggestions for scaling up our work. We thank distinguished visitors to our field sites, Professor Sampurno Bruijnzeel and Professor Keith Beven enriching our project with their wisdom and experience. Dr. Mark Mulligan from Kings College London gave us the opportunity to set up two low cost FREESTATION weather stations and Arduino based soil moisture probes.

We thank Vivek Ramachandran, Rajat R Nayak and Manish Kumar for their contribution to various aspects of instrumentation in the field and in implementing salt-dilution gauging. We thank Vaijayanti Vijayaraghavan and Prachi Ghatwai for their pioneering work on land-cover mapping and infiltration measurements at our sites. We thank Shivona Bhojwani for her contribution towards data analysis and processing. We thank the accounts team – Sridhar Iyengar, Sindhu S. (late), Vartika Saxena, Ashoka B., Bhogaiah B. (all ATREE), Shanthi (FERAL), and Suresh Vardarajan and HR Uma (both NCBS). Dr. Siddhartha Krishnan helped in securing necessary permissions. A special thanks to Nature Conservation Foundation and Agumbe Rainforest Research Station for sharing their weather station data.

A number of individuals extended their support on a personal basis to this project. Mr. Balachandra Hegde, his family and friends provided safe locations for our hydro-met loggers in Aghanashini as did Mr. Vijay (Red Hills), Mr. Hegde (Chamraj and Korakunda tea estates) in the Nilgiris and the management of Travancore Rubber and Tea Estate in Ariankavu.

# CONTENTS

**Chapter 1: Spatial and temporal dimensions of extreme rain events in India** ..... *1*

*Jagdish Krishnaswamy and Srinivas Vaidyanathan*

**Chapter 2: Synoptic typology of rain storms in the Western Ghats: Hydrologic implications** ..... *11*

*Naresh Vissa, Mike Bonell, Nick A Chappell, Wlodek Tych, Page Trevor, Jagdish Krishnaswamy, Ravi Bhalla, and Srinivas Vaidyanathan*

**Chapter 3: Modelling storm flow in sub-surface flow dominated systems of the Western Ghats** ..... *19*

*Nick Chappel, Tim Jones, Wlodek Tych, and Jagdish Krishnaswamy*

**Chapter 4: Impacts of land-cover on catchment hydrology** ..... *19*

*Jagdish Krishnaswamy, Srinivas Vaidyanathan, Ravinder Singh Bhalla, Shrinivas Badiger, Mike Bonell, Nick Chappell, Yogisha Bhat, S. Saravanan and Manohar Kalal*

**Chapter 5: Carbon dynamics in Response to moisture and temperature forcing** ..... *19*

*Mahesh Sankaran, Raghavendra HV, Atul Joshi, Harinandan PV, and Manaswi Raghurama.*

**Chapter 6: Emerging Policy recommendations** ..... *55*

*Nick Chappell, Jagdish Krishnaswamy, and Ravinder Singh Bhalla*

**Chapter 7: Outreach** ..... *59*

*Susan Varghese*

**Chapter 8: Syntheses and conclusions** ..... *67*

*Jagdish Krishnaswamy, Nick Chappel, Mahesh Sankaran and Ravinder Singh Bhalla*

# CHAPTER 1: SPATIAL AND TEMPORAL DIMENSIONS OF EXTREME RAIN EVENTS IN INDIA

*Jagdish Krishnaswamy and Srinivas Vaidyanathan*

## 1.1: INTRODUCTION

Rainfall in India has been declining since the 1950s, even as intense rains have become more frequent (Krishnan et al. 2013; Bollasina et al. 2011; Krishnaswamy et al. 2015; Goswami et al. 2006). These trends have been linked to global warming; teleconnections such as La Nina and Indian Ocean Dipole (IOD); warming of Indian Ocean relative to land (Turner and Annamalai 2012; Saji et al. 1999; Ashok et al. 2004; Cherchi and Navarra 2013; Kumar et al. 1999; Roxy et al. 2015). Additionally, a second set of drivers that include aerosols and land-use change (Bollasina et al. 2011; Douglas et al. 2009; Kishtawal et al. 2010) are known to affect rainfall and its intensity. There is increasing concern in India on the impacts arising from the variability in rainfall levels as well as the increasing frequency of extreme rainfall events (Ghosh et al. 2012; Goswami et al. 2006).

Rainfall in India and the associated high intensity rain events are largely confined within the period of June to November, primarily governed by the South-West Monsoons (SWM) and North-East Monsoons (NEM), each with their spatially coherent signatures (Kripalani and Kumar 2004). Both these Monsoons have distinct, complex and evolving relationships with the two main ocean-atmosphere phenomena, the El Nino Southern Oscillation (ENSO) and the Indian Ocean Dipole (IOD) (Ashok et al. 2004; Saji et al. 1999). La Nina, the positive phase of ENSO is often beneficial for the SWM, especially in the latter half (Gill et al. 2015; Xavier et al. 2007). Positive IOD helps mitigate the negative effects of El Nino on Indian Monsoon and is linked to extreme rainfall events (ERE) in non-El Nino years (Ashok et al. 2004). However, there is concern that warming of oceans and the atmosphere, changes the spatial and temporal influence of these phenomena in complex ways (Krishnaswamy et al. 2015; Roxy et al. 2015). In this context, the increasing spatial variability in rainfall is a matter of major policy concern in India (Kishtawal et al. 2010; Singh et al. 2014).

A spatially explicit analysis of changes in the strength of linkages between intense rain events in India and these ocean-atmosphere phenomena will provide insights into other potential drivers of rainfall trends, and for vulnerability analyses under future climate change (Kumar et al. 2011). This could also provide impetus to develop regional forecast models, rather than country wide forecast models with poor prediction skills. Using time-varying regression models on spatially explicit rainfall data we determine areas witnessing an increase or decline in intense rain events.

## 1.2: METHODS

The annual NINO4 (average SST over 160°E to 150°W and 5°S to 5°N), an ENSO index based on the Extended Reconstructed SST dataset (ERSSTv3) was used. This index was chosen based on recent results which showed this region to have a stronger teleconnection with IM (Kumar et al. 2006). The sign of the index was reversed to give a positive correlation with IM rainfall. Positive values correspond to La Nina, which is associated with higher IM

rainfall. The IOD index is the difference in anomalies in sea surface temperature (SST) between the western (50°E to 70°E and 10°S to 10°N) and eastern (90°E to 110°E and 10°S to 0°S) tropical Indian Ocean (Saji et al. 1999).

To analyze long-term temporal trends in EREs we aggregated data for the entire country (1901 – 2006) using the gridded dataset from Indian Meteorological Department (Rajeevan et al. 2006) ERE frequencies for each year were computed as the number of days for which rainfall exceeding thresholds of 25, 50, 100, 150 and 200 mm per day.

For the spatially explicit analysis we used the APHRODITES's daily gridded data (1951-2007), the only long-term, continent scale, high resolution daily product (0.25°) which is now being used to determine changes in Asian monsoon precipitation (Yatagai et al. 2012). ERE frequencies for each grid cell was computed as the number of days for which rainfall exceeded the 100mm threshold. Additionally, for each cell we defined intense rain as an event, if the daily rainfall total equaled or exceeded the 90% percentile of daily totals during the period 1951-2007.

A spatially explicit version of dynamic models was developed to analyze intense rainfall-LaNina/IOD relationships for each grid. For every APHRODITE grid cell in India, we constructed the time-series of annual counts of intense rain events with the corresponding NINO4 and IOD indices. In these models the regression parameters, the time varying intercept or level ($\beta 0_t$) and the regression slopes ($\beta 1_t$,$\beta 2_t$ ) change with time for every APHRODITE grid in India.

Dynamic regression of ERE against the covariates for each grid for the period 1951-2007 yielded 57 time-varying intercepts and slopes. We estimated the Sen slope (Sen 1968) for the original time-series as well as time-varying intercept and the regression slopes for La Nina and IOD. P-values were estimated to map areas with significant ($p<0.1$) monotonic trends.

## 1.3: KEY FINDINGS

The temporal trend in ERE counts at various thresholds indicates that rain events greater than 100 mm have increased in the last 100 years. The time-varying regression intercept (Fig 1(a-e)) indicates multi-decadal variability, and highlights an overall increasing trend in EREs of 100, 150 and 200 mm exceedance since the early 1900s. However, there is a lot of variability in recent decades. Earlier studies across multi-decadal scales have shown a similar increasing trend in EREs over the Indian subcontinent (Goswami et al. 2006; Rajeevan et al. 2008). The time varying slopes of NINO4 and IOD can be seen in Fig 1(f-j) and Fig 1(k-o), respectively. The influence of IOD has been increasing, while that of NINO4 has been declining, over the last few decades, particularly for the higher exceedance thresholds. The non-stationarity in the influence of NINO4 and IOD on the IM and corresponding EREs is quite clear from DLM – they both point to an increasing influence of IOD on EREs since the 1940s with the slope changing from negative to positive, albeit with a high degree of uncertainty.

At lower exceedance thresholds (25, 50mm day-1), IOD has an influence on frequency of EREs only in its positive phase, but for higher exceedance thresholds, the positive influence of IOD is evident across the range of the IOD index values (Fig 2). Thus, IOD is more important for influencing EREs at higher exceedance levels. Furthermore, for the higher exceedance EREs there is a pronounced non-linear dip in the influence of IOD at the higher end, possibly suggesting the inhibiting influence of un-modelled processes or the influence of different physical processes when compared to lower thresholds.

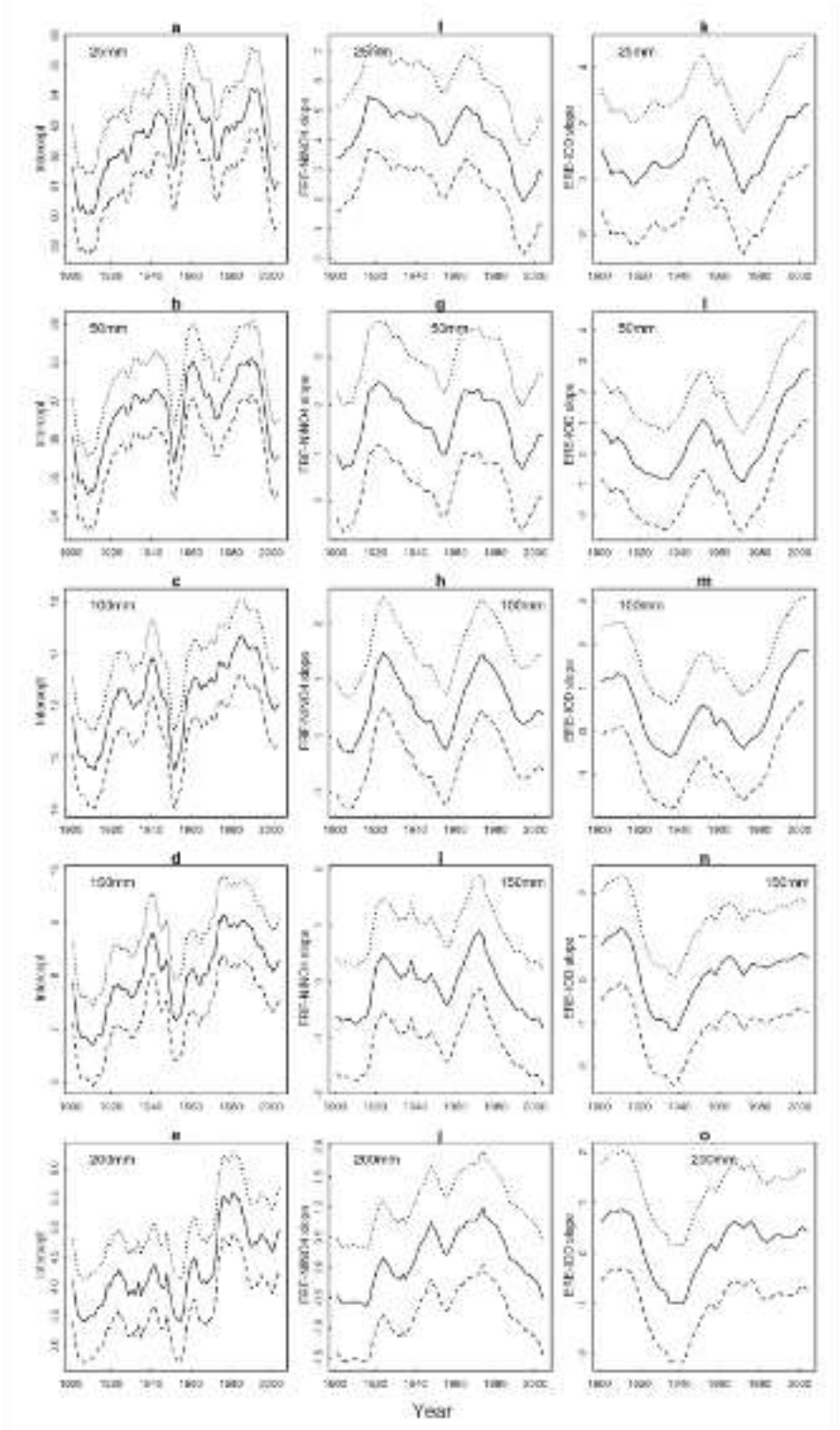


*Figure 1-1 Reproduced from (Krishnaswamy et al. 2015). Time-varying influence of NINO4 and IOD on the annual counts of EREs (square root transformed) for the periods 1901-2004 at different daily exceedance thresholds (25mm, 50mm, 100mm,150mm and 200mm).The time-varying level and regression slope coefficients are plotted (red lines) along with 25th (green line) and 75thintervals (blue line). The first column (a-e) plots the time-varying level or intercept. The third column (f-j) show the time-varying regression slope coefficient of ERE with NINO4, while the last column (k-o) shows the regression coefficient slope of ERE against IOD. Note the increasing influence of IOD in recent decades relative to earlier periods.*

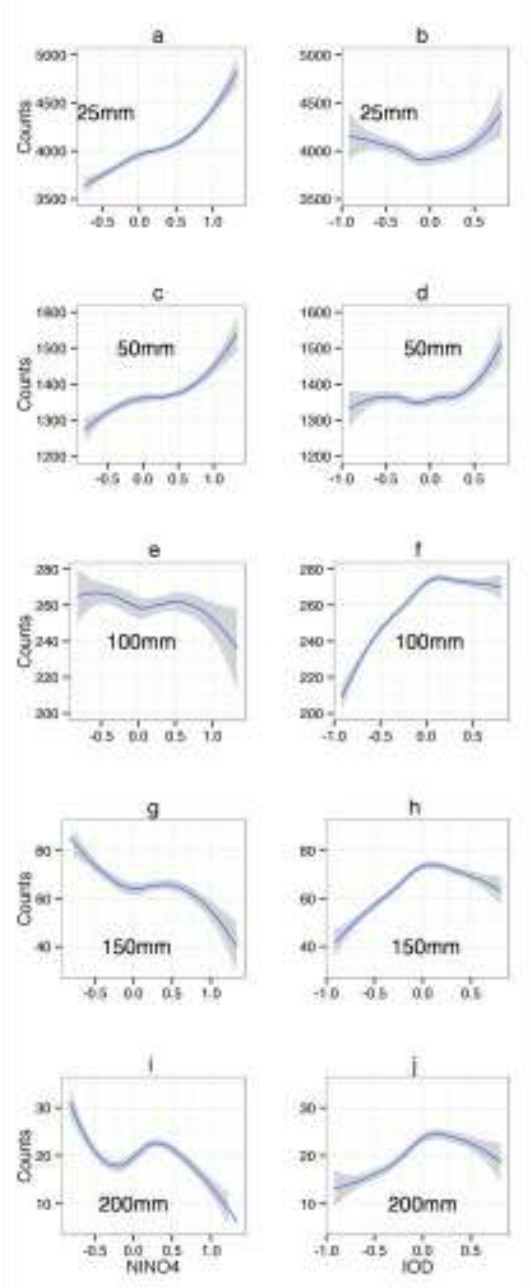


*Figure 1-2 Reproduced from (Krishnaswamy et al. 2015). Non linear response of ERE counts to NINO4 and IOD. Modeled ERE counts as a function of NINO4 (a-e) and IOD (f-j) for time periods 1901-2004 for rainfall exceedance thresholds of 25mm (row 1), 50mm (row 2), 100mm (row 3), 150mm (row 4) and 200mm (row 5). The solid lines represent the fitted values of ERE counts as a function of either NINO4 or IOD based on Generalized Additive Modeling, while the shaded areas represent the standard error bands. IOD emerges as the more monotonic and consistent driver of EREs especially at higher exceedance thresholds.*

Nonlinearities in the relationships are quite apparent. Positive values of IOD are generally associated with an increase in ERE counts (all results were significant at $p < 0.001$), but for 100mm and above, EREs increase with the IOD index, but flatten out at positive IOD values, suggesting that local or regional drivers in addition to the two ocean-atmosphere phenomena could be influencing occurrence of very high EREs.

When we consider spatial trends in annual counts of daily totals exceeding 100 mm day$^{-1}$, the significant trends are few (0.75% of the land area) and scattered across India (Figure 3a).

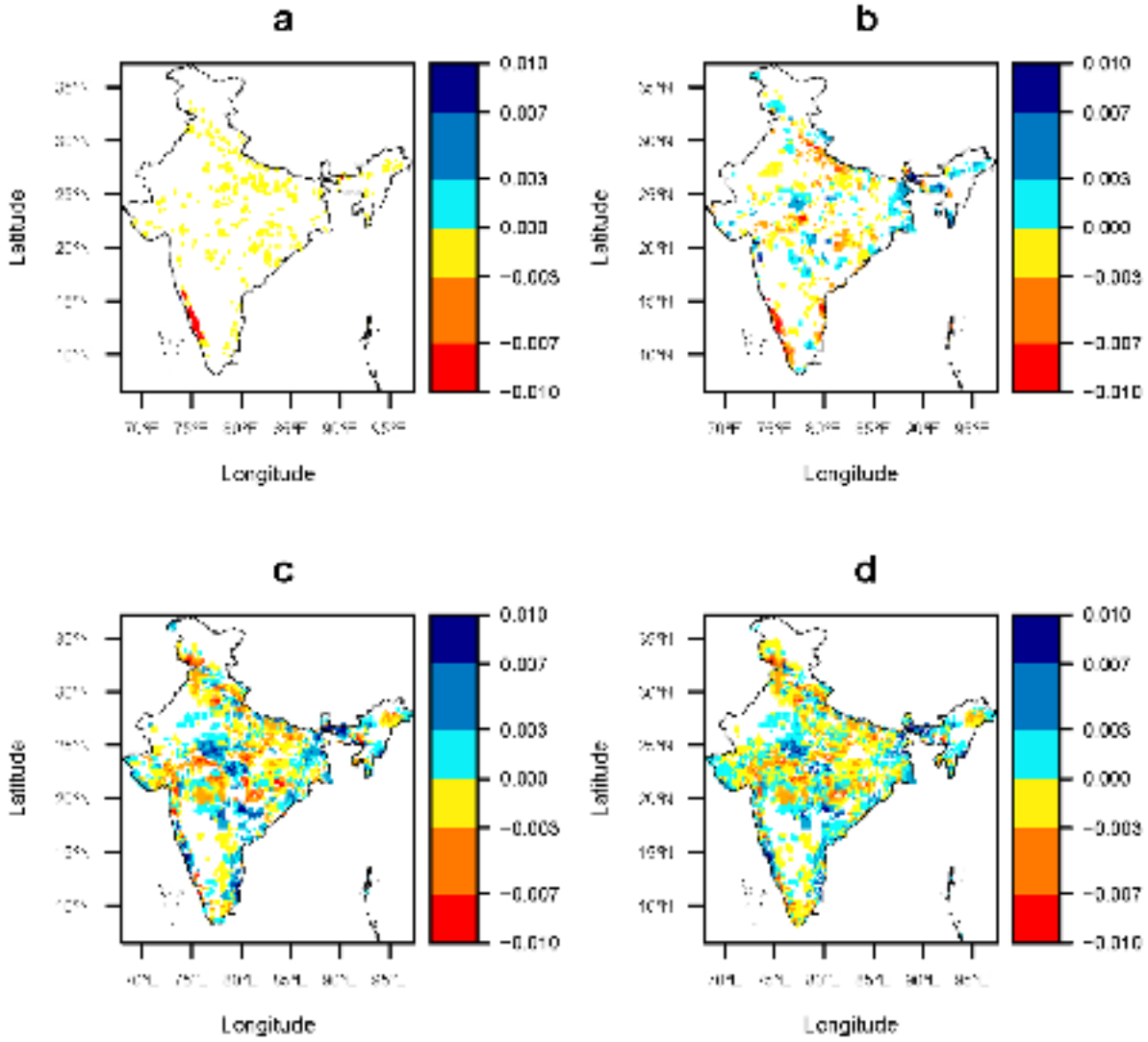


*Figure 1-3 Adapted from Krishnaswamy and Vaidyanathan inprep (a-d) Sen slope trends in the time-varying intercept and regression slopes for La Nina and IOD from the spatial explicit modeling of ERE against La Nina and IOD as covariates. The trends in the time-varying intercept suggest that once the influence of the two ocean-atmosphere phenomena are modeled out, nearly 10% of India is witnessing an increasing trend in rain events>100mm/day. However, the influence of La Nina and IOD is not spatially coherent.*

However, once the influence of ENSO and IOD is accounted for, the time-varying intercept (Figure 1-3b) shows that there are pockets of scattered positive (9% of the land area) and negative trends (11%). Both these ocean atmosphere phenomenon have strong influence on intense rain events in the Western Ghats and Indo-Gangetic plains (Figure 3c-d). Over 25.6% of land area across India shows positive trends for IOD compared to ENSO (21.6%). However, land area showing negative trends with respect to IOD and ENSO are exceeding areas showing a positive trend (30.7% and 24.3% respectively).

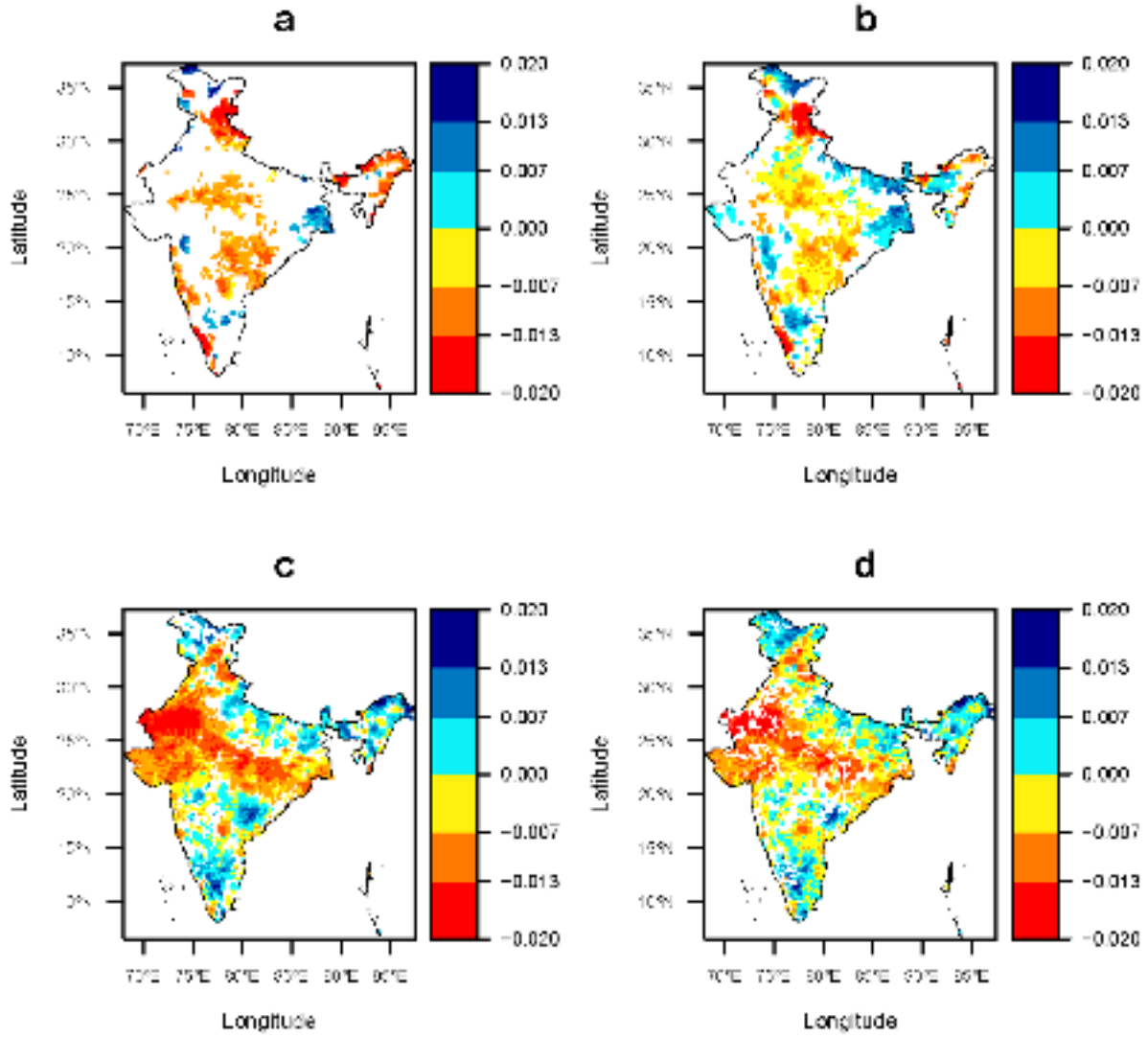


*Figure 1-4 Adapted from Krishnaswamy and Vaidyanathan inprep (a-d) Trends in the time-varying intercept and regression slopes for La Nina and IOD from the spatial explicit modeling of ERE, defined using the 90$^{th}$ percentile of daily totals against La Nina and IOD as covariates. There is a systematic increase in the spatial coherence when compared to the static threshold of 100mm.*

Instead of uniformly applying the 100mm threshold across the country, we defined intense rain as an event if the daily rainfall total equaled or exceeded the 90% percentile of daily totals during the period 1951-2007. The overall patterns and trends are similar to results from the 100mm threshold (Figure 1-4), there is a lot more spatial coherence in areas showing positive (16% of the land area) and negative trends (30% of the land area). EREs are increasingly being defined in terms of their impacts in certain regions or under specific antecedent moisture conditions, and the carrying capacity of the ecosystem rather than based only on absolute or relative values (Pielke and Downton 2000). For example, in the Himalayas, 25 mm day-1 is considered a critical threshold for the occurrence of major landslides once adequate antecedent moisture has accumulated (Gabet et al. 2004). Similarly, other global and regional studies, which define heavy and extreme precipitation for studying long-terms trends or impacts of climate change, have classified events of 25 mm day-1as extreme events (Zhai et al. 2005; Groisman et al. 1999; Hennessy et al. 1997).

Irrespective of the threshold, this still leaves large areas that do not show any significant monotonic trend in the influence of these two drivers on annual counts of intense rain events. The lack of spatial coherence in both indices, suggests that other local and regional drivers are more influential on frequency of intense rain events.

Analysis of rainfall extremes & rainfall-runoff response with respect to meteorological characteristics (Figure 1-5) show contrasting monsoon rainfall totals with Aghanashini at 6457mm and Nilgiris at 2807 mm. The primary data collected during the project suggested that Aghanashini exceed Nilgiris twice the number of extreme rainfall events.

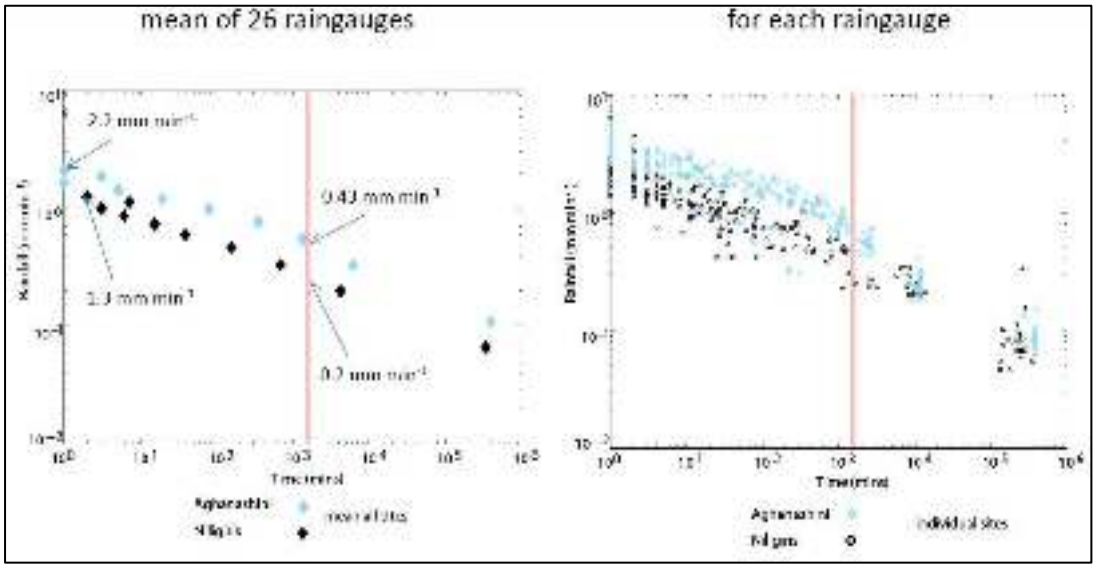


*Figure 1-5: Mean of rainfall per minute for rain gauges in both Aghnashini and Nilgiris.Results also indicate that the potential for predicting maximum rain intensities using daily rain totals is still not established unless we can further tease apart the factors that could influence this relationship over time and space (Figure 1-6).*

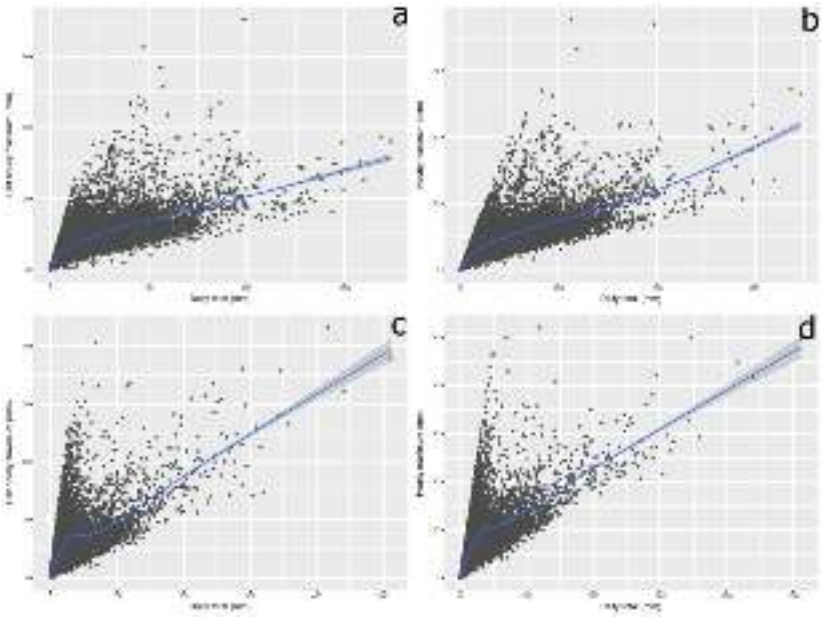


*Figure 1-6: Daily rainfall total for Aghanashini (a & b) and Nilgiris (c & d), on X axis and maximum daily hourly rain intensity recorded on same day on Y axis. There is a positive relationship but the uncertainty and variability in the relationship increases to very high magnitude at higher daily totals, potentially caused by changes in synoptic rain generating mechanisms as the Monsoon progresses, as well as, differences across pre-Monsoon, SW Monsoon and NE Monsoon contributions to rain.*

## 1.4: CONCLUSION

1. Long-term historical data on intense rain events aggregated over the entire country shows an increasing trend in such events. However, the spatio-temporal trends indicate pockets of increase and decrease suggesting that intense rain events are getting restricted to certain parts of the country. Additionally, the spatio-temporal influence of ENSO and IOD suggests that other local and regional drivers are more influential on frequency of intense rain events, except perhaps in the Western Ghats. Our work suggests that the spatially-explicit time-varying influences of major drivers of the Monsoon and EREs such as the ENSO and IOD needs to be considered in assessing which parts of the country are more prone to these influences in order to develop a more region specific forecast.
2. Number of extreme rainfall events in the Aghanashini basin is higher than the Nilgiris basin.
3. The potential for predicting maximum rain intensities using daily rain totals is not yet established unless we can further tease apart the factors that could influence this relationship over time and space.

## 1.5: REFERENCES

Ashok, K., Z. Guan, N. H. Saji, and T. Yamagata, 2004: Individual and combined influences of ENSO and the Indian Ocean dipole on the Indian summer monsoon. *J. Clim.*, **17**, 3141–3155.

Bollasina, M. A., Y. Ming, and V. Ramaswamy, 2011: Anthropogenic aerosols and the weakening of the South Asian summer monsoon. *Science*, **334**, 502–505.

Cherchi, A., and A. Navarra, 2013: Influence of ENSO and of the Indian Ocean Dipole on the Indian summer monsoon variability. *Clim. Dyn.*, **41**, 81–103, doi:10.1007/s00382-012-1602-y.

Douglas, E. M., A. Beltrán-Przekurat, D. Niyogi, R. A. Pielke, and C. J. Vörösmarty, 2009: The impact of agricultural intensification and irrigation on land–atmosphere interactions and Indian monsoon precipitation—A mesoscale modeling perspective. *Glob. Planet. Change*, **67**, 117–128.

Gabet, E. J., D. W. Burbank, J. K. Putkonen, B. A. Pratt-Sitaula, and T. Ojha, 2004: Rainfall thresholds for landsliding in the Himalayas of Nepal. *Geomorphology*, **63**, 131–143.

Ghosh, S., D. Das, S.-C. Kao, and A. R. Ganguly, 2012: Lack of uniform trends but increasing spatial variability in observed Indian rainfall extremes. *Nat. Clim. Change*, **2**, 86–91, doi:10.1038/nclimate1327.

Gill, E. C., B. Rajagopalan, and P. H. Molnar, 2015: Sub-Seasonal Variations in Spatial Signatures of ENSO on the Indian Summer Monsoon from 1901-2009. *J. Geophys. Res. Atmospheres*, 2015JD023184, doi:10.1002/2015JD023184.

Goswami, B. N., V. Venugopal, D. Sengupta, M. S. Madhusoodanan, and P. K. Xavier, 2006: Increasing trend of extreme rain events over India in a warming environment. *Science*, **314**, 1442–1445.

Groisman, P., and Coauthors, 1999: Changes in the Probability of Heavy Precipitation: Important Indicators of Climatic Change. *Clim. Change*, **42**, 243–283, doi:10.1023/A:1005432803188.

Hennessy, K. J., J. M. Gregory, and J. F. B. Mitchell, 1997: Changes in daily precipitation under enhanced greenhouse conditions. *Clim. Dyn.*, **13**, 667–680, doi:10.1007/s003820050189.

Kishtawal, C. M., D. Niyogi, M. Tewari, R. A. Pielke Sr, and J. M. Shepherd, 2010: Urbanization signature in the observed heavy rainfall climatology over India. *Int. J. Climatol.*, **30**, 1908–1916.

Kripalani, R. H., and P. Kumar, 2004: Northeast monsoon rainfall variability over south peninsular India vis-à-vis the Indian Ocean dipole mode. *Int. J. Climatol.*, **24**, 1267–1282.

Krishnan, R., and Coauthors, 2013: Will the South Asian monsoon overturning circulation stabilize any further? *Clim. Dyn.*, **40**, 187–211, doi:10.1007/s00382-012-1317-0.

Krishnaswamy, J., S. Vaidyanathan, B. Rajagopalan, M. Bonell, M. Sankaran, R. S. Bhalla, and S. Badiger, 2015: Non-stationary and non-linear influence of ENSO and Indian Ocean Dipole on the variability of Indian monsoon rainfall and extreme rain events. *Clim. Dyn.*, **45**, 175–184, doi:10.1007/s00382-014-2288-0.

Kumar, K. K., B. Rajagopalan, and M. A. Cane, 1999: On the weakening relationship between the Indian monsoon and ENSO. *Science*, **284**, 2156–2159.

——, ——, M. Hoerling, G. Bates, and M. Cane, 2006: Unraveling the mystery of Indian monsoon failure during El Niño. *Science*, **314**, 115–119.

Kumar, K. K., and Coauthors, 2011: The once and future pulse of Indian monsoonal climate. *Clim. Dyn.*, **36**, 2159–2170, doi:10.1007/s00382-010-0974-0.

Pielke, R. A., and M. W. Downton, 2000: Precipitation and Damaging Floods: Trends in the United States, 1932–97. *J. Clim.*, **13**, 3625–3637, doi:10.1175/1520-0442(2000)013<3625:PADFTI>2.0.CO;2.

Rajeevan, M., J. Bhate, J. D. Kale, and B. Lal, 2006: High resolution daily gridded rainfall data for the Indian region: Analysis of break and active monsoon spells. *Curr. Sci.*, **91**, 296–306.

——, J. Bhate, and A. K. Jaswal, 2008: Analysis of variability and trends of extreme rainfall events over India using 104 years of gridded daily rainfall data. *Geophys. Res. Lett.*, **35**, L18707.

Roxy, M. K., K. Ritika, P. Terray, R. Murtugudde, K. Ashok, and B. N. Goswami, 2015: Drying of Indian subcontinent by rapid Indian Ocean warming and a weakening land-sea thermal gradient. *Nat Commun*, **6**. http://dx.doi.org/10.1038/ncomms8423.

Saji, N. H., B. N. Goswami, P. N. Vinayachandran, and T. Yamagata, 1999: A dipole mode in the tropical Indian Ocean. *Nature*, **401**, 360–363, doi:10.1038/43854.

Sen, P. K., 1968: Estimates of the Regression Coefficient Based on Kendall's Tau. *J. Am. Stat. Assoc.*, **63**, 1379–1389, doi:10.2307/2285891.

Singh, D., M. Tsiang, B. Rajaratnam, and N. S. Diffenbaugh, 2014: Observed changes in extreme wet and dry spells during the South Asian summer monsoon season. *Nat. Clim Change*, **4**, 456–461.

Turner, A. G., and H. Annamalai, 2012: Climate change and the South Asian summer monsoon. *Nat. Clim Change*, **2**, 587–595, doi:10.1038/nclimate1495.

Xavier, P. K., C. Marzin, and B. N. Goswami, 2007: An objective definition of the Indian summer monsoon season and a new perspective on the ENSO–monsoon relationship. *Q. J. R. Meteorol. Soc.*, **133**, 749–764, doi:10.1002/qj.45.

Yatagai, A., K. Kamiguchi, O. Arakawa, A. Hamada, N. Yasutomi, and A. Kitoh, 2012: APHRODITE: Constructing a Long-Term Daily Gridded Precipitation Dataset for Asia Based on a Dense Network of Rain Gauges. *Bull. Am. Meteorol. Soc.*, **93**, 1401–1415, doi:10.1175/BAMS-D-11-00122.1.

Zhai, P., X. Zhang, H. Wan, and X. Pan, 2005: Trends in Total Precipitation and Frequency of Daily Precipitation Extremes over China. *J. Clim.*, **18**, 1096–1108, doi:10.1175/JCLI-3318.1.

# CHAPTER 2: SYNOPTIC TYPOLOGY OF RAIN STORMS IN THE WESTERN GHATS: HYDROLOGIC IMPLICATIONS

*Naresh Vissa, Mike Bonell, Nick A Chappell, Wlodek Tych, Page Trevor, Jagdish Krishnaswamy, Ravinder Singh Bhalla, Srinivas Vaidyanathan*

## 2.1: INTRODUCTION

Western Ghats (WG) are the narrow chain of mountains running parallel to the west coast of India of about 1500 km from Kanyakumari (southern tip) to river Tapi (northern tip) with the exception of Palakkad Gap. Deccan Plateau is situated at the eastern side of the WG, over Deccan Plateau major rivers such as Godavari and Krishna flows towards the east coast of India. Notable features influencing regional atmospheric dynamics include the coastal highlands of the WG. Precipitation is more dominant across the latter, and is characterised by deeper and larger-scale systems (Shrestha et al., 2015). South Eastern Arabian Sea (SEAS) has a significant influence on the meteorology and results of this work. For example, during the winter season thick ocean barrier layer and temperature inversions are the prominent features of the SEAS (Thadathil *et al.,* 2008; Vissa *et al.,* 2013). The extent of BL in the SEAS can be used as a predictor for the onset of summer monsoon (*Masson et al.,* 2005). From February to May sea surface temperatures (SST) in the SEAS region exceeds more than 29° C, which has been refereed as the Arabian Sea mini - warm pool (Vinayachandran *et al.,* 2007) and thus during pre-monsoon (May) season, SEAS are considered as the warmest region in the world (Joseph, 1990; Vinayachandran *et al.,* 2007). Under the influence of strong monsoon winds the circulation of the AS ocean switches direction annually (Beal *et al*., 2013). Rainfall patterns over the west coast of India are significantly impacted by the convection of the AS (Francis and Gadgil, 2006).

Over the WG, annual rainfalls exceed 5000mm with a marked concentration (~80%) occurring in the months June-September, and associated very sharp isohyetal gradients in line with the very complex topography, as reviewed by Gunnell, (1997). The marked rainfall gradients (and associated complex geology and soils) result in the WG being a global biodiversity 'hot spot' linked with a range of forest-types supplemented by a major reforestation programme (Pascal, 1982; Menon and Bawa, 1997; Ramchandra *et al.,* 2004; Sen *et al.,* 2010; reviewed in Bonell *et al.,* 2010). This area also includes a diverse range of agricultural activities and occupied by over 150 million people. All of these functions and communities are vulnerable to extreme rainfall events (and thus floods) which have been reported to be increasing in frequency or projected to do so in India with global warming (Goswami *et al*., 2006; Rajeevan *et al*., 2008, Ghosh *et al*., 2012). Thus a better understanding of the spatial and temporal changes in diurnal and characteristics of rainfalls across seasons towards the identification of the most rainfall impacted areas during extreme events and in turn, flood generation is crucial. In addition, such work may better identify the more favourable areas for rain-fed agriculture, especially during the pre-monsoon when early crop growth is critical. In this context the present chapter is intended to understand the characteristics of extreme rainfall events over WG.

## 2.2: OBJECTIVES

Main objective: To couple the synoptic and mesoscale meteorology with the spatial and temporal dimensions of Extreme Rainfall Events (ERE) in the Western Ghats (Karnataka and Tamil Nadu States): hydrologic responses

To accomplish the main objective the following component objectives are examined

*1.1.Component objectives - the spatial dimension:*

- Over the diurnal cycle (& its seasonal evolution), identify hot spots of rainfall activity over Western Ghats using the recent TRMM 3B42 v7 observations (1998-2015) at the mesoscale – to identify likely hot spots of flood incidence

*2.1.2 Component objectives - the temporal dimension:*

- Typing rain-producing, synoptic-scale systems over the Western Ghats based on satellite outgoing long-wave radiation (OLR) at 0.25 degree and half hourly resolutions.

## 2.3: THE STUDY AREA AND ITS GEOGRAPHIC LIMITS

The topographic (GTOPO30) map of the study area and the names of various locations are shown in Figure 2-1. The study area comprises the geographical boundaries surrounding 8° N - 23° N and 70° E – 78° E; it consider the regions South Eastern Arabian Sea (SEAS), Western Ghats (~ 8° N– 22° N) and Deccan Plateau.

## 2.4: DATA AND METHODOLOGY

### 2.4.1: *Diurnal cycle of rainfall*

In the present study we have utilized rain rates from the latest release of Tropical Rainfall Measuring Mission (TRMM) 3B42 version 7 (V7) available at three hourly with the grid being at spatial resolution of quarter degree (0.25° x 0.25°) for the period 1998-2015. The three hour time block rain rates are the three hourly averaged values centred at the middle of each hour period. The 3B42 algorithm is an optimal product, it considers the various high quality microwave and infrared estimates from different multi satellite passive microwave and geostationary estimates at every three hour interval (for more information about 3B42 algorithm see http:// trmm.gsfc.nasa.gov/3b42.html).

### 2.4.2: *Rainfall indices*

Following Varikoden et al., (2011, 2012) rainfall frequency) or occurrence maps at different octets (0230, 0530, 0830, 1130, 1430, 1730, 2030, and 2330 LST) (LST is UTC + 0530 hrs.), are developed for each of the four seasons. In the present study, at each grid point (i.e., at scale 0.25° x0.25°), is counted as a *rainy day* when rain occurs at any hour during that particular day. Rainfall frequency for each octet is expressed in terms of a *Rain Frequency Percentage (RFP)* at each grid point. The RFP suggests the occurrence of rainfall at that particular hour during in that season as a percentage of the total number of rainy days.

$$RFP = \frac{RN_h}{N} \times 100$$

Where N represents the total number of rainy days in a particular season at a particular grid point, and $RN_h$ represents the total number of rain occurrences at that particular hour. Thus the higher the percentage implies that the chance of rain occurrence is much higher for a particular octet.

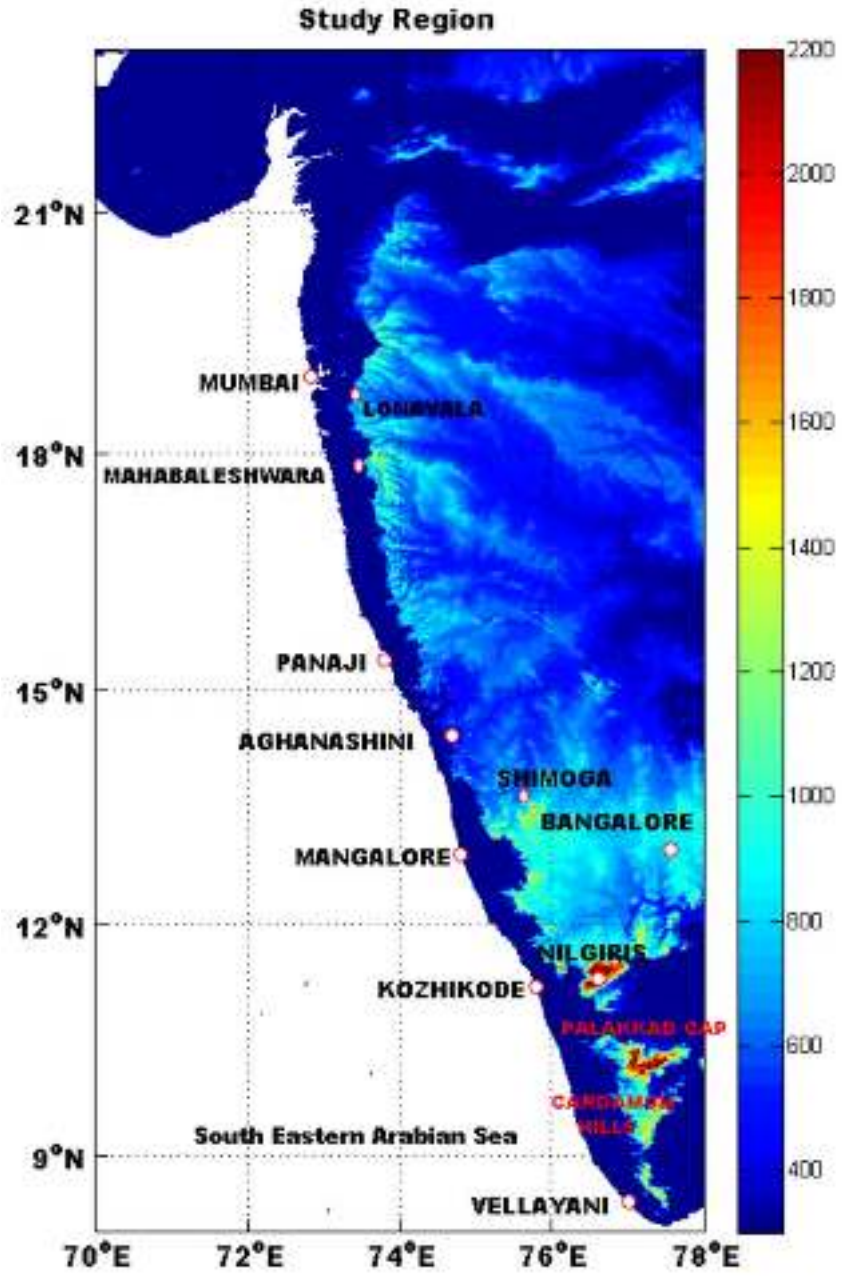


*Figure 2-1: GTOPO30 topography map of study region with locations of important places*

### 2.4.3: *Synoptic typology of rain storms in the WG*

In order to investigate our secondary aim, each discrete storm period was classified as a type of synoptic or mesoscale meteorological event, rather than the typical active and break phases describing wet and dry periods within the monsoon. This was achieved using Outgoing Longwave Radiation (OLR) data from the Indian Satellite ISRO Kalpana I and India Meteorological Department (IMD) reports, using the method described in (e.g. Madan et al. 2005; Francis and Gadgil, 2006) to classify each period into the following synoptic classes, or hybrids/variants of these classes: Tropical Convergence Zone (TCZ); off shore convection (OSC); TCZ embedded with OSC and low pressure systems. As an objective method for identifying storm periods, wavelet analysis of catchment average rainfall was employed.

Wavelet analysis was chosen as it is a robust method for irregularly distributed signals in time, which also have nonstationary power at different frequencies (Daubechies 1990): as is the case for rainfall. Specifically, Mortlet wavelet transformations were used within the software detailed by Torrence and Compo (1998), which allows significant storm periods (i.e. statistically significant from the wavelet analysis) to be delineated. This method was employed to Aghanashini and Nilgiris basin for the period 2013-2014 filed campaign TBRG one-hourly rainfall data.

## 2.5: KEY FINDINGS

### *2.5.1: Diurnal cycle of rainfall over WG*

The diurnal cycle of the maximum RFP and time of primary peak during different octets of the pre-monsoon and monsoon are shown in Figure 2-2.

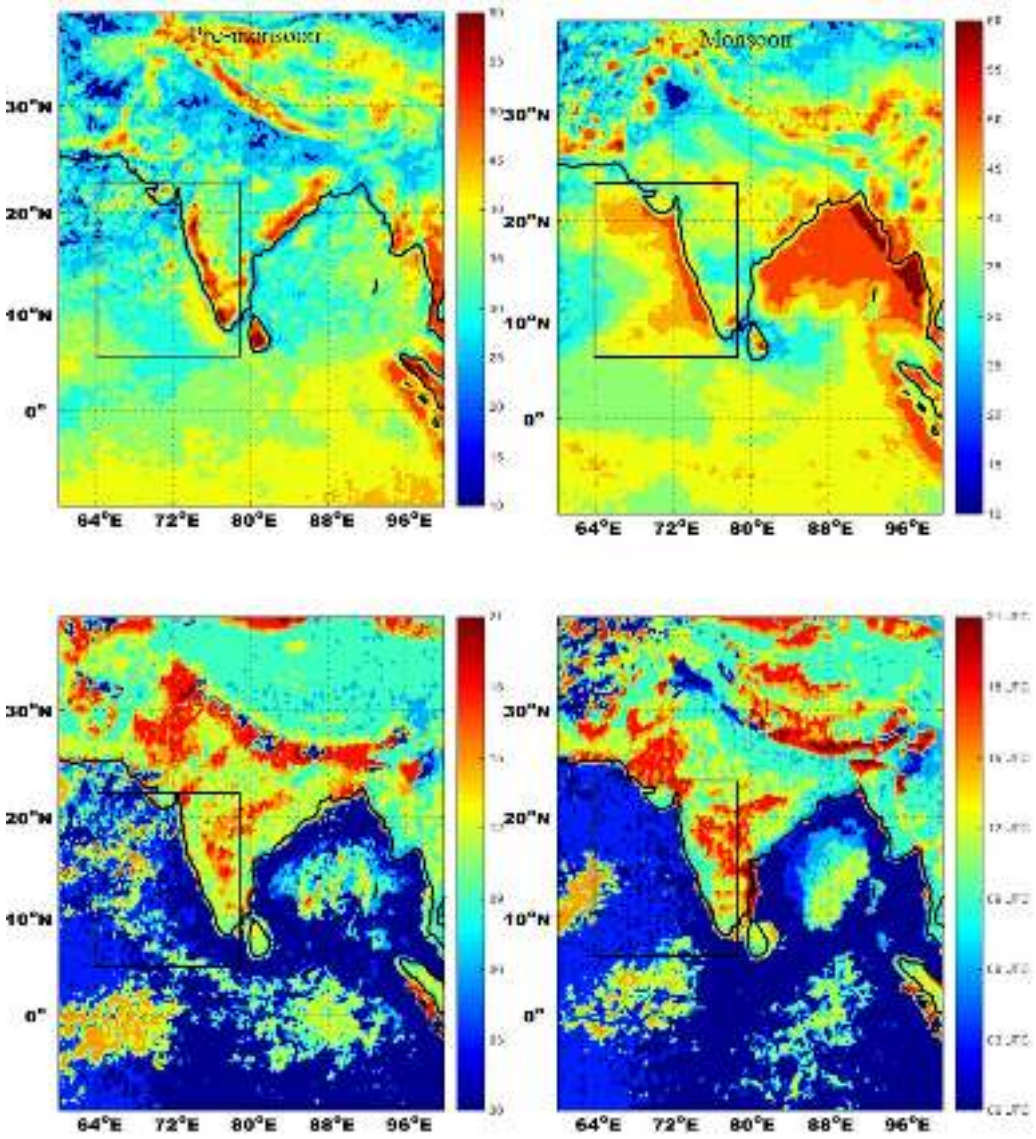


*Figure 2-2: The diurnal cycle of the maximum RFP (top panel) and time of the primary peak during different octets (bottom panel) of the pre-monsoon and monsoon seasons.*

During the pre-monsoon and monsoon season, late-evening to early morning peak is evident over the SEAS, although more predominant during the monsoon season. Findings are concurrent with the Yang and Smith (2006). Over the WG mid-to-late afternoon peak is evident, more significantly during the pre-monsoon season due to the occurrence of thunderstorms (Kandalgaonkar et al., 2005; Vishnu et al., 2013) which are associated with deep and convective cores (Romatschke and Houze, 2010) which could contribute to these hot spots. Subsequently an eastward shift in activity is observed at 1500 and 1800 UTC octets, these events could be attributed to nocturnal thunderstorms triggered by a low level jet (Prabha et al., 2011) during pre-monsoon season. The boundary layer, low level jet induced moisture convergence could be one of the mechanisms responsible for the nocturnal rainfall peak (Murthy et al. 2013) during monsoon season. During monsoon season, an18-year mean and active monsoon periods rain shadow is apparent over the Deccan Plateau (leeward side of the WG). In the present study possible drivers of the diurnal cycle of rainfall over the oceans and continental regions are explored using recently reported observational and modelling studies. This would be useful as such mountainous areas are also the source of floods leading to potentially downstream loss of life or crop damage or inflows of fresh-water, sediment and nutrients into estuaries and coastal and marine environments . Thus the identification of 'hot spots' of preferred high rainfalls during extreme events is required as part of flood forecasting.

### *2.5.2: Storm typing from OLR and wavelet analysis*

Using wavelet analysis, OLR maps analysis and IMD synoptic charts information extreme rainfall events are categorized. Synoptic class for the periods over the basins is classified following Francis and Gadgil (2006).Storm typing for the Aghanashini and Nilgiris basin are given in Table 2-1 & 2-2. Storm typing was done for the composite hourly rainfall datasets for the each basin.

*Table 2-1 Synoptic events classification for Aghanashini basin*

| Year | Storm duration | Storm type |
|---|---|---|
| **2013** | 6 June 2013 to 16 June 2013 | Tropical Convergence Zone (TCZ) |
| | 28 June – 8 July | Off-shore convection (OSC) |
| | 17 July – 3 August | TCZ embedded with OSC |
| | 16 – 19 August | TCZ |
| | 15 – 22 September | TCZ – monsoon retrieving phase |
| **2014** | 16- Jun- 2014 to 23-Jun-2014 | Offshore Convection (OSC) |
| | 11-Jul-2014 to 23-Jul-2014 | OSC with Low Pressure |
| | 24-Jul-2014 to 25-Jul-2014 | Local convection |
| | 26-Jul-2014 to 08-Aug-2014 | OSC |
| | 23-Aug-2014 to 01-Sep-2014 | Tropical Convergence Zone (TCZ) with OSC |

Over the Aghanashini basin the synoptic systems are associated with extreme rainfall events are largely OSC, TCZ and local convection. Over the Nilgiris basin, extreme rainfall events are mostly associated with the active phases of monsoon, onset and retrieval phase of monsoon season. Daily OLR maps over the Western Ghats for the period 2013-2014 are shown in Figure 2-3.

*Table 2-2 Synoptic events classification for Nilgiris basin*

| Year | Storm duration | Storm type |
|---|---|---|
| **2013** | 2 – 4 June | TCZ – monsoon onset phase |
| | 10 – 15 June | TCZ |
| | 18 – 29 June | OSC |
| | 2-5 July | OSC |
| | 15 July – 8 August | TCZ embedded with OSC |
| | 5 – 10 September | TCZ |
| **2014** | 16-Jun-2014 to 22-Jun-2014 | OSC |
| | 05-Jul-2014 to 06-Jul-2014 | TCZ |
| | 09-Jul-2014 to 26-Jul-2014 | OSC with Low Pressure |
| | 28-Jul-2014 to 09-Aug-2014 | OSC |
| | 11-Aug-2014 to 12-Aug-2014 | TCZ |
| | 28-Aug-2014 to 02-Sep-2014 | TCZ |
| | 27-Sep-2014 to 28-Sep-2014 | TCZ |

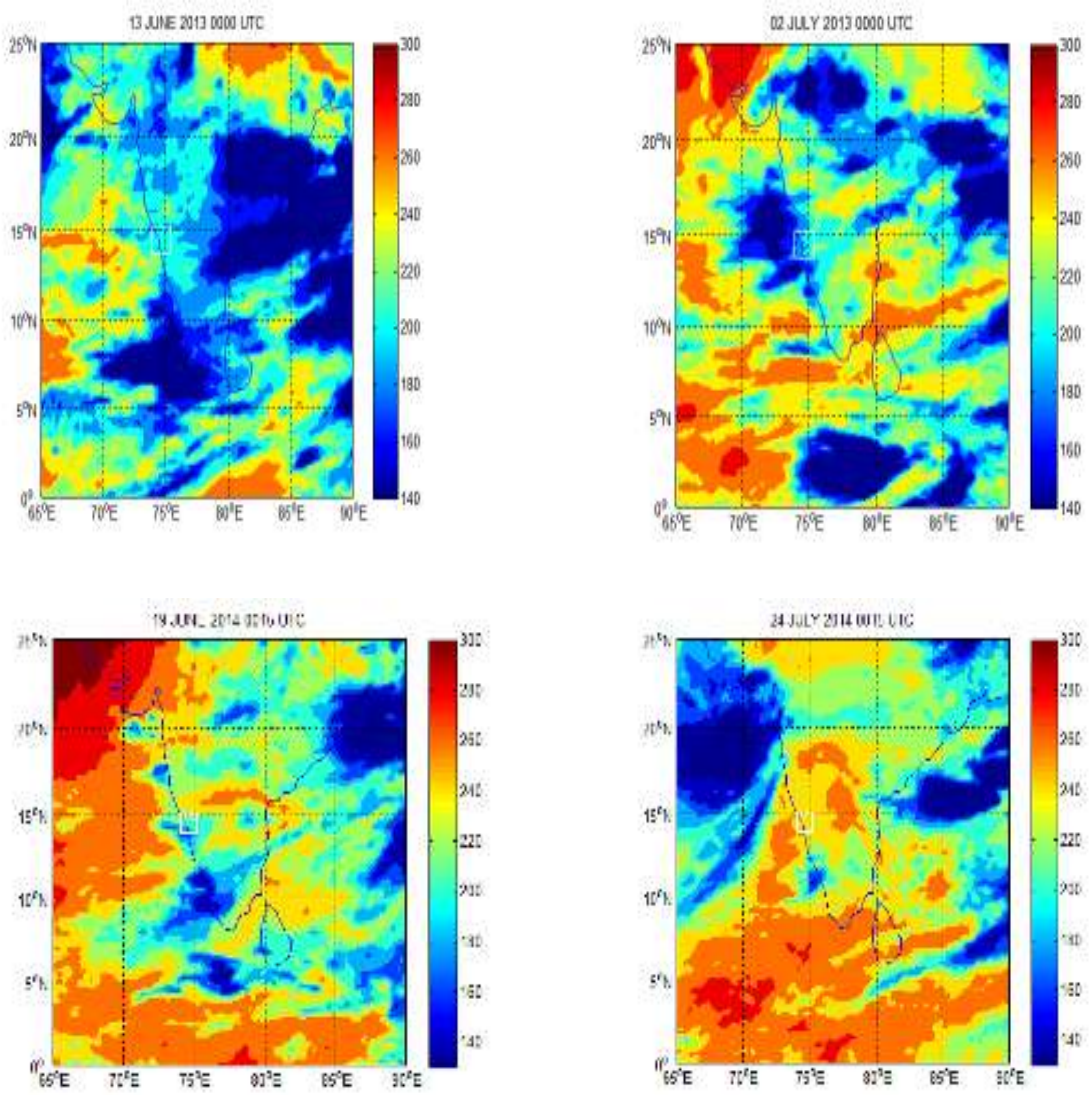


*Figure 2-3: OLR maps for the extreme rainfall events based on storm classification for the Aghanashini basin.*

## 2.6: REFERENCES


Bonell M, Purandara BK, Venkatesh B, Krishnaswamy K, Acharya HAK, Singh UV, Jayakumar R, Chappell N. 2010. The impact of forest use and reforestation on soil hydraulic conductivity in the Western Ghats of India: Implications for surface and sub-surface hydrology. Journal of Hydrology. 391(1): 47-62.

Daubechies, I. (1990). The wavelet transform, time-frequency localization and signal analysis. IEEE Transactions on Information Theory. 36(5), 961-1005.

Murthy BS, Latha R, & Sreeja P. 2013. Boundary layer jet on the lee side of Western Ghats during southwest monsoon as revealed by high resolution sodar winds. Journal of Atmospheric and Solar-Terrestrial Physics. 105: 101-109.

Pascal JP. 1982. Bioclimates of the Western Ghats on 1/500,000, 2 sheets, Institut Français de Pondichéry, Travaux de la Section Scientifique et Technique, Hors seÂrie No. 17.

Prabha TV, Goswami BN, Murthy BS, & Kulkarni JR. 2011. Nocturnal low-level jet and 'atmospheric streams' over the rain shadow region of Indian Western Ghats. Quarterly Journal of the Royal Meteorological Society. 137(658): 1273-1287.

Rajeevan M, Bhate Jyoti, Jaswal AK. 2008. Analysis of variability and trends of extreme rainfall events over India using 104 years of gridded daily rainfall data. Geophysical Research Letters. 35: L18707. DOI: 10.1029/2008GL035143.

Romatschke U, Medina S, Houze RA. 2010. Regional, Seasonal, and Diurnal Variations of Extreme Convection in the South Asian Region. Journal of Climate. 23: 419–439. DOI: 10.1175/2009JCLI3140.1.

Sam NV, Mohanty UC, & Kaur PS. 2005. Conserved variable and observational analysis over the west coast of India during ARMEX-2002. Mausam. 56(1): 201-212.

Sen S, Skaria R, Muneer PA. 2010. Genetic diversity analysis in Piper species (Piperaceae) using RAPD markers. Molecular Biotechnology 46(1): 72-79.

Thadathil P, Thoppil P, Rao RR, Muraleedharan PM, Somayajulu YK, Gopalakrishna VV, Raghu M, Reddy GV, Revichandran C. 2008. Seasonal variability of the observed barrier layer in the Arabian Sea. Journal of Physical Oceanography 3: 624–638.

Torrence, C., & Compo, G. P. (1998). A practical guide to wavelet analysis. Bulletin of the American Meteorological Society, 79(1), 61-78.

Varikoden H, Preethi B, Revadekar JV. 2012. Diurnal and spatial variation of Indian summer monsoon rainfall using tropical rainfall measuring mission rain rate. Journal of Hydrology, 475: 248-258

Varikoden, H, Preethi, B, Samah, A.A, Babu, C.A, 2011. Seasonal variation of rainfall characteristics in different intensity classes over peninsular Malaysia. Journal of Hydrology. 404, 99–108.

Vinayachandran PN, Shankar D, Kurian J, Durand F, Shenoi SSC. 2007. Arabian Sea mini warm pool and the monsoon onset vortex. Current Science 93(2): 203-214.

Vishnu R, Anil Kumar V, Varikoden H, Sarath Krishnan K, Sreekanth TS, Subi Symon VN, Mohan Kumar G. 2013. Convective thundercloud development over the Western Ghats mountain slope in Kerala. Current Science. 104 (11).

Vissa NK, Satyanarayana ANV, Prasad KB. 2013. Comparison of mixed layer depth and barrier layer thickness for the Indian Ocean using two different climatologies. International Journal of Climatology. 33(13): 2855-2870.

Yang S, Smith EA. 2006. Mechanisms for diurnal variability of global tropical rainfall observed from TRMM. Journal of Climate. 19: 5190–5226

# CHAPTER 3: MODELLING STORM FLOW IN SUB-SURFACE FLOW DOMINATED SYSTEMS OF THE WESTERN GHATS

*Nick Chappel, Tim Jones, Wlodek Tych, Jagdish Krishnaswamy*

## 3.1: NEED FOR INNOVATION IN FLOOD MODELLING

Within most Indian and indeed global catchments, the rainfall to streamflow response is nonlinear, in that the addition of a particular amount of rainfall to a catchment does not always produce a consistent amount of streamflow (even if evaporation is consistent between periods). The theory established in Engineering Hydrology for the last 80 years or so, is that this nonlinearity arises from variations in the amount of soil moisture content that affects the rate of infiltration, and so amount of overland flow on slopes that has failed to infiltrate. The closer is the soil to saturation at a particular point in time, the greater the amount of overland flow produced (Horton, 1933). The overland flow produced by this mechanism is then assumed to be linearly related to the amount of overland flow and streamflow produced, with the whole process described as the Unit Hydrograph concept (Sherman, 1932). Most flood forecasting models used around the world, e.g., HEC-1 in the USA or PDM (in ISIS) in the UK are based on these assumptions, and combine a transformation of the rainfall due to varying soil moisture content (i.e., an initial nonlinear component) with linear overland flow routing on slopes to predict flood flows observed in upstream channels.

Since the 1930s forest hydrologists have challenged the generality of this explanation of the primary cause of rainfall to streamflow nonlinearity, presenting evidence that overland flow on slopes does not need to be present in catchments to produce flood flows (e.g., Hursh, 1944), yet the responses are still non-linear. Over the decades the evidence has grown to show that in many catchments rainfall reaches channels during floods almost entirely by subsurface flow pathways and this has been particularly clear for forested catchments (e.g., Bonell and Balek, 1993; Kumagai *et al*., 2017).

More recently researchers have demonstrated that at the same soil moisture content or catchment wetness the flood response may not be linear, but nonlinear with respect of the time-distribution of rainfall intensity, i.e., type of rainfall event (e.g., Rodríguez-Iturbe *et al.*, 1982). *Such a rainfall-related nonlinearity (separate from the acknowledged effects of wetness-infiltration nonlinearity) is not explicitly incorporated into current flood models. If such rainfall-related nonlinearities are significant, then the effect of more extreme types of rain-event on flood magnitude and flashiness would be under-predicted by current models.* The importance of studying the role of rain-event types on the magnitude of flood responses has been highlighted by only a few researchers, notably Professor Mike Bonell whilst leading tropical hydrological research programmes at UNESCO and after (e.g., Bonell and Balek, 1983; Bonell and Callaghan, 2008; Chappell *et al.*, 2012), but this has yet to receive the acknowledgement and incorporation into flood models that it potentially warrants.

One of the central objectives of this MoES/NERC Changing Water Cycle project in the Western Ghats of India has to been to identify if flood responses of headwater catchments are affected by the type of rainstorm characteristics even after the affects antecedent catchment wetness are modelled. The ultimate objective being to demonstrate this climate driver should be better incorporated into flood models to provide better prediction of extreme events in India, and indeed elsewhere in the globe.

## 3.2: ESSENTIAL ASPECTS OF OUR METHODS

We have attempted to identify a mechanism missing from flood models almost universally composed of a nonlinear rainfall transform (due to antecedent catchment wetness) and a linear relationship between the transformed rainfall (called 'effective rainfall' by convention) and the observed streamflow response. It is increasingly acknowledged that identification of processes (or missing processes) with models, or changes in processes with models, is very difficult due to errors associated with all observations and because of uncertainties in model structure and parameters that arise from making models more and more complex (e.g., Beven and Smith, 2014).

*Figure 3-1: An example of a rain gauge installation (left) and headwater stream gauge (right) within our network in the Nilgiris area of the Western Ghats.*

Consequently, to be able to see the presence of a missing mechanism, we needed both high quality observations of rainfall and streamflow (see Chapter 1; Figure 3-1) and models where modelling uncertainties were constrained by keeping complexity to a minimum, i.e., so called 'parsimonious models' (Box and Jenkins, 1970). One such modelling approach utilises Lancaster University's RIVC algorithm (Taylor *et al.*, 2007) applied in a 3-stage Data-Based Mechanistic Approach. The first stage of this approach involved transforming the observed rainfall signal to capture the effects of varying catchment wetness using the store-surrogate equation (Beven and Young, 1994) and then identifying linear transfer function models of a wide range of complexity and type using RIVC. The second stage then involved evaluating all identified models against a range of statistical and mathematical criteria, rejecting as many as possible; the first two stages forming the 'Data-based' aspect of the modelling. Lastly, the statistically acceptable models were then evaluated against hydrological theory, with any at odds with hydrological principles being rejected; hence the 'Mechanistic' aspect of the modelling.

The periods of observed rainfall and streamflow modelled covered the monsoon seasons of 2013 and 2014. To show whether the typical form of flood model did not fully capture the effects of variations in rainstorm characteristics within the monsoon, each monsoon period was divided into separate storm periods (often described as 'active phases' by those studying the Indian monsoon). This division of the monsoon period was achieved using an objective Wavelet Approach (see Chapter 2; Figure 3-2).

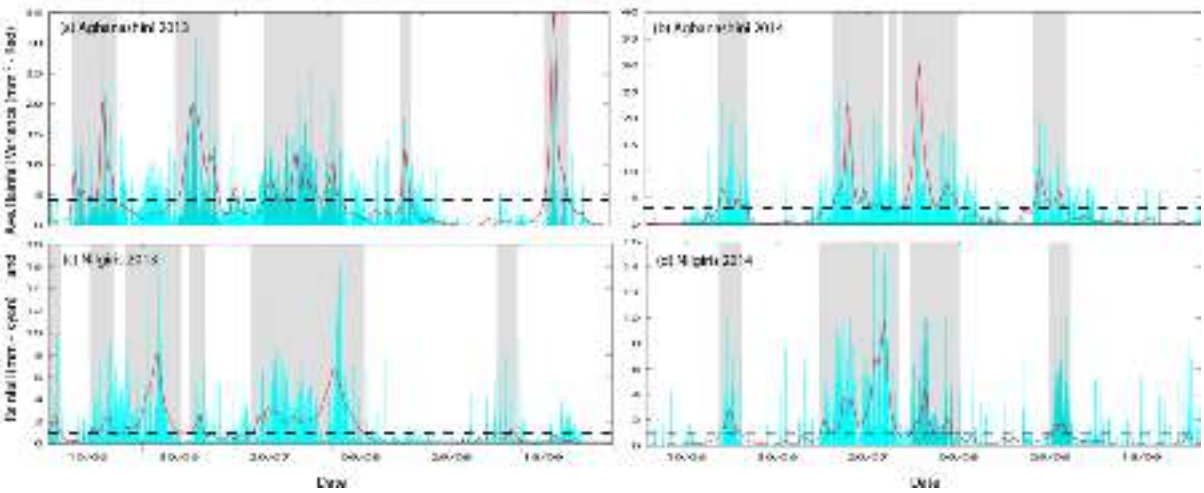

*Figure 3-2: Rainstorm periods (grey shading) identified for the catchments in the Aghanashini and Nilgiris areas of the Western Ghats using Wavelet Analyses (adapted from Page et al., in prep). The turquoise lines are the regionally-integrated 15-min rainfall totals, while the red lines are the spectral densities used to define the periods above the threshold (dashed line) – see Chapter 2.*

For each of these storm periods, the rainstorm characteristic derived was the effective rainfall intensity for 15-minute periods receiving rainfall averaged over the whole storm period ($RI_{WETeff}$). The synoptic type of rainstorm was also characterized (see Chapter 2).

## 3.3: FINDINGS SHOWING THE PRESENCE, SIGNIFICANCE AND NEED FOR EXPLICIT FLOOD MODEL QUANTIFICATION OF VARIATIONS IN RAINSTORM CHARACTERISTICS BETWEEN DIFFERENT STORM PERIODS

Our modelling of rainstorms through the 2013 and 2014 monsoons was able to capture most of the observed dynamics in 15-minute observed streamflow across the gauged headwater catchments in the Western Ghats (Chappell et al., 2017; Page et al., in prep). Models no more complicated than second-order transfer functions (interpreted as a combination of one fast pathway and one slow pathway) were able to capture the dynamics. Models incorporating a slow pathway were needed because of the presence of groundwater in the surficial geology of all of the studied catchments (Page et al., in prep). This was independently shown in the very dynamic water-table observations in shallow wells in the study area (Figure 3-3).

Utilising data from a range of our studied catchments in the Western Ghats area, we were able to show that the flashiness of the critical fast component of the flood hydrographs was strongly correlated with our measure of the rainfall intensity across each storm period (Figure 3-4). This is indeed at odds with the theory that forms the basis of most flood models (Sherman, 1932; Rodríguez-Iturbe et al., 1982) where the flashiness should be constant with respect of rainfall intensity, once antecedent wetness effects have been removed/captured (as we did in the initial stage of our modelling). The identified relationship is monotonically and strongly curvilinear (Figure 3-4), and the implications profound. This finding says that current flood models with their fixed flashiness values for the linear component of model structure ($TC_f$) will under-predict particularly extreme rainstorm events, and over-predict lower intensity events.

*Figure 3-3: A private well in the Aghanashini area of the Western Ghats where shallow groundwater level dynamics were monitored during the 2013 and 2014 monsoons.*

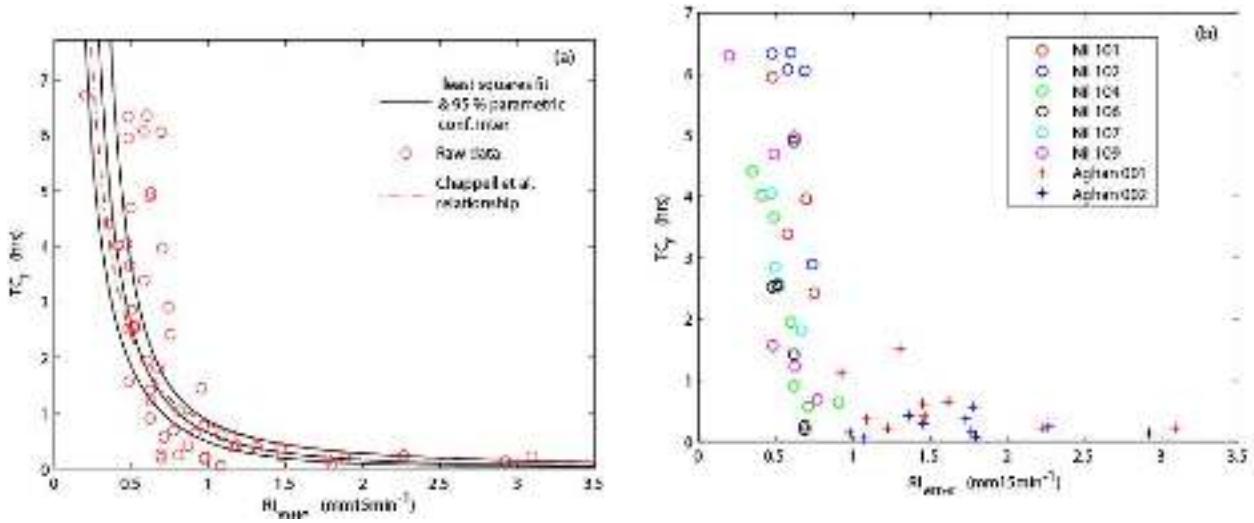


*Figure 3-4: The relationship between the fast component of storm hydrograph flashiness (TCf) and average rainstorm intensity based in 15-minute periods with rainfall (RIWETeff), where (a) shows the trend and its uncertainty (and consistency with Chappell et al., 2017 trend), while (b) shows the catchments utilised in the relationship, where 'Nil' refers to a catchment in the Nilgiris area, and 'Aghan' and catchment in the Aghanashini area (adapted from Page et al., in prep).*

## 3.4: CONCLUSION

What is needed to improve the models is to explicitly incorporate the nonlinearity associated with changing rain-event intensity into the model structure, in addition the nonlinearities associated with antecedent wetness.

## 3.5: REFERENCES


Beven, K., Smith, P., 2014. Concepts of information content and likelihood in parameter calibration for hydrological simulation models. Journal of Hydrologic Engineering. A4014010.

Bonell, M. and Callaghan, J. 2008. The synoptic meteorology of high rainfalls and the storm runoff—response in the wet tropics. In: Living in a Dynamic Tropical Forest Landscape (ed by N. Stork and S. Turton), 23–46. Blackwell Publishing, Oxford.

Bonell, M. and Balek, J., 1993. Recent scientific developments and research needs in hydrological processes of the humid tropics. In: Bonell, M., Hufschmidt, M.N., Gladwell, J.S. (Eds.), Hydrology and Water Management in the Humid Tropics. Cambridge University Press, Cambridge, pp. 167–260.

Box, G.E.P., and Jenkins, G.M., 1970. Time Series Analysis: Forecasting and Control. Holden-Day, San Francisco.

Chappell, N.A., Sherlock, M., Bidin, K., Macdonald, R., Najman, Y., and Davies, G. 2007. Runoff processes in Southeast Asia: role of soil, regolith and rock type. In: Forest Environments in the Mekong River Basin. Sawada, H., Araki, M., Chappell, N.A., LaFrankie, J.V., and Shimizu A. (eds) Springer Verlag, Tokyo. p 3-23.

Chappell, N.A., Bonell, M., Barnes, C.J., and Tych, W. 2012. Tropical cyclone effects on rapid runoff responses: quantifying with new continuous-time transfer function models. In: Revisiting Experimental Catchment Studies in Forest Hydrology, Webb, A.A., Bonell, M. Bren, L. Lane, P.N.J., McGuire, D., Neary, D.G., Nettles, J., Scott, D.F., Stednik J. & Wang, Y. (eds) IAHS Publication 353, Wallingford, IAHS Press. 82-93.

Chappell, N.A., Jones, T.D., Tych, W. and Krishnaswamy, J. 2017. Role of rainstorm intensity underestimated by data-derived flood models: emerging global evidence from subsurface-dominated watersheds. Environmental Modelling and Software, 88: 1-9. DOI: 10.1016/j.envsoft.2016.10.009

Horton, R.E. 1933. The role of infiltration in the hydrologic cycle. Trans. Amer. Geophys. Union 14: 446–460.

Hursh, C.R. 1944. Report of the sub-committee on subsurface flow. Trans. AGU 25: 743-746.

Kumagai T., Kanamori, H., and Chappell, N.A. 2016. Tropical Forest Hydrology. In: Forest Hydrology: Management and Assessment, Amatya, D.M., Williams, T.M., Bren, L. and de Jong, C. (eds), CABI, Wallingford. ISBN: 9781780646602.

Rodríguez-Iturbe, I., Gonzales-Sanabria, M., Camano, G., 1982. On the climatic dependence of the IUH: a rainfall-runoff theory of the Nash model and the geomorphoclimatic theory. Water Resour. Res. 18: 887e903.

Sherman, L.K. 1932. Stream flow from rainfall by the unit graph method. Engineering News-Record 108: 501-505.

Taylor, C.J., Pedregal, D.J., Young, P.C. & Tych, W. 2007. Environmental time series analysis and forecasting with the CAPTAIN toolbox. Environ. Model. Software 22: 797–814.

Young, P.C. & Beven, K.J. 1994. Data-based mechanistic modelling and the rainfall-flow nonlinearity. Environmetrics 5: 335-363.

# CHAPTER 4: IMPACTS OF LAND-COVER ON CATCHMENT HYDROLOGY

*Jagdish Krishnaswamy, Srinivas Vaidyanathan, Ravinder Singh Bhalla and Shrinivas Badiger*

## 4.1: INTRODUCTION

Properties and functions of natural forest ecosystems regulate how rainfall is partitioned into surface flow, sub-surface flow, ground-water and evapotranspiration and also the export of sediment in streams. They also determine how and how much carbon is fixed, stored and lost from these ecosystems. In general, the more carbon that a forest stores in its biomass, the less water that the forest releases into the stream. However, this is not necessarily true under tropical mixed landscapes subject to long-term and intense human use and also as degraded sites are reforested over decades.

Information on how these two different types of functions are linked is sparse for tropical forest ecosystems, especially when these ecosystems are degraded by human-use. We know even less about how hydrologic and carbon functions of ecosystems respond to extreme rain events (lots of rain per hour) and high intensity rain. This is occurring with greater frequency and is likely to increase under future climate change in the Western Ghats and adjacent Deccan Plateau which supports livelihoods and needs of 160 Million people. Furthermore, the effects of such extreme rain events on agroecosystems in tropical landscapes are also largely unstudied, especially in relation to crop damage and soil loss.

One of the gaps in our knowledge is how such extreme rain storms are distributed over space and time, and how this spatial distribution of rain events interacts with different land-use and land-cover in large landscapes to influence hydrology and carbon dynamics. India is one of the global leaders in forestation including experimenting with exotic species and large areas of land has been restored or reforested over the past several decades for various economic benefits. Furthermore alien invasive species have also spread in many head-water catchments.

Currently India is planning to reforest over 10 Million Hectares as part of a national plan (Green India Mission) to sequester carbon and help regulate global atmospheric CO2. These initiatives can transform the water and carbon budgets over large areas and also influence availability of water for agricultural use downstream.

Although the impact of deforestation on enhancing flood risk is well known (Bradshaw et al. 2007; Laurance 2007), the effects of forest degradation and reforestation on floods and the hydrological cycles are less well established, especially under scenarios of climate change. Certain combinations of land-cover and soil types in the WG are already vulnerable to increased surface flows under current rainfall regimes (Bonell et al. 2010), but the responses of these and other land-cover and soil types to future changes in rainfall regimes is less well understood. Further, data and analysis of rain intensity and hydrologic responses to high intensity rainfall events in the tropics, including the WG, are severely lacking (Bonell and Bruijnzeel 2005; Bonell et al. 2010). Thus far, studies on trends in ERE have relied on daily or coarser time resolution data (Goswami et al. 2006; Pattanaik and Rajeevan 2010). However, understanding surface and sub-surface hydrologic and sediment transport in response to stochastic rainfall intensity processes at finer time-steps is probably more critical to our ability to predict consequences of future ERE regimes on the water cycle and

associated carbon dynamics (Medvigy et al. 2010). At present, there is considerable uncertainty in linking finer resolutions of rain intensities (<3 hr) to daily totals and the spatial and temporal dimensions of ERE in regions such as the Western Ghats. Another over-arching issue while studying ERE is that of scales at which the impacts of land cover change (LCC) are overridden by the characteristics of rain-producing systems in terms being the primary source of flood runoff. Blöschl et al. (2007) proposed the concept of a variable "threshold scale". The latter separates the two dominant controls (viz, LCC, rain-producing systems) across different ecosystems (the spatial dimension) and within an ecosystem (the temporal dimension) depending on antecedent hydrological conditions. However such a concept remains to be proven and is the focus of this study in the context of inter-relating the impacts of ERE with the suite of complex land covers in the Western Ghats.

The objectives of the work are based on the following a priori hypotheses:

1. Natural forests mitigate the effects of floods, sediment and carbon transport during ERE within a critical threshold as compared to degraded and agro-ecosystems. However this is likely to be a function of spatial scale.

2. Plantations and Agro-ecosystems will be particularly vulnerable to extreme rainfall events, especially reduction in net infiltration, recharge and increase in annual loss of soil fertility due to erosion.

## 4.2: METHODS

### *4.2.1: Frame-work*

The methodological frame-work will be nested and hierarchical to enable an integrated assessment of the inter-play of spatial and temporal scale and land-cover in modulating the hydrologic and carbon functional response to rainfall of different intensities, especially extreme events. There will be a nested system of water level recorders from upstream to downstream from homogeneous land-cover basins of low order to more heterogeneous basins downstream, as well as adjacent sub-basins under contrasting land-cover wherever feasible. Each cluster of sub-basins in Upper Bhavani in the Nilgiris (Figure 4-1) and Aghanashini, Uttara Kannada (Figure 4-2) had a weather station.

Land-cover and land-use: Land-use and Land-cover will be generated for the basins using both hard-classification using Landsat as well as continuous measures of forest type such as NDVI (Krishnaswamy et al. 2009) for each year using MODIS time-series satellite data.

### *4.2.2: Mapping land use and land cover*

Available topographic maps and ASTER digital elevation models were used to demarcate catchment boundaries for each of the three water level recorders. These were overlaid on a recent land cover map prepared through supervised classification of atmospherically corrected Landsat 8 imagery. Over 430 ground control points collected through a hand held GPS receiver combined with high resolution GoogleEarth imagery were used to train the image. Nine classes of land cover were identified to coincide with a map produced two decades ago. This provided a means to measure changes in land cover in the region.

LANDSAT 8 imagery was also used to prepare normalised difference vegetation index (NDVI) maps for the months of January, March and May. This provided an index of vegetation greenness, which is used as a proxy for evapotranspiration.

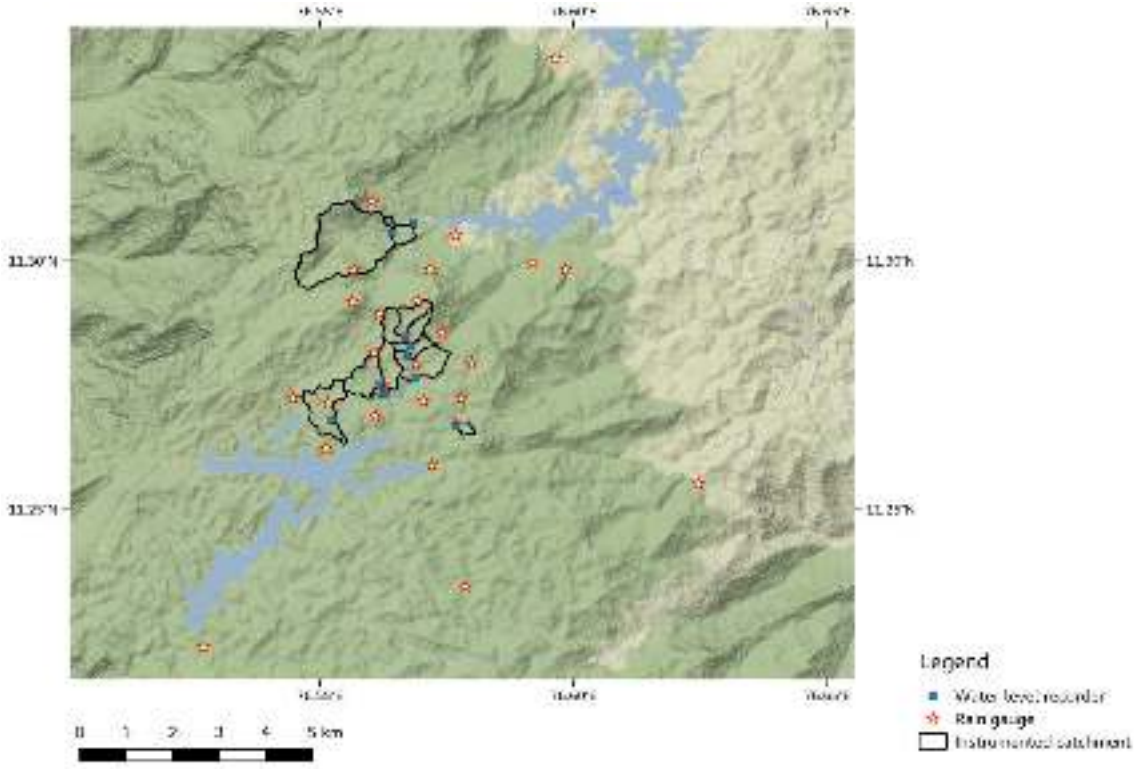


*Figure 4-1: Sampling locations and catchments in the Nilgiri basin*

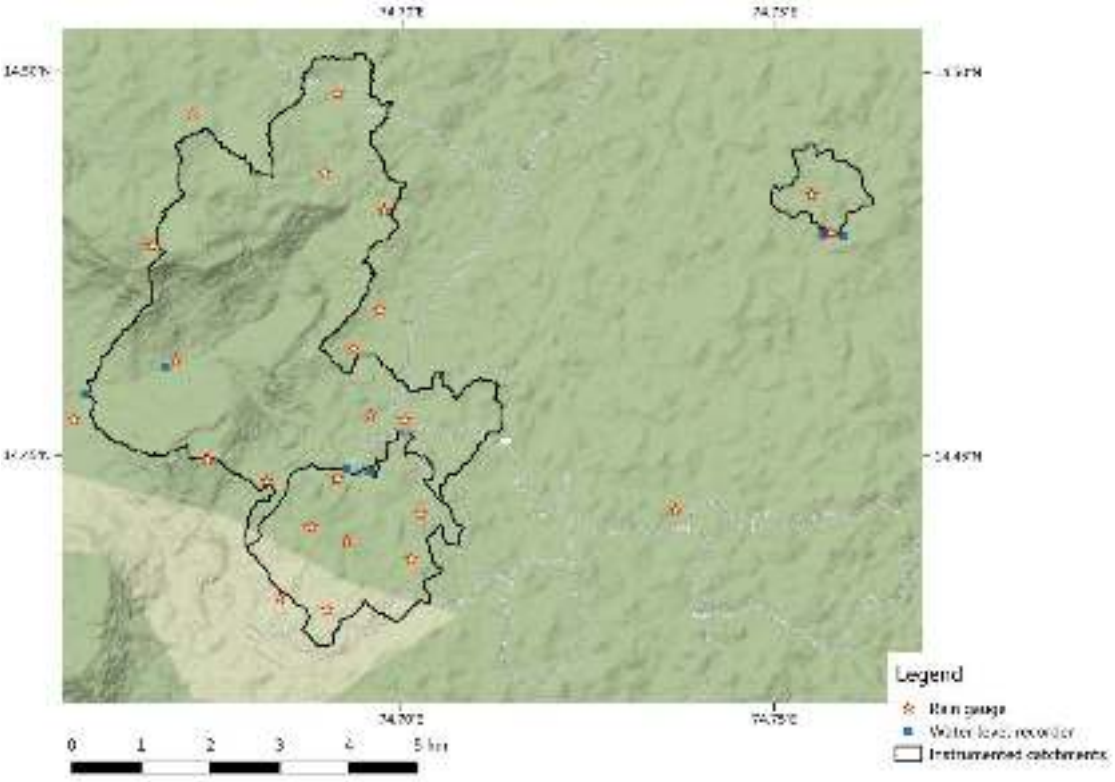


*Figure 4-2: Sampling locations and catchments in the Aghnashini basin*

Catchment level land cover classification was done by combining on-ground GPS tracks and waypoints with GoogleEarth imagery as the 30 meter resolution LANDSAT 8 images were too coarse to differentiate the intermixed patches of grassland, scotch broom and gorse.

### *4.2.3: Field Methods*

Each sub-basin was instrumented with a calibrated capacitance probe based stilling well for measurement of stage and tipping bucket rain gauges.Spot discharges for determining stage-discharge relationships was obtained using velocity-area methods and salt dilution method. Non-linear stage-discharge equations were fit using the equations:

Q = a(stage-b)c which often reduced to a(stage)c, where the parameters were estimated using iterative least squares method using nls routine in R.

In the dry-season this was supplemented with Montana flumes for direct estimation of discharge. Infiltration was measured using the mini infiltrometer (Decagon) under different land-cover in the Nilgiris and in Aghnashini using the disc permeameter (Bonell et al. 2010).

### *4.2.4: Water sample collection and analysis*

Stream water samples were collected at the water discharge measurement locations during a range of flow conditions. Duplicate 1 litre suspended sediment samples (grab samples) were manually collected using a depth integrated sampler. The depth integrated sampler was fabricated in the design of US DH-81 (Figure 4-3a). For more details: https://water.usgs.gov/fisp/products/4107002.html. This provided a representative and integrated estimate of sediment concentrations.

Samples for storm events were collected using a modified siphon sampler, fabricated locally, as per USGS siphon sampler design (https://pubs.usgs.gov/sir/2007/5282/pdf/sir20075282.pdf). This captured sediment at different stream stages and automatically sealed itself after the event (Figure 4-3b). This intensive synoptic sampling was designed to capture the sediment flux responses during storm events, thereby assess the difference in concentration associated with the rising and falling limb of the stream hydrograph.


*Figure 4-3: (a) Depth integrated sampler; (b) Stage sampler; (c) Demonstration of Systronics water analyzer in the field site.*

A total of 304 samples from Aghnashini and 707 samples from Nilgiris were collected between April 2014 to February 2016. We had six monitoring locations at Aghnashini, of

which only two were perennial streams. In Nilgiris, we were monitoring eleven perennial streams for water quality. Each sample was analysed for six basic physico-chemical parameters in the field itself. Two sets of water samples (acidified and non-acidified) were sent to ATREE office, Bangalore in iceboxes for further analysis. Further analysis for Total Suspended Sediments, Total Nitrate, Phosphate, Total Dissolved Carbon and Total Dissolved Nitrogen were done in Bangalore.

- Each sample was analysed on site for six physico-chemical parameters (pH, EC, salinity, turbidity, dissolved oxygen, total dissolved solids) using **Systronics** Portable Water Analyzer (Figure 6-1c).
- Total Suspended Sediments – TARSON Hand pumped **vacuum filtration unit** was used for sediment analysis. It comprise of an upper chamber into which a measured quantity (300ml) of the raw sample is decanted and a lower chamber into which the filtrate is collected. The two chambers are separated by a filter bed on which the filter is placed (here we used Millipore cellulose nitrate membrane of 0.45 micron pore size) (Figure 4-4).

*Figure 4-4: Hand held vacuum filtration unit. (Inset: cellulose nitrate membrane after filtration)*

- Total Nitrate – Total nitrate was measured using **WTW** Nitrate Probe - Ion Selective Electrode. Since our preliminary analysis had shown very low values of nitrate in the freshwater forest streams, we calibrated the electrode with 2 and 5 ppm nitrate standards.
- Nitrate in water samples were measured, as a cross check, by Phenol disulphonic acid method following Trivedy and Goel (1984). Alkali nitrate - N reacts with 2, 4-phenol disulphonic acid and formed yellow colour, which was measured using Microprocessor visible spectrophotometer at 410 nm.

- Phosphate – Phosphate in water sample were measured using the Stannous Chloride method (APHA, 4500–P D) at 625nm with **Microprocessor** visible Spectrophotometer.
- Total Dissolved Carbon and Total Dissolved Nitrogen – The water samples were analysed in the laboratory of Centre for Ecological Studies, Indian Institute of Sciences, Bangalore. Total dissolved carbon and nitrogen were measured using **Shimadzu** TOC- L Analyzer. For the analysis 5 ml of filtered sample was taken in a scintillation vial and freezed. The samples were then directly put in the auto analyzer during the time of analysis.

### *4.2.5: Analytical methods*

Corresponding stream flow time-series from nested stations will be analyzed with respect to rain intensity data and land-use and land-cover patterns from upstream to downstream as a function of spatial scale (stream-order). Hydro-graphs will be generated at the temporal resolution of an individual storm as well as for entire wet season and at various spatial scales from upstream to downstream. Cross-correlation lag plots and lagged regression models (Bonell et al, 1979) were be used to compare stream flow response to rain variables, and antecedent catchment wetness. Time-series plots and boxplots were used to compare land-cover and land-use effects.

## 4.3: KEY FINDINGS

### *4.3.1: Land Use Land Cover*

The instrumented catchment in the Nilgiri basin was devoid of human settlements (Figure 4-5). However, the natural grasslands that occur in the landscape have witnessed historical modifications with the introduction of non-native invasive species. The Aghnashini basin is characterized by a mix of natural evergreen forests, degraded secondary forests, commercial plantations and agricultural fields within human settlements (Figure 4-6). The characteristics of the catchments that are compared in this chapter are provided in Tables 4-1 and 4-2.

*Table 4-1: Land use land cover characteristics of the instrumented catchments in the Nilgiri basin*

| Land use class | Shola | Grassland | Scotch broom/Gorse | Wattle |
|---|---|---|---|---|
| Shola | 65.7% | 1.4% | 3.9% | 14.5% |
| Grassland | 24.7% | 89.8% | 50.7% | 13.9% |
| Wattle | 6.1% | 3.4% | 32.4% | 67.4% |
| Scotch broom | - | - | 8.1% | 0.7% |
| Gorse | - | 5.4% | 4.9% | 2.5% |
| Mixed Eucalyptus and Wattle | 3.0% | - | - | - |
| Rock | 0.3% | - | - | 1.0% |
| Eucalpytus | 0.2% | - | - | - |

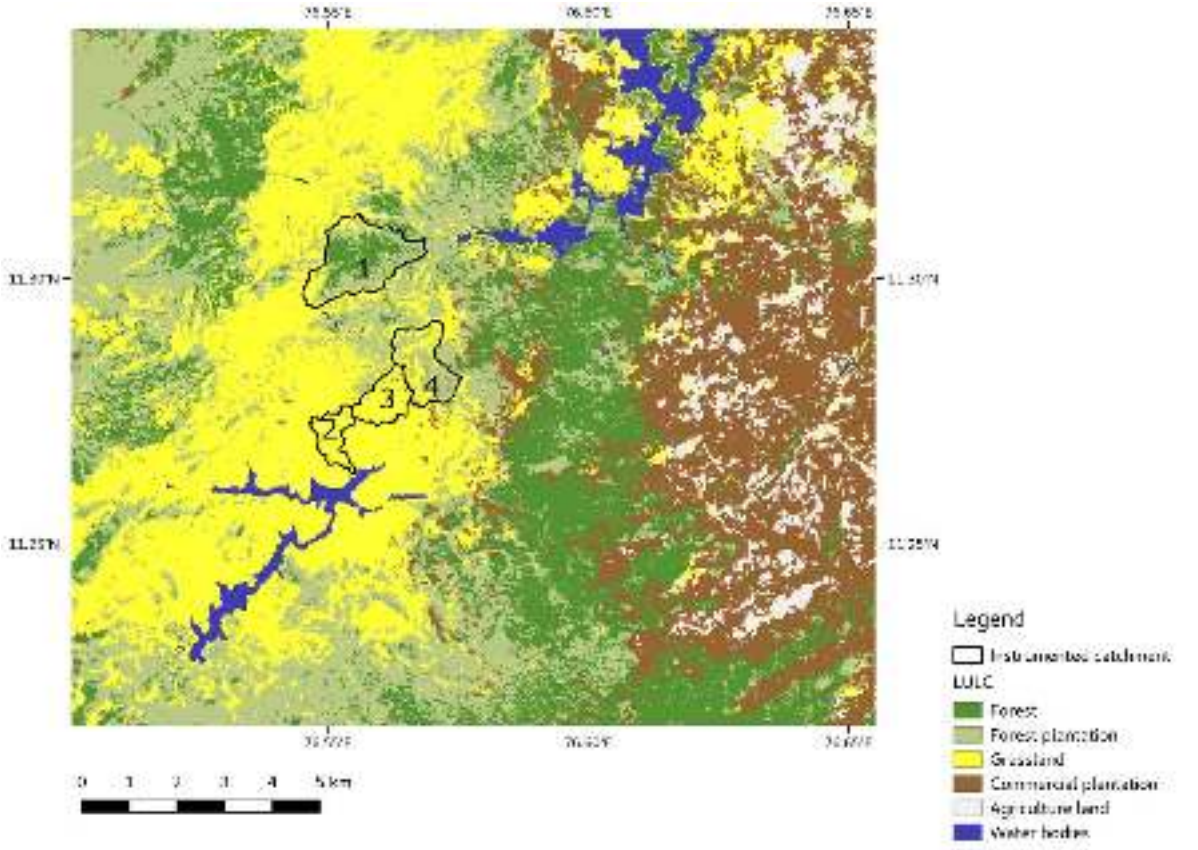


*Figure 4-5: Land use land cover in the Nilgiri basin. Dominant vegetation type of Catchment 1)Shola, 2)Grassland, 3)Scotch broom/Gorse, and 4)Wattle*

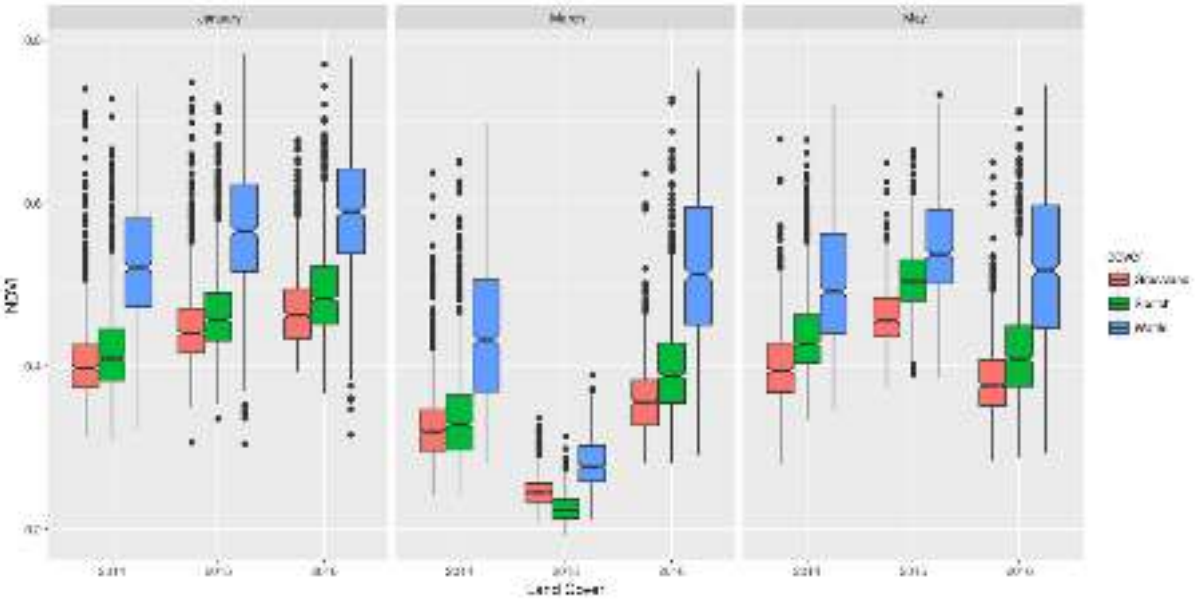


*4-6: Box and Whiskers plots of NDVI dynamics in the dry season across land-cover types. The NDVI values of the wattle dominated catchment remained higher than scotch broom/gorse and grassland dominated catchment across seasons and years. The primary reason for this is that wattle, unlike scotch broom/gorse, forms an unbroken canopy. The latter, however tends to be interspersed with grasslands and bare soil which cause a mixing in the spectral signatures and bring down the NDVI values. There was widespread die back due to fungal infection (Hosagoudar et. al,2007) in the wattle catchment in 2014 which*

*explains the lower NDVIs of wattle that year. Interestingly, the NDVI values did not show any clear relationship with rainfall in the prior dry season or the monsoon.*

*The image for March 2015 had substantial atmospheric interference due to haze and hence the NDVI values were subdued.*

The NDVI dynamics in the Nilgiri basin shows high spatial variability of NDVI during the dry season (Figure 4-6). The results show decline foliar biomass as the dry season progresses each year and a recovery after receiving pre monsoon rains in the month of May. The NDVI values for wattle is highest when compared to grasslands and scotch broom and is attributed to higher LAI and deeper roots. However, 2016 was the significantly drier of the two years in terms of previous wet season and even dry season rainfall and yet NDVI values are higher across all catchments. The spatially averaged rainfall across the catchments show big differences, although they are not far away from each other indicating high spatial variation in rainfall in the Nilgiri basin.

*Table 4-2: Rainfall totals in the Nilgiri basin.*

| Wattle | Preceding wet-season rain (mm) | Dry season rain (mm) |
|---|---|---|
| 2014 | 3380 | 97 |
| 2015 | 2451 | 197 |
| 2016 | 1929 | 31 |
| **Scotch Broom** | | |
| 2014 | 3787 | 90 |
| 2015 | 3151 | 180 |
| 2016 | 2376 | 33 |
| **Grassland** | | |
| | 4022 | 69 |
| | 3149 | 163 |
| | 2233 | 29 |

In both January and March, the wattle dominated catchment shows a much larger NDVI than the other two land covers. This can be attributed to soil moisture availability. Wattle, being a deeper rooted tree is able to access deeper sources of soil moisture, unlike grasslands. As the dry season progresses and the antecedent moisture decreases, the relative difference in the NDVI values increases. In May, the Nilgiris receive pre-monsoon showers leading to the resumption of photosynthesis in the grasslands which is being picked up by the NDVI, hence the differences in the NDVIs in May are not as pronounced.

The lower wattle NDVI's in 2014 can be accounted for due to a large scale wattle die back post 2013 monsoon which gradually recovered in later years (Chayanulu and Balakrishnan, 1980). This has been recorded in earlier periods as well and would probably result in a distinct hydrologic response. Interestingly, even though the rainfall received in 2013 > 2014 > 2015 this does not appear to be reflected in the NDVI response and further investigation is needed to explain this.

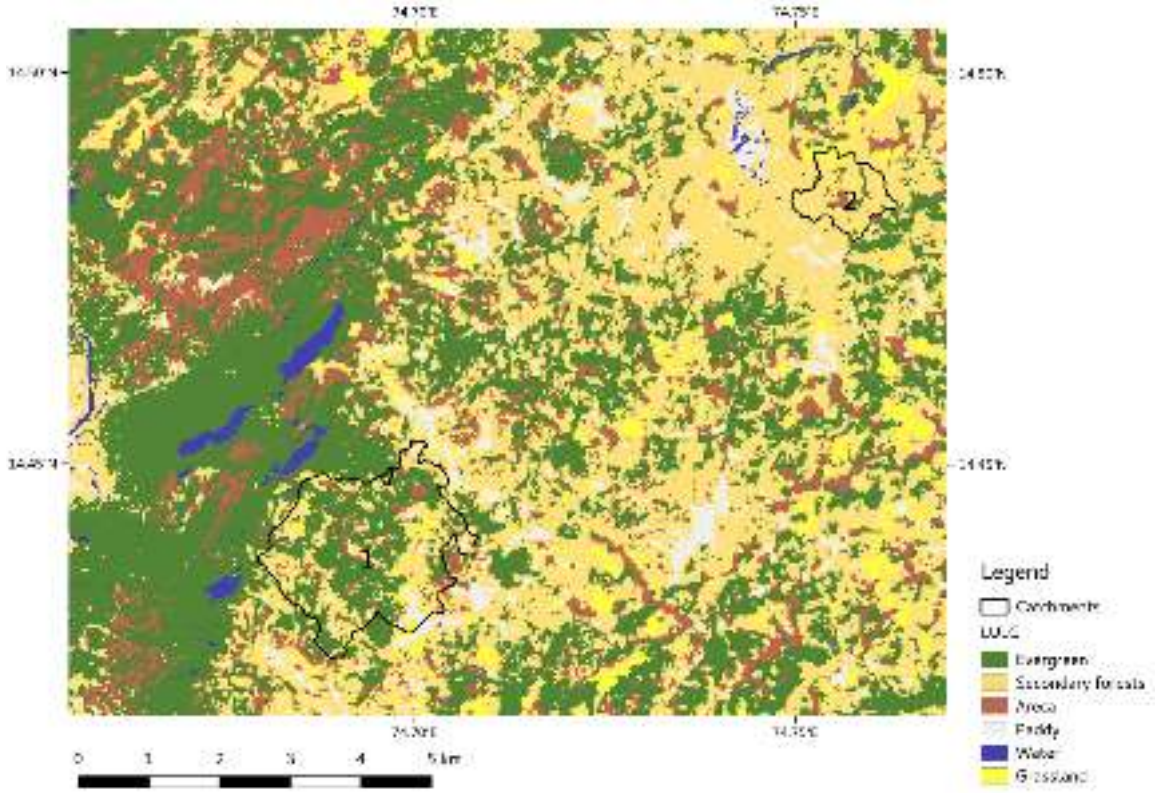


*Figure 4-7: Land use land cover in the Aghnashini basin. Dominant vegetation type of Catchment 1, Saimane, has nearly 12% under cultivation compared to Catchment 2, Hosagadde which has around 6% of the area under cultivation.*

*Table 4-3:Land use land cover characteristics of two catchments in the Aghnashini basin.*

| Land use class | Saimane | Hosagadde |
|---|---|---|
| Evergreen forests | 47.8% | 7.0% |
| Secondary forests | 36.7% | 78.8% |
| Areca plantation | 7.8% | 5.0% |
| Grassland | 3.3% | 8.0% |
| Paddy | 3.5% | 1.0% |
| Water bodies | 0.8% | 0.2% |

The NDVI dynamics in two forest-dominated catchments in Aghanashini shows spatial variability of NDVI in the dry season (Figure 4-8). The results show decline or loss of photosynthetic potential or foliar biomass as the dry season progresses each year. However, there is a significant drop during the dry season of 2016 when the preceding wet season has the driest Monsoon (See Table 4-4). In combination with catchment averaged rainfall data recorded, we note that NDVI in January and the drop of NDVI across the dry season is most sensitive to the preceding Monsoon totals but March NDVI is sensitive to dry-season rainfall.

*Table 4-4: Rainfall totals in the Aghanashini basin.*

| Saimane | Preceding wet-season rain (mm) | Dry season rain (mm) |
|---|---|---|
| 2014 | 6256 | 18 |
| 2015 | 5468 | 29 |
| 2016 | 3331 | 6.3 |
| **Hosagadde** | | |
| 2014 | 5021 | 34 |
| 2015 | 4822 | 15 |
| 2016 | 2534 | 4.3 |

### *4.3.2: Infiltration*

Infiltration of rainwater into soil under different land cover is one of the most fundamental hydrologic processes that determines many other phenomena such as sub-surface flow, recharge of ground-water and potential for flooding. The rate at which rain falls on soil compared to the infiltration rate under different land-cover is an important indicator of the vulnerability of these landscapes to extreme rain events.

Comparison of the observed rainfall intensity to the measured infiltration (Ksat) suggests that natural land cover types have a higher saturated hydraulic conductivity than modified natural systems in both the basins. In the Nilgiris soils in pine and wattle plantationare more vulnerable to infiltration-excess overland flow compared to soil under shola forests and grasslands, which are the native vegetation formations (Figure 4-9). In Aghnashini basin, only the forest soils are able to withstand even the most intense rains without generating infiltration excess overland flow (Figure 4-10).

*Figure 4-8:Infiltrometer used to measure soil infiltration rates in Aghanashini*

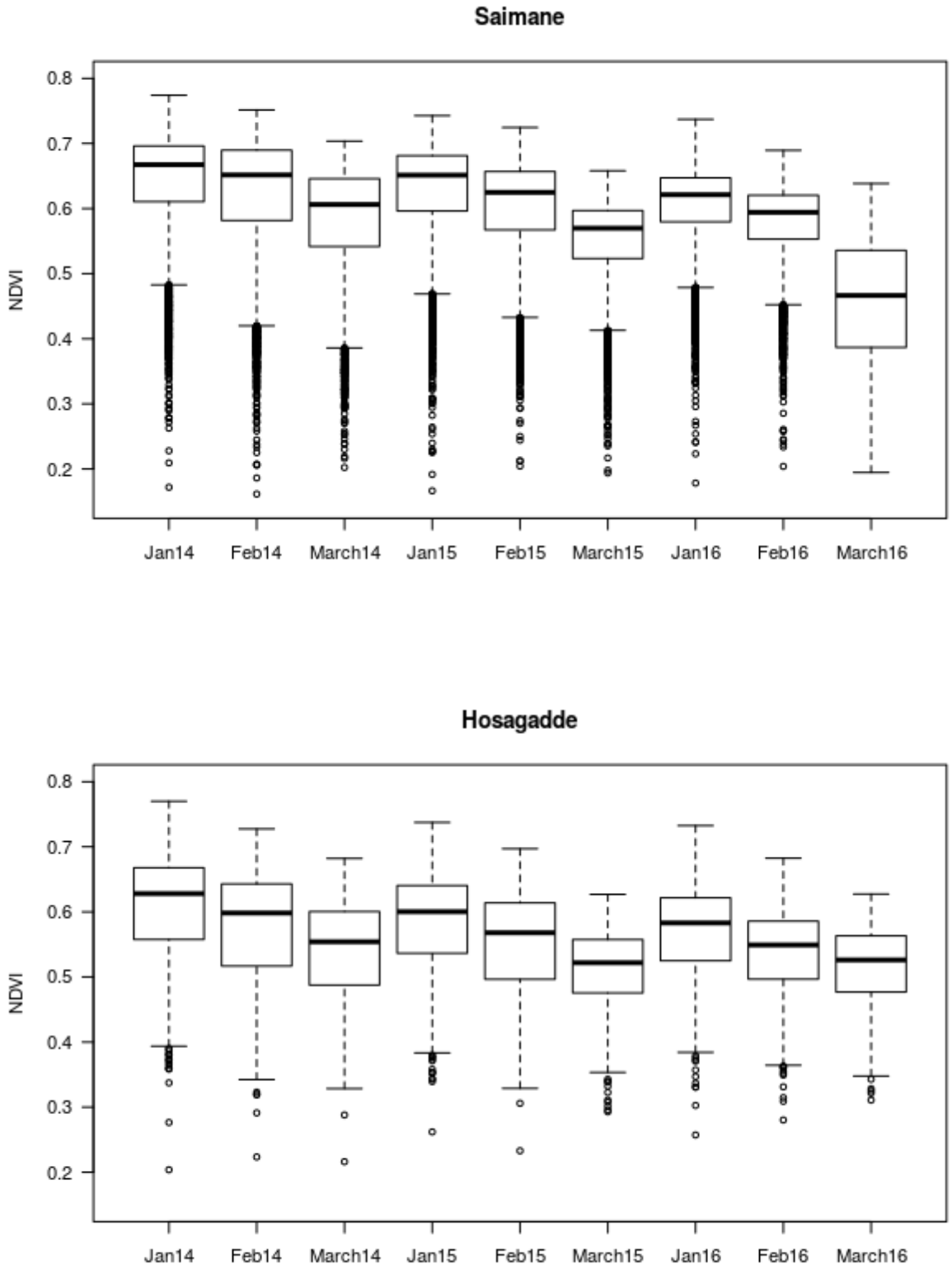


*Figure 4-8: NDVI dynamics in the dry season in two catchments in two forest dominated Aghanashini catchments (~84%) using box and whiskers plots using Landsat 8 data. Each boxplot shows spatial variability of NDVI in the month indicated. Please note the loss of photosynthetic potential or foliar biomass from January to March in each year but particularly note the significant drop across January to March in 2016 when the preceding*

*wet season has the driest Monsoon (See Table 4-4). In combination with catchment averaged rainfall data recorded, we note that NDVI in January and the drop of NDVI across the dry season is most sensitive to the preceding Monsoon totals but March NDVI is sensitive to dry-season rainfall.*

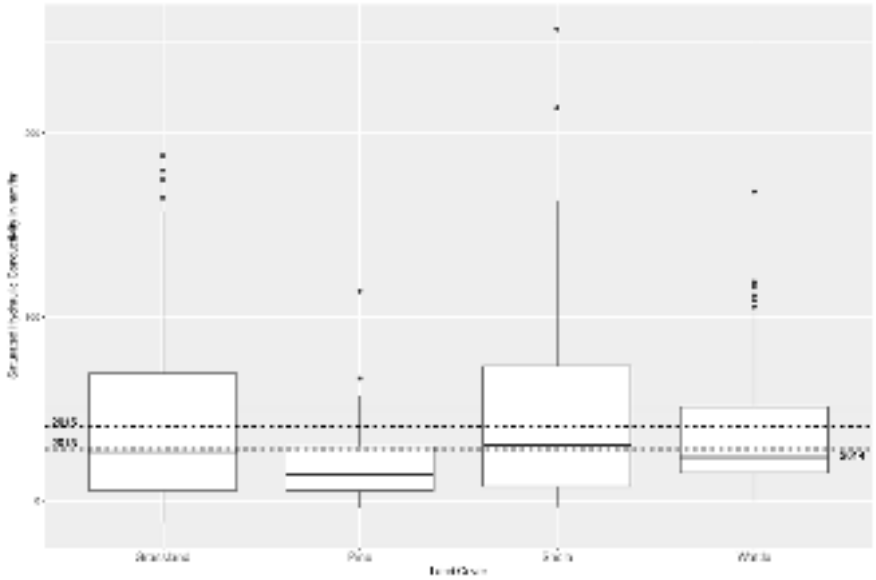

*Figure 4-9: Box and Whiskers plots of Infiltration under different land-cover in the Nilgiris overlayed with maximum rain intensities recorded in 2013, 2014 and 2015. Soils in Pine and Wattle plantation are more vulnerable to infiltration-excess overland flow compared to soil under Shola forests and Grasslands*

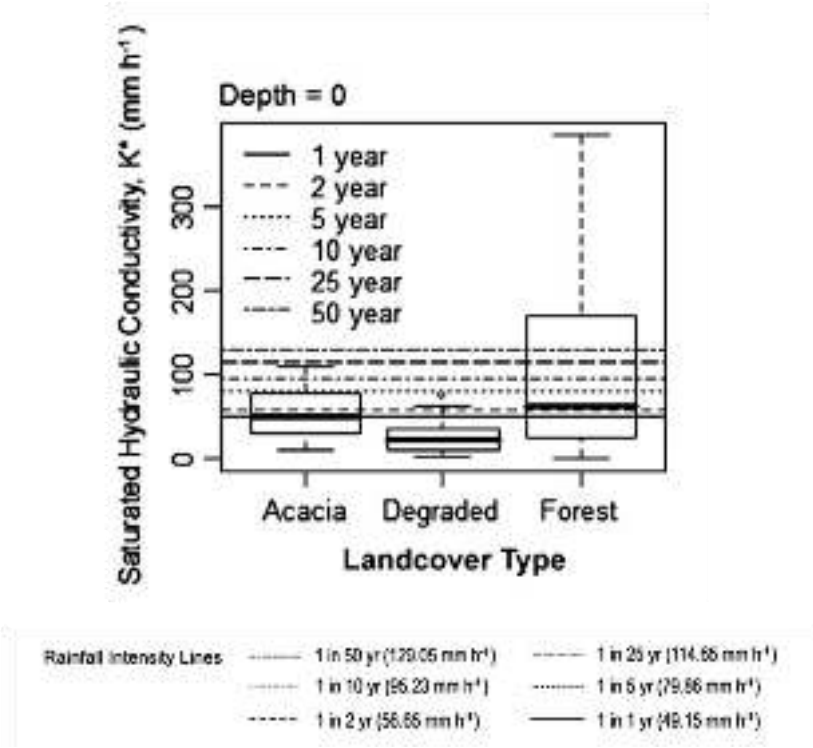


*Figure 4-10: Box and Whiskers plots of infiltration rates in top 10 cm of soil under different land-cover with overlay of rain intensity lines in Aghnashini basin, Uttara Kannada. Only the forest soils are able to withstand even the most intense rains without generating infiltration excess overland flow (Adapted from Bonnel et. al 2010)*

### *4.3.3: Rainfall-flow dynamics*

In the Nilgiris, the higher cross-correlation in grassland relative to Wattle suggests much higher proportion of water from the rainstorm is delivered to the stream by grasslands (Figure 4-11). The first peak at a few hours after the rainstorm peak suggests very good storage capacity for rainwater in soils and sub-surface, as well as sub-surface pathways. The secondary peak in Wattle is more pronounced but in both catchments, there is some indication of ground water contributing to stream flow at ~10-20 hours after the rainstorm. This secondary peak appears in more intense rain episodes (Figure 4-11). We also generated a stage-discharge rating curve to arrive at the final discharge for each water logger in the Aghanashini and Nilgiris. We are still currently investigating the response of stream flow to different thresholds of rainfall each day. Figure 4-13a shows an example rating curve used to arrive at the discharge in m3/second. Figure 4-13b shows a hydrograph with stream flow plotted as a response to precipitation in mm. Figure 4-14 shows pipeflows from the Aghanashini basin.

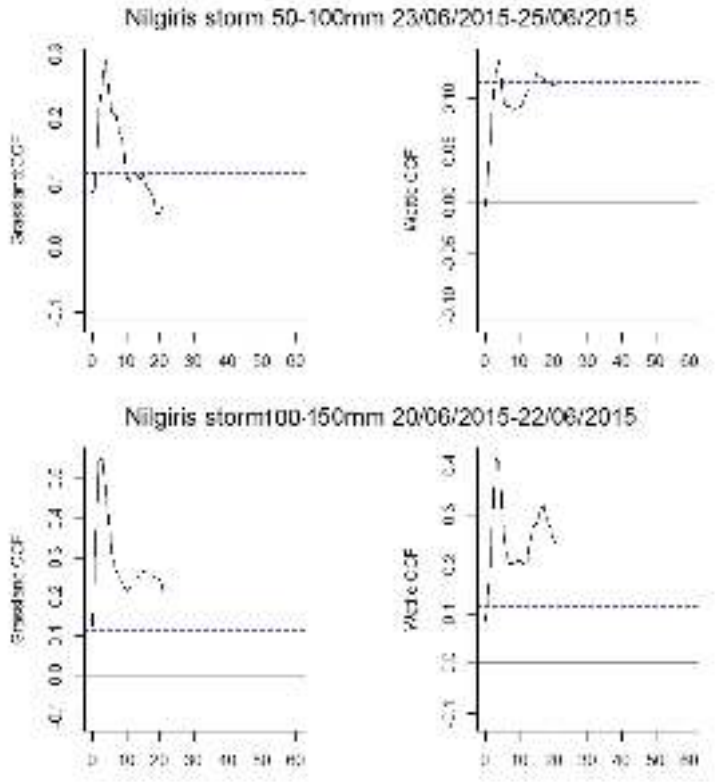


*Figure 4-11: Higher cross-correlation in grassland relative to wattle suggests higher proportion of water from the rainstorm being delivered to the stream by grasslands. The secondary peak in wattle is more pronounced but in both catchments, the initial peak at ~5 hours or less is most likely rapid sub-surface flow but there is indication of deeper ground water contributing to stream flow at ~10-20 hours after the rainstorm.*

In the Aghnashini basin, both catchments have strong rain water storage capacity in the sub-surface with a secondary peak being generated in response to the bigger rain storms (Figure 4-12). The more disturbed Hosagadde catchment shows some evidence of a quicker decay of the cross-correlation at lower intensities but interpretation is difficult as the catchment areas are quite different. Rainstorms totaling over 150 mm per day are likely to generate two flood peaks in these catchments (Figure 4-12).

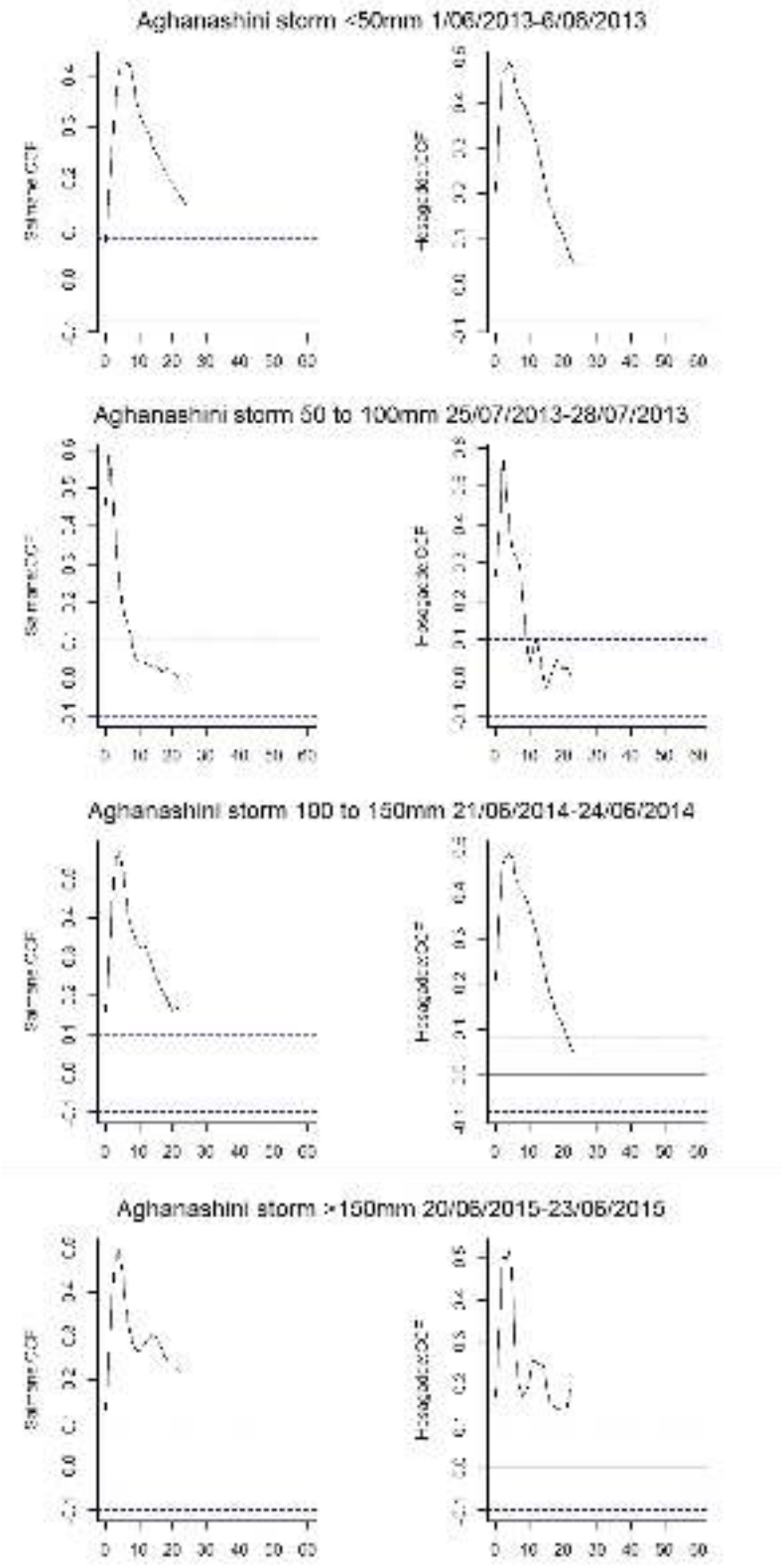


*Figure 4-12: The primary and secondary forest catchments have strong rain water storage capacity in the sub-surface with a primary peak at less than ten hours and a secondary peak being generated in response to the bigger rain storms. Rainstorms totaling over 150 mm per day are likely to generate two flood peaks in these catchments. The primary peak is likely to be generated by shallow rapid sub-surface pathways such as soil pipes.*

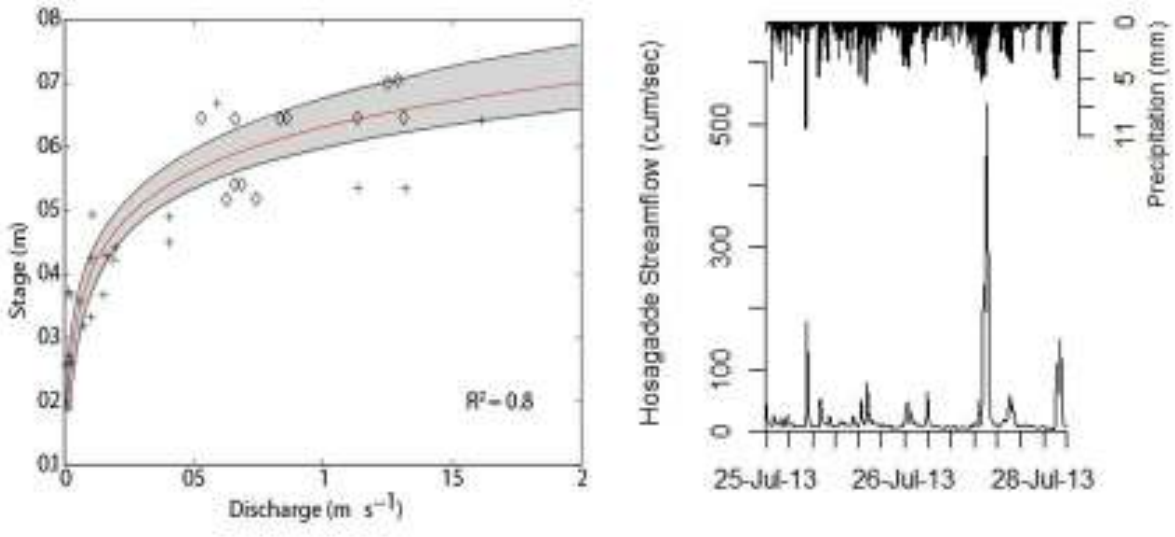


*4-13(a) A variety of field techniques and methods were used to generate stage discharge curves, including salt dilution. However, changes in the relationship due to logistical shifting of water level recorders or accumulation of sediment or debris as well as inability to use ANY technique at very high stage in the floods have made estimate of discharge at high stage difficult. (b) An example of a hydrograph and hyetograph to illustrate hydrologic response to rain in the Monsoon*


*Figure 4-13: It has been recognized by experimental scientists working in temperate environments since the 1930s (often forested) & more recently in humid tropical environments that very peaked or flashy river responses can be generated purely by subsurface or groundwater pathways. Pipe flow is a major hydrologic pathway in the Aghanashini basins. Photos: Chappell, N.A. 2010. Hydrological Processes, 24, 1567-1581*

## 4.4: WATER QUALITY

Grasslands show higher concentration of sediment compared to the more tree or shrub dominated catchments, whereas slightly higher concentration of nitrates are exported by the more tree and shrub dominated catchments (Figure 4-14). In the Aghanashini the catchment with higher percentage of agro-ecosystems (Figure 4-15) has higher export of sediment, nitrates and phosphates. Overall, median sediment and phosphate concentrations are low but large episodic export are evident in the large number of outliers, whereas nitrate concentration seems more even throughout the year, across all catchments.

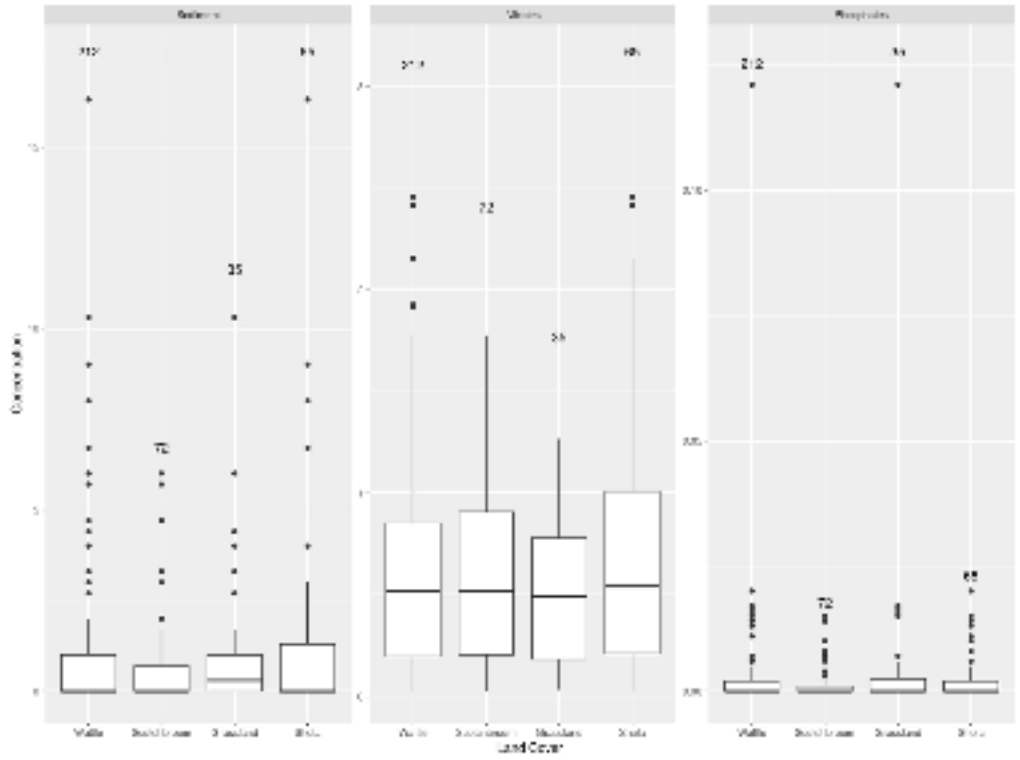


*4-14: Box and Whiskers plots of sediment and nutrient concentration across catchments dominated by major land-cover types in Niligiris with number of samples indicated.*

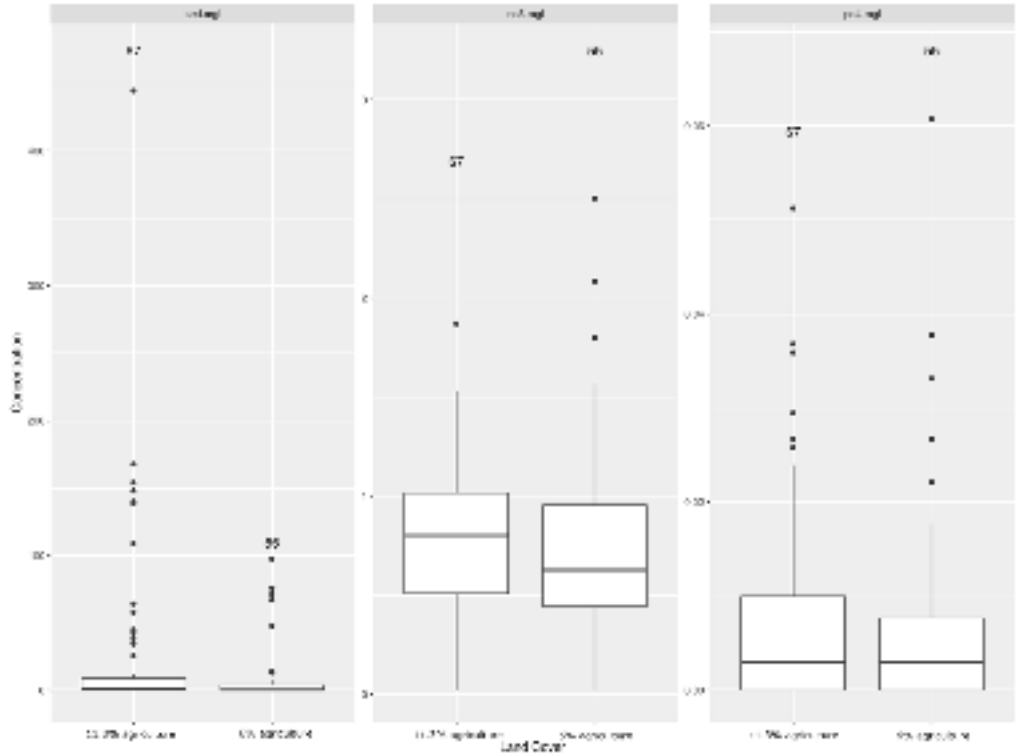


*Figure 4-15: Box and Whiskers plots of sediment and nutrient concentration across catchments dominated by major land-cover types in Aghanashini with number of samples indicated. We can see that the catchment with higher percentage of agro-ecosystems (Saimane on the left in each panel) has higher export of sediment, nitrates and phosphates.*

## 4.5: CONCLUSION

1. The less disturbed upper catchments in the Western Ghats have very high moisture storage capacity with rapid sub-surface flow mechanisms dominating storm response.
2. Soils under less disturbed ecosystems generally have high infiltration capacities in relation to observed rainfall intensities. A few of the more disturbed or degraded sites and plantations are vulnerable to infiltration-excess over-land flow. This could make them more prone to changes in hydrologic pathways in the future under higher rain intensities under climate change.
3. NDVI dynamics suggest that even the high rainfall Aghanashini catchments dominated by forests have a pronounced phenological response to moisture limitation in the dry season. NDVI in January and the drop of NDVI across the dry season is most sensitive to the preceding Monsoon totals but March NDVI is sensitive to dry-season rainfall.
4. The twin peaks that characterize storm responses to higher intensity rain suggest two pathways: one rapid overland and sub-surface pathways (eg pipe-flows in Aghanashini) and a more delayed deeper ground-water dominated pathway.
5. Phosphates are probably limiting in these ecosystems, and all land-covers seem to export very small amounts, but nitrate export is slightly higher in the more tree and shrub covered ecosystems, potentially influenced by nitrogen fixing properties of Wattle. Overall, sediment and phosphate exports are more episodic whereas nitrate seems more even through the year.
6. Catchments with very high and quite similar % of total forest cover (~84%) but with significantly different percentage under disturbed and managed agro-ecosystems such as Areca and Paddy showed very different responses in water quality. The catchment with higher percentage of agro-ecosystems has consistently higher concentration of sediment, nitrates and phosphates as there is greater supply and mobilization of soil and nutrients from these areas located close to the streams.

## 4.6: REFERENCES


Blöschl G, Ardoin- Bardin S, Bonell M, Dorninger M, Goodrich D, Gutknecht D, Matamoros D, Merz B, Shand P, Szolgay J (2007) At what scales do climate variability and land cover change impact on flooding and low flows? Hydrol Process 21:1241–1247.

Bonell M, Bruijnzeel LA (2005) Forests, water and people in the humid tropics: past, present and future hydrological research for integrated land and water management. Cambridge University Press

Bonell M, Purandara BK, Venkatesh B, Krishnaswamy J, Acharya HAK, Singh UV, Jayakumar R, Chappell N (2010) The impact of forest use and reforestation on soil hydraulic conductivity in the Western Ghats of India: implications for surface and sub-surface hydrology. J Hydrol 391:47–62.

Bradshaw CJ, Sodhi NS, PEH KS, Brook BW (2007) Global evidence that deforestation amplifies flood risk and severity in the developing world. Glob Change Biol 13:2379–2395.

Chayanulu, M. V., and K. S. Balakrishnan. "Black wattle mortality-preliminary studies on black wattle Acacia mearnsii (A. mollissima) soils from Nilgiris." Indian Forester 106, no. 7 (1980): 482-489.

Goswami BN, Venugopal V, Sengupta D, Madhusoodanan MS, Xavier PK (2006) Increasing trend of extreme rain events over India in a warming environment. Science 314:1442–1445.

Hosagoudar, V. B., G. R. Archana, and A. Manoj Kumar. "Disease of Wattles (Acacia spp.)-a review." Journal of Mycopathological Research 45, no. 2 (2007): 219-223.

Krishnaswamy J, Bawa KS, Ganeshaiah KN, Kiran MC (2009) Quantifying and mapping biodiversity and ecosystem services: Utility of a multi-season NDVI based Mahalanobis distance surrogate. Remote Sens Environ 113:857–867.

Laurance WF (2007) Environmental science: Forests and floods. Nature 449:409–410.

Medvigy D, Wofsy SC, Munger JW, Moorcroft PR (2010) Responses of terrestrial ecosystems and carbon budgets to current and future environmental variability. Proc Natl Acad Sci 107:8275–8280.

Pattanaik DR, Rajeevan M (2010) Variability of extreme rainfall events over India during southwest monsoon season. Meteorol Appl 17:88–104.

# CHAPTER 5: CARBON DYNAMICS IN RESPONSE TO MOISTURE AND TEMPERATURE FORCING

*Mahesh Sankaran, Raghavendra, H. V., Atul Joshi, Harinandan, P. V & Manaswi Raghurama*

## 5.1: INTRODUCTION

Ecosystem hydrological and carbon cycles are intimately linked, and thus changes in precipitation regimes have the potential to impact ecosystem carbon cycling, with attendant effects that can cascade through the ecosystem. Previously, long-term studies from other parts of the globe have highlighted how the carbon sequestration potential of ecosystems can change in response to inter-annual climatic variability (Philips et al. 2009, Lewis et al. 2011). For example, although Amazonian forests act as C sinks during normal rainfall years, sequestering ~0.89 Mg $ha^{-1}$ $year^{-1}$, they switch to being C sources in drought years (Philips et al. 2009, Lewis et al. 2011). It is estimated that during the severe drought of 2005, between 1.6 – 2.4 Mg C $ha^{-1}$ was lost from Amazonian forests, corresponding to the third greatest annual increase in atmospheric $CO_2$ concentrations in the global record (NOAA 2008). Central African rainforests, on the other hand, appear to have experienced a long-term 'browning' trend, consistent with reduced rainfall and increased temperatures, suggesting a loss of photosynthetic capacity and an erosion of carbon sequestration potential of these forests (Zhou et al. 2014). At present, there are few studies that have evaluated rainfall – C cycling relationships in the Indian context, and our understanding of these linkages as a result remains woefully inadequate.

To this end, as part of this project, we have established long-term initiatives in two contrasting ecosystem types - the wet evergreen forests of Sirsi, Aghanashini basin, Karnataka, and the montane forest-grassland mosaics of the upper Nilgiris, Tamil Nadu - to quantify and monitor ecosystem carbon cycles with the objective of understanding how different components of the carbon cycle respond to inter- and intra-annual climatic variability.

## 5.2: METHODS

### *5.2.1: Carbon cycling in the wet forests of the Aghanashini basin, Sirsi, Karnataka*

We established two 1ha (100 x 100m) long-term forest monitoring plots in Sirsi (Hosagadde&Mulgunda) using internationally accepted protocols (RAINFOR http://www.rainfor.org/, GEM http://gem.tropicalforests.ox.ac.uk/) to quantify:

i) ecosystem carbon budgets, including estimates of carbon pools in vegetation and soils, and
ii) major ecosystem carbon fluxes such as woody growth, litter fall and CO2 respiration from trees and soils.

Within each plot, all trees > 10cm gbh were spatially mapped, tagged and the species identity, height and dbh (at 1.3 m from the ground) recorded (Figure 5-1). In addition, all trees were fitted with dendro-bands to quantify seasonal patterns of growth (Figure 5-2). Wood cores

were collected from 5-10 adult individuals of each species from the surrounding area to estimate wood density (g/cm3) for species within plots.

Above ground carbon stocks were estimated following the general allometric equation proposed by Chave et al. (2005):

Carbon stock = 0.025 X wood density X $DBH^2$ X height

Below ground carbon stocks: To estimate belowground stocks, 10 soil cores (20 cm deep) were collected from different locations within each plot, and total soil C (%) and N (%) quantified using a LECO CN Analyser. Soil % C estimates were converted to soil carbon density (Mg C $ha^{-1}$) based on soil bulk density (kg $m^{-3}$).

Above ground net primary productivity: Trees were re-censused yearly and diameters of marked individuals and new recruits (trees that grew larger than 3 cm DBH between the previous and present census) noted. Further, mortality of individuals between successive censuses were recorded. Annual aboveground net primary productivity (Mg C $ha^{-1}$ $y^{-1}$) was estimated as the change in total aboveground biomass resulting from tree growth, recruitment and mortality from one year to the next.

*Figure 5-3 Photos of a) our long-term wet evergreen forest plot at Hosagadde, Sirsi, Karnataka, b) tagged trees, c) tree fitted with a dendroband to measure seasonal growth increments, and d) monitoring of stem CO2 efflux using the EGM-4 CO2 monitor.*

Belowground net primary productivity: Coarse-root net primary productivity was estimated as 0.21 X aboveground net primary productivity (Malhi *et al.* 2014). Fine root net primary productivity was estimated using root ingrowth chambers. These are cylindrical chambers made of fine mesh that are filled with root-free soil and buried at multiple locations within each plot. Biomass of roots that grew into chambers was

measured every three months. Total belowground net primary productivity was estimated as the sum of coarse and fine root net primary productivity (Mg C $ha^{-1}$ $y^{-1}$).

Litter fall: 25 square mesh nets of $1m^2$ were installed 1 m above the ground within each plot to collect falling leaf litter. Litter was collected from traps every 2 weeks, oven dried and weighed. Fallen litter was assumed to contain 47% carbon. Total carbon in litterfall (Mg C $ha^{-1}$ $y^{-1}$) was quantified by summing estimates of litter fall across a given year.

Tree respiration: Within each plot, stem respiration rates of 25 trees were monitored every 2 weeks using an EGM-4 $CO_2$ analyzer (Figure 5-1). Trees were fitted with PVC collars to facilitate data collection. Respiration rates for individual 2-week periods (g $CO_2$ $m^{-2}$ $h^{-1}$) were summed to estimate annual tree respiration (Mg C $ha^{-1}$ $y^{-1}$).

Soil respiration:Ten soil collars were established within each plot to quantify soil respiration. As before, respiration rates were measured using an EGM-4 $CO_2$ analyzer. Annual soil respiration rates (Mg C $ha^{-1}$ $y^{-1}$) were quantified by summing estimates from individual two-week periods (g $CO_2$ $m^{-2}$ $h^{-1}$).

### *5.2.2: Carbon cycling in the Upper Nilgiris, Tamil Nadu*

We quantified the effects of vegetation type and land-use changes (conversion of grassland to different plantation types) on soil carbon stocks and fluxes in the montane forest-grassland mosaics of the Upper Nilgiris, Tamil Nadu. Soil carbon stocks under different vegetation and land-use types (grassland, shola forest, wattle plantation, & pine plantation) were estimated based on multiple soil cores, as described in the previous section. Soil $CO_2$ fluxes under these different land-use types were estimated bi-weekly using the same methods described in the previous section.

## 5.3: KEY FINDINGS

### *5.3.1: Carbon stocks and fluxes in the wet forests of the Aghanashini basin, Sirsi, Karnataka*

Initial aboveground biomass carbon stocks in our plot at Hossagade, Sirsi was estimated at 121.4 Mg C $ha^{-1}$, while that of the Mulgunda plot was 102.9 Mg C $ha^{-1}$. As expected, trees in our plots showed seasonal patterns of growth, with the greatest stem increments observed in the monsoon months, with little to no growth in the pre- and post-monsoon periods (Figure 5-2).

$CO_2$ efflux from soils and stems showed similar patterns of seasonal variation over time (Figure 5-3). Effluxes tended to be highest during the wet months (May to September) and low during the drier months. However, there was quite a bit of variability in efflux patterns across years. Interestingly, compared to previous years, stem $CO_2$ fluxes were higher during 2015-2016 (Figure 5-3), which was relatively drier and warmer than previous years, suggestive of greater tree respiration during drier and warmer years. These patterns were also evident in the relationships between soil $CO_2$ fluxes, soil temperature and soil moisture (Figure 5-4). Interestingly, soil $CO_2$ fluxes were positively correlated with soil temperature, but unrelated to soil moisture in sites (Figure 5-4) indicating a dominant role for temperature in regulating soil C dynamics in this wet forest ecosystem. While these data suggest that future changes in temperature are likely to affect soil C cycling more than changes in soil moisture, more detailed analyses looking at the interactive effects of moisture and temperature on soil and stem

$CO_2$ effluxes are required in order to draw more definitive conclusions. We will continue to monitor C budgets in our plots in order to get a better idea of how C dynamics of these wet forests respond to inter-annual variation in temperature and precipitation.

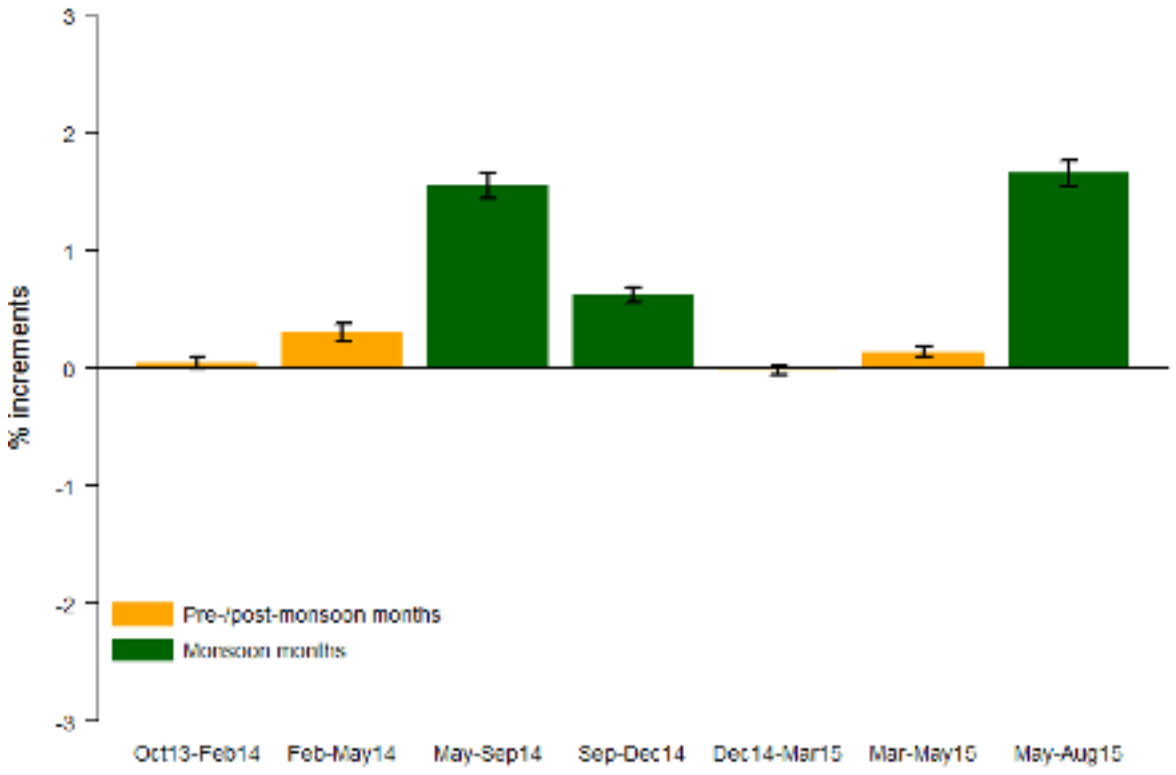


*Figure 5-4 Seasonal patterns of tree growth from our long-term plots in Sirsi as estimated from dendroband measurements. Growth peaked in the monsoon months, with little to no growth observed at other times.*

We have also been able to generate a near-complete carbon budget for the wet-forests of Sirsi, Karnataka (Figure 5-5). To our knowledge, this is the most complete quantification of its kind for any forest ecosystem in the Indian sub-continent. We hope to complete the budget in the coming months by additionally quantifying leaf respiration and woody liter fall.

Finally, the data collected as part of the project also allowed us to evaluate how the C-sequestration potential of the ecosystem and different components of the carbon cycle responded to changes in annual rainfall. Annual rainfall during 2014-15 was almost 2-3 times higher than during 2015-16 (Figure 5-8a). These differences were reflected in the annual net primary productivity of the forests, which were considerably lower in the drier year (Figure 5-8b). The drier year (2015-16) was also associated with greater tree mortality (Figure 5-9a), and higher soil and stem C effluxes (Figure 5-9b, c). Collectively, these data suggest that the C-sequestration potential of these forests are considerably negatively impacted during dry year; not only is NPP reduced, but carbon losses from soils and stems and following tree mortality is also increased. We aim to continue monitoring carbon pools and fluxes in the longer-term in order to get a more

robust idea of the responses and vulnerability of the different pools and fluxes to inter-annual variability in rainfall patterns, particularly drought and above-average wet years.

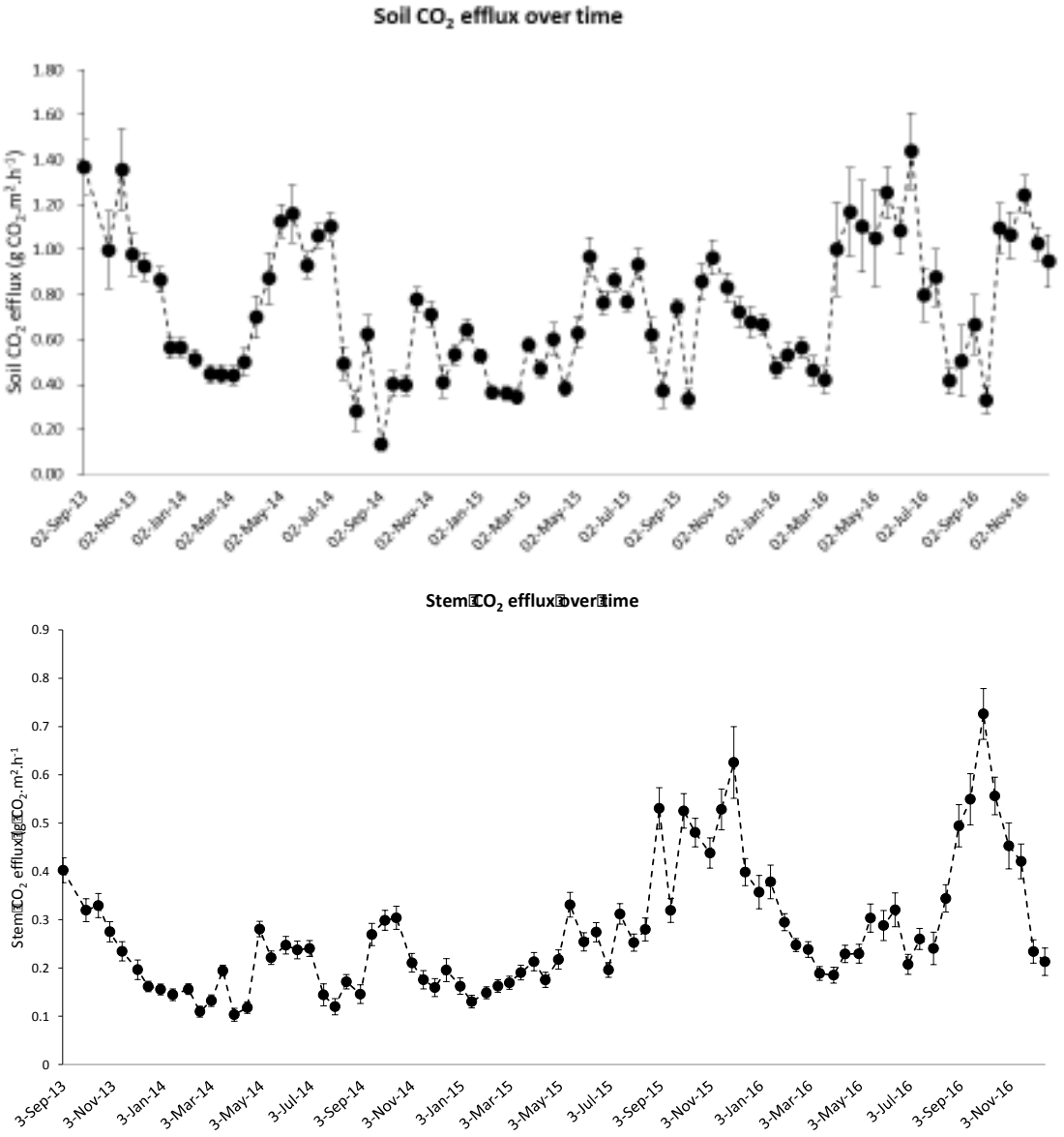


*Figure 5-5 Seasonal and inter-annual patterns of CO2 efflux from soils and tree stems in plots. In general, fluxes tended to be higher during the growing season compared to the non-growing season, with inter-annual differences in the magnitude of peak fluxes.*

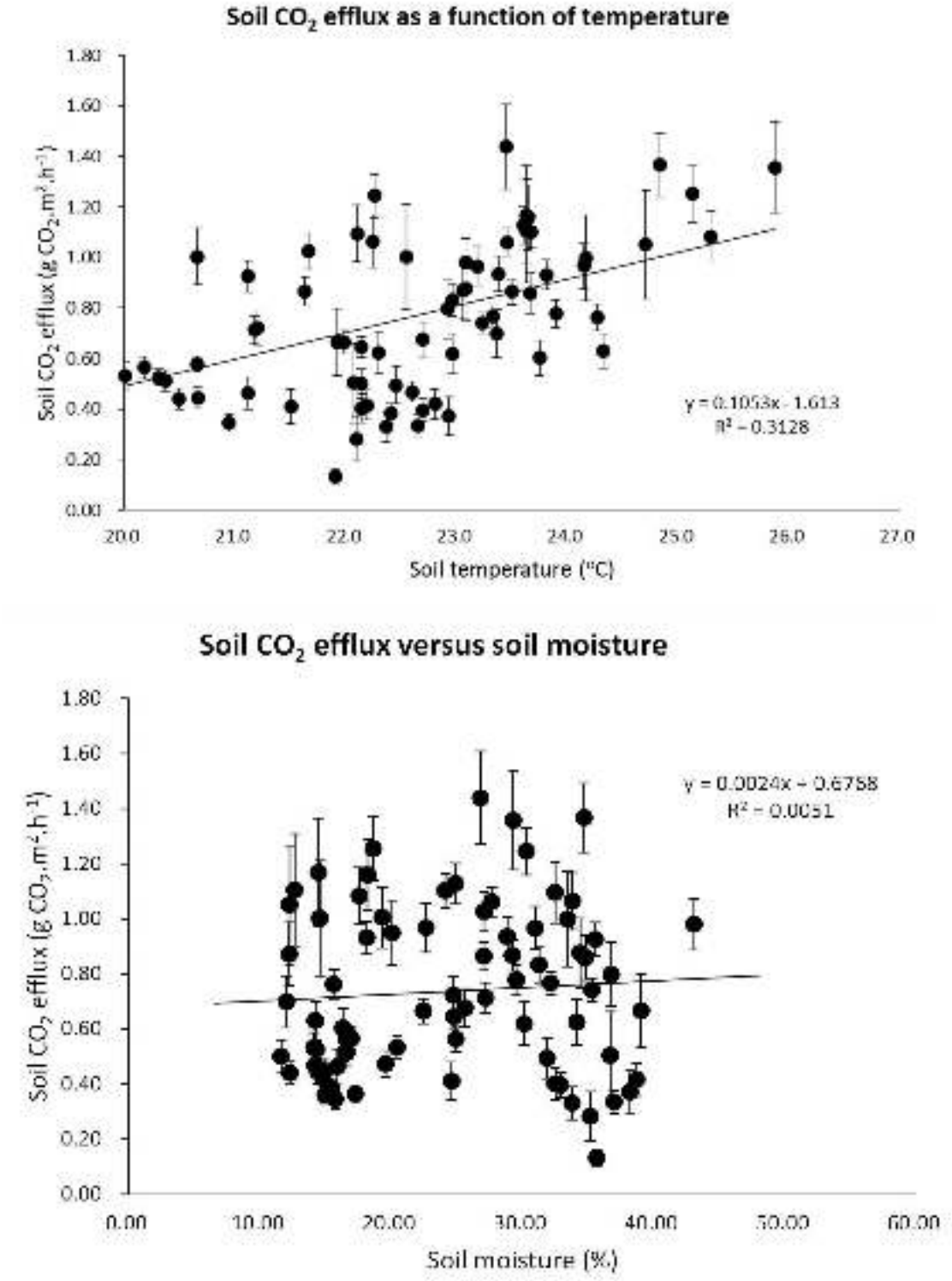


*Figure 5-6: Relationships between soil CO2 efflux and a) soil temperature, and b) soil moisture. Soil C fluxes were positively correlated with soil temperatures but were not related to soil moisture levels in plots.*

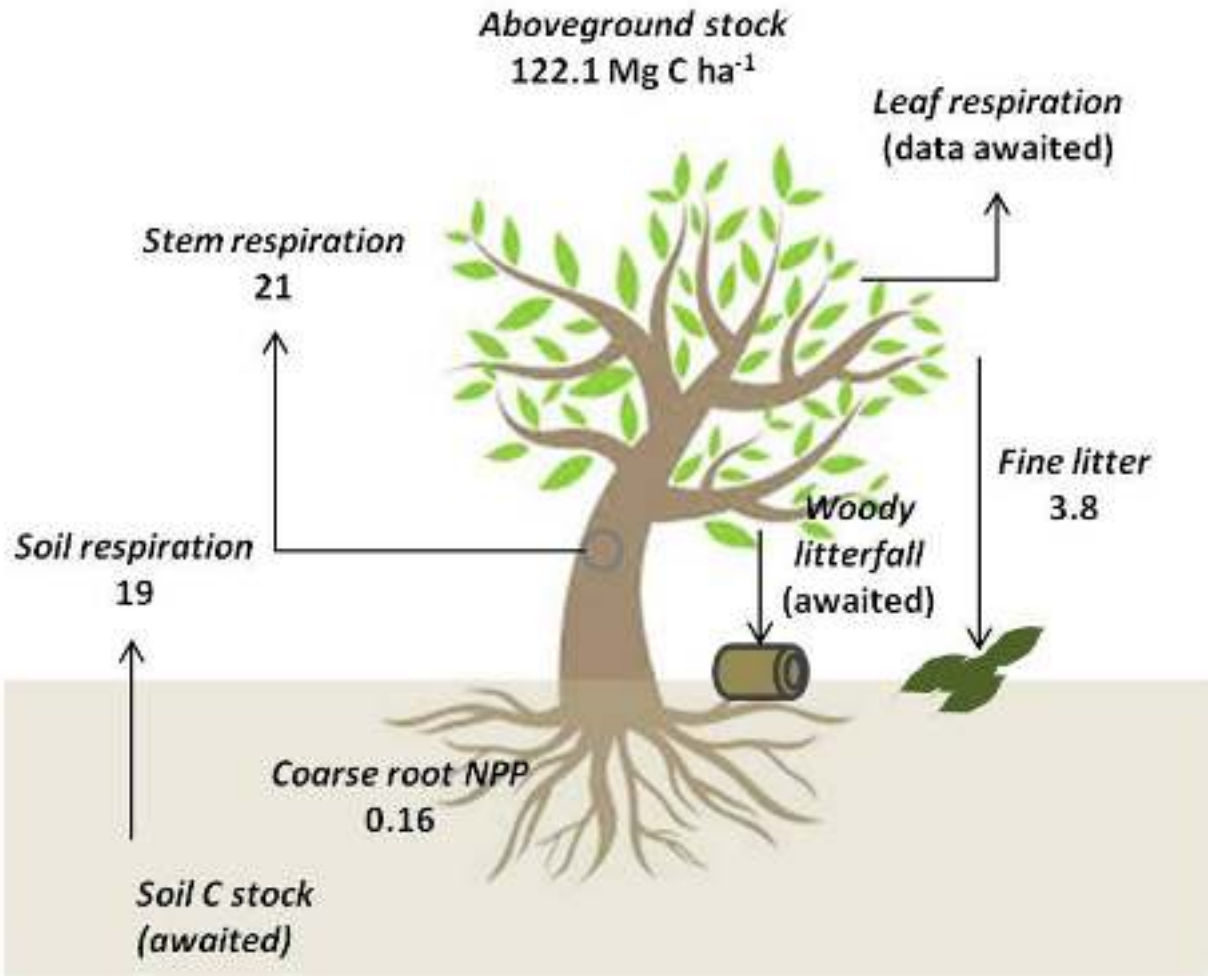


*Figure 5-7 The carbon budget of the wet-forest at Hossagadde, Sirsi, Karnataka. Carbon pools are in Mg C ha-1 and fluxes in Mg C ha-1 yr-1. Data for woody litterfall and leaf respiration are awaited.*

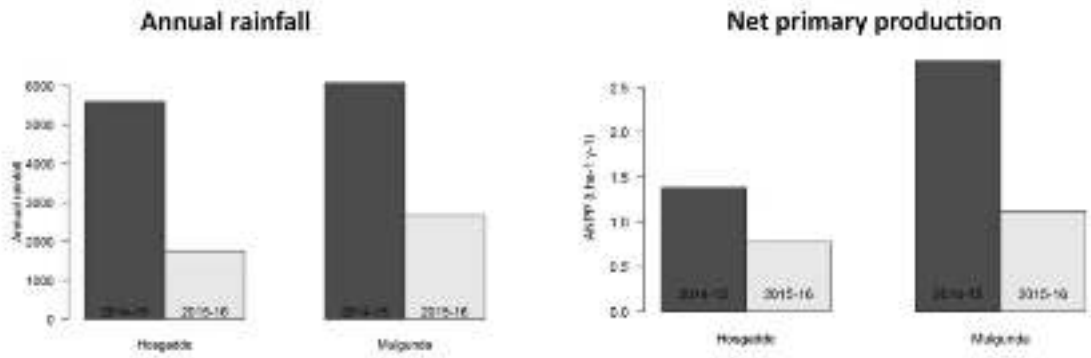


*Figure 5-8 (a)Annual rainfall during 2014-15 and 2015-16 at the Hosagadde&Mulgunda sites, and b) Annual net primary production (ANPP) of the Hosagadde&Mulgunda forests during the 2014-15 and 2015-16. ANPP was considerably lower during the drier year compared to the wetter year.*

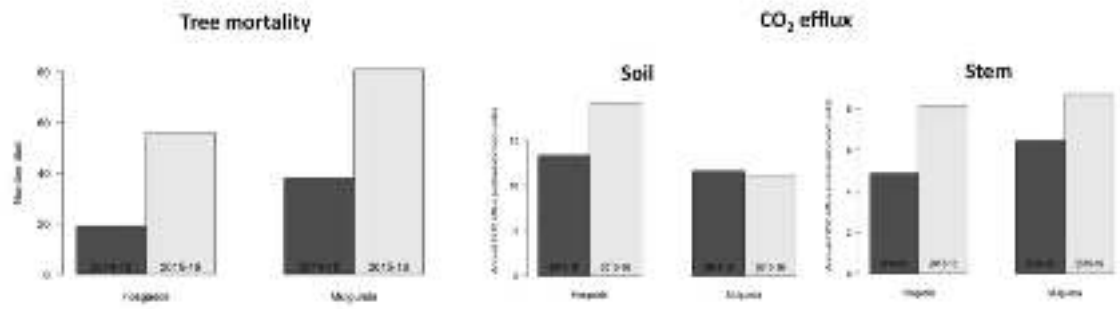


*Figure 5-9 Increased tree mortality (A), soil respiration (B) and stem respiration (C) during the drier year (2015-16) compared to the wetter year (2014-15) at Hosagadde & Mulgunda.*

### *5.3.2: Land-use change and C cycling in the Upper Nilgiris, Tamil Nadu*

Conversion of grasslands to wattle and pine plantations in the upper Nilgiris has significantly affected soil carbon and nitrogen contents (Figure 5-10). In general, soil carbon contents in shola forests and pine plantations were significantly higher than those of wattle soils across depths. Soil C content was lowest in grassland soils (Figure 5-8a). However, patterns differed in the case of soil nitrogen (Figure 5-10). Soil % N was highest in shola forests and lowest in grasslands, with values for pine and wattle plantations intermediate between the two (Figure 5-10)

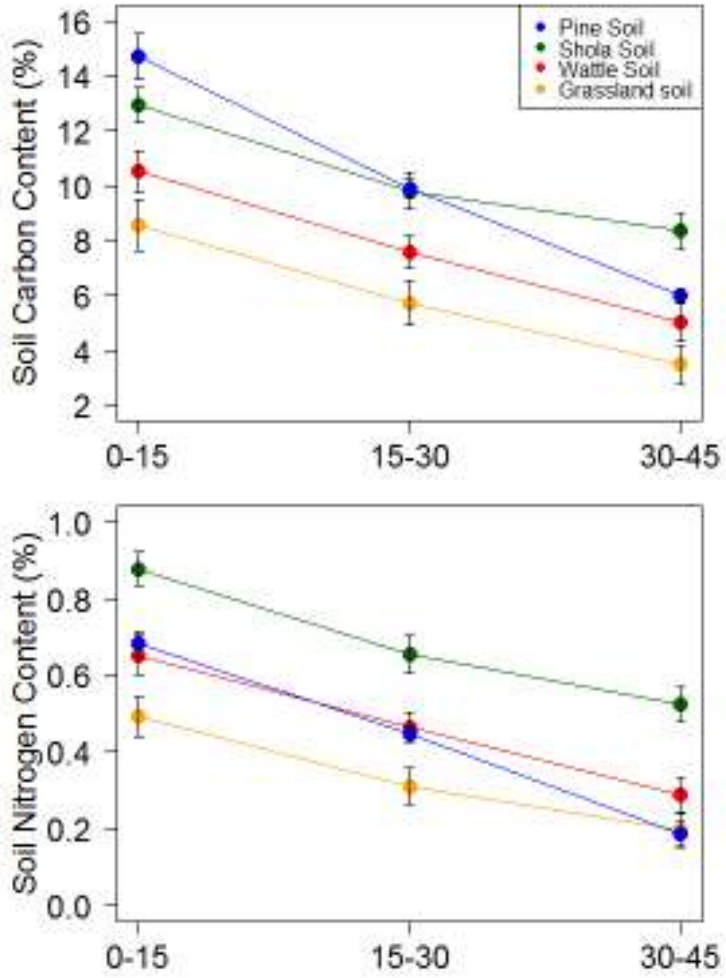


*Figure 5-10 Soil % C and %N at different depths in grasslands, shola forests, wattle and pine plantations in the Upper Nilgiris, Tamil Nadu*

Patterns of soil $CO_2$ efflux were qualitatively similar across different land-use types, and were highest during the monsoon and post-monsoon periods and lowest at the end of the dry season in April (Figure 5-11). In general, soil $CO_2$ efflux rates were lowest in pine plantations, and highest in grasslands (Figure 5-13).

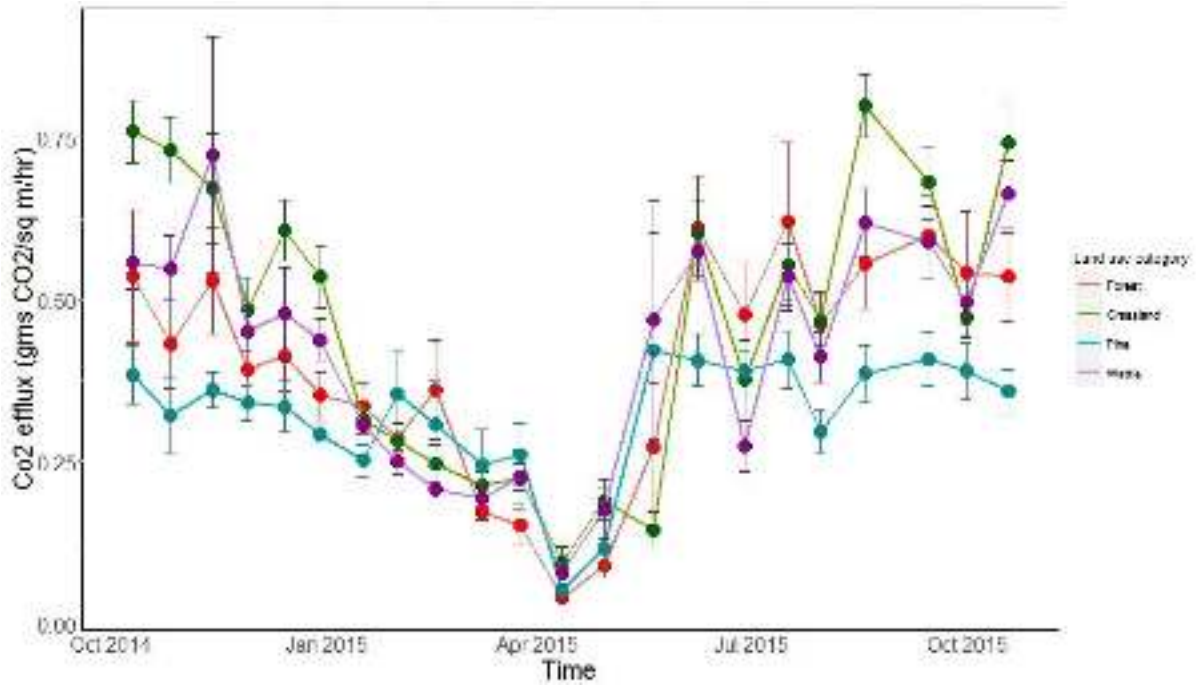


*Figure 5-11 Temporal patterns of CO2 efflux from soils under shola forests, wattle and pine plantations and grassland.*

In contrast to the patterns observed in the wet-forests of Sirsi, Karnataka, where soil $CO_2$ efflux rates were related to temperature but not soil moisture (Figure 5-4), efflux rates across different land-use types in the Nilgiris increased with increasing soil moisture (Figure 5-10), but was unrelated to soil temperatures (Figure 5-11). These results highlight the differential controls over soil C processes in different ecosystems, and suggest that future changes in moisture availability are likely to influence soil C cycling to a greater extent that changes in temperature in this ecosystem. However, more detailed analyses and long-term monitoring efforts are required in order to gain a more robust understanding of carbon dynamics in these ecosystems.

*Figure 5-12 Sediment sampling in the Upper Bhavani basin, Nilgiris*

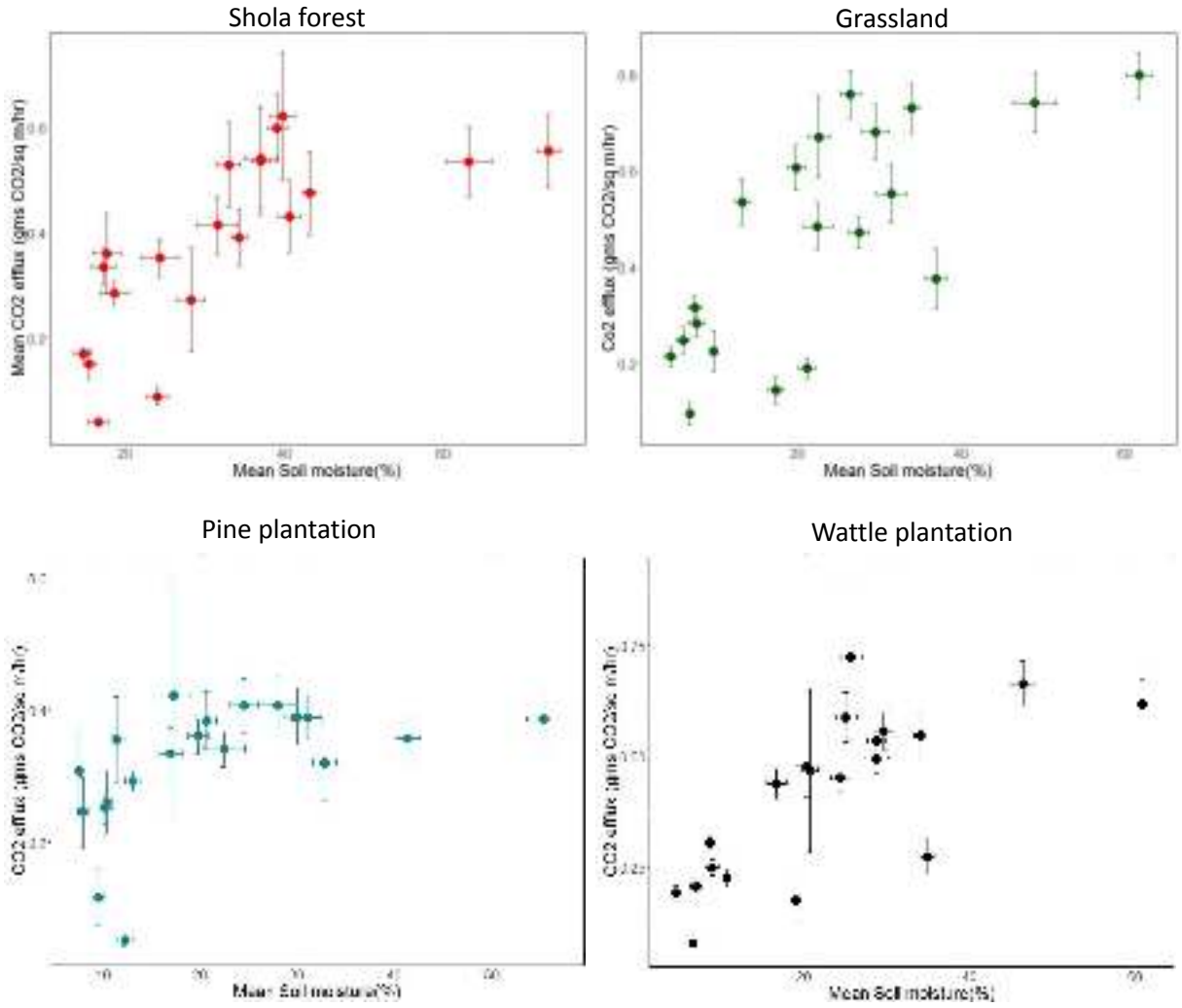


*Figure 5-12 Soil CO2 efflux as a function of soil moisture in (a) shola forests, (b) grasslands, (c) pine plantations and (d) wattle plantations. In general, soil CO2 efflux rates increased with increasing soil moisture in this system.*

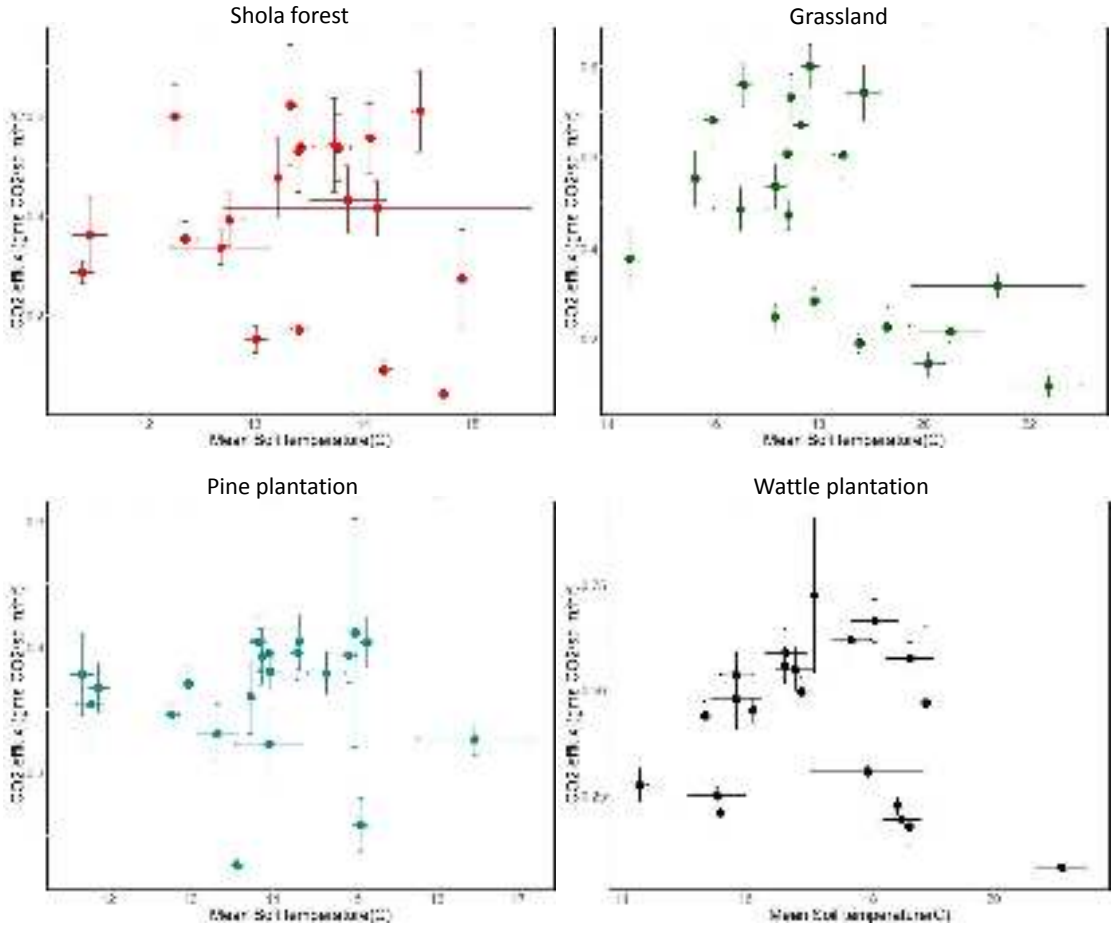


*Figure 5-13 Soil CO2 efflux as a function of soil temperature in (a) shola forests, (b) grasslands, (c) pine plantations and (d) wattle plantations.There was no consistent relationship between soil temperature and CO2 fluxes in this system.*

## 5.4: REFERENCES

Chave, J., Andalo, C., Brown, S., Cairns, M.A., Chambers, J.Q., Eamus, D., Fölster, H., Fromard, F., Higuchi, N., Kira, T. and Lescure, J.P., 2005. Tree allometry and improved estimation of carbon stocks and balance in tropical forests. Oecologia 145:87-99.

Lewis, Simon L., et al. (2011). The 2010 amazon drought. Science 331: 554-554.

National Oceanic and Atmospheric Administration (2008).Trends in Atmospheric Carbon Dioxide, Global (www.esrl.noaa.gov/gmd/ccgg/trends).

Phillips, O.L., Aragão, L.E., Lewis, S.L., Fisher, J.B., Lloyd, J., López-González, G., Malhi, Y., Monteagudo, A., Peacock, J., Quesada, C.A. and Van Der Heijden, G., (2009). Drought sensitivity of the Amazon rainforest. Science 323: 1344-1347.

Zhou, L et al. (2014). Widespread decline of Congo rainforest greenness in the past decade. Nature 509: 86-90.

# CHAPTER 6: EMERGING POLICY RECOMMENDATIONS

*Nick Chappell, Jagdish Krishnaswamy, and Ravinder Singh Bhalla*

## 6.1: EMERGING POLICY RECOMMENDATION NO. 1

ISSUE: Flooding within India costs the economy more than 10 million rupees annually and causes widespread distress, loss of life and impacts on livelihoods. Improved flood prediction would permit more rapid action and better targeting of mitigation measures and so reduce financial and social impact.

FINDINGS: The Western Ghats project via our combined field and parsimonious modelling strategy is providing the first quantitative evidence that the rainfall characteristics associated with different types of rainstorm (synoptic conditions) in the Western Ghats region of India produce very different peak river responses and consequent risks of river flooding.

POLICY RECOMMENDATION: **Flood forecasting models of Indian watersheds, as utilised by the Central Water Commission and state agencies, could be more reliable if the characteristics of the prevailing storm type were to be incorporated explicitly within the model parameterisations.**

## 6.2: EMERGING POLICY RECOMMENDATION NO. 2

ISSUE: A significant proportion of rivers in Peninsular India have dams and reservoirs in their headwaters. These reservoirs provide public water supply and irrigation in the dry season and hydropower throughout the year. Better understanding of the interaction between rainstorms, evapotranspiration and shallow groundwater storage is fundamental to quantifying the amount and seasonal timing of stream inflows to these reservoirs.

FINDINGS: The Western Ghats project has installed and maintained 16 stream gauging stations (supported by 52 rain gauges) in two 30 $km^2$ headwater areas of Peninsular India over two years. From what is now India's most densely gauged headwater area, our modelling can demonstrate the role of differing amounts of both evapotranspiration (resulting from contrasting land-cover) and shallow groundwater storage on flood behaviour and the timing of seasonal flows.

POLICY RECOMMENDATION: **Assessment of the stream inflows prior to a reservoir development or for forecasting reservoir level (to give earlier warning of floods arising from releases) by the Central Water Commission and appropriate state agencies could be improved with the incorporation of observations of both shallow groundwater storage and land-cover impacts on evaporation in addition to rainfall observations.**

## 6.3: EMERGING POLICY RECOMMENDATION NO. 3

ISSUE: Flooding within India costs the economy more than 10 million rupees annually and causes widespread distress, loss of life and impacts on livelihoods. Improved flood prediction would permit more rapid action and better targeting of mitigation measures and so reduce financial and social impact. Given that more than 70 percent of floodwater typically enters the channel network in headwaters accurate rainfall observation in such headwaters is critical to accurate prediction of the amount and timing of flood discharges.

FINDINGS: The Western Ghats project has installed and maintained 52 automatic rain gauges (recording rainfall at a 1-minute resolution) in two 30 $km^2$ headwater areas Peninsular India over two years. From one of India's most dense rain gauge networks at the scale of 60 $km^2$, our analysis demonstrates both the minimum density of rain gauges and minimum recording interval needed to avoid adding biases to models of the stream discharge during flood events. Our new rainfall and streamflow telemetry systems provide further demonstration of the value of high frequency monitoring and data delivery 'real time'.

POLICY RECOMMENDATION: **Regional offices of the Indian Meteorological Department (IMD), notably Karnataka and Tamil Nadu states of Peninsular India, might consider utilising our approach to determining the optimal density of rain gauges (and associated recording interval) needed to simulate flood response in critical headwaters as they deploy the latest generation of automated rain gauges, and consider the value of further telemetry.**

## 6.4: EMERGING POLICY RECOMMENDATION NO. 4

ISSUE: Headwater catchments in humid parts of Peninsular India are often required to support rural water supplies. These supplies are easily contaminated by local agricultural and domestic activities, yet there is little quantitative information on these systems. Hydrologically-based management practices are needed to permit the multiple uses of streams and linked shallow groundwater, including the maintenance of aquatic ecology that provide ecosystem services to support rural communities and biodiversity.

FINDINGS: The Western Ghats project has provided detailed training for NGOs and students in the Western Ghats and other regions in India on measuring aspects of basin hydrology pertinent to rural communities. These skills permit local people to better understand their water resources and improve their own agricultural and agroforestry practices to maximise water use while minimising water pollution.

POLICY RECOMMENDATION: **Giving local communities the skills to measure and better understand water resources within their own communities is a technology transfer activity that other NGOs in collaboration with government agencies and universities might offer to promote improved management of local water resources elsewhere in India.**

## 6.5: EMERGING POLICY RECOMMENDATION NO. 5

ISSUE: The National Mission for Green India of the National Action Plan on Climate Change aims to protect and restore India's forest cover and so improve carbon sequestration, hydrological services, biodiversity and provisioning services in forestlands.

FINDINGS: The Western Ghats team has undertaken extensive investigations on the infiltration capacities of soils under varied natural forest, plantation and grassland cover in the Western Ghats. We found that soils beneath a natural forest cover support greater infiltration capacities, with the notable exception of forests with high cattle densities (due to the extensive trampling impacts).Enhanced infiltration has the potential to improve the water quality of rivers by mitigating soil erosion, while also enhancing dry-season flows in certain circumstances. In other circumstances, notably wattle (*Acacia mearnsii*) plantations the higher evaporation rates offset any infiltration benefits and so lead to reduced dry-season flows.

POLICY RECOMMENDATION: **Forest restoration should be considered a valuable tool at locations of India where there is a focus on restoring the water quality in rivers, but**

**certain forest management activities should be excluded from areas with soils susceptible to compaction. Equally, certain introduced trees that have a negative impact on dry-season flows might be removed from areas where dry-season flows are critical. Such forest interventions are being considered in some of India's biodiversity hot spots, such as the UNESCO World Heritage site of the Western Ghats in Peninsular India, and so should also consider hydrological costs and benefits.**

## 6.6: EMERGING POLICY RECOMMENDATION NO. 6

ISSUE: Tropical headwaters such as the Western Ghats Mountains are hot spots for organic carbon that is transported and transformed along rivers to the oceans, yet little is known about the timing and transformations of carbon delivery in headwater sources. Greater understanding of the functioning of organic carbon in the numerous headwater basins of tropical India would contribute to improvements in the modelling of the global carbon budget.

FINDINGS: The Western Ghats project (particularly the recent extension) has involved measurement of organic carbon in tropical headwater streams at an unprecedented rate comparable to the hydrological changes observed through storm events. This has permitted the development of the first models of these sub-hourly carbon dynamics simulated directly from hydrological observations.

POLICY RECOMMENDATION: **We demonstrate that organic carbon dynamics in tropical headwater streams can be simulated and understood provided that concentrations are monitored continuously. This reinforces the research of the Central Pollution Control Board, notably 'Guidelines for Online Continuous Monitoring System for Effluent, 2014', and should be extended to address carbon and other water quality issues across India's river basins.**

# CHAPTER 7: OUTREACH

*Susan Varghese*

## 7.1: THE MOTIVATION

Sharing the learnings from the project with the research community, students and local stakeholders was an important component of the project. Our outreach activities ran throughout the project period.

Our goal was to build the capacity of civil society to monitor hydrology, water resources and ecological flows, link with important ongoing policy and management initiatives and take the research experience to wider audiences. We achieved this by organizing training workshops, presentations, involving interns and master's students for short term studies and communicating science in popular media. All the project scientists and project recruits have been quite active in disseminating scientific knowledge, promoting field hydrology data collection and management methods.

## 7.2: TRAINING WORKSHOPS & ORIENTATION PROGRAMS:

* In January and July 2012, orientation programs were held to train the project personnel in field data collection, management and troubleshooting.

* In March 2014, annual project meeting cum workshop was held in Bangalore for understanding the dynamics of forest hydrology along with instrumentation and data interpretation.

* In June 2014, an additional workshop on automated analysis of data from rain gauge and water level recorders to derive hydrographs using R statistical package was conducted at FERAL office, Bangalore.

### *7.2.1: Training workshop on "An Introduction to Field Hydrology" from 10th - 14th November, 2014 at FERAL Campus, Pondicherry*

This was the first all India level workshop under the project. The workshop was meant for an audience, particularly non-hydrologists who require basic knowledge about concepts and field methods in surface hydrology. The main target audience, were from non-governmental organizations working in the field of hydrology and/or watershed development.

The aim of the workshop was to help researchers get grounding in the basic concepts of hydrology, help non-hydrologists get up to speed with the collection and analysis of field data and a hands-on on simple, cost-effective ways of visualizing, measuring and calculating discharge.

A total of 23 participants from various non-government organizations from different parts of the country were a part of the workshop (Annex 1).

### *7.2.2: Training workshop in Field Hydrology from 13th to 15th August, 2015 at ATREE field office, Heggarni, Sirsi, Karnataka*

This was the second workshop under the project. The objective of the three day field intensive workshop was to introduce the participants to "state-of-the-art" approaches and

techniques to provide foundation in basic concepts of hydrology. This workshop was mainly focused on capacity building of local stakeholders and those working in and around the study area. Participants included 14 people representing various organizations and 10 participants at the Master's level from the National Centre for Biological Sciences, Bangalore (annex 2).

There were presentations introducing the participants to different topics, discussions, field exercises in stream profiling and velocity measurements, discharge measurements and practical lab sessions.

### *7.2.3: Training Workshop in "Field Hydrology and Basic Data Analysis", from 22nd to 24th February, 2016 at IATC, Meghalaya Water Resources Development Agency, Shillong*

This workshop was organized in Shillong in collaboration with the Meghalaya Water Resources Development Agency, Govt. of Meghalaya (annex 3). The course trained in total 24 government department staff representing 11 districts of Meghalaya Water Resources Development Agency. This was conducted as a part of the training and capacity building exercise for the department. The aim of the workshop was to give an overview of the field hydrology and hands-on on simple field collection methods and analysis.

## 7.3: KNOWLEDGE TRANSFER AND CAPACITY BUILDING:

- Training in Field Hydrology for students of Sirsi College of Forestry on 17th August, 2015 at Hosagadde, Sirsi, Karnataka. A group of 55 students from the Sirsi College of Forestry were trained in field hydrology methods for one day on 17th August followed by a theoretical lecture session in the College by Dr. Jagdish Krishnaswamy on the 21st of August, 2015 (Annex 4). The bachelor level students were introduced to the basics of hydrology with reference to the Western Ghats especially in the Uttara Kannada region. During the field session, the students were taught to measure stream profile and velocity. They were also shown how to measure discharge using the salt dilution technique.
- Independent researchers from various organizations were trained in field hydrology methods enabling them to implement the knowledge in their respective field (Box 1).
- Master's and PhD students were trained helping them in designing their study and data collection (Box 2).
- Vaijayanti Vijayaraghavan, worked as an intern under the project for her M.Sc thesis work, titled "Impact of Extreme Rainfall Events on Land Use/Cover in the Aghanashini Basin, Western Ghats".
- Mr. Kumaran K., working as a project staff completed his M.Sc thesis titled "Relationship between Land Cover and Evapo-Transpiration in the Upper Nilgiris".
- 3 weather stations are being maintained in close collaboration with Tamil Nadu Forest Dept., Nilgiris South. We have also installed rain gauges and a weir on request from the Forest Department for studying the effects of Wattle removal in the Nilgiris.

**Box 1: Capacity building and knowledge transfer for independent researchers and staffs from other organizations**

**Tarun Nair,** Consultant to **FES,** Gujarat: Was involved in a project that attempted to develop a simple methodology for estimating ecological flows in the Son Gharial Sanctuary (Madhya Pradesh). The 'Introduction to Field Hydrology' workshop provided the necessary grounding in hydrological concepts and to enable the collection and analysis of field data for this project.

**Bhupal Singh Bisht,** Development Associate at **CHIRAG**, Uttarakhand: After attending the workshop, he trained team members to use current meter, installing and downloading from water level recorders and calculating discharge.

**Renie Thomas,** Hydrogeologist at **WOTR**, Pune: He found all sessions very informative; especially the practical experiments in the field and the salt dilution discharge measurements technique very interesting. He has initiated a project on the role of natural springs in feeding base flows, taking discharge measurements and water quality studies and working towards formulating management plans for their conservation.

**Walter Kennedy**, Researcher at **ARULAGAM,** Tamil Nadu: He shared his training experience among the NGO participants in the National Environment Awareness Campaign (NEAC). He demonstrated the rainfall measurement technique among the college students.

## 7.4: STAKEHOLDER TRAINING PROGRAMS:

### *7.4.1: Training Program for Forest Department, Ooty, 26-27th October, 2015*

A training program was organized by FERAL, as part of capacity building exercise, at the Cairn Hill Interpretation center, Ooty. The objective was to teach how to operate GPS for creating waypoints and tracks and for navigation, how to manipulate and share the data between GPS units and computers and visualize the same on GIS software such as Quantum GIS and Google Earth. A total of 32 participants were trained consisting of Forest Guards, Watchers and Anti-poaching watchers.

### *7.4.2: Nilgiris Stakeholder Engagement Workshop, Ooty 17th February, 2016*

This stakeholder workshop was to get opinions and views on the data that was being collected in the Nilgiris region since the past 4 years. We wanted to see how the information we collect can contribute to the future management of plantations and restoration of hydrologic services in this region.

Stakeholders included Dr O.P.S. Khola, Principal Scientist and Head, Central Soil and Water Conservation and Training Institute, Mr. Vijay from the Red Hill Nature Resort, Emerald, The Nilgiris, Mr. Vasanthan, independent researcher and Mr. Gokul Halan, Researcher, Keystone Foundation. Reporters from The Hindu and other local media people were also present. As part of the research team, Dr. Ravi S. Bhalla, co-PI along with his research staff

from FERAL organized and coordinated the workshop. From ATREE, Dr. Shrinivas Badiger (Co-PI), Dr. Milind Bunyan (Post-Doctoral Researcher), R. Venkitachalam (Researcher), Ms. Divya Solomon (Researcher), Ms. Prakriti Prajapati (Researcher) and Ms. Revathy (Field Coordinator) attended the workshop.

While everyone shared concerns about extreme rainfall events, increased growths of invasive species (Shola trees and Wattle), shifts in temperatures and rapidly changing landscape, the stakeholders expressed their keen interest in using climate data acquired by the researchers in improving their agricultural practices and yield. Support of a strong economic argument was felt to be imperative in bringing about a significant positive change. The stakeholder workshop was well reported by the press in local language.

## 7.5: COMMUNICATING SCIENCE:

- Krishnaswamy J., Saving India's Rivers and Riverine Ecosystems. December 10, 2015. http://www.fundamatics.net/article/saving-indias-rivers-and-riverine-ecosystems/
- Research into monsoon riddle, Deccan Chronicle, November 30th, 2015
- Bangalore scientists discover changing patterns of El Nino influence, Deccan Herald, August 28th, 2014
- When it rains, it pours, says study, The New Indian Express, September 22nd, 2014
- Krishnaswamy J., was part of a panel discussing the current 'heat wave' in Bangalore, in News9 TV. https://www.youtube.com/watch?v=39stCkVIr9M&feature=youtu.be
- As a part of the extension to the project (WGHATS-Capacity), a website on the trial rain telemetry and high frequency water quality measurements was set up in the Western Ghats alongside those in UK in Malaysia. More details at: http://wp.lancs.ac.uk/basin-network/home-page/map/smart-watersheds-western-ghats/
- A website for the project was set up to showcase the ongoing work. More details at: http://hycase-wg.atree.org/
- Our sites in the Western Ghats were included in the Critical Zone Exploration Network (CZEN).

## 7.6: SCIENTIFIC EXCHANGE:

- A review meeting was held at Oxford in May, 2014 under the MoES-NERC Changing Water Cycle program. Following this, experts (**Prof. Bruijnzeel & Distinguished Prof. Beven**) from the NERC side, visited our sites and provided their useful insights.
- MoES-NERC review meeting was held at Bangalore on 10th March, 2015 where the project outcomes were presented and was appreciated for the amount of efforts being put for collecting the primary data.
- Dr. Jagdish Krishnaswamy and Dr. Ravi Bhalla visited the UK-NERC site under the scientific exchange program in August 2015.
- Dr. Nick Chappell and Dr. Timothy Jones visited Aghnashini and Nilgiris in August, 2015.
- Dr. Mark Mulligan along with Students of King's College, London visited Nilgiris site in December, 2015 and again in December 2016. During his second visit, Dr. Mulligan provided two soil moisture sensors and two FREESTATION Meso-automatic weather stations. The soil moisture sensors have been installed at depths of 20 and 100 cm, while the two FREESTATIONS have been installed in the Nilgiris and Aghanashini, respectively.

## 7.7: CONFERENCES / POSTER PRESENTATIONS:

- Krishnaswamy, J. Ecohydrology in the Anthropocene: Challenges and Opportunities in India. Chapman Conference in Tropical Ecohydrology, American Geophysical Union, 9 June 2016, Cuenca, Ecuador.

  https://agu.confex.com/agu/16chapman3/webprogram/Paper94860.html

- Bonell, M., Krishnaswamy, J., Bhalla, R.S., Badiger, S., Ball, B., Chappell, N.A., Tych, W., Vaidyanathan, S., Sankaran, M., Varghese, S., Vissa, V., Page, T., Jones, T., & Broderick, C., 2016. Hydrologic & carbon services in the Western Ghats: Response of forests & agro-ecosystems to extreme rainfall events. Presentation at India-UK Water Security Exchange Initiative, CEH Wallingford 18 Feb 2016.
- Kumaran K., Bhalla R. S., Devi Prasad K. V. 2016. "Ecological And Anthropogenic Implications Of Two Decades Of Land Cover Changes In The Upper Nilgiris In The Context Of Global Climate Change", International Conference on Sustainable Forest Development in view of Climate Change (SFDCC2016), 8-11th August, Malaysia.
- Chappell, N.A., Jones, T., Young, P., and Krishnaswamy, J. 2015.Demonstrating value of fine-resolution optical data for minimising aliasing impacts on biogeochemical models of surface waters. Presentation in session B14D of the American Geophysical Union meeting AGU Fall Meeting 2015 in San Francisco 14-18 December 2015.
- Jones, T., Chappell, N.A., Tych, W., and Bhalla, R.S., 2015. Importance of high-frequency chemistry for resolving hot moments in headwaters: a combined optical sensor and time-series modelling approach. Presentation in session B53H of the American Geophysical Union meeting AGU Fall Meeting 2015 in San Francisco 14-18 December 2015.
- Krishnaswamy, J. and Vaidyanathan, S. 2015. La Nina and Indian Ocean Dipole influence on distribution of daily rain intensities in India. Poster presentation in session A13A of the American Geophysical Union meeting AGU Fall Meeting 2015 in San Francisco 14-18 December 2015.
- Bhalla, R.S., Kumaran K., Vaidyanathan, S., Krishnaswamy, J., Chappell, N.A., and Jones, T. 2015. Estimating evapotranspiration demands of different land covers using diurnal signals in dry season stream discharge. Poster presentation in session H13D of the American Geophysical Union meeting AGU Fall Meeting 2015 in San Francisco 14-18 December 2015.
- Vissa, N., Bonell, M., Chappell, N.A., Tych, W., Krishnaswamy, J., Bhalla, R.S., Badiger, S. and Vaidyanathan, S. 2014. Effect of extreme rainfall characteristics within differing monsoon synoptic systems on flood response in headwaters. Presentation to the British Hydrological Society meeting BHS2014 Challenging hydrological theory and practice at Birmingham University 2-4th Sept 2014.

**Box 2: Capacity building for MSc and PhD students**

**Vidyadhar Atkore,** PhD student at **ATREE** was supported under the capacity building program of the project for his doctoral thesis titled "Drivers of Fish Diversity and Turnover across multiple spatial scales: Implications for Conservation in the Western Ghats, India".

**Nachiket Kelkar**, PhD student at **ATREE**, Bangalore: He believes what he learned in the workshop was very effective in the long run. He has been able to translate some of the concepts to others as well. He uses the Manning's equation to estimate discharge in some areas of the Ganga River. He shares that learning these methods in the workshop was very useful as there is no simple or cost-effective way to get any estimates for large river discharges otherwise.

**Shishir Rao**, MSc student at **NCBS**, Bangalore: The workshop was extremely effective and helpful for designing his study titled "Response of stream fish assemblages to small hydro-power induced flow alteration in the Western Ghats, Karnataka". He used the Slug discharge method, installed water level recorders and staff gauges. He feels that overall the workshop was very holistic with both hands-on as well as classroom sessions where the data collected from the field was analyzed.

**Suman Jumani**, MSc student at **NCBS,** Bangalore: She found the training was extremely useful specifically the catchment area delineation methods described. Her understanding on stream discharge measurement techniques improved and now knows how to factor it in further studies.

## 7.8: BOOK CHAPTERS:

- Krishnaswamy J. (2016), "Forest Management and Water in India" In: Forest Management and the impact on water resources: a review of 12 nations, IHP - VIII, Technical Document, United Nations Educational, Scientific, and Cultural Organization International Hydrological Programme and International Sediment Initiative, pp: 69-89.

## 7.9: PUBLICATIONS:

- Chappell N.A., Jones T.D., Tych W., Krishnaswamy J. 2017. Role of rainstorm intensity underestimated by data-derived flood models: Emerging global evidence from subsurface-dominated watersheds. *Environmental Modelling & Software*, 88, 1-9. http://dx.doi.org/10.1016/j.envsoft.2016.10.009.

- Krishnaswamy J., V. Srinivas, R. Balaji, M. Bonell, M. Sankaran, R. S. Bhalla, S. Badiger. 2014. Non-stationary and non-linear influence of ENSO and Indian Ocean Dipole on the variability of Indian monsoon rainfall and extreme rain events. *Climate Dynamics* (August 23): 1-10. doi:10.1007/s00382-014-2288-0

- Bhalla, R. S., K. V. Devi Prasad and Neil W. Pelkey. 2014. Impact of India's watershed development programs on biomass productivity. *Water Resources Research* 49 (3): 1568–1580. doi:10.1002/wrcr.20133

- Krishnaswamy. J., M. Bonell, B. Venkatesh, B. K. Purandara, K. N. Rakesh, S. Lele, M. C. Kiran, V. Reddy and S. Badiger. 2013. The groundwater recharge response and hydrologic services of tropical humid forest ecosystems to use and reforestation: support for the "infiltration-evapotranspiration trade-off hypothesis. *Journal of Hydrology* 498 (August 19): 191-209. doi:10.1016/j.jhydrol.2013.06.034

- Krishnaswamy, J., M. Bonell, B. Venkatesh, B. K. Purandara, S. Lele, M. C. Kiran, V. Reddy, S. Badiger, and K. N. Rakesh. 2012. The rain–runoff response of tropical humid forest ecosystems to use and reforestation in the Western Ghats of India. *Journal of Hydrology* 472–473 (November 23): 216–237. doi:10.1016/j.jhydrol.2012.09.016

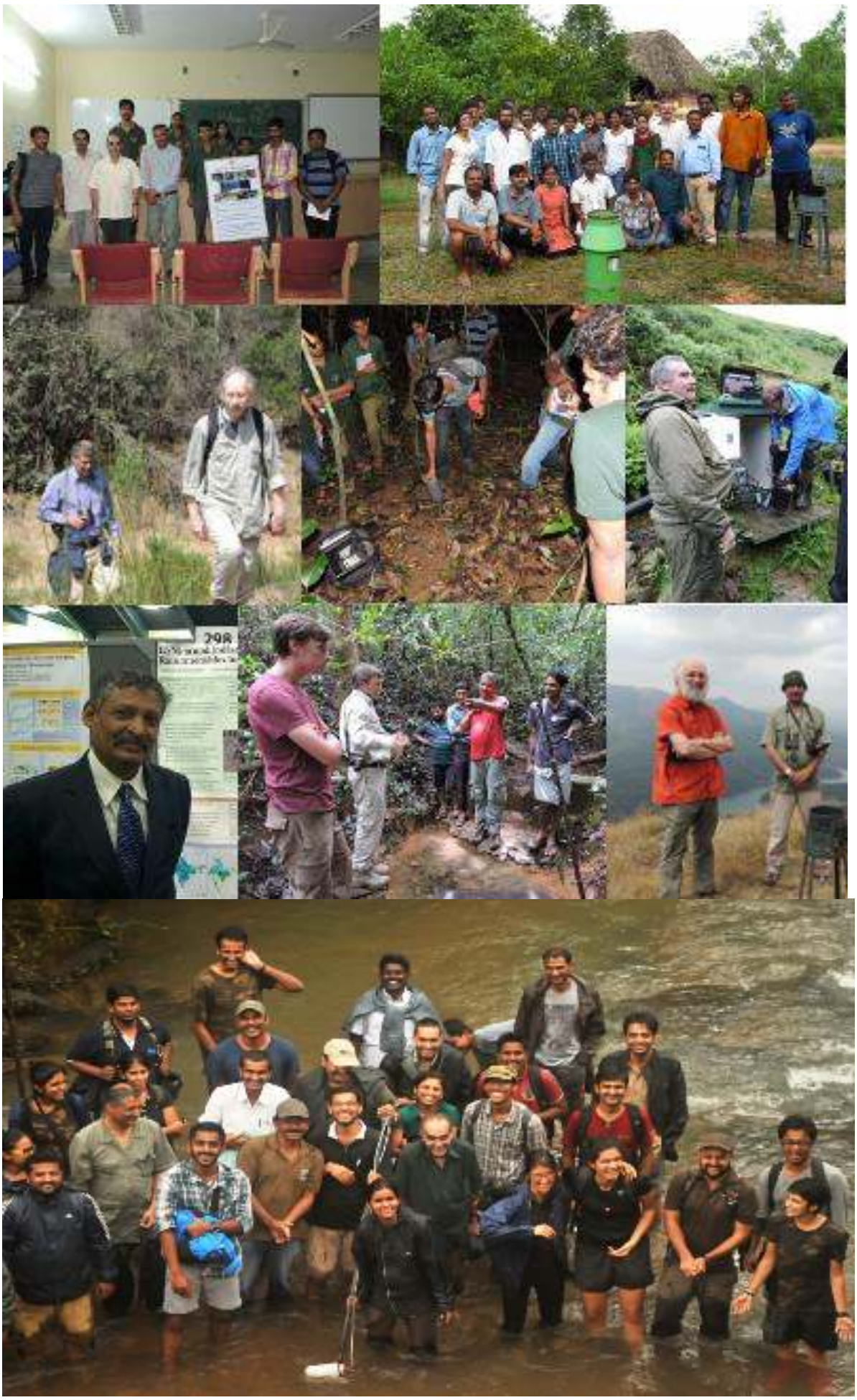

# CHAPTER 8: SYNTHESES AND CONCLUSIONS

*Jagdish Krishnaswamy, Nick Chappel, Mahesh Sankaran and Ravinder Singh Bhalla*

This project leads to some key research, methodological breakthroughs and establishment of long-term monitoring sites and enhancing capacity in civil society.

**Research, methods and data highlights include:**

(1) Our research has focused on the role of extreme rainfall events in generating storm flows and floods in a region of India with perhaps the highest short term rain intensities.

(2) We have used parsimonious methods capable of identifying changing dynamics directly from meteorological & hydrological time-series (from existing government stations & new experimental catchments) so that change can be observed above uncertainties in techniques used (field & numerical).

(3) The application of these techniques have generated key insights such as (a) The changes in the relative role of ENSO and Indian Ocean Dipole (IOD) in the long-term dynamics of the Indian Monsoon as well as a greater role for the IOD in influencing frequency of more intense daily rainfall totals and (b) demonstrated a global monotonically decreasing non-linear relationship between sub-surface watershed residence time and mean rain intensities over a wide range of synoptic conditions. Projected increases in rainstorm intensity would then result in a greater likelihood of river floods in subsurface-dominated watersheds than is currently simulated by systems models omitting this additional nonlinearity.

(4) This is the first ever integrated analyses of high frequency rain data in relation to high frequency streamflow using wavelet analysis, OLR maps analysis and IMD synoptic charts information to categorize extreme rainfall events into synoptic typologies. Key differences between the Aghanashini and Nilgiris emerged: Over the Aghanashini basin synoptic systems that are most associated with extreme rainfall events are OSC, TCZ and local convection. Over the Nilgiris basin, extreme rainfall events are mostly associated with the active phases of monsoon, onset and retrieval phase of monsoon season.

(5) Our carbon dynamics study, one of the first in India integrated with hydro-meteorology has generated some key results with major implications for carbon dynamics under future climate: stem CO2 fluxes were higher during 2015-2016 which was relatively drier and warmer than previous years, suggestive of greater tree respiration during drier and warmer years. These patterns were also evident in the relationships between soil CO2 fluxes, soil temperature and soil moisture. Interestingly, soil CO2 fluxes were positively correlated with soil temperature, but unrelated to soil moisture in sites indicating a dominant role for temperature in regulating soil C dynamics in wet forest ecosystem. These data suggest that future changes in temperature are likely to affect soil C cycling more than changes in soil moisture.

(6) This project has been able to generate a near-complete carbon budget for the wet-forests of Sirsi, Karnataka. To our knowledge, this is the most complete quantification of its kind for any forest ecosystem in the Indian sub-continent.

(7) We have successfully tested and used salt-dilution gauging for estimating spot discharges for stage-discharge curves for head-water streams in Western Ghats under topographic and logistical situations were no other technique is currently accurate, feasible or cost-effective.

(8) The establishment of one of the highest density of rain gauges at the highest sampling frequency (per minute) for any montane tropical environment has resulted in our ability to test satellite based rainfall estimation techniques and assess the potential role of synoptic storm type on rainfall characteristics. This has also enabled us to test various hypotheses related to rainfall-runoff pathways using cross correlation lag characteristics as well spatio-temporal evolution of rain storms and the hydrologic response to these at nested spatial scales.

**Establishment of long-term monitoring sites**

(1) The two clusters of instrumented basins in the Western Ghats are the first of its kind in India and perhaps in the entire humid tropics: highest rain gauge density over a 26-30 $km^2$ area with nested water-level recorders covering diverse land-cover and land-use.

(2) The first ever integrated hydrologic-carbon dynamics studies in the Western Ghats, and perhaps in India.

**Enhancing capacity for research and monitoring**

(1) Trained over a hundred members of civil society including students, NGOs and government staff in hydrologic science and monitoring.

(2) Long-term experimental and observational instrumented catchments for taking forward the field of eco-hydrology in India.

(3) This project has helped transform the field of ecohydrology and integrated hydrology-carbon-water quality dynamics in India and generated valuable data and knowledge that will further develop the capacity of Indian researchers to contribute world class research and data.

# ANNEXURE

ANNEXURE 1: Participant list – Hydrology Training Workshop, 2014 at Pondicherry

| Sl. No. | NAME | ORGANIZATION | Contact No. | Email ID |
|---|---|---|---|---|
| 1 | Manish Kumar | SACON | 9489812154 | manishfisheries@gmail.com |
| 2 | Mr. B. Walter Kennedy | ARULAGAM | 9443592910 | walterkennedyb@gmail.com |
| 3 | Balachander | KEYSTONE | 9442629677 | bala@keystone-foundation.org |
| 4 | Gokul | KEYSTONE | 9442629677 | gokul@keystone_foundation.org |
| 5 | Aditya | ACWADAM | 9765287145 | bhupendradabholi@gmail.com |
| 6 | Tarun Nair | Independant Researcher | 9844234982 | tarunnair1982@gmail.com |
| 7 | Nisarg | NCF | 9035150587 | nisargprakash@gmail.com |
| 8 | Suman Jumani | LIFE | 9886971023 | sumanjumani@gmail.com |
| 9 | Nachiket Kelkar | ATREE (JK lab) | 9880745693 | nachiket.kelkar@atree.org |
| 10 | Mr. S. Sudheer Kumar | FES | 8374209946 | sudheercae.022@gmail.com |
| 11 | Mr. M. Uthanna | FES | 9008744024 | uthannamu@gmail.com |
| 12 | Mr. Bhupal Bisht | CHIRAG | 9627294463 | bhupal@chirag.org |
| 13 | Siddhant Nowlakha | Samaj Pragati Sahayog | 8889616139 | siddhant.n@outlook.com |
| 14 | Medha Hegde | LIFE, Sirsi | 8277517184 | mksirsi@gmail.com |
| 15 | Divya Solomon | CARIAA (Atree) | 8141754659 | divya.solomon@atree.org |
| 16 | Rahul Varier | IDRC (Atree) | 9497274491 | rahulsvarier@gmail.com |
| 17 | Manohar Kalal | ATREE | 8904228088 | manohar.kalal@atree.org |
| 18 | Yogisha Bhat | ATREE | 9480676495 | yogisha.bhat@atree.org |
| 19 | Prachi Ghatwai | ATREE | 9880822244 | prachi.108@gmail.com |
| 20 | Vindhya N. G | ATREE | 9980243232 | vindhya.ng@atree.org |
| 21 | Kumaran K. | FERAL | 9488494601 | kumaran.k@feralindia.org |
| 22 | Siva S. | FERAL | 9488089949 | sivanaturewild@gmail.com |
| 23 | Saravanan S. | FERAL | 9655389379 | saravanan@feralindia.org |

ANNEXURE 2: Participant List – Hydrology Training Workshop, 2015 at Sirsi

| Sl. No. | Name | Organization | Email |
|---|---|---|---|
| 1 | Mohd Zeeshan Malik | SACON | malik908@gmail.com |
| 2 | Pallavi Talware | LIFE | paalavit@gmail.com |
| 3 | Dr. Dheeraj K V | CSIR Pool Officer, KU, Dharwad | dheeraj2k@gmail.com |
| 4 | Renie Thomas | WOTR | renie.thomas@wotr.org.in |
| 5 | Parvathy Menon | IDRC team, ATREE | parvathy.menon@atree.org |
| 6 | Mr.Rajashekhar Barker | Asst. Professor, College of Forestry, Ponnampet | rdbarker11@gmail.com |
| 7 | Vidyadhar Atkore | ATREE | vidyadhar.atkore@atree.org |
| 8 | Ankur Shringi | PhD student, CES, IISc | ankur@ces.iisc.ernet.in |
| 11 | Dina Rasquinha | NCBS | dina.rasquinha@gmail.com |
| 12 | Chidambar Gowda | Sirsi College of Forestry | chidutg@gmail.com |
| 13 | S.D. Bhat | Sirsi College of Forestry | sdbhat.wlvd@gmail.com |
| 14 | Balu Hegde | Independent | blhegde@gmail.com |

**List of NCBS students**

| | |
|---|---|
| 1 | Anisha Jayadevan |
| 2 | Anushka Rege |
| 3 | Biang Syiem |
| 4 | Shivona Bhojwani |
| 5 | Swetha Bashyam |
| 6 | Pradeep Koulagi |
| 7 | Shishir Rao |
| 8 | Binod Borah |
| 9 | Ramchandran |
| 10 | Pooja Rathod |

ANNEXURE 3: Letter from Department of Water Resources, Government of Meghalaya

GOVERNMENT OF MEGHALAYA
OFFICE OF THE CHIEF ENGINEER (WATER RESOURCES)

No: CE/WR/346/2011-16/Pt/208 Dated Shillong, the ___ April. 2016.

**TO WHOMSOEVER IT MAY CONCERN**

The Department of Water Resources, Government of Meghalaya, facilitated a training workshop on "Field Hydrology" from 22nd to 24th February, 2016 in Shillong, Meghalaya.

The workshop was conducted jointly by Ashoka Trust for Research in Ecology and the Environment (ATREE), Bengaluru and Foundation for Ecological Research, Advocacy and Learning (FERAL), Tamil Nadu. It was jointly supported by the Changing Water Cycle Program, Ministry of Earth Sciences, and Government of India and partially by the Department of Water Resources Govt. of Meghalaya.

The resource team conducting the workshop consisted of Dr. Jagdish Krishnaswamy and Dr. Shrinivas Badiger from ATREE and Dr. Ravi Bhalla and Mr. Srinivas Vaidyanathan from FERAL respectively. The team also included Dr. Susan Varughese, Tarun Nair, Vindhya N.G. and Kumaran K. as supporting resource team and coordinating the workshop.

Yours Sincerely

Chief Engineer(WR)
Meghalaya Shillong

ANNEXURE 4: Letter of Appreciation from the Sirsi College of Forestry

University of Agricultural Sciences, Dharwad
**College of Forestry, Banavasi Road, Sirsi**
Uttara Kannada District – 581401.

Shridhar D. Bhat, M.Sc. (Wildlife Science)
*Assistant Professor (Wildlife Management)*
***Zeiss Wildlife Conservation Awardee-2014***

Mobile No.: 09480474740
Email: sdbhat.whrd@gmail.com

To:
Dr. Jagadish Krishnaswamy
Senior Fellow, ATREE
Royal Enclave, Sriramapura,
Jakkur Post, Bengalooru,
Karnataka - 560064

Sub: Gratitude for opportunities for me and students on forest hydrology

Dear Dr. Jagadish,

It is a pleasure to state what the days 13-21 August 2015 were. To start with, I got a life time opportunity to see for myself, witness, participate and learn several things in forest hydrology. It was a dream came true after my readings in Ecology books on Coweeta Field Hydrology Station, about which I had only read and felt fasconated 30 years ago. Thank you and your team for allowing me to participate and learn. It was a learning packed 3 days for me. The guidance by you and your team has made me confident to display practicals to students on stream cross-sectioning, and float method of stream flow measurements. That itself can be a wonderful set of knowledge for our UG, PG students.

Also, on 17.8.2015, our 3rd year B.Sc. (Forestry) students, 58 in number, undergoing Forest Ecology course, visited your field station, and got a wonderful exposure to many of the field hydrology equipments, and hands-on exposure to techniques on steam flow measurements. It was quite an apt exercise. In fact, what they did and learn in the field on that day, they discussed, analysed for over six hours, spread over two practical classes, and submitted as written assignment. 2-3 pages of the assignment, I am emailing photos to you.

Thirdly, it was a privilege for me, students, and colleagues to listen to your lecture titled 'Effects of land cover and land use on hydrologic services in the Western Ghats of India', and interact with you on 21.8.2015.

We would like to associate with you and your team in future years also, for our UG and PG courses on Ecology. Yours is a wonderful set of field laboratories that our students can access.

Our Dean (Forestry) and our Head of Department, Forest Biology, have expressed their pleasure over the matters stated above, and asked me to convey their regards to you. This letter is carrying their wishes.

Thanking you and your team for all the opportunities given and learnings delivered,

Yours sincerely,

Date: 25th September 2015

Shridhar D. Bhat
Assistant Professor (Wildlife)
Department of Forest Biology
College of Forestry
Sirsi - 581 401

Copies submitted to:
1. Dean (Forestry), College of Forestry (CoF), Sirsi, for kind information
2. The Head of the Department, Forest Biology & Tree Improvement, CoF, for kind information.

Journal of Hydrology 472–473 (2012) 216–237

Contents lists available at SciVerse ScienceDirect

Journal of Hydrology

journal homepage: www.elsevier.com/locate/jhydrol

# The rain–runoff response of tropical humid forest ecosystems to use and reforestation in the Western Ghats of India

Jagdish Krishnaswamy [a,*], Michael Bonell [b], Basappa Venkatesh [c], Bekal K. Purandara [c], Sharachchandra Lele [a], M.C. Kiran [a], Veerabasawant Reddy [d], Shrinivas Badiger [a], K.N. Rakesh [a]

[a] Ashoka Trust for Research in Ecology and The Environment, Jakkur Post, Royal Enclave, Sriramapura, Bangalore 560 064, India
[b] The Centre for Water Law, Water Policy and Science Under The Auspices of UNESCO, University of Dundee, Dundee DD1 4HN, Scotland, UK
[c] Hard Rock Regional Centre, National Institute of Hydrology, Belgaum, Karnataka 590 001, India
[d] TERI, WRC, H. No. 233/GH-2, Vasudha Housing Colony, Alto Santa Cruz, Bambolim, Goa 403 202, India

ARTICLE INFO

*Article history:*
Received 16 December 2011
Received in revised form 23 July 2012
Accepted 9 September 2012
Available online 24 September 2012
This manuscript was handled by
Konstantine P. Georgakakos, Editor-in-Chief

*Keywords:*
Rainfall–runoff
Forest degradation and forestation
Western Ghats
India
Monsoon tropics

SUMMARY

The effects of forest degradation and use and establishment of tree-plantations on degraded or modified forest ecosystems at multi-decadal time-scales using tree-plantations on the streamflow response are less studied in the humid tropics when compared to deforestation and forest conversion to agriculture. In the Western Ghats of India (Uttar Kannada, Karnataka State), a previous soil hydraulic conductivity survey linked with rain IDF (intensity–duration–frequency) had suggested a greater occurrence of infiltration-excess overland within the degraded forest and reforested areas and thus potentially higher streamflow (Bonell et al., 2010). We further tested these predictions in Uttar Kannada by establishing experimental basins ranging from 7 to 23 ha across three ecosystems, (1) remnant tropical evergreen Forest (NF), (2) heavily-used former evergreen forest which now has been converted to tree savanna, known as degraded forest (DF) and (3) exotic Acacia plantations (AC, *Acacia auriculiformis*) on degraded former forest land. In total, 11 basins were instrumented (3 NF, 4 AC and 4 DF) in two geomorphological zones, i.e., Coastal and Up-Ghat (Malnaad) and at three sites (one Coastal, two Up-Ghat). The rainfall–streamflow observations collected (at daily and also at a 36 min time resolutions in the Coastal basins) over a 2–3 year period (2003–2005) were analysed.

In both the Coastal and Up-Ghat basins, the double mass curves showed during the rainy season a consistent trend in favour of more proportion of streamflow in the rank order DF > AC > NF. These double mass curves provide strong evidence that overland flow is progressively becomes a more dominant stormflow pathway. Across all sites, NF converted $28.4 \pm 6.41_{stdev\%}$ of rainfall into total streamflow in comparison to $32.7 \pm 6.97_{stdev\%}$ in AC and $45.3 \pm 9.61_{stdev\%}$ in DF.

Further support for the above trends emerges from the quickflow ratio $Q_F/Q$ for the Coastal basins. There are much higher values for both the DF and AC land covers, and their rank order DF > AC > NF. The quickflow response ratio $Q_F/P$ is also the highest for the DF basin, and along with the $Q_F/Q$ ratio, can exceed 90%. The corresponding delayed flow response ratios, $Q_D/P$ clearly show the largest $Q_D$ yields as a proportion of event precipitation from the Forest (NF1). The application of linear model supported these differences (e.g. 10–36% difference between NF and DF, $p < 0.001$) in the storm hydrologic response of the Coastal basins. The exception was $Q_F/P$ where there was a higher uncertainty connected with inter-basin mean differences. Cross-correlation plots for rain–streamflow and corresponding lag regression models for three storm events in the Coastal basins suggested the existence of alternative stormflow pathways with multiple lags with peaks between ~12 and 24 h in NF, compared to respective bimodal peaks at ~1 and 16 h in AC and ~1 and 12 h in DF. The long time lags for NF are suggestive of deep subsurface stormflow and groundwater as the contributing sources to the storm hydrograph. The short time lags in DF and AC are indicative of overland flow and so 'memory' of the previous degraded land cover is retained in AC as supported by previous hydraulic conductivity data. As potential and actual evapotranspiration is likely to be depressed during the monsoon, differences in streamflow and run-off responses between land-cover types is largely attributed to differences in soil infiltration and hydrologic pathways. Enhancing infiltration and reducing run-off in managed ecosystems should be explored in the terms of the context of other ecosystem services and biodiversity.



* Corresponding author.
*E-mail address:* jagdish@atree.org (J. Krishnaswamy).

0022-1694/$ - see front matter © 2012 Elsevier B.V. All rights reserved.
http://dx.doi.org/10.1016/j.jhydrol.2012.09.016

## 1. Introduction

Previous work has highlighted a lack of drainage basin experiments to capture the hydrological responses to multi-decadal land degradation which is now the emerging reality of many humid tropic landscapes (Bruijnzeel, 1989, 2004; Bruijnzeel et al., 2004; Sandstrom, 1998; Giambelluca, 2002; DeFries and Eshleman, 2004; Holscher et al., 2004; Ziegler et al., 2004, 2007; van Dijk and Keenan, 2007; Ilstedt et al., 2007; Malmer et al., 2010). Similarly no such experiments have been established to monitor the hydrological impacts of 'forestation' (Scott et al., 2004) over 'degraded land' (Safriel, 2007) previously occupied by native tropical forests (Scott et al., 2004; Ilstedt et al., 2007; Lamb et al., 2005; Lamb, 2011). As part of the preceding scenarios, earlier work (Bonell et al., 2010; Bonell, 2010) noted that there is comparatively limited information in the humid tropics on the surface and sub-surface permeability of: (i) forests which have been impacted by multi-decades of human occupancy and (ii) forestation of land in various states of degradation. Moreover even less is known about the *dominant* stormflow pathways (as defined by Chappell et al. (2007)) or storm hydrograph characteristics (i.e., quickflow, delayed or baseflow; Chorley, 1978) for these respective scenarios.

Zhou et al. (2001) presented data from experimental first-order basins (up to 6.4 ha) in monsoonal southern China to study the impacts of rehabilitation of barren degraded land using eucalyptus (*Eucalyptus exerta*) as a plantation and separately, by under planting this eucalyptus with indigenous species. Within a 10-year period subsequent to 16 years of forestation, Zhou et al. (2001) noted that there was a progressive reduction in quickflow largely attributed to increasing macroporosity associated with the incorporation of biological matter. Although no soil hydraulic conductivity or hillslope hydrology data were presented, these writers remarked that the quickflow response was the highest from the degraded catchment due to surface soil crusting and showed no trend over the 10-year period, except being sensitive to rainfall variability. Similarly, work in very small basins (0.13–0.25 ha) over karst in Letye, The Philippines (Chandler and Walter, 1998. Chandler, 2006) suggests that that pasture–fallow sites produced high volumes of infiltration-excess overland flow, *IOF* (70–80% of annual rainfall) compared with the minimal volumes of basin streamflow (~3% mostly from subsurface stormflow, *SSF*) from forest.

The above Asian studies are for the most part dealing with multi-decadal to century time scale, human impacted landscapes. In contrast there has been a concentrated effort on the impacts of forest conversion to pasture in the Amazon basin where such land cover changes are more recent. Whilst most of the work (reviewed in Bonell (2010)) has focused on point-scale, field saturated hydraulic conductivity ($K_{fs}$; Bouwer, 1966; Talsma and Hallam, 1980;Talsma, 1987) measurements; the work of de Moraes et al. (2006) was one of the first to present comparative hydrometric evidence (e.g. runoff plots, storm hydrograph response characteristics) from a forested (0.33 ha) and pasture basin (0.72 ha). Forest conversion to pasture 30 years ago had now clearly enhanced the occurrence of saturation-excess overland flow, *SOF* and further introduced *IOF* leading to higher proportions of total flow volumes as quickflow (2.7% forest *vis a vis* 17% pasture). A reduction in macroporosity beneath the pasture when compared with the forest, and a corresponding decrease in $K_{fs}$ in the surface pasture soil, were the causal factors (de Moraes et al., 2006). Similar conclusions from a 3.9 ha basin in Rondonia which drained a cattle pasture were reported by Biggs et al. (2006). They noted quickflow was 16% of rainfall for a 10 rainstorm sample and ~50% of this quickflow resulted from *IOF*. Later Chaves et al. (2008) and Germer et al. (2010) reported on a combined hydrology–hydrochemistry study for respectively a forest (1.37 ha) and pasture (~20 years old, 0.73 ha) basin. These writers reported that overland flow (mostly *SOF*) dominated streamflow from the pasture in contrast to *SSF* in the forest supported by varying proportions of groundwater and soil water. Further evidence at larger scales in the Amazon basin that infer similar changes in the dominant stormflow pathway have also been presented (e.g., Costa et al., 2003; D'Almeida et al., 2007; Rodriguez et al., 2010).

Forest conversion, degradation and reforestation affect both infiltration and evapotranspiration, and there can be a trade-off between the two. These components are encapsulated in the *'infiltration trade-off'* hypothesis of Bruijnzeel (1989, 2004). In the context of this study, this hypothesis suggests that the ability of a degraded forest to allow sufficient infiltration (and thus groundwater recharge via vertical percolation) in the wet-season maybe impaired to such an extent, that the short and long-term effects on delayed flow after storms as well as on dry season flow would be detrimental, even after accounting for 'gains' from reduced evapotranspiration. Further such reductions in infiltration have the ability to change the dominant stormflow pathways (Chappell et al., 2007) on hillslopes from subsurface stormflow (*SSF*) to infiltration-excess overland flow (*IOF*). Under certain conditions and at 'local' scales, there is now emerging evidence in support of this hypothesis when concerning these changes in the storm runoff generation component.

Through the use of a *Comparative Catchment* approach (Blackie and Robinson, 2007), this work will present rainfall–streamflow data from 11 basins (⩽45 ha) in the monsoonal tropics to test hypotheses from an earlier survey of field, saturated hydraulic conductivity, $K_{fs}$ in the Uttar Kannada district (Karnataka State) of the Western Ghats of India (Bonell et al., 2010). The locations of the experimental basins were guided by the landscape groupings of Gunnell and Radhakrishna (2001). Consequently three of the basins were located on the Coastal block and the remainder in the higher interior known as the Up-Ghat block or Malnaad. The rainfall–streamflow data analysed in this work was collected over a 2–3 year period (2003–2005) at a daily time resolution which was supplemented by 36 min data in the case of the Coastal basins.

As a result of degradation of forests over multi-decadal to century time scales, the land cover is complex in Uttar Kannada in common with other parts of the Western Ghats (Menon and Bawa, 1998; Seen et al., 2010). Patches of remnant natural forest, which are less disturbed and less used by people are at one end of the disturbance gradient and whilst at the other end, are a heterogeneous category of disturbed and heavily used forest (known as degraded forest). In addition a mix of State Government and community-based forestation programmes have been implemented for more than two decades within degraded forests and severely degraded, former forest-covered land (Pomeroy et al., 2003; Ramachandra et al., 2004). Consequently the Western Ghats (Karnataka State) provides a basis for evaluating land cover (LC) change impacts on streamflow hydrology at contrasting time scales linked with (i) forest land use and degradation, (ii) forestation over previously degraded land, relative to less used native forest and thus can address the hydrological knowledge gaps connected with these two scenarios (Ilstedt et al., 2007; Malmer et al., 2010). The impacts on the storm runoff hydrology of three of the more common land cover types namely, less disturbed natural–tropical evergreen Forest (NF), heavily impacted, degraded forest (DF) and former degraded land that has undergone 'forestation' (Scott et al., 2004) by way of *Acacia auriculiformis* plantations (AC) will be evaluated. The DF represents severely degraded, former evergreen forest, which has been converted floristically and architecturally into an open tree savanna.

### 1.1. Previous work relevant to the current study

Bonell et al. (2010) had previously provided $K_{fs}$ data for five LCs (natural forests, degraded forests, acacia and teak plantations) and three soil groups, and linked such data with rainfall characteristics (IDF, intensity–duration–frequency). For extreme rainfalls with return periods of 1 in 1 year upwards, these writers inferred that *IOF* was a more dominant stormflow pathway on hillslopes than previously thought when concerning many of the land covers and for many of the return periods of rainfall. Significantly such an inference included some (but not all) of the less disturbed natural forests. Otherwise it was suggested that subsurface stormflow (*SSF*), supplemented by saturation overland flow (*SOF*), was the most prevalent.

One of the few other experimental basin studies previously undertaken in the Western Ghats was by Putty and Prasad (2000a), and later summarised in Putty (2006), based on first order basins (up to 8 ha in area) which were located south of Uttar Kannada within the Dakshina–Kannada district (near Talakaveri, annual rainfall ~6750 mm). Some of the conclusions of Bonell et al. (2010) aligned with the descriptions of Putty and Prasad (2000a). The latter, had noted the occurrence of *IOF* in the multi-decadal impacted, Kannike basin (2.8 ha) of mixed grassland and forestation where final soil infiltrability (Hillel, 1980) could be as low as 6 mm $h^{-1}$. However such *IOF* was supplemented *SOF* from riparian areas adjoining the stream (the Dunne mechanism, Dunne and Black, 1970) and more extensively on slopes, by an additional process termed *pipeflow overland flow, POF* (Putty and Prasad, 2000a). For the less disturbed, natural forest basin (8 ha), Putty and Prasad (2000a) noted that *SOF* is a significant contributor to stream discharge only during short duration events of higher rain intensity (~10–15 mm $h^{-1}$) and pipeflow is the major mechanism generating streamflow for the predominantly low rain intensity-longer storm durations. However these studies did not have detailed $K_{fs}$ or stream hydrograph analyses and these aspects will be addressed in this study.

In the absence of detailed hillslope hydrology studies (a typical situation in most of the humid tropics), the work will analyze the rainfall–streamflow data using up to four analytical methods to assess if there is some coherence across the various interpretations of the results. These analyses will concurrently address the following questions:

1. What are the impacts of the three land covers on the stream discharge hydrograph components, *viz,* total flow, quickflow and delayed flow?
2. What *dominant* stormflow pathways can be inferred from the storm hydrograph characteristics and is there any agreement with the stormflow pathways, as suggested from the earlier $K_{fs}$ survey linked with rain IDF (intensity–duration–frequency) (Bonell et al., 2010)?
3. What is the impact of forestation on the recovery of the rain–streamflow responses towards those observed under the less disturbed, natural forest?

## 2. Description of study area

### 2.1. Geology, landforms, soils and soil hydrology

The locations of the instrumented catchments are shown in Fig. 1. The two sets of sites are located in two distinct landforms: the Coastal plain and adjoining slopes and hilly Up-Ghat or Malnaad region. The geology is mainly Archaen-Proterozoic-Dharwad schist and granitic gneissic, meta-volcanics and some recent sediment in the coastal belt. Greywackes with lateritic caps are prevalent in a cross-section from the Western slopes to the Malnaad (Geological Survey of India, 1981).

Many of the upper geological sequences of this region are lateritised due to their exposure to suitable climatic conditions over a prolonged period. Their thickness ranges from a few cm to as much as 60 m in depth (Geological Survey of India, 2006). Fig. 16b in Bourgeon (1989) provided a simplified latitudinal cross-section of the geology and location of laterite from the coast through to the Malnaad (incorporating Siddapur and Sirsi, Bonell et al., 2010). This cross-section is in proximity to the latitude where the study basins are located.

In the escarpment of the Ghats, the catchments in the Coastal zone are dominated by rocks of the Archean complex. The associated soils are dominated by 1:1 clays associated with iron and aluminium oxy hydroxides. We used the Indian soil classification system (NBSSLUP, 1993; Shivaprasad et al., 1998; Bonell et al., 2010) and these Coastal basin soils belong to the Laterite soil group. Under the FAO system these soils are mixture of Eutric Nitosols and Acrisols (FAO-UNESCO, 1974; FAO, 1998) and would be classified under the USDA system as Alfisols, Ultisols and Oxisols (Soil Survey Staff, 1975, 1999) (Table 1). A separate French survey of the Western Ghats undertaken by Bourgeon (1989) described the soils as being "Lithosols" and "Ferrallitic". A soil description of the evergreen forest within ~5 km of the Coastal basins is provided in Table 2 (Bourgeon, 1989).

The catchments in the Malnaad are on the back slopes of the Western Ghats, deeply dissected, and the geology is dominated by Greywackes. The associated soils have similar clay minerals as above. They are classified as Red and Laterite (Shivaprasad et al., 1998), with similar equivalent classifications of FAO to those soils of the Coastal basins. When concerning the USDA, they are a mixture of Alfisols, Inceptisols and Oxisols (Shivaprasad et al., 1998; Table 1).

The soils in both the Coastal and Malnaad basins are deeply weathered similar to the description of Putty and Prasad (2000a). In the absence of any deep drilling in the basins, however no detailed soil descriptions down to bed rock exist. Exposures in hills and stream banks do suggest that soils extend well beyond 2 m in depth (Fig. 2). Further no detailed mapping of soil pipe occurrence was undertaken. However there was evidence of vertical macropore flow in soil exposures and an example is shown in Fig. 2.

### 2.2. Hydrogeology

Detailed hydrogeological surveys have not been done in the experimental basins. Even across the study area landscape such information is relatively sparse based on two phases of exploration with boreholes up 200 m depth (Central Groundwater Board, CGWB, 2008). The main aquifers in the study area are the weathered and fractured zones of metavolcanics, metasedimentaries, granites and gneisses, laterites, along with the alluvial patches found along the major stream courses. Significantly there is no primary porosity in the hard rocks. It is the secondary structures like joints, fissures and faults present in these formations up to ~185 m below ground level (mbgl) which act as a porous media with an effective porosity of 1–3% and contain groundwater. The transmissivity of aquifer material in general range from 2.09 to 24.41 $m^2$ $day^{-1}$ (CGWB, 2008). At depths $\leqslant$30 mbgl unconfined, groundwater dominates but there is a tendency towards a more confined status at greater depths due to the complexity of the geological formations and associated fracture zones. Spot surveys undertaken in May (pre-monsoon) and November (post-monsoon) 2006 and using a network of 30 of the national hydrograph stations, showed that pre-monsoon water levels between 5 and 10 mbgl were typical over large parts of Uttar Kannada. In the post-monsoon, the

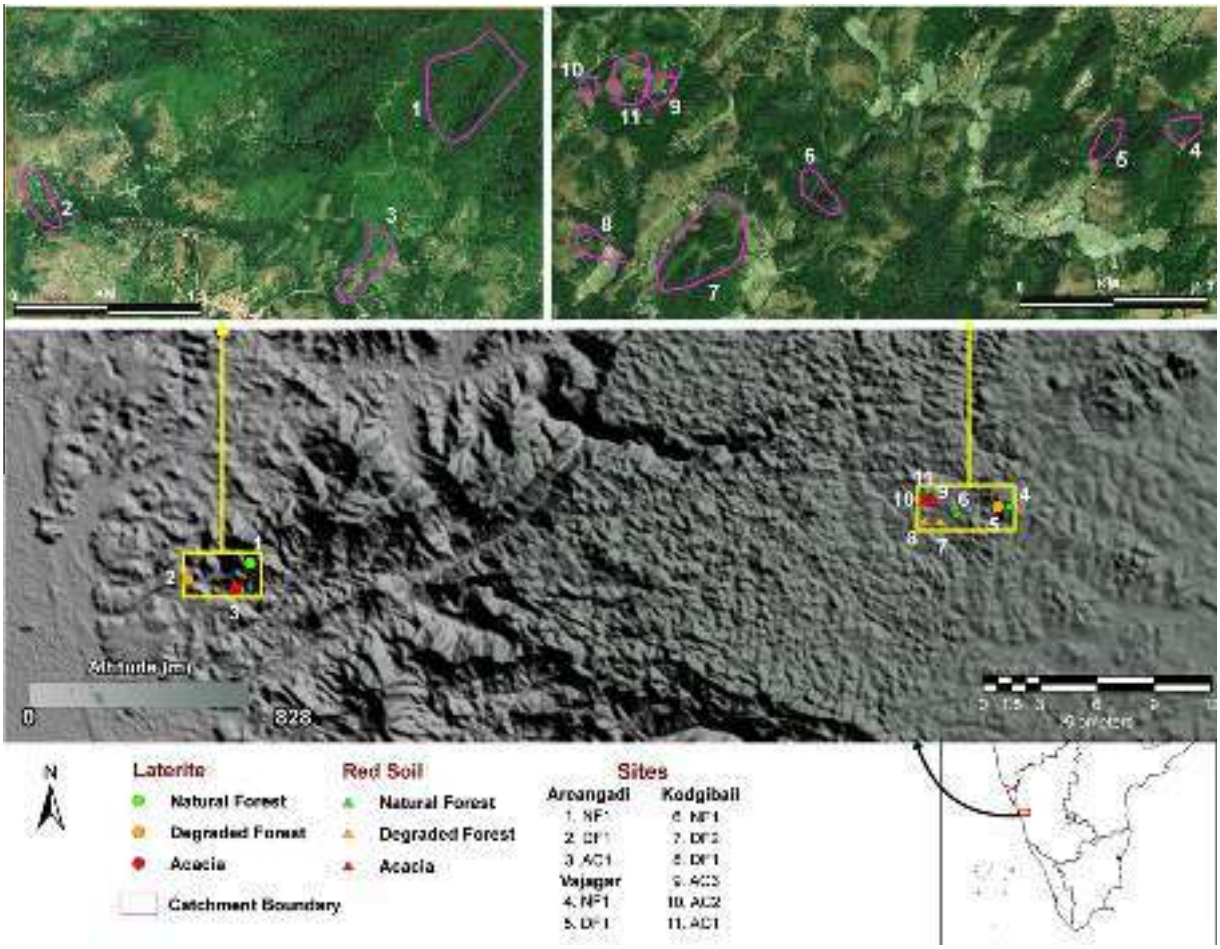


**Fig. 1.** The location, soil types and land covers of the research basins in the Western Ghats, Uttara Kannada District of Karnataka State.

prevailing depths within the Coastal and Malnaad areas were respectively 2–5 and 5–10 mbgl (CGWB, 2008).

### 2.3. Climate

The climate is classified under Koppen as 'tropical wet and dry'. Rainfall is monsoonal and unimodal (June to September). The annual rainfall varies from 3979 mm in the Coastal zone to 3275 mm in the Malnaad (1950–2000 average, derived from Hijmans et al., 2005). Long-term annual reference potential evapotranspiration (PET) is 1482 mm for the Coastal basins and 1527 mm in the Malnaad basins (Hijmans et al., 2005).

On a monthly basis there is marked reduction in PET following the onset of the monsoon in June until its termination from October onwards (Hijmans et al., 2005). This 'dip' in PET is due to persistent high humidity and cloudiness with frequent rainfalls (Bourgeon, 1989; Hijmans et al., 2005).

The dry season lasts from 5 to 6 months and so during this time PET > rainfall. Annual mean temperatures range from 26.4 °C in the Coastal plains and slopes to 24.5 °C in the Malnaad (Hijmans et al., 2005). Annual average relative humidity is ~72.3% in the coastal basins and 70% on the Malnaad slopes ((1960–1990), New et al., 1999).

Maximum rainfall intensities for a duration of 15mins across the study area range from 50 mm $h^{-1}$ (1 in 1 year) to 130 mm $h^{-1}$(1 in 50 year) (Bonell et al., 2010). Overall these short-term rainfall intensities are comparatively low by global standards for the humid tropics (Bonell et al., 2004). In a previous Western Ghats study, despite the high annual rainfalls and the long duration of storms, hourly and 15 min rain intensities >40mm $h^{-1}$ contributed to not more than 15% of total rain and last a mere 2–5% of the total duration of events (Putty, 2006; Putty and Prasad, 2000a,b; Putty et al., 2000).

### 2.4. Aspects of vegetation and land covers

The vegetation of the study area is highly diverse in response to the equally complex geology, geomorphology and climate of the Western Ghats. Based on criteria such as physiognomy, phenology and floristic composition, the vegetation of the study area is classified principally as evergreen and semi-evergreen which are two of the five major floristic types identified in the region (Pascal, 1982, 1984, 1986, 1988; Ramesh and Pascal, 1997; Ramesh and Swaminath, 1999). Within the framework of a highly fragmented land cover/land use system (Blanchart and Julka, 1997; Menon and Bawa, 1998; Pomeroy et al., 2003; Pontius and Pacheco, 2004; Seen et al., 2010), there are typically three principal stable patterns of land use and management, viz:

(i) Less disturbed, dense forest (referred to also as *Natural Forest*, *NF*, *or Forest*) which has resulted from a limited extraction regime, and is commonly associated with Reserve Forest patches.
(ii) Dominantly tree savannas (*Degraded Forest*, *DF*, *or Degraded*) that result from intense harvest of fuelwood, leaf and litter manure and grass, as well as intermittent fires (Rai, 2004;

**Table 1**
The physical characteristics of the experimental basins in the Up-ghat and Coastal regions.

| No. | Site | Type | Area (ha) | Land cover type and code | Average elevation (m) | Average slope (deg) | Mean annual rainfall (1988–1997) (mm) | Soil type as per Indian soil classification and USDA *soil survey staff (1999)*; [a]NBSSLUP (Shivaprasad et al., 1998) |
|---|---|---|---|---|---|---|---|---|
| *Coastal basins* | | | | | | | | |
| 1 | Areangadi | Natural Forest | 23 | NF1 | 255.03 | 17.16 | 3672 | Laterite, Clayey, kaolinitic, *Ultisol* (*Ustic Kandihumults*) |
| 2 | Areangadi | Degraded Forest | 7 | DF1 | 52.71 | 10.38 | 3793 | Laterite, Clayey, kaolinitic, *Ultisol* (*Ustic Kandihumults*) |
| 3 | Areangadi | Acacia | 7 | AC1 | 112.25 | 15.23 | 3793 | Laterite, Clayey-skeletal, kaolinitic, *Ultisol* (*Petroferric Haplustults*) |
| *Malnad (UP-Ghat)* | | | | | | | | |
| 4 | Vajgar | Natural Forest | 9 | NF1 | 618.09 | 7.51 | 2750 | Red, Fine, kaolinitic, *Alfisol* (*Kandic Paleustalfs*) |
| 5 | Vajgar | Degraded Forest | 10 | DF1 | 587.27 | 7.07 | 2750 | Laterite, Fine, kaolinitic, *Alfisol* (*Kandic Paleustalfs* |
| 6 | Kodgibail | Natural Forest | 6 | NF1 | 540.14 | 7.56 | 2750 | Red, Clayey-skeletal, kaolinitic, *Inceptisol* (*Ustoxic Dystropepts*) |
| 7 | Kodgibail | Degraded Forest1 | 9 | DF1 | 522.16 | 4.76 | 2948 | Red, Clayey-skeletal, kaolinitic, *Inceptisol* (*Ustoxic Dystropepts*) |
| 8 | Kodgibail | Degraded Forest2 | 45 | DF2 | 536.50 | 5.10 | 2948 | Red, Clayey-skeletal, kaolinitic, *Inceptisol* (*Ustoxic Dystropepts*) |
| 9 | Kodgibail | Acacia1 | 7 | AC1 | 538.00 | 5.51 | 2948 | Red, Clayey-skeletal, kaolinitic, *Inceptisol* (*Ustoxic Dystropepts*) |
| 10 | Kodgibail | Acacia3[b] | 6 | AC3 | 544.83 | 4.34 | 2948 | Red, Clayey-skeletal, kaolinitic, *Inceptisol* (*Ustoxic Dystropepts*) |
| 11 | Kodgibail | Acacia2 | 23 | AC2 | 544.10 | 3.36 | 2948 | Red, Clayey-skeletal, kaolinitic, *Oxiso l* (*Ustoxic Dystropepts*) |

[a] NBSSLUP – National Bureau of Soil Survey and Land Use Planning.
[b] Acacia3 is nested within Acacia2.

Priya et al., 2007). These tree savannas were previously occupied by mostly evergreen and semi-evergreen forest prior to severe disturbance over decadel to century time scales. The specie composition, tree density and basal area of this land cover however can be highly variable between first-order basins (see Table 3).

(iii) Exotic *Acacia auriculiformes* plantations planted since 1980 (*Acaicia*, *AC*) that are part of the 'forestation' programme of the Karnataka Forest Department (Rai, 1999). Typically these plantations have replaced grazing land, or highly degraded forest land, some of which had further degraded to become barren land. The initial survival of the AC plantings has been ensured through fencing and guarding. The ages of AC plantations in the study basins range from to 7 to 12 years (Table 3).

Historically, people would have used and occupied the more accessible sites, which are currently under degraded forests or are under restoration through establishment of tree plantations.

A description of the dominant vegetation types in the experimental basins are shown in Table 3. It should be noted that the Acacia plantations are not wholly monoculture but do incorporate a few other species.

### 2.5. Vegetation sampling and mapping exercise in the Malnaad

A vegetation sampling and mapping exercise was undertaken in selected Malnaad basins using 100 m × 20 m transects to enumerate tree species, tree girth, tree density and disturbance level (Table 3). Degraded forests still contained significant areas of dense tree vegetation. Further, pure grasslands in small patches exist and are dominated by *Themeda* sp. (Lele and Hegde, 1997). There was also significant difference in the species composition, tree density and basal area of different degraded basins, as well as between natural forests. However, both the NF basins clearly have the highest tree densities and basal areas compared to all other categories.

### 2.6. Tree root depths and surface $K_{fs}$ across the land covers

Examination of selected soil exposures indicated that roots extended well beyond 2 m depth under the Natural Forest. For the young Acacia plantations most roots were $\leqslant$1.5 m in depth and are known to be more densely concentrated between 0.3 and 1.0 m (Kallarackal and Somen, 2008). Depth of roots under the Degraded Forest were more varying, but mostly $\leqslant$0.6 m. depth due to the more extensive low herbaceous cover (dominated by grass species) in between the surviving trees.

Elsewhere Venkatesh et al. (2011) provided complementary evidence of the nature of rooting patterns. They observed that on the basis of soil moisture recessions most plant water use was confined to the upper soil layer ($\leqslant$0.5 m depth) in both the AC1 and DF1 Kodigibail basins (Table 1). This characteristic was attributed to the shallow rooting patterns in these two land covers. In contrast soil moisture recessions were evident throughout the profile down to 1.5 m depth in NF1 due to the greater depth of roots. This significant phase of moisture withdrawal occurred especially in the early stages of the post-monsoon season (Venkatesh et al., 2011), At such times, tree physiological activities take advantage of freely available, soil water combined with a more favourable meteorology that is, less cloudiness and a decrease in air humidity (Kallarackal and Somen, 2008).

The respective $K_{fs}$ for the surface soils were in the range 26.4–187.8 mm $h^{-1}$ for the natural forest compared to 26.8–61.0 mm $h^{-1}$ under the *A. auriculiformes* plantations. The lowest surface $K_{fs}$ occurred under the degraded forests being in the range of only 7.3–24.4 mm $h^{1}$ (Bonell et al., 2010). Further details of the vertical changes in $K_{fs}$ with depth are described in detail in Bonell et al. (2010).

### 2.7. The experimental basins

Additional details of the experimental basins (as shown in Fig. 1) are provided in Tables 1 and 3. The complex mosaic of

**Table 2**
Soil description of the evergreen forest in proximity to the Coastal basins (Bourgeon, 1989).

| Village/location | Tulsani |
|---|---|
| Coordinates | Long: 74°33′25″E; Lat: 14°20′35″N |
| Altitude | 110 m |
| Vegetation | Evergreen forest |
| Geology | Dharwar schists |
| Landscape unit | 3, Ghats |
| Classification | Soil Taxonomy: *Indian* (*NBSSLUP*): Laterite; *USDA*: (Oxic) Eutropept; *French Classification*: Ferrallitic soil, weakly desaturated in B, rejuvenated, reworked. |
| From 0 to 10 cm | Slightly moist. Dark brown (7.5YR 4/4) moist. Humus. No effervescence. 50% of coarse elements, cobbles and gravels of highly weathered schist. Moderate crumb structure, 5 mm size. Coherent, plastic, very friable. Clay with medium sand. Very porous. Plentiful roots. Smooth transition in 2 cm |
| From 10 to 40 cm | Moist. Yellowish red (5 YR 5/6) moist. Humus. No effervescence. 80% of coarse elements, cobbles and gravels of highly weathered schist. Moderate subangular blocky structure, 8 mm size. Coherent, plastic, very friable. Clay with medium sand. Very porous. Plentiful roots. Smooth transition in 10 cm |
| From 40 to 120 cm and more | Moist. Yellowish red (5 YR 5/8) moist. Non-organic. No effervescence. 80% of coarse elements, stones, cobbles and gravels of highly weathered schist. Weak subangular blocky structure, 8 mm size. Coherent, plastic, very friable. Clay loam with fine sand. Very porous. Many roots |

**Fig. 2.** A deeply weathered Red soil profile which is located near the Malnaad (Kodigibail) basins. The depth of the soil profile is in excess of 2 m depth and preferential wetting is also evident. Weathered rock is also visible in the right bottom corner.

land-cover and land-use made it difficult to identify homogeneous catchments of a sufficient area to be sure that inter-basin transfer of groundwater is potentially not significant, and the best possible catchments for a comparative study are less than 50 ha. In many basins the corresponding areas are $\leqslant$10 ha as a result. On the other hand, these basin areas (Table 1) are of the same order of magnitude, or even one to two orders larger, when compared to other studies elsewhere (e.g., Chandler and Walter, 1998; Putty and Prasad, 2000a; Zhou et al., 2001; de Moraes et al., 2006; Chaves et al., 2008). Further because of their limited size, most basins did not have perennial flow. Any shortcomings of using basins of such small area will be later considered.

Despite the higher elevations in the Malnaad (basin numbers 4–11, Table 1), the mean slope angles are low ($\leqslant$7.5°). It is also pertinent that the Vajgar basins 4 and 5 have different soils and higher elvations when compared to basins 6–11. By contrast the Coastal basins (Areangadi, basin numbers 1–3, Table 1) have higher mean slopes varying between ~10–17°. A riparian zone is more evident within the Coastal forest basin from the mid-stream profile towards the gauging station (NF1, Site 1). Whereas this feature is absent in the DF1 (Site 2) and AC1 (Site 3) and the convex hill slopes border the stream channel directly. Overall the Coastal forested catchment is characterised by steeper terrain, especially in upper parts of the basin, when compared to the other land-covers at Areangadi (Table 1).

## 3. Field methods and data

### 3.1. Rain–runoff instrumentation

Stream discharge in each catchment was measured using either weirs or stage-velocity-discharge methods. In addition all catchments in the Coastal zone (Areangadi) were instrumented with stage level, mechanical water-level recorders and an automatic rain gauge. As these three basins were spatially close together, the same data from the one automatic rain gauge was used. The latter was positioned so that it was <2 km from the boundaries of all these Coastal basins. In the Malnaad group, rainfall and streamflow data were collected daily supported by additional manual measurements of stream stage taken up to four times a day.

In summary, daily rainfall and stream discharge data for the years 2003, 2004 and 2005 are available for the Kodigibail and Vajagar catchments in the Up-Ghat (Malnaad), and for 2004–2005 for the three Coastal basins (Table 1). In addition for part of the summer monsoon of 2005 (16 June–26 July), 36 min (0.6 h) data was available for rainfall–streamflow for selected storms in the three Coastal catchments. Such information enabled us to monitor temporal changes in the rain–streamflow response following the onset of the monsoon until maximum basin wetness was attained. However there were equipment malfunctions within at least one of these basins during some of the rain events. This reduced the number of storms where streamflow was measured concurrently across all basins during a rain event to allow an inter-comparison using time series methods. On the other hand, other analytical methods (discussed below) could be undertaken on all events. Further these equipment problems caused us to extend the rain–streamflow monitoring in the Natural Forest basin until 30 September 2005.

### 3.2. Permeability

In the three Coastal zone catchments and in a representative sub-set of basins in the Malnaad zone [i.e., Kodigibail basin nos. 6 (NF1), 7 (DF1), 9 (AC1); Vajagar basin nos. 4 (NF1) and 5 (AC1) in Table 1], field saturated hydraulic conductivity, $K_{fs}$ was measured up to a soil depth of 1.5 m. For the surface and 0.1 m depth, the disc permeameter was used for the determination of soil $K_{fs}$ (Perroux and White, 1988; McKenzie et al., 2002). A Guelph constant head well permeameter, CHWP (Mackenzie, 2002) measured subsoil $K_{fs}$ at depth intervals 0.45–0.60 m, 0.60–0.90 m, 0.9–1.20 m and 1.20–1.50 m. When concerning the presentation of the results, the latter will be abbreviated from here-on using the lower depths, *viz*, 0.6, 0.9, 1.2, 1.5 m.

**Table 3**
Vegetation characteristics of the instrumented basins.

| No. | Site | Type | Land cover type and code | Vegetation type and dominant tree species | Average tree density (per ha) | Average basal area ($m^2$ $ha^{-1}$) |
|---|---|---|---|---|---|---|
| *Coastal basins* | | | | | | |
| | | | | **Low elevation Evergreen and semi-evergreen forest** | | |
| 1 | Areangadi | Natural Forest | NF1 | *Dipterocarpus indicus–Diospyros candolleana–Diospyros oocarpa* type | N/M | N/M |
| 2 | Areangadi | Degraded Forest | DF1 | *Alseodaphne semicarpifolia*, *Lophopetalum wightianum*, *Ixora barcheata*, *Aporosa lindleyana*, *Hopea wightiana*, *Terminalia panniculata*, *and Terminalia alata* | N/M | N/M |
| 3 | Areangadi | Acacia | AC1 | *Anacardium occidentale*, *Garcinia indica*, *Syzigium cumini*, *Buchanania lanzan*, *Holigarna aronottiana*, *Alseodaphne semicarpifolia* | N/M | N/M |
| *Malnad (UP-GHAT)* | | | | | | |
| | | | | **Medium elevation Evergreen and semi-evergreen forests** | | |
| 4 | Vajgar | Natural Forest | NF1 | *Persea macarantha–Diospyros* spp.–*Holigarna* type | 485 | 3536 |
| | | | | *Lophopetalum wightianum*, *Alseodaphne semicarpifolia*, *Gymnonthra conariea*, *Sagereaea listari*, *Holigarna aronottiana* | | |
| 5 | Vajgar | Degraded Forest | DF1 | *Alseodaphne semicarpifolia*, *Lophopetalum wightianum*, *Ixora barcheata*, *Aporosa lindleyana* | 615 | 1896 |
| | | | | **Medium elevation Evergreen and semi-evergreen climax forests** | | |
| 6 | Kodigibail | Natural Forest | NF1 | *Persea macarantha–Diospyros* spp.–*Holigarna* type | 615 | 2632 |
| | | | | *Gymnonthra conariea*, *Sagereaea listari*, *Ixora barcheata*, *Holigarna aronottiana* | | |
| 7 | Kodigibail | Degraded Forest1 | DF1 | *Alseodaphne semicarpifolia*, *Lophopetalum wightianum*, *Ixora barcheata*, *Aporosa lindleyana*, *Hopea wightiana*, *Terminalia panniculata*, *and Terminalia alata* | 352 (DF1) | 2099 (DF1) |
| | | Degraded Forest2 | DF2 | | N/M (DF2) | N/M (DF2) |
| 8 | Kodigibail | Acacia1 Acacia3 | AC1 AC3 | *Acacia auriculiformis*, *Anacardium occidentale*, *Garcinia indica*, *Syzigium cumini*, *Buchanania lanzan*, *Holigarna aronottiana*, *Alseodaphne semicarpifolia* | AC1-132 | AC1-1068 |
| 9 | Kodigibail | Acacia2 | AC2 | *Acacia auriculiformis*, *Buchanania lanzan*, *Holigarna aronottiana*, *Alseodaphne semicarpifolia*, *Syzigium cumini* | 345 | 2053 |

*Notes:* (i) The above DF and AC sites originally belonged to evergreen and semi-evergreen forest type (Pascal, 1984, 1986, 1988). The vegetation cover later changed with the extent of degradation. There is no Leaf Area Index information. (ii) For selected Malnad basins, supplementary information on vegetation composition was obtained from a field survey in addition to taking tree density and basal area measurements. (iii) N/M – Not measured.

## 4. Analytical methods

### 4.1. Analysis of the rain–streamflow data

The rain–streamflow data were analysed using four methods, namely:

#### 4.1.1. Double mass curves (cumulative rainfall ($P_{cum}$) and cumulative stream discharge ($Q_{cum}$) plots)

A double mass curve is a plot of cumulative values of one variable against the cumulative of another quantity during the same time period (Searcy and Hardison, 1960). This concerned an inter-basin comparison of cumulative rainfall ($P_{cum}$) and stream discharge ($Q_{cum}$) plots based on seasonal records at a daily time scale for both the Up-Ghat (Malnaad) and Coastal basins

### 4.2. Outputs from HYDSTRA – Coastal basins

When concerning the continuously monitored Coastal basins, HYDSTRA (2007, previously HYDSYS, 1991, now known as *Hydstra/Times Series Data Management*, 2007, http://www.kisters.com.au) was initially used as a quality control tool to screen the basic rainfall and streamflow data for errors. Subsequently for specific events and using HYDSTRA, the following outputs were produced, *viz*, total rainfall, $P$; maximum rainfall depths, $P_i$, over selected time increments, $i$; volumes of total streamflow, $Q$; quickflow, $Q_F$ and baseflow, $Q_B$ by event and the associated streamflow response ratios $Q_F/P$ (*quickflow response ratio*), $Q_F/Q$ and $Q_B/Q$. The stream hydrograph separation was undertaken following the approach of Moore et al. (1986) whereby a filtering algorithm is applied to hydrographs and separates the flow into "quick", "base" (or "delayed") flows based on certain objective criteria. Despite such filter approaches not being physically based, they are considered better (see review by Furey and Gupta (2001)) than the earlier graphical approaches (e.g. Hewlett and Hibbert, 1967). The streamflow response ratios were then compared across land covers using box plots.

#### 4.2.1. Linear model/ANOVA

The various measures of hydrologic response derived from individual rainfall–streamflow events (% quickflow of total flow, % delayed flow of total flow, % quickflow of total rain, % delayed flow of total rain) within the Coastal basins, were compared across basins using linear model/ANOVA in R Statistical software (www.r-project.org). Mean values and standard errors were generated for each variable for each of the three land-cover types. Subsequently Tukey multiple comparisons of means (HSD, Honestly Significant Differences) were undertaken and 95% family-wise confidence levels generated for the differences.

### 4.3. Time-series lag analyses – Coastal basins

We used a time series methodology previously developed and applied for an Australian rainforest basin (Bonell et al., 1979, 1981) to compare differences in time lags between rainfall and the stream hydrograph by event and between land-cover. The varying time lags which are evident in the rainfall–stream hydrograph peaks within and between basins (and associated different land covers) suggest that possibly there are different dominant stormflow pathways.

The most general rainfall–streamflow (simulation) model, as used by Bonell et al. (1979) is of the form:

$$Y_t = \alpha + \beta_0 X_t + \beta_1 X_{t-1} + \ldots \beta_i X_{t-i} + \varepsilon_t \quad (1)$$

where $X_t$ is the deterministic input series $\log_{10}$(rainfall + 1) and $Y_t$ is $\log_{10}$(stream discharge + 1) at time $t$. The $\varepsilon_t$ is the error, which can have an explicit auto-correlated error structure such as an AR1 of the form:

$\varepsilon_t = \gamma\varepsilon_{t-1} + \eta_t$ i.e., $\varepsilon_t - \gamma\varepsilon_{t-1} = \eta_t$.

Or following Bonell et al. (1981) we further extended Eq. (1)) as a prediction (or forecasting) model in the form:

$$Y_t = a + \sum b_k Y_{t-k} + \sum c_k X_{t-k} + \varepsilon_t \quad (2)$$

where $X_t$ is the deterministic input series (rainfall) and $Y_t$ is stream discharge at time $t$ and $Y_{t-k}$ and $X_{t-k}$ are the rainfall and stream discharge at time $t - k$. Autocorrelation in the error term, $\varepsilon_t$ is similarly treated as described above (under Eq. (1)).

The log transform attempts to achieve normality and homoscedasticity (i.e., homogeneity of variance) of the residuals.

#### 4.3.1. The physical interpretation of the lagged $Y_t$ and $X_t$ variables

The lagged $X_{t-k}$ represent the "direct effect" of rainfall on the response variable, i.e. the stream variable, in the same way as understood for the simulation model in Eq. (1)) (Bonell et al., 1981).

The physical interpretation for the inclusion of any lagged $Y_{t-k}$ in the prediction model (linked with Eq. (2)) reflects the "cumulative effect" of rainfall throughout the storm event. Such cumulative effects are in the context of the requirement for an available soil water store to be filled to capacity in the upper soil layers before any *SOF* can occur on the higher hillslope transects; *and/or* to cause shallow water tables within the lower areas (e.g. riparian zones) to emerge at the surface and thus trigger *SOF* (the Dunne mechanism, Dunne and Black, 1970).

#### 4.3.2. Model selection procedure

We used for model selection, a rigorous information – theoretic approach that estimates likelihood (the probability of the data given by different models) as well as penalizes for model complexity or number of covariates used (Burnham and Anderson, 1998; Johnson and Omland, 2004; Hobbs and Hilborn, 2006). Models were compared and selected using the Bayesian Information Criteria (BIC). Along with AIC (Akaike Information Criteria), the use of the BIC is now increasingly favoured over the traditional regression measures such as $R^2$ and $p$-values, especially in bio-physical applications (Kashyap, 1977; Schwarz, 1978; Johnson, 1999; Hobbs and Hilborn, 2006). We used the BIC values, $p$-values and hydrologic logic to identify and select the best models from amongst the candidate models.

It is well known that when lagged endogeneous variables are included in the model that OLS estimation should not be used except when autocorrelation in the residuals is not significantly different from zero (Davidson and MacKinnon, 1993; White, 2001; Young, 2011). With our inclusion of the AR1 error adjustment, as outlined above, addresses such concerns. Otherwise approaches such as the Standard Instrumental Variable estimation (Young, 2011), or generalised least squares with auto-correlated error structure (Ebbes, 2007), are recommended.

The final models were therefore fitted using the GLS function in R (Pinheiro and Bates, 2000). These functions fit a linear model using generalised least squares (not least squares) and maximum likelihood estimation of coefficients. The errors are allowed to be correlated if needed with an explicit autoregressive structure as described earlier and parameter estimates are done using log-likelihood approaches.

The choice of how many and which rainfall-lag covariates to include was determined by a parsimonious, statistically and hydrologically informed model selection process. This involved looking at the cross-correlation plot between discharge and the rainfall, and the use of BIC criteria to select a subset amongst rainfall lag

and flow lag covariates. The final models were those with positive rainfall lag covariates and both positive and negative flow covariates. However, in the interests of parsimony and with no loss of fit, we retained negative flow covariates only if there were significant (based on *p*-values) corresponding rainfall lag variables at that lag or earlier with a positive coefficient. This pruning was done after ensuring that the signs of the important rainfall terms did not change when the model was simplified and that there was no major loss of goodness of fit.

The goal was to achieve the simplest regression model which could enable us to assess the relative influence of rainfall lag at various time-steps on streamflow response. Once the final model was reached, we checked for autocorrelation in the residuals. If needed autocorrelation was explicitly addressed by including an autocorrelated error structure, as outlined above, as part of the model definition. Comparisons between models with and without autocorrelation were done using likelihood-based diagnostics. Although there are autoregressive and moving average approaches depending on the structure, we chose the first order autoregresive as the most parsimonious choice consistent with the error structure.

We recognize that interpretation of multiple regression coefficients will be difficult when lagged variables are included and we have used the regression models to confirm the interpretation of the cross-correlations lags rather than emphasis on the coefficients. In summary, the steps taken in the work was first to produce cross-correlations between rain and streamflow by storm event for the each basin/land cover type for the detection of time lags followed by regression analyses described above to further strengthen inference on rainfall–streamflow dynamics. Subsequently a brief comparison between the simulation model (based on Eq. (1)) and the prediction model (Eq. (2)) results will be made.

#### 4.3.3. Comparisons between the Coastal basins and NE Australia

The environmental circumstances in the present study are very different from the NE Queensland, Australia work in terms of the synoptic climatology and rainfall characteristics. On the other hand, both the Australian and the current study basins share a seasonal concentration of rainfall and thus have in common near saturated soil profiles at such times (Bonell et al., 1981, 1998; Venkatesh et al., 2011). In addition, the permeability (depth) profiles (discussed below) have some similarities between the two geographic areas, especially the Forest (NF). These suit the application of the time series model as well as being a comparative study.

## 5. Results

### 5.1. The soil hydraulic conductivity profiles

The $K_{fs}$ (depth) profiles as shown in Fig. 3 follow the description previously outlined by Bonell et al. (2010). The Forest profiles are typical of the 'Acrisol-type' (Elsenbeer, 2001; Chappell et al., 2007) which encourages a subsurface stormflow, *SSF* dominant pathway (supplemented by saturation excess overland flow, *SOF*) on hillsides (Elsenbeer, 2001; Chappell et al., 2007). Further there is clear reduction in $K_{fs}$ at the surface when concerning the Degraded Forest and the Acacia plantations. Such a reduction in $K_{fs}$ is confined to the upper 0.2 m layer of soil in line with the description for other sites in the study area (Bonell et al., 2010) as well as findings elsewhere (Hamza and Anderson, 2005; Zimmermann et al., 2006; Zimmermann and Elsenbeer, 2008). The occurrence of *IOF* is possible at such sites. The same effect of land-cover on $K_{fs}$ is consistently observed even in the Malnaad basins (Fig. 3b and c) in spite of differences in soil type.

With the possible exception of one basin each at respectively Kodigibail (DF1) and Vajagar (DF1), the subsoil $K_{fs}$ overall remains comparatively high and in excess of 10 mm $h^{-1}$ across the remaining sites (Fig. 3). The high subsoil $K_{fs}$ must contribute to the rapid translation of the wetting fronts of soil moisture (Venkatesh et al., 2011). It should be noted that the different soil groups are represented across land-covers in Vajagar (Table 1) whereby the Forest and the Degraded Forest are underlain respectively by Laterite and Red. But despite the Red soil group being the more inherently permeable, the impact of long-term forest degradation has reduced the surface $K_{fs}$ (Bonell et al., 2010).

### 5.2. The double mass curves ($P_{cum}$, $Q_{cum}$)

#### 5.2.1. The Kodigibail and Vajagar Up-Ghat basins

The double mass curves are initially shown for the Up-Ghat (NF1, DF1, DF2, AC1, AC2, AC3) basins at Kodigibail (Fig. 4a–c). Despite the varying period of record (Fig. 4), the different basin areas and the variation in total rainfall (i.e. 2252–3663.4 mm), the rank order in percentage (%) of rainfall emerging as streamflow between the basins remains consistent. The lowest streamflow occurs from the Forest and the highest from the Degraded Forest. The Acacia Plantations occupy an intermediate position. For 2004 and 2005 when higher rainfalls occurred, the proportion of streamflow increases across all land covers but is particularly higher in the Acacia plantations, i.e. AC 1 to 3.

The above trends in streamflow production continues with the Vajagar NF1 and DF1 basins (Fig. 5a and b). The Forest covered basin consistently supplies lower streamflow when compared to the Degraded Forest, and these circumstances occur despite differences in soil type and $K_{fs}$ between these basins (Table 1, Bonell et al., 2010).

#### 5.2.2. The Coastal basins (Areangadi)

There is a subtle difference between the Coastal Basins and the Up-Ghat basins. Towards the end of the summer monsoon, stream discharge in the Forest continues whereas flow in both the Acacia and Degraded Forest basins has terminated (Fig. 6a and b). The larger basin area of the Forest is likely be one of the reasons why such a continuation of stream discharge is favoured (Table 1). Thus there is a change in the rank order in percentage (%) of rainfall emerging as streamflow, i.e. DF > NF > AC. However for the bulk of the rainy season, the rank order of streamflow is DF > AC > NF and this is consistent with the Up-Ghat basins.

#### 5.2.3. Comparison between the Up-Ghat and Coastal basins

Overall the double mass curves indicate that there is remarkable consistency in the rank order of basin streamflow yields despite varying monsoon rainfall totals and basin areas. Further the percentages (%) of rainfall emerging as streamflow were similar between years except for 2005 in the Up-Ghat basins. For the latter, all land covers had higher streamflow coefficients in response to the higher summer monsoon rainfall total of 3663.4 mm.

Subsequently the basins identified with the three respective land covers were grouped together across the two geomorphological zones. Overall NF converted a mean of $28.4 \pm 6.41_{stdev\%}$ of rainfall into total streamflow in comparison to $32.7\_ \pm 6.97_{stdev\%}$ in AC and $45.3 \pm 9.61_{stdev\%}$ in DF.

### 5.3. Hydrologic dynamics across land-covers within the Coastal Basins

Focus is now confined to the Coastal basins where continuous records are available to apply HYDSTRA for specific rain events and the application of the ANOVA to ascertain any significant differences in selected HYDSTRA variables. Later for three rain events,

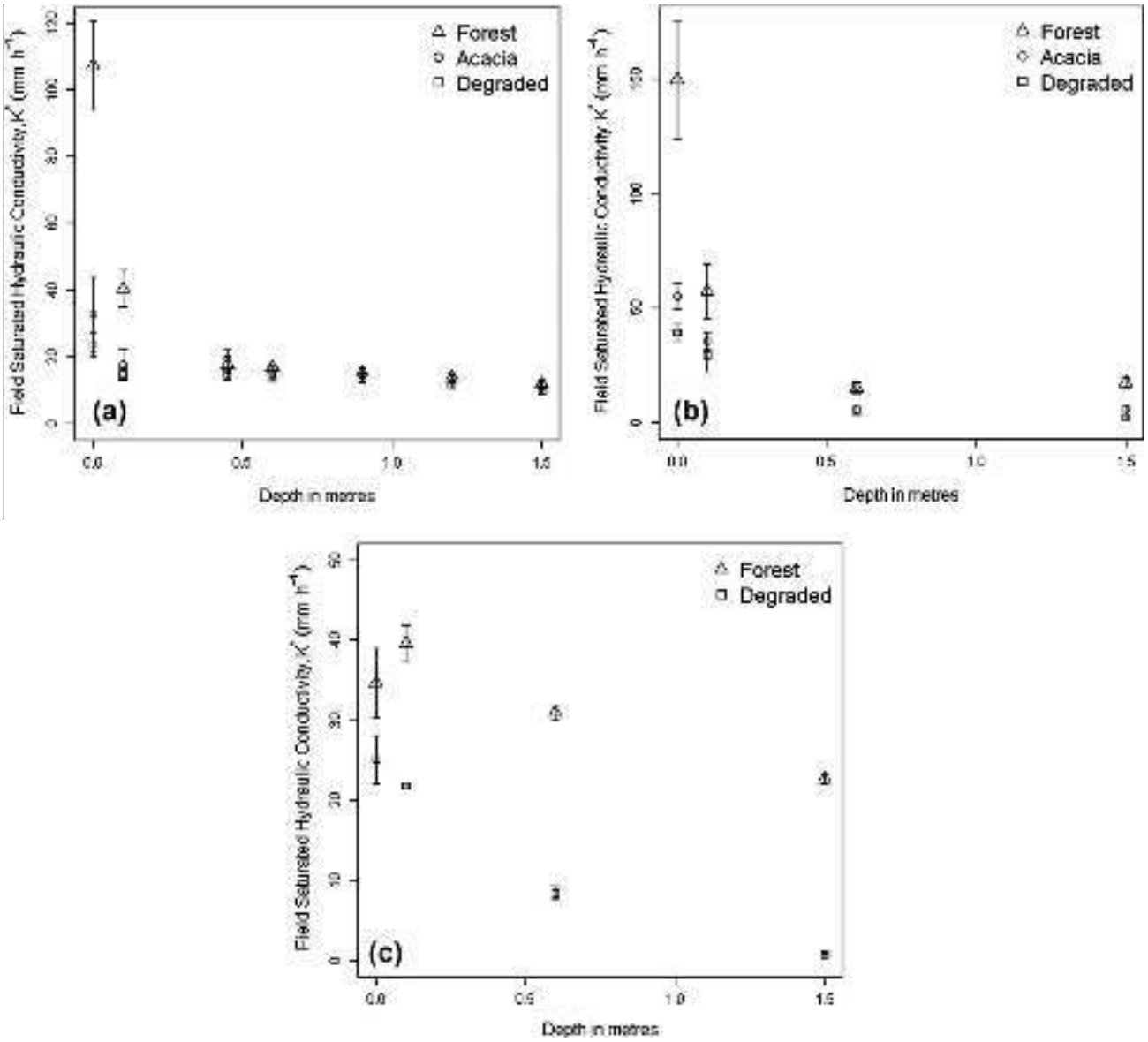


**Fig. 3.** The field saturated hydraulic conductivity $K_{fs}$ and standard deviation against depth ($z$) for the three sites: (a) Areangadi, (b) Kodigibail and (c) Vajagar.

the results from the application of time series-lag regression analyses will be examined.

*5.3.1. A comparison of the storm rainfalls and streamflow characteristics for selected events in the Coastal basins*

A summary of the hydrograph separation results for the above storms using HYDSTRA are presented in Table 4 and the response characteristics also summarised as box plots (Fig. 7). It should be noted that when concerning Table 4, the Event numbers are the same rain storms but the rainfall totals and event definition (start/end times of quickflow) differs between the three basins due to the storm hydrograph separation procedure, as followed by HYDSTRA. Further within Table 4, there are six proportions exceeding 100% when concerning $Q_t/P$ *and* $Q_f/P$, which at face value are physically unrealistic, and four of these are associated with the NF basin. The same issue was noted for a tropical forest basin towards the end of a long duration monsoonal event in north east Australia (Bonell et al., 1991 reproduced in Bonell (2010)). A causal factor put forward to explain such proportions (>100%) is the delayed release of groundwater from subsurface stores of large capacity (Bonell et al., 1991). The latter explanation is also offered here linked with the fissured hydrogeology.

Table 4 also shows the rain events that were selected for later application of the time series analyses where rain–streamflow records were complete. Moreover the nature of hydrograph separation using HYDSTRA causes the duration of quickflow (and thus in some cases, total rainfall) not to be identical across the land covers within a particular event. Further for the smaller storms, the Forest basin proved less sensitive in the streamflow response compared with the other two land covers. That is, HYDSTRA did not detect any streamflow peak to apply hydrograph separation. This aspect also contributed to the uneven sample sizes in Table 4.

Storm totals can be as high as 653 mm but the durations for the larger events (>130 mm) commonly vary between ~2–9 days. By contrast, the maximum 30 min and 1 h rain intensities are comparatively low (equivalent hourly rates $\leqslant$40 mm h$^{-1}$) except for one Event shown as 3NF/4AC/6DF (maximum 30 min, 72.5 mm h$^{-1}$) in Table 4. All these rain characteristics fall in line with the descriptions of Putty and co-workers (Putty et al., 2000; Putty and Prasad, 2000a,b; Putty, 2006).

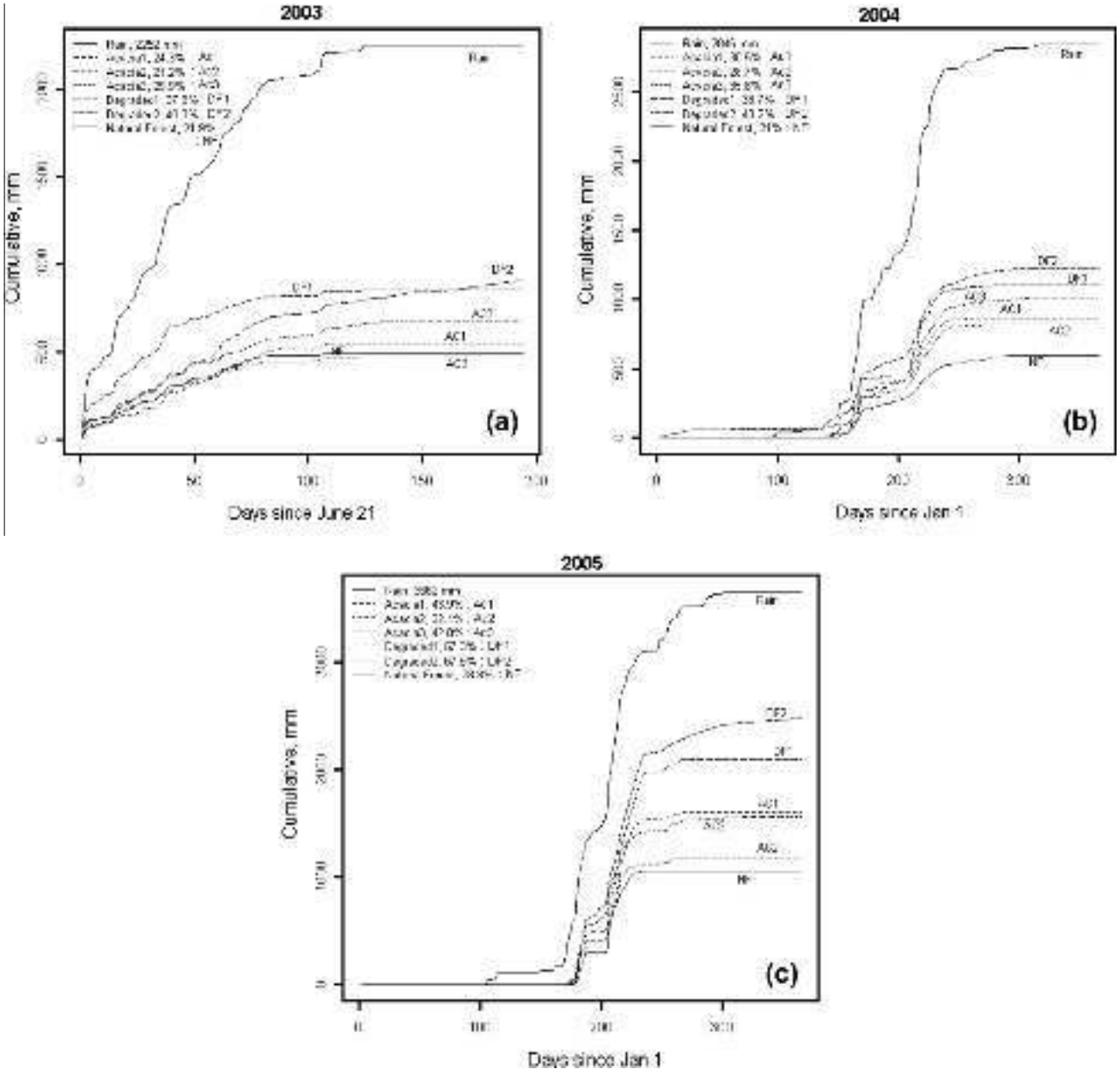


**Fig. 4.** The double-mass plots, $P_{cum}$ ($Q_{cum}$), for the Up-Ghat Kodigibail basins for the years 2003 (a), 2004 (b) and 2005 (c).

The proportion of total flow ($Q$) as quickflow ($Q_F$) (Fig. 7a) shows a clear trend. By far the highest $Q_F/Q$ percentage (median in excess of 90%) emanates from the DF basin (Table 4, Fig. 7a), thus suggesting overland flow occurrence and minimal contributions from deep groundwater (as shown from the inverse % for $Q_D$, Table 4 and Fig. 7b). The Forest has the lowest proportion of $Q$ being represented by $Q_F$ (and in turn greater than 50% of $Q_D$, Table 4) whilst the median of the Acacia Plantation occupies an intermediate ranking (Fig. 7). As expected, the highest quickflow response ratios ($Q_F/P$ up to 90% in Table 4, Fig. 7c) are associated with the Degraded Forest in line with the *a priori* inferred, dominant *IOF* stormflow pathway (Bonell et al., 2010). On the other hand, there are surprisingly only marginal differences between the box plots (Fig. 7c) for the Acacia and the Forest with the middle inter-quartiles in the 20–40% range of $Q_F/P$. This suggests that apart from surface changes in $K_{fs}$ between land covers, there could be other influences controlling storm streamflow which will be examined below.

*5.3.2. The means and standard errors of the hydrologic response characteristics of the storm events*

When concerning Table 5, there is a clear trend for $Q_f/Q_t$, $Q_d/Q_t$ and $Q_d/P$ with the Forest having the expected lowest (i.e., $Q_f/Q_t$) and highest percentages (i.e., $Q_d/Q_t$, $Q_d/P$). The converse applies to the Degraded Forest with the Acacia basins occupying an intermediate rank position. However when concerning the quickflow response ratio ($Q_f/P$), a different ranking exists with a surprising reversal between the Forest and Acacia. Thus the lowest percentage exists for the Acacia basin whilst the Forest occupies an intermediate ranking. The highest $Q_f/P$ for the Degraded is what would be expected. On the other hand, the standard errors for $Q_f/P$ are much higher than for the other response variables and so caution in interpretation of this particular ranking across land covers is required.

The above point is emphasised in the box plots (Fig. 7). When concerning the Forest for $Q_f/P$, there is greater dispersion and more

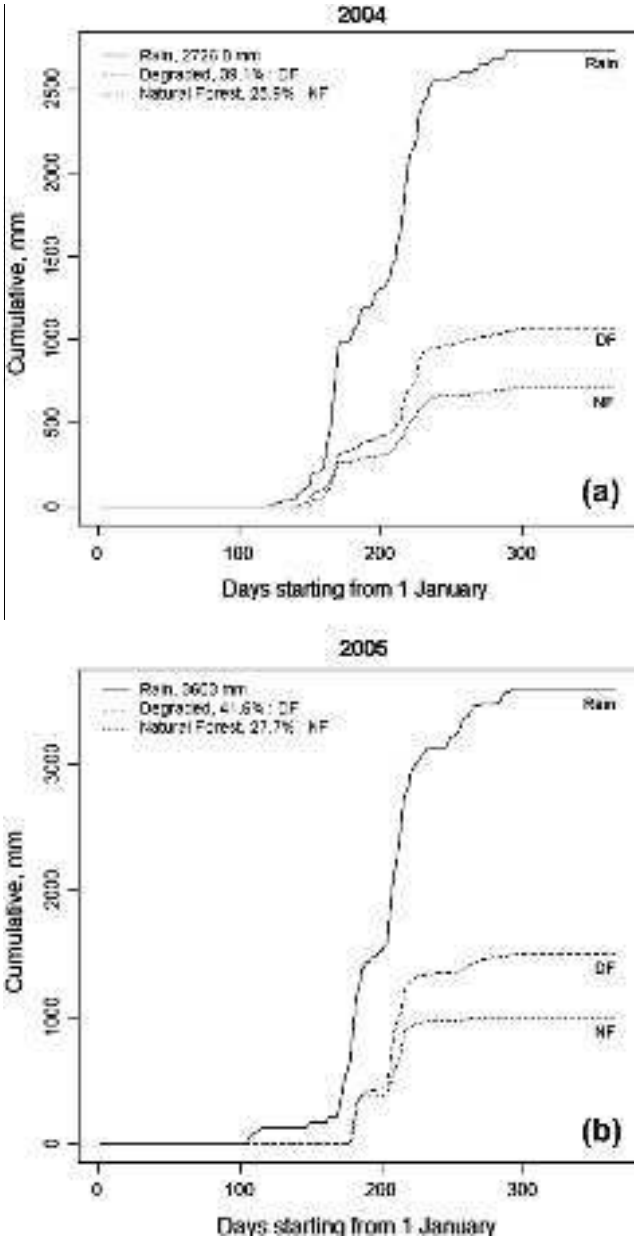


**Fig. 5.** The double-mass plots, $P_{cum}$ ($Q_{cum}$), for the Vajagar Up-Ghat basins for the years 2004 (a) and 2005 (b).

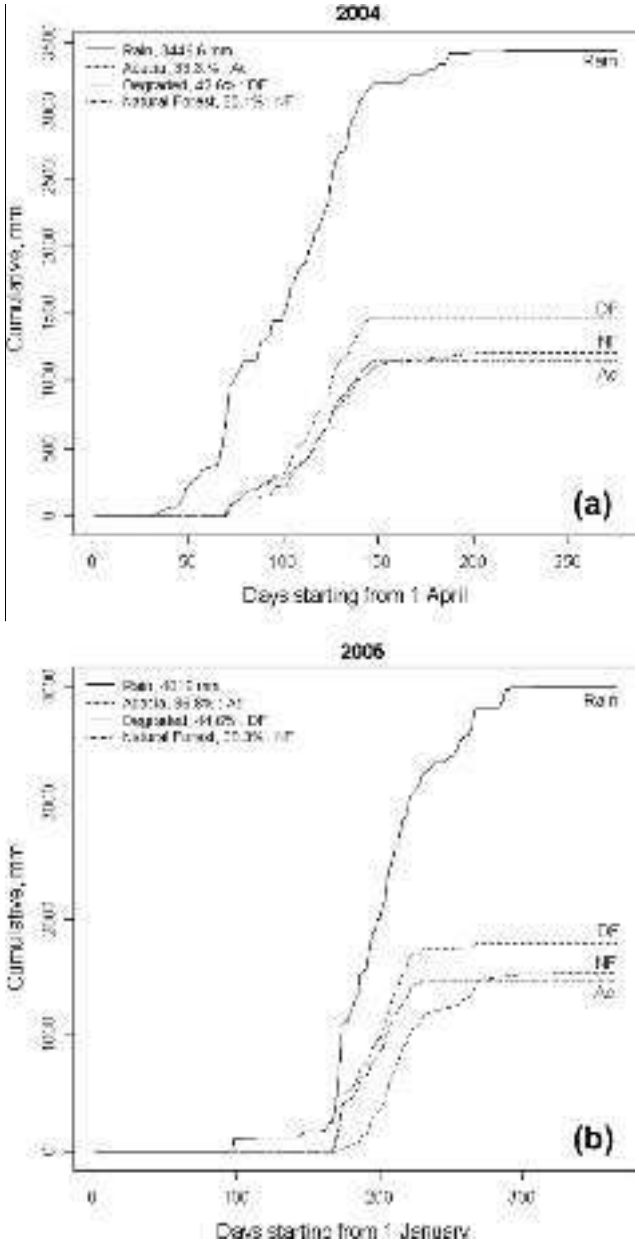


**Fig. 6.** The double-mass plots, $P_{cum}$ ($Q_{cum}$), for the Coastal basins (Areangadi) basins for the years 2004 (a) and 2005 (b).

specifically a greater spread of the lower quartile. Moreover the medians between Forest and Acacia are not that radically different. Furthermore Fig. 7 also highlights there is greater dispersion for other response variables ($Q_f/Q_t$, $Q_d/Q_t$) for Acacia which are not apparent from the standard errors in Table 5. The same comment applies to $Q_d/P$ for the Forest.

*5.3.3. The application of linear model/ANOVA*

Table 6 provides further insights into the differences in hydrologic response. There are sizeable differences in % means (15–40) between all basin pairings across the four response variables, with the exception of $Q_d/P\%$ between Acacia and Degraded.

With the exception of $Q_f/P$, there is a very high certainty of difference based on adjusted $p$ between the Forest and Degraded basins for the other response variables. There is also a high certainty of difference between the Forest with the Acacia. Excluding the $Q_d/P\%$ as above, adjusted $p$ indicates a high certainty of difference between the Acacia–Degraded also exists when concerning $Q_f/Q_t\%$ and $Q_d/Q_t\%$.

It is pertinent that the adjusted $p$ show that there is a low to very low certainty of differences between all combinations of basin pairings when concerning $Q_f/P$.

*5.3.4. Time series analysis: Rain–streamflow cross-correlations*

Data connected with the storm events *1DF/1AC/1NF (16–25 June 2005)*, No. *3DF/2AC/2NF* 2 (*29 June–2 July 2005*) and *9DF/8AC/4NF* (*19–26 July 2005*) (Table 4) were available for all three basins to enable a comparison of the rain–streamflow responsiveness. For reasons of simplification, the above storms will be referred from hereon as respectively, Event 1, 2 and 3.

Two of these events (*Event 1*, range 653–656.5mm; *Event 3*, range 403–430 mm, Table 4) were typical of the long duration storms associated with the SW monsoon. Further the respective maximum 30 min and 1 h rain intensities for the above storms (40 mm $h^{-1}$, 34.3 mm $h^{-1}$; 38.3 mm $h^{-1}$, 32 mm $h^{-1}$, Table 4) were

**Table 4**
The outputs using HYDSTRA for the Coastal Basins - rainfall characteristics and hydrologic response variables.

| Event | Rainfall characteristics | | | | $Q_t/P$ | $Q_f/Q$ | $Q_f/P$ | $Q_d/P$ | $Q_d/Q$ |
|---|---|---|---|---|---|---|---|---|---|
| | Duration (days) | Max.30 min (mm $h^{-1}$) | Max.60 min (mm $h^{-1}$) | Total $P$ (mm) | % | % | % | % | % |
| *Degraded* | | | | | | | | | |
| Event 1DF[a] | 8.68 | 40.0 | 34.3 | 653.0 | 70.26 | 78.33 | 55.03 | 15.23 | 21.67 |
| Event 2DF | 1.63 | 14.2 | 9.2 | 33.0 | 39.24 | 93.51 | 36.70 | 2.55 | 6.49 |
| Event 3DF[a] | 2.88 | 16.7 | 13.3 | 71.0 | 84.54 | 94.32 | 79.73 | 4.80 | 5.68 |
| Event 4DF | 4.33 | 22.5 | 16.5 | 135.5 | 82.12 | 94.00 | 77.19 | 4.93 | 6.00 |
| Event 5DF | 1.17 | 5.8 | 3.5 | 13.0 | 32.15 | 92.82 | 29.85 | 2.31 | 7.18 |
| Event 6DF | 1.96 | 72.5 | 47.2 | 219.8 | 32.31 | 92.93 | 30.02 | 2.28 | 7.07 |
| Event 7DF | 3.46 | 40.0 | 33.3 | 70.0 | 105.90 | 85.71 | 90.77 | 15.13 | 14.29 |
| Event 8DF | 3.08 | 23.3 | 18.3 | 51.0 | 81.27 | 90.54 | 73.59 | 7.69 | 9.46 |
| Event 9DF[a] | 5.75 | 38.3 | 32.0 | 403.2 | 62.81 | 78.43 | 49.27 | 13.55 | 21.57 |
| *Acacia* | | | | | | | | | |
| Event 1AC[a] | 9.32 | 40.0 | 34.3 | 656.5 | 60.13 | 64.51 | 38.79 | 21.34 | 35.49 |
| Event 2AC[a] | 2.71 | 16.7 | 13.2 | 71.0 | 47.89 | 92.91 | 44.49 | 3.39 | 7.09 |
| Event 3AC | 4.75 | 22.5 | 16.4 | 189.5 | 64.95 | 86.44 | 56.14 | 8.81 | 13.56 |
| Event 4AC | 1.63 | 72.5 | 47.1 | 175.0 | 26.38 | 89.80 | 23.69 | 2.69 | 10.20 |
| Event 5AC | 3.04 | 40.0 | 33.1 | 121.5 | 36.93 | 69.27 | 25.58 | 11.35 | 30.73 |
| Event 6AC | 1.42 | 6.7 | 5.0 | 8.0 | 22.50 | 28.89 | 6.50 | 16.00 | 71.11 |
| Event 7AC | 1.54 | 23.3 | 18.3 | 42.5 | 37.91 | 56.36 | 21.36 | 16.54 | 43.64 |
| Event 8AC[a] | 6.10 | 38.3 | 31.7 | 402.7 | 50.64 | 72.44 | 36.69 | 13.96 | 27.56 |
| *Natural Forest* | | | | | | | | | |
| Event 1NF[a] | 9.32 | 40.0 | 34.3 | 656.5 | 5.70 | 47.90 | 2.73 | 2.97 | 52.10 |
| Event 2NF[a] | 2.71 | 16.7 | 13.2 | 71.0 | 141.96 | 75.49 | 107.17 | 34.79 | 24.51 |
| Event 3NF | 5.71 | 72.5 | 47.1 | 232.0 | 69.18 | 65.19 | 45.10 | 24.08 | 34.81 |
| Event 4NF[a] | 7.92 | 38.3 | 31.7 | 429.9 | 59.37 | 47.37 | 28.12 | 31.25 | 52.63 |
| Event 5NF | 7.75 | 24.2 | 15.2 | 183.9 | 88.83 | 52.38 | 46.53 | 42.29 | 47.62 |
| Event 6NF | 17.33 | 30.0 | 22.8 | 188.0 | 67.62 | 38.14 | 25.79 | 41.83 | 61.86 |
| Event 7NF | 9.13 | 25.0 | 15.0 | 157.5 | 51.43 | 41.30 | 21.24 | 30.19 | 58.70 |
| Event 8NF | 2.29 | 13.3 | 10.6 | 37.1 | 39.35 | 37.19 | 14.64 | 24.72 | 62.81 |
| Event 9NF | 7.50 | 23.3 | 16.9 | 84.5 | 162.15 | 67.76 | 109.87 | 52.28 | 32.24 |

*Note: P* – Total precipitation by total storm event (mm), *Q* – Total stream discharge (mm), $Q_f$ – quickflow (mm), $Q_d$ – delayed flow (mm).
[a] Storms used in the time series analyses.

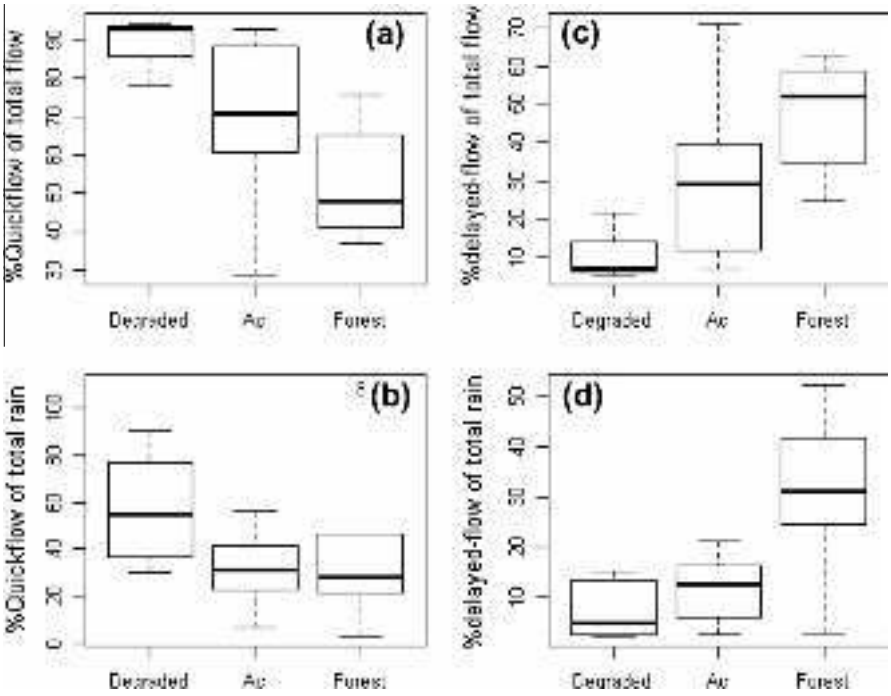


**Fig. 7.** Box plots showing for storm events (Table 4) occurring in the Coastal basins using HYDSTRA: the % quickflow, $Q_F/Q$ (a),% delayed flow (baseflow)/total flow, $Q_B/Q$ (b),% quickflow/total rain, $Q_F/P$ (c) and % delayed flow/total rain, $Q_{DF}/P$ (d).

also typical of the ranges cited by Putty and co-workers (Putty et al., 2000; Putty and Prasad, 2000a,b; Putty, 2006). Event 2 by contrast was weaker with a total rainfall of 33.0mm and maximum 30 min and 1 h rain intensities of only 14.2 mm $h^{-1}$ and 9.2 mm $h^{-1}$ respectively. Further Event 1 was the first major event during the opening stages of the summer monsoon. The other two

events were typical of those that occur once basin antecedent soil moisture attains optimal wetness, similar to the description of Venkatesh et al. (2011) for the Kodigibail basins.

The cross-correlations for these events are shown respectively in Figs. 8–10 and one lag unit represents a time increment of 0.6 h. There is some consistency in the distribution of peak coefficients for both the Degraded Forest and the Acacia Plantation in spite of the noted differences in rainfall characteristics. The highest cross-correlations occur with short time lags (0–2 time units) which suggest the existence of comparatively a faster delivery mechanism of stormflow to the stream hydrograph. Further secondary peaks are also are shown, most notably in the AC basin, which vary between lag 20 and lag 60 (12–36 h) which could be reflecting a slower stormflow pathway.

The Forest by contrast shows less consistency between the three storms in the distribution of peak lags. Multiple peak lags are shown for Event 1 from lag 1 (which has the highest cross-correlation coefficient) up to ~lag 75 (45 h) which could be due streamflow emanating from multiple sources and pathways during the opening phase of the monsoon. For Events 2 and 3 more distinct peak lags are evident, although in the former the coefficients take the form of a flatter peak ~lag 30–40 (18–24 h). For Event 3 when more optimal, catchment wetness exists, the peak lag is shorter and more distinct at ~lag 15 (8 h).

Thus overall the Forest is much less responsive when compared to the other land covers and much slower (multiple) pathways of streamflow are indicated.

*5.3.5. Time series: Lag regression analysis*

Table 7 summarizes the outputs using the simulation model (Eq. (1)) and Figs. 8–10 include the summary of the forecasting/prediction model (Eq. (2)).

For the Forest there are multiple rain lags, and the overall description for the cross-correlation coefficients above is reflected again in these results. A series of longer response delays occur when compared to the other two land covers which suggest multiple contributions from subsurface sources. For Events 1 and 2 there is also shorter response at lag 1, c.f., the cross-correlation, which could be a secondary contribution from the riparian zone which exists in this basin. It is pertinent that the zero time lag for rainfall is never selected for the Forest but almost always for the other two land covers.

By contrast the Degraded Forest and Acacia either show two groups of significant rainfall variables respectively that favour either short and longer lags or short rain lags only (i.e., Event 1, DF; Event 2, Acacia). These results again confirm the trends as shown in Figs. 8–10 for the cross-correlations. The inclusion of short-term rainfalls (in most cases at rain $RF_{t-0}$) with a separate group of longer rain lags infers the juxtaposition of a more rapid pathway of stormflow delivery with the slower, subsurface sources of streamflow characterised by the Forest.

**Table 5**
The means and standard errors of the hydrologic response characteristics for the storm events in the Coastal basins.

| | Catchment type | | |
|---|---|---|---|
| | Degraded | Acacia | Natural forest |
| $\frac{Qf}{Qt}$, % | $89.0 \pm 7.15_{se}$ | $70.1 \pm 5.20_{se}$ | $52.5 \pm 7.15_{se}$ |
| $\frac{Qf}{P}$, % | $58.0 \pm 13.58_{se}$ | $31.7 \pm 9.88_{se}$ | $44.6 \pm 13.58_{se}$ |
| $\frac{Qd}{Qt}$, % | $11.0 \pm 7.15_{se}$ | $29.9 \pm 5.20_{se}$ | $47.5 \pm 7.15_{se}$ |
| $\frac{Qd}{P}$, % | $7.6 \pm 4.67_{se}$ | $11.8 \pm 3.40_{se}$ | $31.6 \pm 4.67_{se}$ |

*Notes:* $P$ = Precipitation (mm), $Q_f$ = total quick flow (mm), $Q_t$ = total streamflow (mm), $Q_d$ = delayed flow (mm), se = standard error.

*5.3.5.1. Brief comparison with the simulation model results.* Figs. 8–10b–f summarize the model fit to the stream hydrograph and the corresponding outputs using Eq. (2)).

Overall when concerning the selected rain variables, the trends as outlined above are reflected again in the equations associated with this model. However with the introduction of the "cumulative effect" of previous rainfalls on regolith available storage capacities (in the form of previous runoff variables or lagged $Y_{t-k}$) reduces the number of rainfall lags and makes the previous interpretations more clear. The importance of antecedent storage capacities (i.e., the inclusion of several lagged $RO_{t-k}$) is also more evident in this study and especially for the Forest than when compared to NE Queensland rainforest (Bonell et al., 1981). On the other hand, for the Degraded Forest (Event 1) has a very simple model, not too different from those reported in the Australian study. Only two short-term rainfall variables are significant, i.e., $RF_{t-0}$ and $RF_{t-1}$ as well as $RO_{t-1}$. In the absence of riparian zone, this result suggests *IOF* occurrence (as well as *SOF*) on the hillslopes which is controlled by short-term, changes in rainfall intensities. Similarly remarks apply to Event 3 for DF and also Event 2 for Acacia except both equations also incorporate a longer rainfall lag as well.

## 6. Discussion

### *6.1. Land cover change impacts on the basin water yield and storm runoff hydrology*

When concerning total streamflow yield, overall the double mass curves, $Q_{cum}$ ($P_{cum}$), at the seasonal time scale show that the highest streamflow yields are in the order DF > AC > NF for both the Coastal and Malnaad (Up-Ghat) basins. The same conclusions emerge when the records from both the Malnaad and Coastal basins are combined. Despite the caution expressed earlier in terms of the problems of using small area basins (e.g., subsurface exchange of groundwater across basin boundaries defined by surface topography), such consistency in rain–streamflow trends is encouraging. Nonetheless because total evapotranspiration was not directly measured on site to factor that component into a water balance, these double mass curves *per se* do not provide conclusive

**Table 6**
Tukey's multiple comparison differences of means for the Coastal storm events along with lower and upper 95% bounds and adjusted $p$-values.

| | Difference | Lower 95% | Upper 95% | $p$ Adjusted |
|---|---|---|---|---|
| $Q_f/Q_t$% | | | | |
| Degraded–Acacia | 18.88 | 0.97 | 36.78 | 0.0375 |
| Natural Forest–Acacia | −17.55 | −35.45 | 0.35 | 0.0554 |
| Natural Forest–Degraded | −36.43 | −53.80 | −19.06 | 0.0000 |
| $Q_f/P$% | | | | |
| Degraded–Acacia | 26.36 | −7.63 | 60.36 | 0.1498 |
| Natural Forest–Acacia | 12.92 | −21.08 | 46.92 | 0.6138 |
| Natural Forest–Degraded | −13.44 | −46.42 | 19.54 | 0.5717 |
| $Q_d/Q_t$% | | | | |
| Degraded–Acacia | −18.88 | −36.78 | −0.97 | 0.0375 |
| Natural Forest–Acacia | 17.55 | −0.35 | 35.46 | 0.0554 |
| Natural Forest–Degraded | 36.43 | 19.06 | 53.80 | 0.0001 |
| $Q_d/P$% | | | | |
| Degraded–Acacia | −4.15 | −15.86 | 7.55 | 0.6529 |
| Natural Forest–Acacia | 19.84 | 8.13 | 31.55 | 0.0009 |
| Natural Forest–Degraded | 23.99 | 12.64 | 35.35 | 0.0001 |

*Notes:* $P$ – Total precipitation by total storm event (mm), $Q_t$ – total stream discharge (mm), $Q_f$ – quickflow (mm), $Q_d$ – delayed flow (mm).

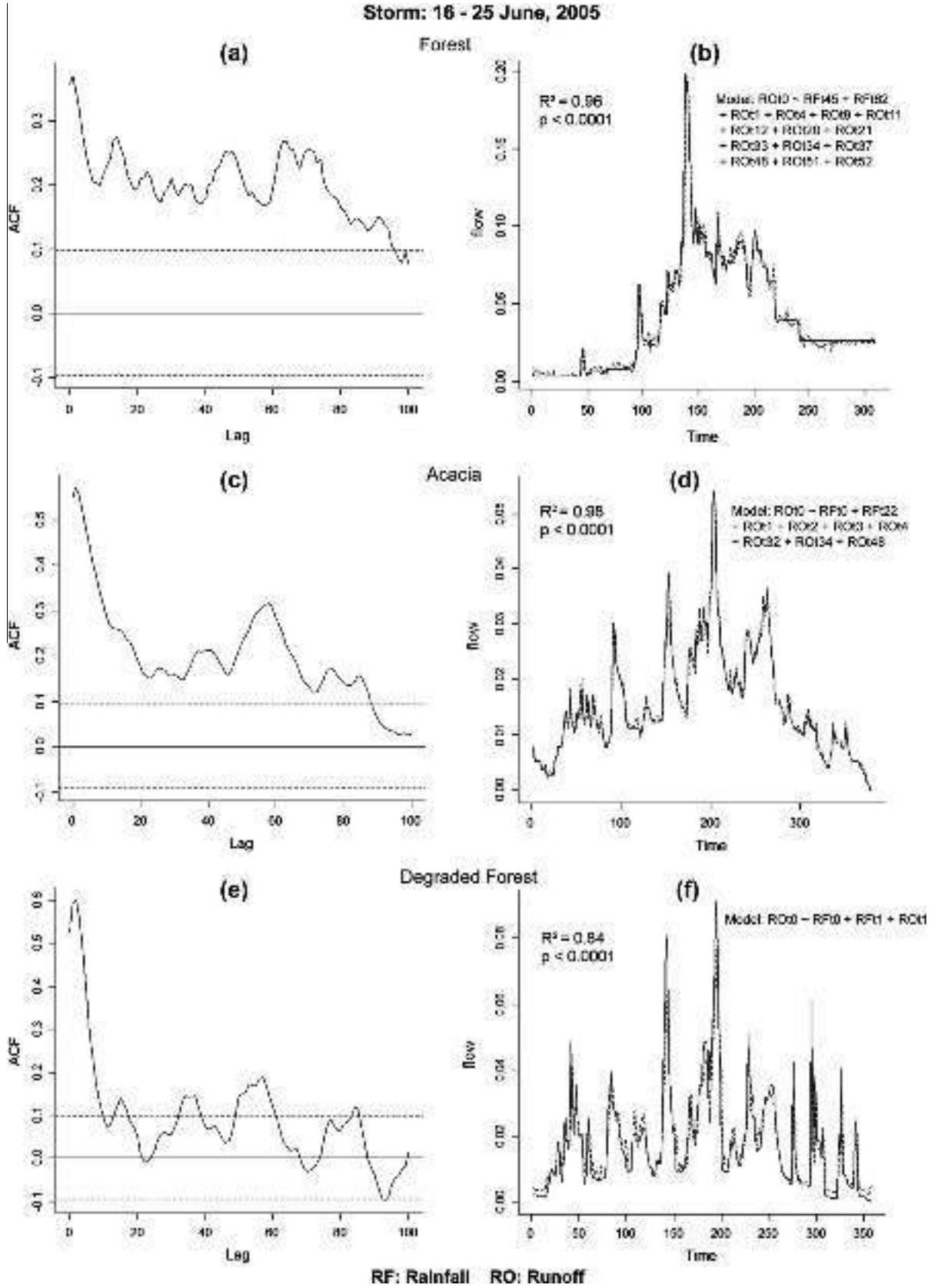


**Fig. 8.** Coastal basins: The cross-correlation coefficients and time series-regression models (Eq. (2)) for the Forest (NF1), Acacia (AC1) and Degraded Forest (DF1) for the Event 1 (16–25 June 2005). *Note:* 1 lag unit is equal to 0.6 h and the time is expressed in lag units.

proof that overland flow progressively becomes a more dominant stormflow pathway in the reverse basin order NF < AC < DF.

On the other hand, there is also additional support for overland flow probably becoming more dominant, when concerning the $Q_F$/

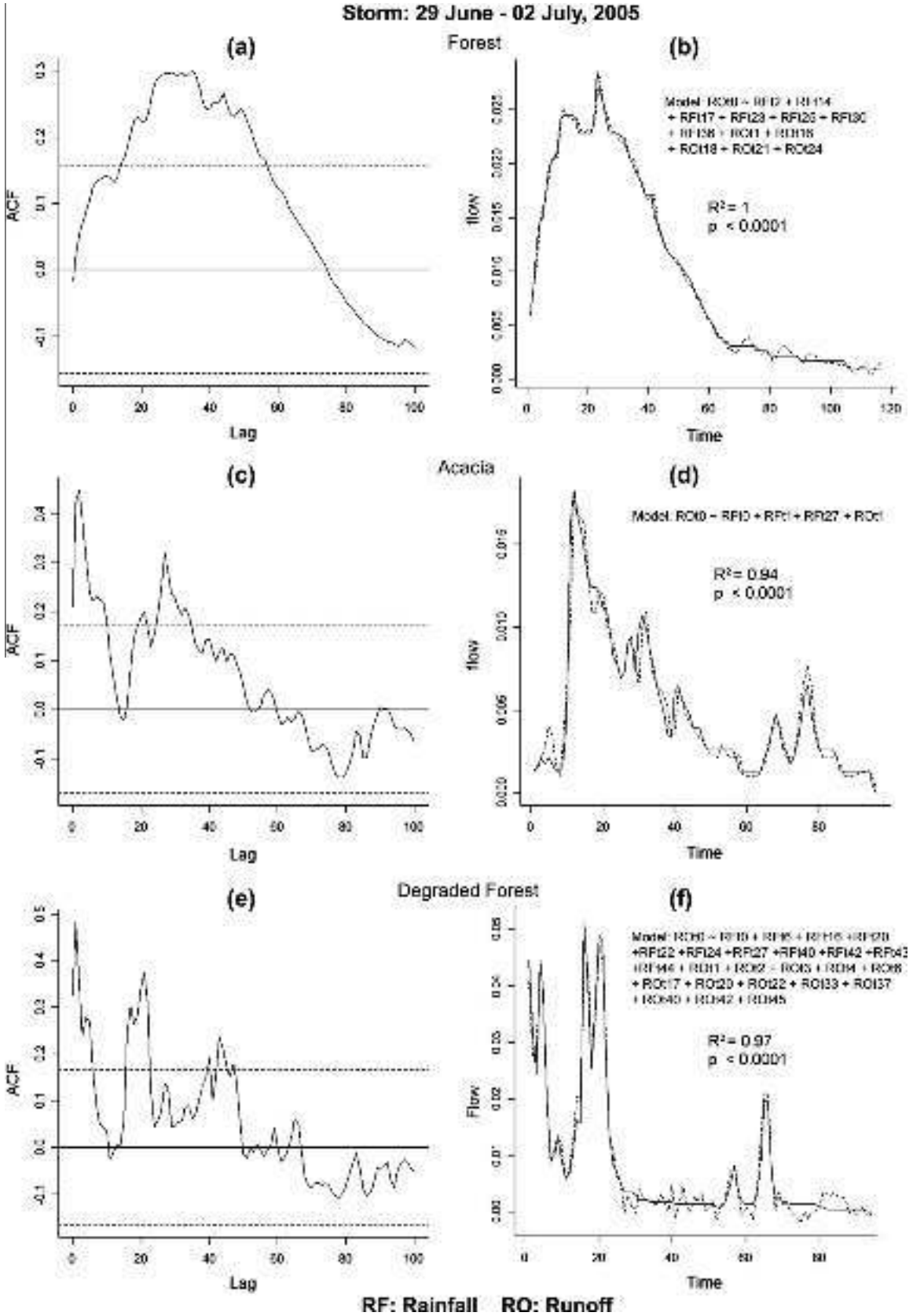


**Fig. 9.** Coastal basins: The cross-correlation coefficients and time series-regression models (Eq. (2)) for the Forest (NF1), Acacia (AC1) and Degraded Forest (DF1) for the Event 2 (29 June 2005–2 July 2005). *Note:* 1 lag unit is equal to 0.6 h and the time is expressed in lag units.

Q ratio by storm event from HYDSTRA for the Coastal basins. For most events, there are much higher values for this runoff ratio for DF and AC, and again, all are in the same rank order NF < AC < DF as for the seasonal double mass curves. Even more

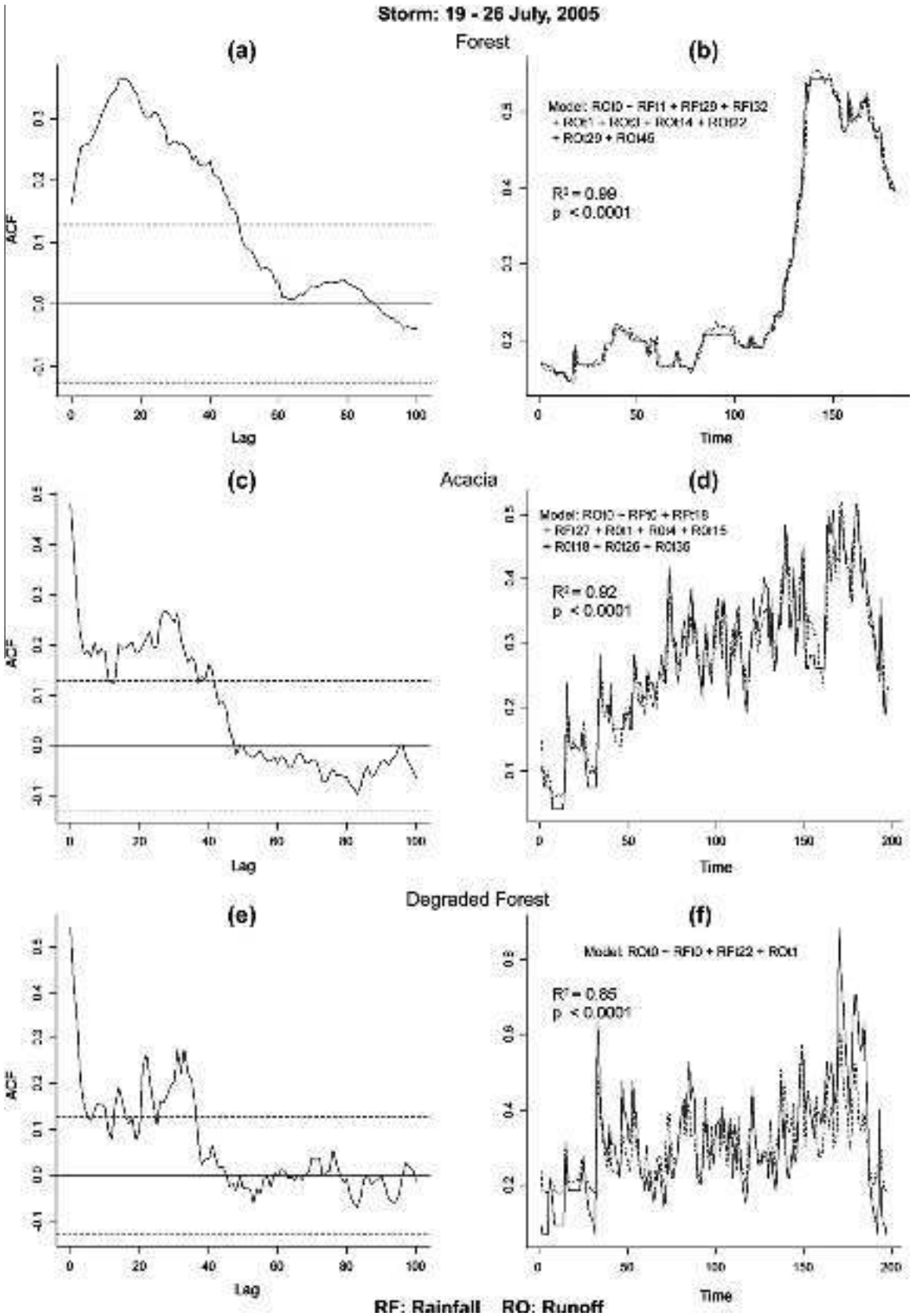


**Fig. 10.** Coastal basins: The cross-correlation coefficients and time series-regression models (Eq. (2)) for the Forest (NF1), Acacia (AC1) and Degraded Forest (DF1) for the Event 3 (19–26 July 2005). *Note:* 1 lag unit is equal to 0.6 h and the time is expressed in lag units.

remarkable is that the $Q_F/Q$ can exceed 90% in the DF basin in selected events. By contrast the $Q_F/P$ ratios are less consistent, with the Acacia rather than the Forest having the lowest mean value. The larger area of the Forest basin may be a cause for this inconsis-

**Table 7**
Streamflow–rainfall regression model terms using rain lag variables.

| Event | Model Regression | | |
|---|---|---|---|
| | Forest | Acacia | Degraded |
| Event 1; 16–25 June | Runoff = rainfallt1 + rainfallt14 + rainfallt36 + rainfallt48 + rainfallt63 + rainfallt74 | Runoff = rainfallt0 + rainfallt1 + rainfallt3 + rainfallt26 | Runoff = rainfallt1 + rainfallt2 |
| Event 2; 29 June – 02 July | Runoff = rainfallt1 + rainfallt4 + rainfallt6 + rainfallt9 + rainfallt11 + rainfallt13 + rainfallt15 + rainfallt17 + rainfallt19 + rainfallt20 + rainfallt22 + rainfallt24 + rainfallt26 + rainfallt27 + rainfallt28 + rainfallt29 + rainfallt30 + rainfallt31 + rainfallt32 + rainfallt33 + rainfallt34 + rainfallt35 + rainfallt36 + rainfallt37 + rainfallt38 + rainfallt40 + rainfallt42 + rainfallt44 + rainfallt46 + rainfallt48 + rainfallt50 + rainfallt51 + rainfallt52 + rainfallt53 + rainfallt55 + rainfallt56 + rainfallt58 + rainfallt60 | Runoff = rainfallt2 + rainfallt0 | Runoff = rainfallt0 + rainfallt1 + rainfallt4 + rainfallt6 + rainfallt16 + rainfallt17 + rainfallt20 + rainfallt22 + rainfallt40 + rainfallt43 + rainfallt45 |
| Event 3; 19–26 July | Runoff = rainfallt11 + rainfallt14 + rainfallt16 + rainfallt19 + rainfallt36 + rainfallt38 + rainfallt43 | Runoff = rainfallt0 + rainfallt1 + rainfallt25 + rainfallt40 | Runoff = rainfallt0 + rainfallt1 + rainfallt2 + rainfallt22 + rainfallt34 |

tency. On the other hand, the statistical analyses showed that there was a low to very low certainty in difference between the three basins when concerning $Q_F/P$. When concerning the remaining hydrologic response variables, there is mostly a high level of certainty in statistical differences between pairs of basins (land cover types).

The corresponding delayed flow response ratios, $Q_D/P$ clearly show the much larger $Q_D$ yield as a proportion of event precipitation from the Forest in contrast to the DF and AC basins. The same trend applies to $Q_D/Q$.

Furthermore the more responsiveness of rain–streamflow time lags from the time series analyses provide further support for a faster dominant storm flow pathway being associated with the DF and AC basins. The regression equations for both the prediction and simulation models are much simpler (notably for the Acacia Plantation) and favour short time lags. Moreover the structure of these regression equations are not too dissimilar from those reported from the NE Queensland tropical forest where shallow *SSF* (supplemented by *SOF*) was the dominant stormflow pathway (Bonell et al., 1979,1981). On the other hand, these results do not give any indication of the spatial and temporal extent of this dominant stormflow pathway. Further the time unit of 0.6 h remains comparatively coarse compared with other tropical hillslope hydrology studies (e.g., reviewed in Bonell (2004)) and even some humid temperate work (Dunne, 1978; Anderson and Burt, 1990) to suggest that the responsiveness of these disturbed basins are not that radically different from many other studies.

It is clear that the impacts of multi-decadal to century time scale degradation or use have reduced surface permeability and so infers that there has been some redirection of the dominant stormflow pathways from previously *SSF* and vertical percolation (Forest) in favour of enhanced *IOF* in the Coastal DF and AC basins. Consequently despite some recovery in surface $K_{fs}$ in the Acacia plantations, the impacts of long-term degradation *a priori* still persist as a 'memory' in the streamflow response. In China, Zhou et al. (2001) also noted the continued retention of more compacted areas in a basin which had previously undergone forestation over more than 20 years previously.

Land cover is thus an important control on streamflow despite two different soil types (Red, Laterite) being represented in the study. The higher volumes of seasonal streamflow and quickflow by event from long-term degradation supports the conclusions from the previous hydraulic conductivity survey that enhanced *IOF* occurs (supplemented by *SOF*) (Bonell et al., 2010). Similar conclusions were also suggested elsewhere (Chandler and Walter, 1998; Zhou et al., 2001; Costa et al., 2003; Bruijnzeel, 2004; Scott et al., 2004; Chandler, 2006; Zimmermann et al., 2006; de Moraes et al., 2006; Chaves et al., 2008; Zimmermann and Elsenbeer, 2008, 2009). Furthermore even though we could not study pipeflow, this work adds much more detail on the storm hydrograph response characteristics impacted by different land covers and thus extends the earlier descriptions given in Putty and Prasad (2000a).

The current results contrast with those from selected controlled experiments in both the humid tropics and the humid temperate latitudes (e.g. Swank et al., 1988; Bruijnzeel, 1990, 1996; Andreassian, 2004; Grip et al., 2004; Brown et al., 2005). In such cases for the most part the soil hydraulic properties at the surface in disturbed basins have retained enough of the pre-disturbed soil hydraulic characteristics, i.e. the 'good' condition status of Bruijnzeel (2004), so the storm runoff process has not been radically altered. In addition, it is evident that several decades will still be required for the rain–streamflow response of forested degraded land (i.e. by way of *A. Auriculiformis* plantations) to return towards the 'background' levels of the Forests. Although the more limited of soil biology associated with these plantations, in contrast to the natural forests, maybe a constraint to complete recovery of the hydraulic conductivity of these soils and thus the storm runoff gen-

eration process (Bonell et al., 2010). In the meantime the runoff generation process remains similar in the Acacia plantations to that found in the Degraded Forest.

Overall there is support from this study for the the 'degraded scenario' of the 'infiltration trade-off' hypothesis of Bruijnzeel (2004) *when concerning the storm runoff generation part of this hypothesis.* At these small basin scales, the surface reduction in soil $K_{fs}$ under the DF land cover, and its persistence in the AC plantations, have clearly enhanced both seasonal streamflow yields and quickflow by rain event. It is to be noted that although this study does not address evapotranspiration and water-balance aspects, we suggest that as potential and actual evapotranspiration are likely to be depressed in the monsoon period when relative humidity is high, differences in stream flow and run-off between land-cover types during the wet-season are largely attributed to soil infiltration and hydrologic pathways.

### 6.2. A comparison of quickflow response ratios linked with synoptic climatology

The quickflow response ratios for the Coastal NF basin are much lower than those reported from north-east Queensland tropical rainforest (e.g. $Q_F/P$ up to 56%) where the Lyne and Hollick (1979) hydrograph separation method was also used (Howard et al., 2010). Aside from differences in soil permeability, a key difference concerns the prevailing short-term rainfall intensities. They are much weaker in the Western Ghats when compared to the Australian study even if the daily totals are comparable (Putty et al., 2000; Putty, 2006; Bonell et al., 2004). The north-east Queensland rainforest is frequently impacted by tropical depressions and cyclones (Bonell et al., 2004; Bonell and Callaghan, 2008) whereas at the synoptic scale, rainfall in the study area emanates more from 'surges' in the wind streamlines of the south-west monsoon. Further orographic uplift of this deep (up to 6 km) and moist, airflow with the topographic barrier of the "Western Ghats-Central Sahyadri" accentuates precipitation. It is this mechanism which is a key driver for the occurrence of such high daily rainfalls (Gadgil and Joshi, 1983; Singh, 1986; Gunnell, 1997).

By contrast the hydrologic response variables associated with quickflow, as reported for the Coastal basins by event, are much higher than the reports from the Amazon basin studies (Biggs et al., 2006; de Moraes et al., 2006; Chaves et al., 2008). Aside from some differences in soil hydraulic conductivity (Bonell et al., 2010), the synoptic climatology is also very different between the two locations. It is not monsoonal in the Amazon basin in the strict sense of cross-equatorial flow over a large latitudinal range (Sadler et al., 1987). Moreover there are a very different suite of rain-producing systems and associated rainfall characteristics in the Amazon basin (Greco et al., 1990; Garstang et al., 1994; Garreaud and Wallace, 1997; reviewed in Bonell et al. (2004)). In addition, land degradation is more recent associated with the above Amazon basin studies (Biggs et al., 2006; de Moraes et al., 2006; Chaves et al., 2008).

### 6.3. The time series analyses and the roles of deep subsurface flow and groundwater

In the Coastal basins the time series analyses also indicated substantial time lags by event in rain–streamflow within the NF basin, and thus deeper, slower pathways being the dominant contributor to the storm hydrograph. Furthermore there was an interesting retention of this characteristic of a longer time lag in the human-impacted AC and DF basins, despite the emergence and juxtaposition of much shorter time lags as well. In contrast no such long time lags were detected in the NE Queensland tropical rainforest study (Bonell et al., 1979, 1981). Thus the more responsive storm hydrographs connected with the latter study (dominated by surface/shallow subsurface streamflow sources, *SOF* and *SSF*), contrasts with the much slower storm hydrograph responses in the NF basin. Much deeper sources of streamflow are suggested via deep *SSF* and groundwater pathways. Remarkably this same characteristic is still retained even within the DF and AC basins, and this is despite human impacts on the surface soils up to a century time scale. Moreover the simulation model indicated larger available storage capacities in the regolith and thus their greater role in the storm runoff generation process in contrast to the NE Queensland tropical rainforest study (Bonell et al., 1981).

One explanation for the above hydrological characteristics is that the subsoil $K_{fs}$ (geometric means $\sim$10–20 mm $h^{-1}$) for all three Coastal basins are comparatively permeable down to 1.50m depth when compared to other Laterite sites in the region (Bonell et al., 2010). Moreover these sub-soils are more permeable than those in the similar 'Acrisol-type' soils of the Australian study (Bonell et al., 1981, 1998) where the geometric mean $K_{fs}$ is an order of magnitude lower. Elsewhere in a similar soil 'Acrisol-type' associated with a Peru study (Elsenbeer and Lack, 1996) there is a lower two order of magnitude difference in subsoil $K_{fs}$. Consequently available soil water storage capacities would be higher under the Forest and in the sub-soil away from the human-impacted surface soil layers. Further percolation to groundwater beneath both the DF and AC land basins would not be impeded, once rainwater entry through the lower surface $K_{fs}$ has occurred. Thus recharge to groundwater, albeit in different proportions of total event rain, can be maintained despite a reduction in surface $K_{fs}$ in the two disturbed land covers. Furthermore in the absence of detailed catchment surveys, the contributions of pipeflow towards a deeper *SSF* pathway cannot be excluded, on the lines of the description by Putty and Prasad (2000a).

The above findings highlight the need for detailed hydrogeology information when concerning rain–streamflow comparative studies linked with LC change. Moreover in addition to evapotranspiration and surface changes in $K_{fs}$, streamflow could potentially be also be affected by subtle differences in the hydrogeology by way of the jointing and fracturing within the underlying parent rock (as mentioned in CGWB (2008)) at such small basin scales. Despite such concerns the overall trend in streamflow yields (DF > AC > NF) for the Coastal basins are in line with the Malnaad basins.

## 7. Conclusions

Following the three questions posed *a priori* the conclusions are:

1. When compared to the less disturbed, baseline evergreen forest the impacts of multi-decadel degradation of forests results in enhanced total stream discharge and quickflow both seasonally and by storm event. Conversely base (delayed) flow is reduced.
2. The work supports earlier conclusions from the hydraulic conductivity survey (Bonell et al., 2010) which suggested that the occurrence of overland flow may have increased as a result of long-term forest degradation. Such comments also apply to (re) forested, former "degraded" land using *A. auriculiformis* plantations. Acacia plantations may thus not be very effective in restoring hydrologic functions in the short-term.
3. On the other hand there is evidence of contributions from deeper, subsurface sources to the storm hydrograph (more associated with the baseline evergreen forest) still continuing under the degraded forest and Acacia plantations. This is partly attributed to the sub-soils being comparatively permeable when compared to other studies. Despite some recovery in the surface hydraulic conductivity, the rain–streamflow response charac-

teristics of the *A. auriculiformis* plantations still retains a 'memory' of the storm hydrograph characteristics described above for the Degraded Forest.

4. As potential and actual evapotranspiration is likely to be depressed during the monsoon, differences in streamflow and run-off responses between land-cover is largely attributed to differences in soil infiltration and hydrologic pathways.
5. Hydrologic functions and services should be viewed in a larger frame-work of multiple ecosystem services and biodiversity of these ecosystems and land-management options to increase infiltration should be explored within this context of trade-offs and synergies at various spatial and temporal scales.

## Acknowledgements

We thank the following for financial and administrative support: Suri Sehgal Centre for Biodiversity and Conservation, ATREE, Bangalore, Ford Foundation, the UNESCO International Hydrological Programme (Paris and Delhi), the Royal Society of Edinburgh, UK (RSE Grant 483.805998), The Carnegie Trust for the Universities of Scotland and the Centre for Water, Law and Policy, Dundee, UK under the auspices of UNESCO. The Crown Research Institute, Manaaki Whenua – Landcare Research in Lincoln (New Zealand) is also thanked for giving us access, and support, in the use of the HYDSTRA software; and to Guy Forrester (Statistician) of the same institution for very useful discussions when concerning the modifications to the time series method. A grant from the Changing Water Cycle programme of the Natural Environment Research Council (NERC, UK) – Ministry of Earth Sciences, Government of India provided support for the revision. We thank WorldClim and International Water Management Institute for making available climate data. Finally we gratefully acknowledge Lex A. (Sampurno) Bruijnzeel, Vrije Universiteit, Amsterdam for his rigorous review and constructive suggestions on an earlier version of this manuscript.

## References

Anderson, M.G., Burt, T.P. (Eds.), 1990. Process Studies in Hillslope Hydrology. Wiley, Chichester, UK, p. 539.

Andreassian, V., 2004. Waters and forests: from historical controversy to scientific debate. J. Hydrol. 291, 1–27.

Biggs, T.W., Dunne, T., Muroaka, T., 2006. Transport of water, solutes and nutrients from a pasture hillslope, southwestern Brazilian amazon. Hydrol. Process. 20, 2527–2547.

Blackie, J.R., Robinson, M., 2007. Development of catchment research, with particular attention to Plynlimon and its forerunner, the east African catchments. In: Neal, C., Clarke, R.T., (Eds.), Special Issue: A View from the Watershed Revisited. Part 1: Catchment Area Research. Hydrol. Earth Syst. Sci., vol. 11(1/1), pp. 26–43.

Blanchart, E., Julka, J.M., 1997. Influence of forest disturbance on earthworm (Oligochaeta) communities in the Western Ghats (South India). Soil Biol. Biochem. 29 (3–4), 303–306.

Bonell, M., 2004. Runoff generation in tropical forests. In: Bonell, M., Bruijnzeel, L.A. (Eds.), Forests, Water and People in the Humid Tropics: Past, Present and Future Hydrological Research for Integrated Land and Water Management. International Hydrology Series, Cambridge University Press, Cambridge, pp. 314–406.

Bonell, M., 2010. The impacts of global change in the humid tropics: selected rainfall–runoff issues linked with tropical forest-land management. Irrig. Drain. Syst. 24 (3–4), 279–325. http://dx.doi.org/10.1007/s10795-010-9104-8.

Bonell, M., Barnes, C.J., Grant, C.R., Howard, A., Burns, J., 1998. High rainfall response-dominated catchments: a comparative study of experiments in tropical north-east Queensland with temperate New Zealand. In: Kendall, C., McDonnell, J.J. (Eds.), Isotope Tracers in Catchment Hydrology. Elsevier, pp. 347–390.

Bonell, M., Callaghan, J., 2008. The synoptic meteorology of high rainfalls and the storm runoff – response in the wet tropics. In: Stork, N., Turton, S. (Eds.), Living in a Dynamic Tropical Forest Landscape. Blackwell Publishing, pp. 23–46 (Chapter 2, Part I).

Bonell, M., Callaghan, J., Connor, G., 2004. Synoptic and mesoscale rain producing systems in the humid tropics. In: Bonell, M., Bruijnzeel, L.A. (Eds.), Forests, Water and People in the Humid Tropics – Past, Present and Future Hydrological Research for Integrated Land and Water Management. UNESCO International Hydrology Series, Cambridge University Press, Cambridge, UK, pp. 194–266.

Bonell, M., Gilmour, D.A., Cassells, 1991. The links between synoptic climatology and the runoff response of rainforest catchments on the wet tropical coast of north-eastern Queensland. In: Kershaw, A., Werran, G. (Eds.), The Rainforest Legacy – Australian National Rainforests Study Report, vol. 2. Australian Heritage Commission, Canberra, pp. 27–62.

Bonell, M., Gilmour, D.A., Sinclair, D.F., 1979. A statistical method for modelling the fate of rainfall in a tropical rainforest catchment. J. Hydrol. 42, 251–267.

Bonell, M., Gilmour, D.A., Sinclair, D.F., 1981. Soil hydraulic properties and their effects on surface and subsurface water transfer in a tropical rainforest catchment. Hydrol. Sci. Bull. 26, 1–18.

Bonell, M., Purandara, B., Venkatesh, B., Krishnaswamy, J., Acharya, H.A.K., Singh, U.V., Jayakumar, R., Chappell, N., 2010. The impact of forest use and reforestation on soil hydraulic conductivity in the Western Ghats of India: implications for surface and sub-surface hydrology. J. Hydrol. 391, 47–62, http://dx.doi.org/10.1016/j.jhydrol.2010.07.004.

Bourgeon, G., 1989. Explanatory Booklet on the Reconnaissance Soil Map of Forest Area: Western Karnataka and Goa, Institut français de Pondichéry, travaux de la section scientifique et technique, hors série 20, Pondicherry, 96p +Annexes.

Bouwer, H., 1966. Rapid field measurement of air entry value and hydraulic conductivity of soils as significant parameters in flow system analysis. Water Resour. Res. 2, 729–738.

Brown, A.E., Zhang, L., McMahon, T.A., Western, A.W., Vertessy, R.A., 2005. A review of paired catchment studies for determining changes in water yield resulting from alterations in vegetation. J. Hydrol. 310, 28–61.

Bruijnzeel, L.A., 1989. (De)forestation and dry season flow in the tropics: a closer look. J. Trop. For. Sci. 1 (3), 229–243.

Bruijnzeel, L.A., 1990. Hydrology of Moist Tropical Forest and Effects of Conversion: a State of Knowledge Review. UNESCO, Paris and Vrije Universiteit, Amsterdam. The Netherlands, pp. 226.

Bruijnzeel, L.A., 1996. Predicting the hydrological effects of land cover transformation in the humid tropics: the need for integrated research. In: Gash, J.D.C., Nobre, C.A., Roberts, J.M., Victoria, R.L. (Eds.), Amazonian Deforestation and Climate. Wiley, Chichester, pp. 15–55.

Bruijnzeel, L.A., 2004. Hydrological functions of tropical forest: not seeing the soil for the trees? Agric. Ecosyst. Environ., 185–228, http://dx.doi.org/10.1016/j.agee.2004.01.015.

Bruijnzeel, L.A., Bonell, M., Gilmour, D.A., Lamb, D., 2004. Conclusion – forests, water and people in the humid tropics: an emerging view. In: Bonell, M., Bruijnzeel, L.A. (Eds.), Forests, Water and People in the Humid Tropics: Past, Present and Future Hydrological Research for Integrated Land and Water Management. International Hydrology Series, Cambridge University Press, Cambridge, pp. 906–925.

Burnham, K.P., Anderson, D.R., 1998. Model Selection and Inference: A Practical Information-Theoretic Approach. Springer-Verlag, New York, USA, pp. 353.

Central Groundwater Board (CGWB), 2008. Groundwater Information Booklet – Uttara Kannada District, Karnataka. Government of India, Ministry of Water Resources, Central Groundwater Board, South Western Region, Bangalore, November 2008, pp. 24 +Appendices.

Chandler, D.G., 2006. Reversibility of forest conversion impacts on water budgets in tropical karst terrain. For. Ecol. Manage. 224, 95–103.

Chandler, D.G., Walter, M.F., 1998. Runoff responses among common land uses in the uplands of Matalom, Leyte, Philippines. Trans. Am. Soc. Agric. Eng. 41 (6), 1635–1641.

Chappell, N.A., Sherlock, M., Bidin, K., Macdonald, R., Najman, Y., Davies, G., 2007. Runoff processes in Southeast Asia: role of soil, regolith, and rock type. In: Swada, H., Araki, M., Chappell, N.A., LaFrankie, J.V., Shimizu, A. (Eds.), Forest Environments in the Mekong River Basin. Springer-Verlag, Tokyo, pp. 3–23. <http://www.es.lancs.ac.uk/people/nickc/ChappellSherlocketal107.pdf>.

Chaves, J., Neill, C., Germer, S., Neto, S.G., Krusche, A., Elsenbeer, H., 2008. Land management impacts on runoff sources in small Amazon watersheds. Hydrol. Process. 22, 1766–1775. http://dx.doi.org/10.1002/hyp.6803.

Chorley, R.J., 1978. Glossary of terms. In: Kirkby, M.J. (Ed.), Hillslope Hydrology. Wiley, Chichester, UK, pp. 365–375.

Costa, M.H., Botta, A., Cardille, J.A., 2003. Effects of large-scale changes in land cover on the discharge of the Tocantins River, Southeastern Amazonia. J. Hydrol. 283, 206–217.

D'Almeida, C., Vorosmarty, C.J., Hurtt, G.C., Marengo, J.A., Dingman, S.L., Keim, B.D., 2007. The effects of deforestation on the hydrological cycle in Amazonia: a review on scale and resolution. Int. J. Climatol. 27, 633–647. http://dx.doi.org/10.1002/joc.1475.

Davidson, R., MacKinnon, J.G., 1993. Estimation and Inference in Econometrics. Oxford University Press, New York.

DeFries, R., Eshleman, K.N., 2004. Land-use change and hydrologic processes: a major focus for the future. Hydrol. Process. 18, 2183–2186.

de Moraes, J.M., Schuler, A.E., Dunne, T., Figueiredo, R.O., Victoria, R.L., 2006. Water storage and runoff processes in plinthic soils under forest and pasture in eastern Amazonia. Hydrol. Process. 20, 2509–2526.

Dunne, T., 1978. Field studies of hillslope flow processes. In: Kirkby, M.J. (Ed.), Hillslope Hydrology. Wilcv, Chichester, UK, pp. 227–293.

Dunne, T., Black, R.D., 1970. An experimental investivagion of runoff production in pemeable soils. Water Resour. Res. 6, 478–490.

Ebbes, P., 2007. A non-technical guide to instrumental variables and regressor-error dependencies. Qunatile 2, 3–20.

Elsenbeer, H., 2001. Hydrologic flowpaths in tropical rainforest soilscapes – a review. Hydrol. Process. 15, 1751–1759.
Elsenbeer, H., Lack, A., 1996. Hydrometric and hydrochemical evidence for fast flowpaths at La Cuenca, Western Amazonia. J. Hydrol. 180, 237–250.
FAO, 1998. World Reference Base for Soil Resources. FAO-UN, Rome.
FAO-UNESCO, 1974. FAO-UNESCO Soil Map of the World. Legend, UNESCO Press, Paris. Later revised as FAO-UNESCO (1988) Soil Map of the World, vol. 1. Revised Legend. World Soil Resources Report 60. FAO, Rome.
Furey, P.R., Gupta, V.K., 2001. A physically based filter for separating base flow from streamflow time series. Water Resour. Res. 37, 2709–2722.
Garreaud, R.D., Wallace, J.M., 1997. The diurnal march of convective cloudiness over the Americas. Mon. Weath. Rev. 125, 3157–3171.
Garstang, M., Massie Jr., H.L., Halverson, J., Greco, S., Scala, J., 1994. Amazon coastal squall lines. Part I: structure and kinematics. Mon. Weath. Rev. 122, 608–622.
Gadgil, S., Joshi, N.V., 1983. Climatic clusters of the Indian region. J. Climatol. 3, 47–63.
Geological Survey of India, 1981. Geological and Mineral Map of Karnataka and Goa. Geological Survey of India. Calcutta.
Geological Survey of India, 2006. Miscellaneous Publication 30. Part VII. Karnataka and Goa.
Giambelluca, T.W., 2002. Hydrology of altered tropical forest. Hydrol. Process. 16, 1665–1669.
Germer, S., Neill, C., Krusche, A.V., Elsenbeer, H., 2010. Influences of land-use change on near-surface hydrological processes: undisturbed forest to pasture. J. Hydrol. 380, 473–480.
Greco, S., Swap, R., Garstang, M., Ulanski, S., Shipham, M., Harriss, R.C., Talbot, R., Andreae, M.O., Artaxo, P., 1990. Rainfall and surface kinematic conditions over central Amazonia during ABLE 2B. J. Geophys. Res. 95, 17001–17014.
Grip, H., Fritsch, J.M., Bruijnzeel, L.A., 2004. Soil and water impacts during forest conversion and stabilization to new land use. In: Bonell, M., Bruijnzeel, L.A. (Eds.), Forests, Water and People in the Humid Tropics: Past, Present and Future Hydrological Research for Integrated Land and Water Management. UNESCO International Hydrology Series, Cambridge University Press, Cambridge, UK, pp. 561–589.
Gunnell, Y., 1997. Relief and climate in South Asia: the influence of the Western Ghats on the current climate pattern of peninsular India. Int. J. Climatol. 17, 169–1182.
Gunnell, Y., Radhakrishna, B.P., 2001. Sahyadri: The Great Escarpment of the Indian Subcontinent (Patterns of Landscape Development in the Western Ghats). Geological Society of India, Bangalore, pp. 1054.
Hamza, M.A., Anderson, W.K., 2005. Soil compaction in cropping systems: a review of the nature, causes and possible solutions. Soil Tillage Res. 82, 121–145.
Hewlett, J.D., Hibbert, A.R., 1967. Factors affecting the response of small watersheds to precipitation in humid areas. In: Sopper, W.E., Lull, H.W. (Eds.), International Symposium on Forest Hydrology. Pergamon, Oxford, pp. 275–290.
Hijmans, R.J., Cameron, S.E., Parra, J.L., Jones, P.G., Jarvis, A., 2005. Very high resolution interpolated climate surfaces for global land areas. Int. J. Climatol. 25, 1965–1978.
Hillel, D., 1980. Fundamentals of Soil Physics. Academic Press, New York, USA, pp. 413.
Hobbs, N.T., Hilborn, R., 2006. Alternatives to statistical hypothesis testing in ecology: a guide to self teaching. Ecol. Appl. 16, 5–19.
Holscher, D., Mackensen, J., Roberts, J.M., 2004. Forest recovery in the humid tropics: changes in vegetation structure, nutrient pools and the hydrological cycle. In: Bonell, M., Bruijnzeel, L.A. (Eds.), Forests, Water and People in the Humid Tropics – Past, Present and Future Hydrological Research for Integrated Land and Water Management. International Hydrological Series, Cambridge University Press, Cambridge, UK, pp. 598–621.
Howard, A., Bonell, M., Cassells, D., Gilmour, D., 2010. Is rainfall intensity significant in the rainfall–runoff process within tropical rainforests of north-east Queensland? The Hewlett regression analyses revisited. Hydrol. Process. 24, 2520–2537.
HYDSYS/TS, 1991. Time Series Data Management. HYDSYS Pty Ltd. Version 4.0, Weston Creek, ACT, Australia.
Ilstedt, U., Malmer, A., Verbeeten, E., Murdiyarso, D., 2007. The effect of afforestation on water infiltration in the tropics: a systematic review and meta-analysis. For. Ecol. Manage. 251, 45–51.
Johnson, D.H., 1999. The insignificance of statistical significance testing. J. Wildlife Manage. 63, 763–772.
Johnson, J.B., Omland, K.S., 2004. Model selection in ecology and evolution. Trends Ecol. Evol. 19, 101–108.
Kallarackal, J., Somen, C.K., 2008. Water loss from tree plantations in the tropics. Curr. Sci. 94 (2), 201–210.
Kashyap, R.L., 1977. A Bayesian comparison of different classes of dynamic models using empirical data. IEEE Trans. Autom. Control AS-22 (5), 715–727.
Lamb, D., 2011. Regreening the Bare Hills. Tropical Forest Restoration in the Asia-Pacific Region. Series: World Forests, vol. 8. Springer, p. 547. ISBN: 978-90-481-9869-6.
Lamb, D., Erskine, P.D., Parrotta, J.A., 2005. Restoration of degraded tropical forest landscapes. Science 310, 1628–1632.
Lele, S., Hegde, G.T., 1997. Potential herblayer productions and grazing effects in anthropogenic savannahs in the moist tropical forests of the Western Ghats. Trop. Grasslands 31, 574–587.
Lyne, V.D., Hollick, M., 1979. Stochastic time-varying rainfall–runoff modelling. In: Hydrology and Water Resource Symposium, Perth, Inst. Eng., Canberra, Australia, pp. 89–92.
Mackenzie, D.H., 2002. Field measurement of saturated hydraulic conductivity using the well permeameter. In: McKenzie, N., Coughlan, K., Cresswell, H. (Eds.), Soil Physical Measurement and Interpretation for Land Evaluation. CSIRO Publishing, Melbourne, pp. 131–149.
Malmer, A., Murdiyarso, D., Bruijnzeel, L.A.(Sampurno), Ilstedt, U., 2010. Carbon sequestration in tropical forests and water: a critical look at the basis for commonly used generalizations. Global Change Biol. 16, 599–604. http://dx.doi.org/10.1111/j.1365-2486.2009.01984.x.
McKenzie, N.J., Cresswell, H.P., Green, T.W., 2002. Field measurement of unsaturated hydraulic conductivity using tension infiltrometers. In: McKenzie, N., Coughlan, K., Cresswell, H. (Eds.), Soil Physical Measurement and Interpretation for Land Evaluation. CSIRO Publishing, Melbourne, pp. 119–130.
Menon, S., Bawa, K.S., 1998. Deforestation in the tropics: reconciling disparities in estimates for India. Ambio 27, 576–577.
Moore, I.D., Mackay, S.M., Walbrink, P.J., Burch, G.J., O'Loughlin, E.M., 1986. Hydrologic characteristics and modelling of a small forested catchment in south eastern New South Wales. Pre-logging condition. J. Hydrol. 83, 307–335.
NBSSLUP, 1993. Land Evaluation for Land Use Planning, Bull No. 42. National Bureau of Soil Survey and Land Use Planning, Nagpur, India.
New, M., Hulme, M., Jones, P., 1999. Representing twentieth-century space–time climate variability. Part I: development of a 1961–90 mean monthly terrestrial climatology. J. Climate 12, 829–856.
Pascal, J.P., 1982. Bioclimates of the Western Ghats on 1/500,000, 2 sheets. Institute francais de Pondichery, travaux de la Section Scientifique et technique, Hors serie No. 17.
Pascal, J.P., with the collaboration of Shyam Sunder, S., & Meher-Homji, V.M., 1984. Forest Map of South India. Sheet: Belgaum-Dharwar-Panaji. Published by the Karnataka and Goa Forest Department and the French Institute of Pondicherry. Institute francais de Pondichery, travaux de la Section Scientifique et technique, Hors serie No.18c.
Pascal, J.P., 1986. Explanatory Booklet on the Forest Map of South India. Sheets: Belgaum-Dharwar-Panaji; Shimoga; Mercara-Mysore. Karnataka Forest Department and the French Institute of Pondicherry, Rapport, Institute francais de Pondichery, travaux de la Section Scientifique et technique, Hors serie No. 18, India.
Pascal, J.P., 1988. Wet Evergreen Forests of the Western Ghats of India. Institute francais de Pondichery, travaux de la Section Scientifique et technique, Tome 20 bis, p. 345.
Perroux, K.M., White, I., 1988. Designs for disc permeameters. Soil Sci. Am. J. 52, 1205–1215.
Pinheiro, J.C., Bates, D.M., 2000. Mixed-Effects Models in S and S-PLUS. Springer, esp. pp. 100, 461.
Pomeroy, M., Primack, R., Rai, S.N., 2003. Changes in four rainforest plots of the Western Ghats, India, 1939–1993. Conserv. Soc. 1, 113–135.
Pontius, R.G., Pacheco, P., 2004. Calibration and validation of a model of forest disturbance in the Western Ghats, India 1920–1990. GeoJournal 61 (4), 325–334. http://dx.doi.org/10.1007/s10708-004-5049-5.
Priya, D., Prita, D., Arjun, M., Pratjeesj, C.M., Carrigues, J.P., Puryavaud, J.P., Roessingh, K., 2007. Forest degradation in the Western Ghats biodiversity hotspot: resources collection, livelihood concerns and sustainability. Curr. Sci. 93 (11), 1573–1578.
Putty, M.R.Y., Prasad, R., 2000a. Runoff processes in headwater catchments – an experimental study in Western Ghats, South India. J. Hydrol. 235, 63–71.
Putty, M.R.Y., Prasad, R., 2000b. Understanding runoff processes using a watershed model—a case study in the Western Ghats in South India. J. Hydrol. 228, 215–227.
Putty, M.R.Y., Prasad, V.S.R.K., Ramaswamy, R., 2000. A study of the rainfall intensity pattern in Western Ghats, Karnataka. In: Varadan, K.M. (Ed.), Proc. Workshop on Watershed Development in the Western Ghats Region of India, 28–29 February 2000, Centre for Water Resources Development and Management, Kozhikode 673 571, Kerala, pp. 44–51 (Summarised in Bonell et al. (2004)).
Putty, M.R.Y., 2006. Salient features of the hydrology of the Western Ghats in Karnataka. In: Krishnaswamy, J., Lele, S., Jayakumar, R. (Eds.), Hydrology and Watershed Services in the Western Ghats of India. Tata-McGraw Hill Publication, New Delhi, p. 65.
Rai, S.N., 1999. Nursery and Planting Techniques of Forest Trees in Tropical South-Asia. Punarvasu Publications Dharwad, Karantaka – Eastern Press, Bangalore, India, 217 pp.
Rai, N.D., 2004. The socio-economic and ecological impact of garcina gumm-gutta fruit harvest in the Western Ghats, India. In: Kusters, K., Becher, B. (Eds.), Forest Products, Livelihoods and Conservation. Case Studies of Non-Timber Forest Product Systems: Asia, vol. 1. CIFOR, pp. 23–42.
Ramachandra, T.V., Kamakshi, G., Shruthi, B.B., 2004. Bio resource status in Karnataka. Renew. Sustain. Energy Rev. 8, 1–47.
Ramesh, B.R., Pascal, J., 1997. Atlas of Endemics of the Western Ghats (India): Distribution of Tree Species in the Evergreen and Semi-Evergreen Forests. Institut Francais de Pondichery, Publications du department d'ecologie 38.
Ramesh, B.R., Swaminath, M.H., with many collaborators, 1999. Assessment and Conservation of Forest Biodiversity in the Western Ghats of Karnataka, India. French Institute of Pondicherry in Collaboration with the Karnataka Forest Department and Fonds Français de l'Environnement Mondial, December 1999, Report available from l'Insitut Français de Pondicherry, 126 pp. (text plus bibliography, maps, colour plates, 5 Annexes).
Rodriguez, D.A., Tomasella, J., Linhares, C., 2010. Is forest conversion to pasture affecting the hydrological response of Amazonian catchments? Signals in the Ji-Parana Basin. Hydrol. Process. 24 (10), 1254–1269.

Sadler, J.C., Lander, M.A., Hori, A.M., Oda, L.K., 1987. Tropical Marine Climatic Atlas, Volume I (Indian Ocean and Atlantic Ocean) and Volume II (Pacific Ocean), Department of Meteorology, University of Hawaii. Available from Dept. Meteorology, University of Hawaii, Honolulu, 96822.

Safriel, U.N., 2007. The assessment of global trends in land degradation. In: Sivakumar, M.V.K., Ndiang'ui, N. (Eds.), Climate and Land Degradation. Springer, pp. 1–38.

Sandstrom, K., 1998. Can forest "provide" water: widespread myth or scientific reality? Ambio 27, 132–138.

Schwarz, G., 1978. Estimating the dimension of a model. Ann. Stat. 6 (2), 461–464.

Scott, D.F., Bruijnzeel, L.A., Mackensen, J., 2004. The hydrological impacts of reforestation of grasslands, natural and degraded and of degraded forest in the tropics. In: Bonell, M., Bruijnzeel, L.A. (Eds.), Forests, Water and People in the Humid Tropics: Past, Present and Future Hydrological Research for Integrated Land and Water Management. UNESCO, Cambridge University Press, Cambridge, UK, pp. 622–651.

Searcy, J.K., Hardison, C.H., 1960. Double Mass Curves. U.S. Geological Survey, Water-Supply Paper 1541-B, 66p.

Seen, D.L., Ramesh, B.R., Nair, K.M., Martin, M., Arrouay, D., Bourgeon, G., 2010. Soil carbon stocks, deforestation and land-cover changes in the Western Ghats biodiversity hotspot (India). Global Change Biol. 16, 1777–1792. http://dx.doi.org/10.1111/j.1365-2486.2009.02127.x.

Shivaprasad, C.R., Reddy, R.S., Sehgal, J., Velayutham, M., 1998. Soils of Karnataka. Soils of India Series, National Bureau of Soil Survey and Land Use Planning (NBSSLUP), Publ. No. 47, 88pp.

Singh, N., 1986. On the duration of the rainy season over different parts of India. Theor. Appl. Climatol. 37, 51–62.

Soil Survey Staff, 1975 (later second edition 1999). Soil Taxonomy: A Basic System of Soil Classification for Making and Interpreting Soil Surveys. US Department of Agriculture Handbook. No. 436, pp. 754.

Swank, W.T., Swift, L.W., Douglass, J.E., 1988. Streamflow changes associated with forest cutting, species conversions, and natural disturbances. In: Swank, W.T., Crossley, D.A. (Eds.), Forest Hydrology and Ecology at Coweeta. Springer.

Talsma, T., 1987. Re-evaluation of the well permeameter as a field method for measuring hydraulic conductivity. Aust. J. Soil Res. 25, 361–368.

Talsma, T., Hallam, P.M., 1980. Hydraulic conductivity measurement of forest catchments. Aust. J. Soil Res. 18, 139–148.

van Dijk, A.I.J.M., Keenan, R.J., 2007. Overview – planted forests and water in perspective. For. Ecol. Manage. 251, 1–9.

Venkatesh, B., Lakshman, N., Purandara, B.K., Reddy, V.B., 2011. Analysis of observed soil moisture patterns under different land covers in Western Ghats, India. J. Hydrol. 397, 281–294.

White, H., 2001. Asymptotic Theory for Econometricians. Academic Press, New York.

Young, P.C., 2011. Recursive Estimation and Time Series Analysis: An Introduction for Student and Practitioner. Springer, New York.

Zhou, G.Y., Morris, J.D., Yan, J.H., Yu, Z.Y., Peng, S.L., 2001. Hydrological impacts of reafforestation with eucalypts and indigenous species: a case study in southern China. For. Ecol. Manage. 167, 209–222.

Ziegler, A.D., Giambelluca, T.W., Plondke, D., Leisz, S., Tran, L.T., Fox, J., Nullet, M.A., Vogler, J.B., Troung, D.M., Vien, T.D., 2007. Hydrological consequences of landscape fragmentation in mountainous northern Vietnam: buffering of Hortonian overland flow. J. Hydrol. 337, 52–67.

Ziegler, A.D., Giambelluca, T.W., Vana, T.T., Nullett, M.A., Fox, J., Tran, D.V., Pitthong, J., Maxwell, J.F., Evett, S., 2004. Hydrological consequences of landscape fragmentation in mountainous northern Vietnam: evidence of accelerated overland flow generation. J. Hydrol. 287, 124–146.

Zimmermann, B., Elsenbeer, H., 2008. Spatial and temporal variability of saturated hydraulic conductivity in gradients of disturbance. J. Hydrol. 361 (1–2), 78–95.

Zimmermann, B., Elsenbeer, H., 2009. The near-surface hydrological consequences of disturbance and recovery: a simulation study. J. Hydrol. 364 (1–2), 115–127.

Zimmermann, B., Elsenbeer, H., de Moraes, J.M., 2006. The influence of land-use changes on soil hydraulic properties: implications for runoff generation. For. Ecol. Manage. 222, 29–38.

Journal of Hydrology 498 (2013) 191–209

Contents lists available at SciVerse ScienceDirect

Journal of Hydrology

journal homepage: www.elsevier.com/locate/jhydrol

# The groundwater recharge response and hydrologic services of tropical humid forest ecosystems to use and reforestation: Support for the "infiltration-evapotranspiration trade-off hypothesis"

Jagdish Krishnaswamy [a,*], Michael Bonell [b], Basappa Venkatesh [c], Bekal K. Purandara [c], K.N. Rakesh [a], Sharachchandra Lele [a], M.C. Kiran [a], Veerabasawant Reddy [d], Shrinivas Badiger [a]

[a] Ashoka Trust for Research in Ecology and the Environment (ATREE), Royal Enclave, Sriramapura, Jakkur Post, Bangalore 560 064, India
[b] The Centre for Water Law, Water Policy and Science under the auspices of UNESCO, University of Dundee, Dundee DD1 4HN, Scotland, UK
[c] Hard Rock Regional Centre, National Institute of Hydrology, Belgaum, Karnataka 590 001, India
[d] TERI, WRC, H. No. 233/GH-2, Vasudha Housing Colony, Alto Santa Cruz, Bambolim, Goa 403 202, India

ARTICLE INFO

*Article history:*
Received 8 October 2012
Received in revised form 7 June 2013
Accepted 19 June 2013
Available online 27 June 2013
This manuscript was handled by Konstantine P. Georgakakos, Editor-in-Chief, with the assistance of Matthew Rodell, Associate Editor

*Keywords:*
Infiltration
Evapotranspiration
Groundwater recharge
Western Ghats
Hydrologic services
Tropical forests

SUMMARY

The hydrologic effects of forest use and reforestation of degraded lands in the humid tropics has implications for local and regional hydrologic services but such issues have been relatively less studied when compared to the impacts of forest conversion. In particular, the "*infiltration-evapotranspiration trade-off*" hypothesis which predicts a net gain or loss to baseflow and dry-season flow under both, forest degradation or reforestation depending on conditions has not been tested adequately. In the Western Ghats of India, we examined the hydrologic responses and groundwater recharge and hydrologic services linked with three ecosystems, (1) remnant tropical evergreen forest (NF), (2) heavily-used former evergreen forest which now has been converted to tree savanna, known as degraded forest(DF), and (3) exotic Acacia plantations (AC, *Acacia auriculiformis*) on degraded former forest land. Instrumented catchments ranging from 7 to 23 ha representing these three land-covers (3 NF, 4 AC and 4 DF, in total 11 basins), were established and maintained between 2003 and 2005 at three sites in two geomorphological zones, Coastal and Up-Ghat (Malnaad). Four larger (1–2 $km^2$) catchments downstream of the head-water catchments in the Malnaad with varying proportions of different land-cover and providing irrigation water for areca-nut and paddy rice were also measured for post-monsoon baseflow. Daily hydrological and climate data was available at all the sites. In addition, 36 min data was available at the Coastal site for 41 days as part of the opening phase of the summer monsoon, June–July 2005.

Low potential and actual evapotranspiration rates during the monsoon that are similar across all land-cover ensures that the main control on the extent of groundwater recharge during the south-west monsoon is the proportion of rainfall that is converted into quick flow rather than differences in evapotranspiration between the different land cover types. The Flow duration curves demonstrated a higher frequency and longer duration of low flows under NF when compared to the other more disturbed land covers in both the Coastal and Malnaad basins. Groundwater recharge estimated using water balance during the wet-season in the Coastal basins under NF, AC and DF was estimated to be 50%, 46% and 35% respectively and in the Malnaad it was 61%, 55% and 36% respectively. Soil Water Infiltration and Movement (SWIM) based recharge estimates also support the pattern (46% in NF; 39% in AC and 14% in DF). Furey–Gupta filter based estimates associated with the Coastal basins also suggest similar groundwater recharge values and trends across the respective land-covers: 69% in NF, 49% in AC, and 42% in DF. Soil water potential profiles using zero flux plane methods suggest that during the dry-season, natural forests depend on deep soil moisture and groundwater. Catchments with higher proportion of forest cover upstream were observed to sustain flow longer into the dry-season. These hydrologic responses provide some support towards the "*infiltration-evapotranspiration trade-off*" hypothesis in which differences in infiltration between land-cover rather than evapotranspiration determines the differences in groundwater recharge, low flows and dry-season flow. Groundwater recharge is the most temporally stable under natural forest, although substantial recharge occurs under all three ecosystems, which helps to

* Corresponding author. Tel.: +91 80 23635555x209; fax: +91 80 23530070.
*E-mail address:* jagdish@atree.org (J. Krishnaswamy).

0022-1694/$ - see front matter 
http://dx.doi.org/10.1016/j.jhydrol.2013.06.034

sustain dry-season flow downstream in higher order streams that sustain local communities and agro-ecosystems. In addition to spatial scale effects, greater attention also needs to be given to the role of hydrogeology within the context of the above hypothesis and its implications for hydrologic services.



## 1. Introduction

Land use and land cover change profoundly transformed terrestrial hydrological budgets and processes (Vorosmarty and Sahagian, 2000; Stonestrom et al., 2009). Although the effects occur at multiple spatial scales from local (small basins) to global, the scale at which local communities and land-use managers are affected is of special concern as decision making on ecosystem services, especially hydrologic services is often at this scale (<10 km$^2$). In tropical landscapes where land-cover and land-use change have been rapid and complex, this issue is of particular interest (Turner et al., 1994). One of the important paradigms that was dominant for much of the 20th century in local scale terrestrial hydrology, and supported by observed and experimental data, is the relationship between accumulation of forest biomass and decrease in stream flow as a result of increased evapotranspiration, or vice versa, in the case of loss of forest cover (Bosch and Hewlett, 1982; Brown et al., 2005). However, based on emerging evidence to the contrary, especially from the tropics, Bruijnzeel (1989, 2004) proposed the "*infiltration-evapotranspiration trade-off hypothesis*". Part of this hypothesis states that under certain conditions of land-cover and land-use change in the seasonal tropics, a degraded forest's ability to allow sufficient infiltration may be impaired to such an extent that the effects on delayed flow or dry-season flow would be detrimental, even after accounting for gains from reduced evapotranspiration. Recent work in the Andes mountains of Columbia by Roa-García et al. (2011) put forward some of the first evidence in support of the *Infiltration- Evapotranspiration 'trade-off'* hypothesis based on a comparative basin study (0.6–1.7 km$^2$), albeit involving volcanic ash deposits i.e., Andisols, that are vastly different than the soils in the Western Ghats. Roa-García et al. (2011) noted in particular that their stream flow frequency–duration curves (FDCs) highlighted that the basin with highest forest cover (68%) showed the smallest reduction in flow during the dry season. Moreover the highest low flows were maintained during the dry season from this forest-dominated basin in contrast to a grassland dominated basin. In addition, soil moisture release curves undertaken in that study showed that the natural forests has a larger capacity to store and release soil moisture in comparison to the grassland. These writers thus concluded that the preceding two findings support the "*infiltration-evapotranspiration trade-off*" hypothesis for tropical environments (for) soils that are subject to compaction (such as highly grazed grasslands) have a reduced rainfall infiltration, which impairs the maintenance of baseflows." (Roa-García et al., 2011, p.11).

In formerly forested regions in the humid tropics, notably in the more densely populated regions of south and south–east Asia such as the Western Ghats of India, major land-cover changes have occurred at a century time scale. The latter have included permanent deforestation and conversion to a variety of agro-forestry and agro-ecosystems, regrowth as well as reforestation. Consequently there is a particular need for decision makers and policy makers to have information from hydrological studies that address the fundamental processes associated with such land cover changes. Over 100 million people depend on surface water sources in streams and rivers that emanate from the Western Ghats. Further this region is a major repository of carbon in its forests and soils (Seen et al., 2010) and is a global biodiversity hotspot (Das et al., 2006). In an era where various ecosystem services are being recognized and valued, it is essential for ecological economists, policy and decision makers to be aware of the synergies and trade-offs between various regulatory and provisioning services (Elmqvist et al., 2010). Thus an investigation of the hydrological effects of specific land-cover changes is a high priority (DeFries and Eshleman, 2004).

### 1.1. Relevant previous work in the study area

In previous work, we established that the soil hydraulic properties (notably field, saturated hydraulic conductivity (Bouwer, 1966)), $K_{fs}$, in the tropical, humid Western Ghats can be significantly altered from land-cover change up to a century time scale from forest conversion or degradation. The enhanced occurrence of infiltration-excess overland flow (*IOF*) was inferred (and thus reduced vertical percolation and groundwater recharge) when comparing selected rainfall intensity–duration–frequency with $K_{fs}$ across both various land covers and soil types. Such changes are sufficient to allow the hill slope hydrology aspects of the infiltration-evapotranspiration trade-off hypothesis to be realized (Bonell et al., 2010).

Later work using experimental catchments also showed how land-cover change from native forest to heavily used forest and its subsequent reforestation have major effects on the rain-runoff process in the wet-season (Krishnaswamy et al., 2012). They showed the highest proportions of rain converted to runoff being associated with the degraded forests whereas the natural forests showed the lowest runoff yields. Using stream hydrograph separation, they also reported much higher quick flow volumes from degraded forest and reforested, former degraded land in the form of *Acacia auriculiformes* plantations when compared to the less disturbed natural forest. Furthermore, time series analysis showed much shorter rainfall-runoff time lags for the degraded forest and *Acacia auriculiformes* plantations when compared to natural forest. This characteristic of a faster rainfall-runoff responsiveness supports the notion of the frequent occurrence of *IOF* within the former two, more human-impacted land covers. Pertinent to the current work, the data in Krishnaswamy et al., 2012, clearly indicates that even assuming the maximum measured annual evapotranspiration (AET) for humid forests globally (~1500 mm, Kume et al., 2011), the estimated water available for recharge from natural forest catchments annually after accounting for both measured runoff and AET was 259 mm (rainfall of 2252 mm) and 978 mm (rainfall of 4016 mm). Thus we concluded from the earlier work that (i) a significant amount of rainfall was potentially available for recharge to groundwater and for downstream baseflow and dry-season flow, (ii) deeper subsurface water or groundwater of possible large capacity, had a significant role in the storm runoff generation process and (iii) the continuation of a secondary, longer rainfall-runoff time lag in the intensely, disturbed land covers indicated that there was a retention of 'memory' of the previous natural forest response.

In the current study, the more detailed aspects of the wet and dry season flows and the water balances of these same catchments were investigated in relation to modelled evapotranspiration, and thus the provision of various estimates of recharge to groundwater.

## 2. Objectives

We will attempt to test the "*infiltration-evapotranspiration trade-off*" hypothesis in the humid Western Ghats by quantifying the groundwater recharge and low flow characteristics components within 11 experimental basins in the Upghat (Malnaad) and Coastal regions across three land covers (Natural Forest, Degraded Forest, Acacia Plantations) within Uttara Kannada. In the absence of detailed process hydrology information, we will use several approaches to evaluate if there is a consistency in the interpretation of the results. The techniques used are as follows:

- The development of basin frequency–duration–curves (FDC).
- The use of basin water balances in the wet season.
- The application of the Furey–Gupta (2001) filter hydrograph model.
- An evaluation of soil water hydraulic potentials in the absence of rainfall and thus confined to dry season only in combination with the application of the zero flux plane (ZFP) method.
- Finally, a brief assessment of the scale issue and downstream dry-season river flow will be subsequently considered.

## 3. Study area

### 3.1. Landscape, soils, geology and hydrogeology

The locations of the 11 instrumented head-water catchments (listed in Table 1) are shown in Fig. 1. In the Malnaad these are located and nested within four larger catchments that supplied irrigation water to downstream areca nut plantations and rice-paddies. As indicated in Table 1, there are two groups of experimental basins which are located in two of the three distinct landforms identified in the classification of Gunnell and Radhakrishna (2001), *viz*, the Coastal plain and the hilly Upghat or Malnaad region (see also Fig. 1 in Bonell et al., 2010; Krishnaswamy et al., 2012). The geology is mainly Archaen-Proterozoic-Dharwad schist and granitic gneissic, meta-volcanic and some recent sediment in the coastal belt. Greywacke prevail from the Western slopes to the Malnaad (Geological Survey of India, 1981).

Many of the upper geological sequences of this region are laterialized due to their exposure to suitable climatic conditions over a prolonged period. Their thickness ranges from a few cm to as much as 60 m in depth (Geological Survey of India, 2006). Figure 16b in Bourgeon (1989) provided a simplified latitudinal cross-section of the geology and location of laterites (known as lateritic caps) from the coast through to the Malnaad (incorporating Siddapur and Sirsi, shown in Bonell et al., 2010). This cross – section is in proximity to the latitude where the study basins are located.

In the escarpment of the Ghats, the catchments in the Coastal zone are dominated by rocks of the Archean complex. The associated soils are dominated by 1:1 clays associated with iron and aluminium oxy hydroxides. We used the Indian soil classification system (NBSSLUP, 1993, Shivaprasad et al., 1998; Bonell et al., 2010) and these Coastal basin soils belong to the Laterite soil group. Under the FAO system these soils are mixture of Eutric Nitosols and Acrisols (FAO-UNESCO, 1974; FAO, 1998) and would be classified under the USDA system as Alfisols, Ultisols and Oxisols (Soil Survey Staff, 1975, 1999) (Table 1). A separate French survey of the Western Ghats undertaken by Bourgeon (1989) described the soils as being "Lithosols" and "Ferrallitic". A soil description of the evergreen forest within ~5 km of the Coastal basins is provided elsewhere (Table 1, Bourgeon, 1989 and reproduced in Krishnaswamy et al., 2012).

The catchments in the Malnaad are on the back slopes of the Western Ghats, deeply dissected, and the geology is dominated by Greywackes. The associated soils have similar clay minerals as above. They are classified as Red and Laterite (Shivaprasad et al., 1998), with similar equivalent classifications of FAO to those soils of the Coastal basins. When concerning the USDA, they are a mixture of Alfisols, Inceptisols and Oxisols (Shivaprasad et al., 1998; Table 1).

The soils in both the Coastal and Malnaad basins are deeply weathered similar to the description of Putty and Prasad (2000a).

**Table 1**
The physical characteristics of the experimental basins in the Up-ghat (Malnaad) and Coastal regions. Land-cover types include natural forest (NF), acacia (AC) and degraded forest (DF).

| Basin | Site | Land cover | Area (ha) | Land cover code | Average elevation (m) | Average slope (deg) | Mean annual rainfall (1988–1997) (mm) | Soil type as per Indian Soil Classification and USDA *Soil Survey Staff* (1999)[a]; NBSSLUP (Shivaprasad et al., 1998) |
|---|---|---|---|---|---|---|---|---|
| *Coastal basins* | | | | | | | | |
| 1 | Areangadi | Natural Forest | 23 | NF1 | 255.03 | 17.16 | 3672 | Laterite, Clayey, kaolinitic, *Ultisol (Ustic Kandihumults)* |
| 2 | Areangadi | Degraded Forest | 7 | DF1 | 52.71 | 10.38 | 3793 | Laterite, Clayey, kaolinitic,*Ultisol (Ustic Kandihumults)* |
| 3 | Areangadi | Acacia | 7 | AC1 | 112.25 | 15.23 | 3793 | Laterite, Clayey-skeletal, kaolinitic, *Ultisol (Petroferric Haplustults)* |
| *Malnaad (UP-GHAT)* | | | | | | | | |
| 4 | Vajgar | Natural Forest | 9 | NF1 | 618.09 | 7.51 | 2750 | Red, Fine, kaolinitic, *Alfisol(Kandic Paleustalfs)* |
| 5 | Vajgar | Degraded Forest | 10 | DF1 | 587.27 | 7.07 | 2750 | Laterite, Fine, kaolinitic, *Alfisol(Kandic Paleustalfs* |
| 6 | Kodigibail | Natural Forest | 6 | NF1 | 540.14 | 7.56 | 2750 | Red, Clayey-skeletal, kaolinitic, *Inceptisol(Ustoxic Dystropepts)* |
| 7 | Kodigibail | Degraded Forest1 | 9 | DF1 | 522.16 | 4.76 | 2948 | Red, Clayey-skeletal, kaolinitic, *Inceptisol(Ustoxic Dystropepts)* |
| 8 | Kodigibail | Degraded Forest2 | 45 | DF2 | 536.50 | 5.10 | 2948 | Red, Clayey-skeletal, kaolinitic, *Inceptisol(Ustoxic Dystropepts)* |
| 9 | Kodigibail | Acacia1 | 7 | AC1 | 538.00 | 5.51 | 2948 | Red, Clayey-skeletal, kaolinitic, *Inceptisol, (Ustoxic Dystropepts)* |
| 10 | Kodigibail | Acacia3[b] | 6 | AC3 | 544.83 | 4.34 | 2948 | Red, Clayey-skeletal, kaolinitic, *Inceptisol, (Ustoxic Dystropepts)* |
| 11 | Kodigibail | Acacia2 | 23 | AC2 | 544.10 | 3.36 | 2948 | Red, Clayey-skeletal, kaolinitic, *Oxisol(Ustoxic Dystropepts)* |

[a] NBSSLUP – National Bureau of Soil Survey and Land Use Planning.
[b] Acacia3 is nested within Acacia2.

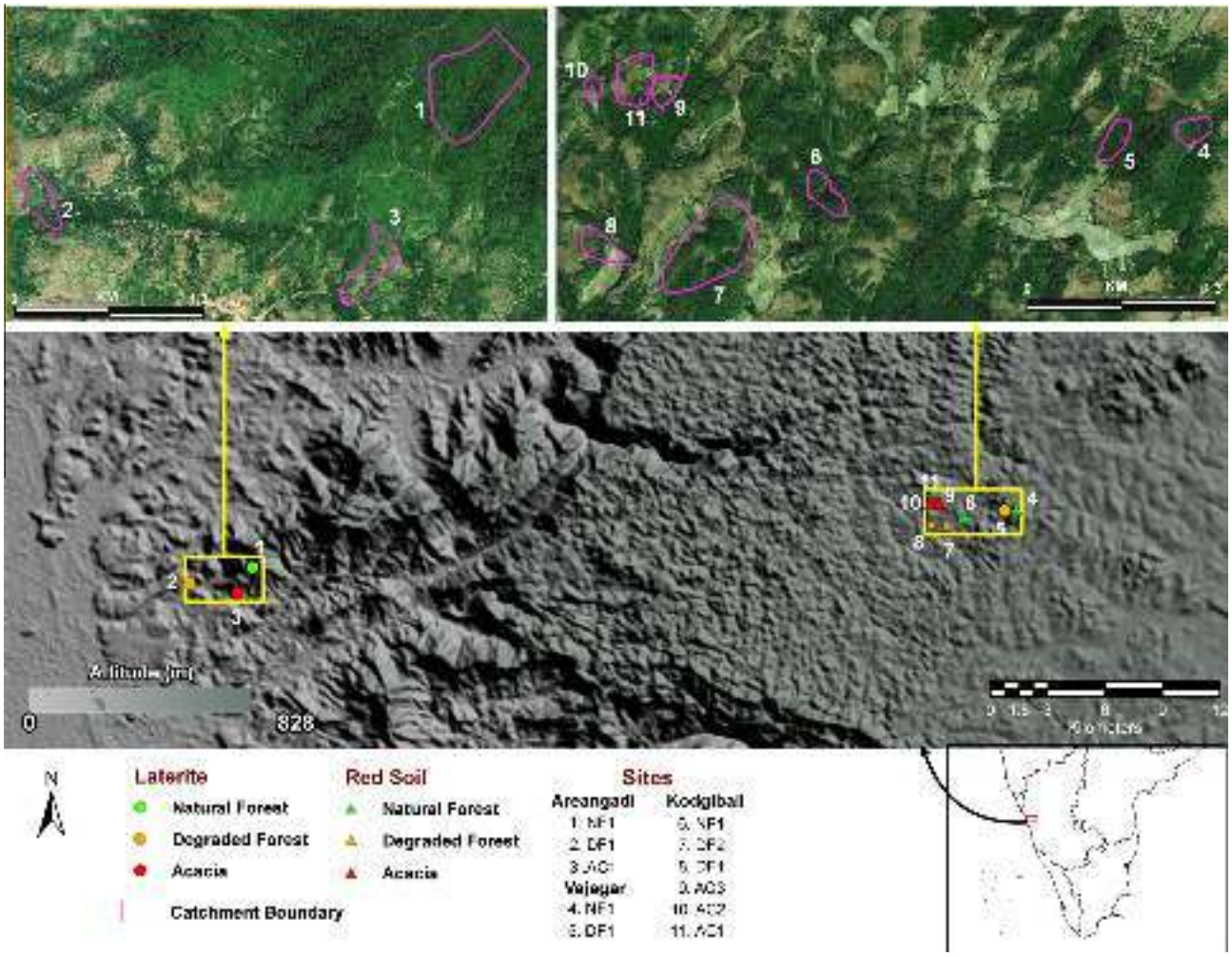


**Fig. 1.** The location, soil types and land covers of the research basins in the Western Ghats, Uttara Kannada District of Karnataka State.

In the absence of any deep drilling in the basins, however no detailed soil descriptions down to bed rock exist. Exposures in hills and stream banks do suggest that soils extend well beyond 2 m in depth. Further no detailed mapping of soil pipe occurrence (Putty and Prasad, 2000a,b) was undertaken, although we have observed soil pipes in the forested catchments in the region and there was evidence of vertical macro-pore flow in soil exposures and an example is shown in Fig. 2 of Krishnaswamy et al., 2012.

The main aquifers in the study area are the weathered and fractured zones of metavolcanics, metasedimentaries, granites and gneisses, laterites, along with the alluvial patches found along the major stream courses. Significantly there is no primary porosity in the hard rocks. It is the secondary structures like joints, fissures and faults present in these formations up to ~185 m below ground level (mbgl) which act as a fractured rock aquifer (e.g., Cook, 2003) with an effective porosity of 1.0 – 3.0% and contain groundwater. The transmissivity of aquifer material are in the general range from 2.09 to 24.41 $m^2\ day^{-1}$ (CGWB, 2008). At depths $\leqslant$30 mbgl unconfined, groundwater dominates but there is a tendency towards a more confined status at greater depths due to the complexity of the geological formations and associated fracture zones. Spot surveys undertaken in May (pre-monsoon) and November (post-monsoon) 2006 and using a network of 30 of the national hydrograph stations, showed that pre-monsoon water levels between 5 and 10 mbgl were typical over large parts of Uttara Kannada. In the post-monsoon, the prevailing depths within the Coastal and Malnaad areas were respectively 2–5 and 5–10 mbgl (CGWB, 2008).

### 3.2. Climate

The climate is classified under Koppen as 'tropical wet and dry'. Rainfall is monsoonal and unimodal (June to September). The annual rainfall varies from 3979 mm in the Coastal zone to 3275 mm in the Malnaad (1950–2000 mm average, derived from Hijmans et al., 2005). Long-term annual reference Potential evapotranspiration (PET) is 1482 mm for the Coastal basins and 1527 mm in the Malnaad basins (Hijmans et al., 2005).

On a monthly basis, and pertinent to this paper, there is marked reduction in PET following the onset of the monsoon in June until its termination from October onwards (Hijmans et al., 2005) and shown in Fig. 2. This 'dip' in PET is due to persistent high humidity and cloudiness with frequent rainfall (Bourgeon, 1989; Hijmans et al., 2005). Of high relevance to the current work, there have been no studies undertaken in the Western Ghats that have made direct measurements of actual evapotranspiration (AET) using micrometeorological methods. Consequently AET estimates will be derived from modelling.

The dry season lasts from 5 to 6 months and so during this time PET > rainfall. The annual mean temperature ranges from 26.4 °C in the Coastal plains and slopes, to 24.5 °C in the Malnaad (Hijmans et al., 2005). Annual average relative humidity is ~72.3% in the

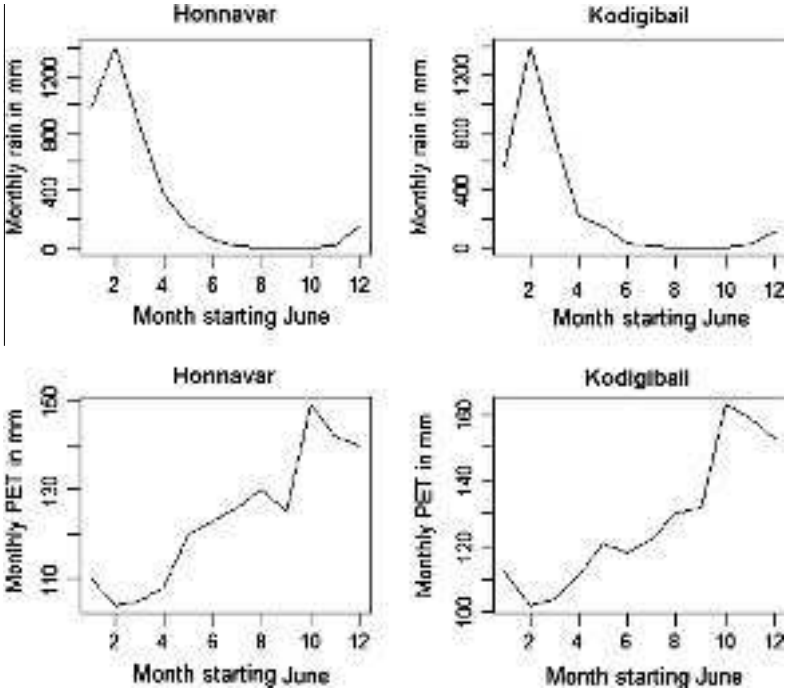


**Fig. 2.** Time series of rainfall and Potential evapotranspiration, PET for the Coastal and Malnaad (Up-Ghat) sites (after Hijmans et al., 2005).

Coastal basins and 70% on the Malnaad slopes (1960–1990, New et al., 1999).

Maximum rainfall intensities for a duration of 15 min across the study area range from 50 mm $h^{-1}$ (1 in 1 year) to 130 mm $h^{-1}$ (1 in 50 year) (Bonell et al., 2010). Overall these short-term rainfall intensities are comparatively low by global standards for the humid tropics (Bonell et al., 2004). On the other hand, the long duration of rain events (often over several days) ensures very high precipitation totals (Putty and Prasad, 2000a,b) and the latter was also shown in Krishnaswamy et al. (2012).

### 3.3. Vegetation and land-cover/land-use

The natural and modified vegetation of the study area is highly diverse in response to the equally complex geology, geomorphology and climate of the Western Ghats. Based on criteria such as physiognomy, phenology and floristic composition, the vegetation of the study area is classified principally as evergreen and semi-evergreen which are two of the five major floristic types identified within several detailed studies of the region (Pascal, 1982, 1984, 1986, 1988; Ramesh and Pascal, 1997; Ramesh and Swaminath, 1999). Within the framework of a highly fragmented land cover and land use system (Blanchart and Julka, 1997; Menon and Bawa, 1998; Pomeroy et al., 2003; Pontius and Pacheco, 2004; Seen et al., 2010), there are typically three principal stable patterns of land use and management, *viz*:

- Less disturbed, dense forest (referred to also as *Natural Forest, NF, or Forest)* which has resulted from a limited extraction regime, and is commonly associated with Reserve Forest patches.
- Dominantly tree savannas (*Degraded Forest, DF, or Degraded*) that result from intense harvest of fuel wood, leaf and litter manure and grass, as well as intermittent fires (Rai, 2004; Priya et al., 2007). These tree savannas were previously occupied by mostly evergreen and semi-evergreen forest prior to severe disturbance over decadal to century time scales. The specie composition, tree density and basal area of this land cover however can be highly variable between first-order basins (see Table 1).
- Exotic *Acacia auriculiformes* plantations planted since 1980 (*Acacia, AC*) that are part of the 'forestation' programme of the Karnataka Forest Department (Rai, 1999). Typically these plantations have replaced grazing land, or highly degraded forest land, some of which have become barren land. The initial survival of the AC plantings has been ensured through fencing and guarding. The ages of AC plantations in the study basins ranged from to 7 to 12 years at the time of the hydrological data collection (Krishnaswamy et al., 2012). Historically, people would have used and occupied the more accessible sites, which are currently under "degraded" forests or are under "restoration" through establishment of tree plantations.

Detailed description of the dominant vegetation types in the experimental basins are given elsewhere (Krishnaswamy et al., 2012). It should be noted that the Acacia plantations are not wholly monoculture but do incorporate a few other species. One of the Acacia basins (Kodigibail, *Acacia 3* in Table 1) is nested within another (i.e. *Acacia 2*) and the latter basin also includes some agriculture.

In the Malnaad the head-water basins are nested within more heterogeneous catchments that supply water to local communities and provide irrigation water to areca nut plantations, home gardens, orchards and rice paddies.

### 3.4. Tree root depths

Krishnaswamy et al. (2012) summarised knowledge of tree root patterns in the study area. Roots extend well beyond 2 m depth under the Natural Forest. For the young Acacia plantations most roots were located at <1.5 m depth and are known to be more densely concentrated between 0.3 and 1.0 m (Kallarackal and Somen, 2008). Depth of roots under the Degraded Forest were more varying, but mostly <0.6 m, depth due to the more extensive low

herbaceous cover (dominated by grass species) in between the surviving trees.

### 3.5. The experimental basins

Krishnaswamy et al. (2012) provided details of the experimental basins. In summary, the complex mosaic of land use in the study area resulted in most basins having small areas (⩽10 ha) to ensure as close as possible 'homogeneity' in land cover for each basin. Moreover the sub-soil field, saturated hydraulic conductivity, $K_{fs}$ down to 1.5 m depth is comparatively permeable (in excess of 10 mm $h^{-1}$) when compared to other reports elsewhere in similar soil groups (Bonell et al., 2010; Krishnaswamy et al., 2012). This combination of a marked concentration of rainfall in few months, small basin areas, comparatively permeable sub-soils and a fissured hydrogeology results in most of the study basins having intermittent flow regimes (i.e., no perennial flow). Streamflow terminates after the end of the monsoon at different times within each basin and will be later considered in this paper and the recharge during the monsoon at smaller scales aggregates and contributes to baseflow in higher order perennial streams.

## 4. Methods

### 4.1. Rainfall-runoff

Stream discharge in each of the 11 catchments (Table 1) was measured using either weirs or stage-velocity-discharge methods. In addition all catchments in the Coastal zone (Areangadi, Table 1) were instrumented with staff gauge, mechanical water-level recorders and a self-recording rain gauge. As these three basins were spatially close together, the same data from the one self-recording rain gauge was used. In the Malnaad group, rainfall and runoff data were collected daily supported by additional manual measurements of stream stage taken up to four times a day.

In summary, daily rainfall and stream discharge data for the years 2003, 2004 and 2005 are available for the Kodigibail and Vajagar catchments in the Upghat (Malnaad), and for 2004–2005 for the three Coastal basins (Table 4). In addition for part of the summer monsoon of 2005 (16 June–26 July, i.e., a total of 41 days), 36 min (0.6 h) data was available for rainfall-runoff for selected storms in the three Coastal catchments. Such information enabled us to monitor temporal changes in the rainfall-runoff response following the onset of the monsoon until maximum basin wetness was attained.

As indicated in Fig. 1, some of the small and relatively homogeneous catchments in the Malnaad sites were nested within larger basins (1.0–2.5 $km^2$) with different proportions of forest cover (as shown in Table 2). Downstream, these larger basins were instrumented with V-notches from December 14, 2004. Such steps will enable an assessment of the dry season flows at these larger scales.

**Table 2**
Summary of the downstream basins in terms of area and land-cover. These basins are located downstream of the more homogeneous head-water basins and typically have mixed land-cover.

| Catchment | Total area ($km^2$) | Percent of area (%) | | |
|---|---|---|---|---|
| | | Forest | Acacia | Others |
| Golikai | 1.05 | 27.2 | 5.2 | 67.6 |
| Kodigibail[a] | 2.42 | 26.5 | 6.6 | 66.9 |
| Nirmundagi | 1.64 | 15.3 | 7.4 | 77.3 |
| Vajgar[b] | 1.06 | 62.4 | 1.1 | 36.5 |

[a] the Kodgibail basins listed in Table 1 as basins 9 to 11 and shown in Fig. 1 are nested within this basin.
[b] The Vajgar sub-basins (4 and 5) in Table 1 are nested within this basin.

### 4.2. Potential evapotranspiration

Reference potential evapotranspiration (PET) was estimated at both the Coastal and Malnaad sites using available daily weather data. Data for more variables were available from an Indian Meteorological Department station close to the Coastal site so PET was calculated using the Penman–Monteith equation following the FAO approach (Allen et al., 1998, http://www.fao.org/). For the Malnaad sites where available weather data was more limited, the much simple empirical equation of Turc (1961) was adopted. In this context, an earlier comparative study of up to twenty different PET methods was undertaken by Jensen et al. (1990). Their work compared estimated PET against carefully selected lysimeter data from eleven stations across a range of climates. Jensen et al. (1990) noted that the Turc method compared very favourably with combination methods at their humid lysimeter locations. More pertinent, the Turc method was ranked second only to the Penman–Monteith method when only the humid locations were considered in that study (Jensen et al., 1990). Elsewhere another comparative study of reference ET methods by Yoder et al. (2005) came to similar conclusions.

#### 4.2.1. Data inputs

More specific details on the data inputs, as part of using the above methods are now provided. In the absence of a meteorological station on site for the Coastal basins, we followed the FAO manual (Allen et al., 1998), which recommended that data from nearest meteorological station be used. Daily climate data (temperature, wind speed and relative humidity) were obtained from the Honnavar station of the Indian Meteorological Department (IMD) which is located about 10 km from the catchments. The variables solar radiation and maximum sunshine hours were not available from this station. Thus the use of a global formula which only requires latitude –longitude as the input for each specific catchment was adopted for this purpose (Allen et al., 1998, http://www.fao.org/). PET will be then plotted over the wet season and the initial stages of the post-monsoon season (May –December 2005, incl.).

**Table 3**
The Furey–Gupta Filter coefficients for the three land-cover types in the Coastal catchments.

| Type | Recession constant | $C1_{mean}$, sd | C2 | $C3_{mean}$, sd | $\frac{C3}{C1}$ median, IQR | $Q_B$ | $Q_F$ |
|---|---|---|---|---|---|---|---|
| *D*, delay = 1 time unit (36 min) | | | | | | | |
| Forest | 0.98 | 0.0067, 0.019 | 0.69 | 0.31, 0.019 | 329, 1910 | 0.95 | 0.05 |
| Acacia | 0.91 | 0.1, 0.134 | 0.47 | 0.43, 0.109 | 6.88, 18.01 | 0.76 | 0.24 |
| Degraded | 0.89 | 0.21, 0.263 | 0.35 | 0.45, 0.197 | 4.22, 15.83 | 0.55 | 0.45 |

*Note*: C1 is the overland flow coefficient; C2 is the evapotranspiration and basin storage coefficient; and C3 is the ground-water recharge coefficient; C3/C1 indicates the fraction of precipitation that becomes recharge and is the ratio of ground-water recharge to the overland coefficient; sd is the standard deviation of C1 and C3; IQR stands for inter-quartile range; $Q_B$ is the proportion of total flow *Q* estimated as baseflow and $Q_F$ is the proportion of total flow *Q* estimated as Quickflow.

**Table 4**
The basin water balances for the wet seasons 2004 and 2005.

| Period (Month/Year) | Land cover | *P* | *Q* | AET | Recharge – (% *P*) | Date in which the stream discharge stopped |
|---|---|---|---|---|---|---|
| *Kodigibail water balance summary* | | | | | | |
| 06/2004 to 09/2004 | Forest | 2514 | 541 | 352 | 1621 (64.5) | 06-10-2004 |
| | Acacia | 2514 | 728 | 369 | 1417 (56.4) | 13-09-2004 |
| | Degraded | 2514 | 1028 | 364 | 1122 (44.6) | 06-10-2004 |
| 06/2005 to 09/2005 | Forest | 3392 | 1056 | 367 | 1969 (58.0) | 24-08-2005 |
| | Acacia | 3392 | 1186 | 364 | 1842 (54.3) | 24-09-2005 |
| | Degraded | 3392 | 2096 | 373 | 923 (27.2) | 25-09-2005 |
| *Coastal basins water balance summary* | | | | | | |
| 06/2004 to 08/2004 | Forest | 2842 | 1132 | 284 | 1426 (50.2) | Continues |
| | Acacia | 2842 | 1148 | 282 | 1412 (49.7) | 27-08-2004 |
| | Degraded | 2842 | 1468 | 268 | 1106 (38.9) | 26-08-2004 |
| 06/2005 to 08/2005 | Forest | 2976 | 1226 | 288 | 1462 (49.1) | Continues |
| | Acacia | 2976 | 1476 | 273 | 1227 (41.2) | 22-08-2005 |
| | Degraded | 2976 | 1750 | 276 | 950 (31.9) | 25-09-2005 |

*Notes*: (i) All values in mm and (ii) wet season = June to September 2004 and 2005.
*Notes*: (i) All values in mm and (ii) wet season = 2004 and 2005: June to August.

In the Malnaad, there was no IMD station data available. A meteorological observatory was established close to the Acacia basins (AC1 and AC2) in the study area at Kodigibail. The observatory was equipped with self-recording and ordinary rain gauges to measure rainfall. Air temperatures (maximum and minimum) and wet and dry bulb temperatures were also measured. The measurements were initiated from October 2004 onwards. Due to the non-availability of radiation and wind speed data, daily records of air temperature and relative humidity were used to compute potential evapotranspiration using the Turc method as recommended for sub-humid climates of India (Venkatesh et al., 2011; Nandagiri and Kovoor, 2006).

### 4.3. Actual evapotranspiration and daily water balance

When taking the appropriate reference PET (i.e., FAO or Turc methods), actual evapotranspiration (AET) in the wet-season was then estimated based on the following criteria:

- An initial condition is that AET can at most equal reference PET (Chiew and McMahon, 1991; Limbrick, 2002).
- The reference PET that we have used as an upper bound for daily AET for forest in subsequent water balance calculations are twice that are reported on a daily basis when compared with reports from a west Africa tropical forest study (Ledger, 1975). The latter had a similar rainfall regime to the Western Ghats with very high annual rainfall which is also concentrated in 4 months and then followed by a marked dry season (Ledger, 1975). Such lower AET values in the wet season also align with the noted wet season 'dip' in PET.

Thus the reference PET values on an annual basis used here are more generous and close to or above the highest values recorded for AET of tropical humid forests anywhere (Kume et al., 2011). They are assumed to be appropriate as the upper bound of actual evapotranspiration for the forest in the wet season. This is especially true for the wet-season when soil water is not limiting but energy is (Fig. 2). Differences in maximum AET between land-covers would be suppressed as they all would be constrained by available energy and not soil moisture and thus their AET would all be less than or equal to PET.

- Based on the water balance equation, AET would be smaller than the difference between rainfall (P) – streamflow (Q) because there is also a groundwater recharge component, viz:

$$P - Q = \mathrm{AET} \pm \mathrm{Gw}(\text{i.e., Gw recharge}) \quad (1)$$

- For the conditions if $P - Q > \mathrm{PET}$ then AET = PET, and if $P - Q < \mathrm{PET}$ then AET = $P - Q$. Basically, this means that groundwater recharge would only occur when AET demands of the vegetation are met and when there is a surplus over and above AET.
- During days when it is not raining but streamflow occurs, then it is assumed that the partitioning of soil moisture in the unsaturated zone is between contributions to AET and Q. Thus water will drain from soil to sustain streamflow only when the soil is sufficiently wet to meet AET demands and contribute to streamflow. Consequently, we assumed that AET was equal to PET under these conditions (Oishi et al., 2010; Palmroth et al., 2010). This assumption is supported by Venkatesh et al. (2011; Fig. 2) who showed that the matric potentials were close to saturation during the wet season with ample supplies of "free water" for sustaining AET at PET levels.

Following the estimation of AET (as outline above), groundwater recharge is calculated using the water balance Eq. (2):

$$\text{Groundwater recharge} = \text{Rainfall}\,(P) - \text{Streamflow}(Q) - \mathrm{AET} \quad (2)$$

where, Rainfall and Streamflow are known over daily time steps for both Coastal and Malnaad basins.

### 4.4. Soil moisture and soil water hydraulic potential

Soil moisture was sampled twice per month for gravimetric soil moisture during the water year (May 2004–April 2005) within the Coastal basins. These were taken at depths from 0.15 m to 1.5 m at 0.15 m intervals using a soil auger at three sampling points located in the upper/mid/lower reaches of each land-cover basin. Subsequently the mean values of the soil moisture parameters (highlighted below) were derived from these three points.

The gravimetric soil moisture values were converted to volumetric moisture based on field sampling of bulk density at the same depths .The available moisture content at different depths (0–0.15 m, 0.15–0.30 m, ... 1.35–1.50 m) was calculated by finding the difference of volumetric moisture content between two consecutive months. Such differences were then converted to volume of available moisture by multiplying the moisture content value by the depth of soil column (0.15 m). Total volume of available moisture content for a given month is calculated by adding the volume of moisture at each of the depth ranges, that is, (0–0.15 m) + (0.15–0.30 m) + (0.30–0.45 m) + ... + (1.35–1.50 m). These were then

summed up to estimate monthly volumes of available moisture content. The latter calculations provide inputs to the zero flux plane estimates (see below).

Furthermore in the absence of soil water pressure transducers, we used the pressure plate data on cores taken from these soils at the same depths to estimate the soil water hydraulic potential (using the soil surface as the reference position, see below) corresponding to the volumetric moisture contents.

### 4.5. Analytical methods

#### 4.5.1. Water yields

The rainfall and discharge data were used to estimate annual water yields which were plotted against basin area and land-cover.

#### 4.5.2. Flow duration curves

Flow duration curves, FDC (Vogel and Fennessey, 1994, 1995) were plotted using the daily discharge time-series data in depth units (mm day$^{-1}$). Essentially these have the magnitude of flow on a log scale on the y axis and the percentage of total number of days in which that flow was equalled or exceeded on the x axis. The FDC are extremely useful in comparing the distribution and magnitude of flows especially low and dry-season flow across sites and land-cover types (Smakhtin, 2001; Roa-García et al., 2011). The FDCs were computed and plotted using the FDC function in the HydroTSR package in R statistical package. These FDCs were computed and plotted on a comparative basis with some land-cover sustaining low flows when others did not have any flow and so are plotted on a log scale after removing zero flows.

#### 4.5.3. The Furey–Gupta (F–G) filter analyses

The filter analysis of Furey and Gupta (2001) was applied to the continuous rainfall–runoff data of 41 days (16 June–25 July 2005) in the Coastal basins.

The method is derived from a basic physical equation for a hill; a simple representation of stream flow; and by partitioning precipitation into overland flow, evapotranspiration, and groundwater recharge, where recharge is time lagged (Furey and Gupta, 2001). Thus, it is a physically-based digital filter that uses time-series of rainfall and streamflow to estimate the recession constant and three diagnostic basin coefficients: $C_1$ is the proportion coefficient of rainfall that becomes overland-flow, $C_2$ is the coefficient corresponding to evapotranspiration, and $C_3$ is the coefficient corresponding to groundwater recharge. These coefficients are constrained to conserve mass such that $C_1 + C_2 + C_3 = 1$. An input to the filter analysis is the estimation of D (see Eq. (11) in Furey and Gupta, 2001) which is the assumed delay time in time-steps between infiltration and ground-water recharge. The small size of the catchments and the high groundwater levels during the monsoon in Uttar Kannada (Central Groundwater Board, 2008) justifies the choice of smaller values of the delay factor, D. Such reasoning for the selection of small values of D is also in agreement with Furey and Gupta (2001). In our case, we assumed 0.6 h for the final reporting, the smallest time-step although we did a sensitivity analysis using varied values of D from 0.6 to 24 h for each of the land-covers and found that the patterns in relative comparisons of estimates of% quick-flow and baseflow between land-cover at different assumed values of D remained consistent throughout. In theory, D could be a function of land-use and land-cover, but hydro-geology is likely to play a major role, and given the spatial proximity of the catchments, we expect the values to be similar. The filter (equation 22 in Furey and Gupta, 2001) also gives the recession constant, 1- for $(t/T)$ in $Q_t = Q_0\, e^{-t/T}$, where $Q_t$ is discharge at time $t$ and $Q_0$ is discharge at time zero.

The above filter of Furey and Gupta (2001) is based on four assumptions which these writers critically evaluated. Such an evaluation will now be placed in the context of the present work. The assumptions are namely: (a) the routing of water from hillside to stream gauge is near-instantaneous and will progressively degrade with increasing basin scale. In that context, the small scale of the Coastal basins may prove an advantage; (b) the ratio of $C_3/C_1$ is assumed to be constant in time and so does not allow for temporal variability in soil moisture and rainfall rate. Furey and Gupta (2001) noted that the estimates for $C_1$ are highly sensitive to error in the estimation of precipitation, and this error increases with increasing basin scale. As with assumption a), the small basin areas in the current work should reduce the error in precipitation measurement and thus the error in $C_1$. Moreover following the wetting up phase at the beginning of the summer monsoon, soil moisture in the study basins is close to maximum conditions of wetness, (as shown by Venkatesh et al., 2011); (c) the delay time, D between precipitation and groundwater recharge is constant. This assumption, however, can only be an approximation due to the variable depth to groundwater table. Further the lack of knowledge on the hydrogeology and the possibility of varying pathways and sources of deeper groundwater contributions (not just from the water table *per se*) to runoff from the underlying fractured rock (discussed in Krishnaswamy et al., 2012), could potentially affect D and thus the $C_3$ estimates across the basins; d) groundwater recharge is proportional to precipitation in a "damped" form.

Furey and Gupta (2001) concluded that the method is best applied at 'long' time scales for the more reliable estimates of baseflow or delayed flow (linked with $C_3$) and small basins. Preliminary analyses of the daily rainfall-runoff records over the wet season linked with the Malnaad basins showed that at the daily time resolution, in conjunction with the small size of these basins, the F-G method proved insufficient to capture all aspects of the flashy hydrograph responses. Thus the assumptions of this approach were not met and the recession constants, $C_1$, $C_2$ and $C_3$ could not be reliably estimated. We thus confined the application of the F-G method to the Coastal basins where rainfall-runoff time series were available at the 0.6 h time resolution.

### 4.6. Estimating groundwater recharge in wet-season using the Furey–Gupta coefficient, $C_2$

The Furey–Gupta filter analysis as applied to 0.6 hourly data for the monsoon of 2005 (41 days) yielded the coefficient $C_2$ which can be considered *as scaling coefficient* to compare and estimate evapotranspiration (and some temporary storage) across land-cover types. Following the short period of "transient wetting up" at the opening of the monsoon (16–25 June 2005, Krishnaswamy et al., 2012), the magnitude of transient storage is likely to stabilise so that AET will dominate $C_2$ for most of the 41 day record. We assume that the ratio of the $C_2$ coefficient values for any two land-covers will approximate the ratio of actual evapotranspiration of these land-covers during the period of the time-series data i.e.,

$$\frac{C2\ \text{Acacia}}{C2\ \text{Forest}} = \frac{\text{AET Acacia}}{\text{AET Forest}} \tag{3}$$

$$\frac{C2\ \text{Degraded}}{C2\ \text{Forest}} = \frac{\text{AET Degraded}}{\text{AET Forest}} \tag{4}$$

The use of these approximations (i.e. Eqs. (3) and (4)) requires that we have some independent reference AET for the Forest on which the relative scaling can be applied to obtain corresponding AET estimates for the Acacia and Degraded Forest. The AET are then applied to the water balance Eq. (2)) along with the respective total P and total Q for each basin, over the 41 days period, to estimate groundwater recharge for each land cover.

The independent estimate of AET for the Forest was taken from the water balance ET estimates of Ledger (1975) based on a study in Sierra Leone where very high rainfalls (7 year mean, 5795 mm)

are concentrated in 3 months of the year (7 year mean rainfall, July – September, 4523 mm) (Bruijnzeel, per comm). As discussed (under Methods), such a rainfall total and its seasonal distribution are climatically similar to the present study sites as well as the Western Ghats (as described by Gunnell, 1997). When compared with most lowland forest ET estimates, the annual ET was found however to be low and only 1011 mm for a 7 year record (Ledger, 1975). As Roberts et al. (2004) noted elsewhere a typical annual estimate of ~1400 mm (Bruijnzeel, 1990) for AET is close the net radiation equivalent of evaporation (1500–1550 mm; Calder, 1999) for the drainage basin experiments.

The average daily ET over the wettest 3 months (July – September, total ET, 139 mm) was low at 1.5 mm $d^{-1}$ (Ledger, 1975) *and it is this figure that will be used as the reference AET for Forest in equations 3 and 4).* It should be noted that use of this reference AET estimate acts as a scaling factor and is restricted to the Coastal basins which are very close to each other so that climate differences are negligible. The $C_2$ coefficient of the Furey–Gupta filter analysis is a surrogate estimate of differences in land cover characteristics (e.g., species composition, crown cover) on AET.

### 4.7. The SWIM model for estimating the water balance

We applied the CSIRO SWIMv2 (Soil Water Infiltration and Movement) model (Verburg, 1996; www.clw.csiro.au/products/swim/) SWIM v2.0 over a water year April 2004–May 2005 for the Coastal basins.

SWIM is based on a numerical solution of the Richards' equation and the advection–dispersion equation. Of relevance to this study, SWIM can be used to simulate runoff, infiltration, redistribution, plant uptake and transpiration, soil evaporation and deep drainage (Verburg, 1996). However the model deals only with a *one-dimensional profile* and assumes that there is one hydraulic conductivity function (based on data from Bonell et al., 2010) for each soil horizon so that macropore flow can only be accounted for in a limited way. Moreover previous work (Bonell et al., 2010; Krishnaswamy et al., 2012) has reported the existence of 2-Dimensional flow (i.e., sub-surface storm flow) within the soil profile during storms so the assumption of 1-Dimensional flow will break down at such times during the wet season. Nonetheless, its application will provide some useful insights into the impacts of land cover on evapotranspiration as well as runoff and groundwater recharge which can then be compared with the results for other methods.

The outputs of SWIM will also be compared with the daily water balances of the Malnaad and Coastal basins.

### 4.8. The zero flux plane method

The zero-flux plane (ZFP) method provides a point estimate of plant-water use and drainage to deeper layers (e.g., Cooper, 1980; Wellings and Bell, 1980; Kirsch, 1993; reviewed in Khalil et al., 2003). The method involves estimating a depth profile of total hydraulic potential of soil moisture and then the identification of a "zero flux plane" which separates the zones of upward and downward movement of water in a thoroughly wetted soil with evaporation and drainage occurring simultaneously. The ZFP separates upward movement of soil water to evapotranspiration from downward drainage towards the deeper soil and water table in the one-dimensional plane. Moreover the method is based on the premise that soil water recharge plus continued downward drainage under gravity is equal to changes in soil-moisture storage below the ZFP and that plant-water use above this zone is similarly estimated. In such circumstances, it is assumed that root extraction of soil moisture for AET below the ZFP is negligible, i.e. there is only drainage below the ZFP (Cooper, 1980). On the basis of the description of tree rooting patterns above, clearly the latter assumption of the ZFP method will not always be met. This notion applies especially once uptake for AET demands of freely available and shallow soil water has been completed in the early stages of the dry season (Venkatesh et al., 2011). Subsequently deeper root extraction is then more favoured especially when concerning the deeper-rooted, natural forest. In such circumstances the ZFP method would potentially over-estimate soil water drainage below the zero flux plane, and conversely under-estimate AET. The review of Khalil et al. (2003) suggested that in similar circumstances elsewhere errors in ZFP estimates were not considered large. But the latter rests on the premise that water is readily available most of the time in the upper soil layers.

As with SWIM above, the existence of 2-dimensional lateral flow during the monsoon (Bonell et al., 2010; Krishnaswamy et al., 2012), will cause a breakdown in the assumptions of the ZFP method. In addition the water table has to be deeper than the ZFP and the occurrence of perched water tables also during the wet season is another problem (Venkatesh et al., 2011; Krishnaswamy et al., 2012). Thus the application of the method is *restricted to the dry season only when no rainfall was recorded.* The method requires data on the soil matric potential ($\Psi$) with depth ($z$) to locate the ZFP as well as soil–water content to measure changes in storage. We used periodic (once a month) measurements of gravimetric soil moisture at various depths up to 2 m from the end of the wet-season in November 2005 through the dry-season until April 2006. As earlier indicated, these gravimetric data were then converted into volumetric soil moisture using bulk-density measured at the sites. Subsequently the matric potentials were obtained from the pressure plate data on soil cores taken at the same depths as the gravimetric moisture data. The total hydraulic potential ($\Phi$) (i.e., total soil water potential) was then calculated at each depth, where $\Phi = \Psi - z$, and taking the surface as the reference datum ($z = 0$). Finally the total hydraulic potential – depth relation was then plotted to identify whether a ZFP exists and if so, evapotranspiration and recharge can be estimated for each land-cover using Eq. (1) in Khalil et al. (2003).

$$E = R + \int_0^{z_0(t_1)} \theta(t_1)dz - \int_0^{z_0(t_2)} \theta(t_2)dz + \frac{1}{2}\int_{z_0(t_1)}^{z_0(t_2)} [\theta(t_1) + \theta(t_2)]dz \quad (5)$$

where $E$ is the Evaporation over the time period $t_1$ to $t_2$; $R$ the Rainfall over the same period; $t$ the time; $z$ the depth measured positively downward; $Z$ the Depth at which drainage is calculated; $\theta$ the Volumetric Moisture Content and $z_0(t)$ the ZFP depth at time $t$.

## 5. Results

### 5.1. Summary of the meteorological data

The annual rainfall for the Coastal site during the hydrologic year (June 2005–May 2006) was 3879 mm. The average rainfall for the hydrologic years 2004 and 2005 during the wet season (June–August) was 2751 mm and for the early the dry season period (September–December), the average was 386 mm. The average relative humidity for the hydrologic year 2005–2006 was 76.8% and average for the wet and dry seasons, as defined above (for the years 2004 and 2005) were 89% and 72.2% respectively. The PET estimated for the hydrologic year 2005–06 was 1479 mm (FAO, Penman–Monteith). The average wet season (June–August) PET for the years 2004 and 2005 was 309 mm (low for reasons stated earlier) and for the early dry season period(September–December), the PET (FAO, Penman–Monteith method) for the same years was 579 mm. The mean daily temperature for the year 2005–06 was 27.4 °C and the maximum and minimum daily temperature recorded was 37.5 °C and 15.9 °C respectively.

The Malnaad recorded an annual rainfall of 2724 mm during the 2004–2005 hydrologic year. The average rainfall during the wet season (June–September) and early part of the dry season (October–December) in 2004 was 2514 and 79 mm respectively and in 2005, 3392 and 140 mm respectively. The average daily relative humidity for the period 2005–2006 was 88.1%, and wet and dry season average for the years 2005 and 2006 were 93% and 89% respectively. The average of annual PET using the Turc method, for the hydrologic years 2004–2005 and 2005–2006 was 1560 mm. The wet season average PET for the years 2004, 2005 and 2006 was 401 mm and early dry season period (October–December) average was 412 mm. The mean daily temperature for 2004–05 was 24.8 °C, and the maximum and minimum daily temperatures were 40 °C and 11 °C, respectively.

For both the Coastal and Malnaad, it is important to note that these PET estimates for the wet season on a daily basis are more *than double* the daily AET cited by Ledger (1975) that will be used later in the F-G analysis. This supports the assumption that estimated PET used in the study is *well above* forest AET in the wet-season. The annual PET estimated for the sites are 1479–1560 mm, just above or close to the maximum measured ET of tropical rain forests (as reviewed in Kume et al., 2011). Thus we are confident of using our reference PET as the upper bound of actual forest ET in general and especially in the wet-season.

### 5.2. Basin area and flow

Fig. 3 shows the annual water yield as a percentage of annual rainfall for the three years 2003–2005, incl. It is evident that the basin area is not a major factor influencing the water yield. On the other hand over the same period, the impact of land cover is as much stronger driver as shown in Fig. 4.

### 5.3. Flow duration curves

As shown in Fig. 5, overall at both the Coastal and Malnaad (Kodigibail, Vajagar) sites, the NF sustains a higher proportion of low flows (depth units) and the most sustained and longer flowing is NF, Coastal (see also Table 4). These low flows also occupy a large proportion of total Q, consistent with observations of Roa-García et al. (2011). Flows below 20 mm day$^{-1}$ in the Coastal, 40 mm day$^{-1}$ in Kodigibail and 80 mm day$^{-1}$at Vajagar are largely confined to the forest and thus are the approximate thresholds for departure of the forest from the other land-covers. However in the Malnaad sites, NF does not necessarily maintain the lowest flow in mm and neither is it the longest flowing after the monsoon in a consistent manner (Fig. 5 and Table 4).

In the Coastal area flows below 0.5 mm day$^{-1}$ are non-existent in the non-natural forest land-covers (AC, DF) sites) whereas the forest sustains flows as low as 0.01 mm day$^{-1}$. Most of the stream discharge is associated with storm events in AC and DF coupled with the more flashy nature of the hydrograph responses and the very low Q in between storms (as reported in Krishnaswamy et al., 2012). In combination, the latter results in a FDC biased towards the ⩽20% of flow spectrum.

Moreover despite differences in soil type at Vajagar, the trends between NF and DF are the same as described above. On the other hand when concerning the DF basin, the flows are sustained longer within this Vajagar basin when compared to this same land cover at Kodigibail and the Coastal site. These results indicate then the importance of differences in soil hydraulic properties (e.g., $K_{fs}$, Bonell et al., 2010) between soil groups as well as basin size but with land-cover playing the dominant role. Overall, the FDC and the duration of flow beyond the monsoon suggests that the Coastal site is most representative of the *infiltration-evapotranspiration trade-off* hypothesis.

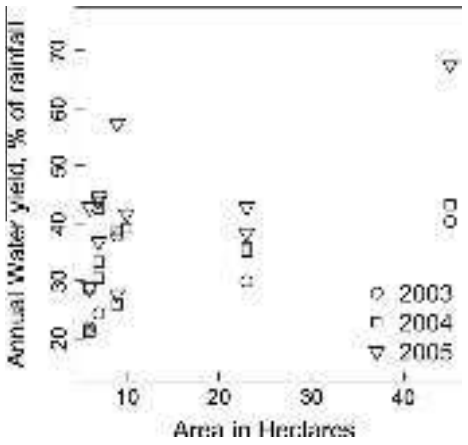


**Fig. 3.** The relationship between annual water yield and catchment area (as given in Table 1).

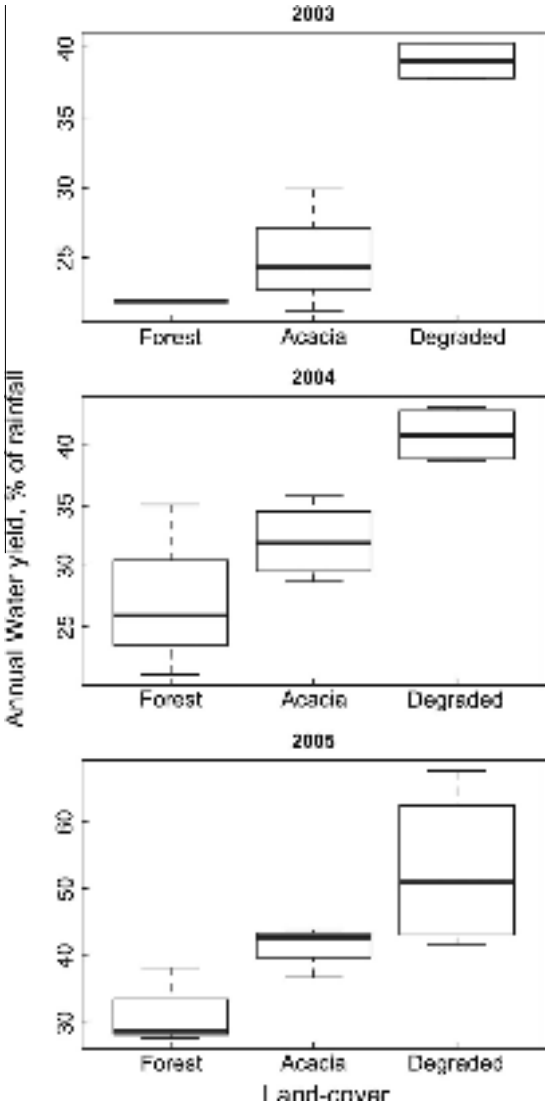


**Fig. 4.** The annual water yield for the different land covers.

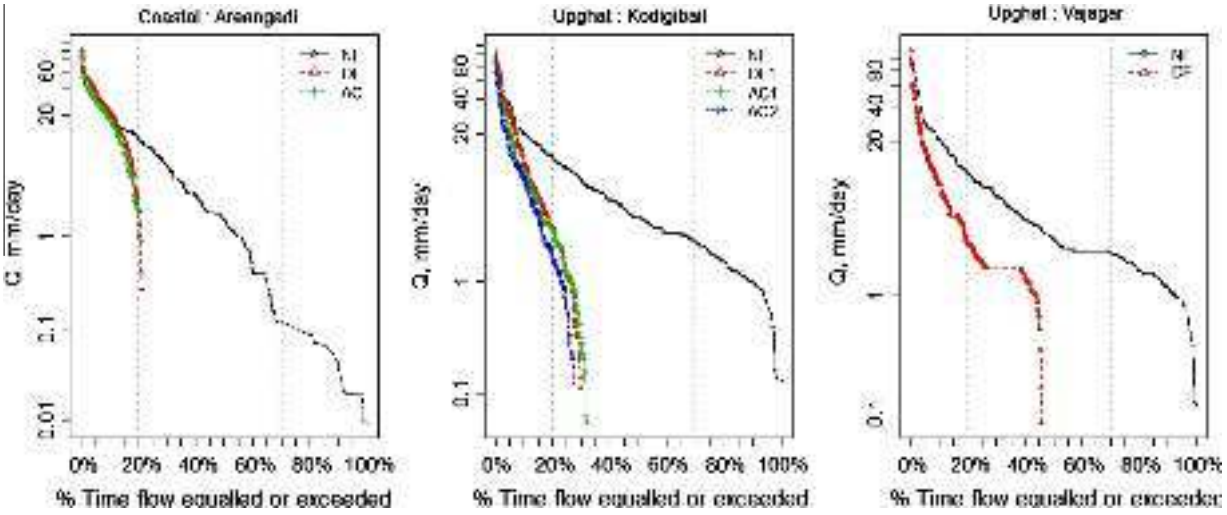


**Fig. 5.** The flow duration curves (FDC) of the Coastal and Up-Ghat basins. These are done on daily time-series data on a comparative basis across the land-cover types in each site using the entire period of record available and not including zero-flow values.

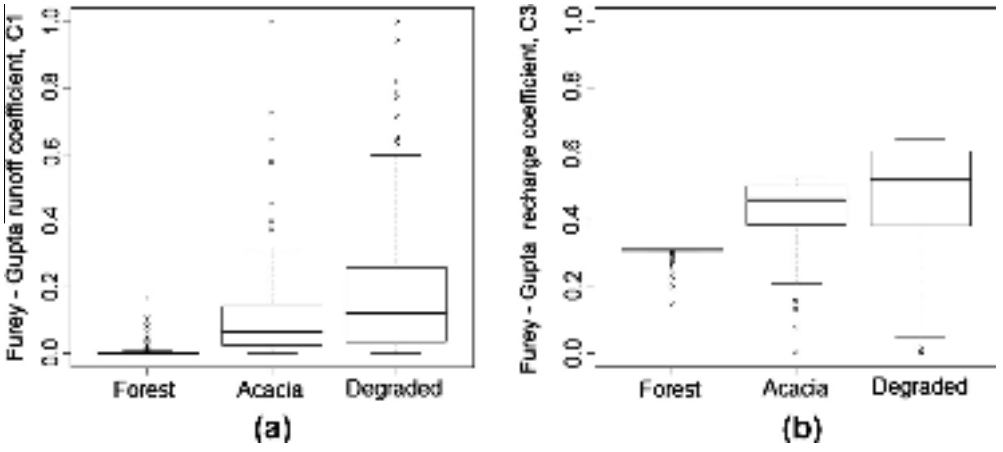


**Fig. 6.** The Furey Gupta filter coefficients, C1 (runoff) and C3 (recharge to ground-water), for the different land covers in the Coastal basins.

### 5.4. The Furey–Gupta filter analysis

It is encouraging that the rank order of the C2 coefficients (evapotranspiration plus some changes in storage), is in line with what would be expected, with the NF having the highest value (0.69) (Table 3). This Table 3 and Fig. 6 also show that the mean C1 is very low (0. 0067) under the Natural Forest and the highest under the Degraded Forest (0.21). The Acacia plantation also has a C1 value much closer to the DF1 basin with a mean of 0.10. Moreover in line with the findings of Furey and Gupta (2001) the variability (as shown by the standard deviation) in the mean C1 estimates remain high, most notably under the Natural Forest. The trend in these C1 estimates is what would be expected from with the previous hydraulic conductivity survey, that is, a greater frequency of overland flow in both the DF1 and AC1 basins (Bonell et al., 2010). Moreover this result is also in line with the higher $Q_F$(-quick flow)/$Q$ (total flow) ratios from specific events, as determined from HYDSTRA, for the DF1 and AC1 (Krishnaswamy et al., 2012).

On the other hand, the median C3 (recharge to groundwater) was higher under DF1 and AC1 when compared to natural forest which is a surprising result. The box plots however show that there is a greater variability in C3 from storm to storm for DF1 and AC1 when compared to the Natural Forest. Thus despite the larger means and medians associated with the latter two basins, such variability *implies that groundwater recharge is inconsistent and more variable, especially under degraded forest*. Furthermore as C2 may include some temporary storage over shorter periods of time, it is likely to suppress somewhat the values of C3, especially for the less-disturbed forest catchment. The lower variability in C3 for NF1 suggests that this land cover has the most stable groundwater recharge mechanism. Such consistency in groundwater recharge maybe partly due the higher surface $K_{fs}$ being receptive to higher infiltration in the Forest when compared to the other land covers. Further the duration of streamflow continued the longest within the Coastal forest after the summer monsoon had terminated, as indicated by the flow duration curves (Fig. 5), which favours the notion of a larger subsurface water storage capacity beneath the Forest. The latter would sustain AET and contribute towards the highest C2 value being associated with the NF1. In addition, the C3/C1 ratios are very similar for the degraded forest and the Acacia plantation with a low IQR (Table 3). These results are encouraging as they suggest a similar hydrogeology, hydro-pedology and climatic environment (Furey and Gupta, 2001). Conversely, the Forest is radically different with a C3/C1 ratio and an associated IQR that are two orders of magnitude higher.

Furthermore, the Natural Forest is also associated with the highest recession constant (0.98) and $Q_B$ (0.95) respectively which,

as one might expect, infers higher recharge to groundwater. The low standard deviation (SD) for C3 for this basin also lends confidence to this interpretation. Further this basin has also the advantage of being larger in area (23 ha) for groundwater storage. Nonetheless the proportion of $Q$ as $Q_B$ still remains at 0.55 or greater for DF1 and AC1 (Table 2), even after taking into account the larger SD in the C3 estimates and the basin areas (7 ha each) being smaller than the Forest. Such $Q_B$ results indicate *that substantial groundwater recharge still occurs* under these land covers despite the lower surface $K_{fs}$.

However as the Forest is approximately three times larger in area when compared to the other two basins, the above conclusions about the relative role of land-cover needs to be made with some caution. Nonetheless all our analyses have been undertaken using depth units (mm) which takes care of some of the area effect and we are thus mostly attributing the differences in $Q_B$ to land-cover rather than basin area.

### 5.5. The wet season water balances

Table 4 indicates that the percentage of precipitation as recharge to groundwater is highest in the Forest basins, followed by Acacia and Degraded Forest. This trend is consistent between the Coastal and Malnaad basins.

### 5.6. The water balance using the F–G C2 coefficient and Ledger (1975) AET estimates

Between 16 June and 26 July 2005, a total rainfall of 2181.6 mm was recorded and the respective total stream flows for NF1, AC1 and DF1 were 600.92 mm, 1073.89 mm and 1241.75 mm.

If the reference AET for the wet evergreen forest is taken as 1.5 mm $d^{-1}$ (Ledger, 1975) during the wet season, then the approximate AET over the 41 days period for the Forest (NF1) is 62 mm. Then applying Eqs. (3) and (4) provides the corresponding AET estimates for AC1 and DF1 (Table 5). Finally Table 5 shows the resulting water balance (using Eq. (2)) and the proportions of rainfall as recharge to groundwater. So the estimated rainfall as recharge over the 41 days in the Coastal basins is highest under Forest (69.63%), followed by Acacia (48.85%) and lowest under Degraded Forest (41.65%).

### 5.7. SWIM

Table 6 indicates that recharge to groundwater is also highest in the Forest (NF1), followed by Acacia and the Degraded Forest in the Coastal basin at an annual time scale. This agreement in rank order of recharge to groundwater, c.f., Tables 4 and 5, is despite the method being constrained by its one-dimensional assumption. The latter may also account for the radical differences in proportions of groundwater recharge when compared to the other approaches (Tables 4 and 5).

**Table 5**
The water balances of the coastal basins (16 June – 26 July 2005) using the Furey–Gupta C2 coefficients and using the mean daily actual evapotranspiration (AET) (Ledger, 1975) for the Forest as the scaling factor.

| Land Cover | Rainfall (mm) | Stream flow (mm) | AET (mm) | Groundwater recharge (mm) | %Groundwater Recharge of Rainfall |
|---|---|---|---|---|---|
| NF1 | 2181.6 | 600.92 | 61.5[a] | 1519.18 | 69.63 |
| AC1 | 2181.6 | 1073.89 | 41.89[b] | 1065.82 | 48.85 |
| DF1 | 2181.6 | 1241.75 | 31.20[c] | 908.66 | 41.65 |

[a] Based on a mean daily estimate from Ledger (1975).
[b] Calculated using Eq. (3).
[c] Calculated using Eq. (4).

**Table 6**
The Soil Water Infiltration and Movement (SWIM) model results for Coastal catchments for the period May 2004–April 2005.

| Land-cover | Rainfall (mm) | Run-off (mm) | AET (mm) | GW recharge (mm) |
|---|---|---|---|---|
| Forest | 3568.6 | 1001.7 (28.1%) | 1555.0 (43.6%) | 1647.3 (46.2%) |
| Acacia | 3568.6 | 1409 (39.5%) | 1312.9 (36.8%) | 1404.4 (39.4%) |
| Degraded | 3568.6 | 2058.7 (57.7%) | 1215.8 (34.1%) | 494.9 (13.9%) |

*Note*: The percentages express the proportion of each water balance component of total rainfall.

### 5.8. Soil water hydraulic potential profiles and the zero flux plane

The profiles of soil water hydraulic potential with depth are shown in Figs. 7 and 8) for respectively the three Coastal basins and Kodigibail (Sites 1–3 and 6–9 in Table 1). The following features are evident:

- The hydraulic potential through the dry-season is higher under the forest at Kodigibail when compared to all other land-covers and basins. Moreover, the hydraulic potential under the Kodigibail forest is consistently maintained at a higher level between 0.60 and 1.20 m depth throughout the dry-season.
- There is evidence of the development of a ZFP in all the land-covers. The ZFP is more pronounced at shallow depths ($\leqslant$0.5 m) but it can also be detected at some sites even at greater depths ($\geqslant$1.2 m),e.g., Kodigibail forest. This suggests that soil water is being extracted from at least two parts of the deep profile to meet transpiration demand and as acknowledged above, will affect both the AET and drainage estimates.
- Table 7 shows the estimates of evapotranspiration and drainage for the Coastal basins for the period mid-December 2005 – mid-March 2006 where the ZFP is more marked. Further Table 7 refers to ZFP evident between 0.45 and 0.60 m and does not take into account any weaker reversals in hydraulic potential gradients at greater depths. *This period coincides with part of the dry season in the absence of any rainfall.* The ZFP was located at 0.45 m for natural and degraded forest and 0.6 m for Acacia. The evapotranspiration above the ZFP during the above period was 24.08 mm for Natural Forest, 34.80 mm for Degraded Forest and 32.58 mm for Acacia. The drainage for the period was 98.02, 66.92, and 70.91 mm respectively for Natural Forest, Degraded Forest and Acacia catchments.. As noted above, however, the deeper rooting patterns below the ZFP under the Natural Forest potentially introduces some unknown error into both the AET and drainage estimates.

Taking into account the above, two characteristics are evident. First, over this period the depths of the ZFP's are relatively fixed under all land covers and do not show temporal variability, and despite no rainfall occurring, and thus a simplified version of the ZFP Eq. (5)) was used (i.e., the rainfall and the 3rd term to account for a variable ZFP were both zero in Khalil et al., 2003). Second, the amounts of evaporation over three months are very low across all land covers (<34 mm), but as expected the rank order is NF > AC > DF. Conversely, the amounts of drainage are at least double the amounts of evaporation. One can conclude from these results that Forest at least must be drawing on much deeper subsurface water (>1.5 m depth) to meet its transpiration

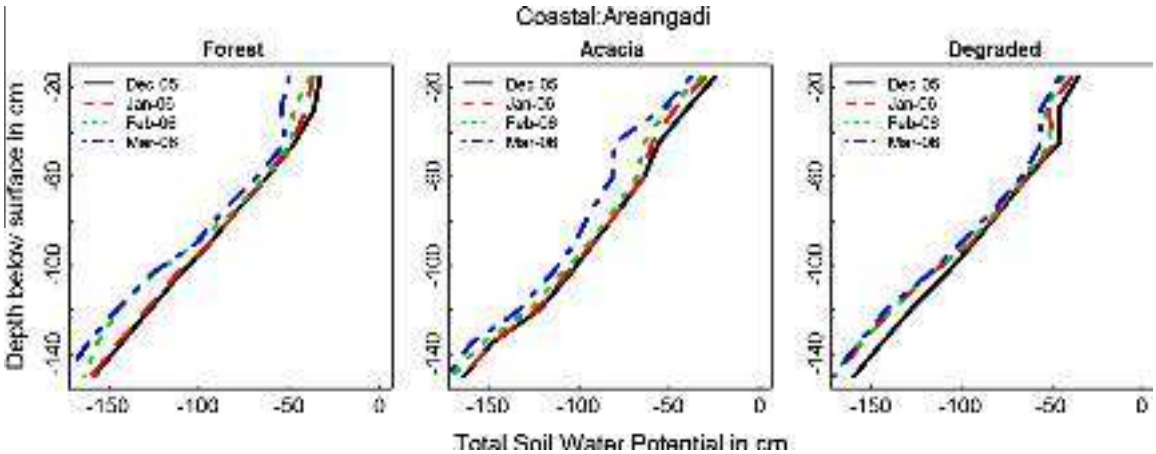


**Fig. 7.** The total soil water hydraulic potential ($\Phi$) versus depth ($z$) relationsat selected dates during the dry season for the Coastal basins (Sites 1–3, Table 1, Fig. 1), where $\Phi = \Psi$ (matric potential) – $z$(gravitational potential), taking the surface as the reference datum.

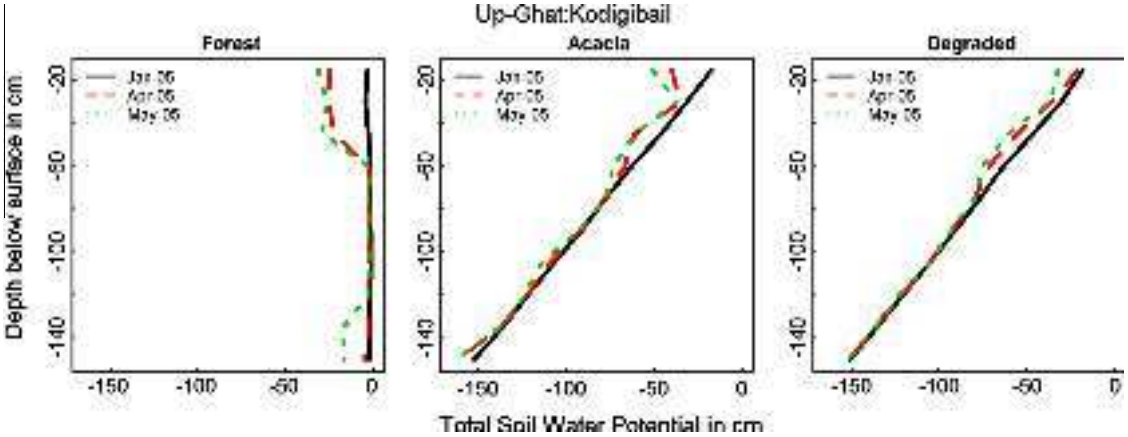


**Fig. 8.** The total soil water hydraulic potential ($\Phi$) versus depth ($z$) relationsat selected dates during the dry season for the Up-Ghatbasins (Sites 6–9, Table 1, Fig. 1)where $\Phi = \Psi$ (matric potential) – $z$ (gravitational potential), taking the surface as the reference datum.

**Table 7**
Estimated evaporation and drainage in the coastal basins, December 2005–March 2006, using the zero flux plane method (ZFP stationary at 0.45 m.depth for NF /DF and 0.60 m depth for AC).

| Catchment | Total depth (m) | ZFP depth (m) | January-06 | February-06 | March-06 | Totals |
|---|---|---|---|---|---|---|
| | | | Evaporation (mm) | | | |
| Degraded Forest | 1.5 | 0.45 | 10.88 | 9.00 | 4.20 | **24.08** |
| Forest | 1.5 | 0.45 | 8.95 | 4.29 | 21.56 | **34.80** |
| Acacia | 1.5 | 0.60 | 8.16 | 7.68 | 16.74 | **32.58** |
| | | | Drainage (mm) | | | |
| Degraded Forest | 1.5 | 0.45 | 61.38 | 18.92 | 17.72 | **98.02** |
| Forest | 1.5 | 0.45 | 14.85 | 36.12 | 15.95 | **66.92** |
| Acacia | 1.5 | 0.60 | 14.75 | 28.61 | 27.55 | **70.91** |

demands. Bourgeon (1989) recorded many roots in a soil pit in this region under evergreen forest up to 1.2 m and beyond. Our field observations of soil exposures in the vicinity of the experimental basins also suggest Natural Forest rooting depths extend beyond 2 m (Krishnaswamy et al., 2012). As noted above, Kallarackal and Somen (2008) reported that Acacia rooting patterns are mainly in the upper 1 m, and further suggest their inability to tap deeper groundwater. Thus it appears that the Natural Forest has the greatest ability to support higher transpiration rates in the dry-season using deeper sources of water.

### 5.9. Dry-season flow in the larger catchments

The time-series of dry-season flow in the basins 1–2 km$^2$ downstream of the smaller instrumented basins indicates that flow is sustained longer into the dry-season in the basin with the highest percentage forest cover, that is, the Vajagar (Fig. 9, Table 2). On the other hand, the basin with the lowest forest cover, namely Nirmundagi (NRM), ranks second in sustaining flow the longest into the dry season. Another interesting feature is that the Kodigibail basin terminates flow early in the record, despite having the

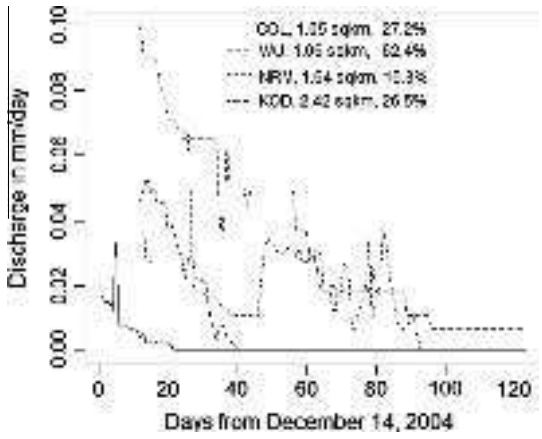


**Fig. 9.** Streamflow discharge in the larger catchments (shown in Fig. 1 and Table 2) duringthe early stages of the dry season. Area and % forest cover are indicated for each catchment. These higher order catchments are located downstream of the smaller and more homogeneous head-water catchments which are the main focus of the study.

advantage of the being the largest in area. On this basis, it could be inferred that Natural Forest is most influential on dry season flow when its areal coverage is very high.

## 6. Discussion

### *6.1. Groundwater recharge and the role of groundwater – a missing link*

The independent results from the different water balance analyses suggest that groundwater recharge is substantial under all three ecosystems during the wet-season, and is the highest under Forest (46.2–69.6%), and is considerably lower under Acacia (39.4–56.4%) and Degraded Forests (13.9–44.6%). The main control on the amount of recharge in these high rainfall areas in the Western Ghats during the monsoon *is not the amount of actual evapotranspiration (AET)* (which is very limited by climatic conditions in the wet-season in all the three ecosystems) but by the soil hydraulic conductivity and the resultant partitioning of rainfall into quickflow, baseflow (delayed flow) and deep-percolation (see also Krishnaswamy et al., 2012). Moreover if one uses the Natural Forest cover over both the Laterites (*EutricNitosols* and *Acrisols*) and Red soils (*EutricNitosols*) as a baseline, the $K_{fs}$ can be used as an indicator of the degree of degradation. It was reported (Bonell et al., 2010; Krishnaswamy et al., 2012) that the Degraded Forest and the Acacia plantations have up an order of magnitude decline in $K_{fs}$ at the surface as result of human impacts at decadal to century time scales. *Nonetheless these results indicate that significant groundwater recharge seems to continue even under these more human – impacted land covers (AC, DF), despite some re-direction of rainfall as overland flow in response to land degradation.* The recharge process is nonetheless suggested to be complex, as indicated by the Furey–Gupta results when concerning the C3 coefficient. In that regard the larger inter–quartile variability shown in the C3 box plots for the more disturbed land covers (Degraded Forest, Acacia) as against those of the Natural Forest is critical. Such variability could be attributed to temporal changes of within - storm rain intensities. When the rain intensities are below the surface $K_{fs}$ threshold for overland flow to occur, recharge dominates. Above this threshold a greater proportion of rain is re-directed laterally over the surface as overland flow and a lesser proportion is available for groundwater recharge. The negligible role of C1 for the Forest in conjunction with the low inter-quartile variability in the box plots for C3 indicates that groundwater recharge is *more consistent under this land cover.*

Furthermore the subsoil $K_{fs}$ (geometric means ~10–20 mm $h^{-1}$) for all three Coastal basins are comparatively permeable down to 1.50 m depth when compared to other Laterite sites in the region (Bonell et al., 2010). These sub-soils are also more permeable than reports from other rainforest studies with 'Acrisol-type' soils in Australia (Bonell et al., 1981, 1998) and Peru (Elsenbeer and Lack, 1996) where the geometric mean $K_{fs}$ are respectively one and two orders of magnitude lower than in the current study. Thus percolation to groundwater beneath both the DF1 and AC1 land basins would not be impeded, once rainwater entry through the lower surface $K_{fs}$ had occurred. Thus recharge to groundwater can be maintained despite a reduction in surface $K_{fs}$ in the two disturbed land covers. Under the Forest, the percolated water can still be intercepted for transpiration or storage (Fig. 9) and thus less is available for recharge for many events in spite of much higher infiltration. However the Forest has emerged as the most stable and consistent land cover to act as a "recharger" of groundwater. The latter is also reflected by the flow duration curves (FDC) where low flows occupy a much greater proportion of total flow from the Forest, when compared to the other land covers. Moreover such low flows are shown to be sustained for a longer period of time, especially in the Coastal region.

The preceding key attributes of the Forest (also previously noted by Roa-García et al., 2011) have important implications when concerning "provisioning" ecosystem services (MA, 2005) linked with a more reliable community water supply to downstream communities and agro-ecosystems such as Arecanut, home gardens and Paddy-rice. This work has shown that one cannot focus entirely on the surface hydrology to explain the impacts of land cover change. All our analyses based on different approaches have highlighted the importance of subsurface pathways and subsurface water bodies (including possibly deep groundwater) as contributing sources to streamflow. Thus at such small basin scales, in addition to surface changes in $K_{fs}$ affecting stormflow pathways, runoff can also be affected by subtle differences in the hydrogeology by way of the jointing and fracturing within the underlying parent rock (as mentioned in CGB, 2008). Consequently, this work highlights the importance and the need for detailed knowledge not only on the evapotranspiration component of the water balance but also on the hydrogeology within the forest-land cover change debate – an issue commonly not strongly highlighted in the forest hydrology literature (e.g., Scott et al., 2004; Bruijnzeel, 2004). Consequently, there is a need for caution when attributing differences in the rainfall–runoff response to land cover change impacts on surface $K_{fs}$ *per se* and that applies to the present study.

The higher and consistent recharge under natural forest at smaller spatial scales leads to longer dry-season flows in basins downstream as supported from measurements of dry-season flow in downstream basins of 1–2 $km^2$. For the specific examples used here only such conclusions apply where forest cover *exceeds* 60% of basin area. However in the absence of other replication studies in the Western Ghats such a figure cannot be taken as universal. Nonetheless qualitative observations on the duration of stream flow within higher order stream networks downstream during the study also suggested that substantial recharge occurs in less disturbed catchments. Thus dry-season flows in these less disturbed basins are more sustained within the long dry season. Elsewhere James et al. (2000) also reported similar characteristics from a comparative, small catchment study (0.15–2.95 $km^2$) within the Western Ghats of Kerala. The densely forested basins produced streamflow ranging from 24.2 to 32.8 mm/unit area in contrast to 1.6–6.4 mm/unit area in "partially exploited" basins and 0 mm/unit area from "fully exploited" basins during the January–May period (James et al., 2000).

The importance of groundwater is also suggested by the ZFP results. Despite potential violation of one ZFP method assumption (*viz*, soil water extraction by roots is mostly confined to above the zero flux plane in the Natural Forest), nonetheless only very small amounts of soil water (<35 mm) in the top 1.5 m of the soil profiles are suggested as contributing towards AET during the protracted dry season. Such small amounts of soil water use must be made up by much larger contributions from deeper groundwater to meet transpiration-physiological demands notably beneath the forest. Some support for the latter comes from the previously mentioned study in the Kodigibail basins by Venkatesh et al. (2011). These writers reported that the use of soil moisture for physiological activities in the Acacia and Degraded Forest was mostly confined to the upper layer (up to 0.50 m depth) due to the shallow nature of the rooting systems, notably beneath the Acacia (Kallarackal and Somen, 2008). Further the upper layer is also more favoured as a soil water source for physiological activities, especially during the early part of the post monsoon season when water is freely available (Kallarackal and Somen, 2008). Furthermore, the maintenance of high soil water hydraulic potentials throughout the dry-season beneath the Kodigibail forest is also interesting. This could be potential evidence of hydraulic redistribution of moisture from deeper to shallower soil by tree-roots, as reported by Prieto et al., 2012), and the process merits a deeper study.

### 6.2. The 'infiltration-evapotranspiration trade-off' hypothesis: a perspective from this study

In the model simulations of Van der Weert, 1994, (reviewed in Bruijnzeel, 2004), the indications were that delayed flow would not be affected if the 'surface runoff coefficients' (i.e. infiltration-excess overland flow) remain below 15% of rainfall. If the latter however, attains 40% then delayed flow (dry season flow) would be halved (Bruijnzeel, 2004). When concerning the heavily-impacted Coastal basins, the estimated overland flow from the F-G analyses (C1 coefficient, max 0.21) lies in- between these 15% and 40% limits, as mentioned by Bruijnzeel (2004).

This analysis however does indicate aspects which support the '*infiltration-evapotranspiration trade-off*' hypothesis. These include the following points:

- From the F–G analysis, there is a reduction in delayed flow of 40% between the Forest and the degraded forest, and conversely an increase in $Q_F$ of 40%.
- Groundwater recharge is the highest for the Forest (natural forest, NF1), followed by AC1 (*Acacia auriculiformis* plantation) and lowest for DF1 (degraded forest) using three independent techniques to estimate the water-balance
- A comparison of the frequency duration curves (FDC) across land covers also suggests less groundwater recharge and baseflow within the disturbed land covers and a greater potential for infiltration excess-overland flow. Thus in the more disturbed land covers (DF, AC), the occurrence of sustained low flows do not occur in contrast to the Forest FDC.
- Elsewhere (Krishnaswamy et al., 2012) it was noted that there is a shift from long to the shorter time lags in rainfall-runoff when comparing the Natural Forest with the AC and DF land covers for specific rain events. Such changes infer reduced infiltration and an 'apparent' transformation from a previously dominant and slower stormflow pathway emanating from subsurface sources towards a more rapid surface pathway. This aspect supports the earlier conclusions from the soil hydraulic conductivity survey (Bonell et al., 2010).

The data from Krishnaswamy et al. (2012) clearly indicates that annual recharge from natural forests can range from 259 mm (rainfall 2252 mm) to nearly 1000 mm when the rainfall is over 4000 mm. On the other hand, there is also evidence that recharge to deeper soil water and groundwater stores still remains significant under all three ecosystems, including the Degraded Forest and the Acacia plantation. The latter are contrary to what might be expected for the 'degraded scenario' of the '*infiltration-evapotranspiration trade-off*' hypothesis (Bruijnzeel, 2004). In terms of this extra recharge not being reflected in the rain-runoff totals, this paradox may be explained by scale. One is dealing here with very small headwater basins. Thus there remains the strong possibility that some of the recharge in the monsoon maybe contributing to a much deeper, regional groundwater flow and storage in the ecosystem that extends well beyond the topographic boundaries of these small basins, as supported by perennial or longer duration flows in higher order catchments downstream that supply water to downstream agro-ecosystems (Fig. 9) .Thus such regional groundwater sustains vegetation water use and other ecosystem services in the dry season.

A principal message from this study is that to make significant progress in the humid tropics on this land cover change – hydrological impacts issue, such basin studies need to be coupled with parallel, hydrogeology, soil moisture and eco-physiological investigations. Further such studies ideally should be undertaken at larger scales subject to the constraint of land cover fragmentation.

#### 6.2.1. Infiltration-evapotranspiration trade-off: a dynamic process?

The "infiltration-evapotranspiration trade-off" conditions are not static for an ecosystem but are a dynamic function of its evolving biomass and structure and the prevailing land-use, all of which influences at any time the infiltration characteristics in relation to the prevalent rainfall regime as well as its evapotranspiration levels (Fig. 10). Our study shows that these conditions can change from storm to storm within a monsoonal season as well as across monsoon seasons (Krishnaswamy et al., 2012). In addition, climate change is likely to further increase the frequency of higher intensity rainfall in the Western Ghats and other parts of India (Rakhecha and Soman, 1994; Lal et al., 2001; Goswami et al., 2006 and Pattanaik and Rajeevan, 2010). This scenario suggests that many ecosystems which are currently just above or at the threshold of the "*infiltration-evapotranspiration trade-off*" levels of $K_{fs}$ will be tipped over to a condition that enhances overland flow at the expense of deep percolation. Furthermore certain soil types and land-covers are particularly sensitive to overland flow occurrence (Bonell et al., 2010). We illustrate the trajectory of forest degradation and land-use and land-cover change in relation to the "*infiltration evapotranspiration trade-off*" *hypothesis* and changes in the rainfall intensity regimes using a conceptual diagram, as shown in Fig. 10, which is based on insights gained from this study. As an example, converting natural forest into other categories implies changes in both infiltration characteristics and evapotranspiration, and in the case of tree-plantations it would be a function of tree-density and age. Grazing may further reduce infiltration compared to well-maintained grassland. We further note that natural forest may be able to cope with increased rain intensities in the future compared to the other land-cover types. The overall impact of these various trajectories on hydrologic functions and services is also scale dependant as mentioned earlier.

### 6.3. Infiltration-evapotranspiration trade off: some implications for forest ecosystem restoration and services

A fundamental message of the work is the need to protect and safeguard the natural forests in headwater areas. Such steps are

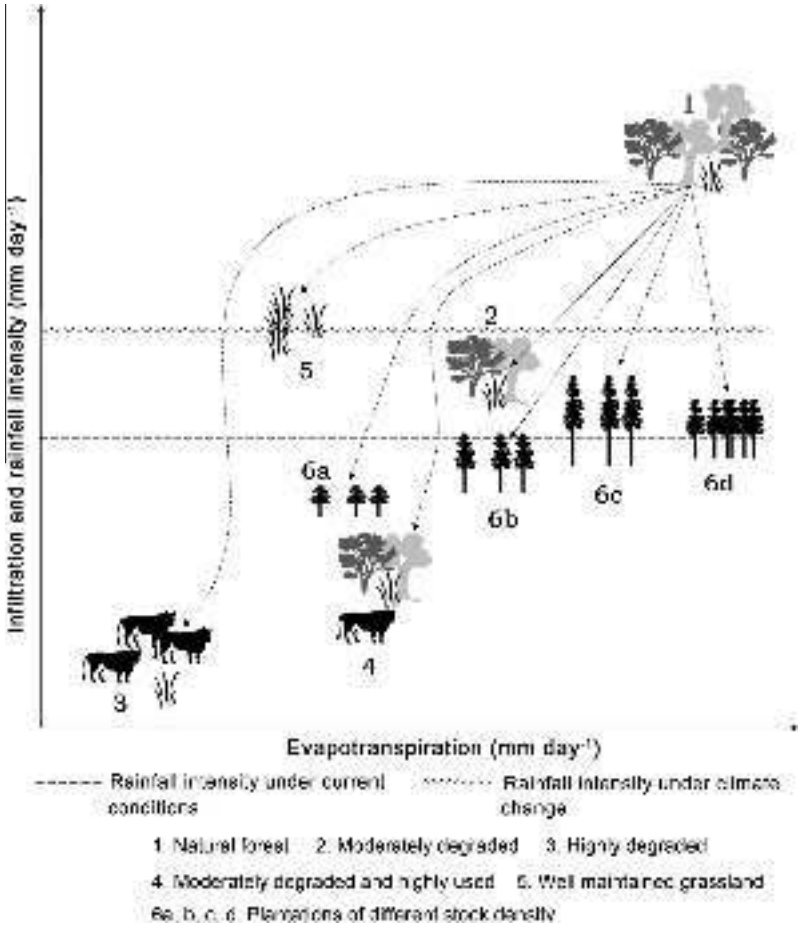


**Fig. 10.** A conceptual diagram ofthe Evapotranspiration-infiltration 'trade-off' as applicable to the study sites and also linked with the hypothesis of Bruijnzeel (1989, 2004). For example conversion of natural forest (1) to over-grazed grassland (3) will reduce both evapotranspiration and infiltration considerably, whereas some young, fast-growing plantations of high density (6d) may match the natural forest (1) in evapotranspiration but will have reduced infiltration. If rainfall intensity exceeds the infiltration the land-cover types are prone to infiltration-excess over run-off and recharge to ground-water will decrease. Under climate change, increase in rainfall intensities will enhance this vulnerability, with consequent changes to hydrologic services.

critical in ensuring that low flows are sustained during the long dry season and thus allow the natural forests to maintain low flows as key "provisioning" ecosystem services (MA, 2005) linked with a more reliable community water supply. It is also evident that the time to recover anywhere close to the natural forest hydrological characteristics (i.e., water balance, FDC) by way of forestation using Acacia may take several decades, or if not at all. The latter is because monocultures for example do not encourage the same diversity of soil biology and ecology (and thus enhanced macro-porosity and resulting effects on infiltration) (Rossi and Blanchart, 2005; Bonell et al., 2010). Despite the paucity of direct measurements of AET of *Acacia sp. /Eucalyptus sp* under humid tropic conditions, the AET of the young and vigorously growing plantations will also possibly be higher than the Natural Forest on the basis of work elsewhere (see review of Scott et al., 2004).

Overall, the management of ecosystems in the Western Ghats needs to take into account the possibility of shifts in hydrologic pathways in the future (Fig. 10) and to local and downstream ecosystem services, such as baseflow of rivers sustaining coastal ecosystems and livelihoods. Furthermore, the planned reforestation and restoration of 6 Million hectares by the Government of India under the Green India Mission initiative (http://www.pib.nic.in/release/release.asp?relid=36449) needs to consider the consequences for hydrologic services under different hydro-climatic conditions. The remarks of Chazdon (2008) that when concerning approaches to restoring forest ecosystems, these "depend strongly on levels of forest and soil degradation, residual vegetation, and desired restoration outcomes" also apply to the hydrologic consequences of such impacts, as highlighted in this work. This study has revealed the potential of certain tropical landscapes characterized by a combination of geo-physical, bio-physical and land-use history to respond hydrologically to forest use, degradation and reforestation in support of the "*infiltration-evapotranspiration trade-off*" hypothesis. The positive role of upstream natural forest in recharging groundwater in the monsoon for downstream sustenance of communities and ecosystems in the Western Ghats is suggested. The implications of these findings, however, remain preliminary. The nature of land cover fragmentation has been a severe constraint in terms of confining such basins studies to comparatively small scales. The critical issue of 'upscaling' results from this type of work still remains a global challenge if it is to realise the objective of comprehensively contributing towards a hydrological basis linked with "provisioning" ecosystem services (Costa et al., 2003; Bruijnzeel, 2004; D'Almeida et al., 2007; MA, 2005; Elmqvist et al., 2010; Rodriguez et al., 2010).

## 7. Conclusions

Through the use of various analytical techniques, the work established some support for the infiltration-evapotranspiration 'trade-off' hypothesis up to basin scales of ~2 km$^2$. Conclusions

from the small basin studies (⩽23 ha) which can be grouped under 1–4 are as follows:

- The frequency–duration–curves (FDC) of streamflow showed the existence of much longer durations of low flows from Forest in contrast to the Acacia and Degraded Forest. These low flows also occupy a large proportion of total Q. Flows below 20 mm day$^{-1}$ in the Coastal, 40 mm day$^{-1}$ in Kodigibail and 80 mm day$^{-1}$ at Vajgar are the approximate thresholds for departure of the Forest from the other land-covers. In contrast, most of the stream discharge emerging from the Acacia and Degraded Forest is associated with storm events coupled with the more flashy nature of the hydrograph responses and very low Q in between storms (as reported in Krishnaswamy et al., 2012). In combination, the latter two factors results in a FDC biased towards the ⩽20% of the flow spectrum.
- The above flashy nature of hydrograph responses is reflected in higher C1 estimates (overland flow) for the Acacia and Degraded Forest basins based on the Furey–Gupta analysis. Such findings are in line with the previous hydraulic conductivity survey that inferred a greater frequency of infiltration-excess overland flow within these land covers (Bonell et al., 2010). Moreover this result is also in line with the earlier reports of higher Quickflow ($Q_F$)/total storm ($Q$) ratios based on hydrographs for specific events for the Degraded Forest and Acacia (as described by Krishnaswamy et al., 2012). Thus the *Acacia auriculiformis* plantations still retains a 'memory' of the storm hydrograph characteristics described above for the Degraded Forest.
- The independent results from the application of three different water balance approaches, which included the use of two modeling techniques (Furey –Gupta, SWIM), all suggest a consistent ranking in priority of groundwater recharge, viz, Forest > Acacia > Degraded Forest. In terms of percentage of rainfall as groundwater recharge however there is some variation, partly due to the assumptions in the methods adopted. Thus for Forest the percentage of rainfall as groundwater recharge ranged from 46.2% to 69.6%, under Acacia (39.4–56.4%) and Degraded Forests (13.9–44.6%). Nonetheless overall, groundwater recharge is substantial under all three ecosystems in the wet-season and is attributed to the specific caveat of soils and hydrogeology found in this environment namely the comparatively high subsoil hydraulic conductivities (Bonell et al., 2010) as well as the nature of the hydrogeology (i.e., fractured rock aquifers). Once rainwater penetrates the surface soil layers of lower permeability in the disturbed land covers, substantial recharge to groundwater can occur. Not all this recharge however becomes streamflow within the headwater experimental basins (which are intermittent), but instead it is considered to emerge downstream in higher-order sub-basins from regional groundwater (point 5 below).
- The zero flux plane analysis highlighted the very low amounts of soil water (< 34 mm) from the top 1.5 m layer across all land covers which were able to service the needs of transpiration and other physiological activities during the dry season. It is suggested that deeper subsurface water sources (deeper soil moisture and groundwater) must compensate for such low amounts in the shallow surface layers. Such findings highlight the importance and need of hydrogeology knowledge which is commonly not mentioned in the context of the infiltration-evapotranspiration 'trade-off' hypothesis.
- Finally at the ~2 km$^2$ basin scale, there is a suggestion of low flows being sustained into the dry season even where the Forest cover exceeds 60% of basin area, thus providing further support for the trade-off hypothesis. Further replications of other similar work are still required in order to derive a more regional figure for the Western Ghats.

## Acknowledgments

We thank the following for financial and administrative support: Suri Sehgal Centre for Biodiversity and Conservation, ATREE, Bangalore, the Ford Foundation, the UNESCO-International Hydrological Programme (Paris and Delhi), the Royal Society of Edinburgh, UK (RSE Grant 483.805998), and The Carnegie Trust for the Universities of Scotland (Carnegie Grant 483.807239). Tim Davie, formerly of the Crown Research Institute, Manaaki Whenua – Land care Research in Lincoln (New Zealand) is also thanked for giving us access, and support (along with Alex Watson), in the use of the HYDSTRA software. A current grant from the Changing Water Cycle programme of the Natural Environment Research Council (NERC, UK, Grant Ref.: NE/I022450/1) – Ministry of Earth Sciences (MoES), Government of India provided support for the revision. We thank WorldClim and International Water Management Institute for making available climate data (Hijmans et al., 2005; New et al., 1999). Finally we gratefully acknowledge Sampurno Bruijnzeel, Vrije Universiteit, Amsterdam for his rigorous review and constructive suggestions on an earlier version of this manuscript.

## References

Allen, R.G., Pereira, L.S., Raes, D., Smith, M., 1998. Crop Evapotranspiration – Guidelines for Computing Crop Water Requirements–FAO Irrigation and Drainage Paper 56, FAO, Rome, Italy.

Blanchart, E., Julka, J.M., 1997. Influence of forest disturbance on earthworm (Oligochaeta) communities in the Western Ghats (South India). Soil Biol. Biochem. 29 (3–4), 303–306.

Bonell, M., Gilmour, D.A., Sinclair, D.F., 1981. Soil hydraulic properties and their effects on surface and subsurface water transfer in a tropical rainforest catchment. Hydrol. Sci. Bull. 26, 1–18.

Bonell, M., Barnes, C.J., Grant, C.R., Howard, A., Burns, J., 1998. High rainfall response-dominated catchments: a comparative study of experiments in tropical north-east Queensland with temperate New Zealand. In: Kendall, C., McDonnell, J.J. (Eds.), Isotope Tracers in Catchment Hydrology. Elsevier, pp. 347–390.

Bonell, M., Callaghan, J., Connor, G., 2004. Synoptic and mesoscale rain producing systems in the humid tropics. In: Bonell, M., Bruijnzeel, L.A. (Eds.), Forests, Water and People in the Humid Tropics – Past, Present and Future Hydrological Research for Integrated Land and Water Management, UNESCO International Hydrology Series. Cambridge University Press, Cambridge, UK, pp. 194–266.

Bonell, M., Purandara, B., Venkatesh, B., Krishnaswamy, J., Acharya, H.A.K., Singh, U.V., Jayakumar, R., Chappell, N., 2010. The Impact of forest use and reforestation on soil hydraulic conductivity in the Western Ghats of India: implications for surface and sub-surface hydrology. J. Hydrol. 391, 47–62. http://dx.doi.org/10.1016/j.jhydrol.2010.07.004.

Bosch, J.M., Hewlett, J.D., 1982. A review of catchment experiments to determine the effects of vegetation changes on water yield and evapotranspiration. J. Hydrol. 55, 3–23.

Bourgeon, G., 1989. Explanatory Booklet on the Reconnaissance Soil Map of Forest Area: Western Karnataka and Goa, Institutfrançais de Pondichéry, travaux de la section scientifiqueet technique, hors série 20, Pondicherry, 96p +Annexes.

Bouwer, H., 1966. Rapid field measurement of air entry value and hydraulic conductivity of soils as significant parameters in flow system analysis. Water Resour. Res. 2, 729–738.

Brown, A.E., Zhang, L., McMahon, T.A., Western, A.W., Vertessy, R.A., 2005. A review of paired catchment studies for determining changes in water yield resulting from alterations in vegetation. J. Hydrol. 310, 28–61.

Bruijnzeel, L.A., 1989. (De)forestation and dry season flow in the tropics: a closer look. J. Trop. For. Sci. 1 (3), 229–243.

Bruijnzeel, L.A., 1990. Hydrology of Moist Tropical Forest and Effects of Conversion: A State of Knowledge Review. UNESCO, Paris and VrijeUniversiteit, Amsterdam, The Netherlands, p. 226.

Bruijnzeel, L.A., 2004. Hydrological functions of tropical forest: not seeing the soil for the trees? Agric. Ecosyst. Environ. 104, 185–228. http://dx.doi.org/10.1016/j.agee.2004.01.015.

Calder, I.R., 1999. The Blue Revolution, Land Use and Integrated Water Resources Management. Earthscan, London, ISBN 1 85383634 6.

Central Groundwater Board, 2008. Groundwater Information Booklet – Uttara Kannada District, Karnataka. Government of India, Ministry of Water Resources, Central Groundwater Board, South Western Region, Bangalore, November 2008, pp. 24 +Appendices.
Chazdon, L.R., 2008. Beyond deforestation: restoring forests and ecosystem services on degraded lands. Science 5882 (320), 1458–1460.
Chiew, F.H.S., McMahon, T.A., 1991. The applicability of morton's and penman's evapotranspiration estimates in rainfall-runoff modeling. JAWRA, J. Am. Water Resour. Assoc. 27, 611–620. http://dx.doi.org/10.1111/j.1752-1688.1991.tb01462.x.
Cook, P.G., 2003. A Guide to Regional Groundwater Flow in Fractured Rock Aquifers. CSIRO-Seaview Press, South Australia, p. 108.
Cooper, J.D., 1980. Measurements of Water Fluxes in Unsaturated Soil in Thetford Forest. Report 66. Institute of Hydrology, Wallingford.
Costa, M.H., Botta, A., Cardille, J.A., 2003. Effects of large-scale changes in land cover on the discharge of the Tocantins River, Southeastern Amazonia. J. Hydrol. 283, 206–217.
D'Almeida, C., Vorosmarty, C.J., Hurtt, G.C., Marengo, J.A., Dingman, S.L., Keim, B.D., 2007. The effects of deforestation on the hydrological cycle in Amazonia: a review on scale and resolution. Int. J. Climatol. 27, 633–647. http://dx.doi.org/10.1002/joc.1475.
Das, A., Krishnaswamy, J., Bawa, K.S., Kiran, M.C., Srinivas, V., Kumar, N.S., Karanth, K.U., 2006. Prioritisation of conservation areas in the western ghats, India. Biol. Conserv. 133, 16–31, http://dx.doi.org/10.1016/j.biocon.2006.05.023.
DeFries, R., Eshleman, K.N., 2004. Land-use change and hydrologic processes: a major focus for the future. Hydrol. Process. 18, 2183–2186.
Elmqvist, T., Tuvendal, M., Krishnaswamy, J., Hylander, K., 2010. Ecosystem Services: Managing trade – offs between provisioning and regulating services. In: Kumar, P., Mike Wood, M. (Eds.), Valuation of Regulating Services of Ecosystems: Methodology and Applications. Routledge, London, New York.
Elsenbeer, H., Lack, A., 1996. Hydrometric and hydrochemical evidence for fast flowpaths at La Cuenca, Western Amazonia. J. Hydrol. 180, 237–250.
FAO, 1998. World Reference Base for Soil Resources. FAO-UN, Rome.
FAO-UNESCO, 1974. FAO-UNESCO Soil map of the world. Legend, UNESCO Press, Paris (Later revised as FAO-UNESCO, 1988. Soil Map of the World, vol. 1. Revised Legend. World Soil Resources Report 60, FAO, Rome).
Furey, P.R., Gupta, V.K., 2001. A physically based filter for separating base flow from streamflow time series. Water Resour. Res. 37, 2709–2722.
Geological Survey of India, 1981. Geological and Mineral Map of Karnataka and Goa.Geological Survey of India, Calcutta.
Geological Survey of India, 2006. Miscellaneous Publication 30. Part VII. Karnataka and Goa.
Goswami, B.N., Venugopal, V., Sengupta, D., Madhusoodanan, M.S., Xavier, P.K., 2006. Increasing trend of extreme rain events over India in a warming environment. Science 314, pp. 1442–1445.
Gunnell, Y., 1997. Relief and climate in South Asia: the influence of the Western Ghats on the current climate pattern of peninsular India. Int. J. Climatol. 17, 1169–1182.
Gunnell, Y., Radhakrishna, B.P., 2001. Sahyadri: The Great Escarpment of the Indian Subcontinent (Patterns of Landscape Development in the Western Ghats). Geological Society of India, Bangalore, p. 1054.
Hijmans, R.J., Cameron, S.E., Parra, J.L., Jones, P.G., Jarvis, A., 2005. Very high resolution interpolated climate surfaces for global land areas. Int. J. Climatol. 25, 1965–1978.
James, E.J., Kumar, P.K.P., Nandeshwar, M.D., Kandasamy, L.C., Ranganna, G., 2000. Investigations on the hydrology of forest watersheds in the Western Ghats. In: Varadan, K.M. (Ed.), Proc. Worskhop on Watershed Development in the Western Ghats Region of India, 28–29 Febraury 2000. Centre for Water resources Development and Management, Kozhikode 673 571, Kerala, pp. 30–43.
Jensen, M.E., Burman, R.D., Allen, R.G., 1990. Evapotranspiration and Irrigation Water Requirements. ASCE Manuals and Reports on Engineering Practice No. 70, ASCE, New York.
Kallarackal, J., Somen, C.K., 2008. Water loss from tree plantations in the tropics. Curr. Sci. 94 (2), 201–210.
Khalil, M., Sakai, M., Mizoguchi, M., Miyazaki, T., 2003. Current and prospective applications of zero flux plane (ZFP) method. J. Jpn. Soc. Soil Phys. 95, 75–90.
Kirsch, S.W., 1993. A field Test of a soil-based measure of evaporatranspiration. Soil Sci. 156, 396–404.
Krishnaswamy, J., Bonell, M., Venkatesh, B., Purandara, B.K., Lele, S., Kiran, M.C., Reddy, V.B., Badiger, S., Rakesh, K.N., 2012. The rain runoff response of tropical humid forest ecosystems to use and reforestation in the western ghats of India. J. Hydrol. 472, 216–237.
Kume, T., Tanaka, Nobuaki, Kuraji, Koichiro, Komatsu, Hikaru, Yoshifuji, Natsuko, Saitoh, Taku M., Suzuki, Masakazu, Tomo'omiKumagai, 2011. Ten-year evapotranspiration estimates in a Bornean tropical rainforest, Agri. For. Meteorol. 151(9), 1183–1192. ISSN 0168-1923, 10.1016/j.agrformet.2011.04.005. <http://www.sciencedirect.com/science/article/pii/S0168192311001183>.
Lal, M., Nozawa, T., Emori, S., Harasawa, H., Takahashi, K., Kimoto, M., Abe-Ouchi, A., Nakajima, T., Takemura, T., Numaguti, A., 2001. Climate change: implication for indian summer monsoon and its variability. Curr. Sci. 9 (81), 1196–1207.
Ledger, D.C., 1975. The water balance of an exceptionally wet catchment area in West Africa. J. Hydrol. 24, 207–214, http://dx.doi.org/10.1016/0022-1694(75)90081-5.
Limbrick, K.J., 2002. Estimating daily recharge to the Chalk aquifer of southern England – a simple methodology. Hydrol. Earth Syst. Sci. 6 (3), 485–496.
MA, 2005. Millennium Ecosystem Assessment (2005) General Synthesis Report. Island Press, Washington, DC.
Menon, S., Bawa, K.S., 1998. Deforestation in the tropics: reconciling disparities in estimates for India. Ambio 27, 576–577.
Nandagiri, L., Kovoor, G., 2006. Performance evaluation of reference evapotranspiration equations across a range of Indian climates. J. Irrig. Drain Eng. 132 (3), 238–249, doi: 10.1061/(ASCE)0733-9437(2006)132:3(238).
NBSSLUP, 1993. Land Evaluation for Land Use Planning. Bull. No. 42, National Bureau of Soil Survey and Land Use Planning, Nagpur, India.
New, M., Hulme, M., Jones, P., 1999. Representing twentieth-century space–time climate variability. Part I: Development of a 1961–90 Mean Monthly terrestrial climatology. J. Climate. 12, 829–856.
Oishi, A.C., Oren, R., Novick, K.A., Palmroth, S., Katul, G.G., 2010. Interannual invariability of forest evapotranspiration and its consequence to water flow downstream. Ecosystems 13 (3), 421–436.
Palmroth, S., Katul, G.G., Hui, D., McCarthy, H.R., Jackson, R.B., Oren, R., 2010. Estimation of long-term basin scale evapotranspiration from streamflow time series. Water Resour. Res. 46, W10512.
Pascal, J.P., 1982. Bioclimates of the Western Ghats on 1/500,000, 2 Sheets. Institute Francais de Pondichery, Travaux de la Section Scientifiqueet technique, Hors. Serie. No. 17.
Pascal, J.P., 1984. (with the collaboration of Shyam Sunder, S. & Meher – Hornji, V.M.). Forest Map of South India-Sheet: Belgaum–Dharwar–Panaji. Published by the Karnataka and Goa Forest Department and the French Institute of Pondicherry. Inst. Fr. Pondichery, Trav. SEC. Sci. Tech. Hors. Serie. 18c.
Pascal, J.P., 1986. Explanatory Booklet on the Forest Map of South India- Sheets: Belgaum–Dharwar–Panaji; Shimoga; Mercara-Mysore. Karnataka Forest Department and the French Institute of Pondicherry, Rapport Institut français Pondichéry, Trav.Sec.Sci.Tech. Hors.Serie. 18.
Pascal, J.P., 1988. Wet evergreen forests of the Western Ghats of India. Inst. fr.Pondichery, Trav. Sec. Sci. Tech., Tome 20 bis, p. 345.
Pattanaik, D.R., Rajeevan, M., 2010. Variability of extreme rainfall events over India during southwest monsoon season. Meteorol. Appl. 17, 88–104.
Pomeroy, M., Primack, R., Rai, S.N., 2003. Changes in four rainforest plots of the Western Ghats, India, 1939–1993. Conserv. Soc. 1, 113–135.
Pontius, R.G., Pacheco, P., 2004. Calibration and validation of a model of forest disturbance in the Western Ghats, India 1920–1990. GeoJournal 61 (4), 325–334. http://dx.doi.org/10.1007/s10708-004-5049-5.
Prieto, I., Armas, C., Pugnaire, F., 2012. Water release through plant roots: new insights into its consequences at the plant and ecosystem level. New Phytol. 193, 830–841.
Priya, D., Prita, D., Arjun, M., Pratjeesj, C.M., Carrigues, J.P., Puryavaud, J.P., Roessingh, K., 2007. Forest degradation in the Western Ghats biodiversity hotspot, Resources collection, livelihood concersn and sustainability. Curr. Sci. 93 (11), 1573–1578.
Putty, M.R.Y., Prasad, R., 2000a. Run off processes in head water catchment – an experimental study in Western Ghats in South India. J. Hydrol. 235, 63–71.
Putty, M.R.Y., Prasad, R., 2000b. Understanding runoff processes using a watershed model—a case study in the Western Ghats in South India. J. Hydrol. 228, 215–227.
Rai, S.N., 1999. Nursery and Planting Techniques of Forest Trees in Tropical South-Asia. Punarvasu publications, Dharwad, Karantaka – Eastern Press, Bangalore, India. 217 pp.
Rai, N.D., 2004. The Socio-economic and ecological impact of Garciniagumm-gutta fruit harvest in the Western Ghats, India. In: Kusters, Koen, Belcher, Brian (Eds.), Forest Products, Livelihoods and Conservation. Case Studies of Non-Timber Forest Product Systems, vol. 1. CIFOR, Asia, pp. 23–42.
Rakhecha, P.R., Soman, M.K., 1994. Trends in the annual extreme rainfall events of 1–3 days duration over India. Theor. Appl. Climatol. 48, 227–237.
Ramesh, B.R., Pascal, J., 1997. Atlas of endemics of the Western Ghats (India): Distribution of Tree Species in the Evergreen and Semi-evergreen Forests. Institut Francais de Pondichery, Publications du department d'ecologie, p. 38.
Ramesh, B.R., Swaminath, M.H., (with many collaborators), 1999. Assessment and Conservation of Forest Biodiversity in the Western Ghats of Karnataka, India. French Institute of Pondicherry in Collaboration with the Karnataka Forest Department and FondsFrançais de l'EnvironnementMondial, December 1999, Report available from l'InsitutFrançais de Pondicherry, 126 pp (text plus bibliography, maps, colour plates, 5 Annexes).
Roa-García, M.C., Brown, S., Schreier, H., Lavkulich, L.M., 2011. The role of land use and soils in regulatingwater flow in small headwater catchments of the Andes. Water Resour. Res. 47, W05510. http://dx.doi.org/10.1029/2010WR009582.
Roberts, J.M., Gash, J.H.C., Tani, M., Bruijnzeel, L.A., 2004. Controls on evaporation in lowland tropical rainforest. In: Bonell, M., Bruijnzeel, L.A. (Eds.), Forests, Water and People in the Humid Tropics – Past, Present and Future Hydrological Research for Integrated Land and Water Management. International Hydrological Series, Cambridge University Press, Cambridge, UK, pp. 287–313.
Rodriguez, D.A., Tomasella, J., Linhares, C., 2010. Is forest conversion to pasture affecting the hydrological response of Amazonian catchments? Signals in the Ji-Parana Basin. Hydrol. Process. 24 (10), 1254–1269.
Rossi, J.P., Blanchart, E., 2005. Seasonal and land-use induced variation of soil macro fauna composition in the Western Ghats, southern India. Soil Biol. Biochem. 37 (6), 1093–1104.
Scott, D.F., Bruijnzeel, L.A., Mackensen, J., 2004. The hydrological impacts of reforestation of grasslands, natural and degraded and of degraded forest in the tropics. In: Bonell, M., Bruijnzeel, L.A. (Eds.), Forests, Water andPeople in the

Humid Tropics: Past, Present and Future Hydrological Research for IntegratedLand and Water Management. UNESCO-Cambridge University Press, Cambridge, UK, pp. 622–651.

Seen, D.L., Ramesh, B.R., Nair, K.M., Martin, M., Arrouay, D., Bourgeon, G., 2010. Soil carbon stocks, deforestation and land-cover changes in the Western Ghats biodiversity hotspot (India). Glob. Change Biol. 16, 1777–1792. http://dx.doi.org/10.1111/j.1365-2486.2009.02127.x.

Shivaprasad, C.R., Reddy, R.S., Sehgal, J., Velayutham, M., 1998. Soils of Karnataka, Soils of India Series, National Bureau of Soil Survey and Land Use Planning (NBSSLUP), Publ. No. 47, 88 pp.

Smakhtin, V.U., 2001. Low flow hydrology.arivew. J. Hydrol. 240, 147–186 <http://dx.doi.org/10.1016/S0022-1694(00)00340-1>.

Soil Survey Staff, 1975 (later 2nd ed. 1999). Soil Taxonomy: A Basic System of Soil Classification for Making and Interpreting Soil Surveys. US Department of Agriculture Handbook No. 436, 754 pp.

Stonestrom, D.A., Scanlon, B.R., Zhang, L., 2009. Introduction to special section on impacts of land use change on water resources. Water Resour. Res. 45. http://dx.doi.org/10.1029/2009WR007937, 2009.

Turc, L., 1961. Evaluation de besoins en eau d'irrigation, ET potentielle. Ann. Agron. 12, 13–49.

Turner, M.G., Hargrove, W.W., Gardner, R.H., Romme, W.H., 1994. Effects of fire on landscape heterogeneity in Yellowstone National Park, Wyoming. J. Veg. Sci. 5, 731–742.

Venkatesh, B., Lakshman, N., Purandara, B.K., Reddy, V.B., 2011. Analysis of observed soil moisture patterns under different land covers in Western Ghats, India. J. Hydrol. 397, 281–294.

Verburg, K., 1996. Methodology in soil water and solute balance modelling: an evaluation of the APSIM-Soil Wat and SWIMv2 models ISBN 0 643 05868 0. Adelaide: CSIRO Division of Soils. Divisional Report.

Vogel, R.M., Fennessey, N.M., 1994. Flow Duration Curves I: New interpretation and confidence intervals. J. Water Resour. Plann. Manage. 120, 485–504.

Vogel, R.M., Fennessey, N.M., 1995. Flow Duration Curves II: a review of application in water resource planning. JAWRA 31, 1029–1039.

Vorosmarty, C.J., Sahagian, D., 2000. antropogenic disturbance of the terrestrial water cycle. Bioscience 50 (9), 753–765.

Wellings, S.R., Bell, J.P., 1980. Movement of water and nitrate in the unsaturated zone of Upper Chalk near Winchester Hants, England. J. Hydrol. 48, 119–136.

Yoder, R.E., Odiahambo, L.O., Wright, W.C., 2005. Evalaution of methods for estimating daily reference crop evapotranspiration at a site in humid south east United States. Appl. Eng. Agri. (ASAE) 21, 197–202.

WATER RESOURCES RESEARCH, VOL. 49, 1–13, doi:10.1002/wrcr.20133, 2013

# Impact of India's watershed development programs on biomass productivity

R. S. Bhalla,[1] K. V. Devi Prasad,[2] and Neil W. Pelkey[3]

Received 18 October 2012; revised 4 February 2013; accepted 8 February 2013.

[1] Watershed development (WSD) is an important and expensive rural development initiative in India. Proponents of the approach contend that treating watersheds will increase agricultural and overall biomass productivity, which in turn will reduce rural poverty. We used satellite-measured normalized differenced vegetation index as a proxy for land productivity to test this crucial contention. We compared microwatersheds that had received funding and completed watershed restoration with adjacent untreated microwatersheds in the same region. As the criteria used can influence results, we analyzed microwatersheds grouped by catchment, state, ecological region, and biogeographical zones for analysis. We also analyzed pre treatment and posttreatment changes for the same watersheds in those schemes. Our findings show that WSD has not resulted in a significant increase in productivity in treated microwatersheds at any grouping, when compared to adjacent untreated microwatershed or the same microwatershed prior to treatment. We conclude that the well-intentioned people-centric WSD efforts may be inhibited by failing to adequately address the basic geomorphology and hydraulic condition of the catchment areas at all scales.

**Citation:** Bhalla, R. S., K. V. Devi Prasad, and N. W. Pelkey (2013), Impact of India's watershed development programs on biomass productivity, *Water Resour. Res.*, *49*, doi:10.1002/wrcr.20133.

## 1. Introduction

[2] Watershed development (WSD) in India is largely governed by a set of guidelines released by the Ministry of Rural Development that are revised regularly, the latest revision being in 2008. Successive guidelines have used a remarkably consistent set of implementation arrangements and criteria through which areas are selected for restoration [*Bhalla et al*., 2011]. WSD is an important component of India's poverty alleviation and rural development efforts with livelihoods being considered a "core objective" [*Joshi*, 2006]. Restoration activities recommended by the guidelines are designed to generate local employment. They target recharge of aquifers, afforestation of catchment areas, rain water harvesting for increasing soil moisture and irrigation, stabilization of slopes, sediment retention, and revegetation of degraded lands [*Government of India*, 2008]. These activities often result in obstruction of natural flows and increasing evapotranspiration [*Batchelor et al*., 2003; *Calder et al*., 2008].

[3] WSD elsewhere, particularly in North America, differs in being largely concerned with meeting water quality standards and protecting water resources. In this respect the western version of WSD is centered on restoration of watershed function [*Cairns*, 1989]. Much literature on watershed restoration is therefore related to hydraulic function and processes, covering transport of sediments [*Anbumozhi et al*., 2005; *Behera and Panda*, 2006; *Fowler and Heady*, 1981; *Tripathi et al*., 2003], nutrients and pollutants [*Cullum et al*., 2006], and impacts of land use changes on stream flow and ground water recharge [*Allan*, 2004; *Bonell et al*., 2010; *Bruijnzeel*, 2004; *Cao et al*., 2009; *Randhir and Hawes*, 2009; *Scanlon et al*., 2007]. Geographic information system (GIS) and remote sensing applications have been used extensively in hydrological modeling [*Setegn et al*., 2008; *Tobin and Bennett*, 2009] with examples from India as well [*Gosain and Rao*, 2004; *Gosain et al*., 2006; *Jain et al*., 2000; *Rao et al*., 1991; *Rao and Kumar*, 2004], albeit with some limitations [*Madon and Sahay*, 1997].

[4] Comprehensive datasets to facilitate scientific management and long-term monitoring of watershed restoration are increasing in number [*Frissell and Ralph*, 1998]. This has led to studies where analysis has been undertaken with the broad objective of "preserving ecosystem integrity while maintaining sustainable benefits for human populations" [*Montgomery et al*., 1995]. This approach to WSD moves from treating symptoms to treating causal processes that operate at landscape scales. Various authors have highlighted the advantage of watershed level restoration as opposed to microinterventions [*Frissell and Ralph*, 1998;

Additional supporting information may be found in the online version of this article.

[1]Foundation for Ecological Research, Advocacy, and Learning, Puducherry, India.
[2]Department of Ecology and Environmental Science, Pondicherry University, Kalapet, Puducherry, India.
[3]Environmental Science and Information Technology, Juniata College, Huntingdon, Pennsylvania, USA.

Corresponding author: R. S. Bhalla, Foundation for Ecological Research, Advocacy, and Learning Pondicherry Campus, 170/3 Morattandi, Auroville Post Vanur Tk, Villupuram Dt., Puducherry 605101, Tamil Nadu, India. (bhalla@feralindia.org)


0043-1397/13/10.1002/wrcr.20133

*Kerr*, 2007; *Wohl et al*., 2005] l however, the latter remains a norm in India.

[5] Stakeholder-based collaborative watershed management has become part of national policy in many countries. This includes Australia and North America [*Curtis et al*., 2005; *Ferreyra and Beard*, 2007] and more recently in Europe under the European Union (EU) Water Framework Directive [*Bruen*, 2008]. The Indian policy for watershed management took a similar route since the Hanumantha Rao Committee report in 1994 [*Government of India*, 1994]. However, there is a fundamental difference. In the west, stakeholders operate at a policy level leaving the implementation to technical teams. In India, stakeholders are expected to act as implementers while policy decisions are left to experts.

[6] The dependence of rural poor on natural resources is well documented internationally [*Bruce and Mearns*, 2002; *Jodha*, 1995; *Millenium Ecosystem Assessment*, 2005; *World Resources Institute*, 2005]. This is the basic premise for linking WSD and poverty alleviation. The latest set of guidelines emphasizes increased returns from natural resources through interventions in areas that have higher productivity potential [*Wani et al*., 2006]. The National Rainfed Area Authority has been created as a crucial component of the new watershed policy. There are some reservations to this approach [*Reddy et al*., 2004; *Reddy*, 2006] and the association made between WSD and increased agricultural productivity [*Hope*, 2007; *Turton et al*., 1998]. Studies on WHD programs in India have raised a number of fundamental concerns that contribute to their poor performance. These include iniquitous sharing of benefits [*Kerr*, 2002; *Kerr et al*., 2002], overemphasis on institutional aspects at the expense of application of appropriate technology [*Vaidyanathan*, 2006], contradictions in management and restoration that arise from different scales at which optimal interventions can be made [*Kerr*, 2007], failure to address functional aspects of watershed restoration [*Joy et al*., 2006], inconsistencies in criteria used to select microwatersheds for treatment [*Bhalla et al*., 2011], and added cost and liability due to overreliance on nongovernment organizations [*Chandrashekar*, 2005; *Deshpande*, 2008].

[7] The primary objective of this paper is to determine whether India's WSD programs have succeeded in their major premise of increasing primary productivity.

## 2. Material and Methods

### 2.1. Hypothesis

[8] We tested the above premise of WSD, namely—that it leads to higher productivity. We adopted an approach based on remote sensing and a spatially explicit all India data set on completed watershed projects. Normalized difference vegetation index (NDVI) in treated, and adjacent, untreated microwatersheds were compared before and after restoration (Figure 1). The NDVI provides a robust index of productivity as it measures chlorophyll content on a scale from $-1$ to 1. It is calculated using the formula $\mathrm{NDVI} = (\mathrm{NIR} - \mathrm{Red})/(\mathrm{NIR} + \mathrm{Red})$ where NIR is the near infrared band and red corresponds to the red band in the image. It has been used in studies on net primary productivity [*Matsushita and Tamura*, 2002] and related ecosystem and hydrological services [*Krishnaswamy et al*., 2009] extensively across the world (see *Pettorelli et al*. [2005] for a brief glossary). NDVI values have also been used extensively for land cover mapping. Various studies have deduced values corresponding to thick vegetation, scrub, barren soils, and water bodies and moist soils.

[9] Successful WHD projects are expected to result in an increase in biomass (grazing lands, fuel, fodder, tree cover), agricultural productivity, reduced soil erosion, increased soil moisture, and increased ground water recharge [*Government of India*, 2006]. All these positively influence vegetative cover, albeit, there can be seasonal effects or lags. For instance, increasing groundwater recharge should lead to increasing NDVI as rising water table will improve tree growth as well as bringing shallow wells back into production for nonsurface supplies of water [*Heuperman et al*., 2002].

[10] NDVI data have been used for a range of land use/land cover change detection studies [*Lunetta et al*., 2006]. Our application, however, is simpler as it merely looks at whether NDVI has increased or decreased and the marked response of NDVI in vegetated as opposed to unvegetated areas is sufficiently sensitive for the purpose [*Friedl et al*., 2002]. We have dealt with seasonal aspects by using 16 day composites for four periods of the year and used the higher 250 m resolution images to ensure there were sufficient pixels per sampling unit, the microwatershed.

[11] We were faced with a rather daunting set of subhypotheses—there were 1025 prewatershed and postwatershed comparisons and 4839 pairs of treated and untreated microwatersheds in our data set. Each microwatershed contained hundreds to thousands of NDVI pixels. Within those comparison there was the issue of choice of a test statistic. The explicit hypothesis was that the posttreatment watershed would have greater productivity, and thus we initially used the greater than criterion as a baseline. The one-tailed criterion exacerbates the chance of finding significance where none really exists, so we also ran two-sided tests for all comparisons. The data regularly failed standard tests of normality, but not always. So we also used Wilcoxon tests. Consistent results across the tests would confirm that the signal in the data was consistent, and inconsistent results would suggest that method might be driving the results.

[12] The following hypothesis was tested:

[13] 1. NDVI values for the treated microwatersheds would show a greater increase than the control microwatersheds, or $\delta\mathrm{NDVI}_{\mathrm{ctrl}} < \delta\mathrm{NDVI}_{\mathrm{treated}}$ where $\delta\mathrm{NDVI} = \mathrm{NDVI}_{\mathrm{post}} - \mathrm{NDVI}_{\mathrm{pre}}$.

[14] 2. The NDVI values of treated watersheds should not be significantly different from untreated watersheds before the treatment but should be higher than control watersheds after WSD, or

[15] i. $\mathrm{NDVI}_{\mathrm{ctrl(pre)}} \sim \mathrm{NDVI}_{\mathrm{treated(pre)}}$

[16] ii. but $\mathrm{NDVI}_{\mathrm{ctrl(post)}} < \mathrm{NDVI}_{\mathrm{treated(post)}}$.

[17] 3. NDVI values of treated watersheds should be higher after treatment, but this should not be so for control watersheds, or

[18] i. $\mathrm{NDVI}_{\mathrm{ctrl(pre)}} \sim \mathrm{NDVI}_{\mathrm{ctrl(post)}}$

[19] ii. but $\mathrm{NDVI}_{\mathrm{treated(pre)}} < \mathrm{NDVI}_{\mathrm{treated(post)}}$.

### 2.2. Data Preparation

[20] The list of microwatersheds where work had been completed in the period between 31 December 2006 and 31

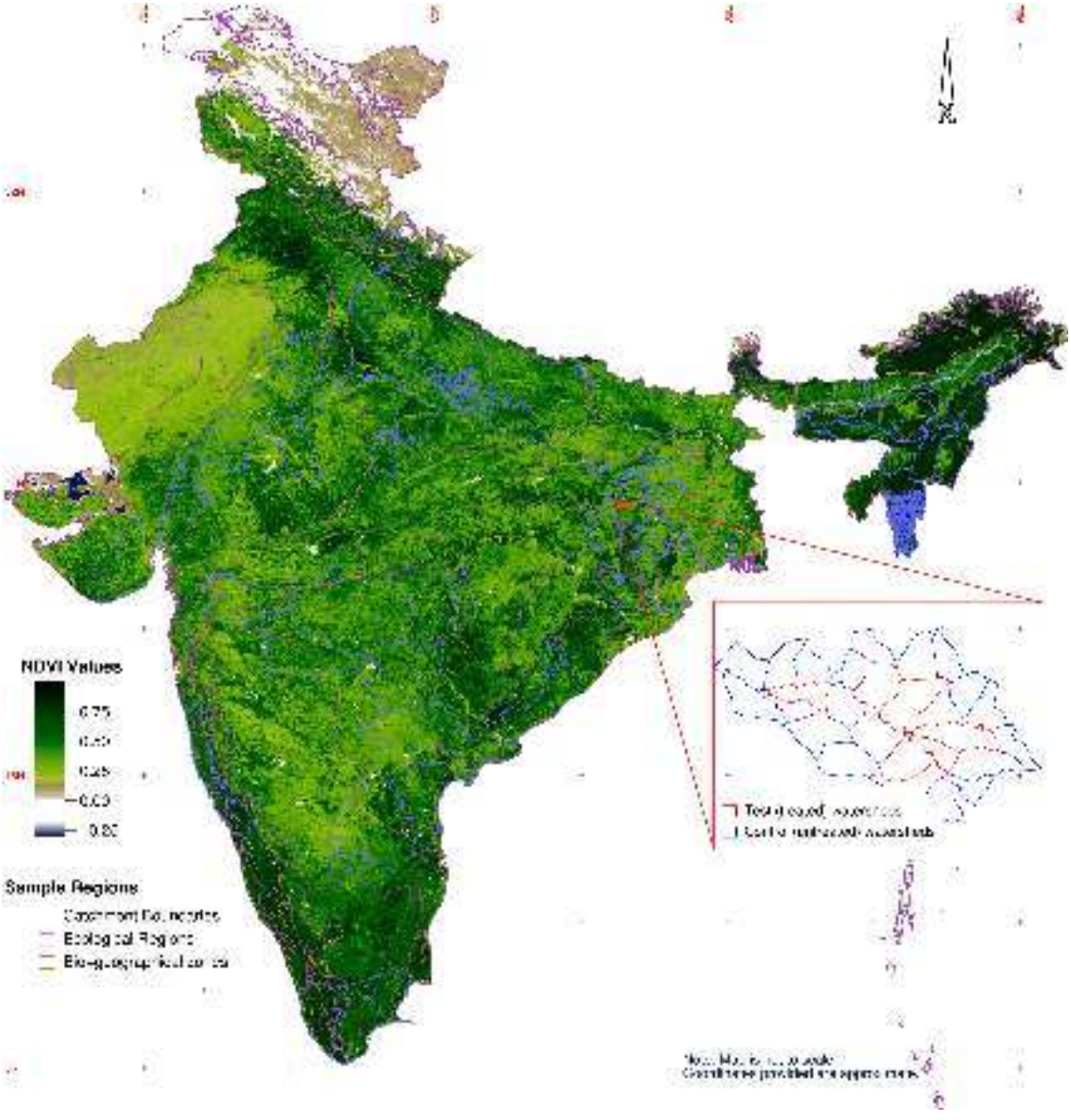


**Figure 1.** Mosaicked MODIS-Terra NDVI values on a map of India showing the boundaries for biogeographical zones, catchments, ecological regions, and states.

December 2010 was compiled from the watershed programs monitoring information system [*Department of IT, Ministry of Communications and Information Technology, GOI*, 2012]. We selected pairs of treated and neighboring untreated (control) microwatersheds to account for local variations. The analysis was grouped across administrative boundaries of states, catchment boundaries, ecological regions [*Olson et al*., 2001], and biogeographical zones [*Rodgers and Panwar*, 1988]. We thereby tried to capture any patterns that were on account of different state policies, watershed catchments, and ecological or climatic factors. To ensure that seasonal variations in NDVI were covered, we used images composites for the dates of 23 April, 29 August, and 19 December for the years 2006 and 2011. We used the minimum, maximum, and mean values of NDVI for all the data sets to ensure that aggregation of values did not bias the results. Only those microwatersheds that contained over 30 pixels were selected. Further, we removed all data sets where there were fewer than 30 pairs to ensure the statistical analysis was more reliable. We then categorized the NDVI values into four responses corresponding to water (NDVI$<0$), barren areas ($0<$NDVI$\leq 0.1$), shrub and grassland ($0.1<$NDVI$\leq 0.3$), and green vegetation and crops (NDVI$>0.3$) [*Herring and Weier*, 2000], and reran the analysis.

[21] Microwatershed maps and administrative boundaries from the National Remote Sensing Center's BHUVAN facility [*NRSC/ISRO*, 2011] were used along with MODIS/Terra Vegetation Indices 16-Day L3 Global 250m SIN Grid [*NASA Land Processes Distributed Active Archive Center (LP DAAC)*, 2011]. These images are preprocessed and are suitable for analytical purposes. They have a range

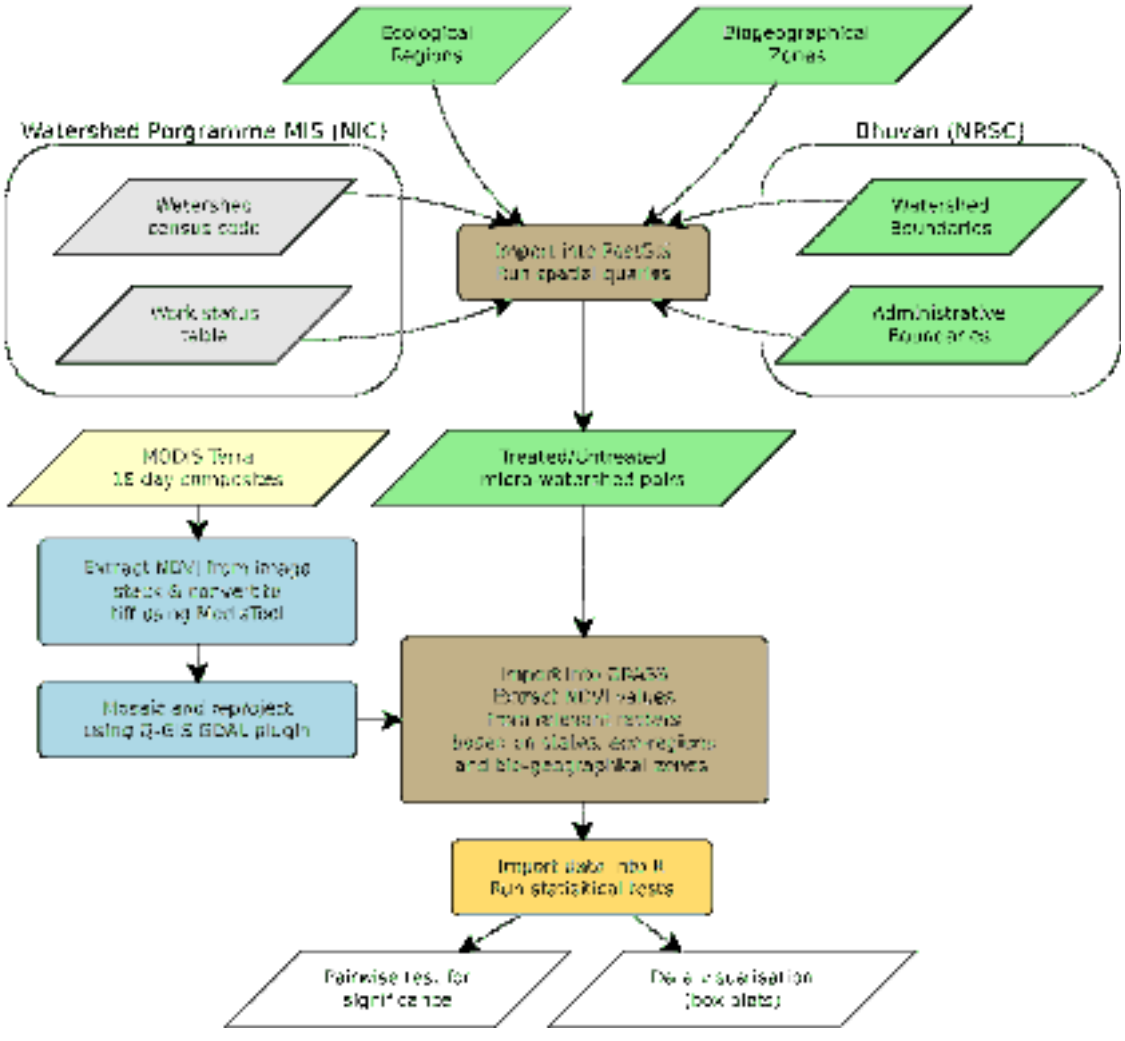


**Figure 2.** Procedure followed for compilation of data and analysis. The steps involved: (1) Downloading relevant datasets, both vectors (green), data (gray), and imageries (yellow). (2) Spatial queries (brown) to derive control and treated microwatersheds based on date of project completion and adjacent (control) microwatersheds. (3) Raster operations (blue) to extract minimum, mean, and maximum NDVI values falling under catchment areas, biogeographical zones, ecological regions, and state boundaries. (4) Importing data into R and performing statistical tests (orange) (5) Exporting aggregated results as box plots and histograms (white).

of −2000 to 10,000 and can be rescaled to actual NDVI values by multiplying with a scale factor of 0.0001. A map showing some of the data sets is presented in Figure 1.

### 2.3. Analysis

[22] Software used for the analysis included the PostGIS geospatial database system [*Ramsey*, 2005], the Geographical Resource Analysis and Support System [*GRASS Development Team*, 2008], and the R system for statistical computing with additional packages [*Conway et al.*, 2012; *Fox*, 2005; *R Development Core Team*, 2008]. The steps involved in the analysis are provided in Figure 2, and the data and R script used for analysis are presented in the supporting information. The script loops through all the factors, namely states, biogeographical zones, ecoregions, and catchments and outputs the results to database tables. In addition, it tests for the two-sided, less and greater alternative of the paired and unpaired tests. This generated thousands of results (Table 1) and over 300 graphical outputs for each of the hypothesis and permutations of the options listed above. The script executes a number of SQL statements, and a compressed backup of the database has been included so the reader may validate the analysis and modify the queries.

## 3. Results

[23] Figures 3–12 present a comparison of the $P$ values for the three hypothesis using a two-sided alternative for pairwise and unpaired comparisons of $t$ test and paired Wilcoxon tests (signed rank tests with and without continuity correction) and unpaired Wilcoxon rank sum test (equivalent to the Mann-Whitney test).

[24] We summarized the results of all the tests by transforming the $P$ values using a $\log(1/P - \text{value})$ transform. This spreads out the values falling in the significant range.

**Table 1.** Summary of Results Showing Proportion of Significant and Nonsignificant Results for the Less and Greater Alternative at a *P* Value of 0.025 and 0.05 (Corresponding to 0.05 and 0.1 on a Two-Sided Alternative)

| Hypothesis | Result | Number of *P* Values | *P* Value ≤ 0.025 (%) | | *P* Value ≤ 0.05 (%) | |
|---|---|---|---|---|---|---|
| | | | Less | Greater | Less | Greater |
| Hyp. 1: $\delta\text{NDVI}_{\text{ctrl}} < \delta\text{NDVI}_{\text{treatment}}$ | Raw NDVI | 6370 | 9 | 5 | 11 | 7 |
| where $\delta\text{NDVI} = \text{NDVI}_{\text{post}} - \text{NDVI}_{\text{pre}}$ | Responses | 1288 | 1 | 2 | 2 | 4 |
| Hyp. 2a: $\text{NDVI}_{\text{ctrl(pre)}} \sim \text{NDVI}_{\text{treated(pre)}}$ | Raw NDVI | 4947 | 7 | 8 | 9 | 12 |
| | Responses | 847 | 1 | 13 | 2 | 15 |
| Hyp. 2b: $\text{NDVI}_{\text{ctrl(post)}} < \text{NDVI}_{\text{treated(post)}}$ | Raw NDVI | 6341 | 8 | 6 | 10 | 8 |
| | Responses | 1325 | 0 | 14 | 0 | 18 |
| Hyp. 3a: $\text{NDVI}_{\text{ctrl(pre)}} \sim \text{NDVI}_{\text{ctrl(post)}}$ | Raw NDVI | 2958 | 12 | 16 | 13 | 18 |
| | Responses | 1197 | 3 | 17 | 4 | 21 |
| Hyp. 3b: $\text{NDVI}_{\text{treated(pre)}} < \text{NDVI}_{\text{treated(post)}}$ | Raw NDVI | 2847 | 12 | 16 | 13 | 18 |
| | Responses | 1097 | 3 | 17 | 4 | 22 |

Box plots of the *P* values were then plotted for the various hypothesis using the less alternative on the negative and greater alternative on the positive *x* axis. The region between the dashed lines indicates nonsignificant values at $P = 0.05$ (0.025 at either tail). Paired *t* tests and the signed rank test with continuity correction provided similar results while the other tests, namely, one sample *t* test, Wilcoxon signed rank test, and the rank-sum test with continuity correction showed varying results. Part of this is due to the effect of binning the data into responses, which resulted in ties that violate one of the assumptions of the Mann-Whitney test, i.e., the data should be continuous variables and therefore have no ties. Also, the paired Wilcoxon test depends on pairwise differences that are zero for some of the pairs, which invalidated some of the comparisons.

### 3.1. Do Treated Watersheds Show a Higher Positive Change in NDVI?

[25] Tests for difference in NDVI values before and after treatment ($\delta\text{NDVI} = \text{NDVI}_{\text{post}} - \text{NDVI}_{\text{pre}}$) for control and treated watersheds showed that there was no significant difference for the majority of microwatersheds irrespective of grouping (Figure 3) or response (Figure 4).

### 3.2. Are Pretreatment NDVI Values for Treated/Control Watershed Any Different Than Posttreatment?

[26] Tests between control watersheds and treated watersheds in 2011 (posttreatment) and 2006 (pretreatment) are summarized in Figures 5–8. The differences between NDVI values prior to treatment of both the treated and nontreated watersheds were not significant for the bulk of the microwatersheds across both grouping (Figure 5) and after binning the NDVI into responses (Figure 6). A comparison of NDVI values of treated and control microwatersheds after the treatment period showed that the bulk of the values was nonsignificant across groups (Figure 7) and when binned into responses (Figure 8).

### 3.3. Are NDVI Values Higher Posttreatment for Treated but Not for Control Microwatersheds?

[27] Results for the third hypothesis are summarized in Figures 9–12. Most microwatersheds did not show a significant difference between 2006 and 2011, regardless of treatment. NDVI values of tests between control watersheds in 2006 and 2011 were expected not to be significantly different. This was the case regardless of whether the microwatersheds were grouped (Figure 9) or the NDVI values binned into response categories (Figure 10). On the other hand, the treated watersheds were expected to exhibit lower NDVI values in 2006 when compared to 2011. This was not the case either when NDVI values were tested across groups (Figure 11) or binned into responses (Figure 12).

### 3.4. Summary of Results

[28] The majority of comparisons showed that the differences between the combination of control and treatment and before and after were nonsignificant. Furthermore, many of the results showed a greater proportion of control or pretreatment responses had higher significance than treated microwatersheds or posttreatment microwatersheds (Table 1). In other words, there is no evidence that productivity of microwatersheds treated as part of WHD projects is greater than untreated regions nor has there been an increase in productivity of the same microwatersheds after WHD when compared to a period prior to treatment.

## 4. Discussion and Conclusions

[29] The poverty-alleviation centric approach to WSD in India would lead one to expect that performance of such projects is measured in enhanced delivery of ecological services, if hydrologic and ecological goals are more than nominal. Changes in hydrologic services associated with improved ecological function of watersheds are used to justify a number of large restoration programs. Such an approach cannot work in India as information required to measure changes in hydrological and ecosystem functions is severely lacking, both on a temporal and a spatial scale. Most online portals for India, which are expected to provide such information remain bereft of data and most agencies, still share their information through paper maps, and hydrological gaging stations are usually limited to dam and barrage sites on major rivers. The resolution of other datasets, such as meteorological measurements, soil, geology, land use, and topography, is insufficient for most models forcing researchers to interpolate or derive "reasonable" values through modeling routines provided by software. This diminishes the accuracy of model predictions and therefore renders them less useful for planners.

[30] Given these limitations, the easiest way to measure the success of interventions in watersheds is to determine their impacts on overall productivities rather than hydrological

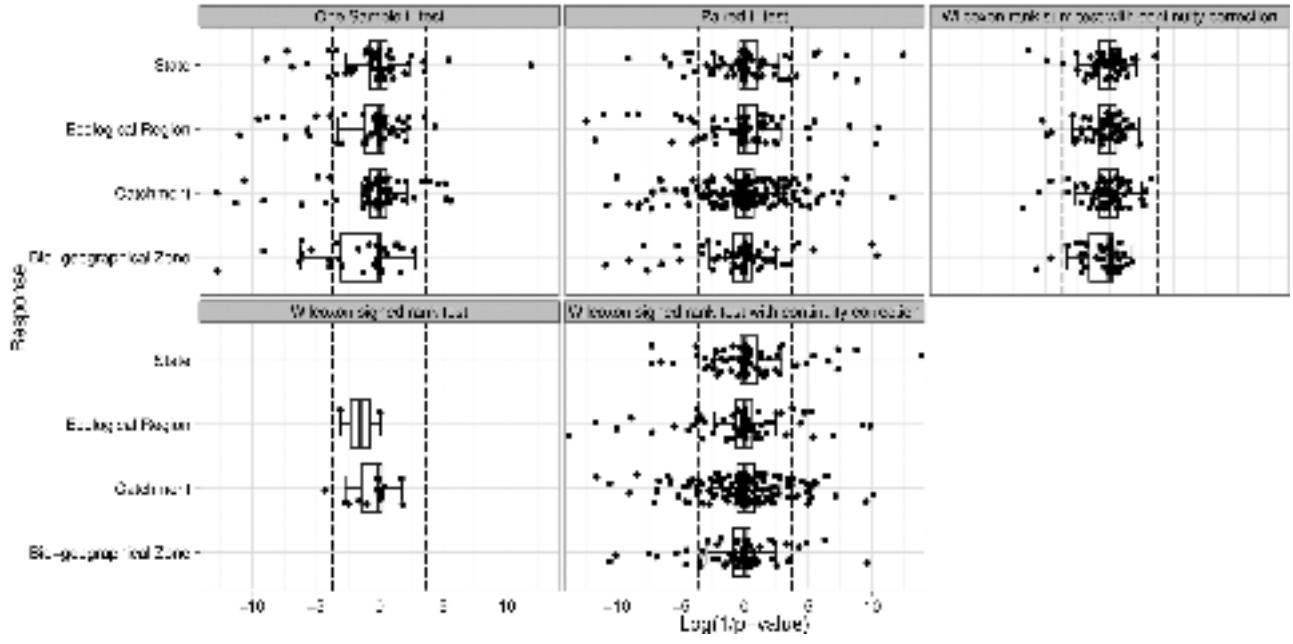

**Figure 3.** Box plots of $P$ values for pairwise and unpaired tests using the less alternative on the negative and greater alternative on the positive $x$ axis. Regions outside the dashed lines are significant at $P = 0.05$. Hypothesis 1: $\delta\text{NDVI}_{\text{ctrl}} < \delta\text{NDVI}_{\text{treatment}}$ where $\delta\text{NDVI} = \text{NDVI}_{\text{post}} - \text{NDVI}_{\text{pre}}$ on NDVI values. Most values lie between the dashed lines showing they were nonsignificant. Similar number of values lie on other sides of showing that the number of microwatersheds where NDVI values increased after treatment was similar to the numbers showing a significant decrease in NDVI.

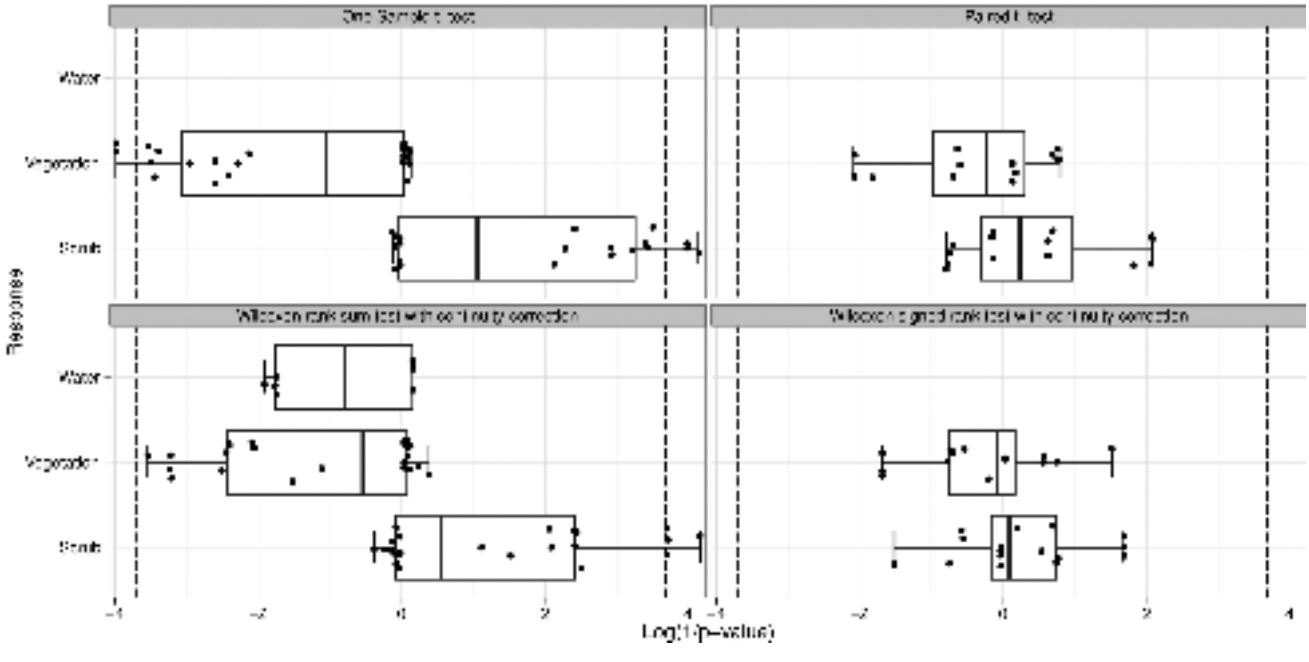

**Figure 4.** Box plots of $P$ values for pairwise and unpaired tests using the less alternative on the negative and greater alternative on the positive $x$ axis. Regions outside the dashed lines are significant at $P = 0.05$. Hypothesis 1: $\delta\text{NDVI}_{\text{ctrl}} < \delta\text{NDVI}_{\text{treatment}}$ where $\delta\text{NDVI} = \text{NDVI}_{\text{post}} - \text{NDVI}_{\text{pre}}$ on responses. Bulk of the values lies between the dashed lines indicating they are nonsignificant. Some microwatersheds show a significant decrease in vegetation and a significant increase in scrub.

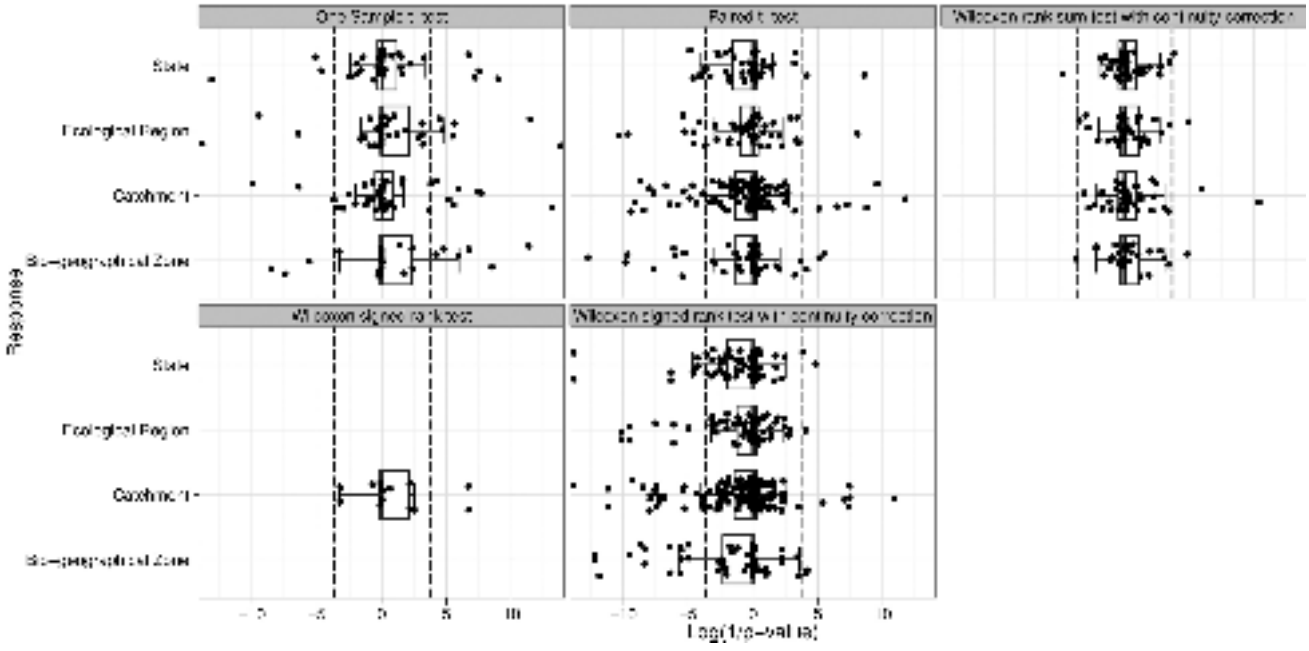

**Figure 5.** Box plots of $P$ values for pairwise and unpaired tests using the less alternative on the negative and greater alternative on the positive $x$ axis. Regions outside the dashed lines are significant at $P = 0.05$. Results for hypothesis 2a: $\mathrm{NDVI}_{\mathrm{ctrl(pre)}} \sim \mathrm{NDVI}_{\mathrm{treatment(pre)}}$ on NDVI values. A large number of points lie between the dashed lines showing they are no significant differences between the control and treatment prior to watershed restoration. Of the significant values, the majority lie to the left of the dashed line, indicating that some control microwatersheds had higher NDVI values prior to treatment.

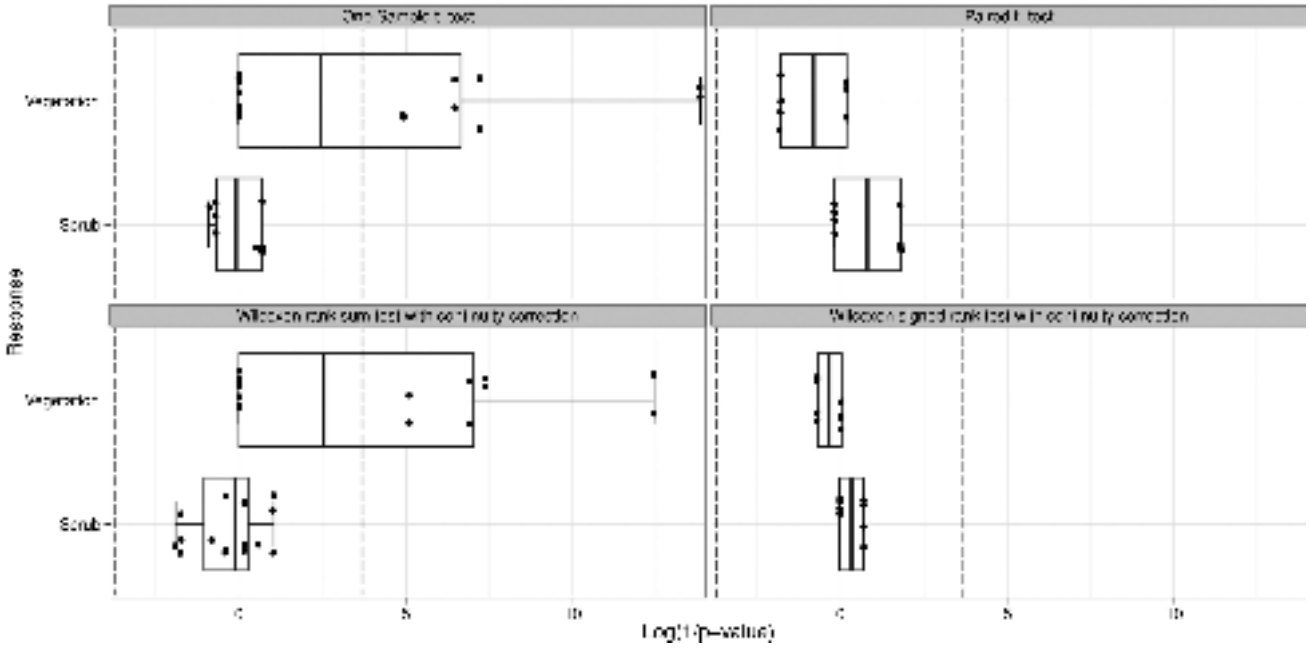

**Figure 6.** Box plots of $P$ values for pairwise and unpaired tests using the less alternative on the negative and greater alternative on the positive $x$ axis. Regions outside the dashed lines are significant at $P = 0.05$. Results for hypothesis 2a: $\mathrm{NDVI}_{\mathrm{ctrl(pre)}} \sim \mathrm{NDVI}_{\mathrm{treatment(pre)}}$ on responses. Most microwatersheds showed no significant difference in NDVI values between control and treatment prior to watershed activities. Among the significant values, a greater number of microwatersheds in the treatment group showed more vegetation prior to watershed restoration activities.

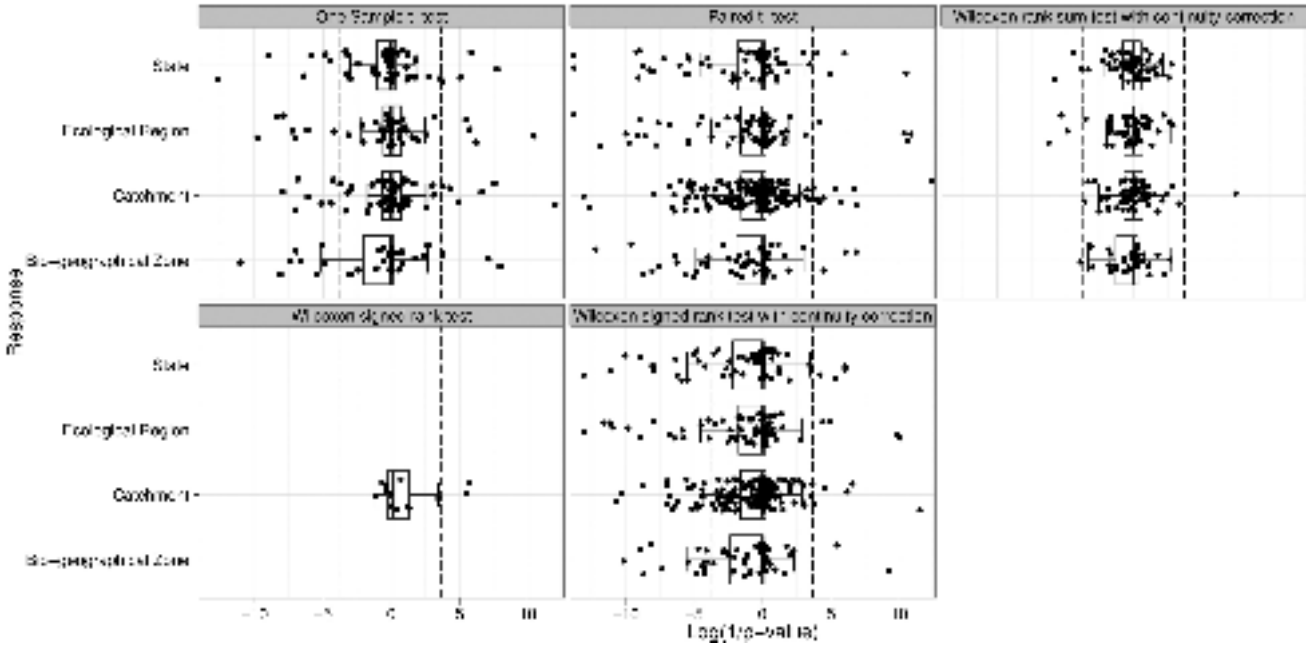

**Figure 7.** Box plots of $P$ values for pairwise and unpaired tests using the less alternative on the negative and greater alternative on the positive $x$ axis. Regions outside the dashed lines are significant at $P = 0.05$. Results for testing hypothesis 2b: $\mathrm{NDVI}_{\mathrm{ctrl(post)}} < \mathrm{NDVI}_{\mathrm{treatment(post)}}$ on NDVI values. Bulk of the values is not significant. Among the significant values, most lie to the left of the dashed line, indicating that control (untreated) microwatersheds showed a greater increase in NDVI than those that were treated under the watershed program. The results are very similar to those of microwatersheds prior to WHD.

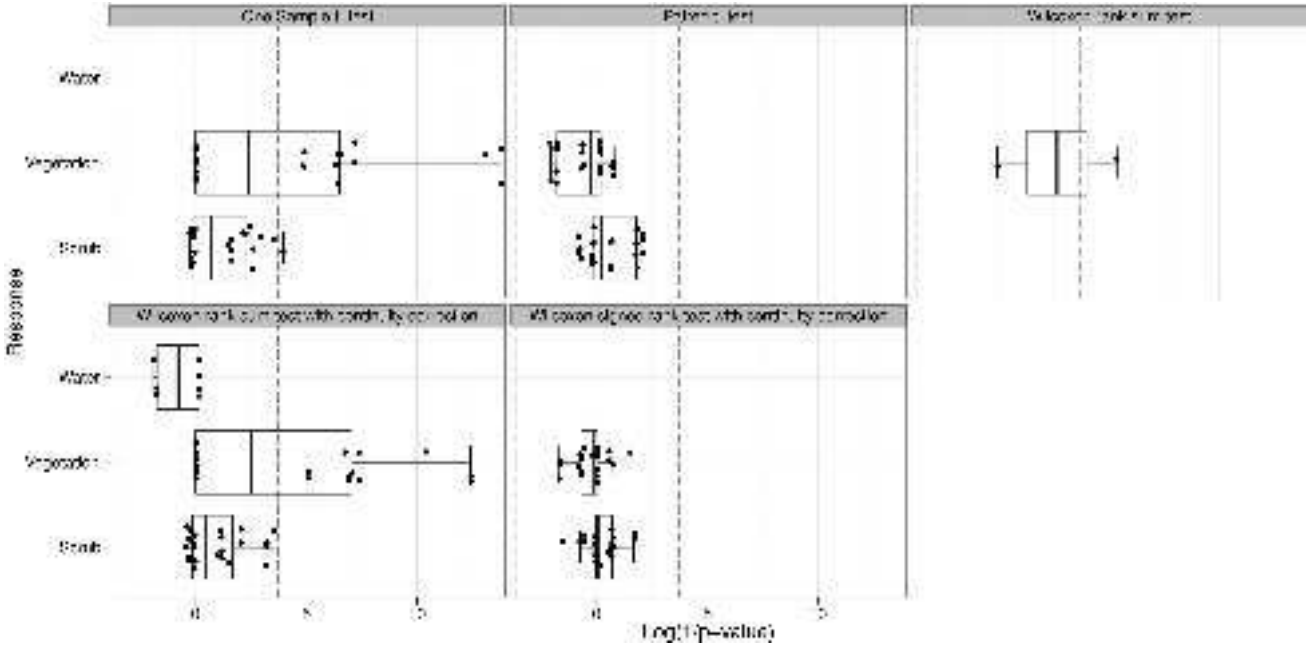

**Figure 8.** Box plots of $P$ values for pairwise and unpaired tests using the less alternative on the negative and greater alternative on the positive $x$ axis. Regions outside the dashed lines are significant at $P = 0.05$. Results for testing hypothesis 2b: $\mathrm{NDVI}_{\mathrm{ctrl(post)}} < \mathrm{NDVI}_{\mathrm{treatment(post)}}$ on responses. Most treated microwatersheds do not show any significant difference after watershed restoration when compared to untreated (control) watersheds. Some however show that there is an increase in vegetative cover and scrub in the treated watersheds when compared to the untreated controls. The results are nearly identical to those prior to initiation of watershed restoration.

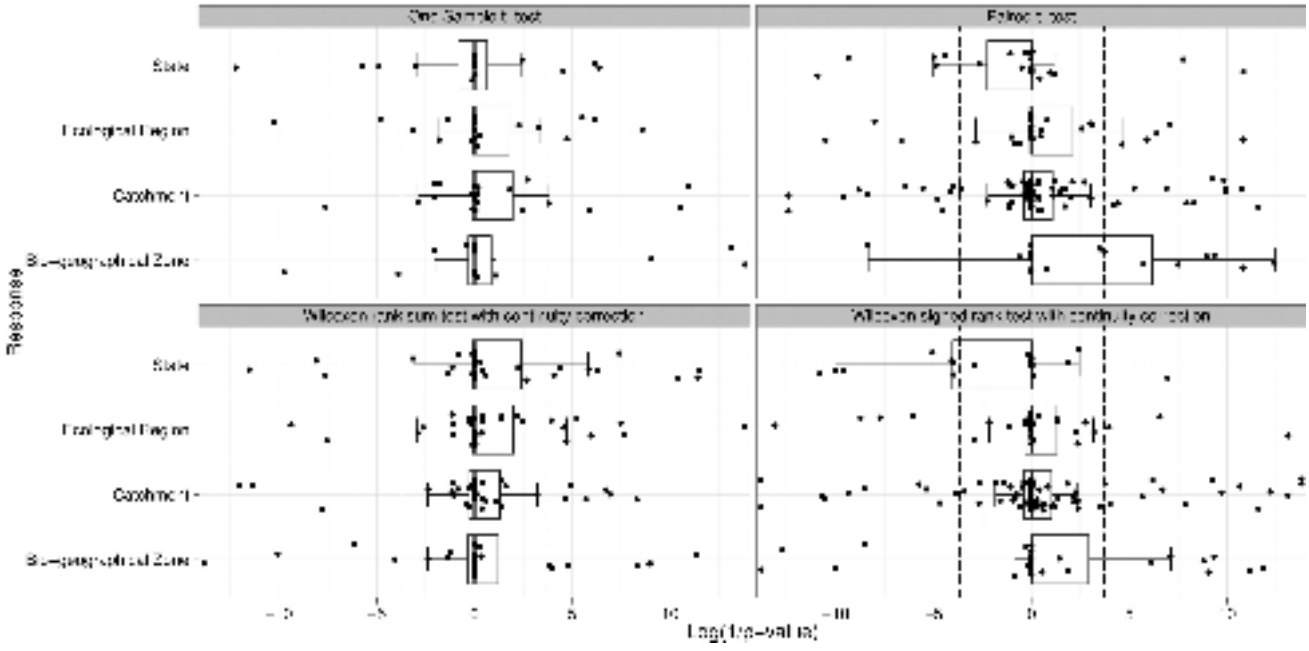

**Figure 9.** Box plots of $P$ values for pairwise and unpaired tests using the less alternative on the negative and greater alternative on the positive $x$ axis. Regions outside the dashed lines are significant at $P = 0.05$. Hypothesis 3a, $\text{NDVI}_{\text{ctrl(pre)}} \sim \text{NDVI}_{\text{ctrl(post)}}$ on NDVI values. Results show that a similar number of points are significant as are nonsignificant. Also these points are equally spread out on the positive and negative $x$ axis showing that the number of microwatersheds with significantly higher NDVI values in control areas were similar in 2006 and 2011.

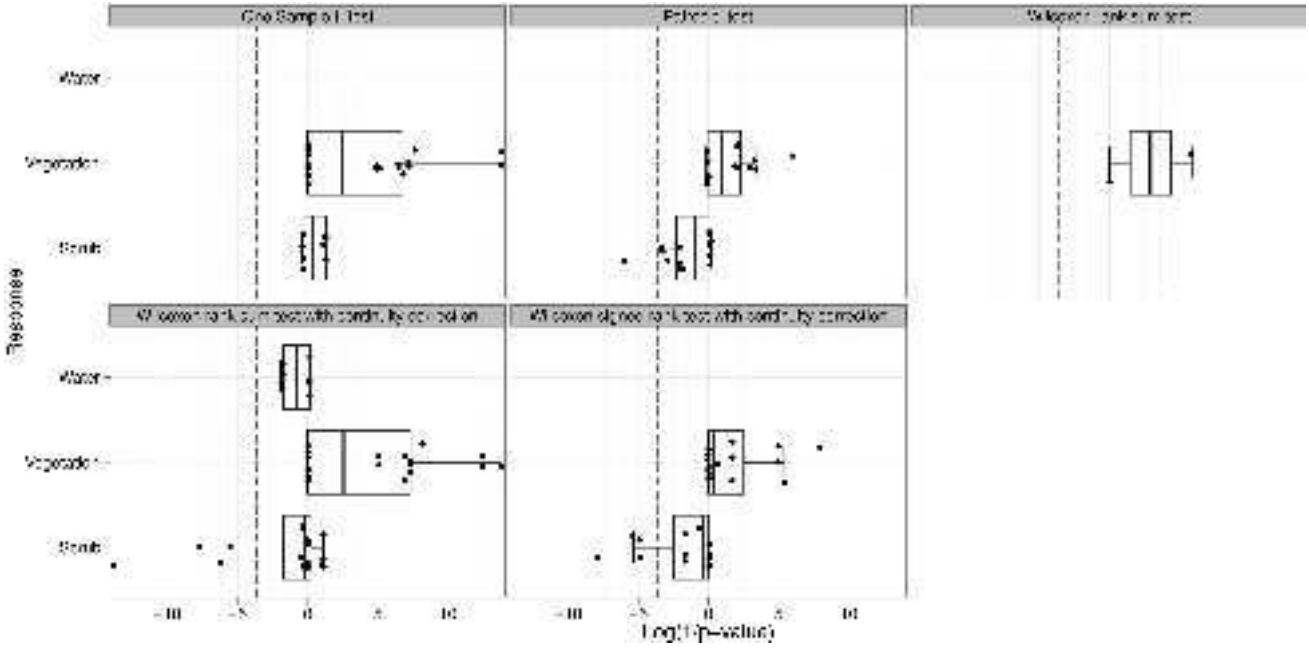

**Figure 10.** Box plots of $P$ values for pairwise and unpaired tests using the less alternative on the negative and greater alternative on the positive $x$ axis. Regions outside the dashed lines are significant at $P = 0.05$. Hypothesis 3a, $\text{NDVI}_{\text{ctrl(pre)}} \sim \text{NDVI}_{\text{ctrl(post)}}$ on responses. While most of the responses are nonsignificant, some control microwatersheds showed higher amounts of vegetation and less scrub in 2011 than in 2006.

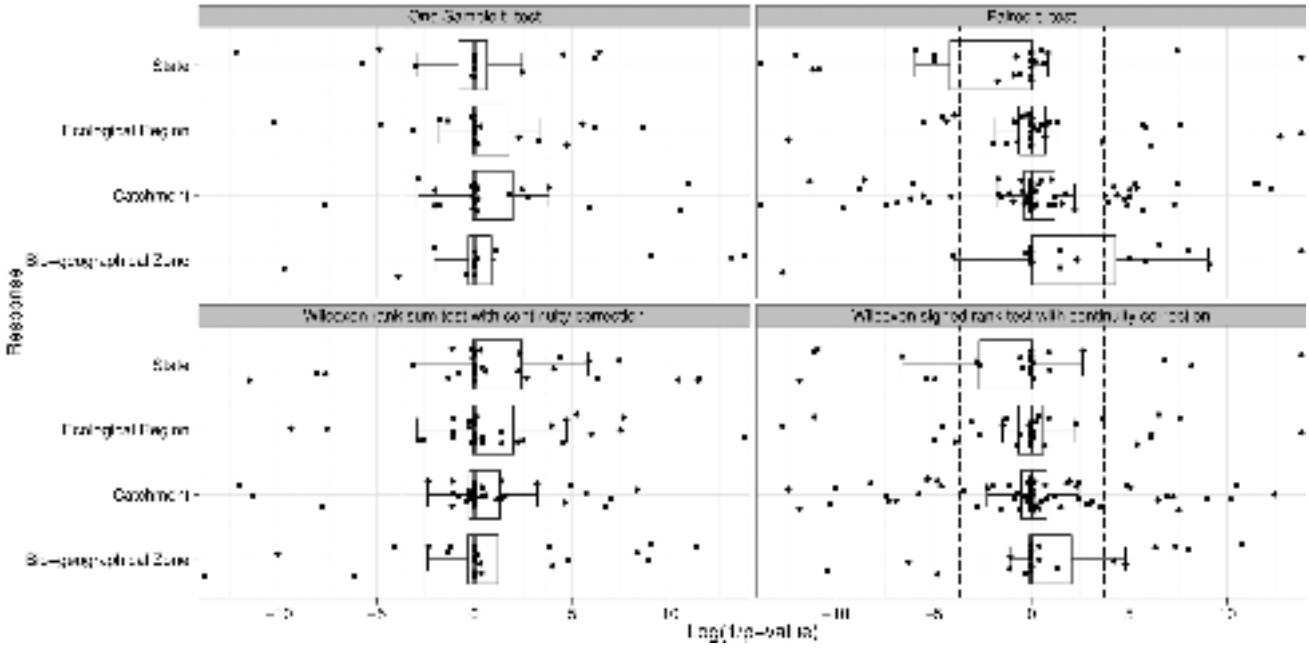

**Figure 11.** Box plots of $P$ values for pairwise and unpaired tests using the less alternative on the negative and greater alternative on the positive x axis. Regions outside the dashed lines are significant at $P = 0.05$. Hypothesis 3b, $\text{NDVI}_{\text{treatment(pre)}} < \text{NDVI}_{\text{treatment(post)}}$ on NDVI values. Results are very similar to Figure 9. A similar number of treated microwatershed showed a significant increase in NDVI after treatment as the numbers show a significant decrease. Also a large proportion of microwatersheds showed no significant difference in NDVI before or after treatment.

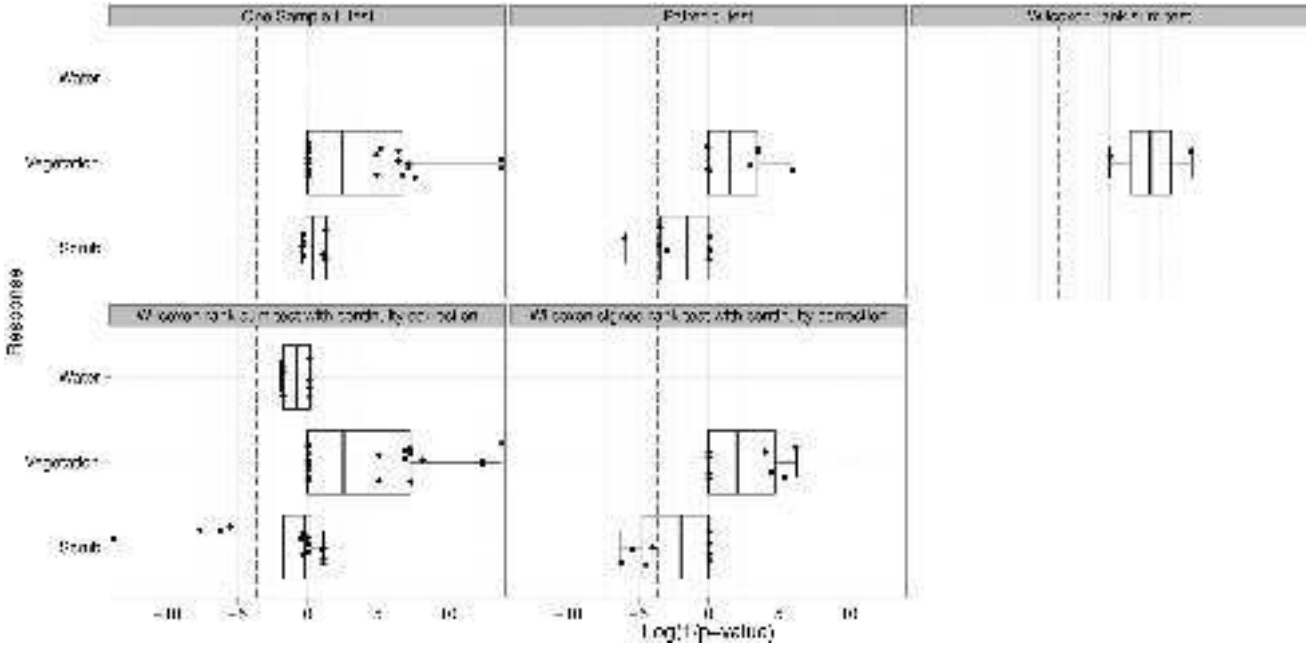

**Figure 12.** Box plots of $P$ values for pairwise and unpaired tests using the less alternative on the negative and greater alternative on the positive $x$ axis. Regions outside the dashed lines are significant at $P = 0.05$. Hypothesis 3b, $\text{NDVI}_{\text{treatment(pre)}} < \text{NDVI}_{\text{treatment(post)}}$ on responses. Results were very similar to Figure 10. Most treated microwatersheds showed no significant difference before or after restoration had taken place. Some however showed significant higher amounts of vegetation but less scrub.

services. Measurements of NDVI values is an inexpensive and robust method. However, this too is limited by the resolution of the satellite imagery [*Lunetta et al*., 2006]. Further, the NDVI does not inform the user about causal factors behind increased productivities that would be revealed by finer grained data on a range of parameters.

[31] The period of the second set of images was selected so that there were two to five years for the treated areas to respond in terms of increased vegetation. Furthermore, we also compared treated and neighboring, untreated (control) watersheds in both 2006 and 2011. Therefore, cases where local conditions, such as poor rains, prevented or delayed a vegetative response to the treatment were accounted for. Comparisons between the cumulative NDVIs of before-after pairs or neighboring treated-untreated (control) pairs were not statistically significant. Paucity of data on completed watershed projects as well as imagery of sufficient resolution did not allow us to test over longer time periods.

[32] Our findings do however show that in terms of productivities, microwatersheds treated through these programs are indistinguishable from those that are not. This holds true across state boundaries, catchment areas, biogeographical zones, and ecological regions, ruling out the possibility of differential performance of the program across state policy, landscapes, and climatic conditions. Our analysis spans seasons and also accounts for local variations by comparing productivities of adjacent untreated microwatersheds. Thus, we conclude that watershed guidelines in India fail to deliver a mechanism to improve local productivities.

[33] In the present arrangement, areas selected for treatment are not watershed units but development units. The program is run more as a rural development initiative rather than a watershed restoration effort. Present institutional structures cater to local requirements, yet restoration work is required at watershed scales, with emphasis on restoration of watershed function. Lack of trained manpower coupled with high technical requirements, very low per hectare outlay, limited time frames for implementation coupled with long gestation periods for project outcomes are other major drawbacks of the program. Further, watershed services are typically low value and highly dispersed. The highest value service, water, is only available to land owners, making these programs inherently iniquitous.

[34] The preparation of watershed restoration plans requires a judicious mix of rural development goals that build upon hydrological and ecologically sound project design. This would change some of the major elements in the guidelines including selection of sites, training and capacity building of implementing agencies as well as the community-based organizations for planning, monitoring, and evaluation of project outcomes. Furthermore, improved hydrologic function will lead to increased ecological goods and services, better access to irrigation water, and increases in livelihoods leading to poverty alleviation. Poverty alleviation schemes are not as likely to lead to increased hydrological function however. There are at least four preconditions to such an approach:

[35] 1. Data accessibility and availability—this refers to hydrological, meteorological, geomorphological, and land-cover data at high spatial resolutions.

[36] 2. Standardized methods and techniques for measuring physical and socioeconomic parameters necessary to design and monitor restoration and management.

[37] 3. Analytical techniques to interpret field measurements for adaptive management. This would necessarily include the ability to set up and utilize hydraulic models and landscape tools as well as stakeholder analysis to ensure equity concerns are addressed.

[38] 4. Design of monitoring strategies, including setting up of measurement stations that track changes, both biophysical as well as socioeconomic.

[39] Ecological goods and services provided by watershed restoration are independent of the local dynamics that determine levels of participation and equity concerns. Pinning watershed restoration funding to local capacity for collaborative activities or governance predisposes the project success to being a function of luck rather than planning. Both collaborative management and watershed restoration have a black eye at the end of the process.

[40] WHD is largely about maximizing ecosystem services from watersheds in a fair, transparent, and sustainable manner. Restoring watersheds to perform these services is therefore bound to underlying hydrological and ecological processes, which, in turn, are governed by a host of environmental parameters including climate and geomorphology. This holds true even if the objective is not to restore natural flows, but to harvest or recharge ground water for agriculture and other uses. We need to identify strategies for physical and ecological restoration of a given watershed before defining institutional frameworks for their management. Trying to fit this reality to social needs is getting the proverbial cart before the horse.

[41] **Acknowledgments.** This study was funded in part by the NRDMS, Department of Science and Technology, New Delhi, through grant NRDMS/11/1083/06 and in part by the Ministry of Earth Sciences, Government of India and Natural Environment Research Council, United Kingdom, under the "Changing Water Cycle" program grant MoES/NERC/16/02/10 PC-ll. The views expressed here are those of the authors and not necessarily those of the funders or their respective institutions. The MODIS/Terra 16-Day L3 Global 250m SIN Grid data were obtained through the online data pool at the NASA Land Processes Distributed Active Archive Center (LP DAAC), USGS/Earth Resources Observation and Science (EROS) Center, Sioux Falls, South Dakota (http://lpdaac.usgs.gov/get_data).

## References

Allan, J. D. (2004), Landscapes and riverscapes: The influence of land use on stream ecosystems, *Annu. Rev. Ecol. Evol. Syst.*, *35*, 257–284.

Anbumozhi, V., J. Radhakrishnan, and E. Yamaji (2005), Impact of riparian buffer zones on water quality and associated management considerations, *Ecol. Eng.*, *24*(5), 517–523, doi:10.1016/j.ecoleng.2004.01.007.

Batchelor, C., M. S. Rao, S. M. Rao (2003), Watershed development: A solution to water shortages in semi-arid India or part of the problem, *Land Use Water Resour. Res.*, *3*(1), 1–10.

Behera, S., and R. K. Panda (2006), Evaluation of management alternatives for an agricultural watershed in a sub-humid subtropical region using a physical process based model, *Agric. Ecosyst. Environ.*, *113*(1-4), 62–72, doi:10.1016/j.agee.2005.08.032.

Bhalla, R. S., N. W. Pelkey, and K. V. Devi Prasad (2011), Application of GIS for evaluation and design of watershed guidelines, *Water Resour. Manage.*, *25*(1), 113–140, doi:10.1007/s11269-010-9690-0.

Bonell, M., B. Purandara, B. Venkatesh, J. Krishnaswamy, H. Acharya, U. Singh, R. Jayakumar, and N. Chappell (2010), The impact of forest use and reforestation on soil hydraulic conductivity in the Western Ghats of India: Implications for surface and sub-surface hydrology, *J. Hydrol.*, *391*(1-2), 47–62, doi:10.1016/j.jhydrol.2010.07.004.

Bruce, J. W., and R. Mearns (2002), Natural resource management and land policy in developing countries, *Lessons learned and new challenges for the World Bank. IIED Drylands Programme Issues Paper*, (115).

Bruen, M. (2008), Systems analysis? A new paradigm and decision support tools for the water framework directive, *Hydrol. Earth Syst. Sci.*, *12*(3), 739–749.

Bruijnzeel, L. A. (2004), Hydrological functions of tropical forests: Not seeing the soil for the trees?, *Agric., Ecosyst. Environ.*, *104*(1), 185–228, doi:10.1016/j.agee.2004.01.015.

Cairns, J. J. (1989), Restoring damaged ecosystems: Is predisturbance condition a viable option?, *Environ. Prof.*, *11*, 152–159.

Calder, I., A. Gosain, M. S. R. M. Rao, C. Batchelor, M. Snehalatha, and E. Bishop (2008), Watershed development in India. 1. Biophysical and societal impacts, *Environment, Development and Sustainability*, *10*(4), 537–557.

Cao, W., W. Bowden, T. Davie, and A. Fenemor (2009), Modelling impacts of land cover change on critical water resources in the Motueka river catchment, New Zealand, *Water Resour. Manage.*, *23*(1), 137–151, doi:10.1007/s11269-008-9268-2.

Chandrashekar, H. (2005), Subsidy and Cost Sharing in Watershed Projects: Role of Panchayats, *Economic and Political Weekly*, *40*(35), 3874–3875.

Conway, J., D. Eddelbuettel, T. Nishiyama, S. K. Prayaga, and N. Tiffin (2012), RPostgreSQL: R interface to the PostgreSQL database system, R package version 0.3-2.

Cullum, R., S. Knight, C. Cooper, and S. Smith (2006), Combined effects of best management practices on water quality in Oxbow lakes from agricultural watersheds, *Soil Tillage Res.*, *90*(1-2), 212–221, doi:10.1016/j.still.2005.09.004.

Curtis, A., I. Byron, and J. MacKay (2005), Integrating socio-economic and biophysical data to underpin collaborative watershed management, *J. Am. Water Resour. Assoc.*, *41*(3), 549–563.

Department of IT, Ministry of Communications and Information Technology, GOI (2012), WPMIS - watershed programmes monitoring information system. [Available at http://watershed.nic.in/Home.asp, accessed 3 July 2012.]

Deshpande, R. S. (2008), Watersheds: Putting the cart before the horse, *Econ. Polit. Weekly*, *43*(6), 74–76.

Ferreyra, C., and P. Beard (2007), Participatory evaluation of collaborative and integrated water management: Insights from the field, *J. Environ. Plann. Manage.*, *50*(2), 271–296.

Fowler, J. M., and E. O. Heady (1981), Suspended sediment production potential on undisturbed forest land, *J.Soil Water Conserv.*, *36*(1), 47–50.

Fox, J. (2005), The R commander: A basic statistics graphical user interface to R, *J. Stat. Software*, *14*(9), 1–42.

Friedl, M. A., D. K. McIver, J. C. F. Hodges, X. Y. Zhang, D. Muchoney, A. H. Strahler, C. E. Woodcock, S. Gopal, A. Schneider, and A. Cooper (2002), Global land cover mapping from MODIS: Algorithms and early results, *Remote Sens. Environ.*, *83*(1), 287–302.

Frissell, C. A., and S. C. Ralph (1998), Stream and watershed restoration, edited by R. J. Naiman and R. E. Bilby, *River ecology and management: lessons from the Pacific Coastal Ecoregion*, Springer-Verlag, New York, 599–624.

Gosain, A. K., and S. Rao (2004), GIS-based technologies for watershed management, *Curr. Sci.*, *87*(7), 948–953.

Gosain, A. K., S. Rao, and D. Basuray (2006), Climate change impact assessment on hydrology of Indian river basins, *Curr. Sci.*, *90*(3), 346–353.

Government of India (1994), Report of the technical committee on drought prone areas programme and desert development programme, Technical Report, Minist. of Rural Dev., Gov. of India, New Delhi.

Government of India (2006), From Hariyali to Neeranchal: Technical committee on watershed programmes in India, Technical Report, Dep. of Land Resour., Minist. Rural Dev., Gov. of India, New Delhi.

Government of India (2008), Common guidelines for watershed development projects, Technical Report, Dep. of Land Resour., Minist. of Rural Development, Gov. of India, New Delhi.

GRASS Development Team (2008), The Geographic Resources Analysis and Support System (GRASS), ITC-irst, Trento, Italy.

Herring, D., and J. Weier (2000), Measuring vegetation (NDVI & EVI): Feature articles. [Available at http://earthobservatory.nasa.gov/Features/MeasuringVegetation/, accessed: 2012-05-10 07:57:40.].

Heuperman, A. F., A. S. Kapoor, and H. W. Denecke (2002), Biodrainage: Principles, Experiences and Applications, (No. 6), Food and Agric. Org., Rome.

Hope, R. A. (2007), Evaluating social impacts of watershed development in India, *World Development*, *35*(8), 1436–1449, doi:10.1016/j.worlddev.2007.04.006.

Jain, A., S. C. Rai, and E. Sharma (2000), Hydro-ecological analysis of a sacred lake watershed system in relation to land-usercover change from Sikkim Himalaya, *Catena*, *40*(3), 263–278.

Jodha, N. S. (1995), Common property resources and the dynamics of rural poverty in India's dry regions, *Unasylva*, *180*(46), 23–29.

Joshi, D. (2006), Broadening the Scope of Watershed Development, *Economic & Political Weekly*, *41*(27/28), 2987–2991.

Joy, K. J., A. Shah, S. Paranjape, S. Badiger, and S. Lele (2006), Issues in restructuring, *Econ. Polit. Weekly*, *41*(27/28), 2994–2996.

Kerr, J. (2002), Watershed development, environmental services, and poverty alleviation in India, *World Development*, *30*(8), 1387–1400.

Kerr, J. (2007), Watershed management: lessons from common property theory, *Int. J. Commons*, *1*(1), 89–110.

Kerr, J. M., G. Pangare, and V. Pangare (2002), Watershed development projects in India: an evaluation, (No.127), *Int. Food Policy Res. Inst.*, Washington D.C.

Krishnaswamy, J., K. S. Bawa, K. N. Ganeshaiah, and M. C. Kiran (2009), Quantifying and mapping biodiversity and ecosystem services: Utility of a multi-season NDVI based mahalanobis distance surrogate, *Remote Sens. Environ.*, *113*(4), 857–867.

Lunetta, R. S., J. F. Knight, J. Ediriwickrema, J. G. Lyon, and L. D. Worthy (2006), Land-cover change detection using multi-temporal MODIS NDVI data, *Remote Sens. Environ.*, *105*(2), 142–154.

Madon, S., and S. Sahay (1997), Managing natural resources using GIS: Experiences in india, *Inform. Manage.*, *32*(1), 45–53, doi:10.1016/S0378–7206(97)00003–7.

Matsushita, B., and M. Tamura (2002), Integrating remotely sensed data with an ecosystem model to estimate net primary productivity in east Asia, *Remote Sens. Environ.*, *81*(1), 58–66.

Millenium Ecosystem Assessment (2005), *Ecosystems and human well-being: General synthesis*, World Resour. Inst., Washington, D. C.

Montgomery, D. R., G. E. Grant, and K. Sullivan (1995), Watershed analysis as a framework for implementing ecosystem management, *Water Resour. Bull.*, *31*(3), 369–386.

NASA Land Processes Distributed Active Archive Center (LP DAAC) (2011), MODIS/Terra Vegetation Indices 16-Day L3 Global 250m SIN Grid, U.S. Geological Survey/Earth Resources Observation and Science (EROS) Center, Sioux Falls, South Dakota.

National Remote Sensing Centre (NRSC)/Indian Space Research Organisation (ISRO) (2011), Bhuvan—Gateway to Indian earth observation. [Available at http://bhuvan.nrsc.gov.in/bhuvan/.]

Olson, D., et al. (2001), Terrestrial ecoregions of the world: A new map of life on earth, *BioScience*, *51*(11), 933–938.

Pettorelli, N., J. O. Vik, A. Mysterud, J. M. Gaillard, C. J. Tucker, and N. C. Stenseth (2005), Using the satellite-derived NDVI to assess ecological responses to environmental change, *Trends Ecol. Evol.*, *20*(9), 503–510.

R Development Core Team (2008), R: A language and environment for statistical computing, Vienna, Austria.

Ramsey, P. (2005), PostGIS manual, Refractions Research Inc., Victoria, British Columbia, Canada.

Randhir, T. O., and A. G. Hawes (2009), Watershed land use and aquatic ecosystem response: Ecohydrologic approach to conservation policy, *J. Hydrol.*, *364*(1-2), 182–199.

Rao, K. H. V. D., and D. S. Kumar (2004), Spatial Decision Support System for Watershed Management, *Water Resour. Manage.*, *18*(5), 407–423, doi:10.1023/B:WARM.0000049135.79227.f9.

Rao, D. P., N. Gautam, R. L. Karale, and B. Sahai (1991), IRS-1A application for land use/ land cover mapping in India, *Curr. Sci.*, *61*(3- 4), 153–161.

Reddy, V. R. (2006), 'Getting the Implementation Right': Can the Proposed Watershed Guidelines Help?, *Econ. Polit. Weekly*, *41*(4), 4292–4295.

Reddy, V. R., M. G. Reddy, S. Galab, J. Soussan, and S. Baginski (2004), Participatory watershed development in India: Can it sustain rural livelihoods, *Dev. Change*, *35*(2), 297–326.

Rodgers, W. A., and H. S. Panwar (1988), Planning a wildlife protected area network in India, Technical Report (Vol 1), Wildlife Inst. of India, Dehra-dun, India.

Scanlon, B. R., I. Jolly, M. Sophocleous, and L. Zhang (2007), Global impacts of conversions from natural to agricultural ecosystems on water resources: Quantity versus quality, *Water Resour. Res.*, *43*(3), W03437, doi:10.1029/2006WR005486.

Setegn, S. G., R. Srinivasan, and B. Dargahi (2008), Hydrological modelling in the Lake Tana basin, Ethiopia using SWAT model, *Open Hydrol. J.*, *2*(1), 49–62.

Tobin, K. J., and M. E. Bennett (2009), Using SWAT to model streamflow in two river basins with ground and satellite precipitation data, *J.Am. Water Resour. Assoc.*, *45*(1), 253–271.

Tripathi, M. P., R. K. Panda, and N. S. Raghuwanshi (2003), Identification and prioritisation of critical sub-watersheds for soil conservation management using the SWAT model, *Biosyst. Eng.*, *85*(3), 365–379, doi:10.1016/S1537–5110(03)00066-7.

Turton, C., M. Warner, and B. Groom (1998), Scaling up Participatory Watershed Development in India: A Review of the Literature, ODI Agric. Res. Ext. Network, 86, 20pp.

Vaidyanathan, A. (2006), Restructuring watershed development programmes, *Econ. Polit. Weekly*, *41*(27/28), 2984–2987.

Wani, S. P., H. P. Singh, T. K. Sreedevi, P. Pathak, T. J. Rego, B. Shiferaw, and S. R. Iyer (2006), Farmer-participatory integrated watershed management: Adarsha watershed, Kothapally India an innovative and upscalable approach, *SAT eJ.*, *2*(1), 327–407.

Wani, S. P., H. P. Singh, T. K. Sreedevi, P. Pathak, T. J. Rego, B. Shiferaw, and S. R. Iyer (2003), Farmer-Participatory Integrated Watershed Management: Adarsha Watershed, Kothapally India An Innovative and Upscalable Approach, *SAT Agricultural Research*, *2*(1), 1–27.

Wohl, E., P. L. Angermeier, B. Bledsoe, G. M. Kondolf, L. MacDonnell, D. M. Merritt, M. A. Palmer, N. L. R. Poff, and D. Tarboton (2005), River restoration, *Water Resour. Res.*, *41*(10), W10301, doi:10.1029/2005WR003985.

World Resources Institute (2005), World resources 2005: The wealth of the poor—Managing ecosystems to fight poverty., Tech. report. (Vol. 11), World Resources Institute (WRI) in collaboration with United Nations Development Programme, U.N. Environ. Prog. and World Bank, Washington, D. C.

# *Non-stationary and non-linear influence of ENSO and Indian Ocean Dipole on the variability of Indian monsoon rainfall and extreme rain events*

**Jagdish Krishnaswamy, Srinivas Vaidyanathan, Balaji Rajagopalan, Mike Bonell, Mahesh Sankaran, R. S. Bhalla & Shrinivas Badiger**

**Climate Dynamics**
Observational, Theoretical and Computational Research on the Climate System

ISSN 0930-7575

Clim Dyn
DOI 10.1007/s00382-014-2288-0

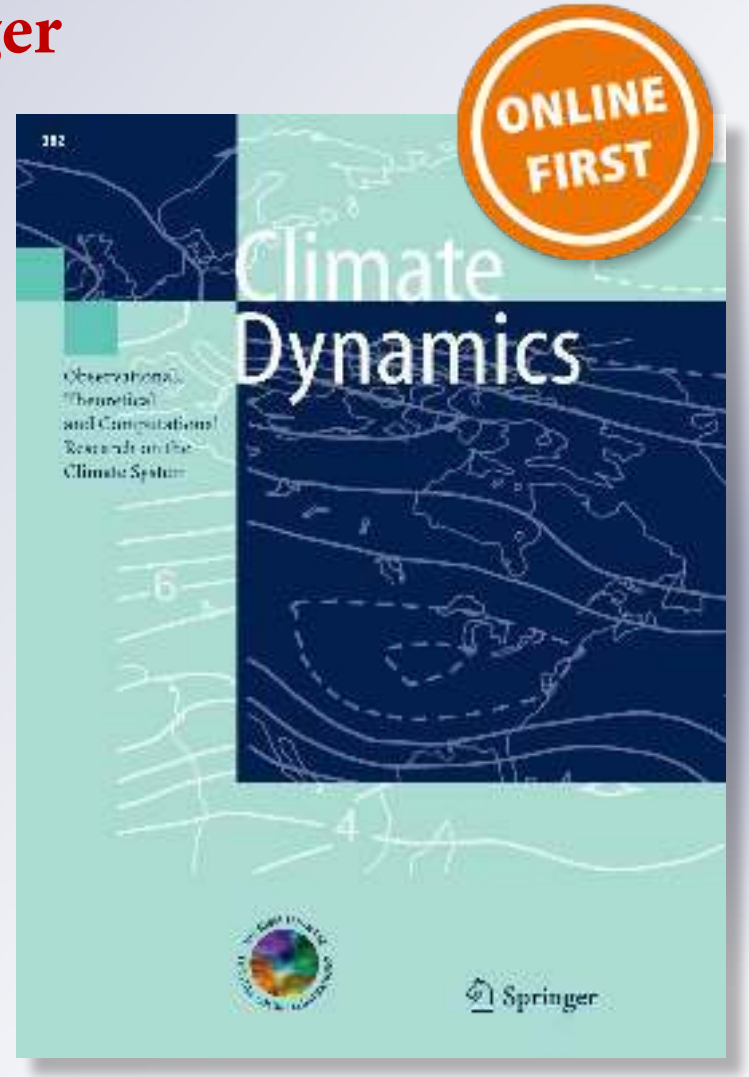


Springer

Clim Dyn
DOI 10.1007/s00382-014-2288-0

# Non-stationary and non-linear influence of ENSO and Indian Ocean Dipole on the variability of Indian monsoon rainfall and extreme rain events

**Jagdish Krishnaswamy · Srinivas Vaidyanathan · Balaji Rajagopalan · Mike Bonell · Mahesh Sankaran · R. S. Bhalla · Shrinivas Badiger**

Received: 6 March 2014 / Accepted: 5 August 2014


**Abstract** The El Nino Southern Oscillation (ENSO) and the Indian Ocean Dipole (IOD) are widely recognized as major drivers of inter-annual variability of the Indian monsoon (IM) and extreme rainfall events (EREs). We assess the time-varying strength and non-linearity of these linkages using dynamic linear regression and Generalized Additive Models. Our results suggest that IOD has evolved independently of ENSO, with its influence on IM and EREs strengthening in recent decades when compared to ENSO, whose relationship with IM seems to be weakening and more uncertain. A unit change in IOD currently has a proportionately greater impact on IM. ENSO positively influences EREs only below a threshold of 100 mm day$^{-1}$. Furthermore, there is a non-linear and positive relationship between IOD and IM totals and the frequency of EREs (>100 mm day$^{-1}$). Improvements in modeling this complex system can enhance the forecasting accuracy of the IM and EREs.

**Keywords** Dynamic linear models · Generalised additive models · La Nina · Western Ghats · Indo-Gangetic plain

## 1 Introduction

The Indian monsoon (IM) and associated extreme daily rain events (EREs) have a major influence on the welfare of over 1.2 billion people (Gadgil and Kumar 2006; Ashfaq et al. 2009). Variability in the IM is known to be modulated by two ocean–atmosphere phenomena, El Nino–Southern Oscillation (ENSO) and the more recently described Indian Ocean Dipole (IOD; Saji et al. 1999; Ashok et al. 2004). The possible linkages between ENSO and IOD are also an active area of investigation (Wang and Wang 2014).

Earlier studies have shown a weakening ENSO–IM relationship in recent decades attributed to a warmer climate

M. Bonell—Deceased on 11 July 2014.

**Electronic supplementary material** The online version of this article (doi:10.1007/s00382-014-2288-0) contains supplementary material, which is available to authorized users.

J. Krishnaswamy (✉) · S. Badiger
Ashoka Trust for Research in Ecology and the Environment (ATREE), Royal Enclave Sriramapura, Jakkur Post, Bangalore 560064, Karnataka, India
e-mail: jagdish@atree.org

S. Vaidyanathan · R. S. Bhalla
Foundation for Ecological Research, Advocacy and Learning (FERAL), Pondicherry Campus, 170/3 Morattandi, Auroville Post, Villupuram 605101, Tamil Nadu, India

B. Rajagopalan
Department of Civil, Environmental and Architectural Engineering and Co-operative Institute for Research in Environmental Sciences, University of Colorado, Boulder, CO, USA

M. Bonell
Centre for Water Law, Policy and Sciences Under the Auspices of UNESCO, University of Dundee, Dundee DD1 4HN, Scotland, UK

M. Sankaran
Ecology and Evolution Group, National Centre for Biological Sciences, TIFR, GKVK Campus, Bellary Road, Bangalore 560065, India

M. Sankaran
School of Biology, University of Leeds, Leeds LS2 9JT, UK

(Kumar et al. 1999; Ashrit et al. 2001; Ihara et al. 2008), and a concurrent strengthening of the IOD–IM relationship (Ashok et al. 2001, 2004; Ashok and Saji 2007; Izumo et al. 2010; Ummenhofer et al. 2011) attributed to non-uniform warming of the Indian Ocean (Ihara et al. 2008; Cai et al. 2009). Extreme rainfall events have also simultaneously increased over parts of India (Goswami et al. 2006; Rajeevan et al. 2008; Ghosh et al. 2012) and the same has been linked to global warming and warming of the Indian Ocean (Goswami et al. 2006; Ajaymohan and Rao 2008; Rajeevan et al. 2008). Interestingly, an overall decline in average IM in recent decades has been reported (Kumar et al. 2011; Krishnan et al. 2013). However certain parts of the country are witnessing an increase in average IM (Guhathakurta and Rajeevan 2008) and in the frequency of EREs (Guhathakurta et al. 2011). The possible role of changes in the land-sea temperature gradient which explain these declines have been reported in earlier studies (Han et al. 2010; Kumar et al. 2011; Krishnan et al. 2013). The evolution of monsoon-IOD feedbacks are also well documented (Abram et al. 2008; Vinayachandran et al. 2009; Luo et al. 2010). Although the overall IM is declining, precipitable moisture for sustaining ERE's could be increasing due to local processes (Trenberth et al. 2003) and also due to larger global phenomena such as SSTs in other ocean basins outside the Indo-Pacific sector (Turner and Annamalai 2012; Cherchi and Navarra 2013; Wang et al. 2013). On the other hand, a recent study (Prajeesh et al. 2013) indicates the possibility of a weakened local mid-tropospheric humidity resulting in reduction in monsoon depression frequency.

Previous studies have looked independently at either overall annual monsoon totals or daily rainfall at high exceedance thresholds (such as above 150 mm day$^{-1}$), rather than as a continuum from low to high and very high exceedance levels. However, the impact of EREs depend on the land-use and land-cover and antecedent moisture status, and thus a daily rainfall of 25 or 50 mm day$^{-1}$ can have an "extreme" impact on people, property, ecosystem response and livelihoods. Existing studies have also addressed changes over time in monsoon and ocean–atmosphere phenomena using moving window correlations, dividing time scale into arbitrary time-periods or linear regression models with time-invariant regression parameters. Most studies, with some exception (Ashok et al. 2001), have focused on specific years, e.g. El Nino, La Nina, positive and negative IOD years, rather than consider the full range of ocean–atmosphere index values to assess their influence on IM and EREs.

There is thus a need for robust methods to model non-stationarity in a continuous and consistent manner across the full range of ocean–atmosphere indices for both Monsoon totals and frequency of EREs across a range of exceedance thresholds with clearly identified parameters that are easy to interpret, along with the quantification of uncertainties. Potential non-linearities in the relationships also need to be identified as the basis for better understanding and forecasting. To this end, we introduce the application of two robust methods to study changes in the relationship between two principal ocean–atmosphere phenomena as well as their evolving influence on monsoon dynamics and annual frequency of EREs at multiple exceedance thresholds over multi-decadal time-scales. We demonstrate that the application of these two methods: *Bayesian dynamic linear regression (DLM) to model non-stationarity based on time-varying regression parameters over multi-decadal scales, and generalized additive models (GAMs) to model non-linearity in the relationships, averaged over larger time periods,* and show how this helps us understand recent shifts and trends in influence of ENSO and IOD on IM and EREs.The scope of this work is primarily to introduce more robust methods for evaluating the impacts of ENSO–IOD on IM extreme rainfall, both for studying and understanding past dynamics as well as for forecasting.

Dynamic state-space models (DLM) including those with time-varying regression parameters (Harrisons and Stevens 1976) have been familiar to statisticians and time-series modellers since the mid-80s when it was applied to economic and industrial output time-series (West et al. 1985; Harrison and West 1997). Dynamic models with time-varying regression coefficients have been used to study changes in stream hydrology and population ecology (Krishnaswamy et al. 2000, 2001; Calder et al. 2003) and more recently to analyze changes in vegetation greenness in response to climate change (Krishnaswamy et al. 2014). Their application in understanding monsoon dynamics in relation to ocean–atmosphere phenomena, however, has been limited (Maity and Nagesh Kumar 2006).

An important statistical development in the last few decades has been advances in GAMs. GAMs (Hastie and Tibshirani 1986, 1990) are semi-parametric extensions of generalized linear models (GLMs), and are based on an assumed relationship (called a link function) between the mean of the response variable and a smoothed, additive, non-parametric function of the explanatory variables rather than a linear function of the covariates as in a GLM.

Data may be assumed to be from several families of probability distributions, including normal, binomial, poisson, negative binomial, or gamma distributions, many of which better fit the non-normal error structures of most ecological and biophysical data. The only underlying assumption made is that the functions are additive and that the components are smooth. The strength of GAMs lies in their ability to deal with highly non-linear and non-monotonic relationships between the response and the set of explanatory variables. GAMs are data rather than model driven. This is because

the data determine the nature of the relationship between the response and the explanatory variables rather than assuming some form of parametric relationship (Yee and Mitchell 1991). Like GLMs, the ability of the method to handle non-linear data structures can aid in the development of models that better represent the underlying data, and hence increase our understanding of biophysical systems. GAMs have been widely used in a range of scientific domains to model non-linearity in regression type data (Lehmann et al. 2002). This provides a better fit to environmental, ecological or meteorological data when compared to linear models (Guisan et al. 2002; Pearce et al. 2011; Wang et al. 2012).

## 2 Data and methods

### 2.1 Data

Datasets used in the study included the following: (1) the homogeneous, area-weighted time-series of annual summer (Jun–Sep) monsoon rainfall totals (JJAS) for the period 1871–2011 (Parthasarathy et al. 1994); (2) summer NINO4 (sea surface temperature (SST) averaged over 160°E–150°W and 5°S–5°N) which is an ENSO index based on the Extended Reconstructed SST dataset (Smith et al. 2008; ERSSTvb3); (3) the summer IOD index-difference in SST anomalies between the western (50°E–70°E and 10°S–10°N) and eastern (90°E–110°E and 10°S–0°S) tropical Indian Ocean (Saji et al. 1999), also computed using the ERSSTvb3 (4) the summer El Niño Modoki Index (EMI; Ashok et al. 2007)-difference in SST anomalies over three regions (165°E–140°W and 10°S–10°N; 110°W–70°W and 15°S–5°N; 125°E–145°E and 10°S–20°N) computed using the ERSSTvb3 (5) NINO4 and IOD indices from the Extended Kaplan SST (Kaplan et al. 1998) dataset and (6) daily gridded rainfall data over India for the period 1901–2004 (Rajeevan et al. 2006). From the latter, ERE frequencies—the number of days of rainfall exceeding a given threshold over all grids in India in each year—were determined. EREs are increasingly being defined in terms of their impacts in certain regions or under specific antecedent moisture conditions and the carrying capacity of the ecosystem rather than based only on absolute or relative values (Pielke and Downton 2000). For example, in the Himalayas, 25 mm day$^{-1}$ is considered a critical threshold for the occurrence of major landslides once adequate antecedent moisture has accumulated (Gabet et al. 2004). Similarly, other global and regional studies, which define heavy and extreme precipitation for studying long-terms trends or impacts of climate change, have classified events of 25 mm day$^{-1}$as extreme events (Zhai et al. 2005; Hennessy et al. 1997; Groisman et al. 1999). In this work, the following exceedance thresholds were therefore selected: 25, 50, 100, 150 and 200 mm per day. The IM data was obtained from http://www.tropmet.res.in/and the indices from http://iridl.ldeo.columbia.edu/.

It is important to note that the NINO4 index was chosen based on recent results that showed this region in the equatorial Pacific to have a stronger teleconnection with the IM (Kumar et al. 2006; Rajagopalan and Molnar 2012). The sign of the index was reversed to give a positive correlation with IM rainfall for easier interpretation and comparison with influence of IOD, whose positive phase is associated with higher rainfall in IM. Positive values of the redefined NINO4 index thus correspond to the La Nina phase, which is associated with higher IM rainfall and potentially higher frequency of EREs and the lower negative end of the scale corresponds to the extreme El Nino phase.

## 3 Methods

### 3.1 Bayesian dynamic linear regression

In a traditional (or static) linear regression model, the regression coefficients estimated based on historical data do not change over time. In contrast, in dynamic linear models the regression coefficients such as intercepts and regression slopes can vary as a function of time, i.e. they allow us to capture the time-varying nature of the relationship. Dynamic linear models (Petris et al. 2009) consider a time series as the output of a dynamical system perturbed by random disturbances. This allows a robust quantification and elegant visualization of the changing influences of covariates. In Bayesian dynamic regression models (Harrison and West 1997; Petris et al. 2009), a type of dynamic state space model, regression coefficients are updated at each time step, conditional on available data and the model using Bayes theorem. The general form of the model is represented as

$$Y_t = \beta 0_t + \beta 1_t X1_t + \beta 2_t X2_t + \ldots + e_t \quad (1)$$

$$e_t \approx N(0, V)$$

where $Y$ is the dependent variable (e.g., IM annual totals and square root of annual counts of EREs in this study) and $X1$, $X2$,… are the independent variables (e.g., NINO4 and IOD in this study), $t$ denotes the time ($t = 1, 2, \ldots, N$) and $\beta 0_t$, $\beta 1_t$, $\beta 2_t$,… are the time varying intercept and slopes, respectively (i.e., regression coefficients). $e_t$ is the noise or error distributed normally with a mean of 0 and variance $V$, and can be obtained from the residual variance from the traditional regression model fitted to the data. The time-varying intercept represents the level at time $t$ corresponding to the covariate model. Its time-trajectory constitutes an overall level/trend that can be interpreted as variability in the response variable that is not captured by the covariates

alone. The trends in the time-varying slope can be directly interpreted as changes in the influence of that covariate on the response variable.

Equation 2 models the time varying regression coefficients—i.e., system dynamics. The parameter $W$ which controls the dynamics of the time-evolution of the regression coefficients is specified a priori by setting $W/V$, the signal to noise ratio. As $V$ is known (obtained from the residual error variance from a traditional regression), assuming the ratio $W/V$ specifies $W$—a conservative value of 0.1 is adopted in our study.

$$\beta 0_t = \beta 0_{(t-1)} + w_t, \beta 1_t = \beta 1_{(t-1)} + w_t, \beta 2_t = \beta 2_{(t-1)} + w_t, \ldots, \text{where} \quad (2)$$

$$w_t \approx N(0, W)$$

The posterior predictive distribution of model coefficients at each time $t$ is based on the distribution of coefficients from the previous time step $t$-1 (i.e., *prior*), and the probability of the data $Y_t$ conditional on the model parameters at time $t$, (i.e., likelihood) using Bayes theorem as:

$$P(\theta_t|Y_t) \propto P(Y_t|\theta_t)P\left(\theta_t|Y_{(t-1)}\right) \quad (3)$$

where $\theta_t$ represents the vector containing the regression coefficients at time $t$.

At the start, the regression coefficients are estimated from a traditional static linear regression which provides the mean value and the variance of the coefficients with a normal distribution—i.e., $\theta_0 \approx N(m_0, C_0)$ where $m_0$ and $C_0$ are the mean vector and the variance–covariance matrix of the regression parameters. Posterior distributions of parameters at any time $t$ can be obtained recursively using a Kalman filtering approach along with Markov chain Monte Carlo simulation approach. Bayesian confidence intervals can be generated from the posterior distributions. Here, we used the library *dlm* in R (Petris et al. 2009).

Although in this study we used a retrospective analysis, DLMs can also be used in forecasting and predictions at time $t + k$ using the regression models conditioning on information known up to a particular time period $t$.

One of the advantages of DLMs is that they offer a frame-work for prediction and forecasting as well, which a moving window correlation cannot. Their ability to have both time-varying intercept and slopes in the model makes it easier to attribute linkages of the response to not only the covariates but also to unmodeled factors. In addition, since a bayesian updating of model parameters evolves

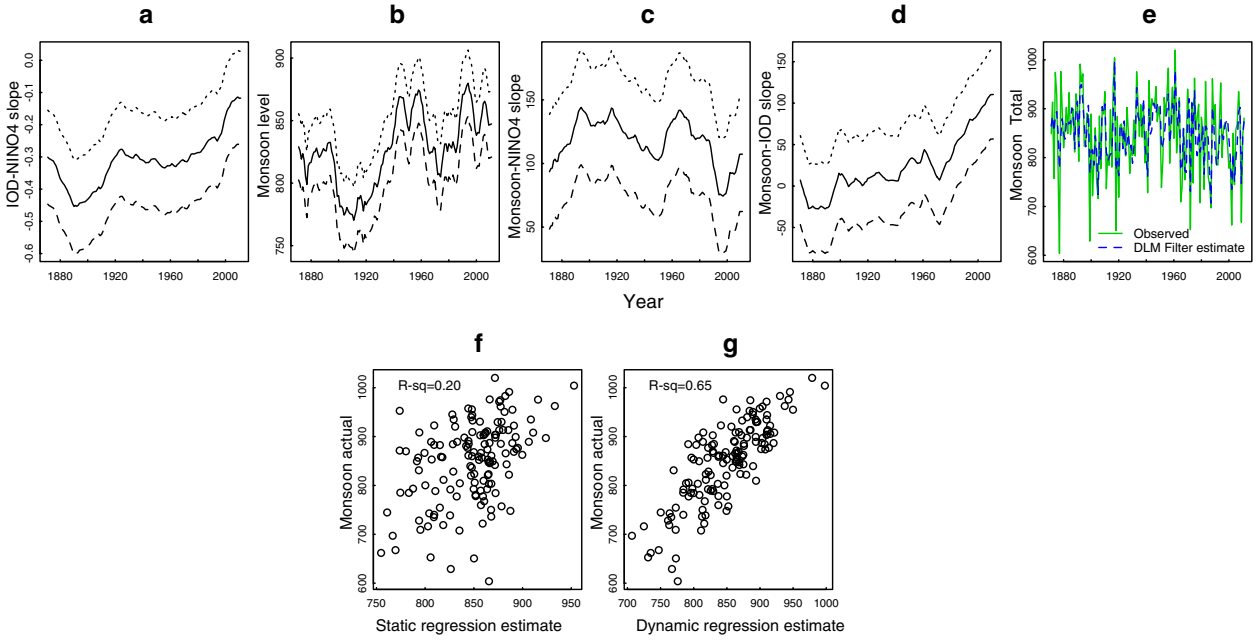


**Fig. 1** Changes in the relationship between IOD and NINO4, and the relationships between these indices and the Indian monsoon over time. Each plot includes a regression parameter (intercept or slope; *solid line*) along with the 25th and 75th percentile credible interval lines (*dotted lines*) estimated using dynamic regression models. **a** Plot of the time-varying slope of the relationship between NINO4 and IOD, **b** Time varying intercept (monsoon level) for the regression of IM with NINO4 and IOD as co-variates, **c** Time-varying slope of the IM–NINO4 relationship, **d** Time varying slope of the IM–IOD relationship, and **e** plot of the estimated rainfall from the dynamic regression model (*dotted blue line*) and the observed rainfall (*solid green line*) over time. **f** Actual and estimated monsoon totals using the ordinary static regression model. **g** Actual and estimated monsoon totals using the dynamic regression model. $p$ values for regression model in **f** and **g** are less than 0.0001

through the time-series, the transition across major changes, whether abrupt or gradual is easily captured.

### 3.2 Generalized additive model (GAM)

Generalised Additive Models were used to detect nonlinearities that might be present in the relationship between covariates (NINO4 and IOD) and monsoon attributes (IM totals, annual frequency of EREs), which are typically hard to capture using traditional linear regression methods. The general form of these models used were:

$$g(E(Y_t)) = \beta_0 + f_1(X_{1t}) + f_2(X_{2t}) \quad (4)$$

The function $g(.)$ is the link function. The functions $f_i$ for each variable $X_i$ used was nonparametric–splines, thus providing the ability to capture appropriate levels of nonlinearities in these variables. The smoothing function for each predictor is derived separately from the data and these are combined additively to generate the fitted values. The covariate range is covered using knots which define segments where the local spline functional form is fitted to define the response. In the case of $Y$ being the monsoon totals, the covariates were the monsoon seasonal average NINO4 and IOD indices for each year and, we used the identity link and Gaussian distribution for the error. In the case of EREs the response variables, $Y$, are the square transformed counts of monsoon seasonal EREs in each year at different exceedance thresholds and the covariates were the same as described above. However, the link function chosen was the log, the standard link function for Poisson distribution appropriate for count data, such as the case here. The difficulty in specifying a probability distribution for the response and error terms is overcome by the use of quasi-likelihood models where only a relationship between mean and variance is specified, and the variance or dispersion is derived from the data. Therefore GAM models are very flexible in accommodating different distributions within the same broad family (i.e. Poisson in the case of count data).The $p$ values obtained from the GAM models are based on the chi square distribution. GAM models are very flexible in being able to accommodate a variety of non-linear shapes and thus are particularly suitable for studying teleconnections between ocean–atmosphere phenomena and climate as these are non-linear and complex (Hoerling et al. 1997).

The output of the GAM models included the fitted values obtained as the expected value of the counts using back-transformation using the link function. The fitted values can be plotted against the covariates and the uncertainty in the scatter quantified using non-parametric smoothing method using the qplot function in R. This enables the interpretation of the response variable in the original units. Uncertainty in fitted GAM models was assessed in two distinct ways: $p$ values from the GAM models, as well as visual interpretation of standard error bands on the fitted values plotted against the individual covariate.

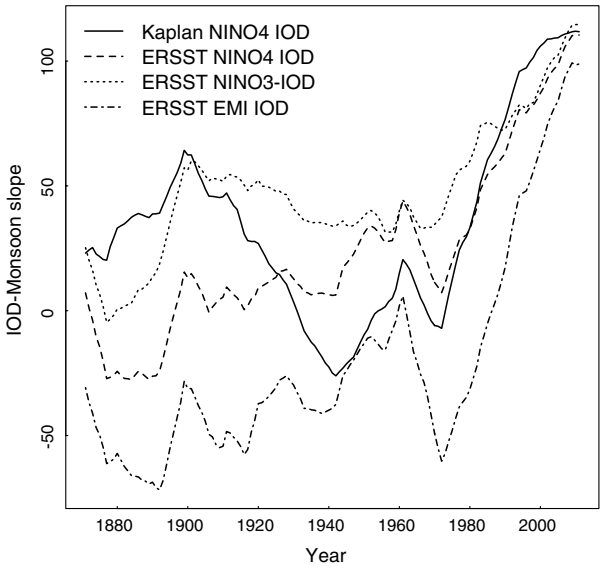


**Fig. 2** Time-varying regression slope coefficient of monsoon-Indian Ocean Dipole (IOD) from dynamic linear models in which the annual Monsoon totals were regressed against NINO indices from different sources and corresponding IOD indices. Note the increase in the monsoon-IOD slope in recent decades across various SST sources and indices

## 4 Results and discussion

We fitted a DLM to IOD with NINO4 as the covariate to investigate the changing relationship between these two indices. Results (Fig. 1a) show a generally negative slope suggesting that that the La Nina phase of NINO4 and the positive IOD positive do not co-occur. It also suggests that IOD's correlation with NINO4 may be weakening in the last decade, indicated by the time-varying slopes tending towards zero. A DLM was fitted to IM as a function of NINO4 and IOD. The time varying intercept (or level) is shown in Fig. 1b, which shows multi-decadal variability with three peaks and troughs. Further, such variability is consistent with multi-decadal variability of the IM rainfall documented by others (e.g., Ummenhofer et al. 2011). The slope of IM–NINO4 shows a recent recovery from the decline from 1960s (Fig. 1c), but the most interesting and clear trend is in the IM–IOD slope which shows a consistent increase since the 1960s (Fig. 1d). Thus, a unit change in IOD is producing proportionately more impacts on the IM relative to earlier periods. Interestingly, the period since 1960s is also the period for which a reduced

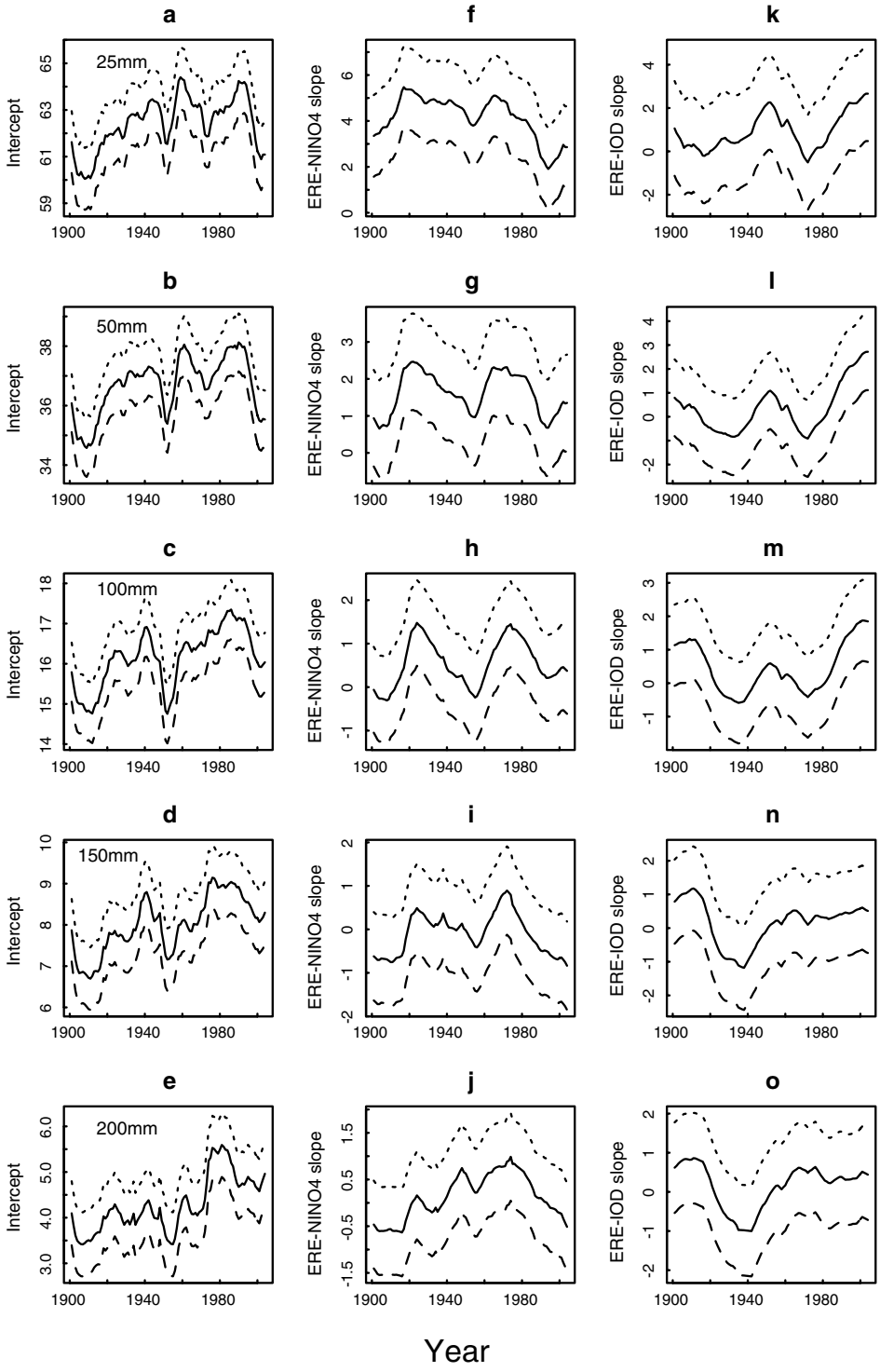


**Fig. 3** Time-varying influence of NINO4 and IOD on the annual counts of EREs (square root transformed) for the periods 1901–2004 at different daily exceedance thresholds (25, 50, 100,150 and 200 mm). The time-varying level and regression slope coefficients are plotted (*solid line*) along with 25th and 75th intervals (*dotted lines*). The first column **a–e** plots the time-varying level or intercept. The third column **f–j** show the time-varying regression slope coefficient of ERE with NINO4, while the last column **k–o** shows the regression coefficient slope of ERE against IOD. Note the increasing influence of IOD in recent decades relative to earlier periods

monsoon-ENSO relationship was reported (Kumar et al. 1999). The mean estimates of IM from the dynamic regression model capture the observed variations in the IM quite well (Fig. 1e). Furthermore, this model outperforms traditional linear regression models (Fig. 1f, g). Additionally, the results were verified using the Kaplan SST dataset for NINO4 and IOD. We also used the NINO3 and EMI indices derived from ERSSTvb3, to verify the increasing influence of IOD on the IM (Fig. 2). Despite some differences, the overall trends and patterns in results are robust over different SST sources and ENSO indices, suggesting the increasing influence of IOD on the IM.

A dynamic regression model was applied to ERE counts at various thresholds and the time varying coefficients are shown in Fig. 3. The time-varying regression intercept (Fig. 3a–e) indicates multi-decadal variability and highlights an overall increasing trend in EREs of 150 and 200 mm exceedance since the early 1900s, however there is a lot of variability in recent decades. Earlier studies across multi-decadal scales have shown a similar increasing trend in EREs over the Indian subcontinent (Goswami et al. 2006; Rajeevan et al. 2008). The time varying slopes of NINO4 and IOD can be seen in Fig. 3f–j and k–o, respectively. The influence of IOD has been increasing, while that of NINO4 has been declining, over the last few decades, particularly for the higher exceedance thresholds. The non-stationarity in the influence of NINO4 and IOD on the IM and corresponding EREs is quite clear from DLM—they both point to an increasing influence of IOD on EREs since the 1940s with the slope changing from negative to positive, albeit with a high degree of uncertainty. The influence of IOD on EREs remains consistent across different sources of SST and ENSO indices (Fig S1).

The non-linear relationship between NINO4 and IOD with IM totals was explored by fitting a GAM (Fig. 4, Fig S2 and S3). Based on the DLM analysis, the early 1940s emerged as a turning point in the relationship between frequency of EREs and IOD (Fig. 3). We thus explored the non-linearity of the IM total NINO4–IOD relationships in the two periods preceding and after the year 1941. The associated $p$ values from the GAM models and standard errors of the fitted values clearly highlight that that the relationships between ENSO and IOD indices and IM changed after the 1940s (Fig. 4, Fig S2 and Fig S3). A similar changing influence of IOD on EREs (above 150 mm) is also evident during the second half (1942–2011) of the study period (Fig. 3n–o and Fig S1). The changing influence of ENSO and IOD on IM since 1940s remains consistent across different types of ENSO indices. However, this is not necessarily true across different SST sources (Fig. 3 and Fig S3). Overall, it's evident that the influence of IOD has strengthened in the 1942–2011 period compared to ENSO, whose relationship with IM seems to be more uncertain and more non-linear relative to 1871–1941 period.

In order to investigate the nature of relationship between NINO4 and IOD with EREs, a GAM was fitted to the ERE counts for different thresholds (Fig. 5). As the number EREs are sparse, especially for higher exceedance thresholds, we applied the GAM model to data from the entire time-period (1901–2007). For lower exceedance thresholds (25, 50 mm day$^{-1}$), IOD has an influence on frequency of EREs only in its positive phase, but for higher exceedance thresholds, the positive influence of IOD is evident across the range of the IOD index values (Fig. 5 and Fig S4). Thus, IOD is more important for influencing EREs at higher exceedance levels. Furthermore, for the higher exceedance EREs there is a pronounced non-linear dip in the influence of IOD at the higher end, possibly suggesting

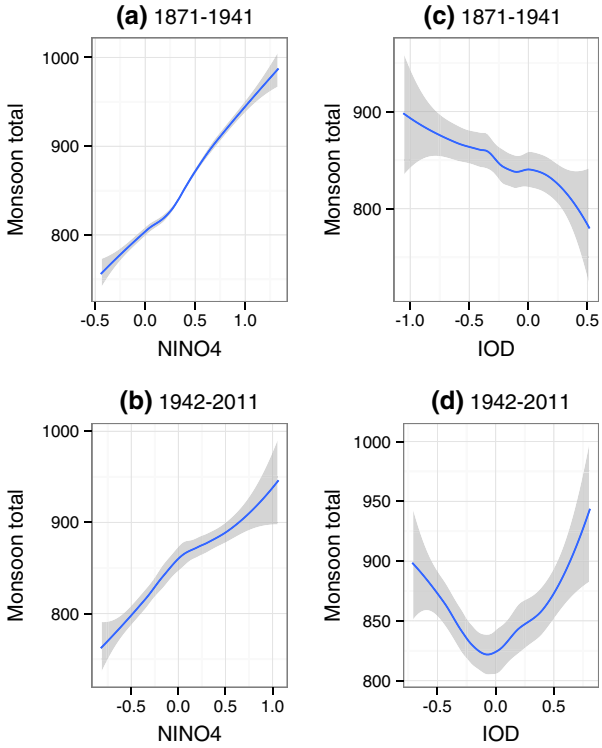


**Fig. 4** Non linear response of annual IM totals to NINO4 and IOD. Modelled IM total as a function of NINO4 (**a**–**b**) and IOD (**c**–**d**). The *solid lines* represent the fitted values of IM total as a function of either NINO4 or IOD based on generalized additive modelling, while the *shaded areas* represent the standard error bands. IOD emerges as the more monotonic and consistent driver of IM especially in the recent decades. The associated $p$ value of GAM model was significant ($p < 0.03$) for influence of IOD for the period 1942–2011, however the standard error bands on the fitted values suggests shifts in the relative role of NINO4 and IOD on the IM between 1942–2011 relative to the earlier period

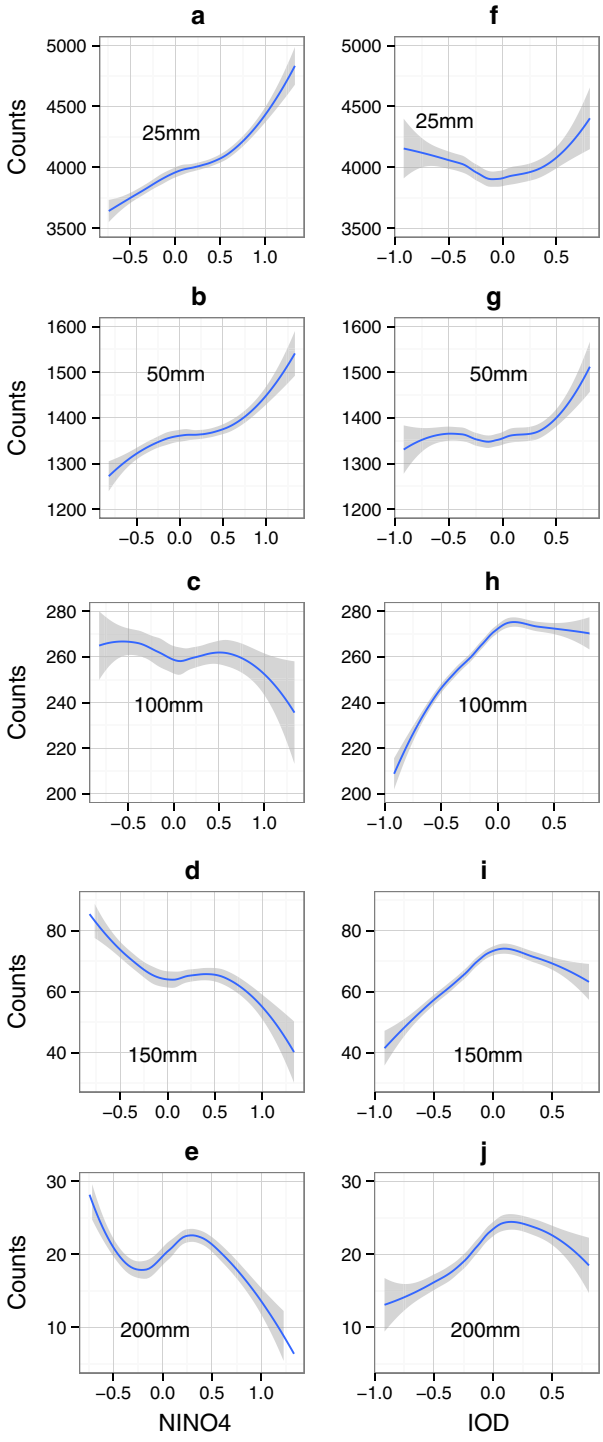


**Fig. 5** Non linear response of ERE counts to NINO4 and IOD. ▶ Modelled ERE counts as a function of NINO4 (**a**–**e**) and IOD (**f**–**j**) for time periods 1901–2004 for rainfall exceedance thresholds of 25 mm (row 1), 50 mm (row 2), 100 mm (row 3), 150 mm (row 4) and 200 mm (row 5). The *solid lines* represent the fitted values of ERE counts as a function of either NINO4 or IOD based on generalized additive modelling, while the *shaded areas* represent the standard error bands. IOD emerges as the more monotonic and consistent driver of EREs especially at higher exceedance thresholds. All models are significant at $p < 0.001$

the inhibiting influence of un-modelled processes or the influence of different physical processes when compared to lower thresholds.

Nonlinearities in the relationships are quite apparent from these plots. Positive values of IOD are generally associated with an increase in ERE counts (all results were significant at $p < 0.001$), but for 100 mm and above EREs increase with the IOD index, but flatten out at positive IOD values, suggesting that local or regional drivers in addition to the two ocean–atmosphere phenomena could be influencing occurrence of very high EREs. The spatial distribution of high EREs (Fig S5) indicates that large areas in India (including upper catchments of major rivers) are prone to flooding. Such areas also incorporate large vulnerable populations including major urban centres. Also in urban landscapes pluvial flooding is a major source of concern and can occur at lower rain intensities (Dawson et al. 2008). As urbanization spreads, vulnerability is predicted to increase in these regions.

The DLM and GAM methods provide a robust approach to modelling non-stationarity and nonlinearity in relationships between large climate features and regional precipitation as well as quantifying the uncertainties. Our approaches can be applied to other regions where ocean–atmosphere phenomenon is known to influence precipitation, and thus evaluate any changes in the pattern of rainfall and EREs. Such analysis should be informed by a comparison across different SST sources used for defining ocean–atmosphere indices. This is especially important as the uncertainty about SST data before 1950 is higher.

Our research and results highlight several exciting and challenging questions. Can dynamic models that include IOD as a covariate improve the predictability of monsoon rainfall and its extremes at time-scales finer than annual? Can we map spatially explicit influences of ENSO and IOD for larger regions to identify vulnerable and sensitive areas? Can we identify local and regional factors that influence EREs apart from ocean–atmosphere phenomena? Can long term simulations from GCM models confirm the shifts in the relative role of ENSO and IOD on the IM? The impact of changing climate and weather extremes on future socio-economic welfare and ecosystem responses in India and elsewhere is a major area of concern for adaptation strategies (Easterling et al. 2000; Meehl et al. 2000; Kundzewicz et al. 2008; Revi 2008; Tubiello et al. 2007). Clearly, advances in these questions will make a meaningful difference to the region's social and economic well-being and the sustainability of its ecosystems and ecosystem services.

**Acknowledgments** We would like to thank the jointly administered Changing Water Cycle programme of the Ministry of Earth Sciences (Grant Ref: MoES/NERC/16/02/10 PC-11), Government of India and Natural Environment Research Council (Grant Ref: NE/I022450/1), United Kingdom for financial support. We thank the two anonymous reviewers and editor for their helpful comments and suggestions on an earlier version of this article. We dedicate this paper to our colleague and co-author Professor Mike Bonell who passed away on July 11th, 2014.

## References

Abram NJ, Gagan MK, Cole JE, Hantoro WS, Mudelsee M (2008) Recent intensification of tropical climate variability in the Indian Ocean. Nat Geosci 1:849–853. doi:10.1038/ngeo357

Ajaymohan RS, Rao SA (2008) Indian Ocean dipole modulates the number of extreme rainfall events over india in a warming environment. J Meteorol Soc Jpn Ser II 86:245–252

Ashfaq M, Shi Y, Tung W, Trapp RJ, Gao X, Pal JS, Diffenbaugh NS (2009) Suppression of south Asian summer monsoon precipitation in the 21st century. Geophys Res Lett 36:L01704. doi:10.1029/2008GL036500

Ashok K, Saji NH (2007) On the impacts of ENSO and Indian Ocean dipole events on sub-regional Indian summer monsoon rainfall. Nat Hazards 42:273–285. doi:10.1007/s11069-006-9091-0

Ashok K, Guan Z, Yamagata T (2001) Impact of the Indian Ocean dipole on the relationship between the Indian monsoon rainfall and ENSO. Geophys Res Lett 28:4499–4502

Ashok K, Guan Z, Saji NH, Yamagata T (2004) Individual and combined influences of ENSO and the Indian Ocean dipole on the Indian summer monsoon. J Clim 17:3141–3155

Ashok K, Behera SK, Rao SA, Weng H, Yamagata T (2007) El Niño Modoki and its possible teleconnection. J Geophys Res 112:C11007

Ashrit RG, Kumar KR, Kumar KK (2001) ENSO-monsoon relationships in a greenhouse warming scenario. Geophys Res Lett 28:1727–1730

Cai W, Cowan T, Sullivan A (2009) Recent unprecedented skewness towards positive Indian Ocean dipole occurrences and its impact on Australian rainfall. Geophys Res Lett 36:L11705

Calder C, Lavine M, Müller P, Clark JS (2003) Incorporating multiple sources of stochasticity into dynamic population models. Ecology 84(6):1395–1402

Cherchi A, Navarra A (2013) Influence of ENSO and of the Indian Ocean Dipole on the Indian summer monsoon variability. Clim Dyn 41:81–103. doi:10.1007/s00382-012-1602-y

Dawson R, Speight L, Hall J, Djordjevic S, Savic D, Leandro J (2008) Attribution of flood risk in urban areas. J Hydroinformatics 10:275–288

Easterling DR, Meehl GA, Parmesan C, Changnon SA, Karl TR, Mearns LO (2000) Climate extremes: observations, modeling, and impacts. Science 289:2068–2074. doi:10.1126/science.289.5487.2068

Gabet EJ, Burbank DW, Putkonen JK, Pratt-Sitaula BA, Ojha T (2004) Rainfall thresholds for landsliding in the Himalayas of Nepal. Geomorphology 63:131–143

Gadgil S, Kumar KR (2006) The Asian monsoon—agriculture and economy. Asian Monsoon. Springer, Berlin Heidelberg, pp 651–683

Ghosh S, Das D, Kao S-C, Ganguly AR (2012) Lack of uniform trends but increasing spatial variability in observed Indian rainfall extremes. Nat Clim Change 2:86–91. doi:10.1038/nclimate1327

Goswami BN, Venugopal V, Sengupta D, Madhusoodanan MS, Xavier PK (2006) Increasing trend of extreme rain events over India in a warming environment. Science 314:1442–1445

Groisman P, Karl T, Easterling D, Knight R, Jamason P, Hennessy K, Suppiah R, Page C, Wibig J, Fortuniak K, Razuvaev V, Douglas A, Førland E, Zhai P-M (1999) Changes in the probability of heavy precipitation: important indicators of climatic change. Clim Change 42:243–283. doi:10.1023/A:1005432803188

Guhathakurta P, Rajeevan M (2008) Trends in the rainfall pattern over India. Int J Climatol 28:1453–1469

Guhathakurta P, Sreejith O, Menon PA (2011) Impact of climate change on extreme rainfall events and flood risk in India. J Earth Syst Sci 120:359–373. doi:10.1007/s12040-011-0082-5

Guisan A, Edwards TC Jr, Hastie T (2002) Generalized linear and generalized additive models in studies of species distributions: setting the scene. Ecol Model 157:89–100

Han W, Meehl GA, Rajagopalan B, Fasullo JT, Hu A, Lin J, Large WG, Wang J, Quan X-W, Trenary LL, Wallcraft A, Shinoda T, Yeager S (2010) Patterns of Indian Ocean sea-level change in a warming climate. Nat Geosci 3:546–550. doi:10.1038/ngeo901

Harrison J, West M (1997) Bayesian forecasting and dynamic models. Springer Verlag, New York

Harrisons PJ, Stevens CF (1976) Bayesian forecasting (with discussion). J Roy Stat Soc Ser B 38:205–247

Hastie T, Tibshirani R (1986) Generalized additive models. Stat Sci 1:297–310. doi:10.1214/ss/1177013604

Hastie T, Tibshirani R (1990) Generalized additive models. Chapman & Hall/CRC, Florida

Hennessy KJ, Gregory JM, Mitchell JFB (1997) Changes in daily precipitation under enhanced greenhouse conditions. Clim Dyn 13:667–680. doi:10.1007/s003820050189

Hoerling MP, Kumar A, Zhong M (1997) El Niño, La Niña, and the nonlinearity of their teleconnections. J Clim 10:1769–1786. doi:10.1175/1520-0442(1997)010<1769:ENOLNA>2.0.CO;2

Ihara C, Kushnir Y, Cane MA (2008) Warming trend of the indian ocean SST and Indian Ocean dipole from 1880 to 2004. J Clim 21:2035–2046

Izumo T, Vialard J, Lengaigne M, de Boyer Montegut C, Behera SK, Luo J–J, Cravatte S, Masson S, Yamagata T (2010) Influence of the state of the Indian Ocean dipole on the following year/'s El Nino. Nat Geosci 3:168–172. doi:10.1038/ngeo760

Kaplan A, Cane MA, Kushnir Y, Clement AC, Blumenthal MB, Rajagopalan B (1998) Analyses of global sea surface temperature 1856–1991. J Geophys Res Oceans 103:18567–18589. doi:10.1029/97JC01736

Krishnan R, Sabin TP, Ayantika DC, Kitoh A, Sugi M, Murakami H, Turner AG, Slingo JM, Rajendran K (2013) Will the South Asian monsoon overturning circulation stabilize any further? Clim Dyn 40:187–211. doi:10.1007/s00382-012-1317-0

Krishnaswamy J, Lavine M, Richter DD, Korfmacher K (2000) Dynamic modeling of long-term sedimentation in the Yadkin River basin. Adv Water Resour 23:881–892. doi:10.1016/S0309-1708(00)00013-0

Krishnaswamy J, Halpin PN, Richter DD (2001) Dynamics of sediment discharge in relation to land-use and hydro-climatology in a humid tropical watershed in Costa Rica. J Hydrol 253:91–109. doi:10.1016/S0022-1694(01)00474-7

Krishnaswamy J, John R, Joseph S (2014) Consistent response of vegetation dynamics to recent climate change in tropical mountain regions. Glob Change Biol 20:203–215. doi:10.1111/gcb.12362

Kumar KK, Rajagopalan B, Cane MA (1999) On the weakening relationship between the Indian monsoon and ENSO. Science 284:2156–2159

Kumar KK, Rajagopalan B, Hoerling M, Bates G, Cane M (2006) Unraveling the mystery of Indian monsoon failure during El Niño. Science 314:115–119

Kumar KK, Kamala K, Rajagopalan B, Hoerling M, Eischeid J, Patwardhan SK, Srinivasan G, Goswami BN, Nemani R (2011) The

once and future pulse of Indian monsoonal climate. Clim Dyn 36:2159–2170. doi:10.1007/s00382-010-0974-0

Kundzewicz ZW, Mata LJ, Arnell NW, Döll P, Jimenez B, Miller K, Oki T, Şen Z, Shiklomanov I (2008) The implications of projected climate change for freshwater resources and their management. Hydrol Sci J 53:3–10. doi:10.1623/hysj.53.1.3

Lehmann A, Overton JM, Austin MP (2002) Regression models for spatial prediction: their role for biodiversity and conservation. Biodivers Conserv 11:2085–2092. doi:10.1023/A:1021354914494

Luo J-J, Zhang R, Behera SK, Masumoto Y, Jin F-F, Lukas R, Yamagata T (2010) Interaction between El Niño and extreme Indian Ocean dipole. J Clim 23:726–742. doi:10.1175/2009JCLI3104.1

Maity R, Nagesh Kumar D (2006) Bayesian dynamic modeling for monthly Indian summer monsoon rainfall using El Niño–Southern Oscillation (ENSO) and Equatorial Indian Ocean Oscillation (EQUINOO). J Geophys Res Atmos 111:D07104. doi:10.1029/2005JD006539

Meehl GA, Karl T, Easterling DR, Changnon S, Pielke R, Changnon D, Evans J, Groisman PY, Knutson TR, Kunkel KE, Mearns LO, Parmesan C, Pulwarty R, Root T, Sylves RT, Whetton P, Zwiers F (2000) An introduction to trends in extreme weather and climate events: observations, socioeconomic impacts, terrestrial ecological impacts, and model projections. Bull Am Meteorol Soc 81:413–416. doi:10.1175/1520-0477(2000)081<0413:AITTIE>2.3.CO;2

Parthasarathy B, Munot AA, Kothawale DR (1994) All-India monthly and seasonal rainfall series: 1871–1993. Theor Appl Climatol 49:217–224. doi:10.1007/BF00867461

Pearce JL, Beringer J, Nicholls N, Hyndman RJ, Tapper NJ (2011) Quantifying the influence of local meteorology on air quality using generalized additive models. Atmos Environ 45:1328–1336. doi:10.1016/j.atmosenv.2010.11.051

Petris G, Petrone S, Campagnoli P (2009) Dynamic linear models. Dyn. Linear Models R. Springer: New York, pp 31–84

Pielke RA, Downton MW (2000) Precipitation and damaging floods: trends in the United States, 1932–97. J Clim 13:3625–3637. doi:10.1175/1520-0442(2000)013<3625:PADFTI>2.0.CO;2

Prajeesh AG, Ashok K, Rao DVB (2013) Falling monsoon depression frequency: A Gray-Sikka conditions perspective. Sci Rep 3

Rajagopalan B, Molnar P (2012) Pacific Ocean sea-surface temperature variability and predictability of rainfall in the early and late parts of the Indian summer monsoon season. Clim Dyn 39:1543–1557. doi:10.1007/s00382-011-1194-y

Rajeevan M, Bhate J, Kale JD, Lal B (2006) High resolution daily gridded rainfall data for the Indian region: analysis of break and active monsoon spells. Curr Sci 91:296–306

Rajeevan M, Bhate J, Jaswal AK (2008) Analysis of variability and trends of extreme rainfall events over India using 104 years of gridded daily rainfall data. Geophys Res Lett 35:L18707

Revi A (2008) Climate change risk: an adaptation and mitigation agenda for Indian cities. Environ Urban 20:207–229. doi:10.1177/0956247808089157

Saji NH, Goswami BN, Vinayachandran PN, Yamagata T (1999) A dipole mode in the tropical Indian Ocean. Nature 401:360–363. doi:10.1038/43854

Smith TM, Reynolds RW, Peterson TC, Lawrimore J (2008) Improvements to NOAA's historical merged land-ocean surface temperature analysis (1880–2006). J Clim 21:2283–2296

Trenberth KE, Dai A, Rasmussen RM, Parsons DB (2003) The changing character of precipitation. Bull Am Meteorol Soc 84:1205–1217. doi:10.1175/BAMS-84-9-1205

Tubiello FN, Soussana J-F, Howden SM (2007) Crop and pasture response to climate change. Proc Natl Acad Sci 104:19686–19690. doi:10.1073/pnas.0701728104

Turner AG, Annamalai H (2012) Climate change and the South Asian summer monsoon. Nat Clim Change 2:587–595. doi:10.1038/nclimate1495

Ummenhofer CC, Gupta AS, Li Y, Taschetto AS, England MH (2011) Multi-decadal modulation of the El Nino–Indian monsoon relationship by Indian Ocean variability. Environ Res Lett 6:034006

Vinayachandran PN, Francis PA, Rao SA (2009) Indian Ocean dipole: Processes and impacts. In: Mukunda, N. (ed) Current trends in science, platinum jubilee special. Indian Academy of Sciences, pp 569–589

Wang X, Wang C (2014) Different impacts of various El Niño events on the Indian Ocean dipole. Clim Dyn 42(3–4):991–1005

Wang P, Baines A, Lavine M, Smith G (2012) Modelling ozone injury to U.S. forests. Environ Ecol Stat 19:461–472. doi:10.1007/s10651-012-0195-2

Wang B, Yim S-Y, Lee J-Y, Liu J, Ha K-J (2013) Future change of Asian-Australian monsoon under RCP 4.5 anthropogenic warming scenario. Clim Dyn 42:83–100. doi:10.1007/s00382-013-1769-x

West M, Harrison PJ, Migon HS (1985) Dynamic generalized linear models and bayesian forecasting. J Am Stat Assoc 80:73–83. doi:10.1080/01621459.1985.10477131

Yee TW, Mitchell ND (1991) Generalized additive models in plant ecology. J Veg Sci 2:587–602. doi:10.2307/3236170

Zhai P, Zhang X, Wan H, Pan X (2005) Trends in total precipitation and frequency of daily precipitation extremes over China. J Clim 18:1096–1108. doi:10.1175/JCLI-3318.1

Environmental Modelling & Software 88 (2017) 1–9

Contents lists available at ScienceDirect

Environmental Modelling & Software

journal homepage: www.elsevier.com/locate/envsoft

# Role of rainstorm intensity underestimated by data-derived flood models: Emerging global evidence from subsurface-dominated watersheds

Nick A. Chappell [a, *], Tim D. Jones [a], Wlodek Tych [a], Jagdish Krishnaswamy [b]

[a] Lancaster Environment Centre, Lancaster University, Lancaster, UK
[b] Ashoka Trust for Research in Ecology and the Environment (ATREE), Bangalore 560064, India

ARTICLE INFO

*Article history:*
Received 29 February 2016
Received in revised form
26 October 2016
Accepted 27 October 2016
Available online 16 November 2016

*Keywords:*
Rainfall intensity
Storm hydrograph
Transfer function
Flood
Nonlinearity

ABSTRACT

Intense rainstorms are a prevalent feature of current weather. Evidence is presented showing that simulation of flood hydrographs shown to be dominated by subsurface flow requires watershed model parameterisation to vary between periods of different rainstorm intensity, in addition to varying with antecedent basin storage. The data show an emerging global relation between flood response and the intensity of rainstorms. Flood responses are quantified as watershed residence times (strictly time constants of nonlinear transfer-function models) identified directly from information contained within 15-min rainfall and streamflow observations. The emerging monotonic, curvilinear relation indicates that (subsurface) watershed residence time decreases as mean intensity rises, and is seen over a wide range of synoptic conditions from temperate and tropical climates. Projected increases in rainstorm intensity would then result in a greater likelihood of river floods in subsurface-dominated watersheds than is currently simulated by systems models omitting this additional nonlinearity.



## Software availability

Program title: CAPTAIN
Developers: Peter Young, Wlodek Tych, Diego Pedregal, James Taylor and Paul McKenna (Lancaster University) Contact e-mail: p.young@lancaster.ac.uk or c.taylor@lancaster.ac.uk
First available: February 2004 (Version 5 released on Internet)
Hardware: PC platforms supporting Matlab™
Software: Captain Toolbox for Matlab™: download from http://www.lancaster.ac.uk/staff/taylorcj/tdc/download.php
Toolbox requirements: Most of the functionality is available using the basic Matlab package

## 1. Introduction

Drainage basins temporarily store each pulse of rainfall to give a streamflow output more damped than that of the rainfall input. With physics-based watershed models the damping is produced primarily by combination of the prevailing antecedent moisture states with the unsaturated permeability distributions (Bear et al., 1968; Ali et al., 2012). With systems models of basins the damping in the rainfall ($r$) or effective rainfall ($r_{eff}$) to streamflow ($q$) signal is often quantified using residence times (or time constants) of a transfer-function or impulse-response function (Young, 1998; Box et al., 2008). The $r_{eff}$ is the rainfall signal after a nonlinear transformation to account for the effects of antecedent watershed storage on hydrograph response (e.g., Whitehead et al., 1979; Young and Beven, 1994; Ye et al., 1998; McIntyre et al., 2011).

There is a general perception that stream hydrographs are flashier and more likely to produce over-bank flows in periods and/or regions experiencing more intense rainfall events. A very small number of studies have demonstrated an apparent link between the properties of hydrograph shape and averaged rainfall intensity characteristics for a specific storm period. Minshall (1960) showed that different measures of the shape of calculated Unit Hydrographs (Sherman, 1932) altered with changes in the hourly rainfall intensity (inches/h) averaged over individual storms. As a specific example, this study showed that the time for the hydrograph to recess to 40 percent of the peak-flow reduced as the average hourly

* Corresponding author. Lancaster Environment Centre, Lancaster University, Lancaster LA1 4YQ, UK.
*E-mail address:* n.chappell@lancaster.ac.uk (N.A. Chappell).

http://dx.doi.org/10.1016/j.envsoft.2016.10.009

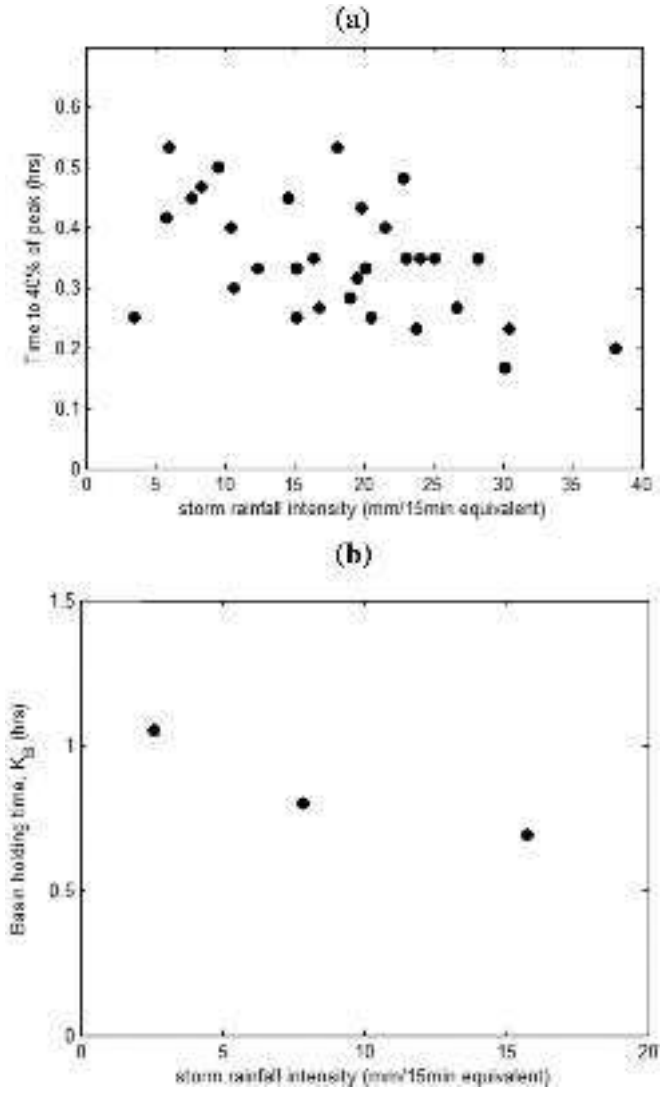


**Fig. 1.** Relationship of measures of hydrograph shape with rainfall intensity averaged over a storm period from two previous studies. (a) Time from the Unit Hydrograph peak to the 'point on the streamflow recession at 40% of the peak' against rainfall intensity (inches/h) averaged over the specific storm (converted to mm/15min equivalent), adapted from Table 3 in Minshall (1960). (b) Basin 'holding time' of the Instantaneous Unit Hydrograph against rainfall intensity (cm/h) averaged over the specific storm (converted to mm/15min equivalent), adapted from Fig. 6 in Wang et al. (1981).

storm rainfall intensity increased (Fig. 1a). Similarly, Wang et al. (1981) showed that the basin 'holding time' ($K_B$) reduced as the average hourly storm rainfall intensity (inches/h) increased (Fig. 1b). In other words, change in hyetograph shape (i.e., temporal evolution of rainfall totals through a storm) between different types of storm can produce different hydrograph shapes and hence nonlinearity in the rainfall to streamflow response (Rodríguez-Iturbe et al., 1982).

Several studies undertaken in regions with more intense tropical rainfall events (e.g., Noguchi et al., 1997; Chappell et al., 2006, 2012; Hugenschmidt et al., 2014) have demonstrated that very flashy stream hydrographs can be produced almost entirely from subsurface flow pathways, i.e., without the need for activation of significant volumes of overland flow (on slopes) during storms. Consequently, nonlinear rainfall-streamflow response generated in such basins would be entirely related to shallow or deeper groundwater flow pathways. Even after correcting for the widely acknowledged nonlinear effects of antecedent wetness on rates of subsurface flow (Graham et al., 2010), it is *our research hypothesis that additional nonlinearities in rainfall-streamflow response dominated only by subsurface flow may be generated by changes in hyetograph shape*. If this hypothesis is valid, it would require explicit model parameterisation or temporal shifts in existing systems model parameterisations to represent and so better simulate streamflow through storms with contrasting conditions. The rainfall intensity regime for a period of contiguous storms is likely to vary with synoptic meteorological typology in time and across the globe. Those in the tropics tend to have greater intensities than those prevailing in temperate regions primarily due to differences in regional convection (Wohl et al., 2012). Equally large variations are seen within the tropics; for example synoptic conditions associated with tropical cyclones tend to have greater average intensities than those associated with local thunderstorms (Francis and Gadgil, 2006; Zipser et al., 2006; Shepherd et al., 2007). To reiterate, non-stationarity in systems model parameters (see e.g., Kundzewicz and Napiórkowski, 1986) characterising rainfall-streamflow responses in subsurface-flow dominated watersheds caused by temporal variations in rainfall intensity regime, would be in addition to those caused by changes in antecedent moisture (or seen in basins with overland flow activation).

While previous studies provide some observational evidence for the potential effects of storm-averaged rainfall intensity on the non-stationarity of hydrograph residence times (Fig. 1ab), the absence of a generic numerical relationship (for basins dominated only by subsurface flow) may be responsible for the lack of a wider recognition of the phenomenon. In part this may be due to the limited range of hydrograph responses and storm-types examined previously (see e.g., Minshall, 1960; Wang et al., 1981; Rodríguez-Iturbe et al., 1982). Consequently, a greater diversity of synoptic meteorological conditions was examined in this study to attempt to *quantify the first approximation of a generic relationship between rainfall intensity characteristics and storm hydrograph shape for subsurface-dominated flood responses.*

## 2. Experimental data sets

In this study selected rainfall and streamflow records were those associated with a set of experimental basin systems (each <5 $km^2$) known to be dominated by shallow subsurface paths (sometimes called 'interflow'), in addition to experiencing a broad spectrum of synoptic conditions. One such system is the South Creek basin in a humid tropical region of Australia (e.g., Chappell et al., 2012). Two other example experimental basins in the tropics (Fig. 2) with hydrograph responses shown to be dominated by shallow subsurface paths, are the Baru basin on Borneo Island (e.g., Kretzschmar et al., 2014) and Saimane basin of the larger Aghanashini basin in India (Bonell et al., 2010; Krishnaswamy et al., 2012). These have contrasting rainfall intensity regimes, with the Baru being dominated by local thunderstorms and Saimane by Tropical Convergence Zone (TCZ) events in the summer monsoon. To capture the effects of typically lower intensity rain-events in temperate regions, three basins from across upland UK are incorporated in the analysis (Fig. 2). The Hafren, Greenholes and Nant-y-Craflwyn basins are dominated by shallow water-paths (Bell, 2005; Chappell and Lancaster, 2007; Jones and Chappell, 2014) and frontal rainfall. Further basin details are given in Table 1. While rainfall-streamflow responses for only six experimental basins are studied, the 16 periods of contiguous storms analysed do cover a diverse range of synoptic conditions (Table 2).

The primary hyetograph characteristic evaluated was the average rainfall depth from all 15-min intervals with measured rainfall in the selected periods of contiguous storms of the same

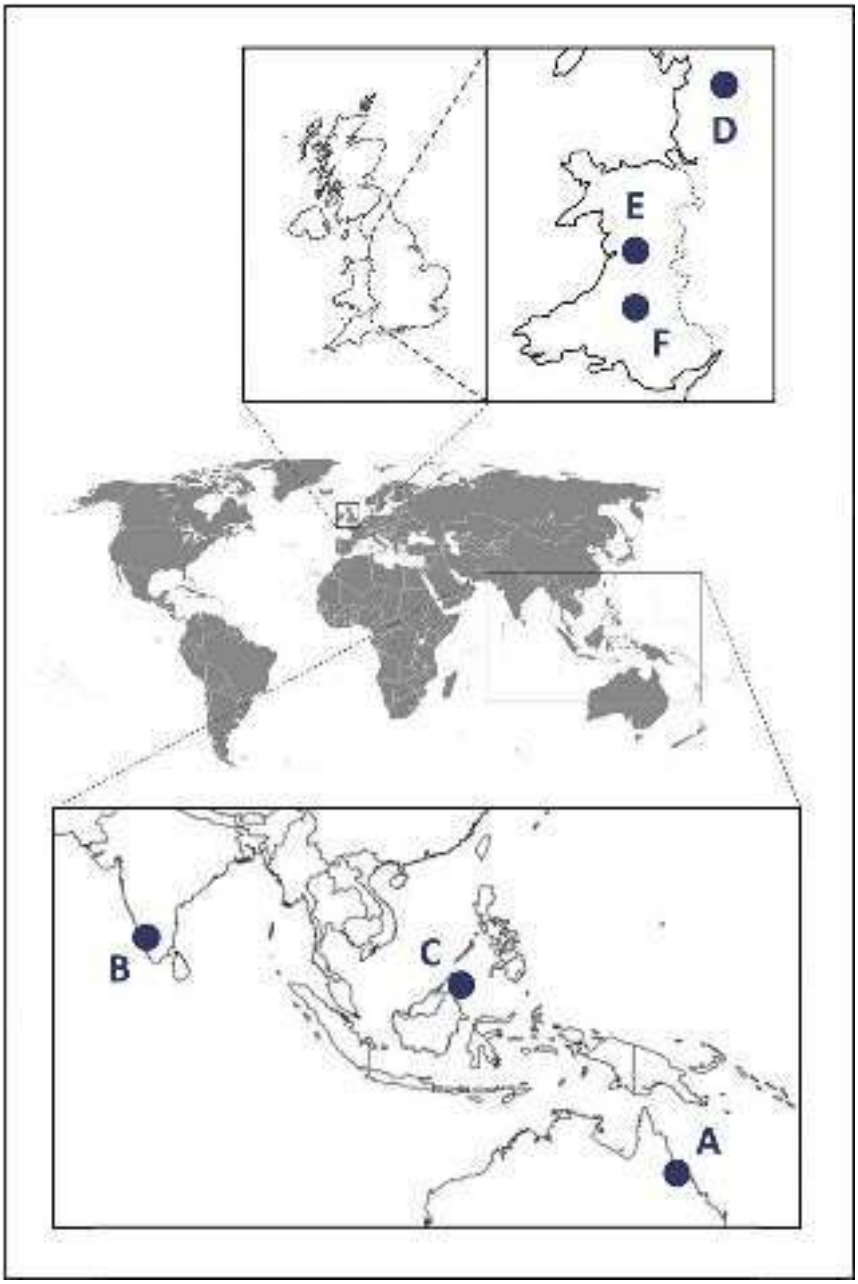


**Fig. 2.** Geographic locations of the experimental basins detailed in Table 1. Location A is the South Creek basin in tropical Queensland, Australia; location B is the Saimane basin in the Western Ghats mountains in Karnataka state of India; location C is the Baru basin in Sabah state of Malaysia on Borneo Island; location D is the Greenholes basin in temperate northwest England, United Kingdom; and locations E and F are the Hafren basin and Nant-y-Craflwyn basin, respectively, in mid-Wales, United Kingdom.

synoptic type ($I_{WET15}$). Thus 15-min periods recording zero rainfall were excluded from the statistics. This removed the confounding influence of differing durations of dry spells within the selected period of contiguous storms on the calculated rainfall characteristic. This also allows for storms of different duration to be characterised (Brommer et al., 2007). A total of 16 separate periods covering a diverse range of synoptic conditions were selected (Table 2).

For the South Creek basin the periods covered are: tropical cyclone 'Ivor'; part of the post-monsoon period; part of the Australian monsoon (December–March); and localized convective events (Klingaman, 2012). The southwest summer monsoon in India comprises of several 'active phases' caused by distinct synoptic systems that may have differing rainfall characteristics (Francis and Gadgil, 2006). Consequently, for the Saimane basin in India, periods comprising of different active phases within the 2013 monsoon, were selected for the modelling. For the Baru basin on Borneo Island, periods of localized convective rainfall (Bidin and Chappell, 2006) were selected for comparison. For a few 15-min sampling increments within the tropical data sets, rainfall intensities were very high, reaching a maximum of 29.25 mm/15min (Supplementary Material Fig. S4ab). This maximum value is equivalent to more than 7 tips per minute of the 0.25 mm/tip tipping-bucket raingauge (Mark II Rimco) used at the South Creek basin (Gilmour et al., 1980). The 15-min sampling increments with such high rainfall intensities are likely to give under-estimates of

**Table 1**
Characteristics of the experimental basins selected to provide the data sets for the 16 periods of contiguous storms.

| Experimental basin | Name of the period of contiguous storms | Basin area (km[b]) | Stream order: Strahler method[g] | Dominant soil type | Surficial geology | Solid geology | Land cover |
|---|---|---|---|---|---|---|---|
| South Creek, Australia[a] | Periods 1 to 4 | 0.3 | 4 | Acrisol | >6 m weathered rock | Basic metamorphic | Tropical evergreen forest (disturbed mesophyll vine forest) |
| Saimane, India[b] | Periods 5 to 8 | 4.9 | 3 | Nitosol | 1-10 m weathered rock | Metamorphic | Tropical evergreen forest (disturbed with agroforestry) |
| Baru, Malaysia[c] | Periods 9 to 10 | 0.4 | 3 | Alisol | <3 m weathered rock | Melange | Tropical evergreen forest (disturbed lowland dipterocarp) |
| Greenholes, UK[d] | Periods 11 to 12 | 1.1 | 2 | Gleysol | 1 to >4 m glacial till | Sedimentary (Carboniferous) | Grassland (heather moorland and improved pasture) |
| Hafren, UK[e] | Periods 12 to 14 | 3.7 | 2 | Histosol & Podzol | 0.1 to ≥10 m solifluction deposit | Metamorphic (Silurian) | Plantation (conifer) & grassland (heather moorland) |
| Nant-y-Craflwyn, UK[f] | Periods 15 to 16 | 0.5 | 2 | Gleysol & Podzol | 1-5 m glacial till | Metamorphic (Ordovician) | Plantation (conifer) |

[a] Gilmour et al. (1980), Chappell et al. (2012).
[b] FAO UNESCO (2004), Bonell et al. (2010), Krishnaswamy et al. (2012).
[c] Chappell et al. (1999, 2012).
[d] Chappell and Lancaster (2007).
[e] Newson (1976).
[f] Reynolds and Norris (1990), Jones and Chappell (2014).
[g] Gregory and Walling (1973).

**Table 2**
Characteristics of the sixteen study periods and models of effective rainfall to streamflow response identified by the RIVC algorithm.

| Period | Regime[a,b] | Experimental basin | $I_{WET15eff}$[c] (mm/15-min) | Model[d] | $R_t^2$[e] | $TC_{fast}$ (hrs)[f] | *fast%*[g] |
|---|---|---|---|---|---|---|---|
| 1 | 1 (Aw) | South Creek | 2.0705 | [2 2 0] | 0.931 | 0.286 ± 0.004 | 50.8 ± 10 |
| 2 | 2 (Aw) | South Creek | 1.5656 | [2 2 0] | 0.855 | 0.116 ± 0.001 | 63.3 ± 9.4 |
| 3 | 3 (Aw) | South Creek | 2.0411 | [2 2 0] | 0.898 | 0.358 ± 0.002 | 40.6 ± 3.7 |
| 4 | 4 (Aw) | South Creek | 0.8721 | [2 2 0] | 0.803 | 1.360 ± 0.003 | 19.7 ± 11 |
| 5 | 5 (Am) | Saimane | 2.1868 | [2 2 0] | 0.777 | 0.355 ± 0.101 | 59.3 ± 38 |
| 6 | 5 (Am) | Saimane | 0.9733 | [2 2 0] | 0.892 | 0.444 ± 0.014 | 37.3 ± 15 |
| 7 | 5 (Am) | Saimane | 0.7374 | [2 2 1] | 0.944 | 0.578 ± 0.024 | 32.5 ± 14 |
| 8 | 5 (Am) | Saimane | 1.2920 | [2 2 0] | 0.929 | 0.270 ± 0.023 | 46.1 ± 19 |
| 9 | 4 (Af) | Baru | 0.7159 | [2 2 0] | 0.927 | 1.702 ± 0.001 | 65.5 ± 44 |
| 10 | 4 (Af) | Baru | 1.3246 | [2 2 1] | 0.884 | 0.830 ± 0.005 | 65.4 ± 19 |
| 11 | 6 (Cfb) | Greenholes | 0.6167 | [2 2 0] | 0.958 | 4.605 ± 0.076 | 74.6 ± 9.2 |
| 12 | 6 (Cfb) | Greenholes | 0.7615 | [2 2 1] | 0.902 | 2.645 ± 0.043 | 55.7 ± 6.3 |
| 13 | 6 (Cfb) | Hafren | 0.7240 | [2 2 3] | 0.985 | 1.375 ± 0.023 | 42.1 ± 7.4 |
| 14 | 6 (Cfb) | Hafren | 0.4822 | [2 2 0] | 0.947 | 1.869 ± 0.017 | 25.8 ± 8.1 |
| 15 | 6 (Cfb) | Nant-y-Craflwyn | 0.4831 | [2 2 2] | 0.966 | 3.209 ± 0.355 | 52.9 ± 26 |
| 16 | 6 (Cfb) | Nant-y-Craflwyn | 0.3305 | [2 2 1] | 0.961 | 3.581 ± 0.038 | 66.3 ± 9.2 |

[a] Storm-type characterizing the regime in period: 1 Tropical cyclone Ivor, 2 post-monsoon period, 3 monsoon period, 4 convective events, 5 Tropical Convergence Zone event, 6 frontal rainfall event.
[b] Köppen-Geiger climate regime: Aw = tropical wet and dry climate, Am = tropical monsoon climate, Af = tropical rainforest climate, Cfb = oceanic climate (Peel et al., 2007).
[c] Average effective rainfall from all 15-min intervals in the selected period receiving rainfall.
[d] Model structure is given as the number of [Denominators, Numerators, Pure Time Delays] as in Chappell et al. (2012).
[e] $R_t^2$ is the simulation efficiency defined as the variance in the model residuals normalised by the variance in the observed streamflow data.
[f] $TC_{fast}$ is the Dynamic Response Component (DRC) of the time constant of the fast response component.
[g] *Fast%* is the DRC of the percentage of response following the fast component (e.g., Jones and Chappell, 2014). Uncertainty in the $TC_{fast}$ and *fast%* values is twice the standard deviation derived from 1000 Monte Carlo realizations using uncertainty information implicit to the RIVC method.

the true 15-min totals (Saidi et al., 2014). Such high intensities are, however, limited to very few increments within the records, and so have little impact on statistics averaged across the periods of contiguous storms. The periods of contiguous storms selected for modelling temperate basins all received rainfall from frontal systems that were expected (Little et al., 2008) and shown (Supplementary Material Fig. S4ab) to have lower mean intensity values. In temperate UK, intense rainfall exceeds 4 mm/h, equivalent to 1 mm/15-min. Consequently, for the study basins in both temperate and tropical regions with a range in $I_{WET15}$ less than 1 mm/15-min, two periods contrasting in rainfall intensity were selected, while for those with a larger range four contrasting periods were used. The rainfall intensity statistic was also calculated for the effective rainfall to be used in the $r_{eff}$-$q$ modelling (i.e., modelling once the effects of antecedent conditions removed), to give $I_{WET15eff}$.

## 3. Model identification methods

The Refined Instrumental Variable in Continuous-time (RIVC) algorithm (Young and Jakeman, 1979; Young and Garnier, 2006; Young, 2015) was used to capture the dominant modes of $r_{eff}$-$q$ response of each period to compare with the $I_{WET15eff}$ statistic. Historically, most rainfall-streamflow models based on transfer functions (TFs) have been discrete-time dynamic models. Discrete-time dynamic models describe a system using difference equations e.g., $q(k) = ar(k-1)$, where $a$ is a recession term and $r(k-1)$ represents the rainfall input at the previous $k$th sampling time. In contrast, continuous-time dynamic models describe a system using differential equations (Young, 2015). These models are generally more

difficult to estimate, but produce more reliable model parameter estimates where the system dynamics are very fast, i.e., where the dynamics are nearly as fast as the sampling increments in the data. Given the likelihood of short residence times for some of the rainfall-streamflow responses in the selected tropical basins (Chappell et al., 2012), a continuous-time modelling approach was used in this study.

The RIVC algorithm was used to identify model structures and parameters following a three-stage Data-Based Mechanistic (DBM) approach. The first stage of this approach is to apply a large range of mathematical relationships that might capture the dynamics of the streamflow from the rainfall or effective rainfall. Thus the model structures identified are based on those that can describe the dynamics between the observed input data and observed output data; hence the models can be defined as *data-based*. This first stage is undertaken without making any *a priori* assumptions about the nature of the processes within the subsurface flow system. It also involves the identification and separate parameterisation of the nonlinear effects on the rainfall-streamflow response caused by changing antecedent subsurface storage between the simulated periods via transformation of rainfall to effective rainfall (Young and Beven, 1994; Chappell et al., 2012; Kretzschmar et al., 2014). The second stage of the DBM approach involves the rejection of as many of the identified models as possible based upon mathematical-statistical criteria. This involves model rejection based upon: 1/an unacceptable degree of correspondence between the observed and simulated streamflow (i.e., poor simulation efficiency), 2/an unacceptable degree of model over-parameterisation (i.e., rejection of models that are more complex than can be warranted by the information contained in the observations), and 3/the failure of various mathematical diagnostic checks, e.g., models exhibiting unstable behaviour. The third and final stage of the approach is the rejection of mathematically acceptable DBM models that do not have a feasible *hydrological process interpretation*. For example, a DBM model of streamflow that is a combination of one water-pathway that adds water to the stream and one that removes it, may be valid statistically, but is not considered consistent with perceptual models of streamflow generation systems. DBM models accepted as having a hydrological interpretation can then be defined as *mechanistic* and therefore, described as data-based mechanistic models.

The DBM approach combined with the RIVC algorithm was used for two principal reasons. First, the constraint on model structural complexity implicit within the DBM approach (so called 'model parsimony') limits the range of possible values of each parameter describing hydrograph shape, notably the $\alpha$ parameter(s) (Eq. (1)), thereby reducing its/their parametric uncertainty (Young, 2013). This allows differences in model parameter values between periods to be identified above the uncertainties and so permits a greater degree of process interpretation (Jones et al., 2014). Secondly, it provides an objective method for separating the effects of antecedent subsurface wetness (that are well known) from the effects of storm-period rainfall intensity on the subsurface response. Without an understanding of how storm-period rainfall intensity affects subsurface flow mechanisms directly, it would not be clear how to modify the structure of a physics-based model to simulate this hypothesised phenomenon. The need for mechanistic (or process) interpretation of all DBM models, combined with their acknowledged parsimony, means that they are considered to be a state-of-the-art approach for gaining process understanding of rainfall-streamflow systems (Beven, 2012; Young, 2013; Jones et al., 2014; Beven and Smith, 2014).

It is the derived RIVC transfer function parameter of the time constant (*TC* or the watershed's residence time of response derived directly from the $\alpha$ parameter) that translates an effective hyetograph to a hydrograph (Young, 1998; Box et al., 2008). For streamflow generation systems lacking more than a few percent of overland flow, the steepest parts of the hydrograph recession (and associated shortest *TC* identified) can be interpreted as the rapid response through the soil-water system (Barnes, 1939), i.e., shallow subsurface flow or 'interflow' pathway. Periods of contiguous storms were selected for the $r_{eff}$-$q$ modelling (and associated $I_{WE\text{-}T15eff}$ determination) to give more reliable parameter estimates than can be achieved for single events with their smaller information content (see Seibert and Beven, 2009).

To capture the nonlinear effects arising from different soil moisture storages at the start of each period of observations, the rainfall observations for each period were first filtered to give $r_{eff}$ (rather than $r$) using an additional, optimized model parameter, $p$, following Chappell et al. (2012) and Kretzschmar et al. (2014). Additional temperature modulation effects on the nonlinearity term (see e.g., Young and Beven, 1994) were not included. The sensitivity of the $r_{eff}$-$q$ model to the $p$-value was estimated with 1000 Monte Carlo realizations of $p$ over the range 0–1.5 (Supplementary Material Fig. S6).

The RIVC algorithm is available in the CAPTAIN Toolbox for Matlab™ (Taylor et al., 2007). Technically, it implements an iterative Instrumental Variable method for estimation of general transfer-functions that capture the dynamic relationship between the $r_{eff}$ input and streamflow output variables using rational polynomial equations in operator $s$ in continuous time (Eq. (1), Young, 2015). These can be directly translated in to differential equations forced by $r_{eff}$ (Eq. (2), see e.g., Jones et al., 2014). To emphasise, the more sophisticated continuous-time version of the algorithm was used as it is less sensitive to the adverse effects of under-sampling of flashy tropical systems, compared to the discrete-time versions in CAPTAIN (i.e., RIVD, e.g., Littlewood and Croke, 2013). The risk of under-sampling effects were further reduced by utilizing rainfall and streamflow observations with a 15-min resolution (Jones et al., 2014). The Instrumental Variables (IVs) are the initial estimates of model output that permit unbiased estimation of the model parameters (i.e., $\alpha_1$, $\alpha_2$, $\beta_0$, $\beta_1$ and $\tau$ in Eq. (2)). These IVs, along with variables $r_{eff}$ and $q$, are then used within Normal Equations to derive the parameter estimates and their covariance matrices (Young, 2015). Model structure is presented as a 'triad' of denominator-numerator-delay within square parentheses, indicating the number of denominator parameters, *den* ($\alpha_1$ and $\alpha_2$ parameters in the lower part of the transfer function equation), the number of numerator parameters, *num* ($\beta_0$ and $\beta_1$ parameters in the upper part of the transfer function equation) and the number of pure time delays, *delay* or $\tau$. The form of the model with a second-order [2 2 τ] structure as an example, can be stated in continuous-time transfer-function form, as:

$$q = \left(\frac{\beta_0 s + \beta_1}{s^2 + \alpha_1 s + \alpha_2}\right) e^{-s\tau} r_{eff} \;\; ; \;\; s \sim \frac{d}{dt} \tag{1}$$

where $q$ is the streamflow (mm/15-min), $r_{eff}$ is the effective rainfall (mm/15-min), $\tau$ is the pure time delay between $r_{eff}$ and an initial $q$ response (given in number of 15-min intervals), $\alpha_1$ and $\alpha_2$ the parameters capturing the rate of soil-water exhaustion or residence time (/15-min), $\beta_0$ and $\beta_1$ the parameters capturing the magnitude of streamflow gain (mm $q$/mm $r_{eff}$), $t$ is time in 15-min periods, and $s$ is the Laplace operator (Young, 2015). Alternatively, the model can be expressed in ordinary differential equation terms (ignoring initial conditions):

$$\frac{d^2 q(t)}{dt^2} + \alpha_1 \frac{dq(t)}{dt} + \alpha_2 q(t) = \beta_0 \frac{dr_{eff}(t-\tau)}{dt} + \beta_1 r_{eff}(t-\tau) \tag{2}$$

To allow physical interpretation, this second-order model of streamflow can be decomposed by partial fraction expansion (Jakeman et al., 1990; Young and Beven, 1994) into two parallel, first-order transfer functions:

$$q = \frac{\beta_f}{s-\alpha_f} e^{-s\tau} r_{eff} + \frac{\beta_s}{s-\alpha_s} e^{-s\tau} r_{eff} \quad (3)$$

where $\alpha_f$ and $\alpha_s$ are the values (specifically roots of the characteristic equation of the differential Eq. (2)) representing the rate of soil-water exhaustion or residence time of the fast and slow components that comprise the total streamflow generation, respectively (/15-min; see Supplementary Material Table S4), and $\beta_f$ and $\beta_s$ the parameters capturing the magnitude of the fast and slow flow components, respectively (mm $q$/mm $r_{eff}$). Hydrological interpretation of the behaviour of these model stores is then made after calculating the Dynamic Response Characteristics, DRCs (e.g., Jakeman et al., 1993; Jones et al., 2014) of the component transfer functions from parameters $\alpha_f$, $\alpha_s$, $\beta_f$, $\beta_s$ and $\tau$ given in Eq. (3). These DRCs include the *TC* for each component flow pathway. For the critical fast path this is given as:

$$TC_{fast} = -\frac{\Delta t}{\alpha_f} \quad (4)$$

where $\Delta t$ is the time-step in the observations (15-min). The uncertainties in the $\alpha_1$, $\alpha_2$, $\beta_0$, $\beta_1$ values and derived $TC_{fast}$ values were estimated using uncertainty information implicit to the RIVC method (Young, 2015) applied in 1000 Monte Carlo realizations.

## 4. Results and discussion

For each of the 16 periods, 36 possible models were evaluated from first-order models with no pure time delays (i.e., [1 1 0] structure) to second-order models with 8 pure time delays (i.e., [2 2 8] structure). To capture the shape of the (total) streamflow recessions, a second-order model structure was needed for most of the 16 periods analysed and was able to simulate 77.7–98.5% of the observed dynamics (Table 2). The lower simulation efficiency for period 5 (77.7%) may have been caused by differences in the rainfall intensity regime within the period, particularly between the single larger event and the series of smaller events.

For consistency, optimal second-order models were selected for interpretation of all periods. This structure can be expressed hydrologically as two parallel water-pathways (i.e., a 'fast' and a 'slow' path) within each basin system (e.g., Jakeman et al., 1990; Jakeman and Hornberger, 1993; Young and Beven, 1994; Littlewood et al., 2007; Jones and Chappell, 2014; Jones et al., 2014). The *TC* of the fastest pathway ($TC_{fast}$) characterizes the shape of the hydrographs surrounding the critical periods of peak streamflow, and as such is a measure of the 'flashiness' of the hydrograph (Table 2). This $TC_{fast}$ was shown to be well-defined by the RIVC approach given the narrow uncertainty in the values (Table 2). Fig. 3bd shows this narrow $TC_{fast}$ uncertainty in period 4 and 11 as examples, together with the observed and modelled streamflow (Fig. 3ac). The results from all other modelled periods are given in the supplementary material.

Table 2 shows the $I_{WET15eff}$ values for each of the 16 periods simulated, while Fig. 4a shows the model-derived $TC_{fast}$ values plotted against $I_{WET15eff}$. The 16 values, comprising of different periods for the same basin and different basins within contrasting climatic regimes, exhibit *shorter TCs (of the fast response component) for higher values of average rainfall intensity integrated over the 15-min intervals where rain was present* (in each period of contiguous storms). This is consistent with the findings of previous studies that have observed faster hydrograph recessions for individual storms with larger hourly rainfall intensities (see Minshall, 1960; Wang et al., 1981; Rodríguez-Iturbe et al., 1982 and Fig. 1ab). For the first time, however, we demonstrate that a strong monotonic, curvilinear relationship is apparent between $TC_{fast}$ and $I_{WET15eff}$ for flood hydrographs dominated by subsurface flow (Fig. 4b). For clarification, this first approximation of a power law relationship was derived using the *lsqcurvefit* and *nlpredci* functions in Matlab™ on log-transformed data.

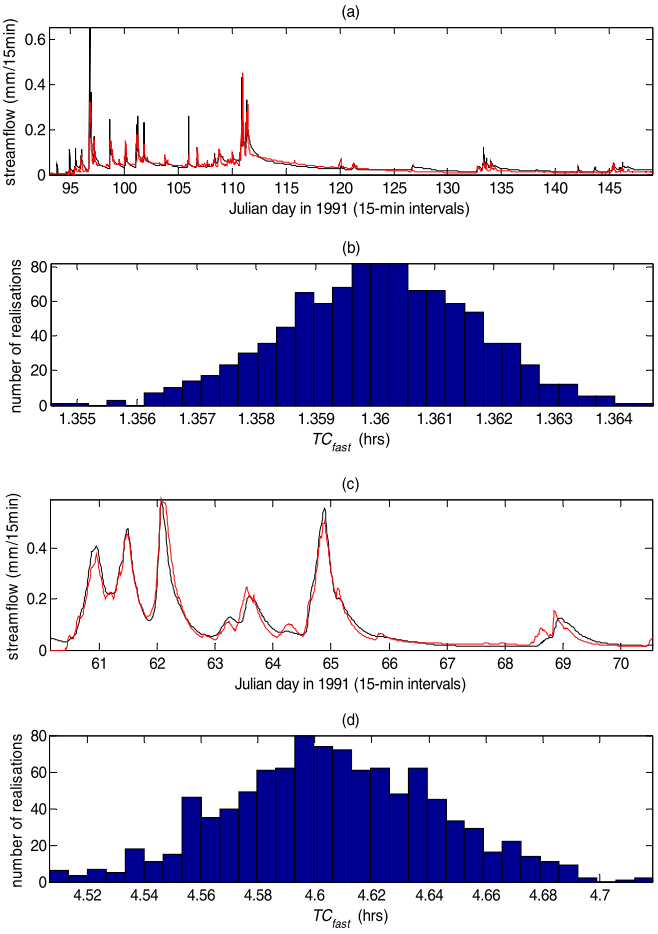


**Fig. 3.** Example observations and model results for period 4 (a tropical basin) and 11 (a temperate basin) shown in Table 1. (a) and (c) Observed (—) and simulated streamflow (——) for periods 4 and 11, respectively. (b) and (d) Frequency distribution of the Dynamic Response Characteristic of the $TC_{fast}$ for periods 4 and 11, respectively, estimated using uncertainty information implicit to the RIVC method applied in 1000 Monte Carlo realizations.

In process terms, the *TC*s of transfer-functions of subsurface-dominated $r_{eff}$-$q$ systems equate to the change of basin storage within each storm, per change of streamflow generated (i.e., $dS/dq$). Consequently, the findings from this study would suggest that for basin systems dominated only by shallow subsurface flow, higher rainfall-intensity regimes deliver more water through the soil-water system to streams within storms rather than accumulate moisture storage within the soil. This effect becomes more pronounced with synoptic systems typically producing lower intensity rainfall, with small changes in the $I_{WET15eff}$ statistic producing large changes in the $TC_{fast}$. The six periods from temperate UK fall along the steeper part of the relation (Fig. 4ab), suggesting that the flashiness of frontal events in temperate streams may be more sensitive to any systematic shifts in the rainfall intensity regime

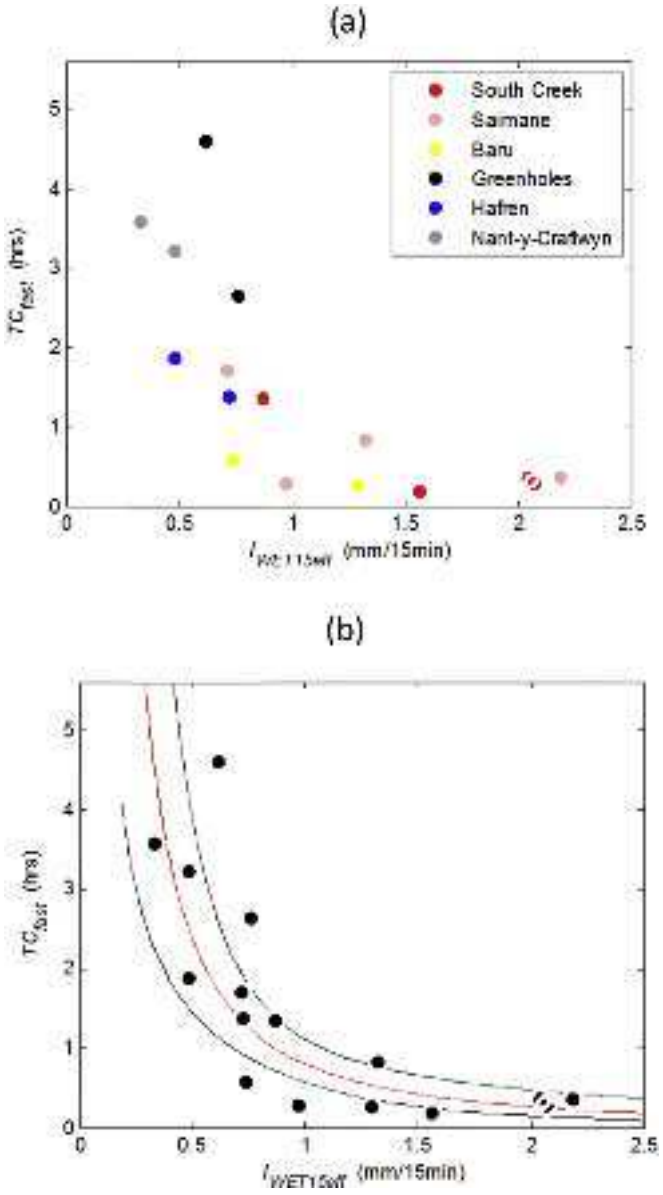


**Fig. 4.** Relationship between $TC_{fast}$ and $I_{WET15eff}$ for the 16 periods of observations pooled from tropical and temperate basins. (a) Values for the same experimental basin are shown using the same colour of solid circle. The tropical basins are: South Creek, Saimane and Baru, while temperate basins are: Greenholes, Hafren and Nant-y-Craflywn. (b) The power model (Eq. (5)) and the 95% confidence intervals are shown with solid lines.

than those of basins with considerably higher rainfall intensities.

The observed relationship is given as:

$$TC_{fast} = 0.80297 I_{WET15eff}{}^{-1.568} \quad ; r^2 = 0.69 \tag{5}$$

where $I_{WET15eff}$ is the average effective rainfall integrated over the 15-min intervals with rain of the selected period of contiguous storms (mm/15min), and $TC_{fast}$ is the associated time constant (hrs) of the fast component of a parallel decomposition of a second-order, transfer function defined by the RIVC algorithm (Fig. 4b). With this model, 69% of the variance in the $TC_{fast}$ could be explained by the variance in the $I_{WET15eff}$ statistic for the 16 periods analysed. The relationship was tested by using the same modelling approach to derive a $TC_{fast}$ value for a different basin during a different monitoring period. For the Nant-y-Bustach basin (UK) over a 25-day period of winter storms an $I_{WET15eff}$ value of 0.4801 mm/15min and a $TC_{fast}$ value of 4.673 h were derived (supplementary material). The point on Fig. 4a associated with these two values lies within the 95% confidence intervals of the power model shown, and so provides some validation of the relationship. For each basin, the trend across periods affected by different intensity regimes, while less clear (Fig. 4a), was not inconsistent with the general power law observed for the whole dataset.

The same degree of explanation of the variations in the $TC_{fast}$ was apparent if the $I_{WET15}$ was used (Supplementary Material Fig. S10) instead of $I_{WET15eff}$ (Fig. 4b). Thus application or not of the nonlinearity transform to the rainfall data to account for the effects of antecedent basin wetness (Young and Beven, 1994) does not impact the ability to identify the relationship with hydrograph flashiness. In some contrast, a much lower degree of explanation of the variations in the $TC_{fast}$ resulted when the median rainfall from all 15-min intervals receiving rainfall ($I_{MED}$) was derived for each period (Supplementary Material Fig. S11). A monotonic relationship was absent between the model parameter $p$ capturing the non-linearities arising from the antecedent moisture conditions and the derived $TC_{fast}$ values (Supplementary Material Fig. S12). A relationship with $TC_{fast}$ was similarly absent with the geomorphic characteristic of basin area (Supplementary Material Fig. S13). Others have attempted to quantify the effects of rainfall intensity characteristics on the proportion of fast-flow during storms (Hewlett et al., 1977; Loague and Freeze, 1985; Bren et al., 1987); this is equivalent to the *fast%* values derived in this study and presented in Table 2. The $I_{WET15eff}$ and $I_{WET15}$ statistic did not, however, produce any systematic relationship with the modelled *fast%* values (Supplementary Material Fig. S14). The shape of the stream hydrograph during storm-events (i.e., $TC_{fast}$ or rainfall-streamflow 'flashiness') was not examined by these other studies. Furthermore, these studies identified only very weak relationships between rainfall intensity characteristics and the proportion of fast-flow during storms. Better correlations were obtained by Howard et al. (2010), but only after subdivision of the rainfall intensity data into several seasonal periods and classes.

For watersheds with subsurface-dominated storm hydrographs, values of systems model watershed parameters representing the residence time of response (i.e., *TC*) are not varied within the current generation of systems models because of differing synoptic storm type (and associated hyetograph shape). Only the separate effects of changing antecedent basin wetness are incorporated into systems model simulations. If watershed model parameters need to be varied between periods of differing storm-averaged intensity (i.e., $I_{WET15eff}$), as our results would suggest (from evidence initially based on subsurface-dominated systems), then models that do not do this will underestimate the fast residence times (i.e., $TC_{fast}$) in periods of higher than average storm intensity. This would mean that simulations of flood events caused by particularly intense storm systems in a long modelled record will be smaller than observed. Additionally, it may mean that locations where the incidence of flooding is particularly sensitive to discrete periods of higher rainstorm intensity (e.g., flooding associated with convective rainfall cells in Southern England in an otherwise frontal rainfall regime: Hand et al., 2004) may not be highlighted sufficiently.

Given that the form and parameters of the relationship are developed from only 16 data periods for initially subsurface-dominated systems, its wider global applicability requires further evaluation of the identified relationship using many combinations of geomorphic setting, as discussed in the closing remarks. The strength of the relationship identified so far is, however, surprising given the diversity of synoptic meteorological conditions

(producing a wide range of rainstorm intensities) examined in this study.

As a working hypothesis, the shallow subsurface systems may be responding differently between periods of contrasting rainfall intensity as a result of activation-deactivation of parts of the soil-macropore systems. It is likely that at higher intensities in a particular basin, more of the macropore system is activated giving a disproportionate and thus nonlinear impact on the shallow subsurface flow (Weiler, 2005) and subsequent rapid loss of moisture storage to streamflow generation. The critical role of soil-macropores in streamflow generation is widely acknowledged. Field methods for their characterization for use in basin modelling does, however, remain poorly understood (Beven and Germann, 2013), thereby restricting the development of physics-based models to show their potential role in explaining the impacts of rain-event characteristics on streamflow generation.

## 5. Conclusions

While a hydrological theory explaining the impact of differences in hyetograph shape (i.e., time-integrated, rain-event characteristics) on hydrograph shape (by a mechanism other than overland flow) may be poorly developed, this is the first study to identify a strong quantitative relationship with rainfall intensity for flashy, subsurface only dominated systems. To reiterate, the strength of the relationship identified so far is, however, surprising given the diversity of synoptic meteorological conditions producing different hyetograph shapes examined in this study. These initial findings do need to be further evaluated (i.e., 'conditional validation': Beven and Young, 2013) against a considerably larger set of experimental basins similarly dominated by shallow subsurface flow. Equally, the presence of relationships for $TC_{fast}$ of experimental basins with significant volumes of deep groundwater-flow (Lesack, 1993; Ockenden and Chappell, 2011) should be evaluated. Furthermore, the link between the rainfall intensity regime and the fast component of streamflow response should be studied with a systematic analysis of storm-type (see e.g., Merz and Blöschl, 2003).

If data-derived model parameters for subsurface-dominated floods need to be varied between periods of differing storm-averaged intensity (i.e., $I_{WET15eff}$), as our results would suggest, then models that do not do this may underestimate the fast residence times (i.e., $TC_{fast}$) in periods of higher than average storm intensity. This would mean that simulations (or long-range forecasts: Pedregal et al., 2009) of flood events caused by particularly intense storm systems in a long record will be less flashy than observed. For larger storm events, if the fast component of flow is delivered more quickly (i.e., shorter $TC_{fast}$), there would be a greater likelihood of floods, caused by over-bank flows, than systems models indicate. This could have profound implications for the subsequent economic and social costs of flooding globally (Arnell and Gosling, 2014).

We are in a period with a greater incidence of extreme rainfall events (e.g., Coumou and Rahmstorf, 2012; de Leeuw et al., 2015) and model projections indicate further intensification through the current century (e.g., Westra et al., 2014). As a result, quantifying the direct impact of more intense storms on flood behaviour (for subsurface-dominated systems and wider), should be an urgent research priority.

## Acknowledgments

The detailed results for this paper are given in the supplementary material, and all data are available by request to the corresponding author. The key stimulus for this modelling work arose from several discussions between N.A.C. and M. Bonell on the role of storm-type in the regulation of hydrograph shape. J. Lancaster is thanked for the collection of the Greenholes basin data when at Lancaster University; M. Bonell for the South Creek data when at James Cook University; Y. Bahat and colleagues at ATREE for the Saimane data; and J. Hanapi of the Yayasan Sabah Group for the Baru data. K. Beven, C.N. Hewitt and P.C. Young of Lancaster University together with the four anonymous reviewers are thanked for their constructive comments. This work was supported by NERC grant WGhats-Capacity (NE/I022450/1) within the NERC Changing Water Cycle programme (in collaboration with Dundee University).

## Appendix A. Supplementary data

Supplementary data related to this article can be found at http://dx.doi.org/10.1016/j.envsoft.2016.10.009.

## References

Ali, M., Fiori, A., Bellotti, G., 2012. Analysis of the nonlinear storage-discharge relation for hillslopes through 2D numerical modelling. Hydrol. Process. 27, 2683–2690.
Arnell, N.W., Gosling, S.N., 2014. The impacts of climate change on river flood risk at the global scale. Clim. Chang. http://dx.doi.org/10.1007/s10584-014-1084-5.
Barnes, B.S., 1939. The structure of discharge recession curves. Trans. Am. Geophys. Union 4, 721–725.
Bear, J., Zaslavsky, D., Irmay, S., 1968. Physical Principles of Water Percolation and Seepage. Unesco, Paris, France.
Bell, J., 2005. The Soil Hydrology of the Plynlimon Catchments. Institute of Hydrology, Wallingford, U.K.
Beven, K.J., 2012. Rainfall-runoff Modelling: the Primer, second ed. Wiley, Chichester.
Beven, K.J., Germann, P.F., 2013. Macropores and water flow in soils revisited. Water Resour. Res. 49, 3071–3092.
Beven, K., Young, P., 2013. A guide to good practice in modeling semantics for authors and referees. Water Resour. Res. 49, 5092–5098.
Beven, K., Smith, P., 2014. Concepts of information content and likelihood in parameter calibration for hydrological simulation models. J. Hydrol. Eng. A4014010. http://dx.doi.org/10.1061/(ASCE)HE.1943-5584.0000991.
Bidin, K., Chappell, N.A., 2006. Characteristics of rain-events at an inland locality in Northeastern Borneo. Hydrol. Process. 20, 3835–3850.
Bonell, M., Purandara, B.K., Venkatesh, B., Krishnaswamy, J., Acharya, H.A.K., Jayakumar, R., Singh, U.V., Chappell, N., 2010. The impact of forest use and reforestation on soil hydraulic conductivity in the Western Ghats of India: implications for surface and sub-surface hydrology. J. Hydrol. 391, 47–62.
Box, G.E.P., Jenkins, G.M., Reinsel, G.C., 2008. Time Series Analysis: Forecasting and Control. Wiley, Hoboken, U.S.A.
Bren, L.J., Farrell, P.W., Leitch, C.J., 1987. Use of weighted integral variables to determine the relation between rainfall intensity and storm flow and peak flow generation. Water Resour. Res. 23, 1320–1326.
Brommer, D.M., Cerveny, R.S., Balling Jr., R.C., 2007. Characteristics of long-duration precipitation events across the United States. Geophys. Res. Lett. 34, L22712. http://dx.doi.org/10.1029/2007GL031808.
Chappell, N.A., Lancaster, J.W., 2007. Comparison of methodological uncertainty within permeability measurements. Hydrol. Process. 21, 2504–2514.
Chappell, N.A., Ternan, J.L., Bidin, K., 1999. Correlation of physicochemical properties and sub-erosional landforms with aggregate stability variations in a tropical Ultisol disturbed by forestry operations. Soil Till. Res. 50, 55–71.
Chappell, N.A., Tych, W., Chotai, A., Bidin, K., Sinun, W., Thang, H.C., 2006. BARUMODEL: combined Data Based Mechanistic models of runoff response in a managed rainforest catchment. For. Ecol. Manag. 224, 58–80.
Chappell, N.A., Bonell, M., Barnes, C.J., Tych, W., 2012. Tropical cyclone effects on rapid runoff responses: quantifying with new continuous-time transfer function models. In: Webb, A.A., Bonell, M., Bren, L., Lane, P.N.J., McGuire, D., Neary, D.G., Nettles, J., Scott, D.F., Stednik, J., Wang, Y., pp82-93 (Eds.), Revisiting Experimental Catchment Studies in Forest Hydrology (IAHS Publication 353). IAHS Press, Wallingford, U.K.
Coumou, D., Rahmstorf, S., 2012. A decade of weather extremes. Nat. Clim. Change 2, 491–496. http://dx.doi.org/10.1038/nclimate1452.
de Leeuw, J., Methven, J., Blackburn, M., 2015. Variability and trends in England and Wales precipitation. Int. J. Climatol. http://dx.doi.org/10.1002/joc.4521.
FAO-UNESCO, 2004. Digital Soil Map of the World and Derived Soil Properties. FAO, Rome.
Francis, P.A., Gadgil, S., 2006. Intense rainfall events over the west coast of India. Meteorol. Atmos. Phys. 94, 27–42.
Graham, C.B., van Verseveld, W., Barnard, H.R., McDonnell, J.J., 2010. Estimating the deep seepage component of the hillslope and catchment water balance within a measurement uncertainty framework. Hydrol. Process. 24, 3631–3647.
Gregory, K.J., Walling, D.E., 1973. Drainage Basin Form and Process. Edward Arnold, London.

Gilmour, D.A., Bonell, M., Sinclair, D.F., 1980. An investigation of storm drainage processes in a tropical rainforest catchment. In: Aust. Water Res. Council Tech. Pap. 56. Aust. Govt. Pub. Ser, Canberra.
Hand, W.H., Fox, N.I., Collier, C.G., 2004. A study of twentieth-century extreme rainfall events in the United Kingdom with implications for forecasting. Met. Apps. 11, 15–31.
Hewlett, J.D., Fortson, J.C., Cunningham, G.B., 1977. The effect of rainfall intensity on storm flow and peak discharge from forest land. Water Resour. Res. 13, 259–266.
Howard, A., Bonell, M., Cassells, D.S., Gilmour, D.A., 2010. Is rainfall intensity significant in the rainfall-runoff process within tropical rainforests of north-east Queensland? : the Hewlett regression analyses revisited. Hydrol. Process. 24, 2520–2537.
Hugenschmidt, C., Ingwersen, J., Sangchan, W., Sukvanachaikul, Y., Duffner, A., Uhlenbrook, S., Streck, T., 2014. A three-component hydrograph separation based on geochemical tracers in a tropical mountainous headwater catchment in northern Thailand. Hydrol. Earth Syst. Sci. 18, 525–537.
Jakeman, A.J., Hornberger, G.M., 1993. How much complexity is warranted in a rainfall-runoff model? Water Resour. Res. 29, 2637–2649.
Jakeman, A.J., Littlewood, I.G., Whitehead, P.G., 1990. Computation of the instantaneous unit hydrograph and identifiable component flows with application to two small upland catchments. J. Hydrol. 117, 275–300.
Jakeman, A.J., Littlewood, I.G., Whitehead, P.G., 1993. An assessment of the dynamic response characteristics of streamflow in the Balquhidder catchments. J. Hydrol. 145 (3–4), 337–355.
Jones, T.D., Chappell, N.A., 2014. Streamflow and hydrogen ion interrelationships identified using Data-Based Mechanistic modelling of high frequency observations through contiguous storms. Hydrol. Res. 45, 868–892.
Jones, T.D., Chappell, N.A., Tych, W., 2014. First dynamic model of dissolved organic carbon derived directly from high frequency observations through contiguous storms. Environ. Sci. Technol. 48, 13289–13297.
Klingaman, N.P., 2012. A Literature Survey of Key Rainfall Drivers in Queensland, Australia: Rainfall Variability and Change. QCCCE Research Report: Rainfall in Queensland. Part 1, Department of Environmental and Resource Management. Queensland Government, Australia.
Kretzschmar, A., Tych, W., Chappell, N.A., 2014. Reversing hydrology: estimation of sub-hourly rainfall time-series from streamflow. Environ. Modell. Softw. 60, 290–301.
Krishnaswamy, J., Bonell, M., Venkatesh, B., Purandara, B.K., Lele, S., Kiran, M.C., Reddy, V., Badiger, S., Rakesh, K.N., 2012. The rain–runoff response of tropical humid forest ecosystems to use and reforestation in the Western Ghats of India. J. Hydrol. 472, 216–237.
Kundzewicz, Z.W., Napiórkowski, J.J., 1986. Nonlinear models of dynamic hydrology. Hydrol. Sci. J. 31, 163–185.
Lesack, L.F.W., 1993. Water balance and hydrologic characteristics of a rainforest catchment in the central Amazon Basin. Water Resour. Res. 29, 759–773.
Little, M.A., Rodda, H.J.E., McSharry, P.E., 2008. Bayesian objective classification of extreme UK daily rainfall for flood risk applications. Hydrol. Earth Syst. Sci. Discuss. 5, 3033–3060.
Littlewood, I.G., Clarke, R.T., Collischonn, W., Croke, B.F.W., 2007. Predicting daily streamflow using rainfall forecasts, a simple loss module and unit hydrographs: two Brazilian catchments. Environ. Modell. Softw. 22, 1229–1239.
Littlewood, I., Croke, B., 2013. Effects of data time-step on the accuracy of calibrated rainfall-streamflow model parameters: practical aspects of uncertainty reduction. Hydrol. Res. 44, 430–440. http://dx.doi.org/10.2166/nh.2012.099.
Loague, K.M., Freeze, R.A., 1985. A comparison of rainfall-runoff modelling techniques on small upland catchments. Water Resour. Res. 21, 229–240.
McIntyre, N., Young, P., Orellana, B., Marshall, M., Reynolds, B., Wheater, H., 2011. Identification of nonlinearity in rainfall-flow response using data-based mechanistic modeling. Water Resour. Res. 47 http://dx.doi.org/10.1029/2010RW009851.
Merz, R., Blöschl, G., 2003. A process typology of regional floods. Water Resour. Res. 39, 1340. http://dx.doi.org/10.1029/2002WR001952.
Minshall, N.E., 1960. Predicting storm runoff on small experimental watersheds. Proc. Am. Soc. Civ. Eng. 86, 28–33.
Newson, M.D., 1976. The Physiography, Deposits and Vegetation of the Plynlimon Catchments. Report Number 30. Institute of Hydrology, Wallingford.
Noguchi, S., Abdul Rahim, N., Baharuddin, K., Tani, M., Sammori, T., Morisada, K., 1997. Soil physical properties and preferential flow pathways in a tropical rain forest, Bukit Tarek, Peninsular Malaysia. J. For. Res. 2, 115–120.
Ockenden, M.C., Chappell, N.A., 2011. Identification of the dominant runoff pathways from the data-based mechanistic modelling of nested catchments in temperate UK. J. Hydrol. 402, 71–79.
Pedregal, D.J., Rivas, R., Feliu, V., Sánchez, L., Linares, A., 2009. A non-linear forecasting system for the Ebro River at Zaragoza, Spain. Environ. Modell. Softw. 24, 502–509.
Peel, M.C., Finlayson, B.L., McMahon, T.A., 2007. Updated world map of the Köppen-Geiger climate classification. Hydrol. Earth Syst. Sc. 11, 1633–1644.
Reynolds, B., Norris, D.A., 1990. Llyn Brianne Acid Waters Project – Summary of Catchment Characteristics. Institute of Terrestrial Ecology, Bangor.
Rodríguez-Iturbe, I., Gonzales-Sanabria, M., Camano, G., 1982. On the climatic dependence of the IUH: a rainfall-runoff theory of the Nash model and the geomorphoclimatic theory. Water Resour. Res. 18, 887–903.
Saidi, H., Ciampittiello, M., Dresti, C., 2014. Extreme rainfall events: evaluation with different instruments and measurement reliability. Environ. Earth Sci. 72, 4607–4616.
Seibert, J., Beven, K.J., 2009. Gauging the ungauged basin: how many discharge measurements are needed? Hydrol. Earth Syst. Sc. 13, 883–892.
Shepherd, J.M., Grundstein, A., Mote, T., 2007. Quantifying the contribution of tropical cyclones to extreme rainfall along the coastal southeastern United States. Geophys. Res. Lett. 34, L23810. http://dx.doi.org/10.1029/2007GL031694.
Sherman, L.K., 1932. Streamflow from rainfall by unit-graph method. Eng. News Rec. 108, 501–505.
Taylor, C.J., Pedregal, D.J., Young, P.C., Tych, W., 2007. Environmental time series analysis and forecasting with the Captain toolbox. Environ. Modell. Softw. 22, 797–814.
Wang, C.T., Gupta, V.K., Waymire, E., 1981. A geomorphologic synthesis of nonlinearity in surface runoff. Water Resour. Res. 17, 343–554.
Weiler, M., 2005. An infiltration model based on flow variability in macropores: development, sensitivity analysis and applications. J. Hydrol. 310, 294–315 (2005).
Westra, S., Fowler, H.J., Evans, J.P., Alexander, L.V., Berg, P., Johnson, F., Kendon, E.J., Lenderink, G., Roberts, N.M., 2014. Future changes to the intensity and frequency of short-duration extreme rainfall: future intensity of sub-daily rainfall. Rev. Geophys. 52, 522–555. http://dx.doi.org/10.1002/2014RG000464.
Whitehead, P.G., Young, P.C., Hornberger, G.M., 1979. A systems model of streamflow and water quality in the Bedford-Ouse: 1. Streamflow modelling. Water Resour. Res. 13, 1155–1169.
Wohl, E., Barros, A., Brunsell, N., Chappell, N.A., Coe, M., Giambelluca, T., Goldsmith, S., Harmon, R., Hendrickx, J., Juvik, J., McDonnell, J., Ogden, F., 2012. The hydrology of the humid tropics. Nat. Clim. Change 2, 655–662.
Ye, W., Jakeman, A.J., Young, P.C., 1998. Identification of improved rainfall-runoff models for an ephemeral low-yielding Australian catchment. Environ. Modell. Softw. 13, 59–74.
Young, P., 1998. Data-based mechanistic modelling of environmental, ecological, economic and engineering systems. Environ. Modell. Softw. 13, 105–122.
Young, P.C., 2013. Hypothetico-inductive data-based mechanistic modeling of hydrological systems. Water Resour. Res. 49, 915–935.
Young, P.C., 2015. Refined instrumental variable estimation: maximum likelihood optimization of a unified Box–Jenkins model. Automatica 52, 35–46.
Young, P.C., Jakeman, A.J., 1979. Refined instrumental variable methods of recursive time-series analysis Part I. Single input, single output systems. Int. J. Control 29, 1–30.
Young, P.C., Beven, K.J., 1994. Data-based mechanistic modelling and the rainfall-flow nonlinearity. Environmetrics 5, 335–363.
Young, P.C., Garnier, H., 2006. Identification and estimation of continuous-time, data-based mechanistic (DBM) models for environmental systems. Environ. Modell. Softw. 21, 1055–1072.
Zipser, E.J., Cecil, D.J., Liu, C.T., Nesbitt, S.W., Yorti, D.P., 2006. Where are the most intense thunderstorms on Earth? B. Am. Meteorol. Soc. 87, 1057–1071.

United Nations
Educational, Scientific and
Cultural Organization

International
Hydrological
Programme

# Forest Management

## and the impact on water resources: a review of 13 countries

IHP - VIII / Technical document N° 37
Latin America and the Caribbean

United Nations Educational, Scientific, and Cultural Organization

International Hydrological Programme

International Sediment Initiative

# Forest management and the impact on water resources: a review of 13 countries












EDITORS

Pablo A. Garcia-Chevesich, Daniel G. Neary,
David F. Scott, Richard G. Benyon, Teresa Reyna.

Published in 2017 by the United Nations Educational, Scientific and Cultural Organization, 7, place de Fontenoy, 75352 Paris 07 SP, France and UNESCO Regional Office for Sciences for Latin America and the Caribbean – UNESCO Montevideo



ISBN 978-92-3-100216-8



Cover photo: CC0 License
Graphic design: Leonardo Alvarez de Ron
Cover design: María Noel Pereyra
Typeset: Pablo García Chevesich
Edition: Miguel Doria, Soledad Benítez, Joaquín Jafif and Tatiana Másmela

# Table of Contents


**Acknowledgements** ..... 6

**Executive summary** ..... 7

**Chapter 1. Forest Management and Water in Argentina** ..... 11

1.1 Introduction ..... 11

1.2 Literature review ..... 14

1.3 Politics ..... 18

1.4 Climate change and the future of forestry & forest research ..... 18

1.5 References ..... 19

**Chapter 2. Forest Management and Water in Australia** ..... 21

2.1 Introduction ..... 21

2.2 Literature review ..... 25

2.3 Politics ..... 28

2.4 Climate change and the future of forestry & forest research ..... 29

2.5 References ..... 29

**Chapter 3. Forest Management and Water in Brazil** ..... 33

3.1 Introduction ..... 33

3.2 Literature review ..... 36

3.3 Politics ..... 38

3.4 Climate change and the future of forestry & forest research ..... 40

3.5 Acknowledgements ..... 41

3.6 References ..... 41

**Chapter 4. Forest Management and Water in Chile** ..... 45

4.1 Introduction ..... 45

4.2 Literature review ..... 47

4.3 Politics ..... 51

4.4 Climate change and the future of forestry & forest research ..... 51

4.5 Acknowledgements ..... 52

4.6 References ..... 52

**Chapter 5. Forest Management and Water in China ..... 55**
5.1 Introduction ..... 55
5.2 Literature review ..... 56
5.3 Politics ..... 60
5.4 Climate change and the future of forestry & forest research ..... 62
5.5 Acknowledgements ..... 63
5.6 References ..... 63

**Chapter 6. Forest Management and Water in the Democratic Republic of Congo ..... 67**
6.1 Introduction ..... 67
6.2 Literature review ..... 68
6.3 Politics ..... 74
6.4 Climate change and the future of forestry & forest research ..... 75
6.5 References ..... 81

**Chapter 7. Forest Management and Water in India ..... 87**
7.1 Introduction ..... 87
7.2 Literature review ..... 88
7.3 Politics ..... 97
7.4 Climate change and the future of forestry & forest research ..... 98
7.5 Acknowledgements ..... 101
7.6 References ..... 101

**Chapter 8. Forest Management and Water in Malaysia ..... 105**
8.1 Introduction ..... 105
8.2 Literature review ..... 110
8.3 Politics ..... 115
8.4 Climate change and the future of forestry & forest research ..... 119
8.5 Acknowledgements ..... 124
8.6 References ..... 125

**Chapter 9. Forest Management and Water in Peru ..... 129**
9.1 Introduction ..... 129
9.2 Literature review ..... 136
9.3 Politics ..... 138
9.4 Climate change and the future of forestry & forest research ..... 140
9.5 Acknowledgements ..... 142
9.6 References ..... 142

**Chapter 10. Forest Management and Water in Romania** ..... **149**
10.1 Introduction ..... 149
10.2 Literature review ..... 153
10.3 Politics ..... 155
10.4 Climate change and the future of forestry & forest research ..... 156
10.5 References ..... 157

**Chapter 11. Forest Management and Water in the Republic of South Africa** ..... **159**
11.1 Introduction ..... 159
11.2 Literature review ..... 162
11.3 Politics ..... 165
11.4 Climate change and the future of forestry & forest research ..... 165
11.5 References ..... 166

**Chapter 12. Forest Management and Water in Spain** ..... **169**
12.1 Introduction ..... 169
12.2 Literature review ..... 173
12.3 Politics ..... 175
12.4 Climate change and the future of forestry & forest research ..... 176
12.5 Acknowledgements ..... 178
12.6 References ..... 178

**Chapter 13. Forest Management and Water in the United States** ..... **181**
13.1 Introduction ..... 181
13.2 Literature review ..... 186
13.3 Politics ..... 195
13.4 Climate change and the future of forestry & forest research ..... 197
13.5 Acknowledgements ..... 198
13.6 References ..... 198

# Acknowledgements

The editors deeply thank all the contributing authors that submitted a chapter representing their country, for all the time and effort invested.

# Executive summary

Trees have been around for more than 370 million years, and today there are about 80 thousand species of them, occupying 3.5 billion hectares worldwide, including 250 million ha of commercial plantations. While forests can provide tremendous environmental, social, and economic benefits to nations, they also affect the hydrologic cycle in different ways. As the demand for water grows and local precipitation patterns change due to global warming, plantation forestry has encountered an increasing number of water-related conflicts worldwide.

This document provides a country-by-country summary of the current state of knowledge on the relationship between forest management and water resources. Based on available research publications, the Editor-in-Chief of this document contacted local scientists from countries where the impact of forest management on water resources is an issue, inviting them to submit a chapter. Authors were instructed to use the following structure:

### *1. Introduction*

Present a brief history of the country's native forests and forest plantations, describing the past and current natural and plantation forest distribution (map, area, main species), as well as main products produced (timber, pulp, furniture, etc.). Characterize the country's water resources and main water uses, discussing the key water resource issues. Finally, describe the forest & water issues that are relevant in the country.

### *2. Literature review*

Write a brief review of water-related forest management studies. Include methods (e.g. paired watershed studies, precipitation/runoff relationship, water balance, hydrological modelling, sap flow meters, etc.) and results. End with a section on best management practices utilized or recommended by the country to increase water yield and/or improve water quality.

### *3. Politics*

Discuss key environmental regulations, laws, and policies related to forestry and water, and evaluate how research results have interacted with politics and *vice versa*, i.e. the creation of new regulations, either enforced by the law, or simply applied by the private sector, to improve water yield and water quality. Also, discuss the role of forest certification systems in managing water quantity and quality.

### *4. Climate change and the future of forestry & forest research*

Evaluate the effects of climate change in the country, especially on water resources, describing how the area occupied by forest plantations is increasing or decreasing, and where. End this section proposing future research and management practices that should be incorporated in the management of forest plantations to improve water quality and water yield.

An excellent group from 13 nations, representing almost half the World's population, submitted chapters (Argentina, Australia, Brazil, Chile, China, Republic of Congo, India, Malaysia, Peru,

Romania, South Africa, Spain, and United States), making this document a relevant contribution to the current state of water and forestry-related issues, management, and policies worldwide.

Differences in historical forest management, climate, vegetation types and socioeconomic conditions driving the use and management of forests mean that forest hydrology research results vary from nation to nation. This makes it difficult to generalise and extrapolate between countries and regions. What seems to be of greatest importance is the combination of watershed characteristics (size, slope and soils), current and prior land uses and local climates, especially the temporal distribution of annual precipitation and temperatures.

In certain climates, for example parts of Australia, Brazil, Chile, China, India, South Africa, Spain and the USA, where natural grassland, shrublands or land previously cleared for agriculture is replaced with fast growing plantations, streamflows and groundwater recharge are often substantially reduced, potentially creating local conflicts between plantations and other water users. In South Africa and Australia, this has led to introduction of legislation to limit plantation developments in some areas. Conversely, reforestation of degraded agricultural land, especially where soils have been heavily compacted, can sometimes increase dry season streamflows by increasing infiltration rates and may also increase the soil's water holding capacity as well as improving water quality. Consequently, flood mitigation is seen as an important role of forests in some countries.

Whereas once forests were thought to bring rain, it is now well documented that at local scales of tens to tens of thousands of ha, replacement of shallow-rooted vegetation with forest usually reduces streamflow but may improve water quality. Permanent clearing of forest will increase streamflow in some regions, albeit often accompanied by reduced water quality. In the few parts of the world where fog drip is an important hydrologic input, forest clearing reduces water yield. At much larger scales, for example in the Amazon Basin in Brazil and Peru, extensive forests can cycle moisture between the land and the atmosphere so that large-scale clearing of natural forest may have detrimental effects on regional and national water cycles.

In many countries, including Brazil, Chile, China, India, Malaysia, Peru, Romania, and Spain, deforestation and soil degradation have created water quality problems, which are now being addressed, or will need to be addressed through reforestation. In China, for example, extensive areas of highly erodible soils have been reforested. However there may be a trade-off between improved water quality through soil restoration and reduced water yield, unless rainfall occurs only during winter months, as is the Chilean case.

Fire in forests can create concerns over water quality, and less commonly, water yield. In Australia, Spain and the USA, fire seasons are becoming longer and more extreme due in part to combinations of drier and warmer climate. Forest management to reduce fire risk and the associated detrimental effects of wildfire on water quality, is now an important consideration in these countries.

Based on the information provided, the countries with the closest links between forest hydrology research and policy-making are Australia, Brazil, China, South Africa, and United States. However, in most of the reminding eight countries, research and political initiatives are rapidly advancing. Importantly, most countries have invested resources and research into climate change adaptations, including its effects on forests and water interactions. In many countries there is still a clear lack of connection between research results and effective forest management policies, a topic that urgently needs to be addressed.

Generally speaking, conflicts between forests and water are increasing worldwide, and future research should focus on how to solve current and future conflicts, considering local climates. As agriculture, mining, and urbanization continue to grow, it is expected that the demands for water resources will increase, leading to more conflicts. However, demands for forest-related products will also increase. Furthermore, the establishment, conservation, and management of forests are tasks that most countries should focus on, in order to ensure healthy watersheds. In this sense, activities such as reforestation, afforestation, and land restoration represent a key factor for the future, since worldwide millions of hectares are deforested every year, with many of them becoming deserts.

Before concluding, it is worth mentioning gender mainstreaming, even though the topic has not been the focus of this work, when remarking the importance of strengthening forests' as an effort to work towards poverty reduction, biodiversity conservation and sustainable development.

Though gender analysis of forest management for water resources is country specific, generally countries have a clear differentiation between the roles of men to those of women, as typically men are in charge of harvesting and manufacturing wood products, whereas women focus more on fruit collection or similar less intense tasks.

A study released by the International Union for Conservation of Nature (IUCN) in the International Year of Forests, 2011, concludes that men and women have different yet complementary knowledge, use and management of the forests. Therefore, in order to achieve sustainable use of forest and land resources, both women and men's needs, knowledge and experience must be valued and considered. This work suggests that despite there has been progress in women´s access to education employment opportunities in development countries, there is still a marked disparity in forest education, employment and career perspectives in forestry. Results indicate that women have poor access to training programmes, official-decision making process as well as property rights of forests. On the other hand, women play an important role in forest resource management and conservation due to their close dependence on forest resources for subsistence (fuelwood, fodder, herbal medicine among others) and income.

A greater focus by future research on the interaction between forest management, water management and gender issues can help to better understand their interconnection and to identify ways to strengthen the management of both resources while fostering gender equality.

# Chapter 7. Forest Management and Water in India

**Jagdish Krishnaswamy**[21] (jagdish@atree.org)

## 7.1 Introduction

India underwent a major transformation of its landscape and land-cover after approximately 1860, when large parts of the country came under the British Colonial rule (Gadgil and Guha, 1993; Goldewijk and Ramankutty, 2004; Kumar, 2010), spurred by demands for timber destined to shipbuilding, railways, expansion of agriculture, and plantations for tea, further continuing in the post-independence period for dams and reservoirs, agricultural expansion, and refugee resettlement.

It is estimated that in the period 1875-1900, roughly one-third of India was cultivated, an equal expanse was forested, and about twenty percent of the land was grassland and savannah-woodlands (Lynch and Talbott 1995; Sivaramakrishnan, 2009).

Overall estimates of deforestation are between 40%-50% of original cover lost between 1860s and 1990s. However, according to Laurance 2007, India has already lost nearly 80% of its original native forest cover. Using the best available datasets, his analyses suggest that the remaining native forests in India are declining at a rapid pace, from 1.5% to 2.7% per year.

According to data from Global Forest Watch (www.globalforestwatch.org), approximately 100,000 hectares of forest were lost from Arunachal Pradesh, between 2001 and 2013, representing more than one percent of the State's entire area.

A report on the forest cover of Arunachal Pradesh, which is India's last remaining massive forest landscape, noted that 70 percent of the state was forested in 1988. By computing projected population growth and its resultant resource extraction pressures, the study estimated 50 percent of the State's forests would be lost by 2021 (Menon et al. 2001).

### *Regional case: The Western Ghats land-cover change*

The Western Ghats is one of the global biodiversity's hotspots and it is an area where some rigorous estimates of forest loss and conversion are available. Menon and Bawa (1997) estimated that out of 81,870 km$^2$ of the southern Western Ghats in Karnataka, Kerala and Tamil Nadu, there was a loss of 40% of the original forest and scrub between 1920 and 1990.

Jha et al. (2000) estimated changes in forest cover between 1973 and 1995 in the southern part of the Western Ghats using satellite data. The study area of approximately 40,000 km$^2$ showed a loss of 25.6% in forest cover over 22 years. The dense forest was reduced by 19.5% and open forest decreased by 33.2%. As a consequence, degraded forest increased by 26.64%.

By the 1990s, estimated forest cover in India was 20%. According to FAO (2006), the area under forests and other wooded land in India has increased from 63.93 mha in 1990 to 67.70 mha in 2005. Thus, FAO estimates do not significantly differ from the Forest Survey of India *(fsi.nic.in)* estimates.

### *State of India' forests*

Periodically, the Forest Survey of India publishes statewide forest cover estimates based on automated algorithms using remotely sensed data. A study by Puyravaud et al. (2010) suggests that India has some of the globally most imperiled forests. They state that even as the Forest Survey of India recently announced that forest cover in India had expanded by nearly 5% over the past

[21] Suri Sehgal Centre for Biodiversity and Conservation, Ashoka Trust for Research in Ecology and the Environment (ATREE)

decade, this is misleading. They state that methodology fails to distinguish native forests from tree plantations, which are often monocultures of exotic species.

They estimate that, since the early 1990s, tree plantations have expanded in India at an estimated rate of roughly 15,400 km$^2$/year. Subtracting plantations from total forest cover shows **that native forests in India have declined by 1.5%–2.7% per year.**

## 7.2 Literary Review

The large scale transformation of India and loss of forest cover raised concerns about the hydrological consequences of these, and while the early discourse was dominated by the effects of this on rainfall, increasingly the effects of land-cover and land-use change within forests on stream flows and sediment load became an area of policy and management interventions by the colonial Forest department. As loss of forest cover mounted, earlier discussions were dominated by the "dessicationist" discourse, a concern about how loss or degradation of forests could reduce rainfall and was also articulate about the "sponge" functions of intact forests (Saberwal, 1999).

The first empirical enquiry into the role of forest cover on sub-surface flows was a "space for time" type of substitution study by Pearson (1907), who measured depth to groundwater in wells located inside and outside forests, and found that depth was 4.74 deeper under forests than outside (Figure 1), perhaps the first empirical study of evapotranspiration by forests in India, even though its value was not recognized as such at that time, even by the author (Saberwal, 1999). Pearson's study took place in Ghodra Forest Range in Panchmahals, what is now "Gujarat". As previously mentioned, the depths to groundwater was shallower under the non-forest site (100m outside a forest) compared to the well in the forest (1200m inside a mixed teak forest) and was much more responsive to rainfall as well. The measurements were taken early in the morning to avoid any effects of water abstraction by local people.

The difference in depths to groundwater between forest and non-forest Wells from Pearson's data (Pearson, 1907) was used as a crude index of forest evapotranspiration and the results are consistent with what we know about phenology and evapotranspiration of a dry deciduous forest, with least ET during dry months (January through June), when moisture is limiting, leaves are progressively being shed, and ET is highest during the Monsoon and early post-Monsoon period (July-December), when moisture is available (Figure 2).

### *India's first forest hydrology experiment*

The consolidation of British colonial administration over the hill and mountain forests of what is now Himachal Pradesh soon after 1865 empowered the government revenue and forest departments with their separate and often conflicting agendas and interests to manage forest resources. This invariably resulted in control over those dependent on them for their needs. One such group of people is the nomadic pastoral communities that ascended with their flocks of sheep and goats to grazing areas near and above the tree line in summers, descending to lower elevation forests during winters. In 1923, a hydro-electric project was constructed at Barot on Uhl River, in what was then the Punjab Himalayas (Saberwal, 1999; and references therein).

Upstream of this site was the Chota Bangahal catchment in The Western Himalayas, in what is now Himachal Pradesh, covering approximately 283 $km^2$ between 2133 m.o.s.l. to over 4900 m.o.s.l., largely forested with high elevation meadows, and some permanent snow cover was the site of an interesting forest hydrologic experiment between 1934 and 1947. In this period, grazing by over 95,000 sheep and goats was stopped, and river discharge and rainfall gauged (see Figure 4). It was fitted a regression model to this data and annual winter rainfall explained 40% of the variability in winter discharge ($p<0.02$). This study was discontinued in 1947 to the detriment of the field of hydrology in India (Saberwal 1999, and references therein).

### *Hydrologic services*

While explicit reference to the term "hydrologic services" is relatively new in India, the concept has been in practice for a long time. One of the earliest examples of a policy decision in India, specifically recognising and valuing hydrologic services, dates back to 1899. The Periyar River in the princely state of Travancore (now in Kerala) was dammed in 1895 to irrigate drylands in Madras Presidency (now in Tamil Nadu). The catchment area upstream of the dam was gazette as a protected sanctuary. Threats to forest cover from the expansion of tea plantations led to the designation of "wildlife sanctuary" to the catchment area of the reservoir, mainly to regulate the sediment inflow into reservoir.

Another well-known example of managing natural systems for the provision of hydrological services was the conservation of forests to protect water sources of Shimla town from pollution and degradation. This was carried out for many decades in the 19th and 20th century, leading to the establishment of the "Shimla water catchment sanctuary" in 1958, under the Municipality of Shimla.

### *The Plantation era*

In the last 150 years, the need for timber and wood-based raw materials led to the establishment of tree plantations on grasslands, converted natural forests, and degraded natural forests. The species consisted of both native species (such as Teak and Sal, but sometimes planted in sites where they were not originally dominant, especially for former species), as well as exotic species from around the world, especially eucalyptus and acacias from Australia.

According to Ravindranath et al. (2006), the area under forests and other wooded land in India has increased from 63.93 mha in 1990 to 67.70 mha in 2005, and if one considers that some deforestation was still occuring in this period, the increase in area under plantations would be even more significant. The authors found that this is similar to estimates from the Forest Survey of India. The estimated cumulative area afforested in India during the period 1980-2005 is about 34 mha, at an average annual rate of 1.32 mha (Ravindranath et al 2008), suggesting that India is one of the globally significant leaders in afforestation and reforestation. A series of studies that are briefly described here were in response to questions related hydrologic effects of tree plantations at various stages of their growth.

### *India's first paired catchment studies*

A pair of small forested catchments (Sal forest clear-felled in 1955 and allowed to regenerate and described as "brush") near Dehradun were calibrated for 8 years (1961-1968) (Gupta et al. 1980). One forested watershed was then clear-cut and re-afforested with Eucalyptus trees. The flow-recording gauge did not function in the first year after cutting but, subsequently, they estimated that reforestation resulted in 28% reduction of streamflow and 73% reduction in peak flows (see Figure 5).

Curiously, many researchers in this period who reviewed the results from such studies did not seem to be aware or under-played the major role of transpiration in determining hydrologic response as evident in this statement: "Some hydrological responses such as soil and water loss through runoff, interception, infiltration, and soil moisture under different forest influences in experimental basins of India were reviewed. These studies show that the moisture regime of basins can be improved with reforestation and controlled grazing, thus improving the productivity of the land and mitigating the effects of droughts and floods". "Rainfall, being the primary source of all water, is influenced in its disposal by the vegetation through interception by the plant canopy and its infiltration into the soil, parts of which go to deep percolation, to streamflow and to channel flow, thus influencing the moisture regime both within and outside the soil profile" (Gupta et al. 1980). To their credit, the authors don't end the review with some possible questions about transpiration demand of trees and

its effects on hydrology. Overall, the emphasis was on peak-flows reductions, and rarely was there an emphasis on low flows or dry-season flows. Furthermore, the size of the catchments studied were often too small in relation to the prevailing climate to sustain perennial flows and this was a constraint that prevented researchers to understand the effects of afforestation on low flows and to better understand evapotranspiration.

emphasis shifted to see the impacts on low flows and reduction in hydrologic services (i.e. hydro-electric power generation).

In addition to the above, Samraj et al. (1977) and Sharda et al. (1998) reported that conversion of grasslands into bluegum plantations reduced annual water yield by 16% during the first rotation and 25.4% during the second rotation, i.e. first generation coppiced bluegum. Moreover, Sikka et al. (2003) emphasized the domination of sub-surface pathways and their implications on low flows. These studies were the first in India to clearly demonstrate at a catchment scale the effects of varying transpiration demands of trees as a function of size-class and age.

### *The Himalayan experience*

The "Kumaon school" of ecosystem ecologists was pioneer in India, in terms of taking a comprehensive view of hydrologic processes, sediment production, and nutrient cycling, all related to the complex vegetation and litter characteristics in the Himalayas (e.g. Pandey et al. 1983, Pathak et al. 1985). They were the first to report that rainfall represnted an important source of nutrient cations to ecosystems. Average overland flow was often below 1% of the total incident rainfall, indicating that these catchments are "subsurface flow systems", attributing sediments to large landslides rather than overland flow (Singh et al. 1983).

Negi et al. (1998) reviewed some aspects of partitioning rainfall into interception, stem-flow, and throughfall across species in the Central Himalayas, concluding that interception from conifers was as high as 30%, compared to 20% or lower in broad-leaved species. Furthermore, the authors emphasized that sub-surface flows are more relevant in the Himalayan systems. Similarly, Pathak et al. (1985) noted the influence of species on streamflow, throughfall, and interception, concluding that interception was between 8.1 to 25% of rainfall. They also conclude that overland flow was low for all forests and that forest hydrology is dominated by subsurface flow systems and, consequently, they are particularly susceptible to the effects of deforestation on the hydrologic cycle. In ther words, after deforestation the pathways could shift more towards overland flow. However, infiltration rates reported in Himalayan studies are generally high, and overland flow is rare. For example, Rai and Sharma (1998) also report very low overland flow in agro-forestry systems compared to agricultural areas on Eastern Himalayas.

Reportedly, the first hydrological monitoring station in the Himalayas in an undisturbed Pine forest catchment of 1.1 $km^2$, at an elevation of 1,615 m.o.s.l. in Central Himalayas, was established by Kumaon University and Oxford Polytechnic at Almora in 1987 (Haigh et al. 1990). The analyses of hourly data from a Himalayan forested catchment were a pioneer contribution from this study. They reported that discharge response to rainfall was quick, within an hour. They also state that "it is, of course, no coincidence that most flow minima are achieved in the late afternoon, when both evaporation and transpiration rates are the highest". To the author's knowledge, this is the first study to explicitly report diurnal cycle in streamflow in India, attributed to evapotranspiration.

### *Direct measurements and modelling of transpiration and evapotranspiration*

The growing concern over the negative effects of Eucalyptus, which was planted all over India, required rigorous measurements of transpiration at the scale of trees and tree-stands. Pioneering independent work by Kallarackal et al. (1997a, 1997b) and Calder et al. (1986, 1993, 1997, 1998), indicated the plasticity of transpiration rates by eucalyptus in response to moisture availability, with annual rates exceeding the total rainfall in semiarid sites, where tree roots had access to groundwater. Stomatal conductance measurements showed that the increase in atmospheric vapor pressure deficit induced stomatal closure and was possibly regulated by leaf-water potential. Kallarackal's (1997a, 1997b) results from a 4-year-old coppiced plantation showed that water loss from plantations ranged between 2.5 and 6.5 mm $day^{-1}$, depending on the season, estimating annual transpiration to

be over 90% of precipitation. The authors concluded, from photosynthesis measurements, that the dry season did not affect photosynthetic rate on a leaf unit area basis. However, the collaboration between ecophysiolgists working on individual trees and wood stands, and catchment hydrologists, in this period could have been very fruitful but it did not occur.

### *The beginnings of ecohydrology in India*

A series of studies using both rigorous measurements and modeling in the last fifteen years, located in humid Western Ghats and dry forests east of the Western Ghats in Karnataka, have added much to our knowledge of hydrologic processes and hydrology from evergreen and deciduous forests. These include the first observations of the relevance of large macro-pores or soil pipes (Putty and Prasad 2000), a distinct feature of humid forests and converted sites in Western Ghats, in determining runoff responses, which is sub-surface but very quick, and could be confused with overland flow by cursory examination of hydrographs. The avobe brought into question the relevance of assuming “average” infiltration characteristics of any landcover type based on limited measurements. Putty and Prasad (2000) also suggested that afforestation activities could damage soil pipes, resulting in substantial overland flow, a new mechanism for generating surface runoff.

The pioneering work of Sekhar et al. (2004) in a semi-arid region, combining well observations and groundwater modeling, showed that groundwater regimes are quite independent of surface catchment boundaries and that over-exploitation of groundwater in agricultural sites could be resulting in deeper groundwater levels under forests in neighbouring basins; this was further supported by simulations and observations in the forest itself.

Hydrologic measurements in the dry forests east of the Western Ghats was initiated for the first time (~2003) by two projects, which were Indo-UK and Indo-French collaborative projects led by ATREE, National Institute of Hydrology-Belgaum and IISc, respectively. The ATREE team indicated the difficulty of selecting catchments of sufficient size for hydrologic studies as even in protected streams with checkdams (Krishnaswamy et al. 2006a, 2006b), sometimes to create water-holes and ostensibly to trap sediment.

Measurements of soil properties and infiltration in Bandipur revealed that the density of human and cattle trails has a major impact on increasing surface runoff in degraded sites (Mehta et al. 2008). The trails occupied a small part of the landscape but had a major impact on runoff because such hydrologic variable is a very small percentage of the total annual hydrologic budget to begin with. Catchments with a higher length of trails and roads showed distinct responses to rainfall, compared to sites with lower density of trails. They estimated that 7-h rainfall events will cause the trails to generate Hortonian overland flow just about every year, but will rarely result in Hortonian flow from the off-trail areas. They show that trail density is also higher in degraded watersheds, thereby increasing the chances and contribution of Hortonian flow in storm runoff events.

In the humid parts of the Western Ghats, infiltration measurements took place in the late 1990s across diverse forest plantations and soil types upto 1.5m. Subsequently, the determined $K^*$ was then linked to rainfall intensity–duration–frequency (IDF) characteristics, to infer the dominant stormflow pathways (Bonell et al. 2010). This study revealed that plantations still retained the “memory” of multi-decadal use and that Black soils (Vertisols), had low permeabilities irrespective of land cover. Furthermore, only the natural forest surface soils had permeabilities high enough to cope with intense rains (one in 25 or one in fifty year storms).

The Indo-French collaborative work in the 4.1-$km^2$ Moolehole experimental catchment in the sub-humid Bandipur forests (Figure 6), has added much to our knowledge of ecohydrology of semi-arid forests in India. In these forests, which are globally recognized for their large mammal wildlife (especially tigers and elephants), the estimated evapotranspiration is between 80 and 90%, and recharge to groundwater from both direct and indirect flashy streamflow is typically less than 10% of annual rainfall. Furthermore, the deep regolith is a major water reservoir that provides upto 100 mm

of water for transpiration by trees in a region where rainfall is only 800-1000 mm $yr^{-1}$. Their work also suggests that regolith depth variability is an important determinant of groundwater table response to rainfall. One could extend this further and suggest that vegetation access to water itself is a function of regolith depth. Figure 7 shows the trends in Bandipur MODIS, indicating a significant decline in leaf area during recent years, with average and one-standard-deviation intervals (based on spatial variability across the 1 $km^2$ pixels, covering 130 $km^2$).

Previous work had established dependence of trees in this site on stored groundwater in the regolith and also possible movement of groundwater from this area to a neighboring agriculture basin, where groundwater extraction is very high. Observations and simulations suggest that groundwater levels may have dropped by 4.5 m between 2004 and 2008 (Ruiz et al. 2010).

Sekhar et al. (2004) reported that exploitation of groundwater in the agricultural areas outside the forest was potentially affecting groundwater levels in a neighboring basin in the Bandipur forests. Whether the negative trends canopy biomass in the Bandipur area shown in Figure 7 are due to loss of access to groundwater, is something that needs to be investigated. If this was the case, forests in semiarid parts of India, adjacent to over-exploited agricultural areas, could suffer ecohydrological and ecological degradation. Furthermore, groundwater levels in observation wells became deeper after around 2004, suggesting possible stress to deep-rooted trees, which depend on groundwater to survive.

The Indo-UK collaborative project looked at (1) remnant tropical evergreen forest (NF), (2) heavily-used former evergreen forest, which now has been converted to tree savanna known as degraded forest (DF), and (3) exotic Acacia plantations (AC, Acacia auriculiformis) on degraded former forest land.

In the humid Western Ghats, land cover differences translated into distinct hydrological responses at various temporal scales (Krishnaswamy et al. 2012): on an annual scale, Natural Forests (NF) converted 28.4% ± 6.41 (st. dev.) of rainfall into total streamflow, in comparison to 32.7% ± 6.97 in Acacia planations (Ac) and 45.3% ± 9.61 in degraded or multiple use forests (DF). However in terms of quickflow, the degraded site had he highest and the natural forest the lowest. Delayed flow was most evident in the natural forest. Their analyses suggested the existence of alternative stormflow pathways with multiple lags, with peaks occurring between ~12 and 24 h. Their cross-correlations and lag regression approaches indicate a lag of 4 h in NF, compared to respective bimodal peaks at 1 and 16 h in AC, and 1 and 12 h in DF. The long time lags for NF are especially suggestive of deep sub- surface stormflow and groundwater, as the contributing sources to the storm hydrograph. They further speculate that “As potential and actual evapotranspiration is likely to be depressed during the monsoon, differences in streamflow and runoff responses between land cover types is largely attributed to differences in soil infiltration and hydrologic pathways”, although no direct evidence is presented. However their study was a space for time substation type, and attributed differences to land cover effects between sites, with different current land cover/land use to be interpreted with some caution.

In the Western Ghats of India, the Indo-UK team (Krishnaswamy et al., 2013) examined the hydrologic responses and groundwater recharge and hydrologic services linked with the three ecosystems mentioned above (1 Instrumented catchments ranging from 7 to 23 ha), representing the three land covers (3 NF, 4 AC, and 4 DF, in total 11 basins). They were established and maintained between 2003 and 2005 at three sites in two geomorphological zones, Coastal and Up-Ghat (Malnaad). Four larger (1-2 $km^2$) catchments downstream of the headwater catchments in the Malnaad, with varying proportions of different land covers and providing irrigation water for areca-nut and paddy rice were also measured for post-monsoon baseflow. They observed higher frequency and longer duration of low-flows under NF, when compared to the other more disturbed land covers. Groundwater recharge was estimated using water balance during the wet season in the Coastal basins under NF, AC, and DF, with values to be 50%, 46% and 35%, respectively, whereas and in the Malnaad it was 61%, 55%, and 36%, respectively. Soil water potential profiles using zero flux plane methods suggest that during the dry-season, natural forests depend on deep soil moisture and groundwater. In some of the same sites, Venkatesh et al. (2011) reported that significant differences in soil moisture with depth were observed under forested watershed, whereas no such changes with depth were noticed under acacia and degraded land covers, hinting at dependence of deep-rooted natural forests on deeper sources of moisture, compared to shallow rooted systems.

Catchments with higher proportions of forest cover upstream were observed to sustain flow longer into the dry-season. These hydrologic responses provide some support towards the ‘‘infiltration-

evapotranspiration trade-off" hypothesis, in which differences in infiltration between land cover and evapotranspiration determines the differences in groundwater recharge, low-flows, and dry-season flow (Bruinjzeel 2004). Groundwater recharge was most temporally stable under natural forest, although substantial recharge occured under all three ecosystems, which helps to sustain baseflow in rivers of higher order downstream.

## 7.3 Politics

Forests and wildlife are on the concurrent list in India and both federal (centre) and states can make laws and policies based on them. The National Forest Policy (1988) explicitly mentions protection of forests for soil conservation and catchment of rivers and reservoirs. These include the various Forest Acts in the state and the central Forest Conservation Act (1981) that requires central permission for diversion of forest land in development projects. There is also provision for protection to upper catchments in hill areas due to state government legislation, such as the Tamil Nadu Hill Areas (Preservation of Trees) Act.

The Wildlife Protection Act (1972) allows for manipulation of vegetation and water bodies inside protected areas (over 5% of India), authorized by the Chief Wildlife Warden of the state *if it is to the benefit of wildlife*. A 1991 amendment to the Wildlife Protection Act specifies that, in wildlife sanctuaries, the chief wildlife warden must certify that any manipulation does not harm wildlife, and that the manipulation needs to be approved by the state government. Under this legal and management umbrella, streams have been dammed, fire-lines cut, grasslands maintained through management, old tree plantations thinned, and weeds or invasive species cleared: all of these have implications on forest hydrology.

Under the 1972 Act, one could argue that manipulation of water resources or vegetation that directly or indirectly harms any protected species, including aquatic species, is prohibited within protected areas and to some extent outside. **Sec 29** states that "No person shall destroy, exploit, or remove any wildlife, including forest products, from a sanctuary, or destroy, damage, or divert the habitat of any wild animal by any act whatsoever, or divert, **stop, or enhance the flow of water into or outside the sanctuary**, except under and in accordance to a permit granted by the Chief Wildlife Warden, and no such permit shall be granted unless the State Government is satisfied in consultation with the Board that such removal of wildlife from the sanctuary **or the change in the flow of water into or outside the sanctuary** is necessary for the improvement and better management of wildlife therein, authorises the issue of such permit". Thus, manipulation of forest and grassland vegetation that indirectly changes the hydrology to the detriment of riparian vegetation of aquatic or terrestrial wildlife is not allowed. However, so far this legal protection for maintaining ecohydrology for the benefit of endangered species has not been invoked to influence forest management practices, but could be used by civil society to legally challenge habitat manipulation that changes ecohydrology.

In 1996, the Supreme Court of India in a landmark judgement based on a citizen's petition, banned the felling of trees without central permission on public or private land that could be defined as "forest". Although it was motivated by the need to stem deforestation, this had and still has implications for any large-scale removal of trees, including invasive or exotic species, even for desirable changes in forest hydrology.

In the state of Tamil Nadu, the government has acted upon a recent ruling of the Madurai High Court (informed by growing realization of the ecological, and to some extent hydrological, consequences of large scale wattle and eucalyptus plantations in the montane grasslands) is cautiously pursuing a policy of experimental removal of these exotic tree plantations.

Finally, in terms of legal aspects of forest-water issues, the recent setting up of the National Green Tribunals under the **National Green Tribunal Act (2010)**, created under an Act of the Parliament of India, enables the creation of a special tribunal to handle the expeditious disposal of the cases pertaining environmental issues. It draws inspiration from the India's constitutional provision of Article

21, which assures the citizens of India the right to a healthy environment. This is likely to inform many aspects of forest-water linkages, including protection of catchments and ecohydrological functions of forests.

## 7.4 Climate change and the future of forestry & forest research

### *Green India Mission*

The National Mission for Green India (GIM) is one of the eight Missions outlined under the National Action Plan on Climate Change (NAPCC). Currently under this programme, India is planning to reforest and restore 10 million hectares in both existing "degraded" forest and non-forested areas as part of the Green India Mission to sequester carbon and help regulate atmospheric $CO_2$ concentrations. However, we know very little about the synergies and trade-offs between carbon and water cycles, and how this is influenced by phenological responses that are driven by changes in climate, both historical and in the future. Establishing monitoring sites to assess the impact of afforestation, especially in semiarid ecosystems, should be a priority and encouraging restoration of grasslands and savannah-woodlands rather than dense tree-plantations should be considered as part of the experiments that would hopefully lead to changes in policy and management.

### *Invasive species in India's forests: A major threat*

Across India, forests have been transformed by invasive species (Singh 2005, Kohli et al. 2006, Hiremath and Sundaram 2005, Kannan et al. 2013). This is particularly evident in sub-humid forests. Species such as Lantana (Figure 8), which is a significant part of the biomass on a per-unit-area basis, could potentially have changed soil moisture regimes through evapotranspiration. The impact of Lantana on linked plant carbon and water relations, and the effects of it on forest hydrological responses should be investigated urgently.

## *Climate change, climate variability, and Indian forests*

The Indian Monsoon systems are changing with shifts in the role of ocean-atmosphere phenomena such as ENSO and Indian ocean Dipole. Additionally, it has been observed a decrease in the Monsoon since the 1950s, but rainfall events are increasing (Krishnaswamy et al. 2014, Guo et al. 2015). Some of these trends are poorly simulated by climate models thus increasing uncertainty about future trends. However, even though there is uncertainty about precipitation, there are no doubts about warming trends, especially in the Himalayas (Shreshta et al. 2012). Browning has been reported in the Himalayan forests in recent decades in response to warming (Krishnaswamy et al. 2014) and supported by ground-observations of leaf-water potential in dry years (Singh et al. 2006); the implications of these for eco-hydrology in the Himalayas needs investigation. Figure 9 shows the findings of Krishnaswamy et al. (2014) on browning trends in the Himalayas. Andermann et al. (2012) reported a deep ground-water reservoir in the Himalayas that regulates streamflow at larger spatial scales. They infer that water is stored temporarily in a reservoir with a response time of about 45 days, hinting at the role of fractured basement aquifers. How warming and precipitation changes will alter the role of Himalayan forests in hydrology (see Figure 10) at different temporal and spatial scales, and whether this groundwater contribution to streamflow will alter in the future is unknown.

## *The way forward*

India and its scientific institutions have lost excellent opportunities to become world leaders in experimental hydrology and eco-hydrology, especially given the long history of the Indian Forest Service and the Forest Research Institute, besides other institutions. Even when some sites were setup by dedicated researchers, they were not maintained beyond 5-10 years. We need to foster a culture of collaboration and shared sites to restore forest hydrologic research to international standards in India.

The failure to maintain long-term monitoring sites in different eco-climatic zones of the country is one of the reasons for our inability to predict future hydrologic responses to land-use and land-cover changes, as well as climate change and other aspects of global change such as nitrogen deposition and aerosols and pollutants. It is obvious that we must quickly establish hydrologic observatories in diverse natural and managed ecosystems at various spatial scales. The entire network of gauging stations maintained by the Central Water Commision (CWC) and state agencies must be open to scrutiny for quality control, especially their rating curves, and calibrations. If we do not improve the quality of data collection at state managed gauging stations, Indian hydrology will be the loser, as no amount of sophisticated modeling can make up for poor quality data. Monitoring of both ground and surface water and soil moisture linked to hydrologic response from transpiration in trees to catchment response at larger scales linked to high-resolution, remotely sensed time-series, should be initiated in different eco-climatic zones immediately. New techniques such as salt-dilution and continuous monitoring of electrical conductivity offer good alternatives to stream gauging in remote sites in the Himalayas (Figure 11).

**Figure 11.** Linking tree water functions with catchment hydrology is an important way forward for ecohydrologists in the Himalayas and the Western Ghats in India (e.g from author's and his student Manish Kumar's instrumented sites in Sikkim, Eastern Himalayas). Photos by: Manish Kumar.

Institutions such as the Ministry of Earth Sciences and state agencies should set aside resources for long-term maintainance of well-instrumented catchments by research institutions and NGOs, which are already in existence. There is an urgent need to train and empower NGOs and local communities to monitor streams and wells with simple but rigorous techniques, as India is very diverse and we need to generate base-line information quickly. Citizen science can play a big role in complementing what detailed hydrologic studies can accomplish.

Finally, India needs a culture of collaboration among hydrologists, with links to experienced hydrologists abroad and establish hydrologic observatories that cater to a range of disciplines and techniques and reach out to communities whose water resources are under threat.

## 7.5 Acknowledgments

The author would like to thank the jointly administered Changing Water Cycle programme of the Ministry of Earth Sciences (Grant Ref: MoES/NERC/16/02/10 PC-11), the Government of India, and the Natural Environment Research Council, United Kingdom (Grant Ref: NE/I022450/1), for their financial support during the course of the preparation of this chapter. The Department of Biotechnology, Government of India, supported our work in Sikkim, which is described in this chapter. The author dedicates this chapter to our colleague and mentor, Professor Mike Bonell, who passed away on July 11th, 2014. The author also thanks Susan Varughese, Manish Kumar, Nachiket Kelkar, and Mayukh Dey for their help editing, adding references, data entry, and finding citations. Finally, many thanks to Joaquin Jafif of UNESCO for his kind help with editing and correcting this chapter.

## 7.6 References

Andermann, C., Longuevergne, L., Bonnet, S., Crave, A., Davy, P., & Gloaguen, R. (2012). Impact of transient groundwater storage on the discharge of Himalayan rivers. *Nature geoscience*, *5*(2), 127-132.

Benskin, E. (1930) Forest and Stream Flow. Indian Forester, 56, p. 440-442 & 521-523.

Bonell M., Purandara B.K., Venkatesh B., Krishnaswamy, J., Acharya H.A.K., Singh U.V., Jayakumar R. & Chappell N. (2010), “The impact of forest use and reforestation on soil hydraulic conductivity in the Western Ghats of India: Implications for surface and sub-surface hydrology”, Journal of Hydrology, Vol. 391, pp: 47–62.

Bruijnzeel, L.A., 2004. Hydrological functions of tropical forest: not seeing the soil for the trees? Agriculture, Ecosystems and Environment 104, 185–228. doi:10.1016/j.agee.2004.01.015.

Calder, I. R. (1986). Water use of eucalypts—A review with special reference to south India. *Agricultural Water Management*, *11*(3), 333-342.

Calder, I. R. (1998). Water use by forests, limits and controls. *Tree physiology*, *18* (8-9), 625-631.

Calder, I. R., Hall, R. L., & Prasanna, K. T. (1993). Hydrological impact of Eucalyptus plantation in India. *Journal of Hydrology*, *150*(2), 635-648.

Calder, I. R., Rosier, P. T., Prasanna, K. T., & Parameswarappa, S. (1997). Eucalyptus water use greater than rainfall input-a possible explanation from southern India. *Hydrology and Earth System Sciences*, *1*(2), 249-256.

Food & Agriculture Organization, (FAO, UN). 2006. Global Forest Resources Assessment 2005, Rome. URL: www.fao.org/docrep/009/a0773e/a0773e00.htm.

Gadgil, M., & Guha, R. (1993). *This fissured land: an ecological history of India*. Univ of California Press.

Goldewijk, K. and N. Ramankutty (2004). Land use changes during the past 300 years, in Natural Resources Policy and Management, ed. by W. Verheye, Encyclopedia of Life Support Systems (EOLSS), Eolss Publishers, Oxford, UK, [http://www.eolss.net]

Guo, L., Turner, A. G., and Highwood, E. J.:2015. Impacts of 20th century aerosol emissions on the South Asian monsoon in the CMIP5 models, Atmos. Chem. Phys., 15, 6367-6378, doi:10.5194/acp-15-6367-2015, 2015.

Gupta VK, Waymire E, Wang CT. 1980. A representation of an instantaneous unit hydrograph from geomorphology. Water Resources Research, 16, 855–862.

Gupta, J.P., Wasi Ullah and V.C. Issac. (1975) A note on some soil moisture changes under permanent vegetative cover. Indian Forester, Sept., 523-526.

Haigh, M., Rawat, J., Bisht H. (1990) Hydrological impact of deforestation in the central Himalaya. Hydrology of Mountainous Areas (Proceedings of the Strbské Pleso Workshop, Czechoslovakia, June 1988). IAHS Publ. No. 190.

Hiremath, A. J., & Sundaram, B. (2005). The fire-lantana cycle hypothesis in Indian forests. *Conservation & Society,* 3, 26-42.

Jha, C. S., Dutt, C. B. S., & Bawa, K. S. (2000). Deforestation and land use changes in Western Ghats, India. *Current Science, 79*(2), 231-237.

Kallarackal, J., & Somen, C. K. (1997a). An ecophysiological evaluation of the suitability of Eucalyptus grandis for planting in the tropics. *Forest Ecology and Management*, *95*(1), 53-61.

Kallarackal, J., & Somen, C. K. (1997b). Water use by *Eucalyptus tereticornis* stands of differing density in southern India. *Tree Physiology*, *17*(3), 195-203.

Kannan, R., Shackleton, C. M., & Shaanker, R. U. (2013). Reconstructing the history of introduction and spread of the invasive species, Lantana, at three spatial scales in India. *Biological invasions*, *15*(6), 1287-1302.

Kohli, R. K., Batish, D. R., Singh, H. P., & Dogra, K. S. (2006). Status, invasiveness and environmental threats of three tropical American invasive weeds (*Parthenium hysterophorus* L., *Ageratum conyzoides* L., *Lantana camara* L.) in India. *Biological Invasions*, *8*(7), 1501-1510.

Krishnaswamy J, Mehta VK, Joshi P, Rakesh KN, Suparsh PN. 2006a. Comparative hydrology in forested South India: methodological approaches to unique challenges. In Hydrology and Watershed Services in the Western Ghats of India. Effects of Land Use and Land Cover Change, Krishnaswamy J, Lele S, Jayakumar R (eds). Tata McGrawHill: New Delhi; 265–295.

Krishnaswamy J., Bonell M., Venkatesh B., Purandara B. K., Lele S., Kiran M.C., Reddy V., Badiger S. & Rakesh K. N. (2012), "The rain–runoff response of tropical humid forest ecosystems to use and reforestation in the Western Ghats of India", Journal of Hydrology, Vol. 472–473, pp: 216–237

Krishnaswamy J., Bonell M., Venkatesh B., Purandara B. K., Rakesh K. N., Lele S., Kiran M.C., Reddy V. & Badiger S. (2013), "The groundwater recharge response and hydrologic services of tropical humid forest ecosystems to use and reforestation: Support for the ''infiltration-evapotranspiration trade-off hypothesis''", Journal of Hydrology, Vol. 498, pp: 191–209

Krishnaswamy J., Milind Bunyan, Vishal K. Mehta, Niren Jain & K. Ullas Karanth (2006b), "Impact of iron ore mining on suspended sediment response in a tropical catchment in Kudremukh, Western Ghats, India", Forest Ecology and Management, Vol. 224, pp: 187–198

**Krishnaswamy, J.,** R. John and S. Joseph. (2014) Consistent response of vegetation dynamics to recent climate change in tropical mountain regions. Global Change Biology, 20, 203-215.

Kumar, V. R. 2010. Colonizing Greens: Political Economy of Deforestation in Colonial South India 1800-1900. *A Biannual Journal of South Asian Studies*, 226.

Laurance, W.F. (2007) Forest destruction in tropical Asia. Curr Sci 93, 1544–1550.

Lynch, O. J., & Talbott, K. (1995). *Balancing acts: community-based forest management and national law in Asia and the Pacific*. World Resources Institute.

Mehta, V. K., Sullivan, P. J., Walter, M. T., Krishnaswamy, J., & DeGloria, S. D. (2008). Impacts of disturbance on soil properties in a dry tropical forest in Southern India. *Ecohydrology*, *1*(2), 161-175.

Menon S and Bawa, K.S. 1997. Applications of geographic information systems, remote sensing and a landscape ecology approach to biodiversity conservation in the Western Ghats.Current Science. 73: 134 – 136.

Menon, S., Pontius, R. G., Rose, J., Khan, M. L. and Bawa, K. S. (2001), Identifying Conservation-Priority Areas in the Tropics: a Land-Use Change Modeling Approach. Conservation Biology, 15: 501–512. doi: 10.1046/j.1523-1739.2001.015002501.x

Negi G. C. S., Rikhari H. C. & Garkoti S. C. (1998), "The hydrology of three high-altitude forests in Central Himalaya, India: A reconnaissance study", Hydrological Processes, Vol. 12, pp: 343-350.

Pandey, A. N., Pathak, P. C., & Singh, J. S. (1983). Water, sediment and nutrient movement in forested and non-forested catchments in Kumaun Himalaya. *Forest ecology and management*, *7*(1), 19-29.

Pathak, P. C., Pandey, A. N., & Singh, J. S. (1985). Apportionment of rainfall in central Himalayan forests (India). *Journal of hydrology*, *76*(3), 319-332.

Pearson, R.S. (1907) The level of subsoil waters with regard to forest. Indian Forester, 33, 57-69.

Putty M.R.Y. & Prasad R. (2000), "Understanding runoff processes using a watershed model—a case study in the Western Ghats in South India", Journal of Hydrology, Vol. 228, pp: 215–227

Putty M.R.Y. & Prasad R. (2000), "Runoff processes in headwater catchments—an experimental study in Western Ghats, South India", Journal of Hydrology, Vol. 235, pp: 63–71

Puyravaud, J. P., Davidar, P., & Laurance, W. F. (2010). Cryptic destruction of India's native forests. *Conservation Letters*, *3*(6), 390-394.

Rai, S. C., & Sharma, E. (1998). Hydrology and nutrient flux in an agrarian watershed of the Sikkim Himalaya. *Journal of Soil and Water Conservation*,*53*(2), 125-132.

Ravindranath, N.H., N.V. Joshi, R. Sukumar and A. Saxena. (2006) Impact of climate change on forest in India Current Science, Vol. 90 No. 3, pp 354-361.

Ravindranath, N H., R K Chaturvedi and I.K. Murthy. (2008) Forest conservation, afforestation and reforestation in India: Implications for forest carbon stocks. Current Science, Vol. 95, No. 2 / 25.

Ruiz, L., Varma, M. R., Kumar, M. M., Sekhar, M., Maréchal, J. C., Descloitres, M., ... & Braun, J. J. (2010). Water balance modelling in a tropical watershed under deciduous forest (Mule Hole, India): Regolith matric storage buffers the groundwater recharge process. *Journal of Hydrology*, *380*(3), 460-472.

Saberwal, V.K. (1999) Pastoral politics. Oxford Univ. Press.

Samra, J. S., Sikka, A. K., & Sharda, V. N. (2001). Hydrological implications of planting bluegum in natural shola and grassland watersheds of southern India. In *Sustaining the Global Farm. Selected papers from 10th International Soil Conservation Organization meeting held at Purdue University* (pp. 338-343).

Samraj, P., S. Chinnamani, and B. Haldorai. (1977) Natural versus man-made forest in Nilgiris with special reference to run-off, soil loss and productivity. Indian Forester, July, 460-465.

Sekhar, M., Rasmi, S. N., Sivapullaiah, P. V., & Ruiz, L. (2004). Groundwater flow modeling of Gundal sub-basin in Kabini river basin, India. *Asian Journal of Water, Environment and Pollution*, *1*(1), 65-77.

Sharda V.N., Samraj P., Samra J.S. & Lakshmanan V. (1998), "Hydrological behaviour of first generation coppiced bluegum plantations in the Nilgiri sub-watersheds", Journal of Hydrology, Vol. 211, pp: 50–60

Shrestha UB, Gautam S, Bawa KS (2012) Widespread Climate Change in the Himalayas and Associated Changes in Local Ecosystems. PLoS ONE 7(5): e36741. doi: 10.1371/journal.pone.0036741

Sikka A.K., Samra J.S., Sharda V.N., Samraj P. & Lakshmanan V. (2003), "Low flow and high flow responses to converting natural grassland into bluegum (*Eucalyptus globulus*) in Nilgiris watersheds of South India", Journal of Hydrology, Vol. 270, pp:12–26

Singh, J. S., Pandey, A. N., & Pathak, P. C. (1983). A hypothesis to account for the major pathway of soil loss from Himalaya. *Environmental Conservation*,*10*(04), 343-345.

Singh, K. P. (2005). Invasive alien species and biodiversity in India. *Current Science*, *88*(4), 539.

*Singh*, *S.P.*, *D.B. Zobel*, S.C. *Garkoti*, A. *Tewari* & *C.M.S. Negi* (*2006*). *Patterns* in *water relations* of *central* Himalayan trees. Tropical Ecology 47, 159-*182*.

Sivaramakrishnan, K. (2009). Forests and the environmental history of modern India. *The Journal of Peasant Studies* **36.2: 299-324.**

Venkatesh B., Lakshman N., Purandara B.K. & Reddy V.B. (2011), "Analysis of observed soil moisture patterns under different land covers in Western Ghats, India", Journal of Hydrology, Vol. 397, pp: 281–294

# IMPACT OF EXTREME RAINFALL EVENTS ON LAND USE/COVER IN THE AGHNASHINI BASIN, WESTERN GHATS

THESIS SUBMITTED TO

Symbiosis Institute of Geoinformatics

FOR PARTIAL FULFILLMENT OF THE M. Sc. DEGREE

By

**VAIJAYANTI VIJAYARAGHAVAN**

**(Batch 2011-2013)**

Symbiosis Institute of Geoinformatics

Symbiosis International University

5th Floor, Atur Centre, Gokhle Cross Road

Model Colony Pune - 411016

# Table of Contents

Acknowledgments ..... 6
List of Figures ..... 7
List of Tables ..... 9
Abbreviation List ..... 10
Preface ..... 11
Chapter 1: Introduction ..... 12
**1.1 Tropical Rain Forests** ..... 12
**1.2 Western Ghats** ..... 12
**1.3 Climate Change** ..... 13
1.3.1.1.1 The increasing concentrations of carbon dioxide in the atmosphere ..... 14
1.3.1.1.2 Alteration in the nitrogen cycle ..... 15
1.3.1.1.3 Land Use/Cover Change ..... 16
**1.4 Extreme Rainfall Events** ..... 17
**1.4.1 Causes of Extreme Rainfall Events** ..... 17
**1.5 Objectives** ..... 18
**1.6 Need for this Study** ..... 19
Chapter 2: Literature Review ..... 21
**2.1 Datasets Used** ..... 21
**2.1.1 Landsat** ..... 21
**2.1.1.1 Landsat 5** ..... 21
**2.1.2 MODIS** ..... 21
**2.2 Image Pre-Processing and Analysis Techniques** ..... 22
**2.2.1 Image Pre-Processing** ..... 22
**2.2.2 Image Analysis** ..... 22
**2.2.2.1 Spectral Reflectance Curve** ..... 22
2.2.2.1.1 Vegetation ..... 23
2.2.2.1.2 Water ..... 24
2.2.2.1.3 Soil ..... 25
**2.2.2.2 Vegetation Indices** ..... 26
2.2.2.2.1 NDVI ..... 26
**2.2.3 Image Classification Techniques** ..... 27
**2.2.3.1 Traditional Pixel-Based Classification** ..... 28
2.2.3.1.1 Classification Techniques ..... 29

**2.2.3.2 Object-Oriented Classification** ..... 31
2.2.3.2.1 Multi-Resolution Segmentation ..... 32
2.2.3.2.2 Classification Process ..... 33
2.2.3.2.3 Classification Criteria ..... 34
**2.2.4 Change Detection** ..... 35
**2.3 Structural Time-Series Model (STM)** ..... 35
Chapter 3: Study Area ..... 36
**3.1 Geography** ..... 36
**3.2 Climate** ..... 37
**3.3 Study Area: Aghnashini Basin** ..... 37
**3.4 Major Land Uses** ..... 38
**3.4.1 Paddy Fields** ..... 38
**3.4.2 Arecanut Plantations** ..... 38
**3.4.3 Soppinabetta Lands** ..... 39
**3.4.3Evergreen Forests** ..... 39
**3.4.4 Semi-Evergreen Forests** ..... 39
**3.4.5 Moist Deciduous Forests** ..... 39
**3.4.6 Grasslands and Tree Savannahs** ..... 39
**3.4.7 Disturbed Forests** ..... 40
**3.4.8 Acacia Plantations** ..... 40
Chapter 3: Methodology ..... 41
**1. Data Collection** ..... 41
**2. Data Processing** ..... 41
**2.1 Landsat Data** ..... 41
**3. Image Classification** ..... 41
**3.1 Field Component** ..... 41
**3.2 Lab Component** ..... 44
**3.2.1 Pixel-Based Supervised Classification** ..... 44
3.2.1.1 Training sets ..... 44
3.2.1.2 Classification Stage ..... 45
**3.2.2 Accuracy Assessment** ..... 45
**3.2.2 Object-Oriented Classification** ..... 45
3.2.2.1 Training Sets ..... 45
3.2.2.2 Segmentation Stage ..... 45
3.2.2.3 Classification Stage ..... 46
3.2.2.3.1 Thresholds ..... 47

3.2.2.4 Accuracy Assessment ..... 48
**3.2.3Change Detection** ..... 48
**4. Time-Series Data Modelling** ..... 48
**4.1 MODIS Data** ..... 48
**4.2. Climate Data** ..... 49
**4.2.1 Model for Batch Conversion of netCDF Files to Shapefiles** ..... 49
**4.2.2 Weighted Average** ..... 50
**4.3 Time-Series Data Analysis Using R** ..... 51
Chapter 5 Results and Discussion ..... 53
**2. Data Collection** ..... 53
**3. Data Processing** ..... 53
**2.1 Landsat Data** ..... 53
**Image Classification** ..... 54
**3.1 Field Component** ..... 54
**3.2 Lab Component** ..... 55
3.2.1 **Pixel-Based Supervised Classification** ..... 55
3.2.1.1 Training Sets ..... 55
3.2.1.2 Classification Stage ..... 56
3.2.1.3 Accuracy Assessment ..... 56
**3.2.2 Object-Oriented Classification** ..... 57
3.2.2.1 Segmentation Stage ..... 57
3.2.2.2 Training Sets ..... 57
3.2.2.3 Classification Stage ..... 59
3.2.2.4 Accuracy Assessment ..... 61
**3.2.3 Change Detection** ..... 61
**4.Time-Series Data Modelling** ..... 65
**4.1 MODIS Data** ..... 65
**4.2 Climate Data** ..... 65
**4.2.1 Model for Batch Conversion of netCDF Files to Shapefiles** ..... 65
**4.2.2 Weighted Average** ..... 65
**4.3 Time-Series Data Analysis Using R** ..... 66
Chapter 6: Conclusion ..... 78
References ..... 81
Appendix 1 ..... 86

# Acknowledgments

I wish to acknowledge the contribution, support and guidance of all the following without which this body of work would not have been possible.

- Symbiosis Institute of Geoinformatics, Pune for providing me this learning platform.
- Dr. Navendu Chaudhary, my guide for M. Sc. Geoinformatics of SIG for leading me to this opportunity.
- Dr. T. P. Singh of SIG for being a steady friend, philosopher and guide.
- ATREE, Bengaluru for enabling this whole exercise.
- Dr. Jagdish Krishnaswamy, my guide at ATREE for this project.
- Dr. Shrinivas Badiger, my co-guide at ATREE for this project.
- Other members of the project: Dr. Michael Bonell, Dr. Mahesh Sankaran, R. S. Bhalla, Dr. Srinivas Vaidyanathan, Naresh Vissa, Rakesh and Susan Varghese.
- Balachandran Hegde, Dr. Sharachchandra Lele and Mr. Kiran for providing me help and guidance in the project.
- Other members of ATREE who helped me in so many ways: Shiju Chako, Ameya Gode, Pranita Sambhus, Samantha Ryder, Pennan Chinnaswamy and Jayalakshmi.
- Mr. Obaiah B, the ever helpful librarian at ATREE
- Manjunath Hebbar, student, Sirsi Forest College, who accompanied me to field and helped me in identifying various forest types.
- K. Narasimhan, for helping me with data compilation.
- My family at Bangalore for putting up with me for six months.
- My parents and brother.

# List of Figures


Figure 1.1 Factors Impacting Global Climate Change
Figure 2.1 Water Reflectance Curve
Figure 2.2 Soil Reflectance Curve
Figure 2.3 Maximum Likelihood Classifier
Figure 3.1 Administrative Boundaries of Karnataka District
Figure 4.1 Acacia Plantations
Figure 4.2 Evergreen Forests
Figure 4.3 Deciduous Forests
Figure 4.4 Paddy Field with Areca Plantation in the Background
Figure 4.5 Semi-Evergreen Forests
Figure 4.6 GCP Collection in Areca Plantation
Figure 4.7 Total Number of Samples Used
Figure 4.8 Multiresolution Segmentation Process Showing the Parameters Used
Figure 4.9 Model for Batch Conversion of netCDF files to Shapefiles
Figure 4.10 MODIS Pixel and 5 Temperature Pixel Near Table Centroids
Figure 4.11 Weighted Average in Excel
Figure 4.12 Weighted Average in Excel
Figure 5.1 RMS Error in Georeferencing the Landsat 1990 image
Figure 5.2 Shift in the Position of Pixel (the darker image is Landsat 1990 and lighter image is the properly georeferenced Landsat 2000)
Figure 5.3 GCP Locations collected for Training the Classifier
Figure 5.4 Samples Selected in ERDAS
Figure 5.5 Transformed Divergence (TD) Separability Statistic
Figure 5.6 Land Use Map 2000
Figure 5.7
Figure 5.8 Segmented 2013 Image
Figure 5.9 Sample Selection Information Tool
Figure 5.10 Samples for the Year 2013
Figure 5.11 Rule Set for Image of Year 2000
Figure 5.12 Extracted Shadow and Water Regions
Figure 5.13 Ruleset for Year 2000
Figure 5.14 Land Use Map 2000 and Land Use Map 2013
Figure 5.15 Accuracy Assessment for Year 2000
Figure 5.16 Accuracy Assessment for Year 2013
Figure 5.17 Change Map
Figure 5.18 Driver for Vegetation Change
Figure 5.19 The left image shows the samples of Areca on MODIS data and the right image shows the extracted and organized values in an Excel sheet

Figure 5.20 Near Table Showing the Distance Weightage(Labelled as NEAR_DIST) Between the 5 Temperature Pixels and Multitude of MODIS pixels
Figure 5.21 Table Showing NDVI, RR and Temperature for Acacia
Figure 5.22 St_Rf1
Figure 5.23 St_T1
Figure 5.24 St_Pa_R1
Figure 5.25 St_Aca_N1 and St_Pa_R1
Figure 5.26 St_Aca_N2 and St_Pa_R1
Figure 5.27 St_Aca_N3 and St_Pa_R1
Figure 5.28 St_Aca_N4 and St_Pa_R1
Figure 5.29 St_Aca_N5 and St_Pa_R1
Figure 5.30 St_Ar_N1 and St_Ar_N2
Figure 5.31 St_De_N2 and St_Pa_R1
Figure 5.32 St_De_N3 and St_Pa_R1
Figure 5.33 St_Ev_N1 and St_Ev_R1
Figure 5.34 St_Se_N1 and St_Se_R1
Figure 5.35 St_Pa_N4 and St_Pa_N1
Figure 7.1 St_De_N1 and St_De_N5
Figure 7.2 St_De_N3 and St_De_N4
Figure 7.3 St_Pa_N1 and St_Pa_N2
Figure 7.4 St_Pa_N3 and St_Pa_N5
Figure 7.5 St_Ev_N1 and St_Ev_N2
Figure 7.6 St_Ev_N5 and St_Ev_N4
Figure 7.7 St_De_N4

# List of Tables

Table 2.1 Classification Criteria

Table 4.1 Region Grow Tool Parameters

Table 4.2 Classification Criteria

Table 5.1 Percentage Increase/Decrease per Class

# Abbreviation List

RR-Rainfall Rate

NDVI-normalized Difference vegetation index

Structural Time-series Model: StructTS Model

# Preface

Extreme rainfall events as defined by the Indian Meteorological Department is rainfall on a said day exceeding 244.5mm. Extremes of weather and climate can have devastating effects on human society and the environment (Goswami et al., 2006). In India, the timely availability of adequate amount of water is essential to meet the various needs of reliant sectors such as agriculture, industrial sector, providing domestic water supply and for hydroelectric power generation and others (Schiermeier, 2007). Global climate changes may influence long-term rainfall patterns impacting the availability of water, along with the danger of increasing occurrences of droughts and floods (Fosse & Changnon, 1993). Thus, understanding past changes in the characteristics of such events, including recent increases in the intensity of heavy precipitation events all over the world, is critical for reliable projections of future changes (Schiermeier, 2007).

Since this is a pioneer project in this region, I looked for the presence of such events by examining 12 year monthly rainfall rate and temperature data. The impact of such events was explored by first classifying Landsat images of years 2000 and 2013 and subsequently carrying out change detection. Areas that have maintained their land use/cover over the years were selected to extract MODIS time-series NDVI data. MODIS NDVI data was available only from November to March and those were used. This thesis tries to understand if the increased rainfall has an impact on forest and agro-ecosystems of this region.
Chapter 1 introduces the project by exploring climate change, its relationship to extreme rainfall events, the objectives and the need for this study. Chapter 2 focuses on literature review. It describes the data used, image pre-processing and analysis techniques, image classification and techniques and time-series data analysis using the Structural Time-Series Model. The remaining chapters deal with methodology, results and conclusion.

# Chapter 1: Introduction

## 1.1 Tropical Rain Forests

As a natural resource, tropical forests are of enormous economic, social, cultural, and scientific value (Wulder & Franklin, 2003). These forests are a source of food, timber and timber products, pharmaceuticals, and land, and represent the major sources of income for the increasing populations of many tropical regions (Ustin, 2004). Over 500 million people live within or in proximity to tropical forests, many of which are among the poorest in the world, and their livelihoods are often linked inextricably to these forests (Wulder & Franklin, 2003). These forests also play a key role in the exchange of atmospheric gases (e.g., carbon dioxide, oxygen), water, and energy, and furthermore strongly influence local, regional and global climates and hydrology (Houghton et al., 1991). They are thus an integral part of the ecosystem.

Over the past few decades, the tropical forests have depleted with a number of factors contributing to it (Wulder & Franklin, 2003). These include large population growth, poverty and poor education, inappropriate government policies (Hecht & Cockburn, 1989), economic crises, weak government institutions, "the quest of individuals or organizations for personal wealth or economic and political power" (Ulsin, 2004), undervaluation of natural forests as a resource, and social factors (Sponsel et al., 1996). Recent increase in fire activity, caused largely by previous degradation along with climate change, have increasingly promoted the loss and degradation of tropical forests in all regions (Laporte et al., 1998; Mayaux et al., 1999).

## 1.2 Western Ghats

The tropical forests of interest in this thesis are those of the Western Ghats, India. The Western Ghats, mountains along the west coast of peninsular India, extend from the southern tip of the peninsula (8°N) northwards about 1600 km to the mouth of the river Tapti (21°N) (Molur et al, 2001). The mountains rise to average altitudes between 900 and 1500 m above sea level, intercepting monsoon winds from the south-west and creating a rain shadow in the region to their east (Menon & Bawa, 1997). The varied climate and diverse topography

provides the elements to make it one of the world's biodiversity hot spots (Menon & Bawa, 1997).

The Western Ghats region, like other parts of the tropics, is undergoing rapid transformation. Compared to the other hotspots, it has the highest human population per unit area (more than 300 humans/km2), making it that much more challenging to conserve (Molur 2009). The deforestation rate is high and forests are being transformed into agriculture and monoculture plantations (Menon & Bawa, 1997). Moreover, there is an increase in the extreme rainfall events over the years.

## 1.3 Climate Change

Climate Change, according to the IPCC report 2007, refers to the "change in the state of the climate that can be identified by changes in the mean and/or the variability of its properties, and that persists for an extended period, typically decades or longer" (Baker, 2007). The reason for this phenomenon garnering so much attention in recent years due to the suddenness of the change and its consequences. It is a global phenomenon that can have devastating impacts.

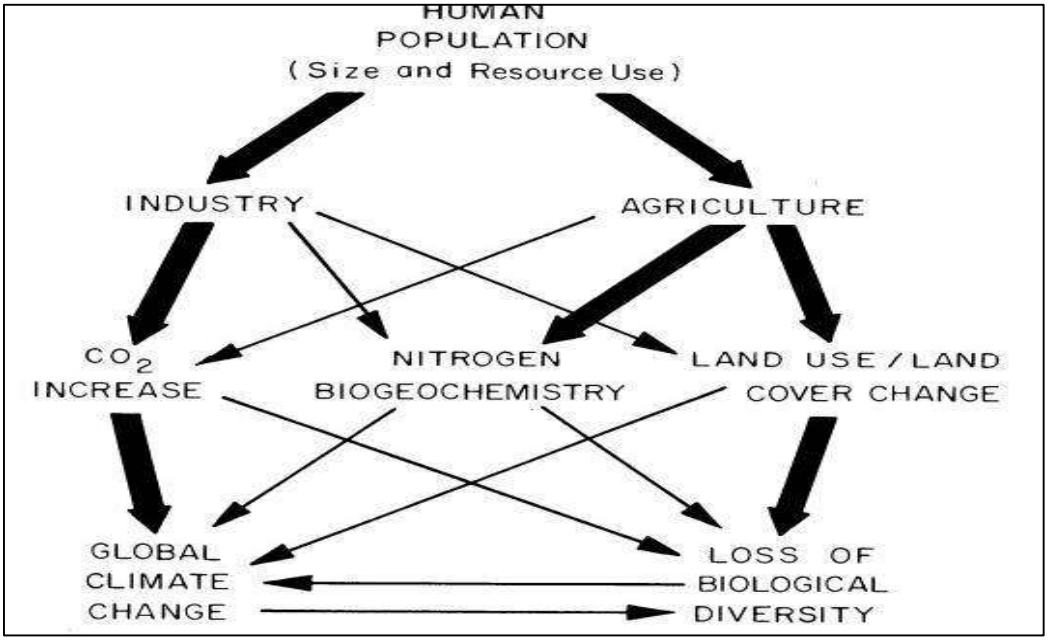


**Figure 1.1 Factors Impacting Global Climate Change**

Several bodies working on this phenomenon share the same understanding of climate change but they disagree as to the causes of climate change (Baker, 2007). For e.g. while IPCC believes that natural and anthropogenic activities may cause global climate change, the UNFCCC defines climate change to be an anthropogenically derived phenomenon. The human causes that have increased the rate at which the climate is changing have been identified. According to Vitousek, increased human population has led to an increase in the amount of resources that have been consumed. This in turn has led to a boom in the number of industries and agricultural plots of land to sustain the growing need of the humungous population. Wide spread deforestation was and is continued to being carried out to make way for these new land uses. The industries and agricultural lands have not only caused wide spread biodiversity loss but also polluted the atmosphere with excessive amounts of reactive nitrogen and $CO_2$. The impact of the change in land use, elevated levels of $CO_2$ and reactive nitrogen is observed as global climate change and has been explained below.

*1.3.1.1.1 The increasing concentrations of carbon dioxide in the atmosphere*

Carbon dioxide is the most important anthropogenic greenhouse gas. The global atmospheric concentration of carbon dioxide has increased from a pre-industrial value of about 280 ppm to 379 ppm[3] in 2005 (Barker, 2007). The atmospheric concentration of carbon dioxide in 2005 exceeds by far the natural range over the last 650,000 years (180 to 300 ppm) as determined from ice cores (Barker, 2007). The primary source of the increased atmospheric concentration of carbon dioxide since the pre-industrial period results from fossil fuel use, with land use change providing another significant but smaller contribution (Bazzaz et al, 1990).

**Effects of elevated carbon dioxide levels**

It was noted by Bazzaz et al (1990) that the rapid increase in carbon dioxide levels has adverse effects on plants. The elevated carbon dioxide levels lead to an increase in the concentration of carbon storage in terrestrial ecosystems (Bazzaz et al, 1990). Carbon dioxide concentrations are important in regulating the openness of stomata, for exchange of gases with the external environment. Open stomata allow $CO_2$ to diffuse into leaves for photosynthesis, but also allow for water to diffuse out of leaves (Taub, 2010). Plants therefore regulate the degree of stomatal opening (also known as stomatal conductance) as a compromise between the goals of maintaining high rates of photosynthesis and low rates of

water loss (Taub, 2010). As $CO_2$ concentrations increase, plants can maintain high photosynthetic rates which allows for faster growth of the plant but with relatively low stomatal conductance. Growth under elevated $CO_2$ decreases stomatal conductance of water by an average of 22% (Ainsworth & Rogers 2007). This would be expected to decrease overall plant water use, which further has a negative impact on plant size, morphology, and leaf temperature (Ainsworth & Rogers 2007). This in turn can have consequences for the hydrological cycle of entire ecosystems, with soil moisture levels and runoff both increasing under elevated $CO_2$ levels (Leakey *et al.* 2009). This increases the likelihood of floods.

*1.3.1.1.2 Alteration in the nitrogen cycle*

The global nitrogen cycle consists of a reservoir of 78% nitrogen in the atmosphere; a smaller quantity of Nitrogen is bonded with C-, H- or O- that cycle among plants, animals, soils and sediments (Vitousek, 1994). An even smaller quantity of Nitrogen is present in the "biologically meditated transfers" (Schlesinger, 1991) between these two pools (Schlesinger, 1991). Moreover, the quantity of Nitrogen available to organisms has an impact on species composition, productivity and the responsiveness of ecosystems to elevated $CO_2$ levels (Vitousek & Howarth, 1991).

Nitrogen is an essential element for organisms to survive. The large reservoir in the atmosphere contains Nitrogen in an unusable form which is fixed into a reactive usable form naturally or through anthropogenic activities. Naturally, nitrogen fixation is carried out by organisms like cyanobacteria in the soil and by lightening (Vitousek, 1994). The Nitrogen is converted to a reactive fixed form that is bonded to carbon, hydrogen, or oxygen, most often as organic nitrogen compounds (such as amino acids), ammonium ($NH_4$), or nitrate ($NO_3$) (Fields, 2004). Animals get their reactive nitrogen from eating plants and other animals somewhere along the food chain. And plants get reactive nitrogen from the soil or water (Fields, 2004).

The past 15 years have seen a huge explosion in the amount of reactive nitrogen that humans have produced and injected into the environment (Townsend, 2003). Industrial nitrogen fixation for nitrogen fertilizer is > 80 Tg/year. An additional 25 Tg of N are fixed by internal combustion engines and released as oxides of nitrogen, and ~ 30 Tg are fixed by legume crops (over and above natural N fixation on those lands) (Smil, 1991). Further, human activity mobilizes N from "long term storage pools" (atmosphere) through biomass burning,

introducing reactive nitrogen fertilizers on farm lands, land use change and drainage of wetlands (Vitousek &Matson, 1993). Both, fixed and mobilized Nitrogen are transported in the atmosphere or in solution, altering the Nitrogen cycle at a certain location which may then spread locally or globally (Vitousek &Matson, 1993). The reactive nitrogen further combines with water and comes down as acid rain. This leads to loss in biodiversity.

*1.3.1.1.3 Land Use/Cover Change*

Land cover change is defined as alteration of the physical nature of a site (Vitousek, 1994), for example, conversion from forest to grassland. Land cover change is the alteration in the way land is utilized by humans (Townsend, 2003) i.e. conversion from agricultural land to urban area. Land use change and land cover change may occur simultaneously or separately, but for convenience, both these processes will be referred to as 'land use change' in this thesis.

It is believed that land use change, currently and for the past few decades, has been the single most important component of global change affecting ecosystems (Vitousek, 1992). Unlike the other two components, it is not a globally homogenous phenomenon. It occurs globally but the extent of change varies locally.

Land use change can also affect climate both locally and regionally by altering the ways that solar energy is partitioned (Townsend, 2003). Conversion of forest to agricultural lands increases albedo and decreases canopy roughness. On a local scale, the net effect is an increase in local temperature and a decrease in humidity; these in turn can affect the potential for forest regeneration, both directly and also by increasing the probability and intensity of a forest fire (Uhl and Kauffman, 1990). The biotic impact of land use change is not restricted to altered land themselves. It causes other issues such as habitat fragmentation and loss of biodiversity (Redford, 1992). Conversion of agricultural land parcels to forests is also observed in areas where the government imposes a reserved forest in a region and evacuates the forest of human settlements as well as the surrounding area (Vitousek, 1994). In recent times though, the former is more common.

Land use change study has gained importance in recent decades so that one can understand the correlation between the rate of land use change and biodiversity loss and subsequently be used as a tool for its prediction. It is necessary to understand that land use change is not the

sole driver for biodiversity loss but it is an important one that interacts with many other components of global climate change. In this thesis, the main land use being focused upon is the tropical forests of the Western Ghats.

The impact of climate change is not limited to those explained above and can be extended to elevated temperatures, increase in number of flood events, increase in duration of the drought season and erratic heavy precipitation all over the world. Of the several effects of climate change, this thesis will focus on extreme rainfall events.

## 1.4 Extreme Rainfall Events

According to the India Meteorological Department, a day is called 'heavy rainfall day' if the rainfall of that day is 64.5 mm or more. This includes very heavy (i.e., 124.5–244.5 mm) and extremely heavy (i.e.>244.5 mm) rainfall (Goswami et al., 2006). Extremes of weather and climate can have devastating effects on human society and the environment (Goswami et al., 2006). Understanding past changes in the characteristics of such events, including recent increases in the intensity of heavy precipitation events all over the world, is critical for reliable projections of future changes (Schiermeier, 2007).

Studying the possible long-term changes in the intensity of extreme events is equally important. The increase in magnitude and frequency of floods and droughts as an impact of extreme rainfall events has become of growing interest to the scientific community (Iwashima and Yamamoto, 1993). As a case study in Africa, Alexander (2003) mentioned that the possibility of collapses of small dams and reservoirs is likely to increase and number of lives to be impacted as a result (only in the floodplains of his study area in South Africa) was up to 1,00,000 people. It has therefore been suggested that tests for climatic change should focus on changes in extreme events rather than on changes in climatic means (von Storch & Zwiers, 1988).

### 1.4.1 Causes of Extreme Rainfall Events

One of the causes of heavy precipitation has been pinned on global warming. Global warming is the rise in the average temperature of Earth's atmosphere and oceans since the late 19th century and this phenomenon has been projected to continue (www1). Since the early 20th century, Global temperatures have increased by about 0.5°C (Folland et al., 1990) with

about two-thirds of the increase occurring since 1980. This sudden increase in global temperatures intensifies the hydrological cycle. The increase in surface air temperature causes an increase in evaporation and higher levels of water vapour in the atmosphere. In addition, a warmer atmosphere is capable of holding more water vapour. The excess water vapour will in turn lead to more frequent heavy precipitation when atmospheric instability is sufficient to trigger precipitation events. Intense precipitation can result in flooding, soil erosion, landslides, and damage to structures and crops. Along with increasing precipitation post the hot and dry months, increased temperatures will also amplify the drying out of soils and vegetation due to increased evaporation in the summer. This is likely to result in more severe and widespread droughts where precipitation doesn't occur.

## 1.5 Objectives

Several studies have highlighted the various damaging possibilities of extreme rainfall events in various parts of the world. Studying the impact of this climatic extreme behaviour would be the first in the Aghnashini basin in the Western Ghats, a biodiversity hotspot. This study area is in a rural setting comprised of agricultural lands, human settlements and reserved forests. As part of my thesis, I wanted to gain an understanding of the changes the extreme rainfall events has had on the land use and land cover (LULC) of the Aghnashini basin (if any).

With that in mind, I have highlighted the following as the objectives of my thesis:

- Creating land use/cover maps for the study area for the years 1990, 2000 and 2013
- Carrying out change analysis
- Analyzing monthly climate data from the year 2001 till 2013 in terms of trend and seasonality
- Using monthly MODIS NDVI time-series data for specific land uses in conjunction with the rainfall time-series data to understand the impact of rainfall on different land uses

## 1.6 Need for this Study

In recent decades, increasing awareness of the depletion of tropical forests and the associated impacts on biodiversity and global climate change in particular have led to regional to global initiatives to halt or slow their decline (Wulder & Franklin, 2003). However, despite these initiatives, forests continue to be cleared, disturbed or degraded at a rapid rate. Coupled with this situation, is the impact of extreme rainfall events.

In India, the timely availability of adequate amount of water is essential to meet the various needs of reliant sectors such as agriculture, industrial sector, providing domestic water supply and for hydroelectric power generation and others (Schiermeier, 2007). Global climate changes may influence long-term rainfall patterns impacting the availability of water, along with the danger of increasing occurrences of droughts and floods (Fosse & Changnon, 1993). The southwest (SW) monsoon, which brings about 80% of the total precipitation over the country, is critical for the availability of freshwater for drinking and irrigation (Goswami, 2006). Changes in climate over the Indian region, particularly the SW monsoon, would have a significant impact on agricultural production, water resources management and overall economy of the country (Schiermeier, 2007). The heavy concentration of rainfall in the monsoon months (June–September) results in scarcity of water in many parts of the country during the non-monsoon periods (Schiermeier, 2007).

Based on the understanding of the severity of the situation, understanding the correlation between land use change and extreme rainfall events will help in realizing the characteristics of such events. This in turn will aid in building of a knowledge base in the Aghnashini basin for the past and current situation and help generate reliable predictions for future events. As a scope for the future, the impact of extreme rainfall events may also be extended to its effects on hydrology, biodiversity and economic well-being of the people. More importantly, the knowledge gained in this thesis may then be used to guide the process of conservation in the Western Ghats.

# Chapter 2: Literature Review

## 2.1 Datasets Used

### 2.1.1 Landsat

Landsat data have helped to improve our understanding of the Earth. Over the past three decades, Landsat has played an increasing role in grasping varied applications such as human population census, growth of global urbanization (Appeaning &Kwasi, 2010) and deletion of coastal wetlands along with understanding coral reefs, tropical deforestation, and Antarctica's glaciers. Today use of Landsat data has evolved from "a fundamental data source for addressing basic science questions", (Chander et al., 2007). to being an invaluable resource for decision makers in several diverse fields such as agriculture, forestry, land use, water resources and natural resource exploration (Appeaning &Kwasi, 2010). Moreover, Landsat has a large archive of data which creates a baseline knowledge for further analysis.

#### 2.1.1.1 Landsat 5

In this thesis, Landsat 5 was used and hence its technical details have been divulged below. Landsat 5 was launched on March 1st, 1984 (Chander et al., 2007). It carries two remote sensing instruments namely, the Multispectral Scanner System (MSS) and the Thematic Mapper (TM). The TM sensor is still operational but the MSS instrument has been decommissioned. It was launched into a 705km high polar, sun-synchronous orbit at an inclination of 98.2° with a temporal resolution of 16 days (Chander et al., 2007).

### 2.1.2 MODIS

MODIS (Moderate Resolution Imaging Spectroradiometer) is sensor on board the Terra and Aqua satellites. Terra orbits the Earth from north to south across the equator in the morning and Aqua passes south to north across the equator in the afternoon (www4). Their temporal resolution is around 1-2 days obtaining data from all over the world in 36 spectral bands. From these 36 bands, MODIS data are dispersed as land products, ocean products and lower atmospheric products. For this thesis, the land product data MOD 13 - Gridded Vegetation Indices (NDVI & EVI) (www4) was downloaded for the years 2001 till 2012. A time-series

was then generated of the NDVI data to understand the changes in seasonality of various land use classes over this time frame.

## 2.2 Image Pre-Processing and Analysis Techniques

### 2.2.1 Image Pre-Processing

Pre-processing of satellite sensor images is necessary for removal of errors, noise and masking out any unnecessary components like clouds that can lead to misinterpretation of the imagery (Coppin et al., 2004). The process of geometric correction helps to eliminate geometric inconsistencies in an image caused due to various reasons. This process uses GCPs to assign map co-ordinates to the image. In this thesis, the image was first clipped to the required extent, the shadow and water bodies were masked out using unsupervised classification and the images were geo-rectified to UTM/ WGS 84 using a LISS 4 image.

### 2.2.2 Image Analysis

Before proceeding to understand how to analyse the satellite imagery, it is important to understand the spectral characteristics of some of the components that will be studied in this thesis.

#### 2.2.2.1 Spectral Reflectance Curve

When electromagnetic energy strikes any given feature on the Earth surface, the three possible interactions are: reflection, absorption and/or transmission of the incoming radiation (Lillesand & Kiefer, 1994). The reflected component is important for remote sensing purposes because this radiation can be measured by the sensor system based in the satellite (Jensen, 2009). The reflected energy is equivalent to the incident radiation on a given feature minus the energy absorbed and/or transmitted by that feature. The reflection of a certain surface depends on different factors. Some of which include (Roth, 1997):

• Nature of the material

• Physical condition (e.g. wet – dry, healthy – stressed)

• Surface roughness of the object

• Exposure to the sun and solar elevation angle

• Spectral features (colour tone) of the object

The amount of reflected energy varies not only with different materials but also with the same materials in having different conditions (Jensen, 2009). Furthermore, for a single Earth's feature, the reflectance varies across the range of wavelengths in the electromagnetic spectrum. As a consequence, each surface material has its characteristic reflection over a range of wavelengths, which is known as spectral signature or profile (Jensen, 2009).

The reflectance characteristics of earth surface features may be quantified by measuring the proportion of incident energy that is reflected by the material for a particular wavelength. This is expressed in a formula as the ratio of energy that is reflected from an object to the energy incident on the object. A graph of the spectral reflectance of an Earth surface feature against wavelength is referred to as the spectral reflectance curve. The spectral reflectance curve is of immense importance as it helps us gain an insight into the spectral characteristics of the feature and heavily influences our choice of wavelength region for obtaining data (Lillesand & Kiefer, 1994). The spectral reflectance curve of the most basic types of Earth surface features has been explained below.

*2.2.2.1.1 Vegetation*

Chlorophyll absorption by plants occurs in the blue and red portion of electromagnetic spectrum as this incident energy is required for photosynthesis. Thus, plants generally have low reflectance in the blue and red portion of the spectrum (Lillesand & Kiefer, 1994). A relative lack of absorption in the green wavelength allows for higher reflection in that electromagnetic spectrum range (Jensen, 2009). Therefore, if a plant becomes diseased or stressed that interrupts its normal growth and productivity, it may decrease or stop chlorophyll production. This results in less absorption in the blue and red bands and more absorption in the green band (Lillesand & Kiefer, 1994).

Near infrared incident energy is strongly reflected from the plant surface. The reason for bulk of the incident NIR energy reflection is that if plants absorbed this energy as efficiently as in the visible spectrum, they could become too warm causing irreversible denaturing of the proteins in their cells. Thus, plants have adapted to not utilize this energy and either reflect or transmit it to the underlying leaves or ground (Jensen, 2009).

The amount of this reflectance is determined by the properties of the leaf tissues like their cellular structure and the "air cell wall-protoplasm-chloroplast interfaces" (Kumar and Silva, 1973). Because structure is highly variable between plant species, reflectance measurements in this range allow for discrimination between plant species which is otherwise difficult in the visible spectrum of electromagnetic radiation (Lillesand & Kiefer, 1994).

Moreover, structural characteristics are affected by environmental factors such as soil moisture, nutrient status, soil salinity, and leaf stage (Ma et al., 2001). Consequently, sensors operating in this range can also detect any stress or disease in the plant.

As wavelength increases to the mid infrared region, both reflectance and transmittance generally decrease. Dips are observed in the spectral response curve at wavelengths 1.4, 1.9 and 2.7 µm (Kumar and Silva, 1973). These wavelengths denote strong absorption by leaves due to presence of leaf water. Since water is a good absorber of mid-infrared energy, the greater the turgidity of the leaf, the lower the mid-infrared reflectance (Ma et al., 2001). A decrease in plant moisture content maybe determined using this wavelength range. When the relative water content decreases below 50%, almost any portion of the visible, near and middle-infrared regions will be useful spectral information regions (Jensen, 2009).

*2.2.2.1.2 Water*

Clear water has excellent transmission properties and poor absorption properties in the visible wavelengths (Belward & Carlos, 1991). The water spectral reflectance curve is characterised by a high absorption at near infrared wavelengths range and beyond (www2). Due of this absorption property, water bodies as well as features containing water can easily be detected, located and delineated with remote sensing data (Belward & Carlos, 1991).

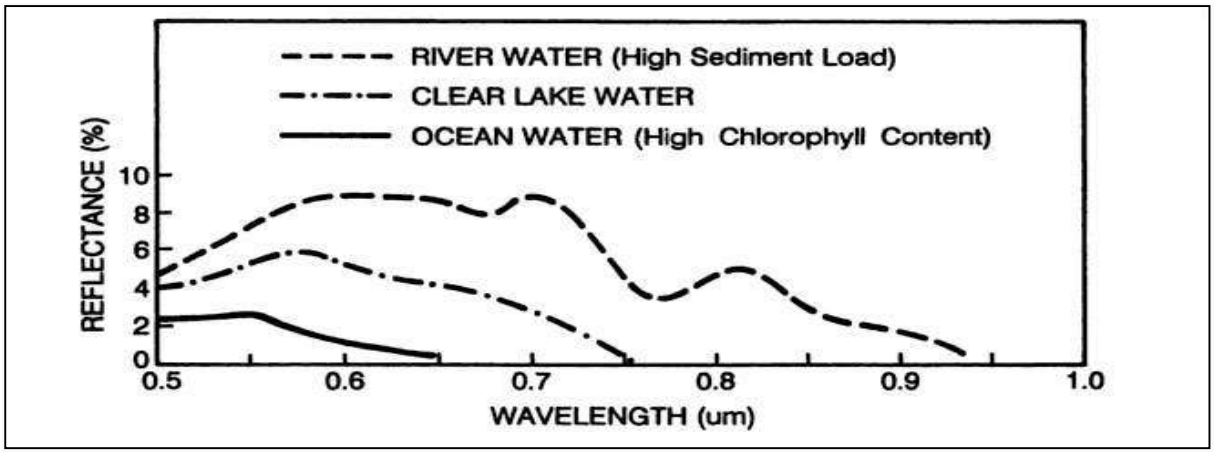


**Figure 2.1 Water Reflectance Curve**

Turbid water has a higher reflectance in the visible region than clear water (www2).Water with high inorganic sediment loads usually has higher reflectance than clear water with a peak seen in the longer red wavelengths (Belward & Carlos, 1991). This is also true for waters containing high chlorophyll concentrations. High chlorophyll content in water will increase reflectance of water in the green spectrum. These reflectance patterns are used to detect algae colonies as well as contaminations such as oil spills or industrial waste water (Lillesand & Kiefer, 1994).

*2.2.2.1.3 Soil*

The spectral properties of soil are simpler than that of water and vegetation in that there is no transmission of the incident radiation (Jensen, 2009). However, the factors that influence soil reflectance are many, some of them are: moisture content, texture, presence of iron oxide and organic content and surface roughness (Belward & Carlos, 1991). These factors are in turn related to one another and highly variable (Lillesand & Kiefer, 1994). For instance, soil reflectance decreases with increase in moisture content.

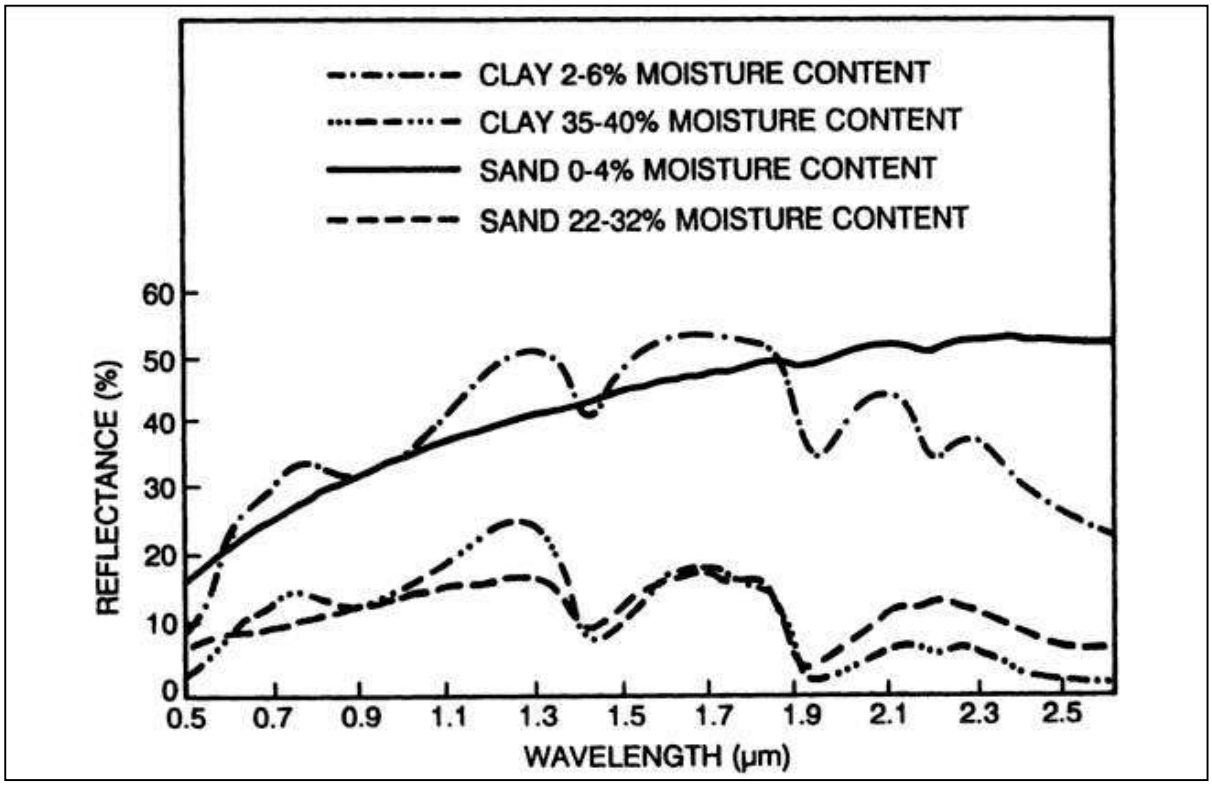


**Figure 2.2 Soil Reflectance Curve**

Furthermore, soil moisture content is strongly related to the soil texture. Under dry circumstances, the curve for both the coarse and fine textured soils is the same though they film of water (Jensen, 2009). Thus, soils with small particle size (fine textured soils), will hold a larger amount of water (Belward & Carlos, 1991). In addition, some of the air spaces in the soil will also be occupied by water. The greater the soil moisture, the more the absorption of incident energy in the mid-infrared region and less energy is reflected. In conclusion, in the presence of soil moisture, coarse grained soils are more reflective than their fine grained counter parts.

#### 2.2.2.2 Vegetation Indices

Vegetation indices are dimensionless, radiometric measurements that help in extraction of useful information pertaining to vegetation in satellite imagery (Huete, 1999). More than 150 VI's have been developed till today that extract and model variables like leaf area index (LAI), biomass, chlorophyll content, absorbed photosynthetically absorbed radiation and others (Huete, 1999). According to Running et al. (1994), a vegetation index must:

1. maximize sensitivity to plant biophysical parameters,
2. eliminate the effect of external parameters such as sun illumination differences, topographic effect, etc. and
3. correlate to various biophysical factors such as biomass, LAI, etc.

The vegetation indices used in this thesis have been explained below.

##### *2.2.2.2.1 NDVI*

Rouse et al (1974) developed the Normalized Difference Vegetation Index (NDVI):

$$NDVI = (NIR-R)/ (NIR+R)$$

Where, NIR and R are the amounts of near-infrared and red reflectance reflected by vegetation and captured by the sensor of the satellite. The NDVI is a numerical indicator that used to analyse remote sensing data, specifically vegetation. NDVI values thus range from -1 to +1, where negative values correspond to an absence of vegetation (Pettorelli, 2005. The formula is based on the fact that chlorophyll absorbs in the red wavelength whereas the leaf structure scatters the incident radiation in the NIR wavelength (Govaerts, 2010). The greater the difference between the reflectance in these wavelengths, the more vegetation there has to

be (Pettorelli, 2005). Unhealthy or sparse vegetation reflects more visible light and less near-infrared light. Bare soils on the other hand reflect moderately in both the red and infrared portion of the electromagnetic spectrum (Holme *et al* 1987).

One importance of this ratio is that it reduces many forms of "multiplicative noise" (Jensen, 2009) (sun illumination differences, topographic variation, cloud shadow) from multiple bands of multi-date imagery (Jensen, 2009). It is often directly related to other ground parameters such as percent of ground cover, photosynthetic activity of the plant, surface water, leaf area index and the amount of biomass and hence finds wide use (Govaerts, 2010). Some of the applications of NDVI in vegetation studies are: estimating crop yields, vegetation type mapping, pasture performance, rangeland carrying capacities and biomass estimation among others (Pettorelli, 2005).

The application of NDVI particularly in this thesis is determination of the various phenological metrics of vegetation. Plotting of time-series MODIS NDVI data will produce a temporal curve that explains the various stages that green vegetation (cropland or forested) undergoes during a complete growing cycle (Reed et al.,2003). From this curve, one can extract information about the start of growing season, peak of season and end of season (Reed et al., 2003). Since the time series will extend for a period of 13 years, we can additionally observe if any climatic variables (temperature and precipitation) have caused a shift in the phenological cycle (if one is witnessed at all) of any of the vegetation types in question.

Some experimental studies showed that the

### 2.2.3 Image Classification Techniques

The overall objective of image classification procedures is to automatically categorize all the pixels in an image into various land cover/ use classes or thematic layers (Chintan et al., 2004). Normally, multispectral data are used to perform classification and the spectral information contained in the pixels is used as the numerical basis (differing DN values) for classification (Lillesand and Kiefer, 1994). As discussed earlier, at various wavelengths, the spectral radiances received by the sensor are recorded for each pixel. Theses spectral radiances are visualized as a combination of DN values (Kiefer, 2001) and differ for every Earth's feature due to dissimilar spectral characteristics. Therefore, the purpose of image

classification becomes the recognition of spectral pattern as formed by the combination of pixels with similar DN values.

Spatial and temporal characteristics of pixels in an image may also be used to categorize pixels into different thematic classes. Time is an important aid in feature identification. This is especially useful when distinguishing forest types like deciduous and evergreen forests and identifying agricultural fields. For example, a field that is freshly sown may not be distinguishable from bare soil but is clearly discernible during harvest season. Interpretation of imagery of such an area using only one date would be unsuccessful, regardless of the number of bands. On the other hand, multi date imagery for the same area will be able to recognize the feature.

Spatial classifiers consider the spatial relationship of pixels with their neighbours and take into account spatial properties such as image texture, pixel proximity, feature shape, size, directionality, repetition and context while classifying. These types of classifiers somewhat imitate the spatial analysis done by the human eye during visual interpretation. These techniques tend to be "more complex in nature and computationally intensive" (Lillesand and Kiefer, 1994) than classification based on spectral properties of pixels.

**Types of Image Classification**

The most frequently exploited type of classification is the pixel-based technique. Pixel-based classification uses multi-spectral classification techniques that assign a pixel to a class by considering the spectral similarities with the class or with other classes (Casals-Carrasco et al. 2000).

Alternatively, object-oriented analysis classifies objects instead of single pixels. The idea to classify objects stems from the fact that most image data exhibit characteristic texture that is neglected in conventional classifications (Blaschke and Strobl 2001). This classification scheme also uses information like context, spatial, morphology of the pixels and its neighbours to classify objects into various thematic classes.

### 2.2.3.1 Traditional Pixel-Based Classification

Over the few past decades, pixel-based procedures have been the main image processing means. Traditional supervised classification and unsupervised classification are all based on

the single pixels. This implies that the overall objective of classical image classification techniques has been to automatically categorize all pixels in an image into land cover classes or themes description (Xiaoxia et al., 2005). To do so, normally, multispectral data are used to perform the classification, and only the spectral information for each pixel is utilized as the basis of categorization description (Xiaoxia et al., 2005).

Pixel-based classification is categorized into supervised and unsupervised classification techniques. In supervised classification, the image analyst "supervises" or guides the computer while it assigns each pixel to a class in the image (Vlek, 2004). The analyst provides the computer with training sets or samples of the various land cover classes. These training samples are numerical descriptors of the thematic classes which help distinguish the classes on the basis of their DN values (Vlek, 2004). The computer then compares the value of each pixel with the DN value range provided in the training sets. The pixel is assigned to the class to which it most "resembles". Having understood supervised classification, let us proceed to unsupervised classification. The main difference between these two classification techniques is the lack of the training stage in the unsupervised classification procedure.

Unsupervised classification techniques involve a two-step procedure. The first step involves a method of clustering the pixels. The image data are first aggregated into the "natural spectral groupings or clusters" (Lillesand & Kiefer, 1994) present in the scene. It enables the user to specify parameters to determine the spatial pattern observed in the data. These patterns need not directly amount to any meaningful land cover class but may merely indicate a cluster of pixels having similar spectral characteristics (ERDAS, 1999). The second stage in this process of classification is the identification of land cover classes by the analyst based on the clusters present in the scene (Vlek, 2004). Using ground reference data, the accuracy of the classification may be determined.

*2.2.3.1.1 Classification Techniques*

**2.2.3.1.1.1 ISODATA Clustering**

ISODATA stands for "Iterative Self-Organizing Data Analysis Technique". It is an unsupervised classification technique and is an iterative procedure. In this process, the first step is the creation of natural clusters. The second step classifies each pixel to the cluster with the closest mean value. In the third step the new cluster mean values are calculated based on

all the pixels in a cluster (www1). The ISODATA iteration repeats the clustering of the image until either:

1. A maximum number of iterations has been performed, or

2. A maximum percentage of unchanged pixels has been reached between two iterations.

The "change" can be defined in several different ways, either by measuring the distances the mean cluster vector have changed from one iteration to another or by the percentage of pixels that have changed between iterations (www1).
The ISODATA algorithm further refines the clusters by their splitting and merging (Jensen, 1996). Clusters are merged if either the number of members (pixel) in a cluster is less than a certain threshold or if the centres of two clusters are closer than a certain threshold. Clusters are split into two different clusters if the cluster standard deviation exceeds a predefined value and the number of members (pixels) is twice the threshold for the minimum number of members (Jensen, 1996).

#### 2.2.3.1.1.2 Maximum Likelihood Classification

It is a parametric supervised classification technique that has been widely used in classification of remotely sensed images. It is assumed that the distribution of the points forming the land cover class training data is Gaussian (normally distributed) (Lillesand & Kiefer, 1994). This assumption of normality is generally reasonable for common spectral response distributions. Based on this assumption, the distribution of a land cover class response pattern can be completely described by the mean vector and the covariance matrix.

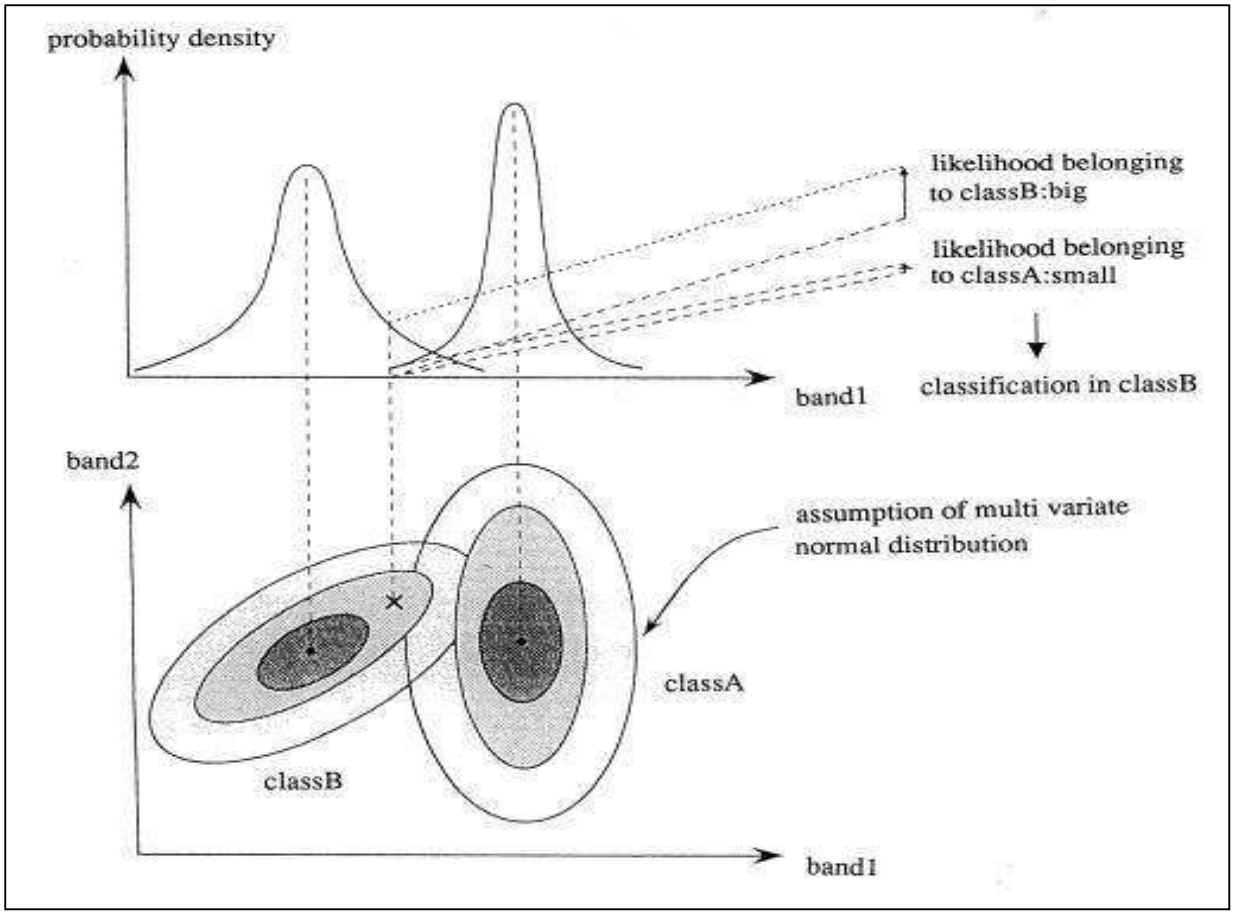


**Figure 2.3 Maximum Likelihood Classifier**

In this technique both the variance and covariance of spectral response patterns of each land cover class is computed. With these parameters, the statistical probability of a given pixel value being a member of all land cover class can be computed. The pixel is assigned to the class with the highest probability. A threshold value may also be provided to the classifier by the analyst. Pixels with probabilities below that threshold are categorized as unclassified.

### 2.2.3.2 Object-Oriented Classification

High spatial resolution imagery is expected to have more accurate classification results (Gua et al., 2004). This expectation is often not met with due to greater spectral variation within a class and a greater degree of shadow (Laliberte et al., 2004). The increase in the amount of spatial information contained in these imagery often leads to an inconsistent classification (Whiteside, 2005). Thus, it is often difficult to classify high resolution imagery on a pixel-by-pixel basis due to the high level of information contained in them (Hofmann, 2001). Spatial information that is also present in these images are not considered during classification by the

pixel-based algorithms. The development of robust object-oriented classification methods suitable for medium to high resolution satellite imagery provides a valid alternative to 'traditional' pixel-based methods (Baatz et al., 2004). An object-oriented approach enables the user to incorporate both spectral information (tone, colour) as well as spatial arrangements (size, shape, texture, pattern and association with neighbouring objects) for image analysis (Gua et al., 2004). For this reason, object oriented analysis has proved to be more useful in classification than its counter-part, pixel based classification by Laliberte et al., 2004. In object oriented classification, individual objects as opposed to single pixels (Thomas et al., 2003) are used.

This process begins with the segmentation stage where objects or 'homogeneous' areas (Baatz et al., 2000) are created based on user defined criteria. These objects have geographical features such as shape and length, and topological characteristics such as adjacency found within them (Gua et al., 2004). These attributes create a knowledge base for the sample objects which are then used for classification (Whiteside, 2005).

*2.2.3.2.1 Multi-Resolution Segmentation*

It is a bottom-up region-growing technique starting with one-pixel objects. It begins by considering each pixel as a single object (Xiaoxia et al., 2005). In numerous subsequent steps the image objects are merged into bigger ones (more pixels) based on the chosen scale, colour, and shape parameters, which define the growth in heterogeneity between adjacent image objects (Gua et al., 2004). This process stops when the smallest growth exceeds the threshold defined by the scale parameter (Benz et al., 2004).

Throughout the segmentation procedure, the whole image is segmented and image objects are generated based upon several adjustable criteria of homogeneity or heterogeneity in factors such as colour, compactness, smoothness and scale (Gua et al., 2004). The scale parameter set by the user is influenced by the heterogeneity of the pixels (Whiteside, 2005). Adjusting the scale parameter influences the average object size: a larger value leads to bigger objects and vice versa (Gua et al., 2004). The colour parameter balances the homogeneity of a segment's colour with the homogeneity of its shape. The form parameter is a balance between the smoothness of a segment's border and its compactness. Addition of weights to these parameters establishes the homogeneity criterion for the object primitives (Whiteside, 2005).

*2.2.3.2.2 Classification Process*

The next step after segmentation is classification. It implies that classes will be generated by assigning to image objects to them based on class description (Xiaoxia et al., 2005). Class description refers to the knowledge-based classification rules that include spectral, spatial, contextual and geometry attributes of the image objects (Xiaoxia et al., 2005). The objects are assigned or classified based on whether they have satisfied the knowledge-based rules or not. eCognition also allows the use of hierarchy. Thus, image objects can inherit object properties from a super-class and also a group. In this thesis, the classification has been carried out using Nearest Neighbourhood Algorithm along with a fuzzy classifier.

Nearest Neighbour (NN) classifier works in 2 stages. First being, the selection of some image objects that are used as representative samples or training sites for a particular class (Gua et al., 2004). The next stage is the actual classification based on the nearest sample neighbours (User Guide, 2011). Each classified object is also provided membership values between 0 and 1 to the various classes. This technique uses fuzzy logic theory combined with user-defined rules. Both act as class descriptors.

Fuzzy classification is a probabilistic approach and a powerful classification technique that uses a knowledge base for classification and is very helpful in distinguishing between different entities that show spectral overlap between classes due to limited spectral resolution (Navulur, 2006). According to Hengl & Reuter (2009) fuzzy logic has emerged as a preferred approach for devising rules for classifying spatial entities using a supervised approach. It also has no statistical requirements for rule creation and can utilize both continuous and discrete input data layers (Hengl & Reuter, 2009). For ‘n’ number of classes, fuzzy classification generates n-dimensional membership degrees, which describe the likelihood of an object being assigned to a certain class (Navulur, 2006).

In contrast, crisp classification assigns every object to a specific class, in spite of the weak correlation between object properties with the rules (Navulur, 2006). On the other hand, the fuzzy rule set contains information about the overall reliability, stability and list of classes the object can belong potentially belong to (Navulur, 2006). An unclassified category is also included to account for those objects that do not meet the required membership function for the ‘n’ classes in the image (User Guide, 2011).

*2.2.3.2.3 Classification Criteria*

**Table 2.1 Classification Criteria**

| Criteria | Explanation | Example |
|---|---|---|
| Mean Layer Values | Mean image layer value of a given image layer within a region (object) is calculated. | The mean layer value of evergreen forest object will be greater than 150 while that of grasslands will be lesser than 60. |
| Standard Deviation of Layer Values | The layer standard deviation of a given image layer within a region (object) is calculated. | Areca plantation layer standard dev. Is low while that of Acacia is high. |
| NDVI | This is a vegetation index that can be used to differentiate vegetated and not vegetated land and to some degree differentiate between vegetation types. Its values range from -1 to +1. **NDVI= (Nir-R)/(Nir+R)** | NDVI of water is lesser than 0 while that of an evergreen forest is generally more than 0.6. |
| Shape | Aspects of shape like elliptical fit, rectangular fit and density are calculated for objects. | Areca plantations are linear and are closer to a rectangular fit than Acacia plantations which are patches of land with no definite shape. |
| Thematic Layers | Various thematic layers may be imported into the software to help in classification or visualization. | Areca plantations are not found in reserved forests. This rule is implemented by using a shapefile of Reserved forests. |
| Relative area of | It is the area covered by image objects of a selected class, found within a user-defined circular area around the selected image object, divided by the total area of image objects inside this area. | Soppinabetta lands are always found within a certain area of areca plantations. |
| Relative Distance to | It is defined as the distance (in pixels) of the image object's centre concerned to the closest image object's centre assigned to a defined class. The image objects on the line between the image objects' centres have to be of the defined class. This acts a buffer zone around objects. | Soppinabetta lands are always found within a certain distance of areca plantations. |
| Slope | A slope map is useful in distinguishing land use classes based on this criteria. | Areca is only found in shallow valley regions while Acacia plantations are mostly located on hills. |

### 2.2.4 Change Detection

In this thesis, I will perform classification of images acquired at different times so a suitable technique for detecting change between them is post-classification change detection. This involves a comparative study of the classification maps produced independently on different dates (Sallaba, 2009). The accuracy of the change map will be the product of the accuracies of each individual classifications (Stow *et al.* 1980). Accuracy of the change in the land use classes depends in turn on spectral separability of classes involved (Mas, 1999). This process will be carried out in the IDRISI which will identify areas that have changed from the previous time step and quantify the change.

## 2.3 Structural Time-Series Model (STM)

An STM is a dynamic model that helps us understand the variation in time-dependent variables. It is assumed that the changes in the variations of variables is due to random disturbances (Ravichandran et al., 2002). One of advantages of STM is the capability of modelling multivariate models. In this thesis, univariant series are only analysed. This model decomposes the univariant time-series into trend (level plus slope), seasonality and an error component (Harvey & Durbin, 1986). Trend and seasonality components are both unobserved components. Thus, the NDVIt = Levelt + Cyclict + et, where et is the error or noise et~N(0,V).

The structural time series models are well represented in the state space form with the state of the system showing the trend and seasonal components while the estimates for these components are provided by the Kalman filter (Harvey, 1993). This makes the trend and seasonality aspects of the model easy to interpret. The Kalman filter is a recursive optimal estimation technique (Durbin & Koopman, 2001) that calculates the current estimate of the state using the observations in the data along with the previous estimate of the state. It is optimal because it provides the best estimate based on all the previous measurements.

# Chapter 3: Study Area

## 3.1 Geography

The Uttara Kannada district of Karnataka is located between north latitudes13.0 55' 02"to 15.0 31' 01" and east longitudes 74.00'35" to 75.010' 23" falling in the survey of India degree sheet numbers –48 I, 48 J, 48 K, 48 M, and 48N (www4). The district has a geographical area of 10222 sq. kms (Deshpande& Kallapur, 2008). It has 4 sub-divisions with my study area falling in the Honavar and Sirsi sub-divisions of this district.

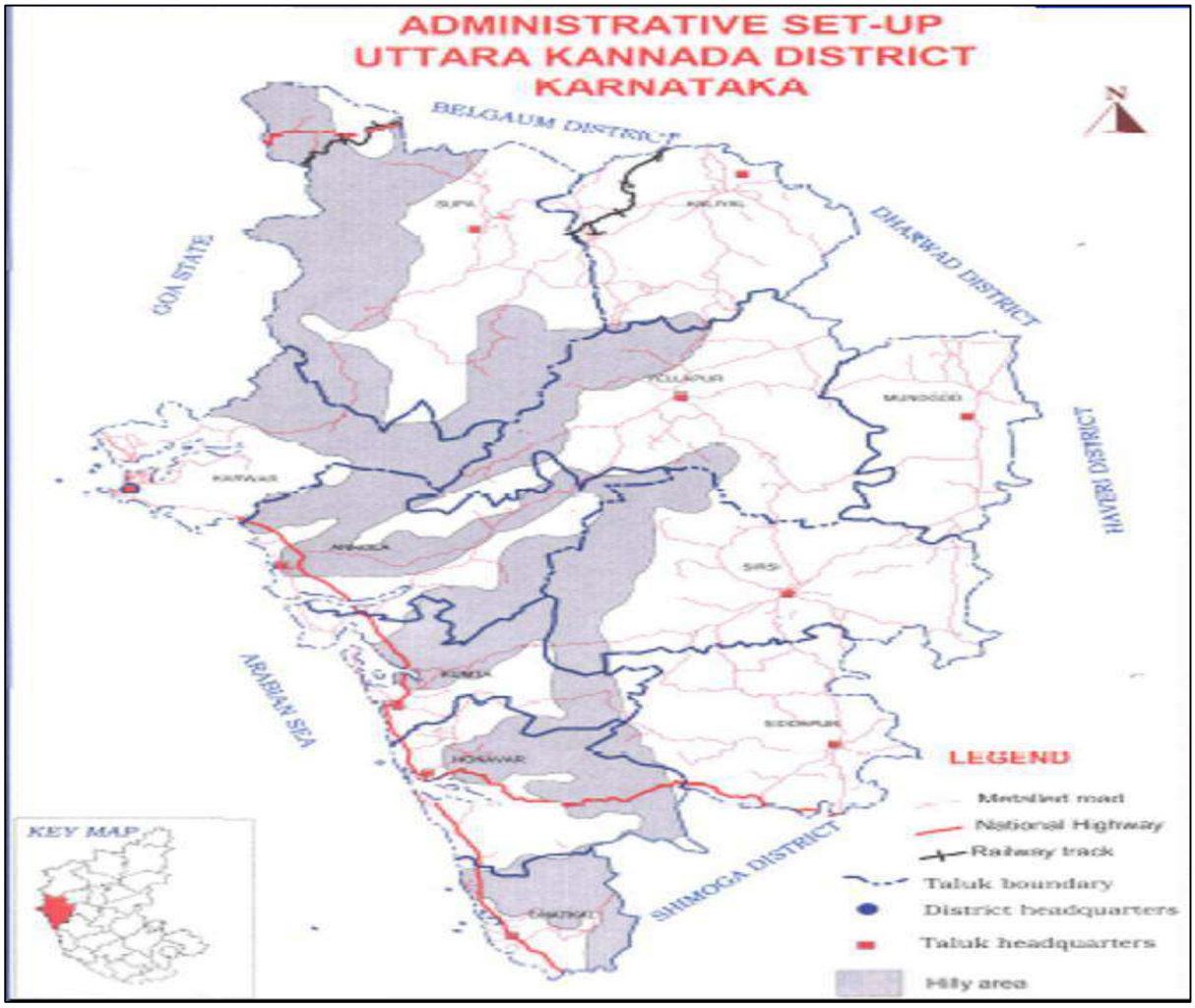


**Figure 3.1 Administrative Boundaries of Karnataka District**

The important rivers in the district are Sharavathi, Kali, Aghnashini, and Gangavali. All these rivers flowing in the westerly direction to join the Arabian Sea (www4). All the rivers in the district, together with their tributaries exhibit dendritic drainage pattern and support a

population of around 14.39 lakhs(as per 2001 census), out of which rural population constitutes 11.40 lakhs(Ramachandra, 2010).

## 3.2 Climate

The district experiences tropical monsoon climate (Krishnaswamy et al., 2012). With the start of the dry season in January, the temperatures start to rise, and it peaks in May. Around 30ºC is the average with highest day time temperatures rising up to 38ºC(Deshpande & Kallapur, 2008).During this season thunderstorms are common in especially in the month of May. The temperature, thereafter declines during monsoons. The humidity is lowest during the dry season and highest during the monsoons which lasts from June to September (Deshpande & Kallapur, 2008). This season brings heavy rainfall to the district ranging between 2000mm-5000mm.

## 3.3 Study Area: Aghnashini Basin

The study area is around 40 km from Sirsi in the Aghnashini basin. It is located between:

North West Corner: Latitude: 14°34'48.55"N
Longitude: 74°32'58.33"E

South East Corner: Latitude: 14°24'35.74"N
Longitude: 74°46'47.58"E

This allows for the continued presence of evergreen, semi-evergreen and deciduous forests. The terrain is hilly interspersed with valleys. The valleys are suitable for cultivation purposes which mainly support paddy fields and arecanut plantations. Coconut and sugarcane plantations are also observed. This Aghnashini river catchment in Uttara Kannada District of Karnataka state does not have many major developmental projects or industries (Avinash & Ashamanjari, 2010). This situation, along with the heavy precipitation are conducive for the presence of evergreen, semi-evergreen, deciduous forests (Champion & Seth, 1968) along with some acacia plantations on the hills. Grasslands may also be seen in this region though they are rapidly being replaced by agricultural land parcels.

## 3.4 Major Land Uses

The district has 8,13,695 ha. of forest (Deshpande & Kallapur, 2008) which constitutes 79 % of the total geographical area of the district.The major occupation in the region is agriculture (Deshpande & Kallapur, 2008). The main food crops grown in the district are paddy, Maize, pulsesgroundnut, and spices. Sugarcane, cotton and arecanut are the maincommercial crops grown in the district(Ramachandra, 2010).

### 3.4.1 Paddy Fields

Rainfed paddy is the major crop in the plains of Uttara Kannada district. Rice cultivation through the transplantation method is common in areas with heavy precipitation (Nayar & Manjappa, 2012). In the Aghnashini basin, heavy rainfall during the early/mid-June, provides sufficient water for paddy cultivation. However, there is scope to grow asecond crop in the dry season of January-April through irrigation (Ramachandra & Nagarathna, 2000)using canals, tanks, and dugwells or tube/bore wells. The second crop maybe paddy, or a type of legume or a vegetation, depending on the availability of water. The yield from paddy in this region is low giving narrow margins of profit. As a result, the area under riceis decreasing year by year(Nayar & Manjappa, 2012).Arecanut on the other hand is very profitable, so a major land use change that has occurred over the years is the change from paddy fields to arecanut plantations.

### 3.4.2 Arecanut Plantations

Arecanut plantations are major commercial crop grown generally found in the shallow valley regions that receive heavy precipitation.These plantations are grown interspersed with other vegetation types like banana, betel-leaf, cardamom and pepper with the areca palm forming the top canopy (Lele, 1993). This provides shade for the younger areca plants and seedlings. Additionally, the arecanut cultivators add tree leaves and twigs on the floor of the plantation to (Lele, 1993):

1. Reduce soil loss during monsoons
2. Provide nutrients to the soil

3. Reduce weeds
4. Reduce soil moisture loss during the dry months

### 3.4.3 Soppinabetta Lands

The tree leaves and twigs used for the Arecanut plantations are obtained from government sanctioned soppinabetta lands. These lands have private access (Lele, 1993).Soppinabetta lands are forest lands provided to the arecanut cultivators around their plantations with privileges like lopping of trees for mulch, manure and fuelwood, for livestock grazing and acquiring fodder, and also using timber from those lands for personal use (Lele, 1993). Since these forests experience much lopping and pruning, their tree canopy cover and tree density is different from those of unlopped forests (Lele et al., 1998).

### 3.4.3Evergreen Forests

Evergreen forests are a dominant forest type found in this region. They are located in areas with very little or no disturbance. These forests are comprised of trees that are 25-30m high with erect, closed dense canopies that cover 95% of the ground (Dash, 2009). Thus, the understory is not very thick as not enough light passes through the dense canopy. Barks of the trees are smooth. Climbers and canesare common.

### 3.4.4 Semi-Evergreen Forests

Along the hills are also present the semi-evergreen forests that are a mixture of tall deciduous trees 15-20m high, with 60-80% closed dense canopy and 40-80% trees are evergreen (Dash, 2009). These trees lack straight tall boles and with irregular canopy. Canes are rare.

#### 3.4.5 Moist Deciduous Forests

Moist deciduous forests may also be found in some regions. They have a moderate height of 10-15m tall trees, closed but not very dense (40-70%) canopy cover (Dash, 2009). Thorny species are commonly found here and canes are not visible.

### 3.4.6 Grasslands and Tree Savannahs

Grasslands and tree-savannahs are ecosystems that have developed in the Uttara Kannada district primarily as a result of clearing of forests and other destructive human activities through centuries of shifting cultivation and cattle grazing (Dash, 2009). The tree savannahs are composed of isolated or clumps of dwarf trees amidst grasses. Studies conducted by Chandran in 1998 indicates that the above ecosystems were initially forests. Climatic conditions in the region would still promote the regeneration of forests but the farmers keep the forests away by periodically burning any woody growth (Chandran et al, 2012).

### 3.4.7 Disturbed Forests

Forest patches around the agricultural plots of land have been greatly altered by humans and the primary forest is not encountered (Reid, 2009). It would be wrong to attribute all disturbances in the forest to anthropogenic activity as natural events like extreme rainfall events may also alter forests (Reid, 2009). A tall forest with an unbroken canopy is generally considered as an undisturbed forest. Disturbed forests may generally have shorter trees with less dense understory as compared to an undisturbed forest (Dash, 2009).

### 3.4.8 Acacia Plantations

Since the passing of Forest Conservation Act in 1980, several programmes and schemes have been developed under to enforce forest conservation in reserved forests (Bhat et al., 2001). The Joint Forest Management programme is one of them and it was primarily initiated to regeneratethe degraded lands with the help of the local community,in exchange for some proportion of the profit from the sales of timber in the final harvest (Kumar, 2008). Karnataka is one of the first states to initiateJFM during 1993 and Uttara Kannadais one of the districts in which this was carried out.The reforestation programme is dominated by the species *Acacia auriculiformis*. In the district, nearly 7000–9000 ha of forest plantations is raised annually (Murthy et al., 2002).

# Chapter 3: Methodology

## 1. Data Collection

For the purpose of creation of land use maps, Landsat images for the years 1990 and 2000 were acquired from the Landsat website (landsat.org) and Glovis website (glovis.usgs.gov). Both images acquired are of March. For the year 2013, a LISS 4 image was resampled to 30m and made use of.

To create NDVI time-series, MODIS data was downloaded from the years 2000-2012.

Climate data (temperature and rainfall) was downloaded from the GLDAS website of 0.25º resolution.

## 2. Data Processing

### 2.1 Landsat Data

All the data obtained for the purpose of creating land use and land cover maps were georectified based on a LISS 4 image of the same area.

## 3. Image Classification

### 3.1 Field Component

Samples for the land use classes areca, acacia, evergreen forests, semi- evergreen forests, deciduous forests, paddy fields, tree savannahs and grasslands were acquired. Classification was being carried out for Landsat images whose pixel size is 30m. So sample sites were located that were larger than 90m x 90m. For the identification of forest types, the assistance of a forestry student was taken. Forests were classified on the basis of: canopy cover, tree height, presence of canes, tree species, and density of undergrowth.

**Figure 4.1 Acacia Plantations**

**Figure 4.2 Evergreen Forests**

**Figure 4.3 Deciduous Forests**

**Figure 4.4 Paddy Field with Areca Plantation in the Background**

**Figure 4.5 Semi-Evergreen Forests**

**Figure 4.6 GCP Collection in Areca Plantation**

## 3.2 Lab Component

### 3.2.1 Pixel-Based Supervised Classification

*3.2.1.1 Training sets*

Training sets were created with the 'Region Grow' tool in ERDAS using the sample locations. The parameters for creating the training sets using this technique varied for each class based on their spectral characteristics. Around 200 samples were used.

**Table 4.1 Showing the Region Grow Tool Parameters**

| Sr. No. | Land Use Class | Parameter | Threshold |
|---|---|---|---|
| 1. | Areca | Spectral Distance | 8 |
| | | Number of Pixels | 100 |
| 2. | Acacia | Spectral Distance | 10 |
| | | Number of Pixels | 200 |
| 3. | Deciduous Forests | Spectral Distance | 15 |
| | | Number of Pixels | 200 |
| 4. | Evergreen Forests | Spectral Distance | 8 |
| | | Number of Pixels | 200 |
| 5. | Semi-Evergreen Forests | Spectral Distance | 10 |
| | | Number of Pixels | 250 |
| 6. | Grasslands/Barren/ Tree Savannahs | Spectral Distance | 15 |
| | | Number of Pixels | 75 |
| 7. | Paddy Fields (Fallow) | Spectral Distance | 8 |
| | | Number of Pixels | 50 |
| 8. | Paddy Fields (Cultivated) | Spectral Distance | 10 |
| | | Number of Pixels | 50 |

These samples were entered into the Signature Editor following which Transformed Divergence Separability Statistic was estimated for the various classes.

Unsupervised classification was carried out in ERDAS and shadow regions were identified. Water bodies were digitized as there was a lot of mixing with shadow and vegetation classes.

*3.2.1.2 Classification Stage*

Shadow and water bodies were masked out from the image prior to supervised classification using maximum likelihood method. Based on the samples, the image was classified.

### 3.2.2 Accuracy Assessment

Around 200 points were used for carrying out accuracy assessment using the tool provided in ERDAS.

| | | | | |
|---|---|---|---|---|
| 187 | ID#187 | 460942.030 | 1596486.720 | 185 |
| 188 | ID#188 | 467419.680 | 1594306.549 | 185 |
| 189 | ID#189 | 462118.181 | 1595942.141 | 185 |
| 190 | ID#190 | 457817.697 | 1595135.808 | 185 |
| 191 | ID#191 | 453076.368 | 1597131.643 | 11 |
| 192 | ID#192 | 452361.260 | 1597607.094 | 185 |
| 193 | ID#193 | 452091.907 | 1598055.041 | 185 |
| 194 | ID#194 | 452332.719 | 1599995.711 | 185 |
| 195 | ID#195 | 457010.504 | 1602111.500 | 185 |
| 196 | ID#196 | 459624.088 | 1602817.559 | 185 |
| 197 | ID#197 | 459828.823 | 1604773.323 | 185 |
| 198 | ID#198 | 458169.881 | 1606415.258 | 70 |
| 199 | ID#199 | 453030.740 | 1607412.906 | 185 |

**Figure 4.7 Total Number of Samples Used**

### 3.2.2 Object-Oriented Classification

*3.2.2.1 Training Sets*

To develop training sets, first some representative areas were identified in the images and then using 'Region Grow' tool in ERDAS, definitive samples were selected and stored in shapefiles. The same 'Region Grow' tool parameters defined earlier for supervised classification are used.

For the 1990 image, training sets were identified based on visual interpretation of the classes. The training sets for image of the year 2000was located using selected points from the Karnataka State Forest Map and visual interpretation of the image. Ground truth points were collected on field for the year 2013, so these GCPs were used to create training sets.

*3.2.2.2 Segmentation Stage*

The first stage was image segmentation. The figure illustrates the parameters assigned for multi-resolution segmentation. Since I'm classifying vegetation, I gave more weightage to the red and nir bands. Slope is an important criteria in differentiating between various classes and

hence it has been assigned weightage of 2 as well. The maximum size of object has been set as 26 (for year 2013) and 5 (for year 2000) based on trial and error method. 0.9 ensures the object will be very compact and 0.1 shape threshold allows spatial aspect of the image to be included while classifying with maximum importance being given to spectral data.

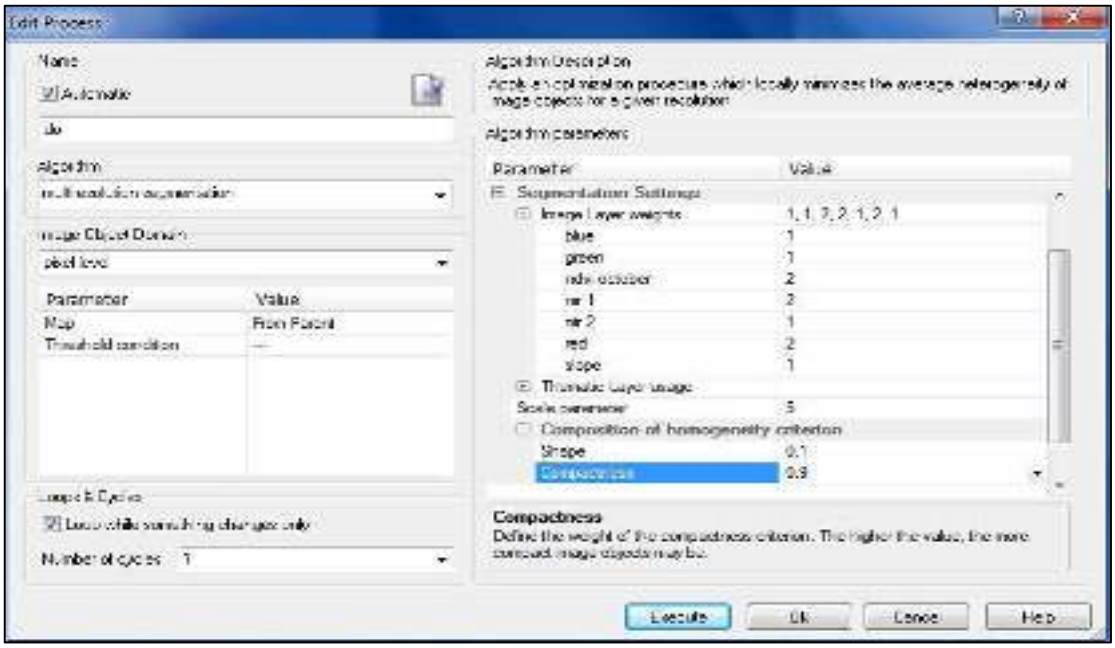


**Figure 4.8 Multiresolution Segmentation Process Showing the Parameters Used**

*3.2.2.3 Classification Stage*

A rule set was created for classification and the nearest neighbourhood algorithm was used for supervised object-oriented fuzzy classification. To further refine the classification, class descriptors have been assigned which act as additional thresholds apart from the ones specified by the samples. Thematic layers such as the digitized water bodies, vectorized shadow class (acquired using unsupervised classification in ERDAS) and a layer specifying areas not included in reserved forests have been used. Further, a slope layer created from a 30m ASTER DEM is stacked along with the main image.

For the year 2000, October and March images were available so an NDVI image from the October one was created and stacked along with March image to improve classification. Similarly, an NDVI image was created from a LISS4 image of the year 2013 and stacked along with the resampled 30m 2013 image.

*3.2.2.3.1 Thresholds*

**Table 4.2**

| Sr. No. | Class | Criteria | Threshold Year 1990 | Threshold Year 2000 | Threshold Year 2013 |
|---|---|---|---|---|---|
| 1. | Fallow* Paddy Fields | Slope | <=10degrees | <=10degree | <=10degrees |
| | | Difference Between March and October Image NDVIs | N.A. | >=0.1 | N.A. |
| | | Mean Green Layer | >=43 | >=39 | >=100 |
| | | Mean Diff to Grasslands/Barren Land (NIR Layer) | Not Defined | >=11 | >=20 |
| 2. | Areca | Slope | <=15degrees | <=15degrees | <=15degrees |
| | | Mean Diff to Paddy Fields (NIR Layer) | >=12 | >=9 | >=40 |
| | | Thematic Object Attribute: Not in Reserved Forests | =1 | =1 | =1 |
| | | Rel. Distance to Paddy Fields | <=300m | <=300m | <=300m |
| | | Shape: Rectangular Fit | >=0.69 | >=0.71 | >=0.67 |
| 3. | Evergreen Forests | NDVI | >=0.6 | >=0.53 | >=0.59 |
| | | Mean Diff to Semi-Evergreen Forests (NIR Layer) | Not Defined | >=12 | >=20 |
| | | Distance to Paddy Fields | >500m | >500m | >500m |
| 4. | Semi-Evergreen Forests | NDVI | <= | <=0.49 | <=0.58 |
| 5. | Deciduous Forests | NDVI | <=0.38 | <=0.43 | <=0.53 |
| | | Difference Between March and October Image NDVIs | N.A | >=0.08 | N.A |
| | | Mean Diff to Grasslands/Barren Land (NIR Layer) | >=13 | >=10 | >=25 |
| 6. | Paddy Fields (Cultiva-ted*) | Slope | <=10degrees | <=10degrees | <=10degrees |
| | | Difference Between March and October Image NDVIs | N.A | >=0.18 | N.A. |
| | | Mean Diff to Grasslands/Barren Land (NIR Layer) | Not Defined | >=13 | >=30 |
| 7. | Water Bodies | Thematic Layer: Number of overlapping objects | =0 | =0 | =0 |
| 8. | Shadow | Thematic Layer: Number of overlapping objects | =0 | =0 | =0 |
| 9. | Disturbed Forests | Distance to Paddy Fields | <=150m | <=150m | <=150m |

| | | | | | |
|---|---|---|---|---|---|
| 10. | Acacia | Thematic Object Attribute: Not in Reserved Forests | =1 | =1 | =1 |
| 11. | Grasslands/Barren Lands | Mean Diff to Fallow Paddy Fields (NIR Layer) | >=13 | >=11 | >=20 |
| | | Difference Between March and October Image NDVIs | N.A | <=0.05 | N.A |
| | | Mean Diff to Cultivated Paddy Fields (NIR Layer) | Not Defined | >=13 | >=30 |

*Paddy fields include fallow land and cultivated land. The spectral range of the class is vast if both are considered together which causes misclassification. So, they have been considered separately and later merged into one class.

Since fuzzy classification is being carried out, a minimum membership function of 0.6 has been set to reduce misclassification. Once the classification was carried out, any visually identifiable misclassifications have been rectified using manual recoding of objects with the help of the fuzzy membership values.

*3.2.2.4 Accuracy Assessment*

A tool provided in eCognition was used to perform this stage by providing sample polygons foreach class. A confusion matrix is created and overall accuracy along with the Kappa coefficient wasestimated.

### 3.2.3Change Detection

Prior to change detection, the images were converted to raster and then imported into IDRISI.

This was carried out in IDRISI software using the Cross Tabulation Method.

# 4. Time-Series Data Modelling

### 4.1 MODIS Data

The MODIS data obtained was converted from HDF format to GeoTIFF, using the 'HEG' tool. The data were then stacked in ArcGIS using the tool 'Composite Bands', clipped based on the study area and converted into a point shapefile. Based on the classification of Landsat images, areas for each land use class that show no change since the year 2000 were identified and the stored in point shapefiles. These were used for extraction of MODIS pixels for each class using the tool 'Sample' in ArcGIS. On extraction, the data was exported to Excel and further organized such that all the NDVI time-series values appear in a single column.

Additional columns of Month and Year are added to the NDVI time-series values to improve clarity of the dataset.

## 4.2. Climate Data

An objective of the project is to understand the seasonality and trends in temperature and rainfall time-series data between 2001 -2012 and then subsequently compare these trends to those observed in MODIS NDVI time-series data. The first step to achieve this is to extract time-series information from climate data.

### *4.2.1 Model for Batch Conversion of netCDF Files to Shapefiles*

The climate data acquired were converted from netCDF format to point Shapefiles as this is the required format for further data processing. The model iterates through all the files in the folder. Each file is first converted to a raster layer using 'Make NetCDF Raster Layer'. The 'Copy Raster' tool is used to convert the raster layer into the TIFF format and subsequently, the file is clipped to the required extent. The clipped file is then reprojected to UTM/WGS84 North Zone 43 and 'Raster to Point' tool is used finally to give the desired output. Usage of the Model tool 'Parse Path' allows for the output to be saved with the same path name as the input. Once the model has produced 1 output, it will iterate through the remainder of the files in the folder till there are no more input files that have been processed.

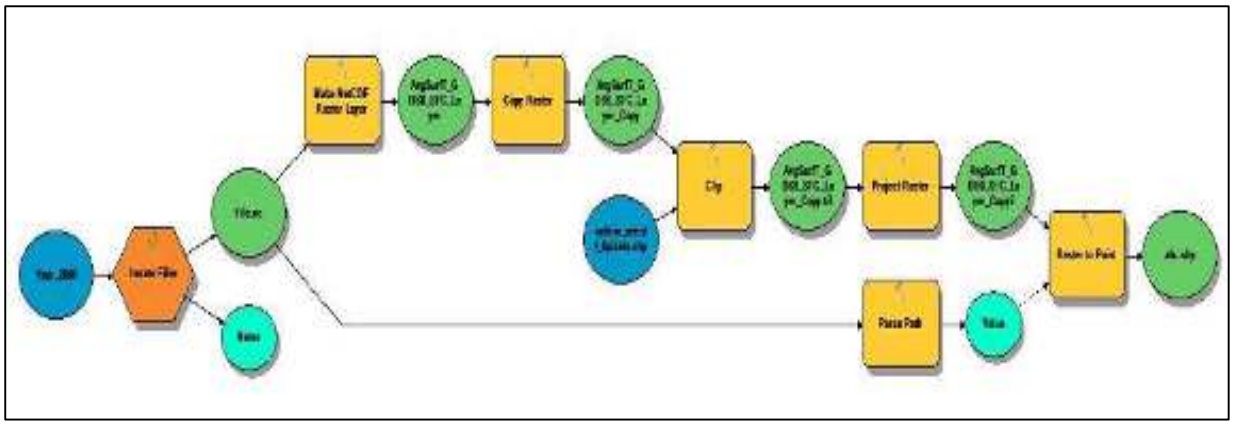


**Figure 4.9 Model for Batch Conversion of netCDF files to Shapefiles**

### *4.2.2 Weighted Average*

Since the resolution of the climate data is 0.25 degrees and that of the MODIS data is 250m, a weighted average method was applied to interpolate climate data values at each MODIS pixel location. For this analysis, the weights used were the distance of centroid of each MODIS pixel to the centroids of the climate variable pixels.

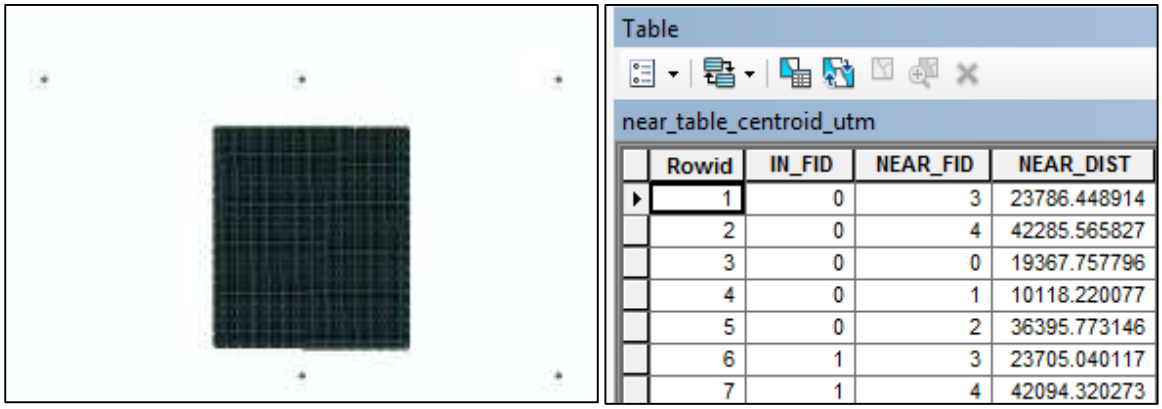

Table

near_table_centroid_utm

| Rowid | IN_FID | NEAR_FID | NEAR_DIST |
|---|---|---|---|
| 1 | 0 | 3 | 23786.448914 |
| 2 | 0 | 4 | 42285.565827 |
| 3 | 0 | 0 | 19367.757796 |
| 4 | 0 | 1 | 10118.220077 |
| 5 | 0 | 2 | 36395.773146 |
| 6 | 1 | 3 | 23705.040117 |
| 7 | 1 | 4 | 42094.320273 |

**Figure 4.10 MODIS Pixel and 5 Temperature PixelNear Table**

**Centroids**

The distance calculation was done using 'GenerateNear Table' in ArcGIS. This table is subsequently exported to Excel. Temperature data was added to this and the following formula was applied to the data.

$$\bar{x}_w = \frac{\sum_{i=1}^{n}(w_i x_i)}{\sum_{i=1}^{n}(w_i)}$$

where as

$\bar{x}_w$ is the weighted mean variable

$w_i$ is the allocated weighted value

$x_i$ is the observed values.

H6 =SUM(G2:G6)/SUM($B2:$B6)

| | A | B | C | D | E | F | G | H | I | J |
|---|---|---|---|---|---|---|---|---|---|---|
| 1 | near_tab_ | x | y | dist | POINTID | Temperature | Weights*Observations | Weighted Average | POINTID | Temperature |
| 2 | 3 | 469353 | 1609670 | 21917.92 | 4 | 299.11999512 | 140392880.8 | | 4 | 300.35000610 |
| 3 | 4 | 469353 | 1609670 | 26872.81 | 5 | 297.17001343 | 139477650.9 | | 5 | 298.57000732 |
| 4 | 0 | 469353 | 1609670 | 37344.28 | 1 | 300.27999878 | 140937332 | | 1 | 301.42999268 |
| 5 | 1 | 469353 | 1609670 | 11888.74 | 2 | 297.73001099 | 140937332 | | 2 | 299.38000488 |
| 6 | 2 | 469353 | 1609670 | 19572.8 | 3 | 296.95999146 | 139379[illegible],5 | 298.7619995 | 3 | 298.51998901 |
| 7 | 3 | 467988.5 | 1598526 | 11761.35 | | 297.12399903 | 139984721.9 | | | |
| 8 | 4 | 467988.5 | 1598526 | 21323.6 | | 296.74799805 | 139072152.9 | | | |
| 9 | 0 | 467988.5 | 1598526 | 39840.47 | | 296.37199708 | 140527590.3 | | | |
| 10 | 1 | 467988.5 | 1598526 | 20214.44 | | 295.99599610 | 140527590.3 | | | |
| 11 | 2 | 467988.5 | 1598526 | 26925.64 | | 295.61999512 | 138973865 | 298.7619995 | | |
| 12 | 3 | 467761.1 | 1597162 | 10622.61 | | | | | | |
| 13 | 4 | 467761.1 | 1597162 | 21015.28 | | | | | | |
| 14 | 0 | 467761.1 | 1597162 | 40298.28 | | | | | | |
| 15 | 1 | 467761.1 | 1597162 | 21395.05 | | | | | | |
| 16 | 2 | 467761.1 | 1597162 | 28045.5 | | | | | | |
| 17 | 3 | 468443.4 | 1596707 | 10828.81 | | | | | | |

**Figure 4.11 Weighted Average in Excel**

As shown in the above figure, weighted average at location 1609670 (X) and 21917.92 (Y) =

**[($D2*F$2) + ($D3*F$3) + ($D4*F$4) + ($D5*F$5) + ($D6*F$6)] / [$D2+$D3+$D4+$D5+$D6]**

This formula is then dragged to the remainder of the cells and the values are further organized. Using the locations of various land use classes, temperature time-series data is extracted. The same process is repeated for rainfall data.

## 4.3 Time-Series Data Analysis Using R

Before importing data to this software, all the time-series data (NDVI, temperature and rainfall) for each land use class was entered into the same data sheet in .txt format. The following code was used to create the Structural Time-Series model which was later analysed:

```
ts<-read.table("D:/MODIS_RF_T/Acacia_TS.txt",header=T)

summary(ts)

Aca_N1<-ts(ts$N1,frequency=5, start=c(2001))

ts.plot(Aca_N1)

St_Aca_N1<-StructTS(Aca_N1,type="BSM")
```

**fitted(St_Aca_N1)**

**plot(fitted(St_Aca_N1))**

This is an example for creating a Structural Time-Series Model for the Acacia NDVI data. This was repeated for rainfall and temperature for all the sample locations for all land use classes.

Once the structural model is obtained, the trend and seasonality of NDVI is analysed. To further understand the changes occurring in NDVI, it was analysed along with the structural models of rainfall rate and temperature.

Time-series of the complete rainfall and temperature data were also modelled to observe the trends in the data.

# Chapter 5 Results and Discussion

## 2. Data Collection

The Landsat images downloaded were acquired in March as those were the only images available for the study area for the given years. For the year 2000, an October image was also available so it was acquired as well and subsequently used along with the March image for analysis. For the year 2010, the Landsat ETM+ and freely downloadable LISS3 images were available but they these images had the problem of striping and more than 50% cloud cover respectively. Due to these radiometric complications, a LISS 4 image was resampled to 30m and used. During classification, this image was stacked along with LISS4 5m data to improve analysis.

Next the MODIS data was downloaded. MODIS data for the months June to October were not acquired as these images had a higher percentage of cloud cover. Some other data containing a higher percentage of cloud cover were also excluded. Climate data was acquired in the netCDF format.

## 3. Data Processing

### 2.1 Landsat Data

Both images of the year 2000 were corrected as required and around 11 GCPs were used for this process The RMS errors were: 0.0054 and 0.0035 for the October and March images respectively. Some problems were encountered while georeferencing the 1990 image. 33 GCPS were used for this task and an RMS error of 0.0027 was achieved but the image still showed a shift from the LISS 4 image. After several unsuccessful attempts to rectify it, the image with the shift was used.

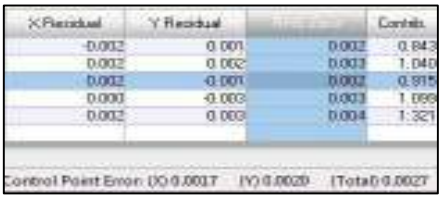


**Figure 5.1 RMS Error in Georeferencing the Landsat 1990 image**

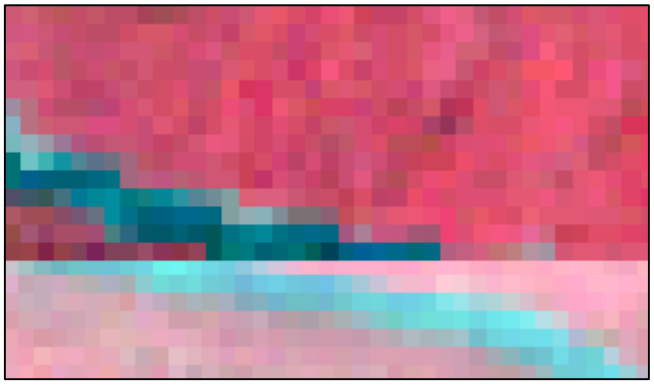

**Figure 5.2 Shift in the Position of Pixel (the darker image is Landsat 1990 and lighter image is the properly georeferenced Landsat 2000)**

## Image Classification

### 3.1 Field Component

Sample locations were around 270 in all for: areca, acacia, paddy, bamboo, sugarcane fields, soppinabetta lands, evergreen forests, semi-evergreen forests, deciduous forests and grasslands.

**Figure 5.3 GCP Locations collected for Training the Classifier**

While on field, many regions of the landscape could not be accessed due to lack of road connectivity and presence of dense forests. Before going on field, a method of identifying a homogenous land cover of size 90mX90m was devised. This ideal site was rarely encountered. The sample sites were mostly of irregular quadrilateral sizes. While taking GPS

readings, it was ensured that the accuracy was 3-4m. Also, at every location, a radius of 40-50m had the same land cover type. This way, even if the ideal 90mx90m was not acquired, legitimate samples were acquired. Some classes have not been considered for classification if the number of samples were too few to train the classifier or if a class has a broad spectral range like soppinabetta lands leading to misclassification. One suggestion was to mask out the soppinabetta lands from the classification using forest maps. Unfortunately, maps of only the year 2000 was available, so this class was not considered.

## 3.2 Lab Component

### 3.2.1 **Pixel-Based Supervised Classification**

*3.2.1.1 Training Sets*

Using the region growing technique in ERDAS, training sets were generated. This process was repeated several times to ensure pure, representative pixels were being used for classification.

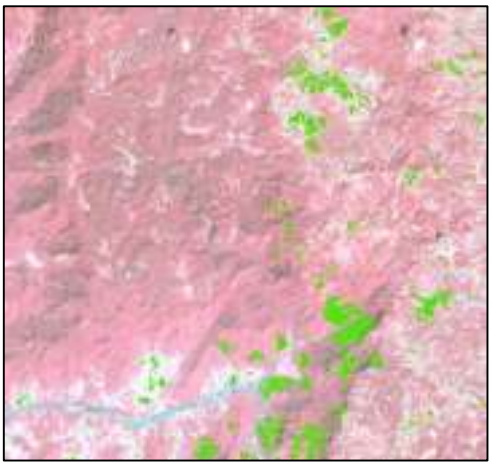

**Figure 5.4 Samples Selected in ERDAS**

Transformed Divergence was used to assess class separability between the various samples. If the index is above 1500, the classes show good separability. The image on the following page shows the matrix of the TD separability index. Spectrally, the samples are quite distinct from each other and display no mixing except for Areca and Acacia.

Separability CellArray

Distance Measure: Transformed Divergence
Using Layers: 1 2 3 4 5 6 7
Taken 7 at a time
Best Average Separability: 1923.4
Combination: 1 2 3 4 5 6 7

| Signature Name | | 1 | 2 | 3 | 4 | 5 | 6 | 7 | 8 | 9 | 10 |
|---|---|---|---|---|---|---|---|---|---|---|---|
| Acacia | 1 | 0 | 1955.05 | 1956.43 | 1970.45 | 2000 | 1998.92 | 2000 | 2000 | 1240.96 | 1998.68 |
| Deci | 2 | 1955.05 | 0 | 1991.01 | 1307.3 | 2000 | 1999.07 | 2000 | 2000 | 1990.03 | 1999.07 |
| Evergreen | 3 | 1956.43 | 1991.01 | 0 | 2000 | 2000 | 2000 | 1999.95 | 1999.95 | 1999.92 | 1999.99 |
| Grasslands/Barren | 4 | 1970.45 | 1997.9 | 2000 | 0 | 1998.37 | 1976.32 | 2000 | 2000 | 1999.68 | 1997.72 |
| Paddy Dry | 5 | 2000 | 2000 | 2000 | 1998.37 | 0 | 1500.19 | 2000 | 2000 | 2000 | 1999.68 |
| Paddy Green | 6 | 1998.92 | 1999.87 | 2000 | 1976.32 | 1500.19 | 0 | 2000 | 2000 | 2000 | 1999.4 |
| Semi | 7 | 2000 | 2000 | 1999.95 | 2000 | 2000 | 2000 | 0 | 0 | 2000 | 2000 |
| Shadow | 8 | 2000 | 2000 | 1999.95 | 2000 | 2000 | 2000 | 0 | 0 | 2000 | 2000 |
| Areca | 9 | 1240.96 | 1990.03 | 1990.02 | 1999.03 | 2000 | 2000 | 2000 | 2000 | 0 | 1999.99 |
| Water | 10 | 1998.68 | 1999.07 | 1999.99 | 1997.72 | 1999.68 | 1999.4 | 2000 | 2000 | 1999.99 | 0 |

**Figure 5.5 Transformed Divergence (TD) Separability Statistic**

*3.2.1.2 Classification Stage*

On carrying out supervised classification, the land use map was dervied. The map for year 2000 has been shown.

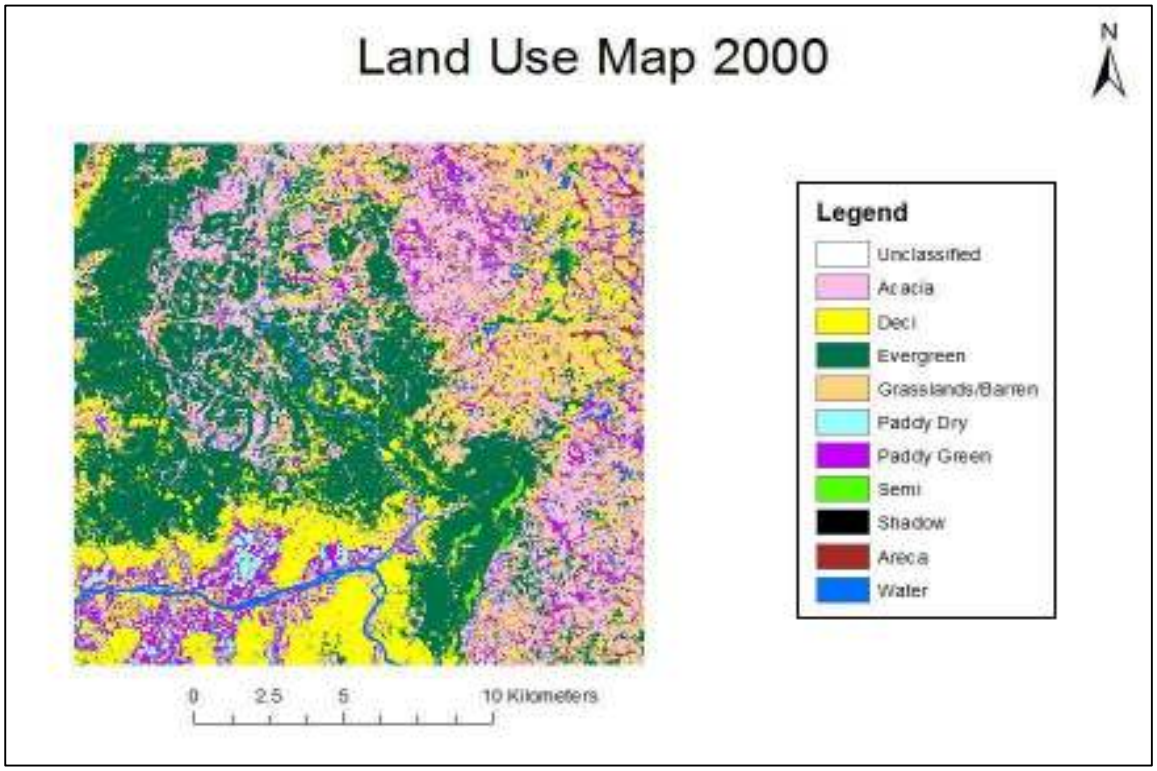


**Figure 5.6 Land Use Map 2000**

*3.2.1.3 Accuracy Assessment*

This was carried out in ERDAS with overall classification accuracy as 71.06% and a Kappa Statistic of 0.6875.

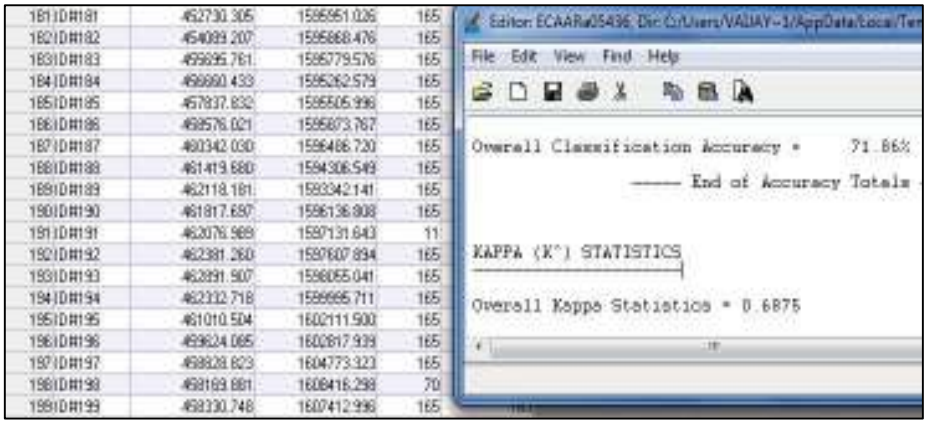


**Figure 5.7 Accuracy Assessment of Pixel-Based Supervised Classification Technique with Total Number of Samples used in the background.**

Although the accuracy is high, I can visually identify some major misclassifications. For example, the presence of Acacia plantations and Areca in reserved forests, classification of grasslands on paddy fields. This prompted me to use a rule based technique to classify my images.

### 3.2.2 Object-Oriented Classification

*3.2.2.1 Segmentation Stage*

The resulting segmented image was able to define objects as desired.

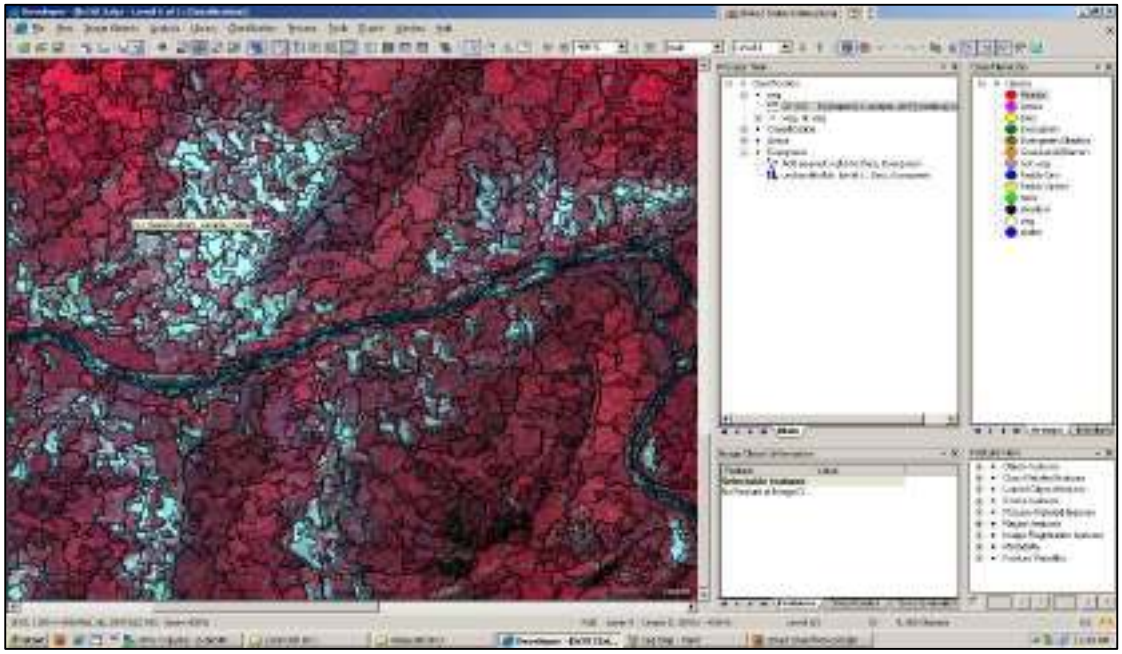

**Figure 5.8 Segmented 2013 Image**

*3.2.2.2 Training Sets*

Samples created in ERDAS were imported to eCognition and instructed by the rules to use them used as training sets. Samples were also generated by using the tools available in

eCognition like 'Sample Selection Information Tool'. This assist the user in selecting the most appropriate samples for classification.

| Class | Membership | Minimum Dist | Mean Dist | Critical Samples | Number of |
|---|---|---|---|---|---|
| Paddy Dry | 1.000 | 0.000 | 696.987 | | 21 |
| | | | | | |
| Deci | 0.000 | 72.156 | 352.998 | 0 | 186 |
| Evergreen | 0.000 | 74.058 | 592.389 | 0 | 106 |
| Areca | 0.000 | 90.230 | 375.435 | 0 | 40 |
| Grasslands/Barren | 0.000 | 118.747 | 392.220 | 0 | 41 |
| Semi | 0.000 | 151.229 | 411.401 | 0 | 62 |
| Acacia | 0.000 | 280.950 | 400.862 | 0 | 25 |
| Paddy Green | 0.000 | 335.627 | 512.321 | 0 | 13 |

**Figure 5.9 Sample Selection Information Tool**

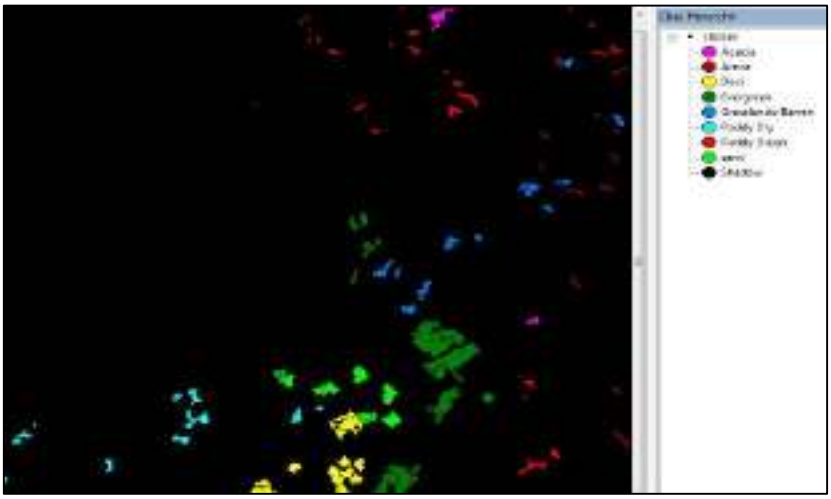

**Figure 5.10 Samples for the Year 2013**

Once the ruleset was run and the classification was generated, the result was examined using the fuzzy classifier membership values to see if my classification has happened as desired. Misclassifications were manually recoded to the desired class.

Image Object Information

| | Value |
|---|---|
| **Current Classificati...** | |
| Semi | 0.972 |
| Acacia | 0.923 |
| | |
| **Alternative Assign...** | **Value** |
| Semi | 0.972 |
| Acacia | 0.923 |
| Evergreen | 0.000 |
| Areca | 0.000 |
| Not Veg | 0.000 |
| Paddy Dry | 0.000 |
| Paddy Green | 0.000 |
| Grasslands/Barren | 0.000 |
| Deci | 0.000 |
| Shadow | 0.000 |
| Veg | 0.000 |
| Water | 0.000 |

**Figure 5.11 Rule Set for Image of Year 2000**

*3.2.2.3 Classification Stage*

First step was the creation of water and shadow masks.

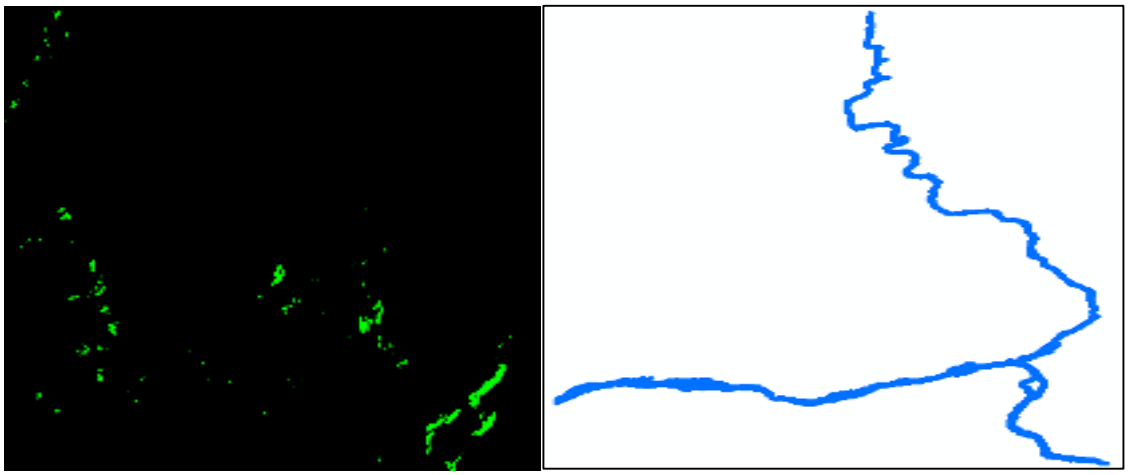

**Figure 5.12 Extracted Shadow and Water Regions**

The image was then classified using the supervised fuzzy classification technique using the following rule set.

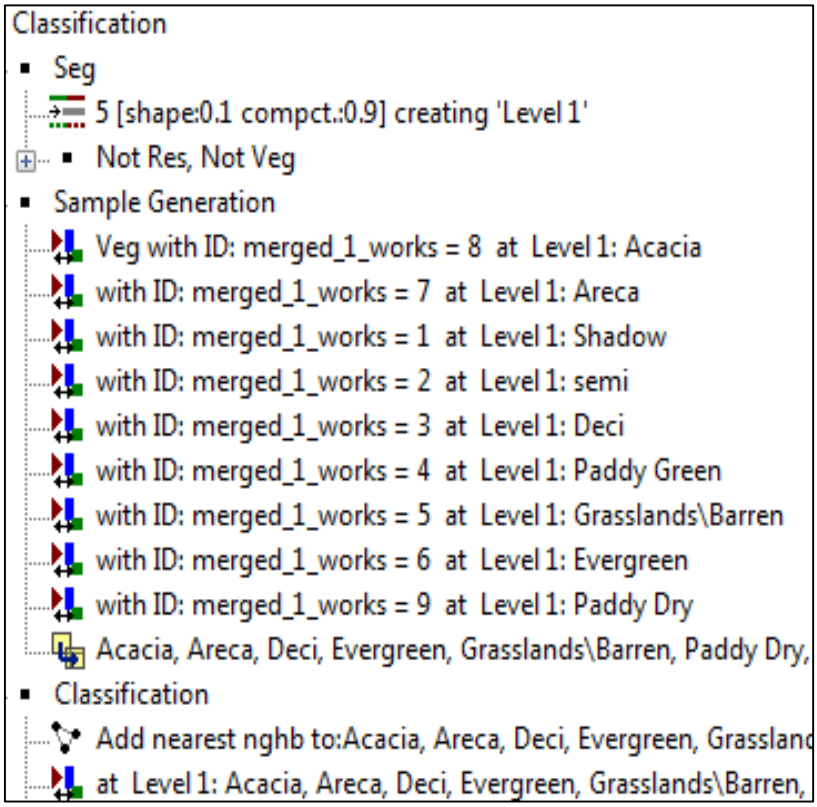


**Figure 5.13 Ruleset for Year 2000**

**Classification Results**

Problems were faced while classifying the 1990 image. There was spectral mixing between semi-evergreen, evergreen and deciduous forests and between grasslands/barren land/tree

savannahs and paddy fields. Setting a threshold to define these classes without any reference map or ground truth points proved to be difficult. Without a reference map, the accuracy assessment would also be based on visually interpretation of the image. This would have led to an element of uncertainty as to the reliability of the image and hence it was this image was discarded from analysis.

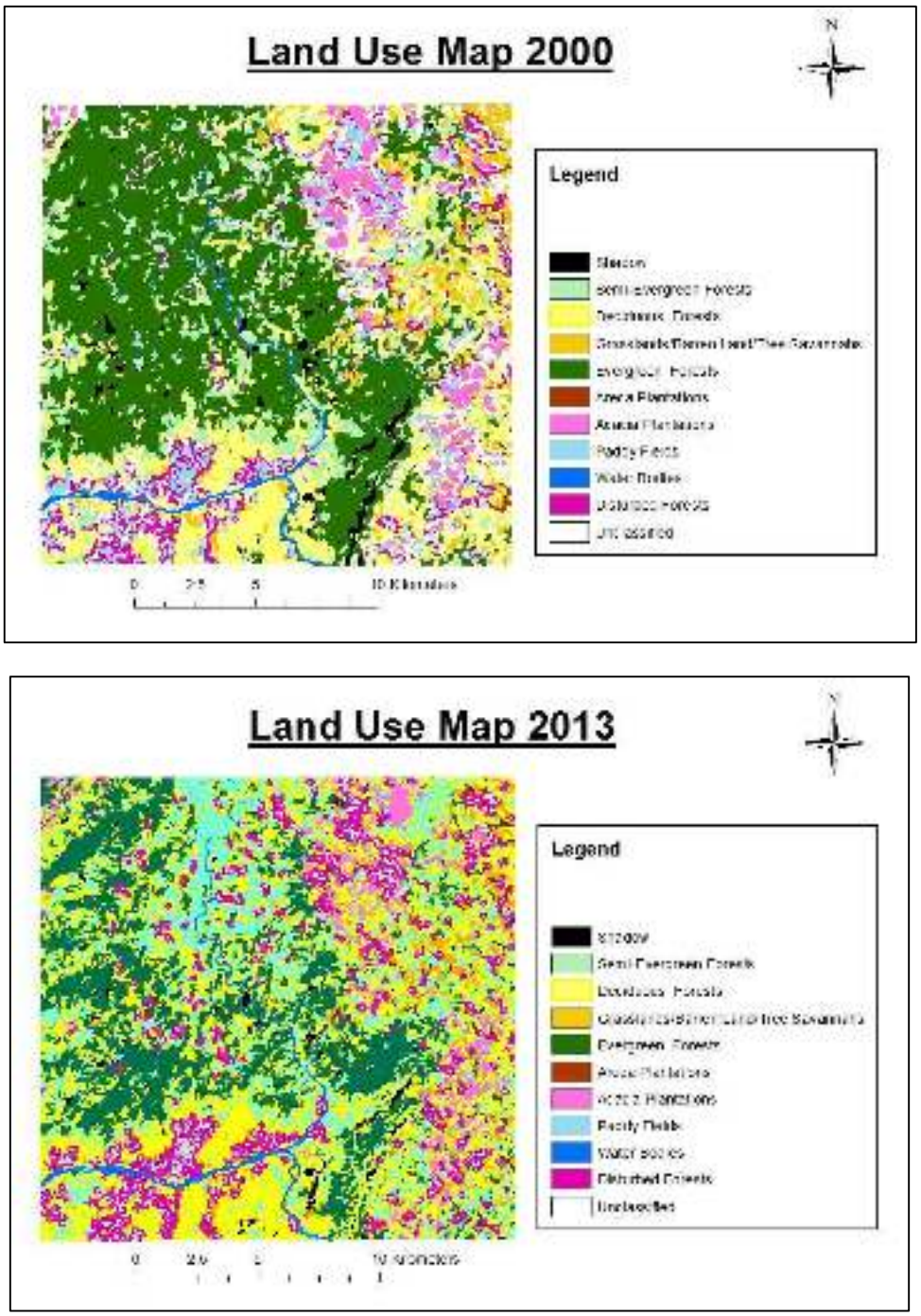


**Figure 5.14 Land Use Map 2000 and Land Use Map 2013**

*3.2.2.4 Accuracy Assessment*

The accuracy assessment was carried out in eCognition itself and the results are displayed in the images below.

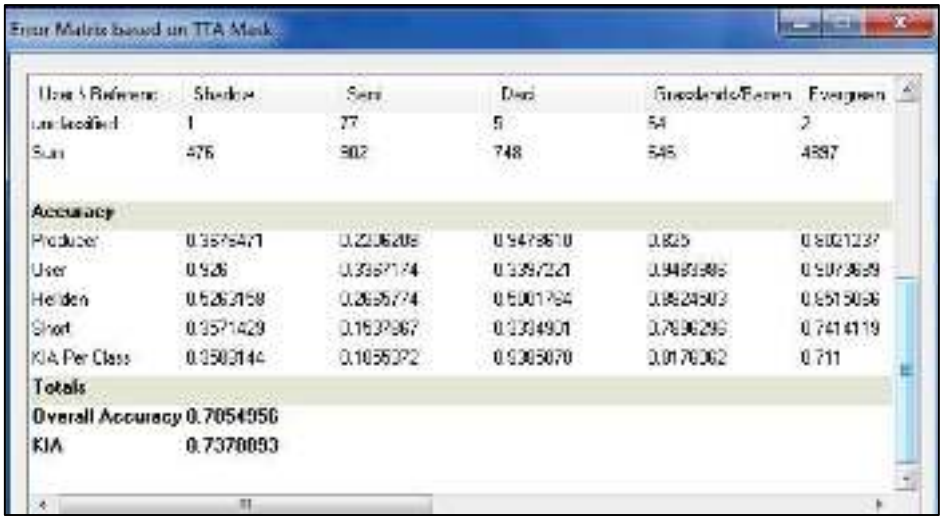


**Figure 5.15 Accuracy Assessment for Year 2000**

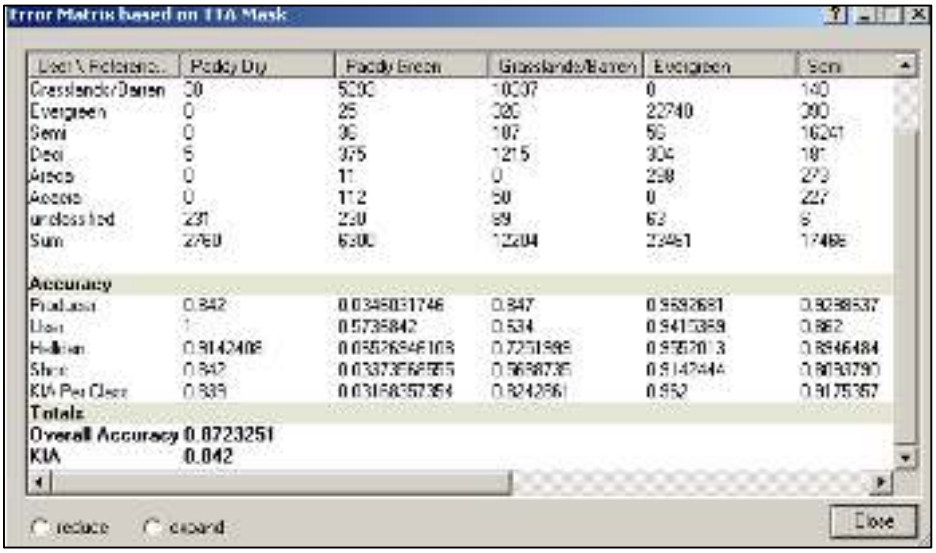


**Figure 5.16 Accuracy Assessment for Year 2013**

### 3.2.3 Change Detection

**Percentage Change Analysis**

The significant classes have been taken for this analysis. Since the focus of the project is forests and argo-ecosystems, the change in their land use has been inspected.

**Table 5.1 Percentage Increase/Decrease per Class**

| LandUse | 2000 Area (ha) | 2013Area (ha) | Percentage Increase/Decrease (%) |
|---|---|---|---|
| **Semi-Evergreen Forests** | 2819.083235 | 7378.765 | 161.7434246 |
| **Deciduous Forests** | 6518.668256 | 13008.635 | 99.55970282 |
| **Evergreen Forests** | 14213.29915 | 8038.415 | -43.44441134 |
| **Areca Plantations** | 213.2614776 | 397.0675 | 86.1881032 |
| **Acacia Plantations** | 1557.908892 | 1417.3175 | -9.024365454 |
| **Paddy Fields** | 2214.772227 | 859.4375 | -61.19521956 |

Using ArcGIS, the areas of classes were computed and the change percentage was calculated. The results indicate that there is a significant increase the area of deciduous and semi-evergreen forests. There is a huge drop in the area under evergreen forests and paddy fields. Areca has increased in area over the years with a 9% drop observed in Acacia plantations.

**Cross Tabulation**

For the purpose of change detection, the vector maps were converted to raster format. The 'Cross Tab' method used for change detection resulted in a change map and a data sheet which indicated how many pixels of one class changed or did not change to another class.

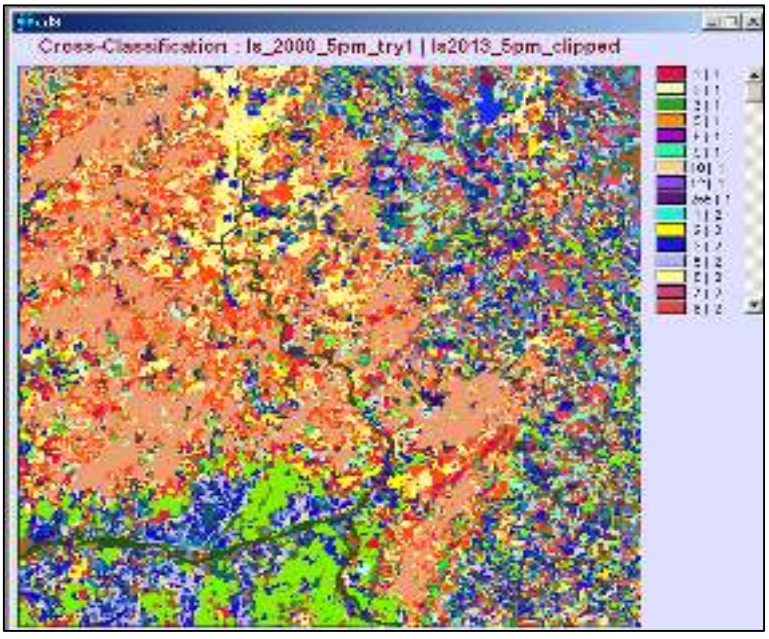


**Figure 5.17 Change Map**

Since there are 11 classes on each land use map, 121 combinations of change variables are depicted in the map. In IDRISI, only the land use changes that we are interested in observing may selected and visualized.

**Table 5.2 Percentage Change from One Class to Another**

| Land Use | Semi-Evergreen (%) | Deciduous (%) | Evergreen (%) | Areca (%) | Acacia (%) | Paddy Fields (%) |
|---|---|---|---|---|---|---|
| **Semi-Evergreen** | 33.86172 | 24.46873 | 22.32005 | 18.621269 | 7.295581 | 6.08075040 |
| **Deciduous** | 40.25682 | 52.63426 | 27.90609 | 20.050441 | 37.93209 | 16.6639478 |
| **Evergreen** | 20.39260 | 7.321852 | 45.24717 | 11.559478 | 3.592334 | 1.71696574 |
| **Areca** | 0.454734 | 1.760777 | 0.201721 | 34.678436 | 0.634666 | 28.955954 |
| **Acacia** | 0.739744 | 2.377601 | 0.810692 | 0.0840689 | 36.90923 | 1.7740619 |
| **Paddy Fields** | 0.166522 | 0.494011 | 0.163026 | 0.4623791 | 0.449812 | 19.796084 |

33.8% of Semi-Evergreen forests have remained from the year 2000 until now. 40% have changed to deciduous forests and 20% seems to have been converted to evergreen forests. Changes have been observed in conversion of deciduous forests to other classes. The largest change is to semi-evergreen forests by 24% and a change to evergreen forests has also been seen by 7%. A small percentage of change is reported to Acacia class. Nearly 50% of the evergreen forests have been converted to semi-evergreen forests or deciduous forests. The areas that are steep show undisturbed evergreen forests even now.

The degradation in forest type maybe due to increased anthropogenic activity with increased disturbance in forests observed in areas with gentle slope. Another hypothesis is that extreme rainfall events may be a factor responsible for the degeneration in vegetation quality. Extreme rain events cause soil erosion and also longer drier periods. Without the optimum conditions for growth, there is a subsequent conversion of forest type. An 'upgradation' in forest type maybe due to favourable climatic conditions with low human activity in the region. Another factor maybe misclassification of pixels as these classes are spectrally close.

The Areca plantations show a 50% change to the forest classes. Acacia shows maximum conversion to deciduous forests and then semi-evergreen forests. Even though the earlier table shows that there is an 89% increase in the area under Areca, the latter table doesn't display such a significant conversion. Through literature review, it is understood that increased percentage value may in fact reflect reality and that there may be some misclassification of Areca.

Acacia plantations are shown to be converted to deciduous forests by around 40%. For an Acacia plantation to be converted to a deciduous forest is unlikely. Recently planted Acacia

may resemble the dry forest or a mature Acacia plantation may be confused for a deciduous forest that hasn't shed its leaves. Either way, I am attributing this conversion in forest type to misclassification.

Paddy fields show a maximum conversion to Areca plantation. This increase is consistent with the increase in the area under Areca plantation in 2013. A conversion to deciduous forest is unlikely and may be attributed to misclassification.

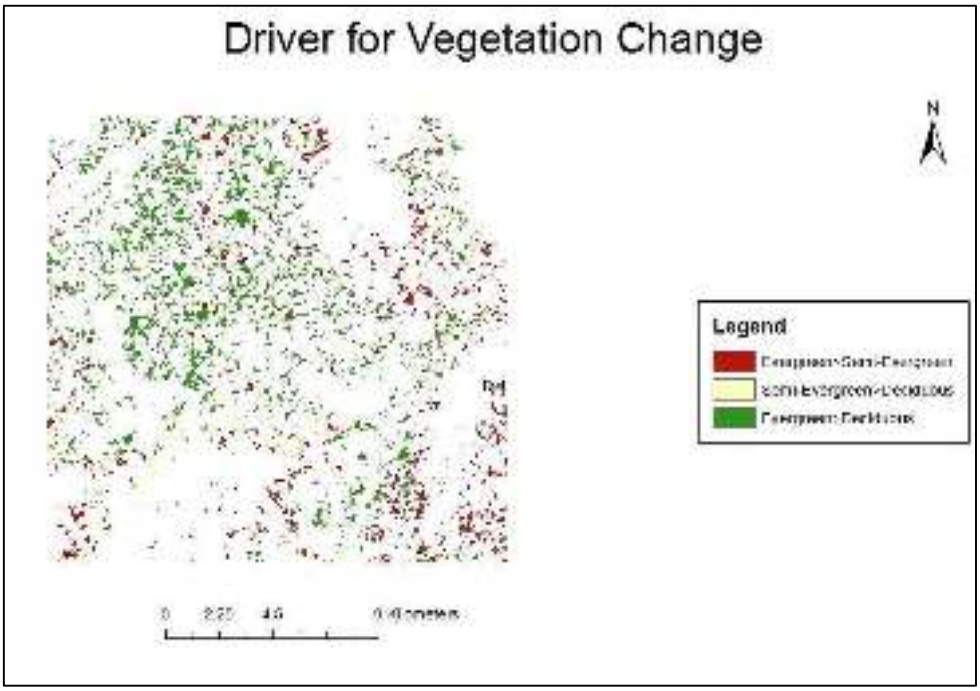


**Figure 5.18 Driver for Vegetation Change**

The above map shows the change that have occurred from evergreen to semi-evergreen and deciduous forests and from semi-evergreen to deciduous forests in regions with less slope. These regions may show the conversion to another forest type maybe be due to human disturbances.

# 4.Time-Series Data Modelling

## 4.1 MODIS Data

The MODIS data was converted to GeoTIFF format, stacked together, clipped to the required extent and converted into point shapefile (to be used later in the project).

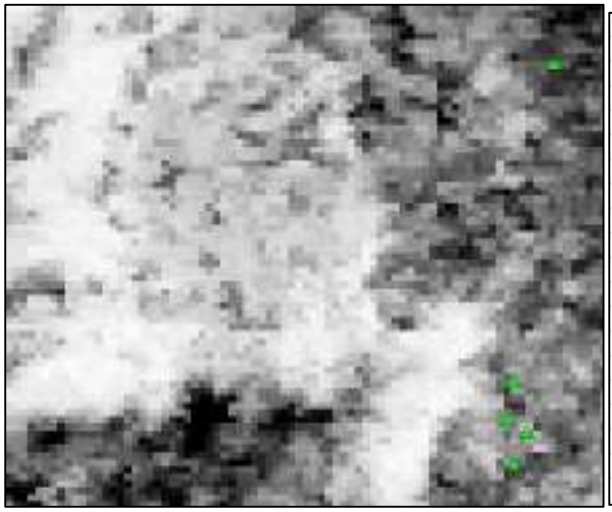

| Year | Month | N1 | N2 | N3 | N4 | N5 |
|---|---|---|---|---|---|---|
| 2000 | nov | 6875 | 7781 | 7768 | 7844 | 7228 |
| 2000 | dec | 7278 | 7822 | 7931 | 7679 | 7383 |
| 2001 | jan | 6987 | 7729 | 7785 | 7827 | 7561 |
| 2001 | feb | 6213 | 7618 | 7565 | 7502 | 7157 |
| 2001 | mar | 6150 | 7020 | 7375 | 7670 | 6570 |
| 2001 | nov | 7419 | 7675 | 7907 | 7978 | 7150 |
| 2001 | dec | 7102 | 7924 | 7712 | 7425 | 7400 |
| 2002 | jan | 6989 | 7810 | 7901 | 7565 | 7407 |
| 2002 | feb | 6305 | 7137 | 8104 | 7803 | 7319 |
| 2002 | mar | 5708 | 7145 | 7307 | 7407 | 7004 |
| 2002 | nov | 7519 | 7931 | 8281 | 8067 | 7815 |
| 2002 | dec | 7067 | 7615 | 7759 | 7682 | 7456 |
| 2003 | jan | 6959 | 6255 | 7763 | 7675 | 6662 |
| 2003 | feb | 7208 | 7610 | 8004 | 7999 | 7605 |
| 2003 | mar | 6968 | 8039 | 7417 | 7903 | 7089 |
| 2003 | nov | 7356 | 7890 | 8133 | 8314 | 7840 |
| 2003 | dec | 7208 | 7610 | 8004 | 7999 | 7605 |
| 2004 | jan | 6990 | 7827 | 7970 | 7659 | 7576 |
| 2004 | feb | 6783 | 7468 | 7821 | 7820 | 6503 |

**Figure 5.19 The left image shows the samples of Areca on MODIS data and the right image shows the extracted and organized values in an Excel sheet**

Using the land use classification maps, areas that have same land cover class since 2000, were identified and the NDVI values from MODIS were extracted. This data was then exported to Excel and organized as shown in the image above.

## 4.2 Climate Data

### *4.2.1 Model for Batch Conversion of netCDF Files to Shapefiles*

The product of the model was288point shapefiles of climate data clipped to the size of the study area and were projected to UTM/WGS 84.

### *4.2.2 Weighted Average*

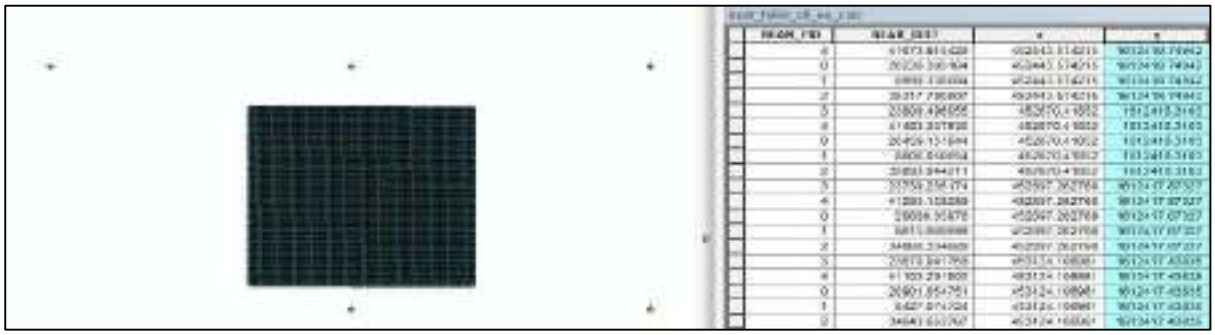

**Figure 5.20 Near Table Showing the Distance Weightage(Labelled as NEAR_DIST) Between the 5 Temperature Pixels and Multitude of MODIS pixels**

Before carrying out a weighted average, the data had to be processed. The result of which is shown in a table with the desired distance weightage between the MODIS pixel centroids and Climate data pixel centroids, the co-ordinates of the MODIS pixel centroids and the Point IDs of the climate data pixel centroids.

Once this data is exported to Excel and the weighted average is calculated for temperature is estimated, the same processing is done for rainfall rate. All this data was then combined based on land use class and visualized as below where N represents NDVI, RF is rainfall rate and T is temperature. This data is then saved in .txt format so as to be input into R.

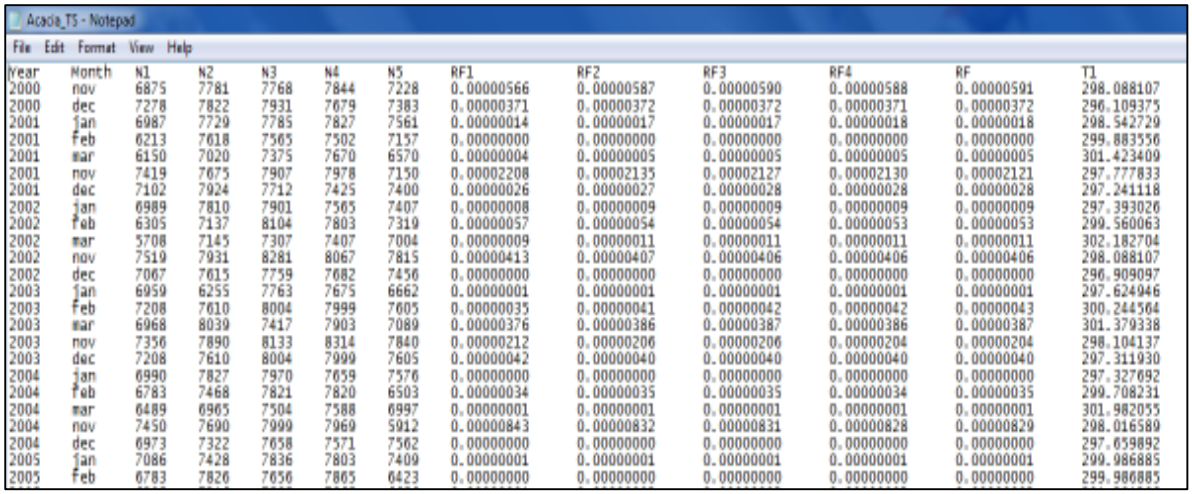
Acacia_TS - Notepad

File Edit Format View Help

| Year | Month | N1 | N2 | N3 | N4 | N5 | RF1 | RF2 | RF3 | RF4 | RF | T1 |
|---|---|---|---|---|---|---|---|---|---|---|---|---|
| 2000 | nov | 6875 | 7781 | 7768 | 7844 | 7228 | 0.00000566 | 0.00000587 | 0.00000590 | 0.00000588 | 0.00000591 | 298.088107 |
| 2000 | dec | 7278 | 7822 | 7931 | 7679 | 7383 | 0.00000371 | 0.00000372 | 0.00000372 | 0.00000371 | 0.00000372 | 296.109375 |
| 2001 | jan | 6987 | 7729 | 7785 | 7827 | 7561 | 0.00000014 | 0.00000017 | 0.00000017 | 0.00000018 | 0.00000018 | 298.542729 |
| 2001 | feb | 6213 | 7618 | 7565 | 7502 | 7157 | 0.00000000 | 0.00000000 | 0.00000000 | 0.00000000 | 0.00000000 | 299.883556 |
| 2001 | mar | 6150 | 7020 | 7375 | 7670 | 6570 | 0.00000004 | 0.00000005 | 0.00000005 | 0.00000005 | 0.00000005 | 301.423409 |
| 2001 | nov | 7419 | 7675 | 7907 | 7978 | 7150 | 0.00002208 | 0.00002135 | 0.00002127 | 0.00002130 | 0.00002121 | 297.777833 |
| 2001 | dec | 7102 | 7924 | 7712 | 7425 | 7400 | 0.00000026 | 0.00000027 | 0.00000028 | 0.00000028 | 0.00000028 | 297.241118 |
| 2002 | jan | 6989 | 7810 | 7901 | 7565 | 7407 | 0.00000008 | 0.00000009 | 0.00000009 | 0.00000009 | 0.00000009 | 297.393026 |
| 2002 | feb | 6305 | 7137 | 8104 | 7803 | 7319 | 0.00000057 | 0.00000054 | 0.00000054 | 0.00000053 | 0.00000053 | 299.560063 |
| 2002 | mar | 5708 | 7145 | 7307 | 7407 | 7004 | 0.00000009 | 0.00000011 | 0.00000011 | 0.00000011 | 0.00000011 | 302.182704 |
| 2002 | nov | 7519 | 7931 | 8281 | 8067 | 7815 | 0.00000413 | 0.00000407 | 0.00000406 | 0.00000406 | 0.00000406 | 298.088107 |
| 2002 | dec | 7067 | 7615 | 7759 | 7682 | 7456 | 0.00000000 | 0.00000000 | 0.00000000 | 0.00000000 | 0.00000000 | 296.909097 |
| 2003 | jan | 6959 | 6255 | 7763 | 7675 | 6662 | 0.00000001 | 0.00000001 | 0.00000001 | 0.00000001 | 0.00000001 | 297.624946 |
| 2003 | feb | 7208 | 7610 | 8004 | 7999 | 7605 | 0.00000035 | 0.00000041 | 0.00000042 | 0.00000042 | 0.00000043 | 300.244564 |
| 2003 | mar | 6968 | 8039 | 7417 | 7903 | 7089 | 0.00000376 | 0.00000386 | 0.00000387 | 0.00000386 | 0.00000387 | 301.379338 |
| 2003 | nov | 7356 | 7890 | 8133 | 8314 | 7840 | 0.00000212 | 0.00000206 | 0.00000206 | 0.00000204 | 0.00000204 | 298.104137 |
| 2003 | dec | 7208 | 7610 | 8004 | 7999 | 7605 | 0.00000042 | 0.00000040 | 0.00000040 | 0.00000040 | 0.00000040 | 297.311930 |
| 2004 | jan | 6990 | 7827 | 7970 | 7659 | 7576 | 0.00000000 | 0.00000000 | 0.00000000 | 0.00000000 | 0.00000000 | 297.327692 |
| 2004 | feb | 6783 | 7468 | 7821 | 7820 | 6503 | 0.00000034 | 0.00000035 | 0.00000035 | 0.00000034 | 0.00000035 | 299.708231 |
| 2004 | mar | 6489 | 6965 | 7504 | 7588 | 6997 | 0.00000001 | 0.00000001 | 0.00000001 | 0.00000001 | 0.00000001 | 301.982055 |
| 2004 | nov | 7450 | 7690 | 7999 | 7969 | 5912 | 0.00000843 | 0.00000832 | 0.00000831 | 0.00000828 | 0.00000829 | 298.016589 |
| 2004 | dec | 6973 | 7322 | 7658 | 7571 | 7562 | 0.00000000 | 0.00000000 | 0.00000000 | 0.00000000 | 0.00000000 | 297.659892 |
| 2005 | jan | 7086 | 7428 | 7836 | 7803 | 7409 | 0.00000001 | 0.00000001 | 0.00000001 | 0.00000001 | 0.00000001 | 299.986885 |
| 2005 | feb | 6783 | 7826 | 7656 | 7865 | 6423 | 0.00000000 | 0.00000000 | 0.00000000 | 0.00000000 | 0.00000000 | 299.986885 |

**Figure 5.21 Table Showing the NDVI, Rainfall Rate and Temperature for all Samples of Acacia**

## 4.3 Time-Series Data Analysis Using R

### Structural Time-Series Model (StructTS Model/STM)

This model segregates the time-series into 2 important aspects, namely, seasonality and trend. An objective of the thesis is to show that the climatic variables may or may not impact NDVI. Before proceeding to that, let us understand the trend and seasonality of the complete 12 year time series of these variables for all 12 months in a year.

**STM of Monthly Rainfall and Temperature Data**

**Rainfall**

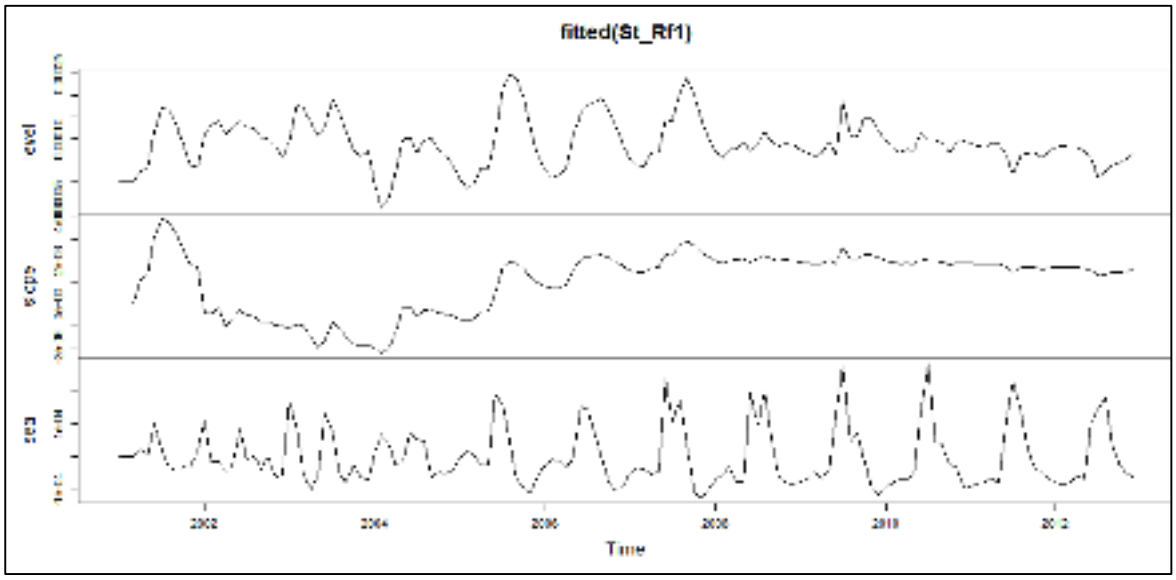


**Figure 5.22 St_Rf1**

Over the years, the amplitude of RR has increased along with the difference between the highest and lowest RR. The RR amplitude is higher after 2009 than the other years but this seems to be declining in 2011 and 2012. The seasonality shows a pattern where the RR increases from January onwards, peaks in July and declines thereafter and reaching a low point in December. In the earlier years, high RR was observed in June, July, September, December and January. Over the years, the RR in January changed from being one of the wettest months to the driest month in the year.

**Temperature**

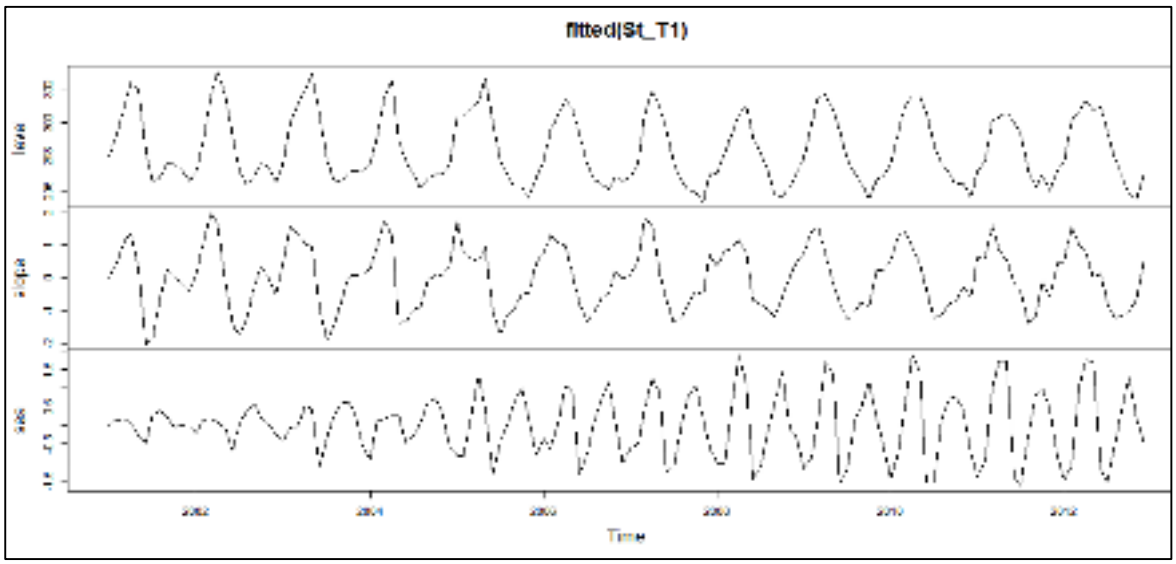


**Figure 5.23 St_T1**

Over the years, the amplitude of the temperature has increased. Each year, shows 2 peaks and valleys. First peak is around April/May and the second is in October. The valleys are seen in July and then January.

While comparing STM of RR with that of temperature, it may be observed that the amplitude of both variables increase with time. The increase is slow at first and then it rises steeply in 2005 and continues to increase. Till 2005, the RR and temperature did not vary greatly in their maximum and minimum values as much as is observed in the later years. The lowest temperatures are observed in January which complements the lowest RR recorded. RR recorded over the years in January has changed from being one of the wettest months to the driest month of the year. The temperature recorded for January shows increasingly low temperature values.

All these aspects together indicate that the elevated temperatures over the years has caused the atmosphere to hold more moisture. The presence of more water vapour in the atmosphere has led to increased rainfall rates. Following the wet months the temperatures can be seen to increase dramatically with very low or no rainfall rate. The subsequent increase in evaporation will most likely cause the drying out of soils and create a moisture strain on vegetation.

**STM of NDVI for Land Use Classes**

The results try to understand if either of the STM components in the MODIS NDVI time-series is impacted by either of these components in the Rainfall Rate (hereafter referred to as RR). Temperature was another aspect that was considered to understand MODIS NDVI time-series. On examining the StructTS model of temperature, the only information made available was a decrease in temperature from November to January and a subsequent increase in the later months. This indicates that the 5 month temperature cycle is inadequate to help with understanding the NDVI. The RR was on the other hand more useful. The StructTS Model of RR for the various land covers are very alike in their trend and seasonality, hence only one Model has been discussed and used repeatedly with the various land cover types.

**StructTS Model for RR**

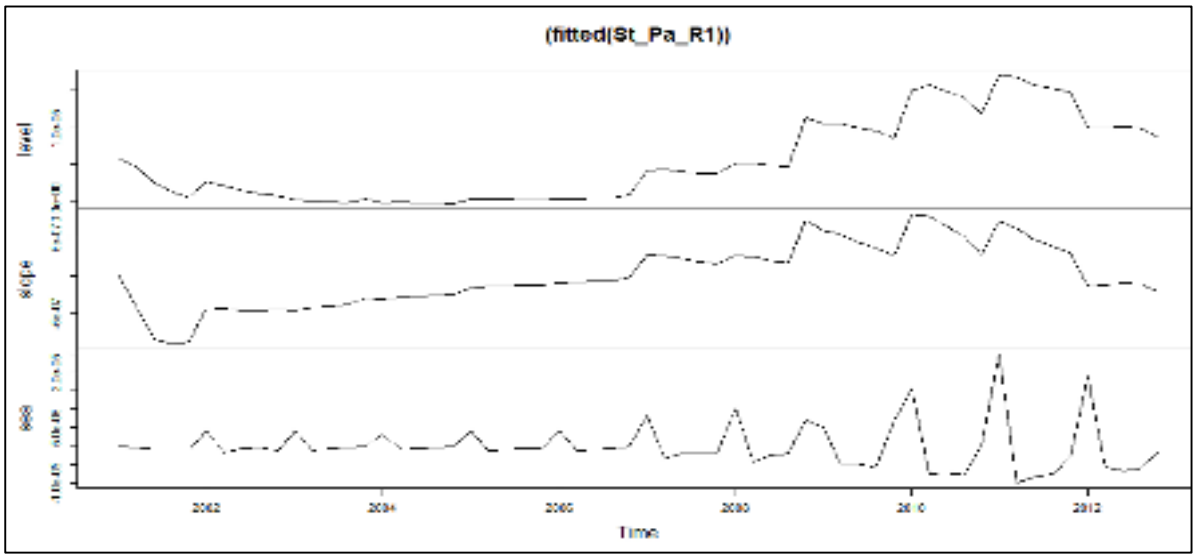


**Figure 5.24 St_Pa_R1**

As an example, StructTS model of RR in paddy fields (above figure) has been used and the remaining RR models are very identical to this one. The level of trend until 2007 shows low NDVI that increases at a steady rate. Post 2007, the level of trend displays rapid increase until 2011. The trend shows a further decline in NDVI in 2012. While observing the seasonality aspect of the model, one can note that November is the month with the highest amplitude and January is the month with the lowest trough in all the years. Until 2007, the maximum amplitudes appear to be constant after which an increase is seen.2011 has the maximum amplitude and then decreases in 2012.

**Acacia**

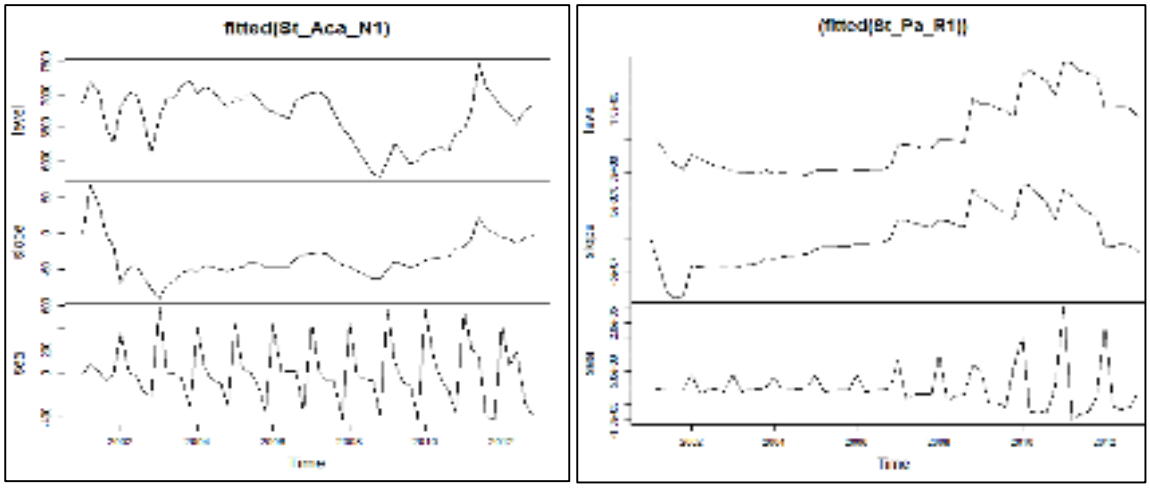


**Figure 5.25 St_Aca_N1(a) and St_Pa_R1(b)**

The model St_Aca_N1 shows initial undulations in trend and then increases after 2004 only to achieve constancy till 2009. Post that, the trend dips and rises again achieving its high NDVI in 2011. The trend shows a rapid decline in 2012. The seasonality of the model shows that the peak of each season is in November, after which there is a rapid decline in the NDVI. A lesser significant peak is observed January in all the years save 2010. In 2012, the peak is seen to decline from 2011 and a lesser significant peak is observed in January. On observing the NDVI StructTS model along with RR StructTS model it may be seen that the increases in amplitude of NDVI seasonal model from 2008 till 2011 and the decline after, is similar to pattern of changes in amplitude in the RR StructTS model. It may thus be safe to say that seasonal maximum amplitudes of the NDVI are influenced by the seasonal maximum amplitudes of RR.

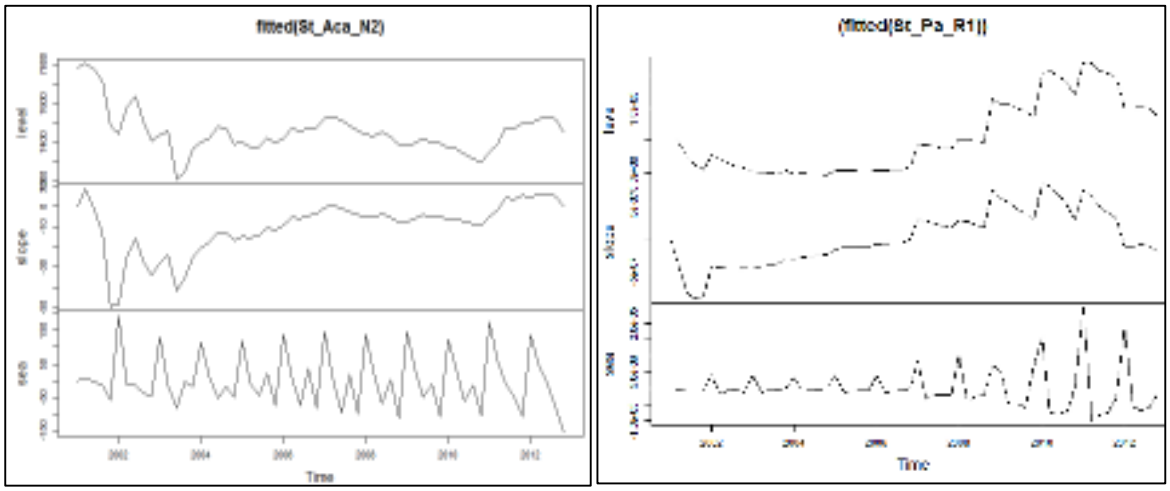

**Figure 5.26 St_Aca_N2 and St_Pa_R1**

In fig. St_Aca_N2, the maximum amplitude in seasonality is achieved in 2002 after which there is a decline only to slowly rise again in 2011. For all the years, the highest amplitude is seen in November. The trend in NDVI shows an initial dip and then it increases rapidly between 2004 and 2005 and achieves constancy till 2011 after which a steady increase is observed. While looking into seasonality, a similar pattern as that observed in fig. St_Aca_N1 is seen here. A dominant characteristic visible here is the smaller peak in February in the seasonality graph which in not visible in 2011 and 2012. While looking at the RR StructTS model, a similar relationship as observed earlier seen here. Additionally, the RR StructTS model indicates that the driest month in this 5 month season is January. This coincides with lack of January peaks in the NDVI StructTS model. It may be possible that the Acacia, due to moisture strain is deviating from this characteristic January peak.

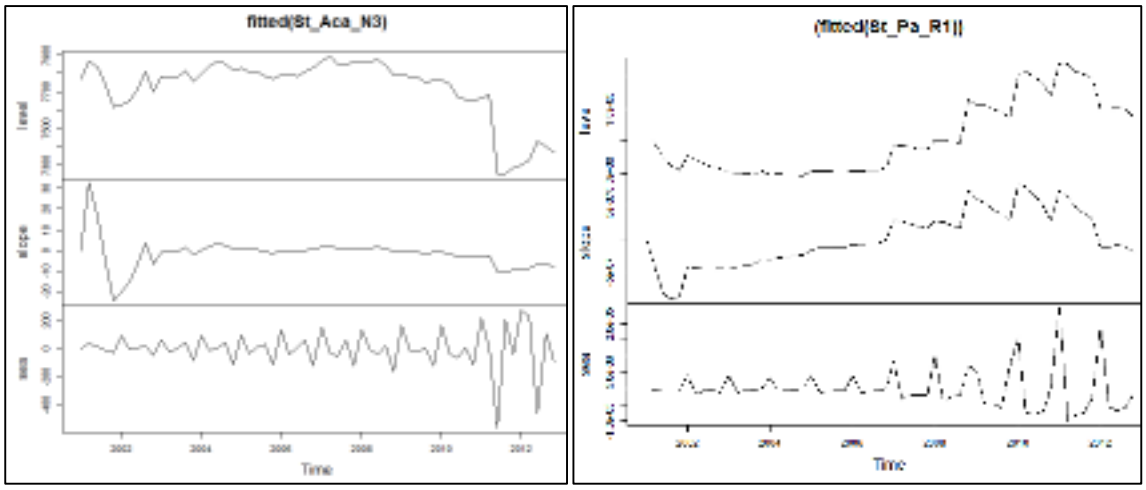


**Figure 5.27 St_Aca_N3 and St_Pa_R1**

The amplitude in Acacia in fig. St_Aca_N3 increases steadily over the years and rises to achieve the highest amplitude in 2012. For all the years, the highest amplitude is achieved in November. In 2011 and 2012, the dip in the temperature in January is dramatic. The trend shows an initial drop in NDVI values, then a constant period and then a decrease in 2011. The seasonality pattern observed here is similar to that observed in evergreen forests (will be discussed later). An interesting observation involving both the NDVI and RR StructTS model is that the lowest troughs in NDVI in January of 2011 and 2012 corresponds to the lowest troughs of RR during the same period. Thus, rainfall has been identified as one of the factors influencing the change in acacia plantation characteristics.

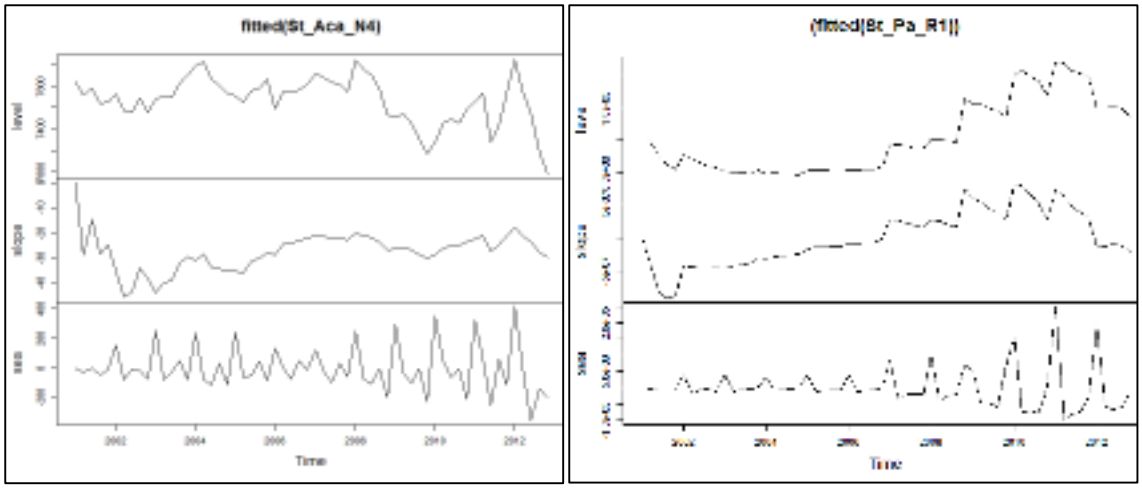


**Figure 5.28 St_Aca_N4 and St_Pa_R1**

In fig. St_Aca_N4, the seasonality amplitude until 2008 shows minor highs and lows. It steadily increases after 2008. For all the years, the highest amplitude is achieved in November. A second minor peak is observed in February. The trend shows several undulations at first then increases and becomes constant. The gradual increase in NDVI could indicate increased maturity of the plantation.

An association between the NDVI and RR StructTS model is visible as RR model shows low troughs when low troughs are seen in the NDVI model. This illustrates the dependency of Acacia on rainfall rate.

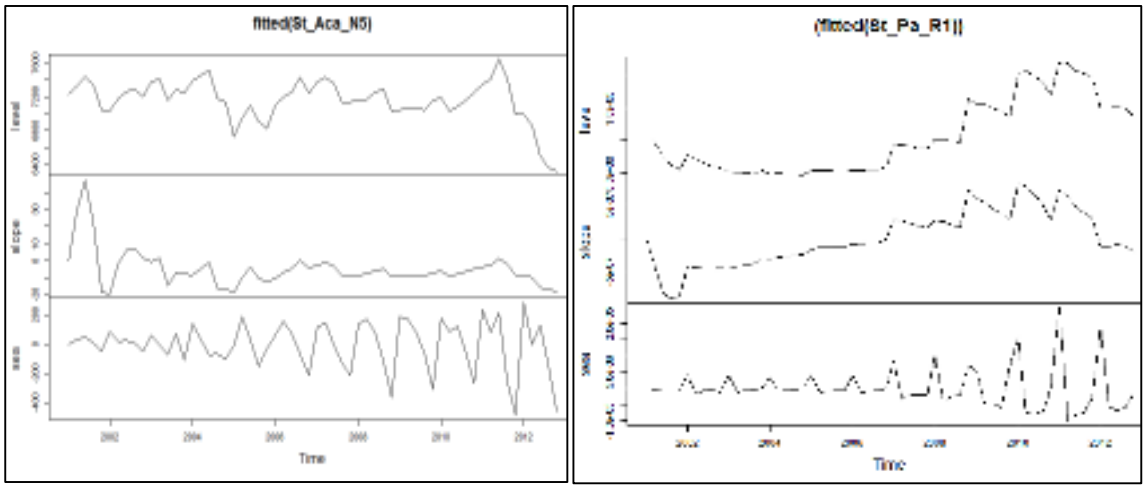


**Figure 5.29 St_Aca_N5 and St_Pa_R1**

In fig. St_Aca_N5, the trend seems to have an added component of the seasonality, so it has not been analsed.The seasonality amplitude shows peaks in November. Initially, the variation

in the 5 monthly NDVI values is low but that increases with time. It may be looked at as an increasing tendency of this platation to change from a state similar to evergreen forests to a deciduous state. This may imply that these Acacia plantations have been exploited for timber.

The impact of RR on NDVI is not as prominent with this sample of Acacia plantation and this factor has not been included in analysis.

**Areca**

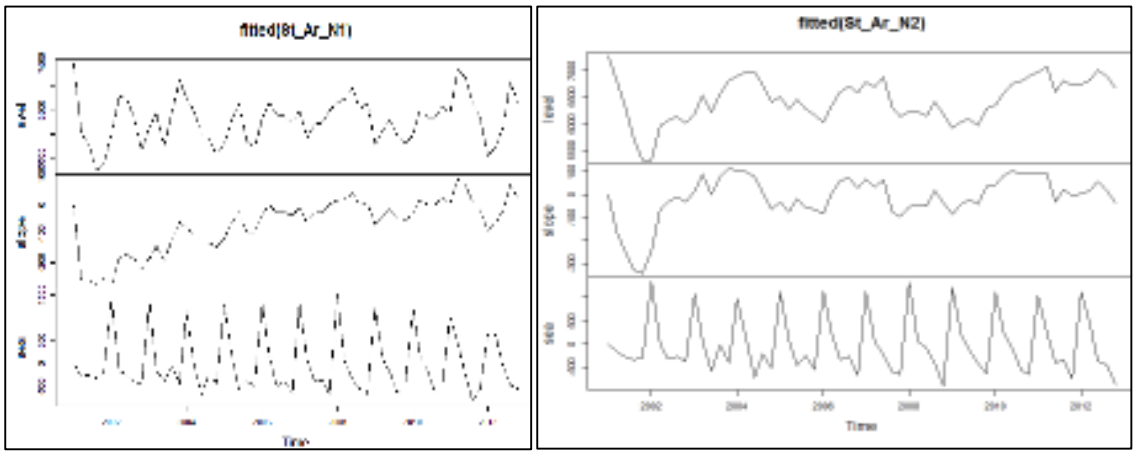


**Figure 5.30 St_Ar_N1 and St_Ar_N2**

In fig. St_Ar_N1, we can observe a steady increase in the trend in NDVI over the years. From 2011, a decline is observed. In the seasonality graph, November stands out as the peak NDVI season and there is a decline in NDVI thereafter. An occasional increase in NDVI observed in January. With respect to seasonality, fig. St_Ar_N2 shows a similar pattern. In the trend graph, the NDVI appears to be fairly constant with gentle peak and valley pattern. This could imply the Areca plantation has matured and its productivity is being maintained. While on the other hand, in fig. St_Ar_N1, the trend could imply that the areca plantation was relatively young in 2000 and with time, it has matured. The constant (or near constant) high and low amplitudes in seasonality in both Areca plantation samples (shown above) emphasize the role of human intervention in the maintenance of this vegetation type. Thus, no dependency has been observed as yet to the changes in the RR.

**Deciduous Forests**

All 5 sample locations were identified under this forest type of which St_De_N1 and St_De_N5 are similar to St_De_N2 and St_De_N4 is similar to St_De_N3. The graphs from the model may be found in the Appendix 1.

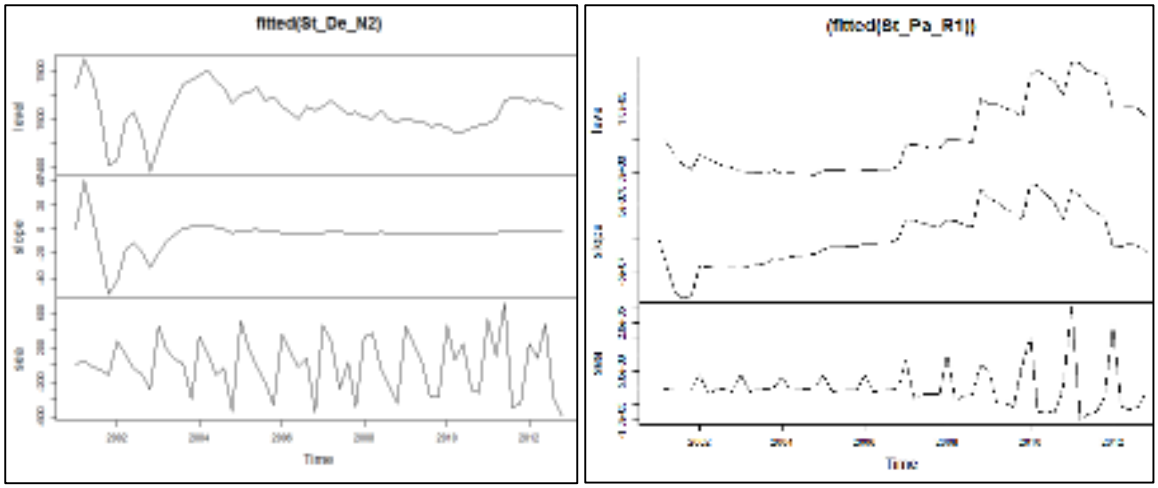


**Figure 5.31 St_De_N2 and St_Pa_R1**

The seasonality graph of fig. St_De_N2 depicts 2011 as the year with the maximum amplitude. November is the peak of the season for most years. In 2009, December emerges as the peak month while in 2011 and 2012 it is January. In the latter years, the NDVI in January is significantly greater than in December. The trend in the data shows initial fluctuations, followed by a constant rate of change of trend.

On comparing this model with the RR StructTS model, it was realized that the NDVI changes were not explained by RR as during the months of peak NDVI values, the RR is the lowest. Some other factors may be at play in this scenario and are beyond the scope of this thesis.

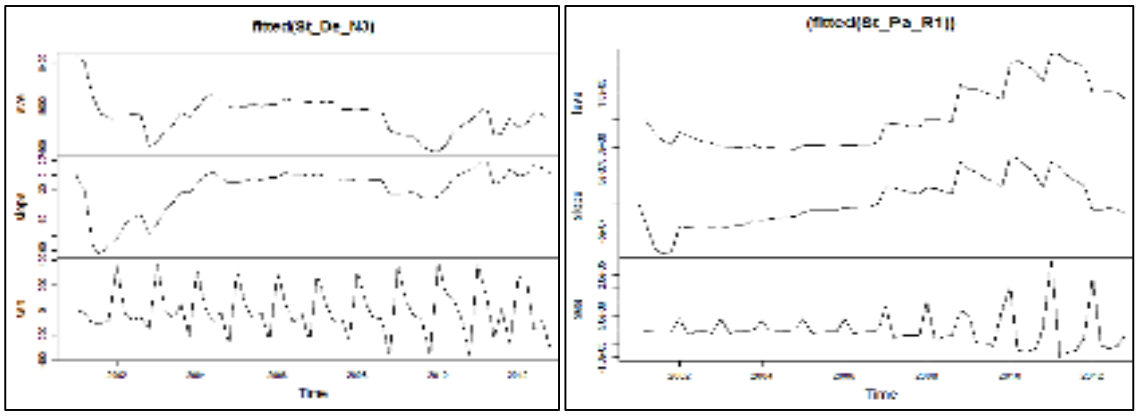


**Figure 5.32 St_De_N3 and St_Pa_R1**

In fig. St_De_N3, the amplitude in seasonality for all years is relatively high and it peaks in November for all years. After the lowest trough is achieved in January, there is a rise in the graph in February and thereafter, it declines again. Since 2009, the decrease in NDVI in January is significantly more than the previous years. 2011 and 2012 show a significant

increase in their amplitude in February. When comparing this to RR data, similarities are observed in aspects like low troughs in January in 2011 and 2012. The decrease in rainfall rate in 2012 corresponds to the decrease in NDVI in 2012. In conclusion, it may be said that decrease in rainfall rate during January has caused reduction in NDVI in that month in deciduous forests due to moisture strain.

**Evergreen Forests**

Five sample locations were in all identified as evergreen forests all of which have close to identical StructTS model properties. St_Ev_N1 has been discussed below and the remaining four may be found in the Appendix 1.

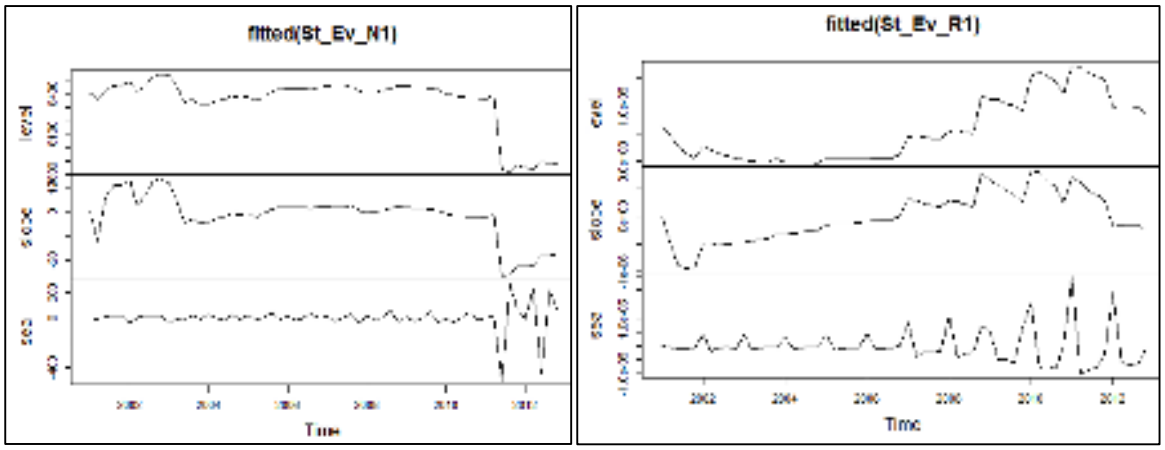


**Figure 5.33 St_Ev_N1 and St_Ev_R1**

Fig. St_Ev_N1 shows initial undulations in trend until 2003, the overall trend is constant up to 2011. Subsequently, the trend observes a steep decline followed by a gradual rise. The seasonality indicates a fairly constant NDVI throughout the 5 months till 2011. The NDVI troughs are lowest for 2011 and 2012 in January, followed by a rapid increase in February.

The rainfall rate (RR) may also be examined of the same region. The trend shows a low rainfall rate that increased steadily till 2007 after which there is an increase in RR. While observing the NDVI data with RR for the years 2011 and 2012, it came to light that the low troughs in January in NDVI corresponds to the low troughs in January of RR. A subsequent increase in NDVI and RR is seen in February. Thus, the low NDVI may be attributed to moisture strain during that period. This seasonal quality is similar to that found in deciduous forests and it may be possible that the evergreen forests have acquired a deciduous nature.

**Semi-Evergreen Forests**

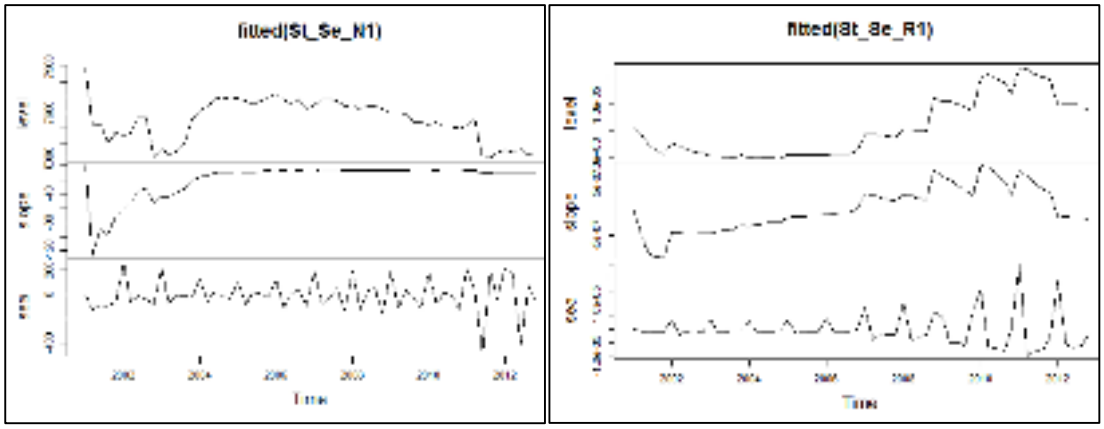


**Figure 5.34 St_Se_N1 and St_Se_R1**

Fig. St_Se_N1 displays undulation initially in the level and then proceeds to increase gradually in trend towards 2004. The trend is constant apart from the initial undulations observed. The seasonal aspect shows maximum NDVI in November and another peak is seen in February. In 2011, the graph dips to -479.23 in January. The graph in February is almost similar to the November peak. A similar high peak and low trough pattern is observed in the following year as well.

Low troughs found in January in RR StructTS model is similar to what is observed in NDVI. Hence, it may be said that moisture strain is the cause of the low NDVI during January. The marked dip in the graph in January, followed by a rise in February and subsequent dip in March is a characteristic seasonal trend of deciduous forests. This pattern in seasonality may indicate a recent increase in the deciduous nature of these forests.

**Paddy Fields**

Five sample locations were in all identified as paddy fields all of which have similar StructTS model properties. St_Pa_N4 has been discussed below and the remaining four may be found in the Appendix.

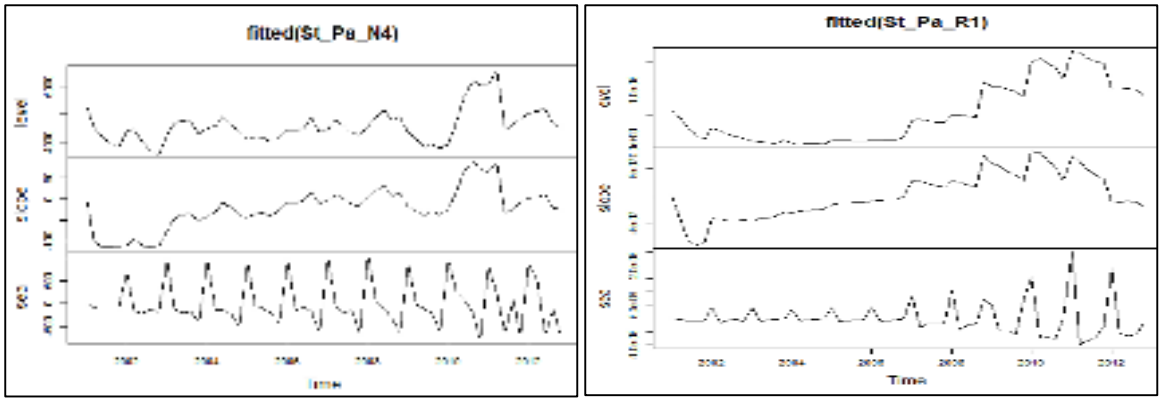


**Figure 5.35 St_Pa_N4 and St_Pa_N1**

Fig. St_Pa_N4 shows a gradual increase in trend till 2009 then dips and steeply increases and dips again. 2011 onwards, a gradual increase is observed again. The seasonality graph shows November contains the maximum NDVI for all years. Evidences of double cropping are visible from 2002 onwards as NDVI values increase for January/February and the troughs decrease after 2005. The absence of a peak in February and presence of relatively high troughs eliminate the presence of paddy prior to 2002.

Since this region is comprised of mostly rainfed paddy, it should show dependence on RR. Higher RR amplitudes in 2011 and 2012 may be responsible higher January/February NDVI peaks by increasing availability of water.

# Chapter 6: Conclusion

In this thesis, land use classification for the years 2000 and 2013 was carried out with emphasis on forest and agro-ecosystems. The aim of the classification was to observe what forest and agricultural classes were present back in 2000 and what has changed now. Additionally, climatic variables were individually analysed for all 12 months for 12 years to understand the trends in the data. Monthly NDVI for these 12 years was observed in conjunction with climate data in the hope to understand the drivers of this change.

The key premise for this study is the presence of heavy rainfall events in the Aghnashini Basin of the Western Ghats region. Since this is a pioneer project in the region studying hydrological components, the presence of heavy rainfall had to be established. Amplitudes in monthly rainfall rate and climate data indicated that there is indeed a dramatic increase in both variables since 2005. The rainfall rates have increased during the monsoon months and have shown drier months in non-monsoonal season.

Rainfall rates have been studied in this thesis, and most of the definitions of extreme rainfall events are measured as absolute amounts. My thesis forms part of a larger project being carried out in this region. Absolute rainfall measurements are being taken using rain gauges. These installations are fairly recent and so the data collected is insufficient for analysis currently. Once this data has been acquired over a period of at least 3 years, this may be compared to rainfall rates observed and ascertained if the increased rates are in fact a result of extreme rainfall events.

The change detection in the land use maps between 2000 and 2013 revealed that 43% of the evergreen forests have been converted to deciduous and semi-evergreen forests and 40% of semi-evergreen forests have been converted to deciduous forests. This large scale degradation in forests implies the presence of very dominant factors driving this change. This could be increased human activity in those regions or drastic climatic changes over the past few years or even both. ‘Upgradation’ of forest types has also been observed where semi-evergreen forests have been converted to evergreen forests and deciduous forests have been converted to semi-evergreen forests. This may be possible provided the forest has been left undisturbed for a long time and the climate has been favorable. On observing the trends in the evergreen

and semi-evergreen forests in the MODIS data, it seems unlikely. So, this change may be attributed to classification error.

Another change that is prominent is that from paddy fields to Areca plantations. This change has occurred by 28%. This just goes to emphasize that Areca is a more profitable crop than paddy. A decrease in the forests in favour of agricultural land parcels was expected. Only a 1.7% change has been observed Areca from deciduous forests. The plains may have already been occupied and the steep hills may be a constraining factor in expansion to other areas in the region.

Study of the change map depicting conversion to "degraded vegetation classes" along with slope shows that large amount of vegetation change has occurred in areas that may be easily accessed by humans. This goes to show that climate change along with human activity has caused land use conversion.

Once the changes in the landscape were quantified, areas that have retained the same land use over the years were identified and used for MODIS NDVI and climate data extraction. The most important premise for this thesis is that extreme rainfall events has caused these changes in The temperature and rainfall time-series data were modelled using STM for 12 years using data for all months. The results

The STM was created for NDVI as well as the corresponding rainfall rate data. What is prominent in all of the data sets is that the rainfall rate has increased dramatically since 2010 showing peaks in November and has decreased dramatically in January. This nature in seasonality has corresponded to patterns in seasonality in all three forest type classes and Acacia. For paddy, the increased rainfall rate in November seems to have helped in the supporting a second winter crop of paddy. Arecanut plantations don't show much dependency on RR.

For evergreen and semi-evergreen forests, a sudden change to deciduous nature has been observed post 2010 with low troughs in January. January is also the month with the lowest RR. This implies moisture strain in these forests. Human intervention has been ruled out as the high amplitude of NDVI is still observed.

In conclusion to this study, it may be said that increased rainfall and temperature have been observed over the years which has certainly had an impact on the land use of the region. This study was limited to one decade. Time-series from 1960 till the present will be able to

highlight the climate changes more accurately and help make projections for the future. Further studies should be carried out to understand the human aspect of this "natural change" so as to help decision makers take informed corrective steps towards conserving the forests in this region.

# References


1. Appeaning Addo, Kwasi. 2010. "Urban and Peri-Urban Agriculture in Developing Countries Studied Using Remote Sensing and In Situ Methods." *Remote Sensing* 2 (2) (February 2): 497–513. doi:10.3390/rs2020497. http://www.mdpi.com/2072-4292/2/2/497/.
2. Avinash, KG, and KG Ashamanjari. 2010. "A GIS and Frequency Ratio Based Landslide Susceptibility Mapping: Aghnashini River Catchment, Uttara Kannada, India." *International Journal of Geomatics* 1 (3): 343–354. http://www.researchgate.net/publication/216521049_A_GIS_and_frequency_ratio_based_landslide_susceptibility_mapping_Aghnashini_river_catchment_Uttara_Kannada_India/file/32bfe50fe6d7696623.pdf.
3. Baatz, M. and Schäpe, A., 2000, Multiresolution segmentation – an optimization approach for high quality multi-scale image segmentation, In: Strobl, J., Blaschke, T. and Griesebner, G. (eds.), Angewandte Geographische
4. Baatz, M., Benz, U., Dehghani, S., Heynen, M., Höltje, A., Hofmann, P., Lingenfelder, I., Mimler, M., Sohlbach, M.Weber, M., & Willhauck, G., (2004), eCognition Professional: User guide 4; Munich: Definiens-Imaging.
5. Belward, Alan S., and Carlos R. Valenzuela, eds. 1991. *Remote Sensing and Geographical Information Systems for Resource Management in Developing Countries (Google eBook)*. Springer. http://books.google.com/books?id=8XvOEfo6fX8C&pgis=1.
6. Benz, U.C., Hoffmann, P., Willhauck, G., Lingenfelder, I. and Heynen, M., 2004, Multi- resolution, object-oriented fuzzy analysis of remote sensing data for GIS-ready information, ISPRS Journal of Photogrammetry and Remote Sensing, 58: 239-258
7. Bhat, D.M., K.S. Murali, and N.H. Ravindranath. 2001. "Formation and Recovery of Secondary Forests in India: A Particular Reference to Western Ghats in South India." *Journal of Tropical Forest Science* 13 (4): 601–620. http://www.cifor.org/publications/pdf_files/articles/ABhat0101.pdf.

8. Blaschke, Thomas. 2003. "Object-based Contextual Image Classification Built on Image Segmentation." *Advances in Techniques for Analysis of Remotely …* 00 (C). http://ieeexplore.ieee.org/xpls/abs_all.jsp?arnumber=1295182.
9. Chander, Gyanesh, Brian L Markham, Julia A Barsi, and Abstract Effective April. 2007. "Revised Landsat-5 Thematic Mapper Radiometric Calibration" 4 (3): 490–494.
10. Chandran, Subash M.D., G.R. Rao, Vishnu Mukri, Prakash Mesta, and T.V. Ramachandra. 2012. "Grasslands of Anshi-Dandeli Tiger Reserve." *ENVIS Technical Report*. http://wgbis.ces.iisc.ernet.in/biodiversity/pubs/ETR/ETR36/chapter3.htm.
11. Dash. 2009. *Fundamentals Of Ecology 3E*. 3rd ed. Tata McGraw-Hill Education. http://books.google.com/books?id=7mW4-us4Yg8C&pgis=1.
12. Dash. 2009. *Fundamentals Of Ecology 3E*. 3rd ed. Tata McGraw-Hill Education. http://books.google.com/books?id=7mW4-us4Yg8C&pgis=1.
13. DEFiNiNENS AG, 2000. eCognition User Guide, http://www.defineiens.com
14. Deshpande, G. S., and B. K. Kallapur. 2008. "GROUND WATER INFORMATION BOOKLET UTTARA KANNADA DISTRICT," (November): 1–24.
15. Durbin, J. and Koopman, S. J. (2001) *Time Series Analysis by State Space Methods*. Oxford University Press.
16. Gao, Bo-cai. 1996. "NDWI A Normalized Difference Water Index for Remote Sensing of Vegetation Liquid Water From Space." *Elsevier* 266 (April 1995): 257–266.
17. Govaerts, Bram. 2010. "The Normalized Difference Vegetation Index ( NDVI ) GreenSeeker TM Handheld Sensor : Toward the Integrated Evaluation of Crop Management Part A : Concepts and Case Studies." *International Maize and Wheat Improvement Center (CIMMYT)*. http://www.plantstress.com/methods/Greenseeker.PDF.
18. Gua, Juan, Jun Chen, and Qiming Zhou. 2004. "A Hierarchical Object-Oriented Aproach for Extracting Residential Areas From High Resolution Imagery." *Image Rochester NY*.)
19. Hengl, T., and H.I. Reuter. 2009. "Geomorphometry: Concepts, Software, Applications." http://www.narcis.nl/publication/RecordID/oai%3Auva.nl%3A301831.
20. Krishnaswamy, Jagdish, Michael Bonell, Basappa Venkatesh, Bekal K. Purandara, Sharachchandra Lele, M.C. Kiran, Veerabasawant Reddy, Shrinivas Badiger, and

K.N. Rakesh. 2012. “The Rain–runoff Response of Tropical Humid Forest Ecosystems to Use and Reforestation in the Western Ghats of India.” *Journal of Hydrology* 472-473 (November): 216–237. doi:10.1016/j.jhydrol.2012.09.016. http://linkinghub.elsevier.com/retrieve/pii/S0022169412008190.

21. Laliberte, A.S., Rango, A., Havstad, K.M., Paris, J. F., Beck, R. F., McNeely, R. and Gonzalez, A.L., 2004, Object-oriented image analysis for mapping shrub encroachment from 1937 to 2003 in southern New Mexico, Remote Sensing of Environment, 93: 198-210
22. Lele, Sharachchandra, G Rajashekhar, Venkataramana R Hegde, G Prevish Kumar, and P Saravanakumar. 1998. “Meso-scale Analysis of Forest Condition and Its Determinants : A Case Study from the Western Ghats Region , India Meso-scale Analysis of Forest Condition and Its Determinants : A Case Study from the Western Ghats Region , India.” *Current Science* 75 (3).
23. Lele, Sharchchandra. 1993. “Degradation, Sustainability, Or Transformation? A Case Study Of Villagers’ Use Of Forest Lands In The Malanaad Region Of Uttara Kannada District, India”. Bangalore: Center for Ecological Sciences.
24. Mas, J.F. 1999. “Monitoring Land-cover Changes: a Comparison of Change Detection Techniques*.” *International Journal of Remote Sensing* 20 (1): 139–152.
25. Murthy, Indu K, K S Murali, G T Hegde, P R Bhat, and N H Ravindranath. 2002. “A Comparative Analysis of Regeneration in Natural Forests and Joint Forest Management Plantations in Uttara Kannada District, Western Ghats” 83 (11): 1358–1364.
26. Navulur, Kumar. 2006. *Multispectral Image Analysis Using the Object-Oriented Paradigm*. CRC Press. doi:10.1201/9781420043075.fmatt. http://www.crcnetbase.com/doi/pdfplus/10.1201/9781420043075.fmatt.
27. Pettorelli, Nathalie, Jon Olav Vik, Atle Mysterud, Jean-Michel Gaillard, Compton J Tucker, and Nils Chr Stenseth. 2005. “Using the Satellite-derived NDVI to Assess Ecological Responses to Environmental Change.” *Trends in Ecology & Evolution* 20 (9) (September): 503–10. doi:10.1016/j.tree.2005.05.011.
28. Ramachandra, T.V, and a.V Nagarathna. 2001. “Energetics in Paddy Cultivation in Uttara Kannada District.” *Energy Conversion and Management* 42 (2) (January): 131–155. doi:10.1016/S0196-8904(00)00052-2. http://linkinghub.elsevier.com/retrieve/pii/S0196890400000522.

29. Ramachandra, T.V., D.K. Subramanian, and N.V. Joshi. 1999. "Hydroelectric Resource Assessment in Uttara Kannada District, Karnataka State, India." *Journal of Cleaner Production* 7 (3) (March): 195–211. doi:10.1016/S0959-6526(98)00076-6. http://linkinghub.elsevier.com/retrieve/pii/S0959652698000766.
30. Reed, BC, M White, and JF Brown. 2003. "Remote Sensing Phenology." *Phenology: An Integrative Environmental* http://phenology.cr.usgs.gov/methods_metrics.php
31. Reid, Fiona. 2009. *A Field Guide to the Mammals of Central America and Southeast Mexico*. Vol. 2009. Oxford University Press. http://books.google.com/books?id=aBEbUaXTWYAC&pgis=1.
32. Sallaba, Florian. 2009. "Potential of a Post-Classification Change Detection Analysis to Identify Land Use and Land Cover Changes . A Case Study in Northern Greece" (159).
33. Thomas, N., Hendrix, C. and Congalton, R.G., 2003, A comparison of urban mapping methods using high-resolution digital imagery, Photogrammetric Engineering and Remote Sensing, 69(9): 963-972
34. User Guide, 2011. "eCognition Developer 8." *Whats New* 74 (1): 43–70. doi:10.1525/hlq.2011.74.1.43. http://www.jstor.org/stable/10.1525/hlq.2011.74.1.43.
35. Van der Sande, C.J., S.M. de Jong, and a.P.J. de Roo. 2003. "A Segmentation and Classification Approach of IKONOS-2 Imagery for Land Cover Mapping to Assist Flood Risk and Flood Damage Assessment." *International Journal of Applied Earth Observation and Geoinformation* 4 (3) (June): 217–229. doi:10.1016/S0303-2434(03)00003-5. http://linkinghub.elsevier.com/retrieve/pii/S0303243403000035.
36. Whiteside, T. 2005. "A COMPARISON OF OBJECT-ORIENTED AND PIXEL-BASED CLASSIFICATION METHODS FOR MAPPING LAND COVER" (September): 1225–1231.
37. Xiaoxia, Sun, Zhang Jixian, and Liu Zhengjun. 2005. "A Comparison of Object-Oriented and Pixel-Based Classification Approachs Using Quickbird Imagery": 1–3. http://citeseerx.ist.psu.edu/viewdoc/summary?doi=10.1.1.184.3501

**References Obtained from the Internet**

www1. Anon. "Unsupervised Classification Algorithms." http://www.yale.edu/ceo/Projects/swap/landcover/Unsupervised_classification.htm.

www2. Anon. "Spectral Reflectance Curve."

http://www.seos-roject.eu/modules/remotesensing/remotesensing-c01-p05.html.

www3. Anon. “Landsat Science - Data.” http://landsat.gsfc.nasa.gov/data/sci_data.html.

www4. Anon. “MODIS Website.” http://modis.gsfc.nasa.gov/.

www5- Anon. “Uttara Kannada - Wikipedia, the Free Encyclopedia.” http://en.wikipedia.org/wiki/Uttara_Kannada

.

# Appendix 1

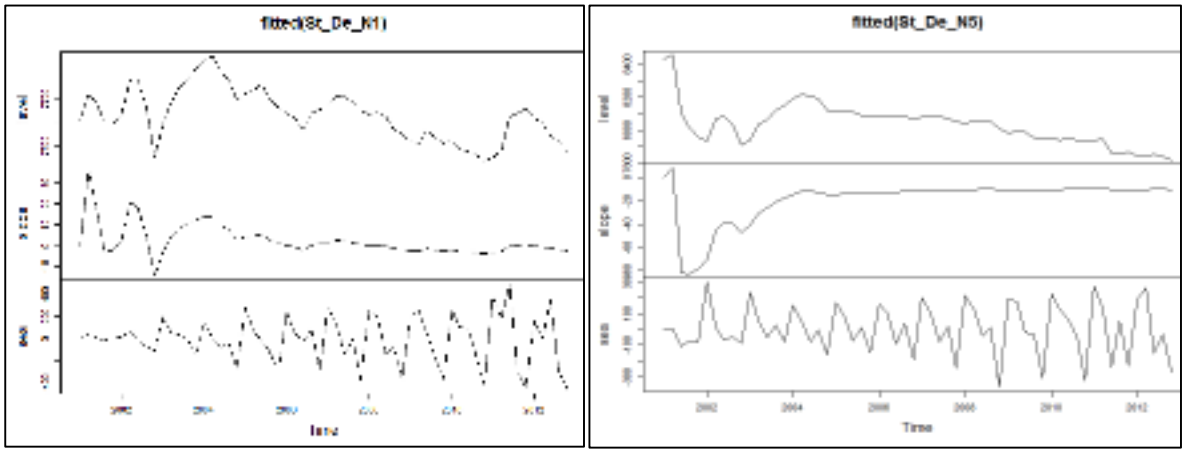


**Figure 7.1 St_De_N1 and St_De_N5**

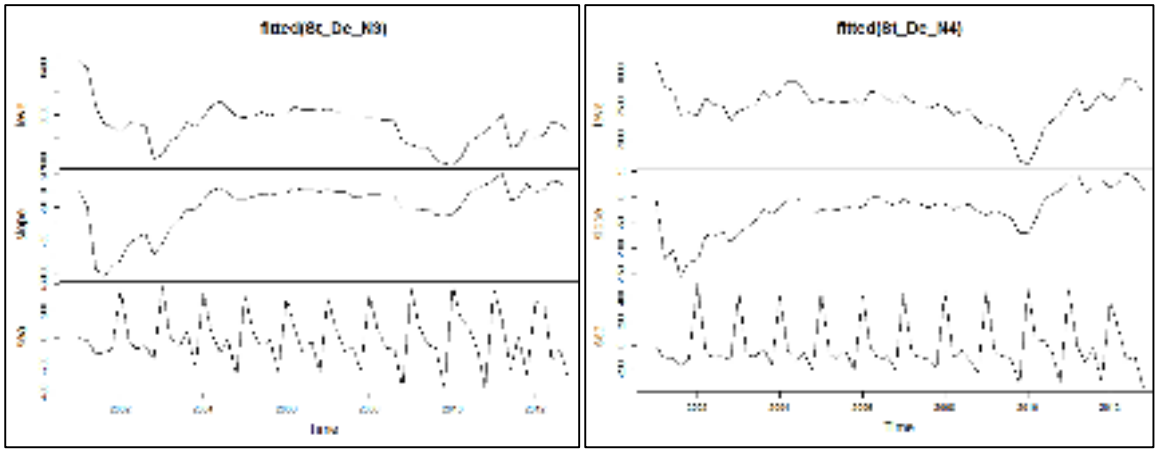


**Figure 7.2 St_De_N3 and St_De_N4**

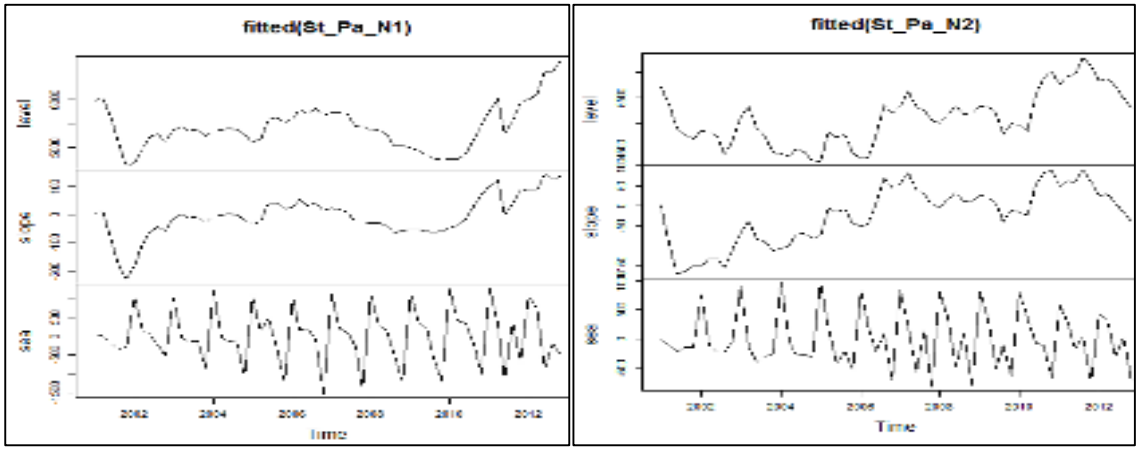


**Figure 7.3 St_Pa_N1 and St_Pa_N2**

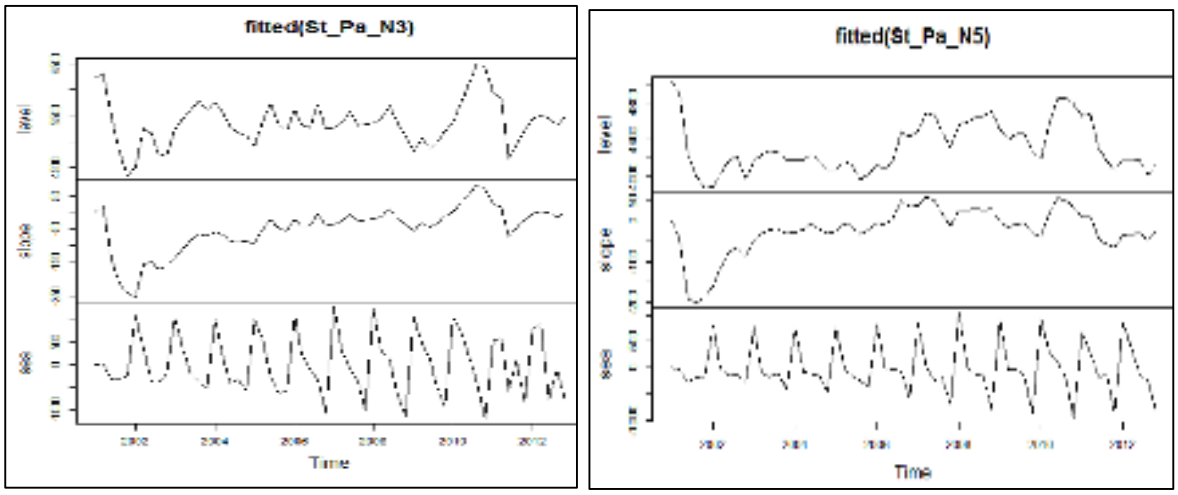


**Figure 7.4 St_Pa_N3 and St_Pa_N5**

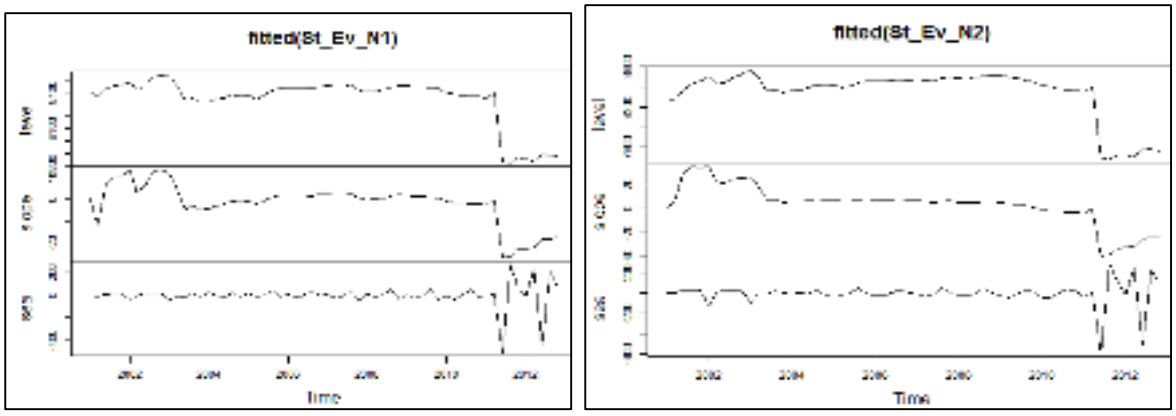


**Figure 7.5 St_Ev_N1 and St_Ev_N2**

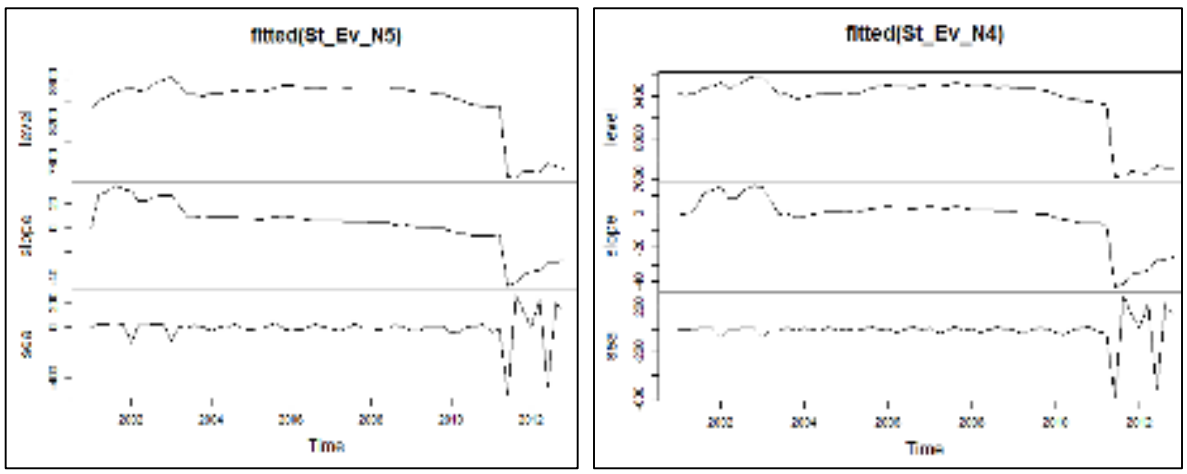


**Figure 7.6 St_Ev_N5 and St_Ev_N4**

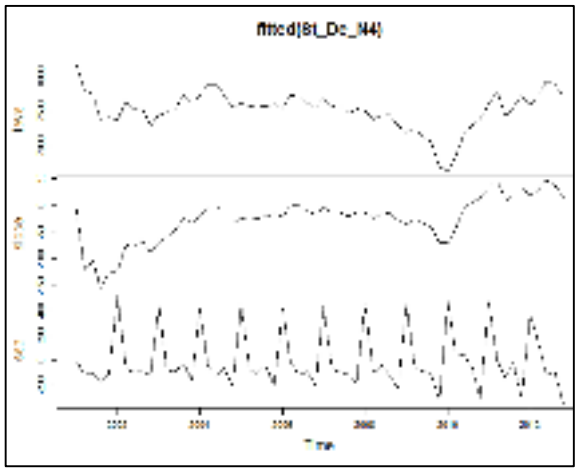

**Figure 7.7 St_De_N4**

# RELATIONSHIP BETWEEN LAND COVER AND EVAPO-TRANSPIRATION IN THE UPPER NILGIRIS

Dissertation submitted to Pondicherry University,
in partial fulfilment of the requirements
for the degree of

**MASTER OF SCIENCE**
**IN**
**ECOLOGY & ENVIRONMENTAL SCIENCES**

**By**
**K. Kumaran**

Under the guidance of
**Dr. K.V. Devi Prasad, Ph. D**
**Professor**


**Department of Ecology and Environmental Sciences,**
**School of Life Sciences, Pondicherry University,**
**Puducherry – 605 014.**

**2015**

**Dr. K.V. Devi Prasad,**
Professor and Head,
Department of Ecology and Environmental Sciences,
School of Life Sciences,
Pondicherry University.

# Certificate

This is to certify that Mr. K. Kumaran has carried out the work embodied in this dissertation title "**RELATIONSHIP BETWEEN LAND COVER AND EVAPO-TRANSPIRATION IN THE UPPER NILGIRIS**" being submitted for partial fulfilment of the requirement for the award of Degree of Master of Science in Ecology and Environmental Sciences, Pondicherry University, during the academic year 2013 – 2015. The work is original and has not been submitted for the award of any certificate, diploma or degree of this or any other university.

Date :

Place : (Dr. K.V. Devi Prasad)

COUNTER SIGNED BY

**Dr. K.V. Devi Prasad, Ph. D**
Head of the Department
Ecology and Environmental Sciences,
Pondicherry University.

**K. Kumaran,**
M. Sc (Ecology and Environmental Sciences),
Department of Ecology and Environmental Sciences,
School of Life Sciences,
Pondicherry University.

## DECLARATION

I hereby declare that the project thesis entitled " **RELATIONSHIP BETWEEN LAND COVER AND EVAPO-TRANSPIRATION IN THE UPPER NILGIRIS** " is submitted by me ,in partial fulfilment of the requirements for requirement for the award of **M. Sc Degree** ,is a record of project work under the guidance of **Dr. K.V. Devi Prasad, Ph. D,** ,during the period of 2013-2015 at Department of Ecology and Environmental Sciences, Pondicherry University .

The project which has been prepared by me is an original work which has not previously formed the basis for the award for any Degree, Diploma and Association, Fellowship or other similar titles.

**Place:** Pondicherry **K. Kumaran**

**Date:**

ACKNOWLEDGEMENT

I express my sincere thanks to **Dr. K.V. Devi Prasad, Ph. D,** professor and Head, Department of Ecology and Environmental Sciences, Pondicherry University. For his guidance, co-operation and facilities provided during the project.

This study was part of an ongoing project entitled **"Hydrologic and Carbon Services in the Western Ghats, Impact of Extreme Rainfall Events"** supported by Ministry of Earth Sciences, New Delhi.

I express my grateful thanks to **Dr. Jagdesh Krishnasami, Ph. D**, principal investigator and the team members of the project.

I am very thankful to **Dr. R.S. Bhalla, Ph. D**, Foundation for Ecological Research, Advocacy and Learning, for giving opportunity to study this course and for academic inputs and support at all stages of the project.

I am very thankful to **Mr. Srinivas V,** Foundation for Ecological Research, Advocacy and Learning, for giving opportunity to study this course and support at all stages of the project.

I am very thankful to **Mrs. Sunita Ram**, (Managing Director) Foundation for Ecological Research, Advocacy and Learning, for giving opportunity to study this course and support.

I express my grateful thanks to **Forest Department of Tamil Nadu, District Forest Officer and Staffs of Forest Department** Nilgiri South.

I express my grateful thanks **Mr. Senthil Babu, Mr. Rajat Nayak, Mr. Gaspard Appavu, Mr. Gopinath Srikandan, Mr. Balu and M/s Anu** for continuous encouragement to complete my study.

I am extremely thankful to my colleagues especially, **Dr. Susan Varghese, Mr. S. Saravanan, Mr. Sivakumar, Mr. T. Siva, Mr. Kamal Raj, Mr. Senthil, Mr. Sathish, Mr. Ganesh, Mr. Rajendran and Mrs. R. Santhi** for their support and their suggestions during the tenure of my project.

Many stage of this study would not have been possible if it was not for my beloved friends, who renders their enduring support thought the course of the study. My hearty thanks to **Sriram, Naveen, Kayalvizhi, Karkuzhali, Nithya, Kathir, Bala** and **Jaya** and whoever I missed here.

Thanks to all the people of the Department of Ecology and Environmental Sciences, Pondicherry University for providing me with relevant information.

I express my grateful thanks to **My Family Members** for their support all along my course.

I feel immensely grateful to the **God Almighty** for having endowed me with the necessary energy and hopes for the successful completion of this work.

Thank you All

# Contents

**Contents** i

**List of Tables** ii

**List of Figures** iii

**1 Introduction** 1
Background . . . 1
Study Area . . . 2

**2 Literature Review** 5

**3 Objectives and Methods** 8
Objectives . . . 8
Methods . . . 8

**4 Observations and Results** 17
Land-cover Mapping . . . 17
Normalised Difference Vegetation Index (NDVI) . . . 20
Catchment Delineation . . . 20
Discharge Measurements . . . 20
Evapotranspiration . . . 23

**5 Discussion and Conclusion** 27

**Bibliography** 30

**A R script for analysing discharge data and plotting the results** 35

**B Photographs of the study and site** 42

# List of Tables

1.1 Summary of catchment statistics. . . . . 4

4.1 Area under different land cover classes. . . . . 19
4.2 Kappa accuracy assessment of supervised classification. . . . . 21
4.3 Summary statistics for discharge. . . . . 26
4.4 Summary statistics for ET in mm per day. . . . . 26

# List of Figures


1.1 Location map of study area. . . . . 4

3.1 Steps in deriving land classes from multispectral LANDSAT8 imagery. 11
3.2 Steps involved in catchment delineation. . . . . 11
3.3 Map of the Lakdihalla watershed (above) and catchment for station 101. . . . . 12
3.4 Steps involved in calculating discharge values for a stream. . . . . 12
3.5 A stream profile showing points at which velocities were measured. 14
3.6 Rating curve used to evaluate the stage-discharge relationship. . . . 14
3.7 Stage-discharge points used to derive a rating curve. . . . . 16
3.8 Steps in deriving ET for diurnal variations in stream discharge. . . . 16

4.1 Proportion of area under different land cover. . . . . 18
4.2 Discharge measurements for the different catchments. . . . . 24
4.3 ET measurements for the different catchments. . . . . 25
4.4 Plot of linear regression between NDVI and ET. . . . . 26

B.1 Study site and instruments. Photo credits: CWC team - FERAL. . . 43
B.2 Landscape panoramas, wildlife and visitors at the Nilgiri South range. 44

## Abstract

A method for estimating plant based evapotranspiration (ET) is presented based on measurements of diurnal variation of stream discharge and land cover analysis of their catchment for the dry season. The relationship between normalised difference vegetation index (NDVI) and ET rates is explored. Implications of large scale land cover changes on the water balance of basins is discussed.

The study is located in the biodiversity hotspot of the Western Ghat mountains in the Nilgiri South division of the Nilgiri Biosphere Reserve. Large scale replacement of grasslands with wattle in the mid twentieth century provide a useful comparison of ET between native grasslands and Shola, a tropical montane forest, and the introduced wattle plantations.

Results suggest an increase in total ET from the reserve on account of wattle plantations is about 650mm per year when extrapolated from dry season daily ET rates. There is a strong relationship between NDVI and ET with grasslands showing the lowest, wattle an intermediate and Shola forests showing the highest rates of ET.

# 1. Introduction

## Background

Changes in stream flow as a result of modifications of land cover in catchment areas is a topic of wide concern in countries such as India where large sections of the population depend on agriculture and where hydroelectric dams contribute a significant component of power generation. Land cover changes have wide ranging impacts on stream-flow (Bonell and Bruijnzeel, 2010). These include changes in flow duration and discharge during the dry season as well as the amount of sediment and nutrient discharge during high flows.

Large scale changes in land cover have been seen in forests across the Western Ghats both before but mostly during and after the British period (Chandran, 1997). The Nilgiris, which lie in the headwaters of the Cauvery basin are no exception. Natural Shola forests and grasslands of the Nilgiris were replaced with plantations of blue gum (*Eucalyptus globulus*) and wattle (*Acacia mearnsii*) by the Indian foresters in the 1960's in order to meet requirements for pulp and tannin (Rangan et al., 2010; Sikka et al., 2003).

The likely impact of this on the hydrology of the region, is a matter of serious concern given that the Nilgiris district alone accounts for nearly 40% of the

state's hydroelectric power generation (Sikka et al., 2003). Other large scale afforestation schemes, such as the Greening India Mission with targets of afforesting ten million ha over a decade (Anon., 2013; Ravindranath and Murthy, 2010) are equally likely to affect basal flows in catchments and potentially impact natural systems in a negative manner. Understanding the relationship between forests and basal flows is therefore important to inform such programmes.

There is a strong positive correlation between ET and photosynthesis (Running et al., 1989). Photosynthetically active vegetation draws its water from available sources, which during the dry season correspond to soil moisture. Vegetation in riparian reaches of streams and rivers can therefore influence the amount of discharge. This effect is most obvious during the dry season and expresses itself as a diurnal variation in discharge.

## Study Area

The study was located in the Nilgiri South Forest Division, falling within the Nilgiri Biosphere Reserve in the Western Ghats. The Western Ghats are a global biodiversity hotspot (Mittermeier et al., 2011) and the Nilgiris harbour a number of endemic species and are of high conservation value (Das et al., 2006). The Nilgiris also are the headwaters of the Bhavani and Moyar rivers, thereby providing substantial hydrologic services.

The study site was located between minimum longitude/latitude 76.4753 E, 11.1917 N and maximum longitude/latitude 76.7485 E, 11.5195 N and an elevation range between 1800 and 2600m and a temperature range between 5 and 25 degrees Celsius. It comprises of a native habitat of grasslands in the hill

slopes and associated Shola forests in the valleys and folds. Vegetation studies in the region documented nearly 90 species of trees, lianas, shrubs and large herbs (Mohandass et al., 2009). The soils of the area are described a lateretic and derived from Charnockites with textures ranging from sandy loam to sandy clay loam (Caner and Bourgeon, 2001).

Three catchments corresponding to the three dominant vegetation types were selected for the study, namely grassland, shola and wattle. Details of the area under the catchments and land cover are provided in table 1.1 .

| Catchment | Area under riparian vegetation (ha) | Stream length (m) | Stream order | Catchment area (ha) |
|---|---|---|---|---|
| Wattle | 0.29 | 140.677 | 1 | 24.29 |
| Grassland | 0.25 | 236.772 | 1 | 43.74 |
| Shola | 266.11 | 6049 | 3 | 266.11 |

Table 1.1: Summary of catchment statistics.

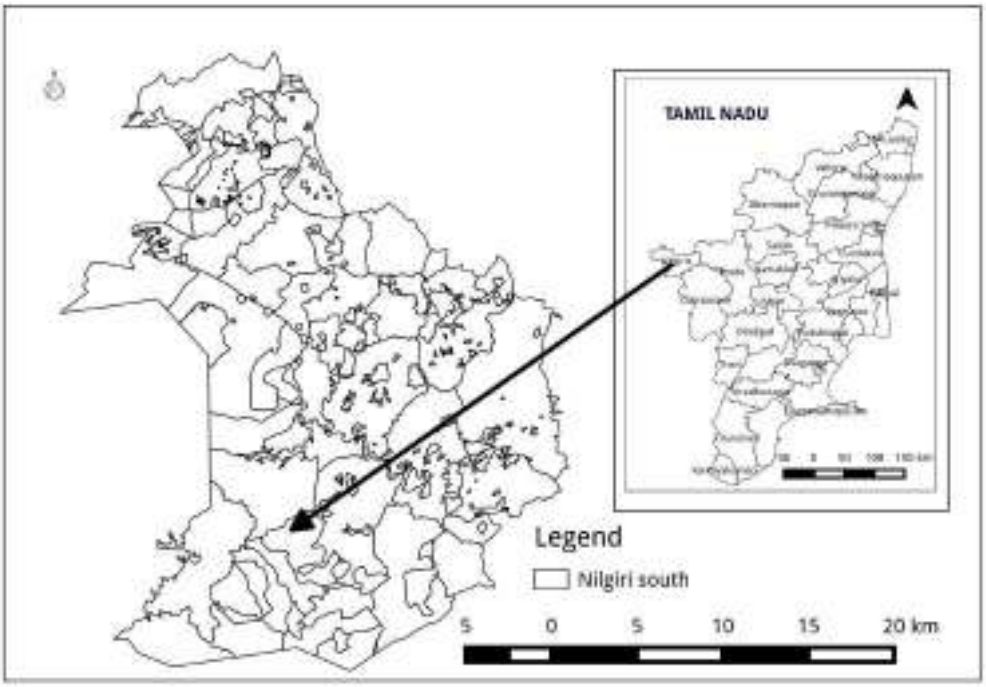


Figure 1.1: Location map of study area.

# 2. Literature Review

The impact of land cover change on hydrologic services is among the most intensively studied topics in forest hydrology (Brauman et al., 2007; Schilling et al., 2008) owing to its relevance to climate change and water resources management (Foley et al., 2005). Studies on land cover change are typically limited to catchment scales where the hydrological effects are most easily noted (Blöschl et al., 2007). Many of these are specific to a given species, for instance, the hydrological impact of eucalyptus plantations (Calder et al., 1999).

ET during the dry season plays a dominant role in the water balance of a catchment. The water balance equation:

$$\Delta S = P - ET - Q - D \tag{2.1}$$

defines this relationship, where $\Delta S$ is the change in water storage in the basin, $P$ is precipitation, $ET$ is evapotranspiration, $Q$ is stream flow and $D$ is recharge of ground water or deep drainage. Equivalently, ET is given by:

$$ET = P - \Delta S - Q - D. \tag{2.2}$$

The water balance equation for a given volume of soil provides another conceptual basis for measuring this. The root zone water balance is given by the

equation:

$$\Delta S = P - I - E - T - RO - DD \tag{2.3}$$

where $\Delta S$ is the change in root zone water storage for the time period of interest, $P$ is precipitation, $I$ is interception loss, $E$ is direct evaporation from the soil surface, $T$ is transpiration by plants, $RO$ is surface runoff and $DD$ is deep drainage (Zhang et al., 2002). In other words, during the dry season, plants meet their water demands from soil moisture or directly from groundwater via their root systems (Gribovszki et al., 2010) resulting is a signature which can be detected in stream discharges.

Total ET is an important component of the hydrological cycle. It is also one of the more complex components to measure as it depends on a number of other variables among which are temperature, relative humidity and land cover. However, one simple way of measuring the contribution of ET to the water balance is to measure the diurnal changes in stream discharge during the dry season (Boronina et al., 2005; Lundquist and Cayan, 2002).

The Normalized Difference Vegetation Index (NDVI) (Rouse Jr et al., 1974) is a remote sensing based index for the amount of green vegetation, which in turn, can be used as a surrogate for actively transpiring plant tissue or plant based ET (Krishnaswamy et al., 2009). NDVI is calculated as the ratio between the reflectance of red and near infra-red as and ranges between -1 (water) and +1 (vegetated) with values close to 0 corresponding to bare soils. It has the advantage that it can be used to monitor changes in vegetation growth and that in its derivation, it reduces some of the errors associated with atmospheric and sun illumination differences in imageries. Among the disadvantages of NDVI are that it saturates in conditions of high biomass and is sensitive to variations in

the background of the canopy, such as bare soils (Jensen, 2009).

Classification of land cover is among the most important applications of remote sensing. Among the earliest application of remotely sensed data to land use planning were in the late 1930s and early 1940s in the USA. The Steering Committee on Land Use information and Classification was formed in 1971 which adopted two land use systems proposed by J.R. Anderson which were based primarily on remotely sensed data (Anderson et al., 1976). A number of image classification algorithms have been developed over the years. Of these the maximum likelihood classifier is the most commonly used parametric approach to image classification (Jensen, 2009). Monitoring of land use and land cover change is an important component of environmental monitoring, (Lambin et al., 2001). Land use dynamics influence the climate change and the climate related impacts such as green house gas regulation genetic and species diversity and biodiversity (Chase et al., 2000). Remote sensing is also used extensively in tracking changes in land cover such as replacement of natural forest by settlements and for agricultural production (Armenteras et al., 2003).

Another application of land cover is hazard and risk assessment, such as the increased risk of landslides from the conversion of forest areas to agriculture. This process has led to the Nilgiris being identified amongst the most shallow landslide prone region in India (Bhagavanulu, 2008).

# 3. Objectives and Methods

## Objectives

1. To determine the impact of land cover on dry season flows with a focus on diurnal variation in surface discharge.

2. To determine the amount of photosynthetically active vegetation (NDVI) across land covers.

3. To determine the relationship between NDVI and diurnal variations in discharge.

4. To determine the relationship between land cover and water balance in the upper watersheds of the Nilgiris.

## Methods

The analysis of spatial data presented here was done using the Geographical Resource Analysis Support System version 7 (GRASS Development Team, 2015) and the Quantum GIS package (QGIS Development Team, 2015). The R pack-

age for statistical computing (R Core Team, 2015) and its various libraries was used for the statistical analysis and graphing.

## Land Cover Mapping

The steps involved in deriving the land cover from the LANDSAT imagery are summarised in figure 3.1.

This study assess the land use and land cover using LANDSAT 8 satellite data for land use classification based on maximum likelihood classification (Neteler et al., 2012). A total of 232 ground control points (GCP) were collected for three major types of land cover, namely, grasslands, Shola forests and wattle plantations. Given that some of the wattle plantations were dead or dormant, separate training sites for each were collected. Two thirds of the GCPs were used for training the image while a third was used as input for the accuracy assessment.

## Normalised Difference Vegetation Index (NDVI)

NDVI calculations were done using the r.mapcalc module in GRASS and the formula:

$$(NIR - R)/(NIR + R) \tag{3.1}$$

where $NIR$ is near infrared or band 5 of LANDSAT 8 and $R$ is red or band 4. The resulting region was then classified using the land cover map generated from the supervised classification procedure. The NDVI layer were also used to demarcate the photosynthetically active vegetation in riparian zones of the

catchment, which was expected to be contributing most to the diurnal signal in discharge.

## Catchment Delineation

The steps involved in delineating the catchment boundaries are summarised in figure 3.2.

Delineation of the catchment for each gauging station of the stream was done using a digital elevation model (DEM) obtained from an ASTER image. Topographic lines from maps of the area were also digitised. Streams were separately digitised and together with the topographic lines, were merged with the DEM. These provided ground controls and improved the accuracy of the DEM. The GRASS7 module *r.watershed* was then used to delineate watershed boundaries and *r.water.outlet* to delineate catchments for specific discharge points. Results were finally vectorised and area statistics added to the attribute tables (figure 3.3).

These area calculations provide the input for determining the "depth of discharge" from a given catchment, which is a fundamental component of the water balance equation.

## Discharge Measurements

The steps involved in measuring discharge have been presented in figure 3.4 and are detailed below.

A number of different techniques were used for the measurement of discharge. The traditional method for calculating stream discharges is based on

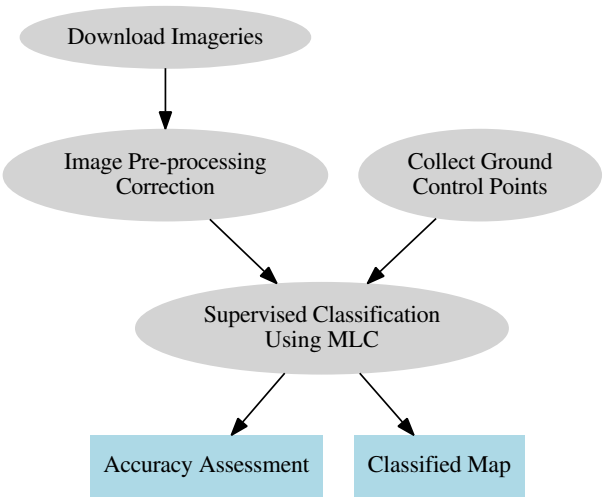


Figure 3.1: Steps in deriving land classes from multispectral LANDSAT8 imagery.

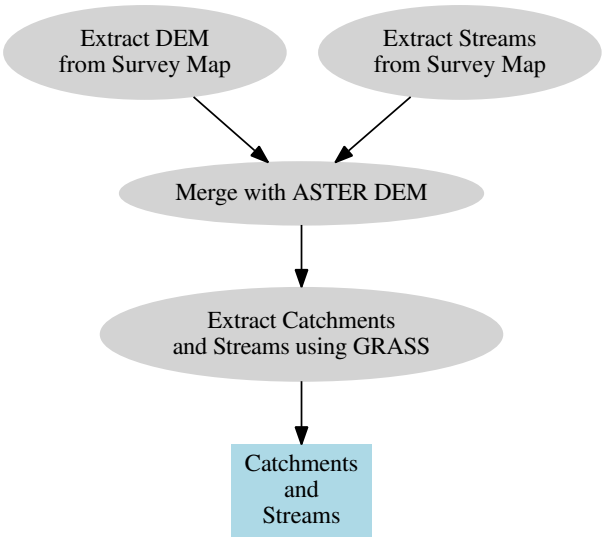


Figure 3.2: Steps involved in catchment delineation.

Figure 3.3: Map of the Lakdihalla watershed (above) and catchment for station 101.

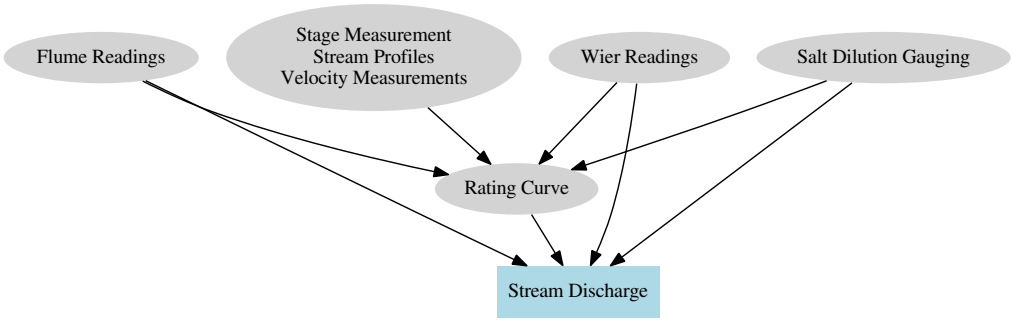


Figure 3.4: Steps involved in calculating discharge values for a stream.

surveying the cross section of the stream at different stages and measuring the velocity of the water using a current meter or floating orange method (figure 3.5). Once a sufficient number of profiles have been collected, a relationship is calculated by fitting an appropriate model to fit values of stage to discharge. This "rating curve" is then utilised to obtain discharge measurements for all other stages (Gordon et al., 2013). Other methods used for determining discharge are salt dilution gauging and controlled structures such as weirs and flumes. The latter are often also added to the points required for calculating the rating curve.

We utilised all of the above for this study. Flumes were uses mostly during low flows when stream velocity measures were unreliable, e.g. in the grassland dominated catchment. Salt dilution gauging, using the slug method, was employed during very high flows during which it was difficult, and in some streams, dangerous to enter the stream for velocity measurements or profiles. This was used in the Shola dominated catchment. A permanent weir was constructed and used for all measurements at the wattle dominated catchment.

The cross sectional profiles and velocity measurements for each stream corresponding to the period of the study were used in combination with readings from flumes and salt dilution gauging. The resulting rating curve is shown in figure 3.6. The discharge for the period of the study (February to April 15$^{th}$, 2014) was then extracted for the selected stations and plotted against time as shown in figure 3.7

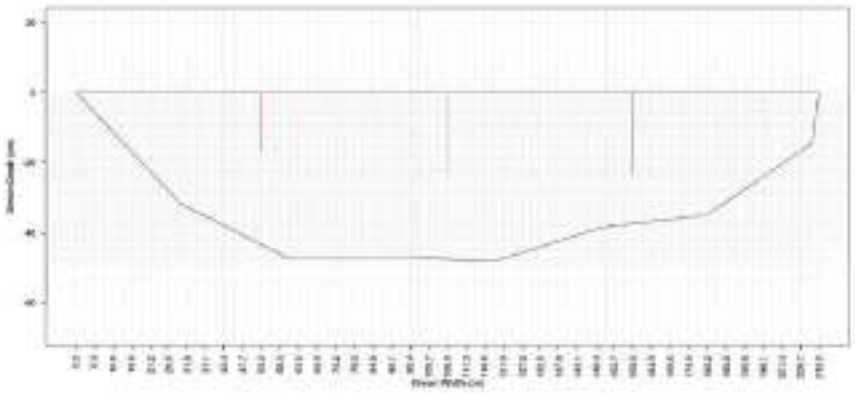

Figure 3.5: A stream profile showing points at which velocities were measured.

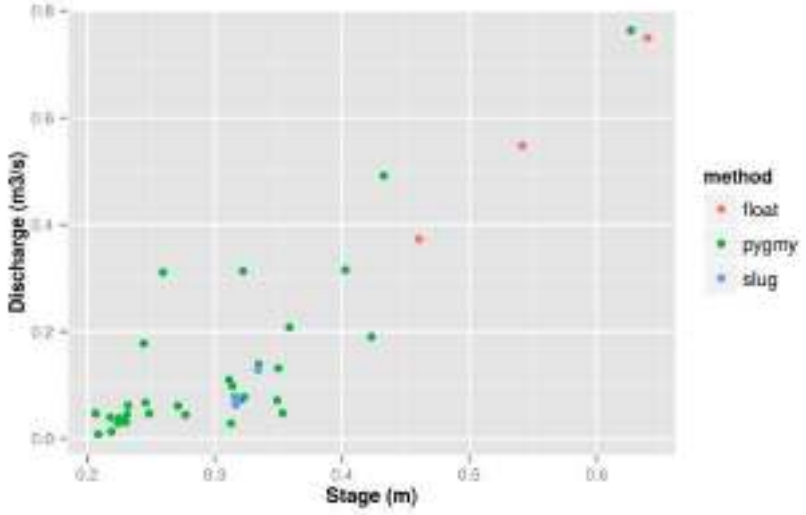


Figure 3.6: Rating curve used to evaluate the stage-discharge relationship.

## Evapotranspiration

The steps involved in extracting the ET from diurnal variations in discharge are shown in figure 3.8. The conceptual basis for the measurement of ET is the work of Boronina et al. (2005) who estimated the ET due to riparian vegetation can be measured by the difference of a potential hydrograph with the observed hydrograph as:

$$ET_{alluv}^{daily} = \sum_{i=1}^{24}(Q_{max} - Q_i)\Delta t \tag{3.2}$$

where $ET_{alluv}^{daily}$ is the daily loss of water from the catchment through ET, $Q_{max}$ is the daily maximum flow rate in the river between noon and 3pm, $Q_i$ is the average flow rate for every hour of the day and $\Delta t$ is one hour (Gribovszki et al., 2010).

Diurnal patterns in stream discharge during the dry seasons reflect the contribution of ET due to vegetation cover in riparian regions. Relative effect of different land cover can therefore also be measured from catchments with known areas under different forest types. An analysis of differences in NDVI from a NDVI value from a reference vegetation class can further allow us to develop a means to measure ET from remotely sensed data (Krishnaswamy et al., 2009).

In order to measure the contribution of this to total stream flow, one needs to calculate the ratio of the amplitude of the diurnal cycle to the average total daily discharge. Here the amplitude of the diurnal cycle is half the difference between the maximum and minimum daily discharge and is averaged over the period being examined (Lundquist and Cayan, 2002).

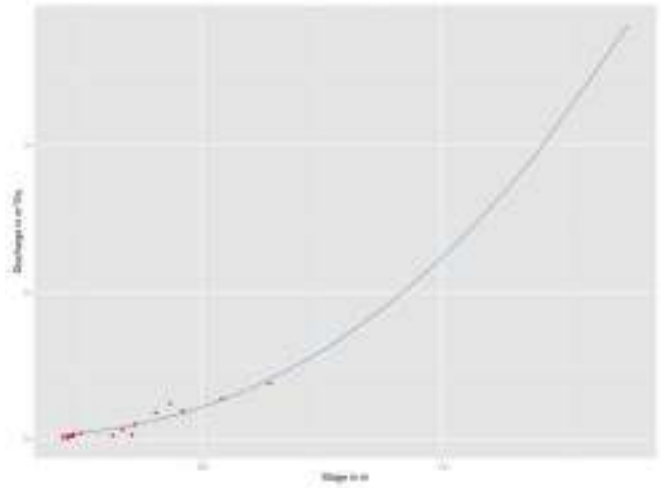

Figure 3.7: Stage-discharge points used to derive a rating curve. Note that over 97% of the readings fall within the range of values for which stage-dischrge measurements were collected.

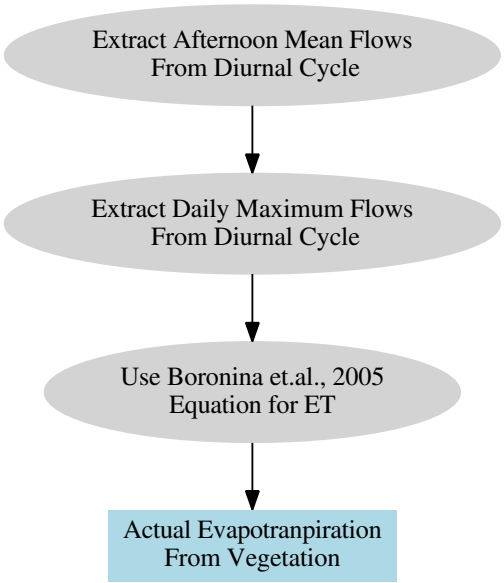


Figure 3.8: Steps in deriving ET for diurnal variations in stream discharge.

# 4. Observations and Results

## Land-cover Mapping

The land cover map for the Nilgiri South reserve is presented in map 4.1 along with the areas under the different classes (table 4.1). Training sites used to generate the map and conduct the accuracy assessments are presented in map 4.2 and the accuracy matrix is presented in table 4.2. This matrix is calculated by cross tabulating the classified map layer with respect to a reference map layer generated from a subset of the GCP which results in a table of commission errors, i.e. errors made by the producer who incorrectly commits pixels to an incorrect land cover class and omission errors, or user errors, where objects classified on the map do not match the actual land cover class on the ground. The former results from insufficient number of ground control points or errors in delineation of training sites while the latter can result from the imagery not having sufficient spectral information to tease apart land cover classes. The Kappa analysis used to conduct accuracy assessments is now considered a standard (Congalton, 1991).

The total area under different land covers as per the supervised map are presented in figure 4.1.

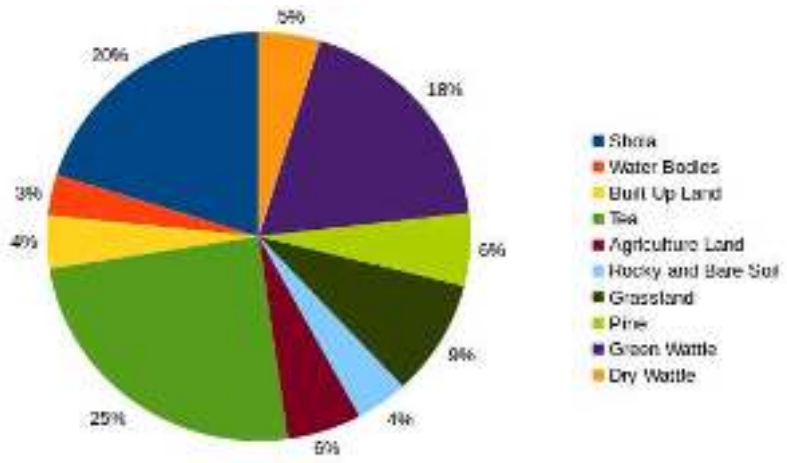


Figure 4.1: Proportion of area under different land cover.

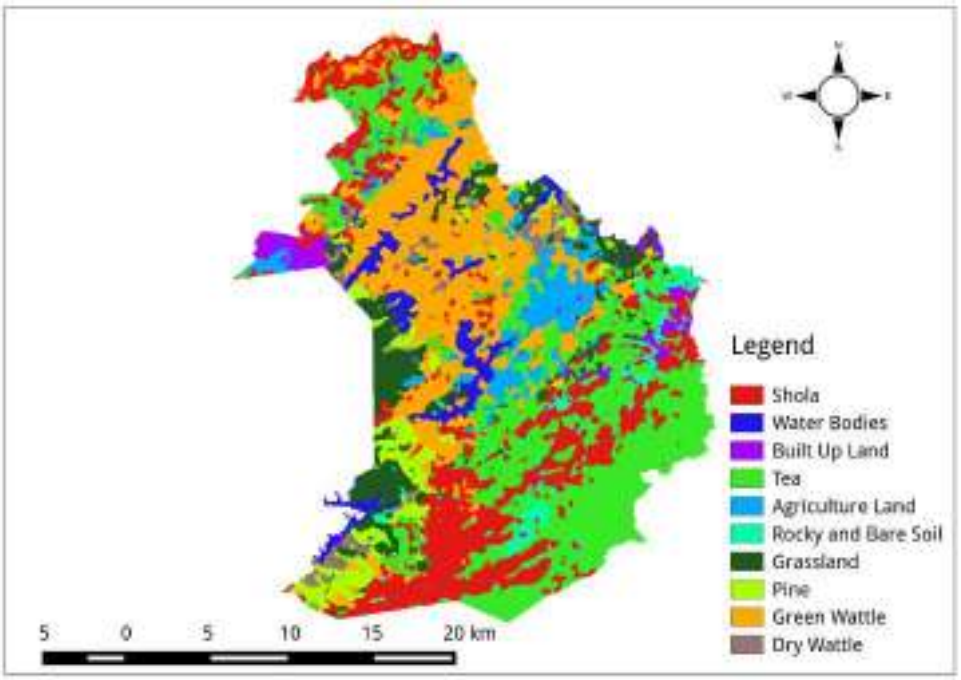


Map 4.1: Supervised classification of land cover in the Nilgiri South range.

| Sl. | Land Cover | Area (ha) |
|---|---|---|
| 1 | Shola | 12097.16 |
| 2 | Water Bodies | 1939.54 |
| 3 | Built Up Land | 2511.47 |
| 4 | Tea | 14829.22 |
| 5 | Agriculture Land | 3431.75 |
| 6 | Rocky and Bare Soil | 2404.76 |
| 7 | Grassland | 5529.59 |
| 8 | Pine | 3449.63 |
| 9 | Green Wattle | 11092.42 |
| 10 | Dry Wattle | 2820.71 |
| | Total | 60106.25 |

Table 4.1: Area under different land cover classes.

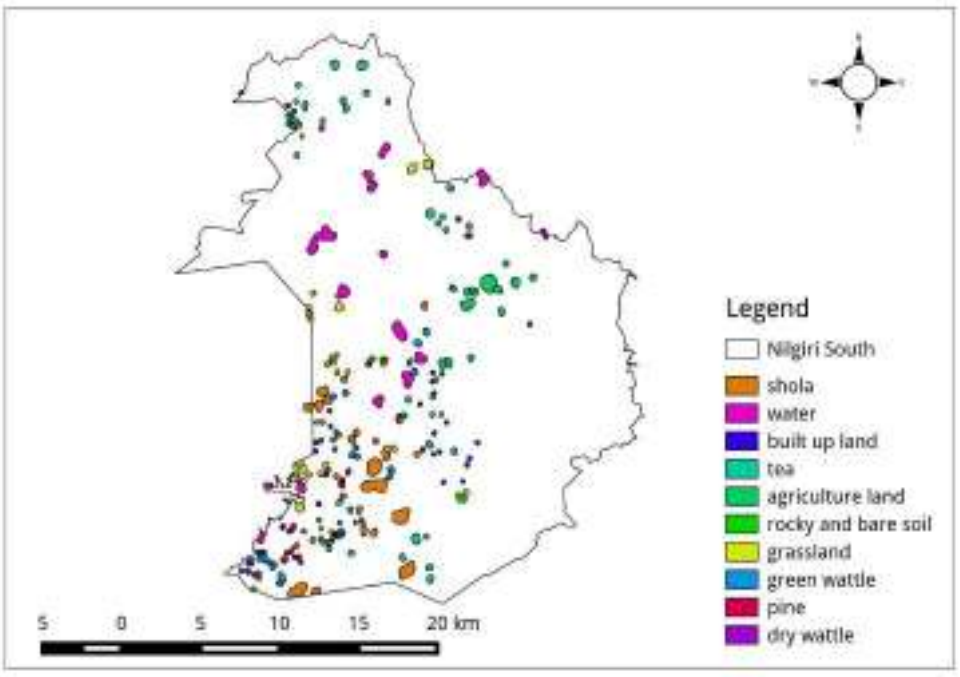


Map 4.2: Training sites used to supervise the land cover map.

## Normalised Difference Vegetation Index (NDVI)

The normalised difference vegetation index for the study area is presented in map 4.3. As the image was taken in the dry months, the bulk of the range forest under grassland showed a low NDVI with the highest values in the Shola patches.

## Catchment Delineation

The areas under the three catchments (map 4.4) were estimated using a digital elevation model (map 4.5). The areas under grassland, wattle and Shola forest were 43.74, 24.29 and 266.1 hectares respectively.

## Discharge Measurements

The discharge data used for this study was obtained from an ongoing project[1]. Data for the dry season, from January to mid April was used which corresponded to the longest period without rain. The script used to analyse the data and generate the results is presented in Appendix A. Figure 4.2 shows the discharge measurements for the period 1st February to 15th April which corresponds to the logest dry spell at the study site. Of the three land cover types, the grassland exhibited the largest and nearly linear drop in percentage discharge during this

[1]This is a Ministry of Earth Sciences supported project under the Changing Water Cycle programme. The project title is "Hydrologic and Carbon Services in the Western Ghats, Impact of Extreme Rainfall Events". The author is a member of the project team and has participated in the installation of equipment and collection of data. The data itself is processed using R scripts written by other members of the team. It has been made available for this thesis with the consent of the principal investigator of the project.

| Cats | Category Description | % Commission | % Ommission | Estimated Kappa |
|---|---|---|---|---|
| 1 | Shola | 9.876543 | 47.857143 | 0.890234 |
| 2 | Water Bodies | 0 | 1.067616 | 1 |
| 3 | Built Up Land | 26.086957 | 32 | 0.734377 |
| 4 | Tea | 12.962963 | 7.843137 | 0.865459 |
| 5 | Agriculture Land | 4 | 17.241379 | 0.959152 |
| 6 | Rocky and Bare Soil | 6.976744 | 10.447761 | 0.92283 |
| 7 | Grassland | 10.11236 | 3.614458 | 0.88524 |
| 8 | Pine | 55.421687 | 57.471264 | 0.408976 |
| 9 | Green Wattle | 42.473118 | 28.187919 | 0.52456 |
| 10 | Dry Wattle | 42.682927 | 12.962963 | 0.556009 |

Table 4.2: Kappa accuracy assessment of supervised classification.

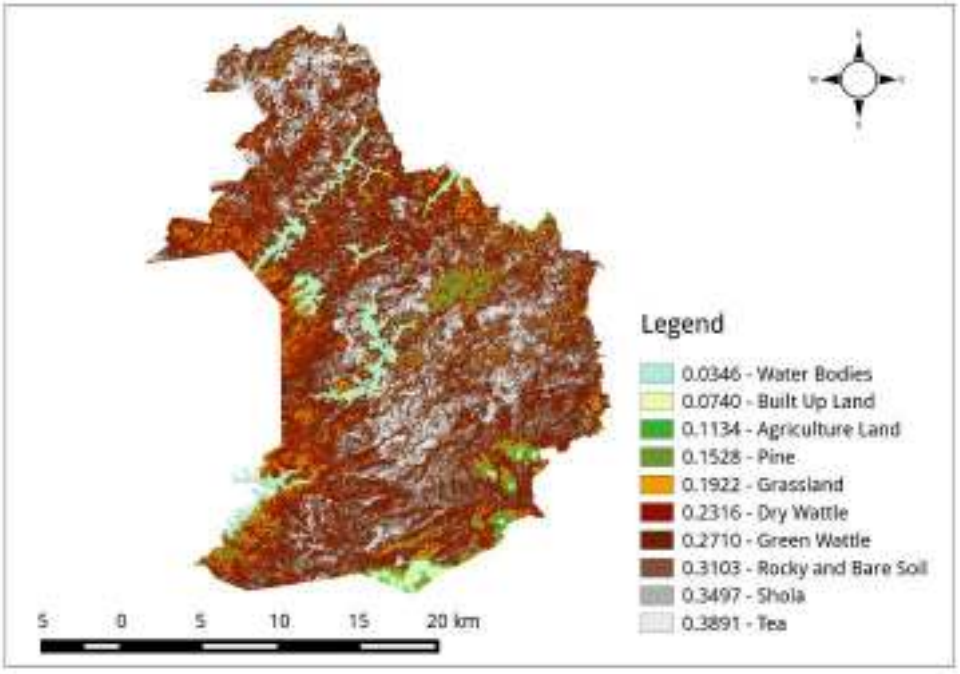


Map 4.3: Normalised Difference Vegetation Index map of the Nilgri South range. The map has been supervised into land cover categories based on the land cover map.

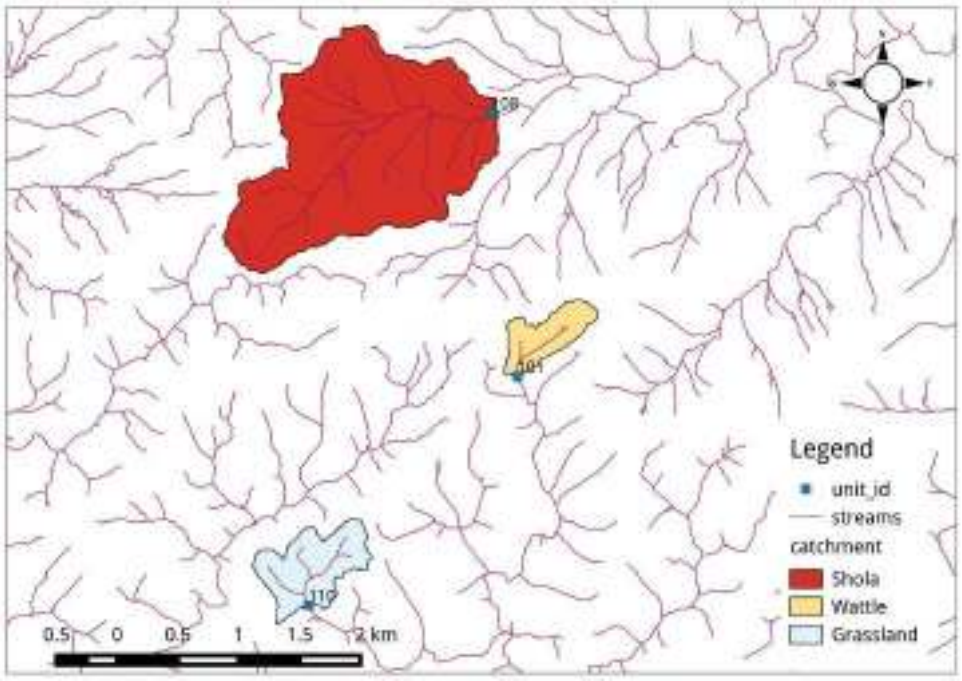


Map 4.4: Study catchments with the stream layer derived from the digital elevation model.

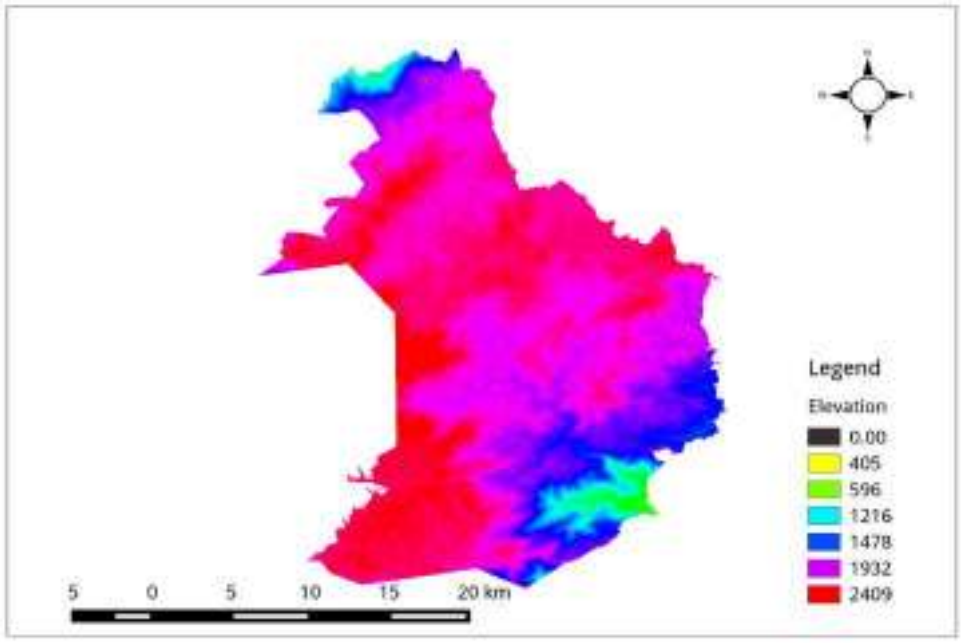


Map 4.5: ASTER based digital elevation model of the study area used to derive the catchment and streams layers.

period while the Shola catchment showed the lowest total decrease in percentage of discharge with the wattle catchment displaying intermediate values.

The amplitude of diurnal discharge variations was the most pronounced in the Shola catchment followed by the grassland and wattle. This pattern was repeated for the total volume of discharge which ranged from 0.09632 to 0.2566$m^3/s$ for Shola, 0.03535 to 0.07797 $m^3/s$ for grassland and 0.00101 to 0.00882 $m^3/s$ for the wattle. The summary statistics for the discharge measurements are presented in table 4.3.

## Evapotranspiration

ET showed an increasing trend from grassland, wattle to Shola. The summary statistics have been provided in table 4.4. The mean ET for the three catchments was 2.975, 4.759 and 6.135 respectively. The diurnal amplitude also follwed an increasing pattern from grassland, to wattle to the Shola dominated catchment. Figure 4.3 presents the results of ET calculations where area for both the entire catchment as well as just the riparian region of the stream were used. The observed ET values were similar to those in published literature both internationally (Allen et al., 1998) and from nearby stations at Coimbatore (Kannappan et al., 2003).

A linear regression between the mean ET and NDVI values from the three land covers (grassland, green wattle and Shola) shows a strong positive relationship (figure 4.4) with an adjusted R-squared of 0.9891 and p-value of 0.0471.

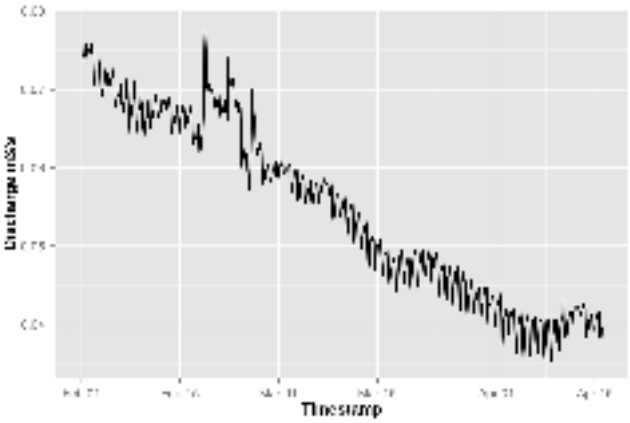


(a) Grassland dominated.

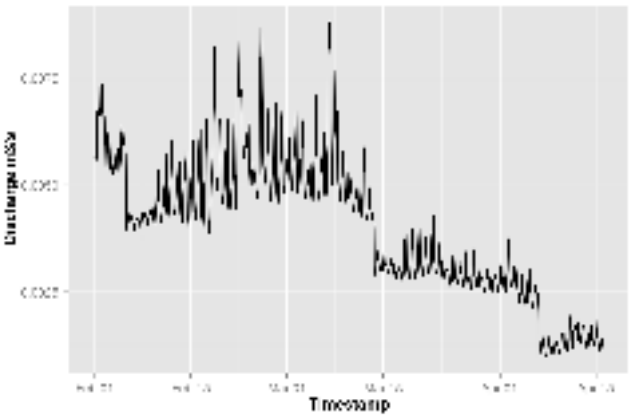


(b) Wattle dominated.

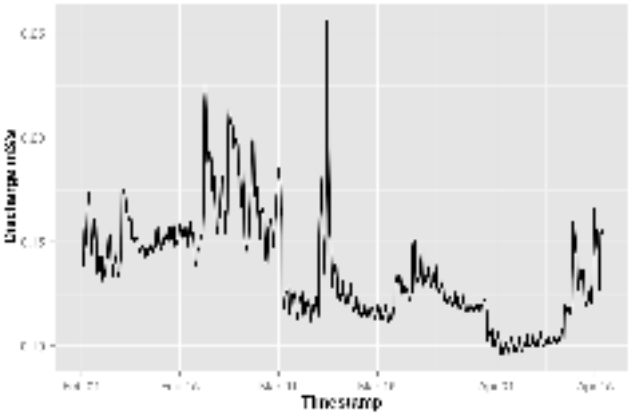


(c) Shola dominated.

Figure 4.2: Discharge measurements for the different catchments.

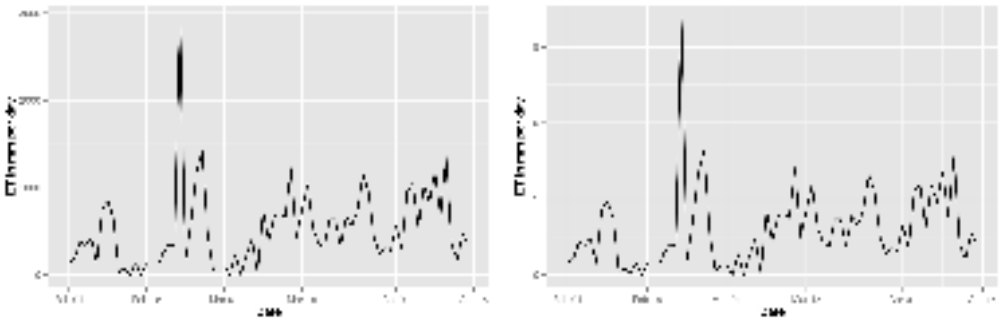

(a) Grassland dominated.

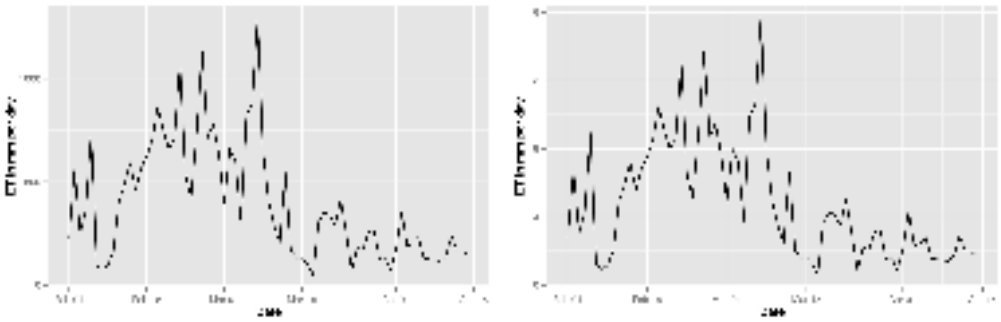

(b) Wattle dominated.

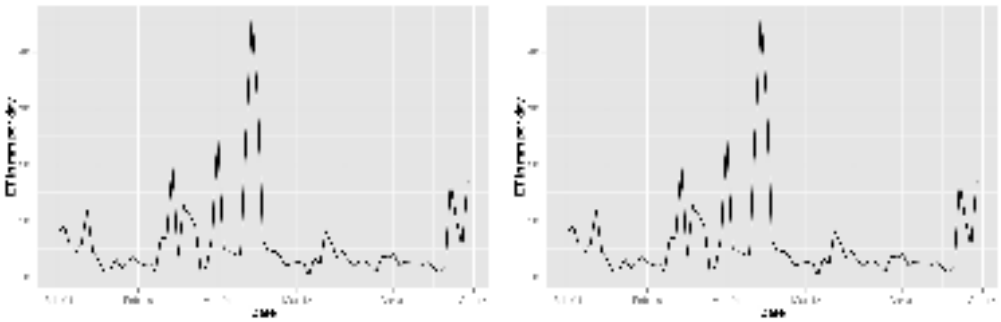

(c) Shola dominated.

Figure 4.3: ET measurements for the different catchments. Figures on the left are ET for the green vegetation in the riparian reaches of the catchment, i.e. along the streams.Those on the right are for the entire catchment area. Note that the entire catchment of the Shola patch comprised of green Shola species.

| | Grassland | Wattle | Shola |
|---|---|---|---|
| Min. | 0.03535 | 0.00101 | 0.09632 |
| 1st Qu. | 0.04364 | 0.00283 | 0.1177 |
| Median | 0.05484 | 0.00422 | 0.1308 |
| Mean | 0.05462 | 0.004019 | 0.136 |
| 3rd Qu. | 0.06638 | 0.00524 | 0.1525 |
| Max. | 0.07797 | 0.00882 | 0.2566 |

Table 4.3: Summary statistics for discharge (top) in $m^3/s$ and depth of discharge in mm (bottom).

| | Grassland | Wattle | Shola |
|---|---|---|---|
| Min. | 0 | 0.5969 | 0.2236 |
| 1st Qu. | 1.072 | 1.955 | 2.346 |
| Median | 2.356 | 3.705 | 3.479 |
| Mean | 2.975 | 4.759 | 6.135 |
| 3rd Qu. | 3.997 | 7.286 | 6.392 |
| Max. | 16.89 | 15.64 | 46.01 |

Table 4.4: Summary statistics for ET in mm per day.

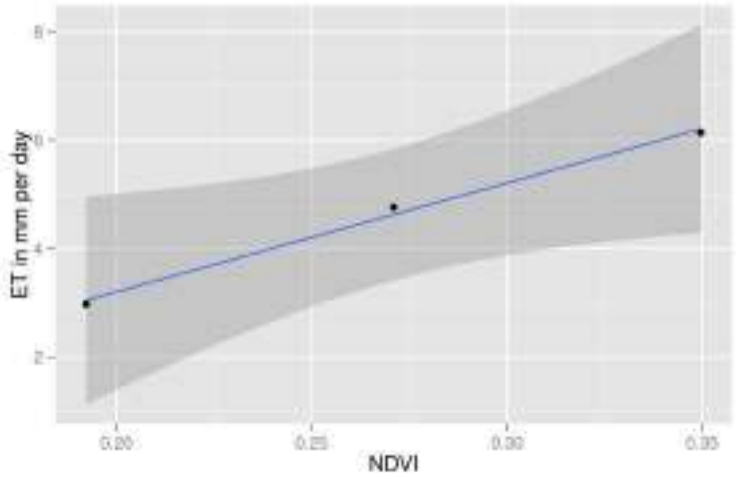


Figure 4.4: Plot of linear regression between NDVI and ET.

# 5. Discussion and Conclusion

Land cover showed a clear relationship with ET where grassland dominated catchment had the lowest ET followed by wattle and Shola. This is consistent with the NDVI values for these three land covers where broad leaved evergreen Shola species had the highest NDVI followed by wattle. Grasslands showed the minimum NDVI as they dry up during the dry season.

Discharge measurements showed that the wattle dominated catchment had the lowest discharge followed by the grassland and finally the Shola dominated catchment. Discharge, however, is a function not only of precipitation, but also of the area under the catchment, its underlying soil and geomorphology which can play a major role in determining sub-surface flows. The lower discharges of the wattle catchment were probably due to its much smaller area. An interesting trend, which requires further investigation, was the decrease in basal flows for the three catchments. Here grasslands showed the sharpest decrease followed by wattle and Sholas, which showed a very shallow reduction.

Diurnal variations in discharge, however, would be more dependent on extraction of water from the soil by vegetation and through evaporation. These showed a clear difference between the three land covers with the variation being the highest in Shola (57.84546), followed by wattle (11.8206) and the lowest in

grassland (7.017668). This is, again consistent with the trend in NDVI of the three land cover types.

The total land cover of the site showed that tea formed the bulk of the vegetation followed by wattle, Shola forests and grasslands. Both tea and wattle were planted over grasslands and have, in all likelihood, played a major role in modifying the hydraulic balance of the area. Tea, like Shola species, is an evergreen plant and is likely to have a higher ET than grassland or even wattle. Even though the wattle in the study catchment partially dry, it has started to recover in the past year and will, in all likelihood result in an increase in the total transpiring vegetation.

The change in land cover from grasslands to evergreen species such as tea and wattle is likely to increase the amount of water withdrawn from these catchments by transpiration. Once a relationship between vegetation cover and ET is established, the likely change in water balance in a catchment as a result of land cover change can be calculated.

Our finding show that even partially dry wattle has an ET rate which is 61% higher than grasslands. For Shola forests this is 68% higher than grasslands, however, unlike Shola forests, wattle offers little in terms of biodiversity services. Converting grasslands to tea and wattle would have therefore increased the water lost due to transpiration to the order of 65%. In terms of total increase of water loss this translates to a loss of 1.784mm per day or 651.16mm a year which corresponds to over half the annual rainfall of Pondicherry.

While these figures are suggestive, the study shows that this approach can be used to evaluate the impact of land cover change on ET and water budgets extrapolated over larger landscapes. The results underline the need for care-

ful planning prior to engaging in large scale land cover changes through programmes such as the Greening India Mission. Headwaters of our major rivers play a crucial role in maintaining ecosystem services such as provisioning of water to downstream communities. Modifications of the land cover in these regions can have negative repercussions on downstream water users.

# Bibliography

Richard G. Allen, Luis S. Pereira, Dirk Raes, Martin Smith, and others. Crop evapotranspiration-Guidelines for computing crop water requirements-FAO Irrigation and drainage paper 56. *FAO, Rome*, 300(9), 1998. URL http://www.engr.scu.edu/~emaurer/classes/ceng140_watres/handouts/FAO_56_Evapotranspiration.pdf.

James R Anderson, Ernest E Hardy, John T Roach, and Richard E Witmer. A Land Use And Land Cover Classification System For Use With Remote Sensor Data. Professional Paper, A revision of the land use classification system as presented in U.S. Geological Survey Circular 671 964, United States Government Printing Office, Washington, 1976.

Anon. *National Mission for Greening India*. Ministry of Environment and Forests, Goverment of India, 2013.

D. Armenteras, F. Gast, and H. Villareal. Andean forest fragmentation and the representativeness of protected natural areas in the eastern Andes, Colombia. *Biological Conservation*, 113(2):245–256, 2003. URL http://www.sciencedirect.com/science/article/pii/S0006320702003592.

S. Vasantha Kumar-DVS Bhagavanulu. Effect of Deforestation on Landslides in Nilgiris District-A Case Study. *J. Indian Soc. Remote Sens.*, 36:105–108, March 2008. URL http://www.springerlink.com/index/pdf/10.1007/s12524-008-0011-5.

Günter Blöschl, Sandra Ardoin-Bardin, Mike Bonell, Manfred Dorninger, David Goodrich, Dieter Gutknecht, David Matamoros, Bruno Merz, Paul Shand, and Jan Szolgay. At what scales do climate variability and land cover change impact on flooding and low flows? *Hydrological Processes*, 21(9):1241–1247, 2007. URL http://onlinelibrary.wiley.com/doi/10.1002/hyp.6669/full.

M. Bonell and L. A. Bruijnzeel. *Forests, Water and People in the Humid Tropics - 2 Part Set: Forests, Water and People in the Humid Tropics 2 Volume Set: Past, Present ... Management*. 2010.

Anastasia Boronina, Sergey Golubev, and Werner Balderer. Estimation of actual evapotranspiration from an alluvial aquifer of the Kouris catchment (Cyprus) using continuous streamflow records. *Hydrological Processes*, 19(20):4055–4068, 2005. URL http://onlinelibrary.wiley.com/doi/10.1002/hyp.5871/full.

Kate A. Brauman, Gretchen C. Daily, T. Ka'eo Duarte, and Harold A. Mooney. The nature and value of ecosystem services: an overview highlighting hydrologic services. *Annu. Rev. Environ. Resour.*, 32:67–98, 2007. URL http://www.annualreviews.org/doi/abs/10.1146/annurev.energy.32.031306.102758.

Ian R. Calder, Paul TW Rosier, K. T. Prasanna, and S. Parameswarappa. Eucalyptus water use greater than rainfall input-possible explanation from southern India. *Hydrology and Earth System Sciences*, 1(2):249–256, 1999. URL http://www.hydrol-earth-syst-sci.net/1/249/1997/hess-1-249-1997.pdf.

Laurent Caner and Gérard Bourgeon. Andisols of the Nilgiri highlands: new insight into their classification, age and genesis. *Sahyadri: The Great Escarpment of the Indian Subcontinent (Patterns of Landscape Development in the Western Ghats).*, pages 905–918, 2001. URL http://hal.cirad.fr/hal-00259435/.

MD Subash Chandran. On the ecological history of the Western Ghats. *Current Science*, 73(2):146–155, 1997. URL http://www.researchgate.net/profile/M_D_Chandran/publication/259105549_On_the_ecological_history_of_the_Western_Ghats/links/53fcd3ed0cf2dca8ffff61b3.pdf.

T. N. Chase, R. A. Pielke Sr, T. G. F. Kittel, R. R. Nemani, and S. W. Running. Simulated impacts of historical land cover changes on global climate in northern winter. *Climate Dynamics*, 16(2-3):93–105, 2000. URL http://link.springer.com/article/10.1007/s003820050007.

Russell G. Congalton. A review of assessing the accuracy of classifications of remotely sensed data. *Remote sensing of environment*, 37(1):35–46, 1991. URL http://www.sciencedirect.com/science/article/pii/003442579190048B.

Arundhati Das, Jagdish Krishnaswamy, Kamaljit S Bawa, M C Kiran, V. Srinivas, N Samba Kumar, and K Ullas Karanth. Prioritisation of conservation areas in the Western Ghats. *Biological Conservation*, 133:16–31, 2006. doi: 10.1016/j.biocon.2006.05.023.

Jonathan A. Foley, Ruth DeFries, Gregory P. Asner, Carol Barford, Gordon Bonan, Stephen R. Carpenter, F. Stuart Chapin, Michael T. Coe, Gretchen C. Daily, Holly K. Gibbs, and others. Global consequences of land use. *science*, 309(5734):570–574, 2005. URL http://www.sciencemag.org/content/309/5734/570.short.

Nancy D. Gordon, Thomas A. McMahon, Brian L. Finlayson, Christopher J. Gippel, and Rory J. Nathan. *Stream hydrology: an introduction for ecologists*. John Wiley & Sons, 2013. URL http://books.google.com/books?hl=en&lr=&id=9ZlOIRNO8s0C&oi=fnd&pg=PT7&dq=stream+ecology+introduction+to+ecologists&ots=kkN3DEhEBq&sig=f3cxP8r9cK9AC_X-inijA_37cCE.

GRASS Development Team. *Geographic Resources Analysis Support System (GRASS GIS) Software version 7*. Open Source Geospatial Foundation, 2015. URL http://grass.osgeo.org.

Zoltán Gribovszki, József Szilágyi, and Péter Kalicz. Diurnal fluctuations in shallow groundwater levels and streamflow rates and their interpretation–A review. *Journal of Hydrology*, 385(1):371–383, 2010. URL http://www.sciencedirect.com/science/article/pii/S0022169410000685.

John R. Jensen. *Remote sensing of the environment: An earth resource perspective 2/e*. Pearson Education India, 2009. URL http://books.google.com/books?hl=en&lr=&id=ge_nwDX-HBEC&oi=fnd&pg=PR13&dq=remote+sensing+of+the+environment+jensen&ots=nEoAOBo7cZ&sig=qCCOK-kyluTZDxzKMKlOBpJTvTU.

K. Kannappan, A. Murugappan, N. Manikumari, and A. Manoharan. Reference Evapotranspiration Models For Certain Locations In Tamilnadu. *Watershed Hydrology*, page 56, 2003. URL http://books.google.com/books?hl=en&lr=&id=73DdflwDU0oC&oi=fnd&pg=PA56&dq=referance+evapotranspiration+models+for+certain+location+in+tamilnadu&ots=MlUV_2RRk0&sig=k8ZAcSkbRRPZv2oLekCFx92sqQU.

Jagdish Krishnaswamy, Kamaljit S. Bawa, K. N. Ganeshaiah, and M. C. Kiran. Quantifying and mapping biodiversity and ecosystem services: Utility of a multi-season NDVI based Mahalanobis distance surrogate. *Remote Sensing of Environment*, 113(4):857–867, 2009. URL http://www.sciencedirect.com/science/article/pii/S0034425708003696.

Eric F. Lambin, Bi L. Turner, Helmut J. Geist, Samuel B. Agbola, Arild Angelsen, John W. Bruce, Oliver T. Coomes, Rodolfo Dirzo, Günther Fischer, Carl Folke, and others. The causes of land-use and land-cover change: moving beyond the myths. *Global environmental change*, 11(4): 261–269, 2001. URL http://www.sciencedirect.com/science/article/pii/S0959378001000073.

Jessica D. Lundquist and Daniel R. Cayan. Seasonal and spatial patterns in diurnal cycles in streamflow in the western United States. *Journal of Hydrometeorology*, 3(5):591–603, 2002. URL http://journals.ametsoc.org/doi/abs/10.1175/1525-7541(2002)003%3C0591:SASPID%3E2.0.CO;2.

Russell A. Mittermeier, Will R. Turner, Frank W. Larsen, Thomas M. Brooks, and Claude Gascon. Global biodiversity conservation: the critical role of hotspots. In *Biodiversity hotspots*, pages 3–22. Springer, 2011. URL http://link.springer.com/chapter/10.1007/978-3-642-20992-5_1.

D. Mohandass, Priya Davidar, and others. Floristic structure and diversity of a tropical montane evergreen forest (shola) of the Nilgiri Mountains, southern India. *Tropical Ecology*, 50(2):219, 2009. URL http://www.tropecol.com/pdf/open/PDF_50_2/J-02.pdf.

Markus Neteler, M. Hamish Bowman, Martin Landa, and Markus Metz. GRASS GIS: A multi-purpose open source GIS. *Environmental Modelling & Software*, 31:124–130, 2012. URL http://www.sciencedirect.com/science/article/pii/S1364815211002775.

QGIS Development Team. *QGIS Geographic Information System*. Open Source Geospatial Foundation, 2015. URL http://qgis.osgeo.org.

R Core Team. *R: A Language and Environment for Statistical Computing*. R Foundation for Statistical Computing, Vienna, Austria, 2015. URL http://www.R-project.org/.

Haripriya Rangan, Christian A. Kull, and Lisa Alexander. Forest plantations, water availability, and regional climate change: controversies surrounding Acacia mearnsii plantations in the upper Palnis Hills, southern India. *Regional Environmental Change*, 10(2):103–117, 2010. URL http://link.springer.com/article/10.1007/s10113-009-0098-4.

N. H. Ravindranath and I. K. Murthy. Greening India Mission. *CURRENT SCIENCE*, 99(4):444, 2010.

J. W. Rouse Jr, R. H. Haas, D. W. Deering, J. A. Schell, and J. C. Harlan. Monitoring the Vernal Advancement and Retrogradation (Green Wave Effect) of Natural Vegetation.[Great Plains Corridor. 1974. URL http://ntrs.nasa.gov/search.jsp?R=19750020419.

Steven W. Running, Ramakrishna R. Nemani, David L. Peterson, Larry E. Band, Donald F. Potts, Lars L. Pierce, and Michael A. Spanner. Mapping regional forest evapotranspiration and photosynthesis by coupling satellite data with ecosystem simulation. *Ecology*, pages 1090–1101, 1989. URL http://www.jstor.org/stable/1941378.

Keith E. Schilling, Manoj K. Jha, You-Kuan Zhang, Philip W. Gassman, and Calvin F. Wolter. Impact of land use and land cover change on the water balance of a large agricultural watershed: Historical effects and future directions. *Water Resources Research*, 44(7), 2008. URL http://onlinelibrary.wiley.com/doi/10.1029/2007WR006644/full.

A. K. Sikka, J. S. Samra, V. N. Sharda, P. Samraj, and V. Lakshmanan. Low flow and high flow responses to converting natural grassland into bluegum (Eucalyptus globulus) in Nilgiris watersheds of South India. *Journal of Hydrology*, 270(1):12–26, 2003. URL http://www.sciencedirect.com/science/article/pii/S0022169402001725.

Lu Zhang, Glen R. Walker, and Warrick R. Dawes. Water balance modelling: concepts and applications. *ACIAR MONOGRAPH SERIES*, 84:31–47, 2002. URL http://www.cossa.csiro.au/aciar/book/PDF/Monograph_84_Chapter_01.pdf.

# A. R script for analysing discharge data and plotting the results

```
1  ## Generate dischages, calculate ET and create plots of
       diurnal cycles using ggplot2
2  ## Author: R.S. Bhalla, 2015
3  ## Released under creative commons, non-commercial, share
       alike.
4  ## Prepared for project "Hydrologic and Carbon Services in
        the Western Ghats,
5  ## Impact of Extreme Rainfall Events",
6  ## Supported by Ministry of Earth Sciences under the
       Changing Water Cycles Programme.
7  ##-- Load required libraries
8  library(ggplot2)
9  library(timeSeries)
10 ##-- Set environment as appropriate
11 setwd(dir="[]")
12 wlr.dir <- "[]"
13 sd.dir <- "[]"
14 stn.no <- c("101", "110", "108")
15 stn.type <- c("Wattle", "Grassland", "Shola")
16 ts.start <- as.POSIXct("2014-02-01␣00:00:00", tz="Asia/
       Kolkata")
17 ts.end <- as.POSIXct("2014-04-15␣23:59:59", tz="Asia/
       Kolkata")
18 ##-- Begin loop
19 for(i in 1: length(stn.no)){
20     pat <- paste(stn.no[i], "_1␣hour.csv", sep="")
```

```
21      wlr.fn <- list.files(path=wlr.dir, pattern=pat, full.
           names=T)
22      wlr.dat <- read.csv(wlr.fn)
23      if(names(wlr.dat)[[3]]=="cal"){
24          names(wlr.dat)[[3]] <- "Stage"
25      }
26      wlr.dat$date_time <- as.POSIXct(wlr.dat$date_time, tz=
           "Asia/Kolkata")
27      wlr.dat <- subset(wlr.dat, subset=(wlr.dat$date_time>=
           ts.start & wlr.dat$date_time < ts.end))
28      if(stn.no[i]=="101"){
29          ar.cat <- 242941.95
30          ar.rip <- 2938.67
31          dis.figname <- paste(getwd(), "/stn101_Dis_vs_Time
               .png", sep="")
32          dis.depth.figname <- paste(getwd(), "/stn101_
               DisDepth_vs_Time.png", sep="")
33          et.catch.figname <- paste(getwd(), "/stn101_ET_vs_
               Time_catchment.png", sep="")
34          et.riper.figname <- paste(getwd(), "/stn101_ET_vs_
               Time_riparian.png", sep="")
35          wlr.lowstage <- wlr.dat[wlr.dat$Stage<=0.603, ]
36          wlr.highstage <-  wlr.dat[wlr.dat$Stage>0.603, ]
37          wlr.lowstage$discharge.m3sec <- 1.09*(1.393799*((
               wlr.lowstage$Stage-0.2065)^2.5))
38          wlr.highstage$discharge.m3sec <- 1.09*((1.394*(((
               wlr.highstage$Stage-0.2065)^2.5) - ((wlr.
               highstage$Stage-0.603)^2.5))) + (0.719*(wlr.
               highstage$Stage-0.603)^1.5))
39          wlr.discharge <- rbind(wlr.lowstage, wlr.highstage
               )
40          wlr.discharge$date_time <- as.POSIXct(wlr.
               discharge$date_time)
41          wlr.discharge.sorted <- wlr.discharge[order(wlr.
               discharge$date_time, na.last=FALSE),]
42          wlr.dat <- subset(wlr.discharge.sorted, select=c("
               raw", "Stage", "date_time", "Discharge"))
43          names(wlr.dat) <- c("Capacitance", "Stage", "
               Timestamp", "Discharge")
44          wlr.dat$Discharge <- round(wlr.dat$Discharge,
               digits=5)
45          wlr.dat$DepthDischarge <- (wlr.dat$Discharge/ar.
               cat)*1e+9
```

```
46          plot(wlr.dat$Stage, wlr.dat$Discharge, type="p",
47               main="Stage␣Discharge␣Curve␣for␣V-notch␣at␣
                    Kolaribetta",
48               xlab="Stage␣(m)", ylab="Discharge␣(m^3/sec)")
49          plot(wlr.dat$Timestamp, log(wlr.dat$Discharge),
                 type="l", main="Hydrograph␣for␣V-notch␣at␣
                 Kolaribetta␣\n␣WATTLE␣CATCHMENT",
50               xlab="Time", ylab="Log␣of␣discharge␣(m^3/sec)
                    ")
51          ## Now do a ggplot
52          wlr.dat <- subset(wlr.dat, select=c("Stage", "
                 Timestamp", "Discharge", "DepthDischarge"))
53          ggtitle.dis <- "Discharge␣versus␣time␣for␣station␣
                 101␣-␣Kolaribetta\n␣WATTLE␣CATCHMENT"
54          ggtitle.et.catch <- "Daily␣ET␣versus␣time␣for␣
                 station␣101␣-␣Kolaribetta\n␣WATTLE␣CATCHMENT"
55          ggtitle.et.riper <- "Daily␣ET␣versus␣time␣for␣
                 station␣101␣-␣Kolaribetta\n␣WATTLE␣RIPARIAN␣
                 AREA"
56      }
57      if(stn.no[i]=="110"){
58          ar.cat <- 437425.5
59          ar.rip <- 2511.30
60          dis.figname <- paste(getwd(), "/stn110_Dis_vs_Time
                 .png", sep="")
61          dis.depth.figname <- paste(getwd(), "/stn110_
                 DisDept_vs_Time.png", sep="")
62          et.catch.figname <- paste(getwd(), "/stn110_ET_vs_
                 Time_catchment.png", sep="")
63          et.riper.figname <- paste(getwd(), "/stn110_ET_vs_
                 Time_riparian.png", sep="")
64          p1 <- 10.3833
65          p3 <- 3.1399
66          wlr.dat$Discharge <- p1*(wlr.dat$Stage)^p3
67          wlr.dat$DepthDischarge <- (wlr.dat$Discharge/ar.
                 cat)*1e+9
68          wlr.dat <- subset(wlr.dat, select=c("Stage", "date
                 _time", "Discharge", "DepthDischarge"))
69          names(wlr.dat) <- c("Stage", "Timestamp", "
                 Discharge", "DepthDischarge")
70          ggtitle.dis <- "Discharge␣versus␣time␣for␣station␣
                 110\n␣GRASSLAND␣CATCHMENT"
71          ggtitle.et.catch <- "Daily␣ET␣versus␣time␣for␣
```

```
            station␣110\n␣GRASSLAND␣CATCHMENT"
72          ggtitle.et.riper <- "Daily␣ET␣versus␣time␣for␣
               station␣110\n␣GRASSLAND␣RIPARIAN␣AREA"
73      }
74      if(stn.no[i]=="108"){
75          ar.cat <- 94454.51
76          ar.rip <- 94454.51
77          dis.figname <- paste(getwd(), "/stn108_Dis_vs_Time
               .png", sep="")
78          dis.depth.figname <- paste(getwd(), "/stn108_
               DisDepth_vs_Time.png", sep="")
79          et.catch.figname <- paste(getwd(), "/stn108_ET_vs_
               Time_catchment.png", sep="")
80          et.riper.figname <- paste(getwd(), "/stn108_ET_vs_
               Time_riparian.png", sep="")
81          p1 <- 1.482 ##  25.5628
82          p3 <- 1.598 ## 3.3999
83          wlr.dat$Discharge <- p1*(wlr.dat$Stage)^p3
84          wlr.dat$DepthDischarge <- (wlr.dat$Discharge/ar.
               cat)*1e+9
85          wlr.dat <- subset(wlr.dat, select=c("Stage", "date
               _time", "Discharge", "DepthDischarge"))
86          names(wlr.dat) <- c("Stage", "Timestamp", "
               Discharge", "DepthDischarge")
87          ggtitle.dis <- "Discharge␣versus␣time␣for␣station␣
               108\n␣SHOLA␣CATCHMENT"
88          ggtitle.et.catch <- "Daily␣ET␣versus␣time␣for␣
               station␣108\n␣SHOLA␣CATCHMENT"
89          ggtitle.et.riper <- "Daily␣ET␣versus␣time␣for␣
               station␣108\n␣SHOLA␣RIPARIAN␣AREA"
90      }
91      ##-- Subset for afternoon flows
92      wlr.aft <- subset(wlr.dat, subset=strptime(Timestamp,
           format="%Y-%m-%d␣%H:%M:%S")$hour > 12 & strptime(
           Timestamp, format="%Y-%m-%d␣%H:%M:%S")$hour < 15)
93      ##---Extract afternoon mean for ET calculation---##
94      wlr.aft <- wlr.aft[complete.cases(wlr.aft),]
95      charvec <- wlr.aft$Timestamp
96      wlr.tsaft <- timeSeries(data=wlr.aft$Discharge,
           charvec=charvec)
97      by <- timeSequence(from=ts.start, to=ts.end, by="day")
98      mean.dis <- aggregate(wlr.tsaft, by, mean)
99      colnames(mean.dis)[1] <- "Mean"
```

```
100     mean.dis$Timestamp<-row.names(mean.dis)
101     mean.dis <- as.data.frame(mean.dis)
102     row.names(mean.dis) <- NULL
103     mean.dis$Timestamp <-  as.POSIXct(mean.dis$Timestamp,
           tz="Asia/Kolkata", origin="1970-01-01")
104     mean.dis$Date <- as.Date(mean.dis$Timestamp, "%Y-%m-%d
           ")
105     ##---Extract daily maximum for ET calculation---##
106     wlr.dat <- wlr.dat[complete.cases(wlr.dat),]
107     charvec <- wlr.dat$Timestamp
108     wlr.ts <- timeSeries(data=wlr.dat$Discharge, charvec=
           charvec)
109     by <- timeSequence(from=ts.start, to=ts.end, by="day")
110     mn.dis <- aggregate(wlr.ts, by, mean)
111     colnames(mn.dis)[1] <- "Mean"
112     max.dis <- aggregate(wlr.ts, by, max)
113     colnames(max.dis)[1] <- "Max"
114     max.dis$Timestamp<-row.names(max.dis)
115     max.dis <- as.data.frame(max.dis)
116     row.names(max.dis) <- NULL
117     max.dis$Timestamp<-  as.POSIXct(max.dis$Time, tz="Asia
           /Kolkata", origin="1970-01-01")
118     max.dis$Date <- as.Date(max.dis$Timestamp, "%Y-%m-%d")
119     max.dis$ET <- max.dis$Max-mean.dis$Mean
120     max.dis$ETcatch <- max.dis$ET*1e+9/ar.cat
121     max.dis$ETriper <- max.dis$ET*1e+9/ar.rip
122     ##--plot using ggplot2--##
123     ##-- Discharge
124     sd.plot <- ggplot(data = wlr.dat, aes(Timestamp,
           Discharge)) +
125          geom_line(data=wlr.dat, aes(Timestamp, Discharge))
                +
126                                          #      ggtitle(
                                                ggtitle.dis) +
127              labs(x = "Timestamp", y = "Discharge␣m3/s") +
128                  theme(axis.title=element_text(size=10,face
                        ="bold"),
129                        axis.text=element_text(size=8))
130     ggsave(sd.plot, filename=dis.figname, width=6, height
           =4, units="in")
131     ##-- Depth of discharge in mm
132     sd.depth.plot <- ggplot(data = wlr.dat, aes(Timestamp,
           DepthDischarge)) +
```

```
133          geom_line(data=wlr.dat, aes(Timestamp,
                DepthDischarge)) +
134                                          #      ggtitle(
                                                ggtitle.dis) +
135              labs(x = "Timestamp", y = "Dept␣of␣Discharge␣(
                    mm)") +
136                  theme(axis.title=element_text(size=10,face
                        ="bold"),
137                        axis.text=element_text(size=8))
138      ggsave(sd.depth.plot, filename=dis.depth.figname,
            width=6, height=4, units="in")
139      ##-- Depth of ET in mm for catchment
140      et.plot.catch <- ggplot(data = max.dis, aes(Date,
            ETcatch)) +
141          geom_line(data=max.dis, aes(Date, ETcatch)) +
142                                          # ggtitle(ggtitle.
                                                et.catch) +
143              labs(x = "Date", y = "ET␣in␣mm␣per␣day") +
144                  theme(axis.title=element_text(size=10,face
                        ="bold"),
145                        axis.text=element_text(size=8))
146      ggsave(et.plot.catch, filename=et.catch.figname, width
            =6, height=4, units="in")
147      ##-- Depth of ET in mm for riparian area
148      et.plot.riper <- ggplot(data = max.dis, aes(Date,
            ETriper)) +
149          geom_line(data=max.dis, aes(Date, ETriper)) +
150                                          #  ggtitle(ggtitle
                                                .et.riper) +
151              labs(x = "Date", y = "ET␣in␣mm␣per␣day") +
152                  theme(axis.title=element_text(size=10,face
                        ="bold"),
153                        axis.text=element_text(size=8))
154      ggsave(et.plot.riper, filename=et.riper.figname, width
            =6, height=4, units="in")
155  }
156  ##-- Run LM and plot
157  Cover <- c("Grassland", "Dry␣Wattle", "Green␣Wattle", "
        Shola")
158  NDVI <- c(0.1922, 0.2316, 0.2710, 0.3497) ## 0.2316
159  ET <- c(2.975, NA, 4.759, 6.135)
160  df.ndvi.et <- data.frame(Cover, NDVI, ET)
161  cleandata <- df.ndvi.et[-2, ]
```

```
lm.ndvi.et <- lm(ET~NDVI, data=cleandata)
summary(lm.ndvi.et)
c <- ggplot(cleandata, aes(NDVI, ET)) +
    stat_smooth(method = "lm") + geom_point() +
      labs(x = "NDVI", y = "ET in mm per day")
ggsave(c, filename="lmplotET_NDVI.png", width=6, height=4,
    units="in")
##-- calculate CV and SD
stn110 <- read.csv(file="stn110_ET.csv")
var(stn110$ETcatch)
sd(stn110$ETcatch)
stn101 <- read.csv(file="stn101_ET.csv")
var(stn101$ETcatch)
sd(stn101$ETcatch)
stn108 <- read.csv(file="stn108_ET.csv")
var(stn108$ETcatch)
sd(stn108$ETcatch)
```

Listing A.1: R code for analysing and plotting results of discharge and ET.

# B. Photographs of the study and site

(a) The grassland dominated catchment with the flume used to measure flows.

(b) The weir at he wattle dominated catchment needed to be maintained by clearing debris regularly.

(c) The shola dominated catchment, survey of the stream.

Figure B.1: Study site and instruments. Photo credits: CWC team - FERAL.

(a) Gaur and the Nilgiri Thar.

(b) Downloading data from rain gauges overlooking the Upper Bhavani reservoir and at Kolaribetta.

(c) Distinguished hydrologists who have visited the study site, Dr. Jagrish Krishnaswamy (P.I.) and Dr.Bruijnzeel (left) and the late Dr.Mike Bonell (UK, P.I.) with Dr.Krishnaswamy and Dr.Badiger (Co.PI.).

Figure B.2: Landscape panoramas, wildlife and visitors at the Nilgiri South range. Photo credits: CWC team - FERAL.